Advances in Natural and Technological Hazards Research

Theo van Asch
Jordi Corominas
Stefan Greiving
Jean-Philippe Malet
Simone Sterlacchini *Editors*

Mountain Risks: From Prediction to Management and Governance

Springer

Mountain Risks: From Prediction to Management and Governance

Advances in Natural and Technological Hazards Research

Volume 34

For further volumes:
http://www.springer.com/series/6362

Theo van Asch • Jordi Corominas • Stefan Greiving
Jean-Philippe Malet • Simone Sterlacchini
Editors

Mountain Risks: From Prediction to Management and Governance

Springer

Editors
Theo van Asch
Department of Physical Geography
Utrecht University
The Netherlands

Stefan Greiving
Institute of Spatial Planning
Technical University of Dortmund
Germany

Simone Sterlacchini
National Research Council of Italy
Institute for the Dynamic of Environmental Processes
Milan, Italy

Jordi Corominas
Department of Geotechnical Engineering
Technical University of Catalonia
Barcelona, Spain

Jean-Philippe Malet
University of Strasbourg
CNRS, Institut de Physique du Globe de Strasbourg
Strasbourg, France

ISSN 1878-9897 ISSN 2213-6959 (electronic)
ISBN 978-94-007-6768-3 ISBN 978-94-007-6769-0 (eBook)
DOI 10.1007/978-94-007-6769-0
Springer Dordrecht Heidelberg New York London

Library of Congress Control Number: 2013944754

Printed on acid-free paper

Springer is part of Springer Science+Business Media (www.springer.com)

Preface

This book offers a cross-disciplinary coverage for the rapidly growing field of integrated approaches in risk assessment in mountain areas. It considers all the aspects related to hazard and risk assessment, risk management and governance, all illustrated with a wide range of case studies. The book associates (1) technical chapters on the state-of-the-art methods for the understanding of mountain processes and quantitative hazard and risk forecasts and (2) case study chapters detailing the integration of natural, engineering and human sciences within multi-scale methodologies for risk management and prevention planning.

Long-term cohabitation of the social, economic and environmental systems in mountain areas necessitates (1) to reflect the 'chain of safety' (e.g. pro-action, prevention, preparation, response and follow-up) and (2) to cover the chain of the 'living with risk' process, from quantitative risk assessment to coping strategies including socio-economic and political decision-making. The observed increase in disastrous events over the last decades, associated with an often low perception of most natural risks by the local communities, along with the lack of efficient, socially accepted and environmentally sound remedial measures are amongst the drivers behind the increasing effects of mountain risks.

Landslides and rockfalls on mountain slopes, debris flows within torrential streams and flooding on river valleys, driven by climatic and anthropogenic factors as well as land mismanagement, all cost the economy dearly, especially in mountain areas. Even today, development is still taking place in many hazardous zones, and even more development is taking place in future hazard zones where planning and predictive assessment are at odds. Growing attention has to be paid also to the impact of climatic and non-climatic changes that will result in changing hazard risk patterns over Europe. The development of viable livelihoods on the long-term also endorses the task of governing the risk assessment process at all levels of spatial planning, and for several spatial and temporal scales.

The assessments of natural hazards and risks are generally carried out by natural scientists from fields such as engineering geology, geomorphology, geophysics, hydrology, soil science and geography; however, while the physical problems associated with risk assessment need continual science and engineering attention

(e.g. development of monitoring techniques, alert systems and protection measures), some of the ongoing questions need to be addressed by other disciplines including social and economic science, cognition science, civil and public law, planning and politics.

Most text books deal with some aspects related to hazard and risk assessments (Turner and Schuster 1996; Lee and Jones 2004; Glade et al. 2005; Landslide Committee – National Research Council 2008; Sassa and Canuti 2008). This book focuses on comparative multi-disciplinary case studies and gives a complete picture of all the aspects related to hazards and risks.

The book provides valuable insights, guidance and advice to research scientists, engineers, people in charge of local and regional risk management, planners and policy makers and all those who share a common interest of effective risk reduction to show them the importance of an integrated approach of all aspects of risks in mountainous areas. It is envisaged that the presented cross-disciplinary approach may extend their vision, add to their understanding and possibly, facilitate their work.

The first part of the book is focusing on new techniques for assessing mass movement and flood hazards. It describes the state-of-the-art techniques for the morphological characterization and the monitoring of displacements. Computational advances are described to understand the physical processes, the interactions within the systems and to quantify the hazard.

In the introduction, *Greiving et al.* (Chap. 1) discuss key issues related to aspects of hazards and risks of natural processes in mountain areas and set up the framework of risk governance, which aims to integrate these elements. *Lu et al.* (Chap. 2) introduce several innovative remote-sensing techniques to monitor and analyse the kinematics of slow moving to moderately moving landslides. These are illustrated in three case studies in Italy and France. *Kniess et al.* (Chap. 3) highlight the interest of combining different techniques obtained from numerous developments in remote-sensing, near-surface geophysics, field instrumentation and data processing. In a number of case studies, they show significant advances in characterizing the landslide morphology and internal structure. *Ferrari et al.* (Chap. 4) give an overview of the recent developments of numerical models to describe the complex behaviour of slow and rapid mass movements which form the basis for hazard and risk assessment and the development of reliable Early-Warning Systems (EWS). Special attention is given to the complex hydrological system of landslides, which controls their dynamic behaviour. Case studies are presented to illustrate the performance of the numerical models detailed in this chapter.

The second part of the book is focusing on methodologies to assess the impact of the natural hazards on the society in terms of risks. It presents methods and tools for a quantitative risk assessment of dangerous rapid mass movements using run-out models and the characterization of the vulnerability of the elements at risk.

Luna et al. (Chap. 5) evaluate several dynamic process-based models able to simulate the propagation of rapid mass flows and forecast the hazard (e.g. delineation of the zones where the elements-at-risk will suffer an impact of a certain level of intensity) and the risk through the application of fragility and

vulnerability curves and the generation of risk curves based on economic losses. *Mavrouli et al.* (Chap. 6) give a review on the current methodologies that are used for the assessment of rockfall susceptibility, hazard and risk. The authors present advances involving the consideration of the magnitude of the events and the intensity of the phenomena at selected locations as well as the incorporation of a quantitative vulnerability into the risk equation. *van Westen et al.* (Chap. 7) discuss the analysis of multi-hazards, especially in terms of their interaction, in mountainous environments at a medium scale (1:25,000). They give an overview of the problem of multi-hazard risk assessment illustrated through a case study for the Barcelonnette area (French Alps). *Sterlacchini et al.* (Chap. 8) discuss how vulnerability assessment plays a crucial role in 'translating' the estimated hazard level into an estimated level of risk. They stated that it is impossible to address risk assessment without assessing vulnerability first, and it appears unquestionable that a multi-disciplinary approach is requested in vulnerability assessment studies. *Garcia et al.* (Chap. 9) present a quantitative survey to evaluate the response capacity of the population in the mountainous environment of the Italian Central Alps, in order to assess the levels of preparedness and the perceived risk. The outcome of the enquiry showed that, in this case study, a gap between the occurred disasters and the possible lessons to be learnt still exist and that an effective method to share and disseminate knowledge is missing.

The third part of the book is focusing on the response of the Society towards the problems of hazard and risk. It highlights the role of spatial planning, Early-Warning Systems and evacuation plans for risk management. It establishes practical thresholds for acceptable and tolerable risks and emphasizes the validity of education and communication towards the Society.

Greiving and Angignard (Chap. 10) discuss options for mitigating risk by spatial planning and highlight the effectiveness of such measures by analysing the example of the municipality of Barcelonette (French Alps). *Mavrouli et al.* (Chap. 11) distinguish two different strategies for corrective and protective measures for the mitigation of landslide risk, namely stabilization/interception measures and control measures. A variety of mitigation measures are presented for three different landslide types: rockfalls, debris flows and shallow to deep seated slope movements. *Angignard et al.* (Chap. 12) discuss the interconnection of factors that determine risk perception through a series of social variables and by concentrating on the relevance of legal frameworks and insurance possibilities. The theoretical implications of risk culture on risk assessment and management in practice are explained by the example of the case study of the region of Valtellina (Italian Central Alps). *Garcia et al.* (Chap. 13) analyse different types of Early-Warning Systems with the aim to connect scientific advances in hazard/risk assessment with local management strategies and practical demands of stakeholders/end-users. An Integrated People-Centred Early Warning System (IEWS) is presented, which is mainly based on prevention as a key element for disaster risk reduction. *Peters-Guarin and Greiving* (Chap. 14) give an analysis about risk acceptability and tolerance, which greatly depend on the existing social, economic, political, cultural, technical and environmental conditions of the society at a given moment in time.

Frigerio et al. (Chap. 15) propose interactive tools by means of a WebGIS service architecture to inform stakeholders about the different stages of risk management, especially the preparation phase and emergency management. Different cases are set up using a common open source environment: multi-hazard risk assessment, risk management with interoperability on spatial data and metadata, collection of information on historical natural events and visualisation of outcomes of multi-hazard risk analyses.

The book chapters are the results of the collaborative work of 19 young researchers of the MOUNTAIN RISKS Project (www.mountain-risks.eu/) carried out during 4 years, from January 2007 to January 2011. This collaborative work was supported by the 6th Framework Program of the European Commission through a Marie Curie Research & Training Network. The focus of the project is on research and training in all aspects of mountains hazards and risks assessment and management. The project has involved 14 partners throughout Europe, each hosting a Post-Doc (ER) and a PhD (ESR) position. The partners have organized a series of intensive courses and workshops to train young scientists in all aspects of natural, social and engineering sciences dealing with mountain risks.

We wish to express our gratitude to all those authors who have made this volume possible and to the staff of Springer for all their support.

Utrecht, The Netherlands — Theo van Asch
Strasbourg, France — Jean-Philippe Malet

References

Committee on the Review of the National Landslide Hazards Mitigation Strategy, National Research Council (2004) Partnerships for reducing landslide risk: assessment of the national landslide hazards mitigation strategy. The National Academies Press, Washington, DC

Glade T, Anderson MG, Crozier MJ (2005) Landslide hazard and risk. Wiley, Chichester

Lee EM, Jones DK (2004) Landslide risk assessment. Thomas Telford, London

Sassa K, Canuti P (2008) Landslides: disaster risk reduction. Springer, Berlin

Turner AK, Schuster RL (1996) Landslides: investigation and mitigation. The National Academies Press, Washington, DC

Contents

Chapter 1
Introduction: The components of Risk Governance

Stefan Greiving, Cees van Westen, Jordi Corominas, Thomas Glade, Jean-Philippe Malet, and Theo van Asch

Abstract This introductory chapter discusses key issues related to aspects of hazards and risks of natural processes in Mountain area's and discusses the framework of risk governance, which aims to integrate these elements.

Hazard assessment intends to make an estimate of the spatial and temporal occurrence and magnitude of dangerous natural processes. The chapter describes different methods to assess hazard in a qualitative and quantitative way including all kind of data driven statistically approaches and the use of coupled hydro mechanical deterministic models.

S. Greiving
Institute of Spatial Planning, TU Dortmund University, August-Schmidt-Straße 10, D-44227 Dortmund, Germany

C. van Westen
Faculty of Geo-Information Science and Earth Observation (ITC), University of Twente, Hengelosestraat 99, 7514 AE Enschede, The Netherlands

J. Corominas
Department of Geotechnical Engineering and Geosciences, Technical University of Catalonia, BarcelonaTech, Jordi Girona 1-3, D-2 Building, 08034 Barcelona, Spain

T. Glade
Department of Geography and Regional Research, Geomorphic Systems and Risk Research Unit, University of Vienna, Vienna, Austria

J.-P. Malet
Institut de Physique du Globe de Strasbourg, CNRS UMR 7516, Université de Strasbourg/EOST, 5 rue René Descartes, F-67084 Strasbourg Cedex, France

BEG, Bureau d'Etudes Géologiques SA, Rue de la Printse 4, CH-1994 Aproz, Switzerland

T. van Asch (✉)
Faculty of Geosciences, Department of Physical Geography, Utrecht University, Heidelberglaan 2, 3584 CS, The Netherlands
e-mail: aschtheo@gmail.com

T. van Asch et al. (eds.), *Mountain Risks: From Prediction to Management and Governance*, Advances in Natural and Technological Hazards Research 34,
DOI 10.1007/978-94-007-6769-0_1, © Springer Science+Business Media Dordrecht 2014

Since statistical approaches, will meet difficulties in future predictions in case of changes of the environmental factors, like land use and climate, special attention is given to the use of physical deterministic models which makes it possible in theory to do predictions about hazard without historical data sets.

An overview is given of the different approaches to come to a final risk assessment. For a risk assessment information on temporal, spatial and intensity probabilities of the endangering processes is required as well as an identification of the vulnerability of the society for the impact of these processes. Vulnerability assessment, which forms a key element in these procedures still knows a lot of difficulties.

Current research on natural risks is fragmented and isolated with natural sciences and engineering disciplines on the one hand and societal sciences on the other hand. The complex, socio-political nature of risk calls for an integrated approach. A discussion is presented about the concept of risk governance, which tries to combine all the physical, technical, socio-economic and political aspects to take the right decisions for a safe and sustainable society.

Abbreviations

IUGS	International Union of Geological Sciences
GIS	Geographical Information Systems
ALARP	As Low As Reasonably Practicable
EIA	Environmental Impact Assessments
EWS	Early Warning Systems
DEM's	Digital Elevation Models
LIDAR	LIght Detection And Ranging
F-N curves	Frequency vs. Number of fatality' graphs
UN	United Nations
UN-ISDR	United Nations International Strategy for Disaster Reduction
EC	European Commission
IRGC	International Risk Governance Council
RG	Risk Governance
RA	Risk Assessment
RM	Risk Management
RC	Risk Communication
MORLE	Multiple Occurrence Regional Landslide Events

1.1 Hazard Assessment

Hazard and risk assessment are prerequisites for a safe and sustainable development of the society in mountainous areas. *Hazard* assessment for example of landslides aims at an estimate of the spatial and temporal occurrence and magnitude of these natural processes (IUGS Working Group on Landslides 1997).

Decisions in the area of so called "traditional" hazards like landslides are normally based on expert expertise, often combined with results from modelling analysis. Hereby, the calculation of the spatio-temporal probabilities of the natural hazards on the basis of recent field monitoring but also related to available historical information is crucial.

Different methods are used to assess landslide hazard in a qualitative and quantitative way (Soeters and Van Westen 1996; Carrara et al. 1999; Guzzetti et al. 1999; Dai et al. 2002). All kind of data driven statistically approaches are used now at days to relate the occurrence of landslides which their causal factors. In recent years there is a growing interest for the use of coupled hydro mechanical models, which can describe quantitatively the frequency and dynamic of landslides.

For the assessment of hazard by the heuristic or statistical approach temporal information is needed in terms of magnitude and frequency of dated historic landslide events that can be related with sufficient long historical records of the most important triggering events: rainfall and earthquakes (Zezere et al. 2004; Corominas and Moya 2008). However, analysed data are only available for a specific period – and are thus not representative for longer periods. This problem is enhanced when using historical data. These add indeed the value of information in particular for frequency and magnitude analysis of the investigated processes. It has to be admitted that historical data are always incomplete information covering in particular the large scale events, but not the events with smaller magnitudes.

Historic information can be completed by landslide interpretation from aerial photographs and satellite imagery. This needs however great skills in field and photo interpretation and even then different experts may deliver different results (Carrara et al. 1992; Van Westen et al. 1999).

Statistical approaches, which are based on correlations between past landslide occurrences and the causative landscape factors will meet difficulties in future predictions in case of changes of the environmental factors, like land use and climate. The observed climate changes related effects on temperature and precipitation will lead to new uncertainties, because past events might be not representative anymore. Similarly, other changes in the catchments (e.g. deforestation, melting of glaciers, surface sealing through settlement development, surface modification by infrastructure, etc.) will also lead to high uncertainties. Here, the perspective changes from probabilities to just possibilities. With public decision-making not having any precise information at hand, restrictions for private property rights are probably not anymore legally justifiable. Hereby, justification of actions and consensus about thresholds for acceptable risks and response actions becomes more important.

1.1.1 Susceptibility Assessment

The spatial component of the hazard assessment is called the susceptibility assessment. A susceptibility map shows the subdivision of the terrain in zones that have

a different likelihood that landslides or other mountain hazards may occur. The likelihood may be indicated either qualitatively (as high, moderate low, and not susceptible) or quantitatively (e.g. as the density in number per square kilometers, area affected per square kilometer, Safety Factor, height or velocity of run-out). Landslide susceptibility maps should indicate both the zones where landslides may occur as well as the run out zones. Therefore the landslide susceptibility methods are divided into two components. The first susceptibility component is the most frequently used, and deals with the modelling of potential initiation areas (susceptibility to failure). The resulting maps will then form the input as source areas in the modelling of potential run-out areas (run-out susceptibility).

Many statistical techniques have been developed and applied successfully to landslide susceptibility assessment and mapping in the last 10 years using bivariate or multivariate approaches, probabilistic approaches (like Bayesian inferences or logistic regression) and artificial neural networks approaches Such techniques are capable to predict the spatial distribution of landslides adequately with a relatively small number of conditioning variables.

Overviews and classification of methods for landslide initiation susceptibility assessment can be found in Soeters and Van Westen (1996), Carrara et al. (1999), Guzzetti et al. (1999), Aleotti and Chowdury (1999), Cascini et al. (2005), Chacon et al. (2006), Fell et al. (2008), Cascini (2008), Dai and Lee (2003).

Landslide susceptibility assessment can be considered as the initial step towards a quantitative landslide hazard and *risk* assessment. But it can also be an end product in itself, or can be used in qualitative risk assessment if there is insufficient information available on past landslide occurrences in order to assess the spatial, temporal and magnitude probability of landslides.

Methods for assessing landslide run-out may be classified as empirical and analytical/rational (Hungr et al. 2005). For susceptibility zoning purposes both methods are widely used given their capability of being integrated in GIS platforms. However, they vary a lot depending on the type of process modelled, the size of the study area (modelling individual events or modelling over an entire area), availability of past occurrences for model validation, and parameterization.

For flood susceptibility assessments, also the two components mentioned for landslides can be differentiated: the initiation component dealing with the runoff modelling in the upper catchment (hydrologic modelling), and the spreading component, dealing with the estimation of the spatial distribution, height and flow velocity in the downstream section (hydraulic modelling).

In near-flat terrain with complex and also in urban environments and in areas with a dominant presence of man-made structures, flood models are required that calculate flow in both X- and Y-direction (2-D models). Such models, like SOBEK (Stelling et al. 1998; Hesselink et al. 2003), Telemac 2D (Hervouet and Van Haren 1996) and MIKE21 can also be applied in the case of diverging flow at a dike breach. They require high quality Digital Elevation Models (DEM's), which ideally are generated using LIDAR data (Alkema and Middelkoop 2005). The flood modelling is usually carried out at a municipal to provincial scale, at a selected stretch of the river. These models provide information on how fast the water will flow and

how it propagates through the area. It is very suitable to assess the effects of the surface topography, like embanked roads and different land cover types on the flood behavior (Stelling et al. 1998).

1.1.2 From Susceptibility to Hazard

Hazard assessment requires information on temporal, spatial and intensity probabilities. The analysis of these probabilities is very different for landslide and flood hazard assessment. In the case of flood hazard assessment, flood inundation scenarios are generated for flood discharges that are related to a specific return period, which can be analyzed using magnitude/frequency analysis of historical discharge data. The resulting flood scenarios already indicate the areas that are likely to be flooded (hence the spatial probability of flooding in these areas is 1), and the intensity of flooding (in terms of water depth, flow velocity or impact pressure).

In the case of landslide hazard assessment the conversion of susceptibility maps into quantitative hazard maps is much more complicated, especially at medium scales of analysis. Conversion of landslide susceptibility maps into landslide hazard maps often requires a separate estimation of the spatial, temporal and magnitude probabilities of landslides (Guzzetti et al. 1999; Fell et al. 2008; Van Asch et al. 2007; Corominas and Moya 2008; van Westen et al. 2008), which may not be correct as these three components are interdependent.

- The spatial probability required for hazard assessment is not the same as the landslide susceptibility. A susceptibility map outlines the zones with a relatively likelihood of landslides. However, only a fraction of the high hazard zones outlined in these maps may actually experience landslides during different scenarios of triggering events. In most of the methods that convert susceptibility to hazards, triggering events and the landslide pattern they cause, play a major role. Hence it is important to obtain event-based landslide inventories or MORLE (Crozier 2005) for which one can determine the temporal probability of the trigger, the spatial probability of landslides occurring within the various susceptibility classes, and the intensity probability. In this approach, which is mostly carried out at medium scales, the susceptibility map is basically only used to subdivide the terrain in zones with equal level of susceptibility.
- Intensity probability is the probability of the local effects of the landslides. Intensity expresses the localized impact of a landslide event, measured in different ways, such as height of debris (e.g. for debris flows), velocity (e.g. of debris flows, or large landslides), horizontal or vertical displacement (e.g. of large landslides), or impact pressure (e.g. for debris flows, rockfalls). Whereas the magnitude of a landslide, which can be represented best by the volume of the displaced mass, is a characteristic of the entire landslide mass, the intensity is locally variable, depending on the type of landslide, the location with respect to the initiation point, and whether an element at risk is on the moving landslide,

in front of it, or directly above it. The quantitative estimation of the probability of occurrence of landslides of a given size is a key issue for any landslide hazard analysis (Malamud et al. 2004; Fell et al. 2008). Magnitude probabilities of landslides can be estimated after performing the magnitude-frequency analysis of landslide inventory data. For estimating landslide magnitudes, the area of landslide (m^2) can be considered as a proxy (Guzzetti et al. 2005b) to the volume, which is often difficult to collect from inventories. The frequency-size analysis of landslide area can be carried out by calculating the probability density function of landslide area using the maximum likelihood estimation method assuming two standard distribution functions: Inverse-Gamma distribution function (Malamud et al. 2004), and Double-Pareto distribution function (Stark and Hovius 2001).

- Temporal probability can be established using different methods. A relation between triggering events (rainfall or earthquakes) and landslide occurrences is needed in order to be able to assess the temporal probability (Corominas and Moya 2008). Temporal probability assessment of landslides is either done using rainfall threshold estimation, through the use of multi-temporal data sets in statistical modeling, or through dynamic modeling. Rainfall threshold estimation is mostly done using antecedent rainfall analysis, for which the availability of a sufficient number of landslide occurrence dates is essential. If distribution maps are available of landslides that have been generated during the same triggering event, a useful approach is to derive susceptibility maps using statistical or heuristic methods, and link the resulting classes to the temporal probability of the triggering events. The most optimal method for estimating both temporal and spatial probability is dynamic modeling, where changes in hydrological conditions are modeled using daily (or larger) time steps based on rainfall data (Van Asch et al. 2007). However, these require reliable input maps, focusing on soil types and soil thickness. The methods for hazard analysis should be carried out for different landslide types and volumes, as these are required for the estimated losses.

1.1.3 Physical Modelling and Monitoring as a Basis for Hazard and Risk Assessment

The use of physical deterministic models plays an essential role in quantitative landslide hazard and risk assessment because these estimate in a quantitative way failure and motion, calculate run-out distances, velocities, impacts and material spreading. The use of physical deterministic models makes it possible in theory to do predictions without historical data sets. However the modeling tools require rather detailed spatial information about the input parameters, sometimes very difficult to obtain, like for example soil thickness. Therefore this deterministic approach is only feasible in more site specific situations or at the catchment scale in rather homogeneous areas with simple landslides (Dietrich et al. 2001; Chen and Lee 2003; Van Beek and Van Asch 2003).

Coupled hydrological slope stability and run-out models can be used to determine the temporal frequency of land sliding. Coupled hydrological catchment models and hydraulic propagation models forms the basis for flood frequency assessment. An estimate of the temporal occurrence of landslides triggered by earthquakes is more problematic. There are many types of hydrological triggering mechanisms dependent on the state of the system, which defines the thresholds for first-time failure and landslide reactivation. Therefore it is a necessity to understand the hydrological triggering mechanisms. Most systems are related to infiltrating water, decrease in suction and increase in groundwater pressures (van Asch and Sukmantalya 1993; Terlien et al. 1995; Fredlund et al. 1996; Sun et al. 1998; Brooks et al. 2004) Also, surface runoff following high-intensity rainfall in steep catchments can infiltrate into accumulated debris and trigger debris flows (Blijenberg 1998; Berti and Simoni 2005; Tang et al. 2011). Difficulties in modelling properly the hydrological triggering system are related to the complexity of real landslides, the difficulty to monitor groundwater levels or soil moisture contents in unstable terrain, and the difficulty to understand the water pathways within the landslide bodies (Brunsden 1999). Especially, the complex morphology of landslides and the presence of fissure systems may result into complex and inter-connected hydrological subsystems (van Asch et al. 1996; Malet et al. 2005).

In hydrological models a coupling between unsaturated and saturated flow and the influence of the vegetation on water losses by evapotranspiration is essential to forecast changes in failure frequency induced by climate and land use changes (Bonnard and Noverraz 2001; Bogaard and van Asch 2002; van Beek 2002).

With respect to the hazard assessment of slow moving landslides, the essence of modelling must be focused on an accurate reproduction of the deceleration and acceleration of landslide bodies and in particularly, a reliable forecast of the potential transformation towards catastrophic, extremely rapid surges. Post-failure movement of landslides is controlled by a complex and dynamic interaction between mechanical and fluid properties and states which results in a spatio-temporal variation in the effective strength and apparent rheological properties of the material (Vulliet 1997, 2000; Picarelli et al. 1995; Leroueil et al. 1996; Pastor et al. 2010).

Due to these complex interactions, the parameterization of hydrological and geomechanical factors by field and laboratory tests is not sufficient to describe the post-failure movement patterns of landslides (Vulliet 2000) and not all the processes can be included in detail in the simulation (van Asch et al. 2006).

The modelling of fast landslides with large run out distances (rock falls, debris flows, rock avalanches) is important because of their intensive impacts and the higher spatial probability to hit elements at risk. The deterministic modelling of these rapid mass movements for a reliable hazard zonation is problematic because of the great variety in and complexity of the triggering processes, the amount of sediment release per event, the related mechanical run out characteristics, the mechanics of entrainment along the run-out track and the spreading in the deposition zone (Quan Luna et al. 2012). The modelling becomes uncertain because direct field measurements of key variables such as pore-pressure and viscosity are impossible. Rheological properties (yield stress, viscosity) determined

from laboratory small-scale samples may not be representative at the slope scale. The parameterisation for a given rheological model is therefore most times determined by back-analyses of observed events (Malet et al. 2004; Hungr et al. 2005; Quan Luna et al. 2012). For a reliable hazard zonation of these flow-like features in the deposition areas, one has to know the detailed DTM's of the dynamic and changing topography of the built-up debris fans to predict adequately the spreading (Hungr et al. 2005; Van Asch et al. 2007).

One of the challenges is to extend our methodologies to get better predictions about the temporal occurrences and magnitudes of landslides making use of statistical and deterministic methods or a combination of this. When there is a lack of temporal information it is promising to couple spatial probability of landslides (susceptibility) acquired by statistical techniques with temporal probabilities obtained by stochastic hydrological slope instability modelling using rainfall with different return periods as input (Thiery 2007).

The last decade shows a rapid development in all kind of geodetic, geoinformation and remote sensing techniques to detect, and monitor landslides and to deliver more precise topographical information and other environmental causative factors (Van Westen et al. 2005). An important task for the future is to further explore develop and evaluate these new techniques because they seem very promising to improve our ability for early warning and for hazard and risk assessment.

1.1.4 Multi-technique On-Site and Remote Monitoring as a Basis for Hazard and Risk Assessment

To develop comprehensive hazard assessment procedures, it is important to incorporate time series, 3-D patterns and deformation analyses in the model-building exercise; it is also essential that the physically-based models be improved so that a greater spatial and temporal description can be included. This goal requires first that rapid-varying factors (rainfall, freeze-thaw, meltwater, ground acceleration) and slow-varying factors (tectonic movements, weathering and associated property changes, erosion, deposition, changing confinement and unloading) are properly specified at adequate spatial and temporal resolutions. The influence of these elementary factors for the different landslide types can be identified through new investigation and monitoring techniques, and detailed analyses of event databases.

The last decade shows a rapid development in all kind of geodetic, geoinformation and remote sensing techniques to detect, and monitor landslides and to deliver more precise topographical information and other environmental causative factors (Fig. 1.1). Displacement monitoring of unstable slopes is a crucial tool for the prevention of hazards. It is often the only solution for the survey and the early-warning of large landslides that cannot be stabilized or that may accelerate suddenly. The choice of an adequate monitoring system depends on the landslide type and size, the range of observed velocity, the required frequency of acquisition, the desired accuracy and the financial constraints.

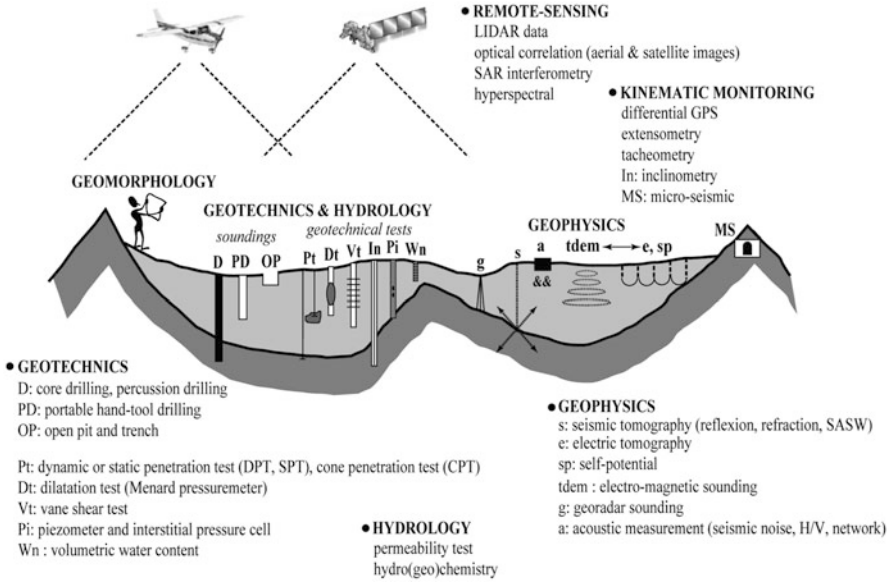

Fig. 1.1 Multi-technique strategy of investigation and monitoring of an active slope movement

Displacement monitoring techniques applied on landslides can be broadly subdivided in two main groups: geodetic and remote-sensing techniques.

Geodetic surveying consist in detecting geometrical changes in the landslide topography by measuring geometric parameters such as angles, distances or differences in elevation (e.g. levelling, tacheometry; Naterop and Yeatman 1995; Jaboyedoff et al. 2004). These techniques necessitate the installation of targets in and outside the landslide and in measuring their position at different times. They have the advantage to be very accurate (0.2–2.0 cm) with a high potential of automation. Furthermore, many authors demonstrated the efficiency of a permanent (Malet et al. 2002) and non-permanent (Squarzoni et al. 2005) differential Global Positioning System (dGPS) for landslide monitoring with a centimetric accuracy during any daytime and weather conditions. However, because landslides can show highly variable displacement rates in time and space according to the local slope conditions (bedrock geometry, distribution of pore water pressures), the major drawbacks of the geodetic techniques are (1) to provide only discrete point measurements of the displacement and (2) the costs of installation and maintenance of the survey network. They are usually only justified in the case of a real risk for the population.

Remote-sensing techniques are interesting tools to obtain spatially-distributed information on the kinematics (Delacourt et al. 2007) and can be operational from spaceborne, airborne and ground-based platforms. Remote-sensing techniques give the possibility to discriminate stable and unstable areas and to map sectors within the landslide with different kinematics from a regional to a local scale. They are

also useful tools for a process-based analysis of the deformation field affecting the slope (Casson et al. 2005; Teza et al. 2008; Oppikofer et al. 2008). In the last decades, the development of ground-based platforms for landslide monitoring at the local scale provided many advantages over spaceborne and airborne platforms despite a shorter spatial coverage (Corsini et al. 2006). The geometry and frequency of acquisitions are more flexible and adaptable to any type of local environment. In addition permanent installations of ground-based platforms allow continuous monitoring (Casagli et al. 2004). Three main categories of ground-based remote sensing techniques are used in landslide monitoring: Ground-Based Synthetic Aperture Radar Interferometry (GB-InSAR), Terrestrial Laser Scanning (TLS) and Terrestrial Optical Photogrammetry (TOP). Detailed reviews of the application of GB-InSAR and TLS to landslides can be found in Corsini et al. (2006), Tarchi et al. (2003), Jaboyedoff et al. (2010), Teza et al. (2007, 2008) and Monserrat and Crosetto (2008). A state-of-the art of the application of TOP to landslide and related geomorphological processes is given in Travelletti et al. (2012).

An important task for the future is to further explore develop and evaluate these new techniques because they seem very promising to improve our ability for early warning and for hazard and risk assessment.

1.2 Risk Assessment

Risk assessment focuses on the consequences of the impact of these processes on society in terms of loss (IUGS Working Group on Landslides 1997). In order to come to a risk evaluation we need to identify the vulnerability of the society for the impact of these flooding and landslide processes and to assess the losses.

1.2.1 The Problem of Vulnerability

There are different types of vulnerabilities and associated losses which are related to physical, economic social and environmental aspects. For analyzing the physical vulnerability various types of approaches can be used, that can be either quantitative (Uzielli et al. 2008) or qualitative (Glade 2003), and based on heuristic, empirical or analytical methods. In the case of flooding, vulnerability curves are available that link the flood intensity (water height, velocity or impact pressure) to the degree of damage for different elements at risk. In the case of landslides vulnerability assessment is much more complicated. First of all because there are many types of landslides, and different measures of intensity (e.g. impact pressure for rock-fall, height for debris flows etc.). Secondly, the spatial variation of the intensity is much more difficult to estimate for landslides than for flooding, as the run-out of mass movements depends on many factors, which are very difficult to predict on a medium scale (e.g. expected initiation volume). There are also much

less historical damage data available for landslides than for flooding that allow the construction of vulnerability curves (Fuchs et al. 2007). Therefore the focus in landslide vulnerability assessment at a medium scale is mostly on the use of expert opinion in defining vulnerability classes, and the application of simplified vulnerability curves or vulnerability matrices. In many situation, when there is not enough information to specify the expected intensity levels of the hazard, or when there is not enough information available to determine vulnerability classes, vulnerability is simply given a value of 1 (completely destroyed). Other types of vulnerability (e.g. social, environmental, and economic) are mostly analyzed using a Spatial Multi-Criteria Evaluation, as part of a qualitative risk assessment.

Damages on physical elements at risks like buildings and infrastructures can be translated relatively easy in direct losses in terms of money. More problematic are the assessments of direct and indirect economic and environmental losses due to the complexity of economic and environmental systems. The most difficult is to define indicators which can express direct and indirect social damages and losses related to for example fatalities, injuries, psychological impact and loss of social cohesion (Glade 2003; Guzzetti et al. 2005a).

1.2.2 From Hazard to Risk

For a direct risk assessment of physical objects the hazard and vulnerability components have to be integrated with an exposure component. This exposure component is based on an analysis of the number of elements at risk that are spatially overlapping with a certain hazard scenario. In the case of flooding, the individual flood extend maps for different return periods can be spatially combined in GIS with the footprints of the elements at risk (e.g. buildings) to calculate the number of buildings affected during that specific scenario. In the case of landslides the hazard map, which has basically the same spatial units as the susceptibility map, is spatially combined with the elements at risk. Here the spatial probability that within a certain hazard class a landslide will occur needs to be included in the analysis, leading to a much higher degree of uncertainty then in the case of flood risk assessment.

To come to a quantitative risk assessment the losses or consequences are calculated by multiplying the vulnerability and the amount of exposed elements at risk for each hazard scenario with a given temporal probability The results is a list of specific risk scenarios, each one with its annual probability of occurrence and associated losses. The specific risk is calculated for many different situations, related to hazard type, return period and type of element at risk. Given the large uncertainty involved in many of the components of the hazard and vulnerability assessment, it is best to indicate the losses as minimum, average and maximum values for a given temporal probability.

The specific risks are integrated using a so-called risk curve in which for each specific risk scenario the losses are plotted against the probabilities, and expressing also the uncertainty as minimum and maximum loss curves. The total risk can then

be calculated as the integration of all specific risks, or the area under the curve. The risk curves can be made for different basic units, e.g. administrative units such as individual slopes, road sections, census tracts, settlements, or municipalities.

A similar approach can be used also for the analysis of population risk (societal risk), although the analysis depends on the spatial and temporal distribution of population and the application of specific population vulnerability curves, either for people in buildings, or in open spaces. The results are expressed as f-n curves (Salvati et al. 2010).

1.2.3 A Summary Related to Aspects of Risk Assessment

Table 1.1 gives a summary of the main aspects related to risk assessment at a medium scale for flooding and different types of mass movements discussed in the earlier part of this section. It is clear from the description of the problems associated with each of the components of quantitative risk assessment, that a hazard and risk assessment often includes a large degree of uncertainty. If the uncertainties in the input factors cannot be evaluated, or if there are simply not enough data to estimate the hazard and vulnerability components, the best option is then to carry out a qualitative risk assessment instead. This could be done in several ways. For instance a set of worst-case scenarios could be used to address the maximum possible losses, without including information on temporal probabilities or vulnerabilities (See for instance the example from the Barcelonnette area in this chapter). Another option is to carry out a qualitative risk assessment using a Spatial Multi-Criteria Evaluation, in which a hazard and a vulnerability index is made using a set of indicators and expert derived weight values.

The results from the risk assessment are subsequently used for evaluating the best disaster risk reduction measures. Some of these measures require quantitative risk assessments, whereas for other qualitative risk assessment can be sufficient. For cost-benefit analysis of physical mitigation measures, quantitative values of annualized risk are required which should be based on the analysis of many different scenarios with respect to their return periods (probabilistic approach). For the development of early warning systems and the design of disaster preparedness programmes, quantitative risk could be calculated for specific hazard scenarios (deterministic approach). For spatial planning and Environmental Impact Assessments, also qualitative risk information could be used.

1.3 Risk Management

Risk management is the systematic application of policies, procedures and practices to the tasks of identifying, analyzing, assessing, monitoring and mitigating risk. It takes the output of the risk assessment and weighs up risk mitigation options

Table 1.1 Main aspects related to risk assessment at medium scale for flooding and different types of mass movements

	Components	Flooding	Rockfall	Shallow landslides	Debrisflows
Input data	Historical data	Direct: discharge data for stations upstream of the study area. Indirect: rainfall-runoff modelling,	Generally only location information is available on past events. Only in few cases also dates and volumes are available	Multi-temporal inventories based on image interpretation. Information of specific event dates and associated sizes/volumes are limited. Event-based inventories are essential	Collection of data historical debrisflow events, with dates and associated areas affected. In most cases this information is very limited.
	Factors	DEM should be very detailed (LIDAR preferably), surface roughness, boundary conditions	Lithology, discontinuities, slope, soils, land cover, protective measures.	Soil thickness, geotechnical properties and slope information is difficult to collect at medium scale.	Initiation volume, hydrological parameters, rheology, detailed topographic profiles.
Susceptibility	Initiation susceptibility	Not needed if discharge data available. Otherwise based on rainfall runoff modelling, depends on availability of (daily or continuous) rainfall data. Spatial variability is an important point	This requires sufficient historical information, and can be done using statistical or numerical approaches.	Depending on the input data simplified physically-based modelling can be carried out. Otherwise statistical analysis is carried out.	Either based on simplified physically-based modelling of shallow landslides, or using hydrological models that include sediment component.
	Runout susceptibility	Good estimate through hydraulic modelling	Application of empirical or simple numerical approaches is possible. More advanced numerical approaches can be applied in smaller areas.	Application of simple empirical approaches is most commonly used.	Regional runout models that are based on reach angles, application of specific runout models for individual catchments. Validation is problematic.
Hazard	Spatial probability	1 for different flood scenarios	If advanced approaches are used a good estimate can be obtained	Depends on the availability of event-based inventories	1 if numerical simulations are used
	Temporal probability	Magnitude-frequency analysis of discharge data	Difficult, because it is based on past records, whereas the link with triggering events is less clear.	Link with return period of triggering event (rainfall or peak ground acceleration)	Link with return period of triggering rainfall event is sometimes difficult.
	Intensity probability	Resulting directly from the modelled scenarios	If advanced approaches are used a good estimate can be obtained, otherwise a reasonable estimation.	Based on frequency-size distribution of event-based inventories	If numerical simulations are used the resulting maps may indicate debrisflow height or velocity.
Risk	Exposure	This can be done by simple GIS overlaying of flood scenarios with elements at risk	This can be done by simple GIS overlaying of rockfall scenarios with elements at risk	Depends on the possibility to obtain estimate of spatial probability.	Depends very much on the quality of the runout model used.
	Vulnerability	Vulnerability curves are available for most elements at risk, including building contents	Even though vulnerability curves are less available, a general indication of vulnerability is possible	Simple approaches are mostly used relating it to expected landslide size.	Some vulnerability curves are available, but actual damage is highly variable. Depends on quality of runout model.
	Type of risk assessment	Quantitative risk assessment is possible, and level of uncertainty is relatively limited	Quantitative risk assessment is possible for deterministic scenarios. Relation with temporal probability is more problematic	Very high degree of uncertainty for quantitative risk assessment. Mostly done qualitatively	Quantitative risk assessment is possible, but with high degree of uncertainty. Relation with temporal probability is more problematic

Colours indicate the degree of uncertainty: *yellow* = high, *orange* = moderate, *green* = relatively low

Table 1.2 Landslide risk mitigation strategies

Strategy	Action	Goal
Risk acceptance	Do nothing	
Hazard avoidance	Reduce exposure	Locate people and structures in safe places
Hazard reduction	Slope maintenance	Control of landslide preparatory factors
	Reduce landslide occurrence: landslide stabilization	Reduce driving forces Increase resisting forces
	Reduce landslide severity	Reduce landslide magnitude and/or intensity
Minimizing consequences	Evacuation	Saving lives and reduce damages
	Reduce vulnerability	Increase resilience of exposed element
	Protection	Avoid damages

Modified from Corominas (2013)

(Fell et al. 2005). Different strategies may be considered to face landslide risk (Corominas 2013): accepting the risk, avoiding hazardous locations, reducing the hazard level, and minimizing the consequences (Table 1.2).

These strategies have different goals and actions, and may be implemented through specific measures, which may be either active or passive (Mavrouli et al. 2012 – this book). Active measures aim at modifying the occurrence or the progression of the landslides and involve earthworks, the construction of concrete structures (structural measures) or the implementation of surface protective works including eco-engineering techniques (non-structural measures). Passive measures do not interfere with the landslide process. They are conceived to either avoid or reduce the adverse consequences of the landslides as in the case of the land use planning or the early warning systems.

1.3.1 Risk Acceptance

Risk acceptability is the predisposition to accept the risk. This occurs when the incremental risk from a hazard to an individual is not significant compared to others risks to which a person is exposed in everyday life. Under the risk acceptability premises, any action for further reducing the risk is usually found as not justifiable. However, risk acceptance may sometimes be forced by the lack of economic resources to reduce landslide hazard or to construct protection works. Risk may then be managed within the ALARP (As Low As Reasonably Practicable) principle and it is considered tolerable only if its reduction is impracticable or if its cost is grossly in disproportion to the improvement gained (Bowles 2004).

Risk acceptance strategy also includes transferring the costs through insurance, compensation, or emergency relief actions. Slow-moving landslides and creep mechanisms may justify taking the option of repair and replacement of the affected structures without adopting specific stabilization or protective measures.

1.3.2 Hazard Avoidance

Hazard avoidance is fundamentally achieved by adopting land use planning measures that aim at reducing the exposure to the hazardous events. This strategy is by far the most efficient and economic option to manage risk. It is also important to consider that some landslides cannot just be controlled by implementing stability or protective measures. This is particularly true for very rapid and high intensity phenomena, such as large debris flows or rock avalanches. Avoidance of hazard requires, first of all, the appropriate identification and mapping of all existing and potential landslides and their potential paths, which is the goal of the landslide susceptibility and hazard maps. The detail and intensity of the analysis will depend on the available resources and, at its turn, it will condition the spatial resolution and reliability of the landslide hazard map and subsequent zoning.

1.3.3 Hazard Reduction

Hazard reduction strategies aim at improving the safety of the elements at risk in areas threatened by landslides. The goal of these strategies may consist (i) to reduce the probability of occurrence of the failure or the reactivation of an existing landslide by means of stabilization works or (ii) to construct structures with the purpose to intercept or constrain the landslide progression, reducing its magnitude, velocity, and run-out. The stabilization of the slopes or the existing landslides may be achieved by either reducing driving forces or by increasing resisting forces. Some recent books present an up to date review of the current practice of landslide stabilization (e.g., Turner and Schuster 1996; Cornforth 2005; Highland and Bobrowsky 2008). Reducing driving forces is mainly achieved by the removal of the unstable mass or by slope regrading. The increase of resisting forces in the slopes may require the use of external loads such as retaining structures or anchoring systems. Drainage is one of the most effective actions in stabilizing slopes by increasing shear strength of soils and reducing cleft water pressures in rock joints. Alternatively, the hazard level may be reduced once the landslide has occurred. To this end, the measures have to be implemented along the potential landslide path. They may have different goals such as diverting the trajectory away from the exposed elements, directly protecting the exposed elements or decreasing the landslide intensity by reducing the magnitude, the velocity or both.

The implementation of these type of active measures require careful engineering design, which must be technically feasible, affordable, environmentally sound, and accepted socially, making sure that they will not divert the problem elsewhere. Numerical models are usually used to facilitate the decision of the location of the structures (e.g. barriers, dissipaters) and for their dimensioning. Despite the recent developments a lot of uncertainties still remain, which concern the rheological parameters of the moving mass and in the assessment of the potential movable volume in order not to overcome the storage capacity of the retention works.

Maintenance and protection of the slope is also part of the hazard reduction strategy. The former aims to control the evolution of preparatory factors such as rock weathering, toe erosion or water infiltration that dispose the slope prone to failure. Measures to restrict the development of instability preparatory factors include slope protection and adoption of best practices (Chatwin et al. 1994; GEO 2003).

1.3.4 Consequence Reduction

Risk may be mitigated by minimizing the damages by avoiding the harmful effects of the hazardous process. Measures for reducing the consequences of the landslides range from the reinforcement of the exposed elements, the implementation of adaptive designs, the active protection, and the evacuation systems. These measures may involve a combination of non-structural and structural measures. Vulnerability of the exposed elements may be reduced by structural reinforcement or with adaptive designs (e.g. large bridge spans, flexible pipes). They must be considered a very last option only as few structures are able to resist high intensity impacts such as those produced by debris flow or rock-fall events. Most frequently, consequence reduction is achieved by the construction of protective works which include structural elements such as galleries, wall, tunnels or earth-works.

Alert systems are a risk mitigation option for places where urban population and infrastructures have expanded into landslide-prone areas. Their goal is to alert the public in order to reduce their exposure to the landslides and to mobilize the emergency teams within government departments. The alert system requires an effective early warning system (EWS) for landslides, as well as operational administrative units and educated population. EWS are commonly based on correlation with triggers (i.e., cumulative rainfall) or on monitoring schemes that use predefined rates of displacement or changes in groundwater levels to launch the alert (Guzzetti et al. 2008). Some landslide triggers such as earthquakes are, however, difficult to predict.

1.3.5 Implementation of Risk Mitigation Measures

The most efficient strategy to manage landslide risk is avoiding hazardous zones by means of an appropriate land-use planning policies. This requires the consideration of the potential hazardous locations, which is the goal of the landslide susceptibility and hazard maps. Despite the impressive development of the landslide mapping methods and the support of the GIS platforms and integrated physically based models, the definition of hazardous zones is still a challenge. The main uncertainties come from our inability to estimate the landslide volume beforehand and the probability of occurrence, particularly considering the climate and the land-use changes. Consequently, landslide maps must be validated and updated whenever possible.

The slope stabilization and protection measures are best recommended in situations where population or infrastructures are subjected to an imminent landslide threat (Mavrouli et al. 2012 – this book). In any case, to stabilize a landslide requires the appropriate understanding of the failure geometry and of the mechanism. Landslide stabilization is a permanent activity that does not stop after the completion of the works and continues with the maintenance of the structural elements and with the monitoring of the whole system.

Operational early warning systems exist only for a few areas and most of those systems are prototypes. Furthermore, inadequate monitoring networks, insufficient personnel and, sometimes, insufficient warning criteria hamper the ability of the existing systems to issue effective warnings (Baum and Godt 2009). Because of this, when considering any type of risk mitigation technique it is important not to generate a false sense of security, particularly in urbanized areas and to inform and educate population properly.

1.4 Risk Governance as an Overall Framework

1.4.1 Introduction

In mountain regions, natural hazards and risks are of major importance. Due to the limited space in the valley floors and the slopes, it is often unavoidable to use exposed areas for susceptible socio-economic activities. Therefore it seemed to be consequent, to focus on this in detail in mountain regions.

Commonly, the link between modelling, consequent prediction of natural processes and risks to management and governance of these is rather weak. This is true for places all over the world, however, more dominant in mountain regions. Consequently, it is important not to stop with the modelling and the production of results, often presented in form of maps. Instead, it has to be carefully evaluated what is really needed. This setting is in particular determined by the local, regional and national legislation. Therefore, it is consequent to include the involved stakeholders' right from the start and get guidance from the relevant institutions throughout the whole procedure of process analysis incl. modelling and presentation of relevant results in required forms in order to allow a sustainable development of the region. Herein, risk governance as a guiding principle is of major importance.

The reduction of disaster risk from multiple hazard sources is an explicitly pronounced aim in several international agendas, for example in the Agenda 21 (from the UN Conference on Environment and Development, 1992), the Johannesburg Plan (adopted at the 2002 World Summit on Sustainable Development) or the Hyogo Framework for Action 2005–2015: Building Resilience of Nations and Communities to Disasters (UN-ISDR 2005). Strategies and actions to "control, reduce and transfer risks" on basis of risk assessments and analyses can be subsumed under the term risk management (UN-ISDR 2009). Linking the relevant

actors and policies throughout the disaster management cycle, but also creating an inventory of information on disasters are propagated as key objectives by the 2009 EC Communication "A Community approach on the prevention of natural and man-made disasters" (European Commission 2007). Here, it becomes clear that available knowledge on disasters is currently limited and suffers from a lack of comparability.

However, this current limitation of research on natural risks, which is fragmented and isolated (i. e. with natural sciences and engineering disciplines on the one hand and societal sciences on the other hand) the importance and difficulty of maintaining trust among all stakeholders, and the complex, socio-political nature of risk call for an amplified approach. The concept of risk governance tries to fill exactly this gap.

The objective of this book is to give an overview of the whole concept of risk governance and its application in the field of natural risks, shed some light at each single component, explaining its significance and inherent challenges. Due to the complexity and multi-disciplinarity, this approach is a first step to identify the main challenges and bridge the existing gaps between natural and social sciences in disaster risk research. Herein, risk governance strategies are of major importance.

1.4.2 A Theoretical Discussion of Risk Governance

'Risk governance' aims to enhance the disaster resilience of a society (or a region) and includes "the totality of actors, rules, conventions, processes, and mechanisms concerned with how relevant risk information is collected, analysed and communicated and management decisions are taken" (IRGC 2005). Risk governance is therefore related to the institutional dimension of resilience, which "is determined by the degree to which the social system is capable of organising itself and the ability to increase its capacity for learning and adaptation, including the capacity to recover from a disaster" (UN-ISDR 2002).

The IRGC definition points at the elements of risk governance (RG): risk assessment (RA, divided into a pre-assessment and a risk appraisal) and risk management (RM on basis of a tolerability and acceptability judgement which is informed by the assessment of risk). The whole procedure has to be embedded in a risk communication (RC) process among scientists, politicians and the public (public and private stakeholders). The whole risk governance framework is explained by the following Fig. 1.2:

This figure clearly indicates that the framework is divided into two spheres, an assessment sphere which is about generation of knowledge and a management sphere where decisions are taken. The latter is of a normative character and thus influenced by cultural beliefs and political preferences. However, even the assessment sphere is influenced by normative factors, because whoever controls the definition of risk and controls risk policy. Thus a concern assessment should

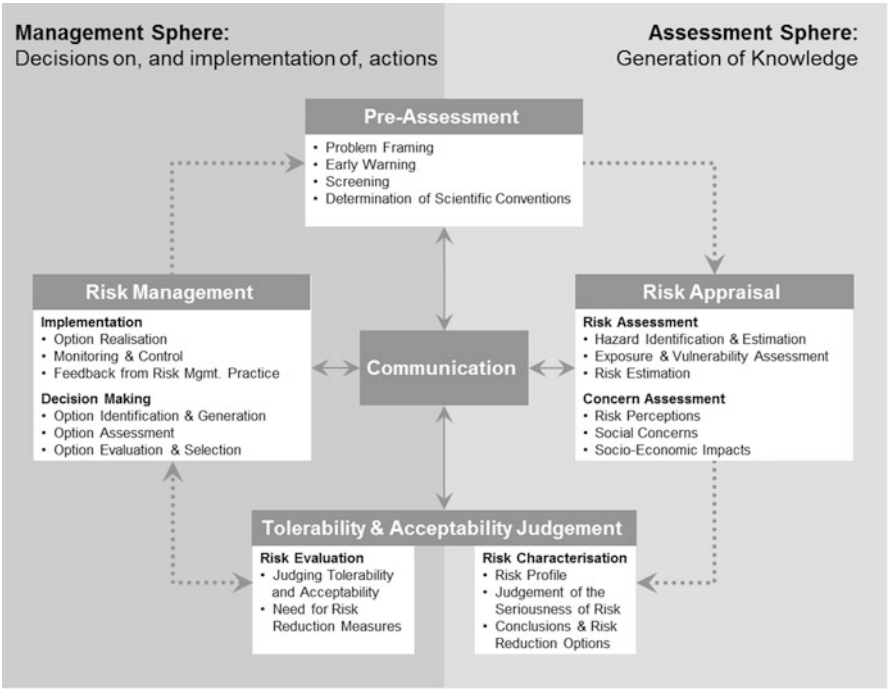

Fig. 1.2 Risk governance framework (Source: Adapted from IRGC 2005)

be part of the risk appraisal. It has to be stressed, however, that there is no clear divide between the two spheres. Although they might also be represented in different institutions (e.g. Geological Surveys – spatial planning unit), their relation and communication has to cross these borders.

Aiming at the development of integrative models and concepts that link the different phases of risk governance mentioned before, attention has to be paid to the given variations in characteristics of the several risk types, both on the collective level and the individual risk perception. There are many factors known to affect an individual's perception of risk, namely familiarity with a risk, control over the risk or its consequences, proximity in space, proximity in time, scale of the risk or general fear of the unknown (the so called "dread factor"). Apart from these factors, individual risk perception is also shaped by how the community or a certain socio-cultural milieu generally deals with a special type of risk or risky situations. Risk perception enters the risk management equation through differing estimations on, for example, how probable in space and time an event may be, and how much money is to be spent on preparedness according to the level of acceptable risk which is a characteristic of each single cultural setting and differs largely from one region to the other. These factors might contribute in each single case in a different manner to the perception and estimation of risk. In addition, they are strongly interlinked with

more collective socio-political factors and form a particular culture of risk. The variation in different cultural (regional, national) contexts is a perspective studied within the cultural risk paradigm.

Risk governance has become increasingly politicised and contentious. The main reasons are controversies concerning risks that are not supported by adequate scientific analysis methods (Armaş and Avram 2009). Rather, risk controversies are disputes about who will define risk in view of existing ambiguity. In many cases policy discourse is not about who is correct about assessment of danger, but whose assumptions about political, social and economic conditions, as well as natural or technological forces win in the risk assessment debate. Thus, the hazard as a potentially damaging physical event is real, but risk is socially constructed.

Scientific literacy and public education are important but not the only aspect necessaries to avoid conflicts about risk. Emotional response by stakeholders to issues of risk is truly influenced by distrust in public risk assessment as well as in risk management. Due to this fact, those who manage and communicate risks to the public need to understand the emotional responses towards risk and the way risk is perceived by the at-risk population. It is a matter of the definition of risk how risk policy is carried out. Moreover, defining risk is an expression of power. Slovic (1999) thereby argues that whoever controls the definition of risk controls risk policy. Within the communication strategies in all approaches, trust can be seen as a central term in this respect (Löfstedt 2005).

Distrust makes institutional settings vulnerable as it lowers the efficiency and effectiveness of management actions. The whole disaster cycle from mitigation, preparedness, response to recovery is embedded in an institutional system. Thus, institutional vulnerability can in principle be understood as the lack of ability to involve all relevant stakeholders and effectively co-ordinate them right from the beginning of the decision-making process. It refers to both organisational and functional forms as well as guiding legal and cultural rules. Consequently, a stakeholder-focused process is needed meaning consulting and involving administrative stakeholders as well as the general potentially affected community. In this regard, research on risk governance has to be understood as co-operative research: a form of research process which involves both researchers and non-researchers in close co-operative engagement. However, any communication has to be tailor-made to the educational background as well as social and cultural beliefs of individuals and groups and adjusted to the given legal-administrative framework of a study site.

The concept of risk governance has been created and adapted in the area of new emerging mostly man-made risks such as nanotechnology. Nonetheless, it is of particular relevance for mountain risks either. Actually the successful management of mountain risks is limited due to the fact that the interactions between individual sectors, disciplines, locations, levels of decision-making and cultures are not known or not considered (IRGC 2005; Greiving et al. 2006). Inadequate public available

information about risks in terms of societal and natural dimensions, inapprehensible procedural steps as well as insufficient involvement of the public in the risk related decision-making process lead to severe criticism and distrust towards respecting relevant decisions in regard to a specific risk.

The risk governance approach has recently been regarded as important by the new Territorial Agenda of the EC, launched in 2007 in Leipzig, Germany by the Member States Ministers for Spatial Planning as part of the priority 5 "Promoting Trans-European Risk Management" (European Commission 2007).

1.4.3 Relevance for Europe

Within the global change debate, the field of climate change in general, but particularly as a triggering factor for many natural hazards, is of special importance for Europe with its existing settlement structures, cultural landscapes and infrastructures which have been developed over centuries. Mitigation actions, carried out i.e. by spatial planning (discussed more in detail in part 3), are under these circumstances less effective than in countries which are still growing rapidly in terms of population and the built environment. Here, disaster prone areas can be kept free from further development whereas most of these areas are in Europe already built-up. However, this calls for authorities to improve public risk awareness and to look for means to mitigate this problem. Moreover, measures based on mandatory decisions of public administration, as well as measures which are in the responsibility of private owners need to be understood and regarded as suitable by their addresses for their implement ability. This is clearly visible when looking at evacuation orders or building protection measures to be taken by private households. Having these facts in mind, the "active involvement", of the population at risk, propagated e.g. by the European Communities Flood Management Directive (European Communities 2007), has to be seen as crucial for the success of the Directive's main objective: the reduction of flood risks.

Within the European Community it has also been recognized, that a risk approach has also to be applied to other natural hazards such as coastal hazards or soil erosion and landslide hazards (e.g. Soil Thematic Strategy 2006). The risk governance approach has recently been regarded as important by the new Territorial Agenda of the EC, launched in 2007 in Leipzig, Germany by the Member States Ministers for Spatial Planning as part of the priority 5 "Promoting Trans-European Risk Management" (European Commission 2007).

The previously addressed issues found the basis for this book. Thus the content includes the traditional assessments of hazards and risks indeed, but it offers information and concepts beyond the purely engineering and natural science solutions.

1.5 Conclusions

Hazard and risk assessment are prerequisites for a safe and sustainable development of the society in mountainous areas. Hazard assessment aims at an estimate of the spatial and temporal occurrence and magnitude of damaging natural processes. Risk assessment focuses on the consequences of the impact of these processes on society in terms of loss.

The observed climate changes related effects on temperature and precipitation will lead to new uncertainties in the assessment of hazard, because past events might be not representative anymore to predict future hazards. Similarly, other changes in the catchments related to land use change will also lead to high uncertainties in the prediction of these processes.

The use of physical deterministic models plays an essential role in quantitative hazard and risk assessment because these estimate in a quantitative way the frequency, spatial extent and impact of these processes without the necessary access to historical data sets.

A major step forward in the assessment of landslide hazard is the further development of all kind of geodetic, geo-information and remote sensing techniques to detect and monitor landslides and to deliver more precise topographical information and other environmental causative factors.

Vulnerability assessment is a crucial step towards a risk assessment. Vulnerability assessment for the different element at risk are especially difficult in case of landslide hazard. Other types of vulnerability assessments (e.g. social, environmental, and economic) are also problematic due to the complexity of economic and environmental systems.

It turned out that a quantitative risk assessment often includes a large degree of uncertainty. If the uncertainties in the input factors cannot be evaluated, or if there are simply not enough data to estimate the hazard and vulnerability components, the best option is then to carry out a qualitative risk assessment instead.

It is not appropriate to focus solely on products of hazard and risk assessment, without a careful evaluation what society really needs. Therefore, it is important to include the involved stakeholders' right from the start and get guidance from the relevant institutions throughout the whole procedure of risk assessment and presentation of relevant results in order to allow a sustainable development of the region. Herein, risk governance as a guiding principle is of major importance.

Risk governance is an important framework which integrates all the aspects related to risk assessment, tolerability and acceptability judgment of risk and risk management. It aims to study how relevant risk information is collected, analysed and communicated and management decisions are taken.

References

Aleotti P, Chowdury R (1999) Landslide hazard assessment: summary review and new perspectives. Bull Eng Geol Environ 58(1):21–44

Alkema D, Middelkoop H (2005) The influence of floodplain compartmentalization on flood risk within the Rhine – Meuse delta. Nat Hazard 36(1–2):125–145

Armaş J, Avram E (2009) Perception of flood risk in Danube Delta, Romania. Nat Hazard 50(2):269–287

Baum RL, Godt JW (2009) Early warning of rainfall-induced shallow landslides and debris flows in the USA. Landslides 7:259–272

Berti M, Simoni A (2005) Experimental evidences and numerical modelling of debris flow initiated by channel runoff. Landslides 2(3):171–182

Blijenberg H (1998) Rolling stones? Triggering and frequency of hill slope debris flows in the Bachelard valley, southern French Alps. Netherlands Geographical Studies 246, Utrecht

Bogaard TA, Van Asch TWJ (2002) The role of the soil moisture balance in the unsaturated zone on movement and stability of the Beline landslide, France. Earth Surf Processes Landf 27:1177–1188

Bonnard C, Noverraz F (2001) Influence of climate change on large scale landslides: assessment of long-term movements and trends. In: Landslides: causes, impacts and counter measures. Verlag Glückhauf, Essen/Davos

Bowles DS (2004) ALARP evaluation: using cost effectiveness and disproportionality to justify risk reduction. ANCOLD Bull 127:89–106

Brooks SM, Glade T, Crozier MJ, Anderson MG (2004) Towards establishing climatic thresholds for slope instability: use of a physically-based combined soil hydrology-slope stability model. Pure Appl Geophys 161(4):881–905

Brunsden D (1999) Some geomorphological considerations for the future development of landslide models. Geomorphology 30:13–24

Carrara A, Cardinali M, Guzzetti F (1992) Uncertainty in assessing landslide hazard and risk. ITC J 192(2):172–183

Carrara A, Guzzetti F, Cardinali M, Reichenbach P (1999) Use of GIS technology in the prediction and monitoring of landslide hazard. Nat Hazard 20(2–3):117–135

Casagli N, Farina P, Leva D, Tarchi D (2004) Application of ground-based radar interferometry to monitor an active rock slide and implications on the emergency management. In: Evans SG, Scarascia-Mugnozza G Strom A, Hermanns RL (eds) Landslides from massive rock slope failure. Proceedings of the NATO Advanced Research Workshop on Massive Rock Slope Failure – New Models for Hazard Assessment, Springer, Celano/Berlin, 16–21 June 2004

Cascini L (2008) Applicability of landslide susceptibility and hazard zoning at different scales. Eng Geol 102(3–4):164–177

Cascini L, Bonnard C, Corominas J, Jibson R, Montero-Olarte J (2005) Landslide hazard and risk zoning for urban planning and development. In: Hungr O, Fell R, Couture R, Eberthardt E (eds) Landslide risk management. Taylor & Francis, London

Casson B, Delacourt C, Allemand P (2005) Contribution of multi-temporal sensing images to characterize landslide slip surface – application to the La Clapière Landslide (France). Nat Hazard Earth Syst Sci 5:425–437

Chacon J, Irigaray C, Fernandez T, El Hamdouni R (2006) Engineering geology maps: landslides and geographical information systems. Bull Eng Geol Environ 65:341–411

Chatwin SC, Howes DE, Schwab JW, Swanston DN (1994) A guide for management of landslide-prone terrain in the Pacific North-West. Research Branch, Ministry of Forests, Victoria

Chen H, Lee CF (2003) A dynamic model for rainfall-induced landslides on natural slopes. Geomorphology 51(4):269–288

Cornforth DH (2005) Landslides in practice: investigation, analysis and remedial/preventative options in soils. Wiley, Hoboken

Corominas J, (2013) Avoidance and protection measures. In: Shroder J (Editor in Chief), Marston RA, Stoffel M (eds) Treatise on geomorphology, vol 7, Mountain and hillslope geomorphology. Academic Press, San Diego, pp 259–272

Corominas J, Moya C (2008) A review of assessing landslide frequency for hazard zoning purposes. Eng Geol 102:193–213

Corsini A, Farina P, Antonell G, Barbieri M, Casagli N, Coren F, Guerri L, Ronchetti F, Sterzai P, Tarchi D (2006) Space-borne and ground-based SAR interferometry as tools for landslide hazard management in civil protection. Int J Remote Sens 27(12):2351–2369

Crozier MJ (2005) Multiple occurrence regional landslide events in New Zealand: hazard management issues. Landslides 2:247–256

Dai FC, Lee CF (2003) A spatial temporal probabilistic modelling of storm induced shallow landsliding using aerial photographs and logistic regression. Earth Surf Processes Landf 28(5):527–545

Dai FC, Lee CF, Ngai YY (2002) Landslide risk assessment and management: an overview. Eng Geol 64(1):65–87

Delacourt C, Allemand P, Berthier E, Raucoules D, Casson B, Grandjean P, Pambrun C, Varel E (2007) Remote-sensing techniques for analysing landslide kinematics: a review. Bull Soc Géol Fr. 178(2):89–100

Dietrich WE, Bellugi D, Real de Asua R (2001) Validation of the shallow landslide model, SHALSTAB, for forest management. In: Wigmosta MS, Burges SJ (eds) Land use and watersheds: human influence on hydrology and geomorphology in urban and forest areas, vol 2, Water science and application. American Geophysical Union, Washington, DC, pp 195–227

European Communities (2007) Directive 2007/60/EC of the European Parliament and of the Council of 23 October 2007 on the assessment and management of flood risks. European Communities, Brussels

European Commission (2007) Territorial Agenda of the European Union. European Commission, Brussels

Fell R, Ho KKS, Lacasse S, Leroi E (2005) A framework for landslide risk assessment and management. In: Hungr O, Fell R, Couture R, Eberhardt E (eds) International conference on landslide risk assessment and management, Vancouver

Fell R, Corominas J, Bonnard C, Cascini L, Leroi E, Savage WZ (2008) Guidelines for landslide susceptibility, hazard and risk zoning for land use planning. Eng Geol 102:85–98

Fredlund DG, Xing A, Fredlund MD, Barbours SL (1996) The relationship of the unsaturated shear strength to the soil-water characteristic curve. Can Geotech J 33(3):440–448

Fuchs S, Heiss K, Hóbl J (2007) Towards an empirical vulnerability function for use in debris flow risk assessment. Nat Hazard Earth Syst Sci 7:495–506

GEO – Geotechnical Engineering Office (2003) Layman's guide to slope maintenance. The government of Hong Kong. Geotechnical Engineering Office, Hong Kong

Glade T (2003) Vulnerability assessment in landslide risk analysis. Beitrage Erdsystemforschung 134(2):123–146

Greiving S, Fleischhauer M, Wanczura S (2006) Management of natural hazards in Europe: the role of spatial planning in selected EU member states. J Environ Plann Manag 49(5):739–757

Guzzetti F, Carrara A, Cardinali M, Reichenbach P (1999) Landslide hazard evaluation: a review of current techniques and their application in a multi-scale study, Central Italy. Geomorphology 31(1–4):181–216

Guzzetti F, Reichenbach P, Cardinali M, Galli M, Ardizzone F (2005a) Probabilistic landslide hazard assessment at the basin scale. Geomorphology 72:272–299

Guzzetti F, Peruccacci S, Rossi M, Stark CP (2008) Rainfall thresholds for the initiation of landslides in central and southern Europe. Meteorol Atmos Phys 98(3–4):239–267

Guzzetti F, Salvati P, Stark CP (2005b) Evaluation of risk to the population posed by natural hazards in Italy. In: Hungr O, Fell R, Couture R, Eberhardt E (eds) Landslide risk management. Taylor & Francis, London

Hervouet JM, Van Haren L (1996) Recent advances in numerical methods for fluid flows. In: Anderson MG, Walling DE, Bates PD (eds) Floodplain processes. Wiley, Chichester

Hesselink AW, Stelling GS, Kwadijk JCJ, Middelkoop H (2003) Inundation of a Dutch river polder, sensitivity analysis of a physically based inundation model using historic data. Water Resour Res 39(9):1234

Highland L, Bobrowsky P (2008) The landslide handbook: a guide to understanding landslides. United States Geological Survey Circular 1325. U.S. Geological Survey, Reston

Hungr O, Corominas J, Eberhardt E (2005) Estimating landslide motion mechanisms, travel distance and velocity. In: Hungr O, Fell R, Couture R, Eberhardt E (eds) Landslide risk management. Taylor & Francis, London

IRGC – International Risk Governance Council (2005) White paper on risk governance: towards an integrative approach. IRGC, Geneva

IUGS Working Group on Landslides, Committee on Risk Assessment (1997) Quantitative risk assessment for slopes and landslides-the state of the art. In: Cruden D, Fell R (eds) Landslide risk assessment. Balkema, Rotterdam

Jaboyedoff M, Ornstein P, Rouiller J-D (2004) Design of a geodetic database and associated tools for monitoring rock-slope movements: the example of the top of Randa rockfall scar. Nat Hazard Earth Syst Sci 4:187–196

Jaboyedoff M, Oppikofer T, Abellan A, Derron M-H, Loye A, Metzger R, Pedrazzini A (2010) Use of LiDAR in landslide investigations: a review. Nat Hazard 2010:1–24. doi:10.1007/s11069-010-9634-2

Leroueil S, Locat J, Vaunat TJ, Picarelli L, Lee H, Fuare R (1996) Geotechnical characterization of slope movements. In: Seneset K (ed) Proceedings of the 7th international symposium on landslides. Balkema, Trondheim/Rotterdam

Löfstedt R (2005) Risk management in post-trust societies. Palgrave Macmillan, Houndmills/Basingstoke/Hampshire/New York

Malamud BD, Turcotte DL, Guzzetti F, Reichenbach P (2004) Landslide inventories and their statistical properties. Earth Surf Processes Landf 29:687–711

Malet JP, Maquaire O, Calais E (2002) The use of global positioning system techniques for the continuous monitoring of landslides. Geomorphology 43(1–2):33–54

Malet JP, Maquaire O, Locat J, Remaître A (2004) Assessing debris flow hazard associated to slow-moving landslides: methodology and numerical analyses. Landslides 1:83–90

Malet JP, Van Asch TWJ, Van Beek LPH, Maquaire O (2005) Forecasting the behaviour of complex landslides with a spatially distributed hydrological model. Nat Hazard Earth Syst Sci 5:71–85

Mavrouli O-C, Corsini A, Corominas J (2012) Chapter 11: Disaster mitigation by corrective and protection measures. In: Van Asch TV, Corominas J, Greiving S, Malet J-P, Sterlacchini S (eds) Mountain risks: from prediction to management and governance. Springer, London, pp 303–326

Monserrat A, Crosetto M (2008) Deformation measurement using Terrestrial Laser Scanning data and least squares 3D surface matching. ISPRS J Photogramm Remote Sens 63:142–154

Naterop D, Yeatman R (1995) Automatic measuring system for permanent monitoring: Solexperts Geomonitor. In: Proceedings of the 4th international symposium on field measurements in geomechanics (FMGM-1995), Bergamo, 18–23 April 1995

Oppikofer T, Jaboyedoff M, Kreusen H-R (2008) Collapse at the eastern Eiger flank in the Swiss Alps. Nat Geosci 1(8):531–535

Pastor M, Manzanal D, Fernǘndez Merodo JA, Mira P, Blanc T, Drempetic V, Pastor MJ, Haddad B, Sanchez M (2010) From solids to fluidized soils diffuse failure mechanisms in geostructures with applications to fast catastrophic landslides. Granul Matter 132:211–228

Picarelli L, Russo C, Urcioli G (1995) Modelling earth flow movement based on experiences. In: Proceedings of the 11th European conference on soil mechanics and foundation engineering. Balkema, Copenhagen/Rotterdam

Quan Luna B, Remaître A, Van Asch TWJ, Malet J-P, Van Westen CJ (2012) Analysis of debris flow behavior with a one dimensional run-out model incorporating entrainment. Eng Geol 128:63–75

Salvati P, Bianchi C, Rossi M, Guzzetti F (2010) Societal landslide and flood risk in Italy. Nat Hazard Earth Syst Sci 10:465–483

Slovic P (1999) Trust, emotion, sex, politics, and science: surveying the risk-assessment battlefield. Risk Anal 19(4):689–701

Soeters R, Van Westen CJ (1996) Slope instability recognition, analysis and zonation. In: Turner AK, Schuster RL (eds) Landslides, investigation and mitigation, Transportation Research Board, National Research Council, Special report 247. National Academy Press, Washington, pp 129–177

Soil Thematic Strategy (2006) Communication from the Commission to the Council, the European Parliament, the European Economic and Social Committee and the Committee of the Regions. Brussels

Squarzoni C, Delacourt C, Allemand P (2005) Differential single-frequency GPS monitoring of the La Valette landslide (French Alps). Eng Geol 79(3–4):215–229

Stark CP, Hovius N (2001) The characterisation of landslide size distributions. Geophys Res Lett 28:1091–1094

Stelling GS, Kernkamp HWJ, Laguzzi MM (1998) Delft Flooding System, a powerful tool for inundation assessment based upon a positive flow simulation. In: Babovic VM, Larsen LC (eds) Hydro-informatics. Balkema, Rotterdam

Sun HW, Wong HN, Ho KKS (1998) Analysis of infiltration in unsaturated ground. In: Slope engineering in Hong-Kong. Balkema, Rotterdam

Tang C, Renger N, van Asch TWJ, Yang YH, Wang GF (2011) Triggering conditions and depositional characteristics of a disastrous debris flow event in Zhouqu city, Gansu Province, Northwestern China. Nat Hazard Earth Syst Sci 11:1–10. doi:10.5194/nhess-11-1-2011

Tarchi D, Casagli N, Fanti R, Leva DD, Luzi G, Pasuto A, Pieraccini M, Silvano S (2003) Landslide monitoring by using ground-based SAR interferometry: an example of application to the Tessina landslide in Italy. Eng Geol 68(1-2):15–30

Terlien MTJ, Van Westen CJ, Van Asch TWJ (1995) Deterministic modelling in GIS: landslide hazard assessment. In: Carrara A, Guzetti F (eds) Geographical information systems in assessing natural hazards. Kluwer, Rotterdam, pp 57–77

Teza G, Galgaro A, Zaltron N, Genevois R (2007) Terrestrial laser scanner to detect landslide displacement fields: a new approach. Int J Remote Sens 28(16):3425–3446

Teza G, Pesci A, Genevois R, Galgaro A (2008) Characterization of landslide ground surface kinematics from terrestrial laser scanning and strain field computation. Geomorphology 97(3–4):424–437

Thiery Y (2007) Susceptibilité du Bassin de Barcelonnette (Alpes du Sud, France) aux 'mouvements de versant': cartographie morphodynamique, analyse spatiale et modélisation probabiliste. PhD thesis, University of Caen, Caen

Travelletti J, Delacourt C, Allemand P, Malet J-P, Schmittbuhl J, Toussaint R, Bastard M (2012) Correlation of multi-temporal ground-based optical images for landslide monitoring: application, potential and limitations. ISPRS J Photogramm Remote Sens 70:39–55

Turner AK, Schuster RL (1996) Landslides, investigation and mitigation. Transportation Research Board, National Research Council, Special Report 247, National Academy Press, Washington, DC

United Nations-International Strategy for Disaster Reduction (UN-ISDR) (2002) Natural disasters and sustainable development: Understanding the links between development, environment and natural Background Paper No. 5. Geneva. http://www.johannesburgsummit.org/html/documents/backgrounddocs/unisdr%20report.pdf

United Nations-International Strategy for Disaster Reduction (UN-ISDR) (2005) Hyogo Framework for Action 2005-1015: Building the Resilience of Nations and Communities to Disasters, Tech. Report, World Conference on Disaster Reduction. Geneva

United Nations-International Strategy for Disaster Reduction (UN-ISDR) (2009) Terminology on Disaster Risk Reduction. Geneva. http://www.unisdr.org/eng/terminology/terminology-2009-eng.html

Uzielli M, Nadim F, Lacasse S, Kaynia AM (2008) A conceptual framework for quantitative estimation of physical vulnerability to landslides. Eng Geol 102:251–256

Van Asch TWJ, Sukmantalya IN (1993) The modelling of soil slip erosion in the upper Komering area, South Sumatra-Province, Indonesia. Geogr Fisica Dinam Quat 16:81–86

Van Asch TWJ, Hendriks MR, Hessel R, Rappange FE (1996) Hydrological triggering conditions of landslides in varvedclaysin the French Alps. Eng Geol 42:239–251

Van Asch TWJ, Van Beek LH, Bogaard T (2006) Problems in predicting the rate of slow moving landslides. Eng Geol 88:59–69

Van Asch TWJ, Malet JP, VanBeek LPH, Amitrano D (2007) Techniques, issues and advances in numerical modelling of landslide hazard. Bull Soc Geol Fr 178(2):65–88

Van Beek LPH (2002) Assessment of the influence of changes in climate and land use on landslide activity in a Mediterranean environment. Geographical Studies 294, Utrecht

Van Beek LPH, Van Asch TWJ (2003) Regional assessment of the effects of land-use change on landslide hazard by means of physically based modelling. Nat Hazard 31:289–304

Van Westen CJ, Seijmonsbergen AC, Mantovani F (1999) Comparing landslide hazard maps. Nat Hazard 20(2–3):137–158

Van Westen CJ, Van Asch TWJ, Soeters R (2005) Landslide hazard and risk zonation—why is it still so difficult? Bull Eng Geol Environ 65(2):167–184. doi:10.1007/s10064-005-0023-0

Van Westen CJ, Castellanos Abella EA, Sekhar LK (2008) Spatial data for landslide susceptibility, hazards and vulnerability assessment: an overview. Eng Geol 102(3–4):112–131

Vulliet L (1997) Three families of models to predict slowly moving landslides. In: Klubertanz G, Laloui L, Vulliet L (eds) Computer methods and advances in geomechanics. Balkema, Rotterdam

Vulliet L (2000) Natural slopes in slow movement. In: Zaman M, Gioda G, Booker J (eds) Modeling in geomechanics. Wiley, Chichester, pp 653–676

Zezere JL, Rodrigues ML, Reis E, Garcia R, Oliveira S, Vieira G, Ferreira AB (2004) Spatial and temporal data management for the probabilistic landslide hazard assessment considering landslide typology. In: Lacerda WA et al (eds) Landslides, evaluation and stabilization. Proceedings of the 9th international symposium on landslides, Rio de Janeiro

Part I
New Techniques for Assessing Mass Movement Hazards

Chapter 2
Innovative Techniques for the Detection and Characterization of the Kinematics of Slow-Moving Landslides

Ping Lu, Alexander Daehne, Julien Travelletti, Nicola Casagli, Alessandro Corsini, and Jean-Philippe Malet

Abstract Remote sensing has been proven useful for landslide studies. However, conventional remote sensing techniques based on aerial photographs and optical imageries seem to be more suitable for detecting and characterizing rapid-moving landslides. This section introduces several innovative remote sensing techniques aiming at the characterization of the kinematics (e.g. displacement pattern, deformation, strain) of slow- to moderate-moving landslides. These methods include Persistent Scatterers Interferometry (PSI), automatic surveying using total station integrated with GPS, Ground-Based Synthetic Aperture Radar Interferometry (GB-InSAR), image correlation of catalogues of optical photographs (TOP) and Terrestrial Laser Scanner (TLS) point clouds. Three case studies, including the Arno river basin (Italy), the Valoria landslide (Italy) and the Super-Sauze landslide (France) are presented in order to highlight the usefulness of these techniques.

P. Lu (✉) • N. Casagli
Department of Earth Sciences, University of Firenze, Via G. La Pira 4, IT-50121 Florence, Italy
e-mail: luping.office@gmail.com

A. Daehne • A. Corsini
Department of Earth Sciences, University of Modena and Reggio Emilia University, Largo Sant' Eufemia 19, IT-41100 Modena, Italy

Department of Geosciences, University of Missouri – Kansas City, 5110 Rockhill Road, Kansas City, MO 64110, USA

J. Travelletti • J.-P. Malet
Institut de Physique du Globe de Strasbourg, CNRS UMR 7516, Université de Strasbourg/EOST, 5 rue René Descartes, F-67084 Strasbourg Cedex, France

BEG, Bureau d'Etudes Géologiques SA, Rue de la Printse 4, CH-1994 Aproz, Switzerland

T. van Asch et al. (eds.), *Mountain Risks: From Prediction to Management and Governance*, Advances in Natural and Technological Hazards Research 34,
DOI 10.1007/978-94-007-6769-0_2,

Abbreviations

ALS	Airborne Laser Scanner
CPT	Coherent Pixels Technique
DInSAR	Differential InSAR
EW	Early Warning
GB-InSAR	Ground-based Synthetic Aperture Radar Interferometry
IPTA	Interferometric Point Target Analysis
LOS	Line-of-Sight
PS	Persistent Scatterers
PSI	Persistent Scatterers Interferometry
InSAR	SAR Interferometry
SBAS	Small Baseline Subset
SPN	Stable Point Network
StaMPS	Stanford Method for Persistent Scatterers
TLS	Terrestrial Laser Scanner
TOP	Terrestrial Optical Photogrammetry
DEM	Digital Elevation Model
GPS	Global Positioning System

2.1 Introduction

Data products of remote observing systems are increasingly available with higher spatial and temporal resolution and offer new opportunities for the detection, mapping, characterization and monitoring of landslides. The application of advanced sensors and analysis methods can help to significantly increase the quantity and quality of our understanding of potentially hazardous areas and helps to reduce associated risk.

The choice of an adequate observing system depends on the landslide type and size, the range of observed velocity, the required frequency of acquisition, the desired accuracy and the financial constraints. Displacement monitoring techniques applied on landslides can be broadly subdivided in two main groups: geodetic and remote-sensing techniques.

– Geodetic surveying techniques consist in detecting geometrical changes in the landslide topography by measuring geometric parameters such as angles, distances or differences in elevation (levelling, tacheometry; Naterop and Yeatman 1995). These techniques necessitate the installation of targets in and outside the landslide and in measuring their position at different times. They have the advantage to be very accurate (0.2–2.0 cm) with a high potential of automation (Malet et al. 2002; Jaboyedoff et al. 2004; Foppe et al. 2006). Furthermore, many authors demonstrated the efficiency of permanent (Malet et al. 2002) and non-permanent (Squarzoni et al. 2005; Brunner et al. 2007) differential Global

Positioning System (dGPS) for landslide monitoring with a centimetric accuracy during any daytime and weather conditions. However, because landslides can show highly variable displacement rates in time and space according to the local slope conditions (bedrock geometry, distribution of pore water pressures), the major drawbacks of the geodetic techniques are (1) to provide only discrete point measurements of the displacement and (2) the costs of installation and maintenance of the survey network. They are usually only justified in the case of a real risk for the population.

– Remote sensing surveying techniques are interesting tools to obtain spatially-distributed information on the kinematics (Delacourt et al. 2007) and can be operational from spaceborne, airborne and ground-based platforms. Remote-sensing techniques give the possibility to discriminate stable and unstable areas and to map sectors within the landslide with different kinematics from a regional to a local scale. They are also useful tools for a process-based analysis of the deformation field affecting the slope (Casson et al. 2005; Teza et al. 2008; Oppikofer et al. 2008). In the last decades, the development of ground-based platforms for landslide monitoring at the local scale provided many advantages over spaceborne and airborne platforms despite a shorter spatial coverage (Corsini et al. 2006). The geometry and frequency of acquisitions are more flexible and adaptable to any type of local environment. In addition permanent installations of ground-based platforms allow continuous monitoring (Casagli et al. 2004; Delacourt et al. 2007). Three main categories of ground-based remote sensing techniques are used in landslide monitoring: Ground-Based Synthetic Aperture Radar Interferometry (GB-InSAR), Terrestrial Laser Scanner (TLS) and Terrestrial Optical Photogrammetry (TOP).

In this section, several of the above mentioned innovative remote sensing techniques are introduced and their usefulness in the detection and characterization of the kinematics (e.g. displacement pattern, deformation, strain) of slow- to moderate-moving landslides is highlighted through three case studies.

2.2 Detection and Characterization of Slow-Moving Landslides from Persistent Scatterers Interferometry (PSI)

2.2.1 The Principle of Persistent Scatterers Interferometry (PSI)

For studies of slow-moving landslides, SAR interferometry (InSAR), which uses the phase content of radar signals for estimating surface deformation, regardless of weather and night condition, has recently already become a widely-used technique (Gens and Van Genderen 1996). In particular, satellite InSAR represents a typical example of repeat-pass interferometry, combining two or more SAR images of

similar scene of terrain from slightly displaced passes of SAR sensor at different times (Massonnet and Feigl 1998). Besides, side-looking imaging radar ensures improvement of pixel resolution in viewing direction. Traditional satellite InSAR technique is mainly focusing on differential InSAR (DInSAR) approach which primarily employs two corresponding interferograms for differential measurements (Massonnet and Feigl 1998; Rosen et al. 2000). DInSAR was proven useful in studies of slow-moving landslides (e.g. Fruneau et al. 1996; Singhroy et al. 1998; Xia et al. 2004; Strozzi et al. 2005). It largely fills the gap of conventional remote sensing techniques of aerial photos and optical images, which are chiefly used for mapping rapid-moving shallow landslides and debris flows (Lu et al. 2011).

However, the conventional DInSAR approach, which is based on the assumption that surface deformation change is linear, is often affected by temporal decorrelation and atmospheric disturbances (Massonnet and Feigl 1998; Ferretti et al. 2001). These disturbing factors, which produce a significant bias during the phase measurement and the difficulty in fulfilling baseline criteria, bring the need for further advanced processing of SAR images. One possible solution is to include multi-temporal SAR images for a long-term interferogram processing, known as the technique of Persistent Scatterers Interferometry (PSI). Over recent years, several PSI approaches have been developed for the purpose of extracting long-term stable radar benchmarks, namely Persistent Scatterers (PS), from some multi-interferogram analysis of SAR data based on different statistical approaches.

For instance, a PSInSARTM technique was firstly developed by Ferretti et al. (2001) and then improved by Colesanti et al. (2003). Another approach, known as Stanford Method for Persistent Scatterers (StaMPS), which calculates a time series of deformation with spatially-correlated nature of ground deformation, was initially developed by Hooper et al. (2004) and further modified by Hooper et al. (2007) for improvement of measuring accuracy. Besides, the approach of Interferometric Point Target Analysis (IPTA), which detects persistent benchmarks in low-coherence regions and includes large baselines for phase interpretation, was suggested by Werner et al. (2003) and Strozzi et al. (2006). In addition, two small baseline approaches were developed, including the Coherent Pixels Technique (CPT) proposed by Mora et al. (2003) and Blanco-Sanchez et al. (2008), and Small Baseline Subset (SBAS) indicated by Berardino et al. (2002), Casu et al. (2006) and Lanari et al. (2004). Similarly, a stable point network (SPN) mode was also reported by Crosetto et al. (2010) and Duro et al. (2003). These approaches mentioned above enable a measurement of ground motion with millimeter accuracy (Lu et al. 2010).

2.2.2 Detection and Characterization of Slow-Moving Landslides from PSI at Catchment Scale

Due to its large spatial coverage, PSI technique can be useful in detecting landslide at regional scale. In this section, a case study for detecting and characterizing slow-moving landslides at catchment scale is illustrated on the Arno river basin (central

Italy). The whole basin covers about 9,130 km^2 with 78 % (7,190 km^2) area across the mountainous and hilly areas. Previous researches have mapped more than 27,000 landslides within the whole basin, most of which are slow-moving deep-seated landslides (Catani et al. 2005; Farina et al. 2006).

The PS data were processed from the technique of PSInSAR^{TM} (Ferretti et al. 2001) by Tele-Rilevamento Europa (TRE) on behalf of the Arno River Basin Authority. In total 102 RADARSAT-1 images with incidence angle of 30°–37°, covering the period from 2003 to 2006 with the acquisition interval of 24 days, were analyzed. Among these images, 54 of them are ascending data and 48 of them are descending data. More than 700,000 PS were finally derived with a pre-defined coherence threshold above 0.60. The precision of displacement rates is ranging between 0.1 and 2.0 mm·year^{-1} along Line-of-Sight (LOS). The geocoding accuracy is within 10 m in east–west and 5 m in the north–south direction.

Lu et al. (2012) proposed a semi-automatic approach for detecting slow-moving landslides. At its initial stage, a flat mask was used on PS data in order to focus on PS exclusively located in the mountainous and hilly areas. Then two statistical approaches were applied in the following analyses: (1) the Getis-Ord G_i* Statistics (Getis and Ord 1996) and (2) the kernel density estimation (Silverman 1986). The G_i* statistics (Getis and Ord 1996) was mainly employed to estimate the clustering level of PS data. It specified a single PS at a site i, and its neighbours j within a searching distance d. For each single PS at a site i, the G_i* index was calculated as:

$$G_i^*(d) = \frac{\sum x_j + x_i - n_{ij}\,\bar{x^*}}{s^*\left\{\left[(n \cdot n_{ij}) - {n_{ij}}^2\right]/(n-1)\right\}^{0.5}} \tag{2.1}$$

where n is the number of calculated PS datasets. n_{ij} is the number of PS within the searching distance d, which is actually the sum of PS at the site i and its neighbours j. x is the velocity of each single PS. s^* is the standard deviation of PS velocity for the entire dataset. The searching distance d was defined as 114 m, calculated by the average distance of the shortest path to a channel and the shortest distance to a ridge pixel calculated based on steepest descent direction as proposed by Tucker et al. (2005).

The kernel density estimation was then used to fit a smoothly tapered surface as a hotspot using a kernel estimator defined as

$$f(x) = \frac{1}{nh}\sum_{i=1}^{n} K\left(\frac{x - X_i}{h}\right) \tag{2.2}$$

where h is the searching window width, x–X_i is the distance of each calculating pixel to each PS i. K is the quadratic kernel function defined as:

$$K(x) = \frac{3}{4}(1 - x^2), |x| \le 1$$
$$K(x) = 0, x > 1 \tag{2.3}$$

This kernel estimator was calculated on all PS datasets, with the corresponding G_i* index as the weighting factor. The final output was a smooth kernel density map that represents PS hotspots for an easier and straightforward visualization for landslide detection.

Figure 2.1 is the derived hotspot map reported by Lu et al. (2012), indicating where potential slow-moving landslides might exist. It covers part of the Arno river basin of Pistoia-Prato-Firenze and the Mugello areas. Hotspots with high positive kernel density values are displayed with blue color whereas hotspots with low negative values are given in red color. These blue and red hotspots reveal those areas which are potentially affected by slow-moving landslides within the detection precision of PSI technique. The deeper the color is, the more intense high-velocity PS datasets are clustered, thus suggesting the presence of high density of mass movements. The color of hotspots renders the information of moving direction. Clustering of PS moving towards LOS (positive velocity) is represented by blue hotspot whereas clustering of PS moving away from LOS (negative velocity) is rendered in red hotspot. In addition, the radius of each hotspot suggests the extent of a potential landslide-affected area.

2.3 Ground-Based Multi-instruments Monitoring of Slow- to Moderate-Moving Landslides

2.3.1 The Combination of Geodetic and Remote Sensing Techniques for Monitoring at the Slope Scale

In the case of reactivation of slow- to moderate-moving landslides, the mechanism of failure and evolution at the slope scale is governed by a combination of different processes. Continuous monitoring systems were used for uncovering such complex movement patterns (Malet et al. 2002; Petley et al. 2005a). For such studies, the critical components to assess landslide hazard are efficient information on the velocity and acceleration of the moving masses (Hervás and Bobrowsky 2009). In some cases, early-warning based on real-time continuous monitoring is in principle possible by exploiting empirical relationships linking the progressive acceleration to the timing of failure (Petley 2004; Petley et al. 2005b).

In order to compare the performance of real-time continuous geodetic (automated total station measurements) and ground-based remote sensing techniques (GB-InSAR measurements), a field test was carried out from 23 to 25 February 2009 at the Valoria landslide (Northern Apennines). The particular focus was to document the spatial and temporal patterns of slope movements during reactivations and to compare the instrument's pros and cons in the perspective of surveying and early warning.

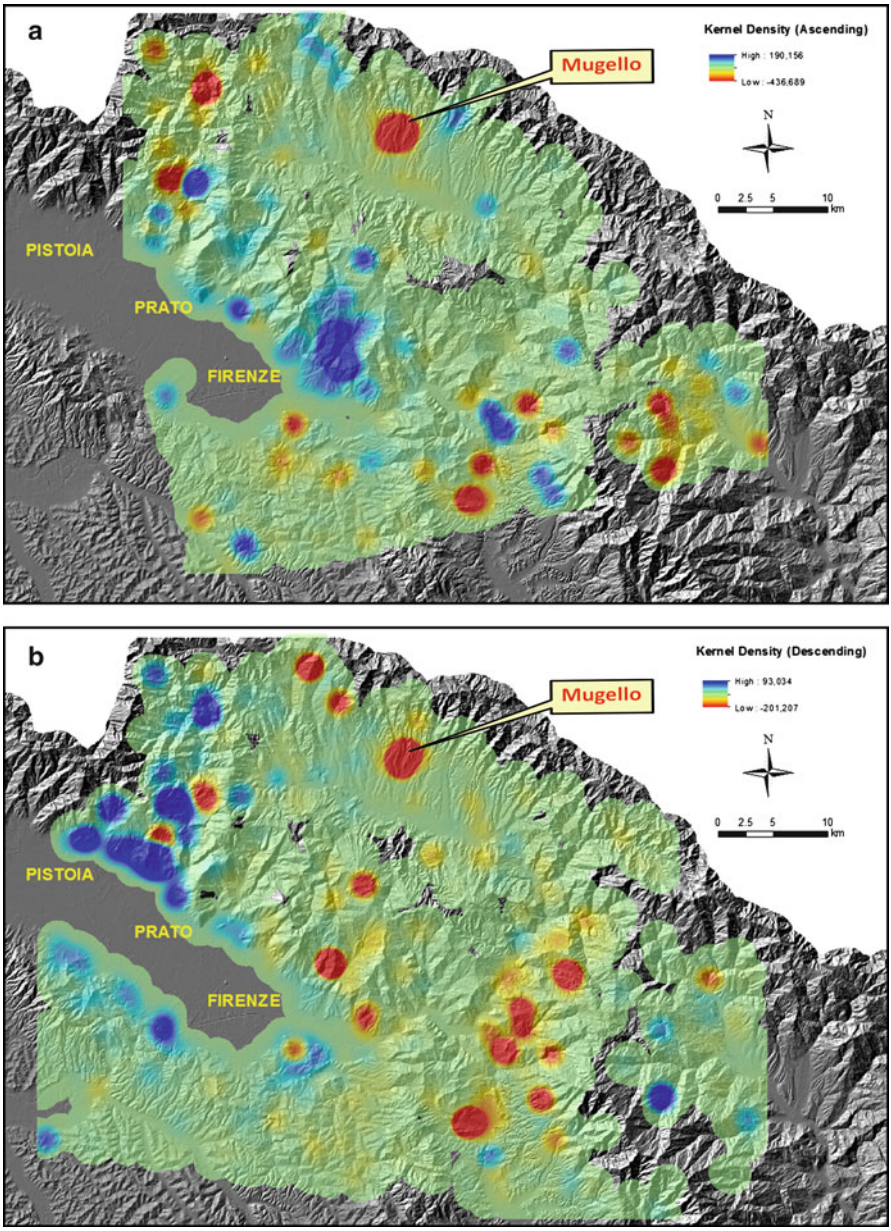

Fig. 2.1 The landslide hotspot map of Pistoia-Prato-Firenze and Mugello basin (central Italy), generated from: (**a**) ascending RADARSAT PSI; (**b**) descending RADARSAT PSI (Lu et al. 2012)

The landslide is a complex and composite mass movement. Rotational and translational slides in the source area and subsequent earthflows in the track and accumulation zones are associated (Fig. 2.2). The landslide activity since 2001 ranges from persistent slow movements, associated with relatively low hazard and risk levels, to phases of accelerated movements in the scale of some $m \cdot h^{-1}$ to $m \cdot day^{-1}$ (Ronchetti et al. 2007; Corsini et al. 2009).

A continuous topographic monitoring system, based on a Leica TCA2003 automated total station is operated since March 2008. The system was installed in response to the repeated reactivations that affected the landslide since 2001 and it was designed to cover the whole landslide from the main upper scarp to the toe. The monitored area extends over more than 3 km in length and ranges from altitudes between 1,390 and 520 m. The automated total station is located midway in the slope, on a panoramic position located a few hundred meters northeast of the landslide (Fig. 2.2). More than 40 prisms were placed inside the landslide and 6 prisms were placed in stable areas as reference points for measurements correction. The hardware setup includes a control unit (industrial computer) that is also used for a permanent GPS network which was installed nearby the topographic survey station (Fig. 2.3 I–III). The technical characteristics of the system (total station and GPS) are summarized in Table 2.1.

The total station is mounted on a tribrach on top of a reinforced concrete pillar that is anchored 1 m into the ground. The instrument is protected from environmental impacts through a ventilated case made of 5 mm thick glass (Fig. 2.3 I, II). This hardware solution was set to perform a measuring cycle in a 3 h duty schedule. During movement, prisms are followed by the total station using the instrument's Automatic Target Recognition functionalities. The search window was set to 10 m, so that the system is potentially capable of measuring velocities up to 3 $m \cdot h^{-1}$ assuming the prism remains visible to the laser beam. Daily and seasonal climatic conditions produce variations in distance measurements that are corrected by applying p.p.m. corrections and using the reference prisms installed outside of the landslide body as fixed locations.

From 23 to 25 February 2009, during a complete reactivation event, a ground-based synthetic aperture radar interferometry (GB-InSAR) test was carried out. For this purpose, an IBIS-L device, manufactured by IDS (Ingegneria dei Sistemi, Pisa, Italy) was used (Fig. 2.4).

GB-InSAR was tested to assess if it can be used to complement measurements obtained by the total station for movement rates up to cm to $m \cdot day^{-1}$. The high water content in the landslide mass during the reactivation is particularly challenging for GB-InSAR since phase ambiguity and loss of coherence due to ground moisture changes data processing (Tarchi et al. 2003; Antonello et al. 2004; Corsini et al. 2006). To cover the entire slope, the radar was first directed toward the upper slope for 17 h, and then toward the lower slope for 24 h (Fig. 2.2). In order to have the possibility to compare results between radar and total station, new topographic prisms were installed in the moving deposits within the radar scene coverage.

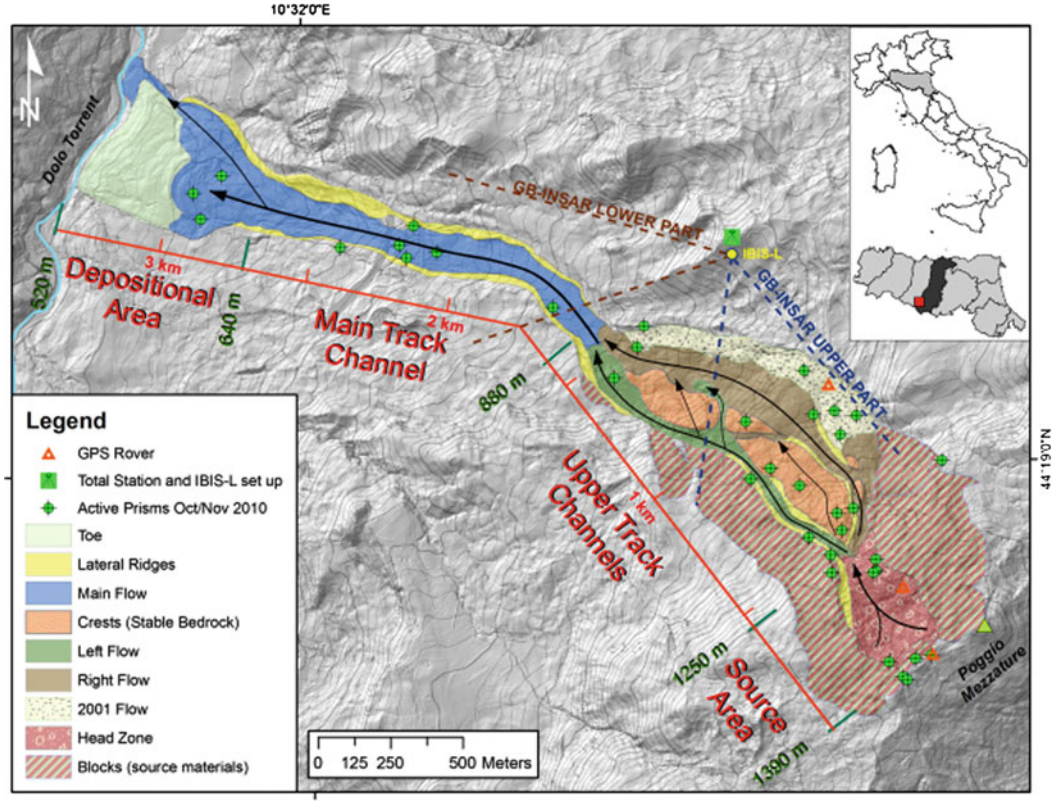

Fig. 2.2 The Valoria landslide (Northern Apennines, Italy). Slope deformations are characterized by earthflows developing in the source area and transporting materials around two stable crests downslope. The locations of prisms targets automatically surveyed by a total station since March 2008 along with GPS rover stations are marked. The site monitoring is complemented by two InSAR surveys conducted in February 2009 and targeting the upper and lower landslide body, respectively

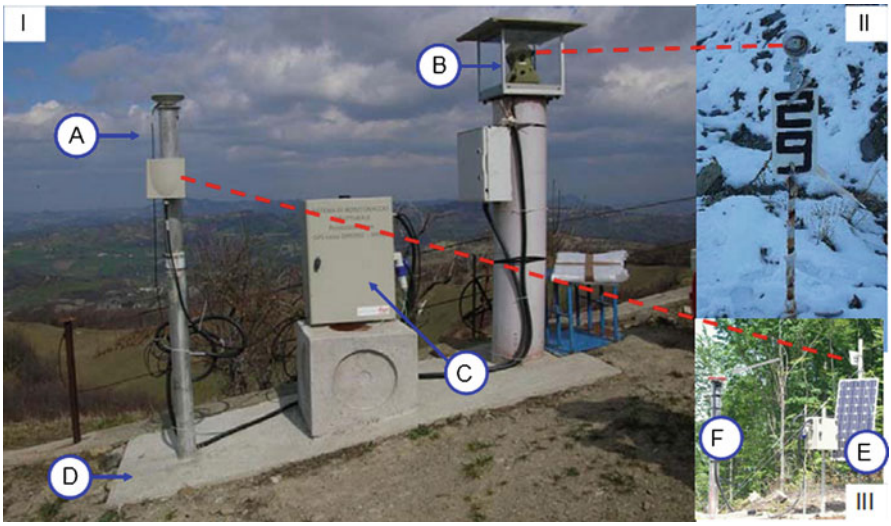

Fig. 2.3 Automated topographic monitoring station with integrated GPS system. **I**. (*A*) GPS Master and WLAN Antenna, (*B*) Automated total station, (*C*) Controller unit with OEM computer, power supply and modem for data transmission, (*D*) Foundation with GPS and total station monuments; **II**. Optical prism installed inside the landslide, target acquisition via laser beam; **III**. Rover GPS installed inside landslide materials: (*E*) Autonomous power supply through solar panel with controller and backup battery, WLAN streaming data transmission, (*F*) GPS Antenna mounted on GPS monument

The IBIS-L consists of "Stepped Frequency Continuous Wave" radar unit (Fig. 2.4). The main features of the device can be found in Table 2.2, while specific operational parameters for the two surveys conducted at the Valoria landslide are summarized in Table 2.3. The IDS developed software (GRAPeS) was used to process data. A calibration dataset was created using about 30 raw images and a coherence threshold of 0.6. This calibration set includes pixels that are above the coherence threshold in all the 30 scenes. Displacement is then calculated for each coherent pixel by stacking all the collected scenes, computing phase differences between subsequent scenes and using stable areas as proxies for estimating atmospheric correction. The results can be visualized as raster maps of displacement or velocity, or as time series for each single coherent pixel.

2.3.2 Comparison of the Monitoring Datasets

The evaluated Leica robotic total station and IBIS-LGB-InSAR systems performed well in detecting movements covering almost the entire case study site (Fig. 2.5). While highly LOS velocities of few mm·h^{-1} were noted for both techniques the surveyed prisms generally contained a higher level of noise for slow movements

Table 2.1 Main parameters of the automated total station set-up with integrated GPS system

	Instrument parameter	Description
Total Station	Type	1 Leica TCA 2003 (Leica Geosystems 2004)
	Operating distance	<2,000 m
	Survey mode	Automatic target recognition ATR, custom defined intervals, *e.g.* 3 h
	Total station position control	Bi-directional Leica Nivel 210 (mrad, temperature, sampling 300 ms)
	Angular standard deviation	0.01 mgon
	Distance standard deviation	1 mm + 1 ppm/3.0 s
	Survey targets	41 prisms: 35 inside and 6 for control
	External communication	GSM modem/satellite link
GPS	Master station	1 Leica GMX902 GG (L1,L2) dual frequency receiver, antenna Leica AX1202GG, grid connected (220 V) with back-up battery
	Rover	3 receivers Leica GMX901 GG (L1, 12 CH.,1Hz), autonomous power supply (solar panel + battery)
	Data transmission link	Continuous data streaming via GMX902 WLAN modena
Master unit	Operating system	Windows XP
	Total station/GPS integration	Software based, direct link to monitoring equipment and data storage
	Power supply	220 V grid-tied with 12 V battery as backup power
	Remote data transmission	GPRS modem

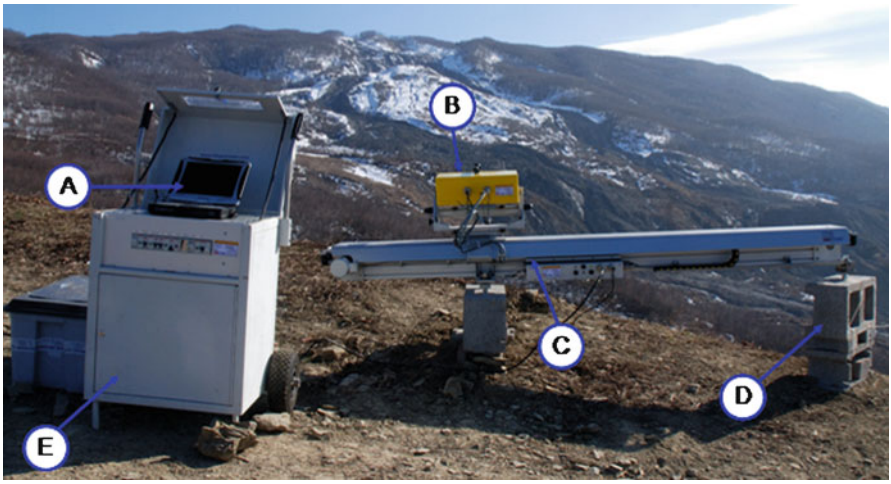

Fig. 2.4 GB-InSAR survey of the upper part of the Valoria landslide. Set-up: (*A*) Control unit (Mobile PC with software), (*B*) Radar sensor head, (*C*) Linear scanner (2.5 m rail with sled), (*D*) Support system (temporary or permanent mounts allowing for repeated observations), (*E*) Power module (controller, fuses, 12 V batteries connected in serial)

Table 2.2 GB-InSAR technical characteristics (IDS, IBIS-L model)

Instrument parameter	Description
Frequency	Ku band (available also in X band)
Radar type	Stepped Freq. Cont. Wave (SF-CW)
Operative range	[10–4,000] m
Range resolution	0.75 (0.5) m
Cross-range resolution	4.38 mrad
Displ. accuracy	up to 0.1 mm
Acquisition time	≥5 min
Phase ambiguity limit	∼4.4 mm
Installation time	∼2 h
Power supply	24 VDC or electrical network
Size	250 × 100 × 100 cm
Weight	∼200 kg
Power consumption	70 W

Table 2.3 Operational parameters of the IBIS-L ground-based InSAR surveys conducted at the Valoria landslide

	Upper part	Lower part
Date	25/02/2009	24/02/2009
Distance to hillslope [m]	300–1,900	450–1,300
Horizontal antenna aperture [degree]	38	38
Range resolution [m]	0.5	0.5
Cross-range resolution [mrad]	4.5	4.5
Acquisitions per hour [−]	8	9
Duration [h]	17	24

(Fig. 2.5; Prisms 42, 44). The observed higher noise levels in the observations of slow moving events are due to the lower limit of detection of the total station. Maximum velocity values measured in the upper part at the right flow by the GB-InSAR reached about 99 mm over a period of 17 h and about 336 mm over 24 h in the central part of the main flow. Thus, an average maximum LOS velocity of about 5.8 mm·h^{-1} was measured in the upper and about 14 mm·h^{-1} in the lower part. Higher velocities in the lower part were evidenced by prisms surveyed by the total station with maximum rates of 52 mm·h^{-1} (Prism 28a) and 10.7 mm·h^{-1} (Prism 51). Further, the data acquisition for the entire field-of-view at once allows for apparent distinction of zones of high and low displacements on qualitative scales using GB-InSAR while topographic surveys are restricted to few discrete observations. However, flow movements can be variable within just a few meters yielding better absolute measurements when using prims targets compared to GB-InSAR measurements without corner reflectors. It should be noted from the plots in Figure 2.5 that closer LOS of InSAR to the slope movement direction produces a better fit between InSAR displacement and "real" displacement measured by prims (Prism 28a).

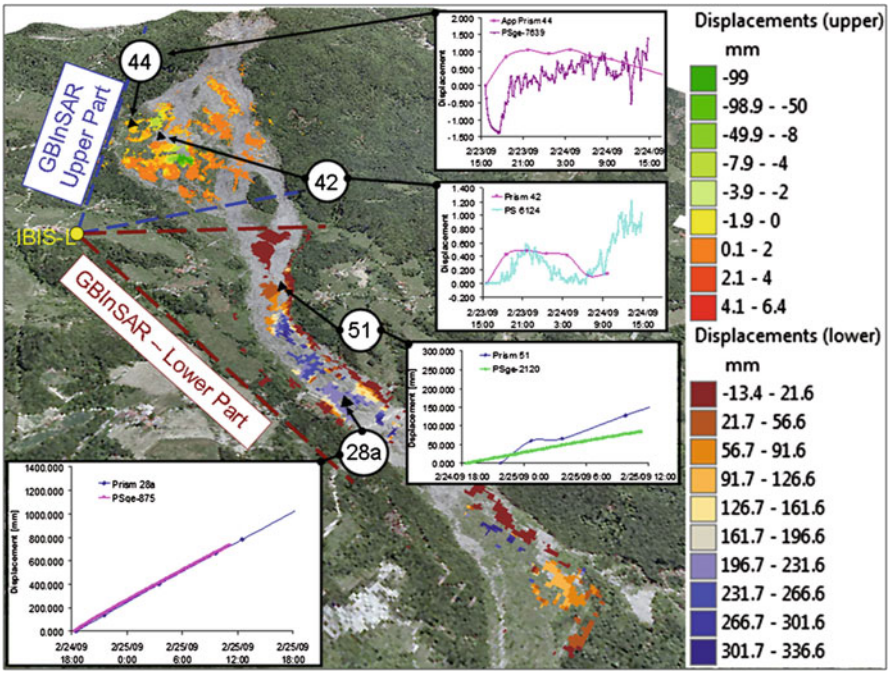

Fig. 2.5 Results of displacement monitoring at the Valoria landslide during the winter 2009 reactivation. Prisms were measured by an automated total station from nearby the position of the IBIS-L ground-based InSAR. Using an IBIS-L terrestrial Radar instrument, surveys of the *upper* and *lower* landslide body were obtained. The displacements shown are in the Line-of-sight (*LOS*) direction with respect to the location of the instrument reaching maximum values of about 336 mm over 24 h of observation

Both adopted monitoring systems can be compared on the basis of general knowledge, as well as on the basis of the information gathered during the field tests. The assessment of several relevant issues for each system is summarized in Table 2.4. During the set-up phase of topographic and ground-based InSAR monitoring surveys, field and installation logistics are crucial. For both instruments, operational cost during the initial phase of landslides monitoring are high due to the unit and site development costs. Therefore, view shed, distance, incidence angle between line-of-sight and slope displacement vector, power supply, accessibility, and instrument safety need to be factored in to ensure a successful survey. Where highly precise measurements are necessary due to slow movements (mm·month^{-1}), both the total station and the IBIS-L instrument require a stable and firm foundation. As regards spatial coverage, the evaluated Leica robotic total station system has an angle of operation of 360° covering almost the entire case study site with some line-of-site restrictions. Although line-of-sight restrictions also affect GB-InSAR, in good coherence conditions, spatially distributed and continuous information can be obtained for one LOS direction at a time. In practice this means that for the

Table 2.4 The comparison between the total station and the GB-InSAR for the Valoria landslide monitoring

Evaluation criteria	Total station with integrated GPS	GB-InSAR
Unit cost	Approx. 40.000 €	Approx. 150.000 €
Initial installation and setup	1 week, min. 1 m^2 of property with good line of sight coverage (elevated point)	2–3 h, portable unit requires min two persons for set up and transport
Autonomous operation mode	Yes, requires 220 V power supply (alternatively with solar panels)	Yes, requires 220 V power supply (alternatively with solar panels)
Spatial coverage (extent and resolution)	Point targets (optical prisms), max observation distance 2 km, line of site contact necessary but 360° angle of operation	Up to 4 km range distances. Movements are pixel-averaged for the entire field of illumination, Spatial resolution decreases with increasing distance. Operational on a 60° view
Temporal resolution	Near-real-time (a cycle of 40 prisms takes about 20 min to complete)	Near-Real-time observations (scene every 6–10 min depending on the max range distance) independent of dormant or active state of landslide
Displacement resolution	mm (ang. St.dev. 0.01 mgon, dist. st. dev 1 mm + 1 ppm)	mm to sub-mm
Displacement range	mm to max range distance. However, stability of targets makes it so that in Valoria we managed to measure max up to 120 m before losing the point	Theoretically limited only by maximum distance of operation (4 km). However, the "real object" captured in the pixel may change in time
Velocity range	Up to m/h. However, loss of prims is likely in a few days if velocities exceed m/h → active state	4.4 mm/10 min. Maximum detection range limited by wavelength
Remote data accessibility	Yes, if using a router/modem to connect to the on-site PC	Yes, if using a router/modem to connect to the on-site PC
Data processing	On-site, windows based OEM PC, on-site post processing possible	On-site, windows based laptop PC, on-site post processing possible
Maintenance	Frequent visits prism targets necessary when landslide is active to replace or reorient the prisms (2 operators needed: 1 at the total station and 1 in the field)	After installation no maintenance necessary, visits only for retrieval of data
Reliability	High, after initial phase, autonomous operation continues for more than 3 years. Minor interruptions only in remote data transmission. Maintenance at prism targets to ensure line-of-sight contact with survey station	To be tested in the long term
Early warning capability	Yes, transmission of automated warning messages possible based on "rules" that account for displacement and/or velocity of individual prisms or group of prisms	Yes, transmission of automated warning messages possible based on max velocity in the scene

total station the number of prisms determines the availability of displacement data (generally no more than for 100 discrete targets), while the radar output maps contain thousands of pixel, each with its own time series of LOS displacements. The temporal resolution for both instruments ranges from near-real-time (duty cycles of few minutes) to long-term monitoring (duty cycles of some years). The measurement cycles are determined mainly by the type of landslide and its dynamics. Displacement range and resolution differs slightly based on the different approaches both instruments apply. GB-InSAR is characterized by a sub-millimeter detection limit whereas the total station may identify movements only in the range of few millimeters depending on the distance to the optical prism and atmospheric effects. This is due to the lower limit of detection and generally higher positional inaccuracy compared to the IBIS-L instrument.

At the upper limit, absolute movements over 100 m could be tracked with the Leica TCA2003, whereas InSAR-based techniques tend lose the original target for very large displacements. The high detection capabilities and spatial coverage of the IBIS-L comes at the cost of averaging displacements for each pixel rendering an exact (absolute) displacement measure impossible without the use of corner reflectors. On the other hand, the data acquisition for the entire field-of-view at once allows for apparent distinction of zones of high and low displacements on a qualitative level.

Topographic surveys are restricted to few discrete observations obtaining absolute measurements from within moving deposits. Since movements can be variable within just a few meters prime targets may yield more exact measurements of maximal values compared to radar derived displacements. With respect to the velocity range, a highly sensitive detection level of the IBIS-L instrument resolved Line-of-Sight displacements of only few $mm \cdot h^{-1}$ during field tests. At the Valoria landslide, an average maximum LOS velocity of about 5.8 $mm \cdot h^{-1}$ was measured in the upper and about 14 $mm \cdot h^{-1}$ in the lower part at the main flow. The automatic total station is well suited for slow ($mm \cdot day^{-1}$) to moderate ($m \cdot h^{-1}$) movements whereas it is not ideal for monitoring very slow moving landslides ($mm \cdot year^{-1}$). Using a GB-InSAR approach maintenance efforts during longer operation periods are in theory very low and field visits are required only for data retrieval. For the total station autonomous and almost maintenance-free functioning is possible on the long-term for very slow movements but when reactivations occur, frequent field visits may be necessary to reorient the prisms. A particular advantage is possibility to remotely access the computer that controls the total station ensuring long-term autonomous operation and remote collection of data.

During the years of operation the automated total station was found to be a reliable and constantly improving technology and a perspective tool for early-warning at the Valoria landslide. During landslide reactivations, measurements were taken in near real-time (3 h interval) and transmitted to an off-site computer. Based on displacement or velocity information critical movement patterns can be determined for individual prisms or for group of prisms. During autonomous operation the IBIS-L detects automatically the highest velocity of a scene between acquisitions and allows for a text message to be send in the case a predetermined threshold is exceeded.

2.4 Distributed Ground-Based Monitoring of Moderate-Moving Landslide Using Image Correlation Techniques

2.4.1 The Principle of Image Correlation (IC) Technique Applied to Landslide Analysis

The focus of this section is to highlight the possible applications and limitations of Image Correlation techniques applied both on terrestrial optical images and on Terrestrial Laser Scanner (TLS) point clouds. Using matching techniques, two-dimensional displacement fields can be derived by tracking objects in time series of images. The technique is based on the automatic identification of identical texture patterns within an image by maximizing a correlation function (Lewis 1995). Its principle adapted for landslide kinematics analysis is described in Delacourt et al. (2007).

Visible ground features have to be superimposed on two successive images on stable parts located outside the landslide. On the areas affected by landslide movements, the visible and recognizable features are shifted by the displacements. In order to quantify the ground displacements, a correlation window is defined on a reference (often the oldest) image. The corresponding window is searched in a pre-defined explored area belonging to the second image. The starting point of this explored area is the expected position of the window with the assumption that no displacement occurred between two acquisitions. The process is repeated for each pixel of the reference image. The Euclidean distance between the reference point and the matching point represents the displacement amplitudes in the image plane. By modifying the zone of interest, it is then possible to determine the displacements at various positions within the images. It is important to note that the normalized cross-correlation technique cannot track objects that start to rotate significantly or are affected by important perspective distortions (Lewis 1995).

The size of the correlation window is a compromise between the desired accuracy on the displacement estimates and the spatial resolution of the velocity field (Delacourt et al. 2007). An increase of the size of the correlation window ensures a good signal to noise ratio and thus a good precision, but the accuracy on the displacement estimates decreases because of their averaging on a larger correlation window. So far, Image Correlation techniques have been applied only on aerial and satellite images (e.g. SPOT, QuickBird, OrbView, EROS) for the creation of landslide displacement maps (Casson et al. 2003; Delacourt et al. 2004; LePrince et al. 2008; Debella-Gilo and Kääb 2010).

The correlation results consist in matrices of displacement Δu and Δv along the u- and v-axes in the image plane with their associated correlation index. In case of orthorectified airborne images, the pixel size is constant, only the effective pixel size at the ground has to be calculated to estimate metric displacements. In case of terrestrial images, the pixel size is not constant in the image due to the oblique

acquisition; the displacements field correlated in the image plane cannot be directly interpreted in terms of metric displacements and an orthorectification procedure is compulsory for a quantitative analysis.

Several datasets of multi-source images acquired at the Super-Sauze landslide (South French Alps) over the period 2007–2010 from different platforms are analyzed to highlight the usefulness of the technique.

2.4.2 *Image Correlation of Terrestrial Optical Photographs (TOP)*

A set of images acquired at the Super-Sauze landslide over the period May–July 2008 is used to illustrate the potential of the technique for the characterization of the kinematics during an acceleration period (Travelletti et al. in review).

Figure 2.6 presents the monitoring system installed in front of the landslide. The instrumentation consists in a low-cost D70 Nikon reflex digital camera installed on a concrete pillar located at a distance of 300 m from the lower part and 900 m from the main scarp. The acquisition system is controlled by a datalogger powered by a 40 W solar panel. Every 4 days, a serie of images is acquired at 11:00, 12:00, 13:00 and 14:00 GMT.

Figure 2.7A details an example of displacement rates (in pixel·day^{-1}) of the ground surface in the image plane derived from image pairs of 1–4 June 2008. The reference is the image of 20 May 2008. The contrast in displacement rates between the landslide area and the stable area gives confidence on the calculated velocity field. One can notice that the pattern of displacement rate is heterogeneous spatially and temporally. The upper part of the landslide displays the highest velocity ranging from 1 to 7 pixels·day^{-1} while the lower part displays velocity of less than 4 pixels·day^{-1}. The maximum of displacement rate is observed around the 1 June 2008. Then the landslide decelerates to displacement rate of about 1 pixel·day^{-1}. No quantitative comparisons can be carried out at this stage because the pixel sizes vary strongly in the image.

The displacement fields computed in the image plane are then orthorectified in a local geographic coordinate system by transforming the central projection of the image into an orthogonal view of the ground using the collinearity equations (Kraus and Waldhäusl 1994). The details of the methodology are explained in Travelletti et al. (2012). Figure 2.7B presents the amplitude of the 3D orthorectified displacement rates for the period 1–4 June. The difference of kinematics between the upper (until 3 m·day^{-1}) and the lower (until 1 m·day^{-1}) parts is important. The performance of the method has been evaluated by comparing the displacements derived from the image correlation, and the displacement monitored by dGPS on several benchmarks distributed in the stable parts and on the landslide. A correlation coefficient of $r = 0.95$ is found on 219 measurements and an average relative accuracy of 20 % is determined (Travelletti et al. 2012).

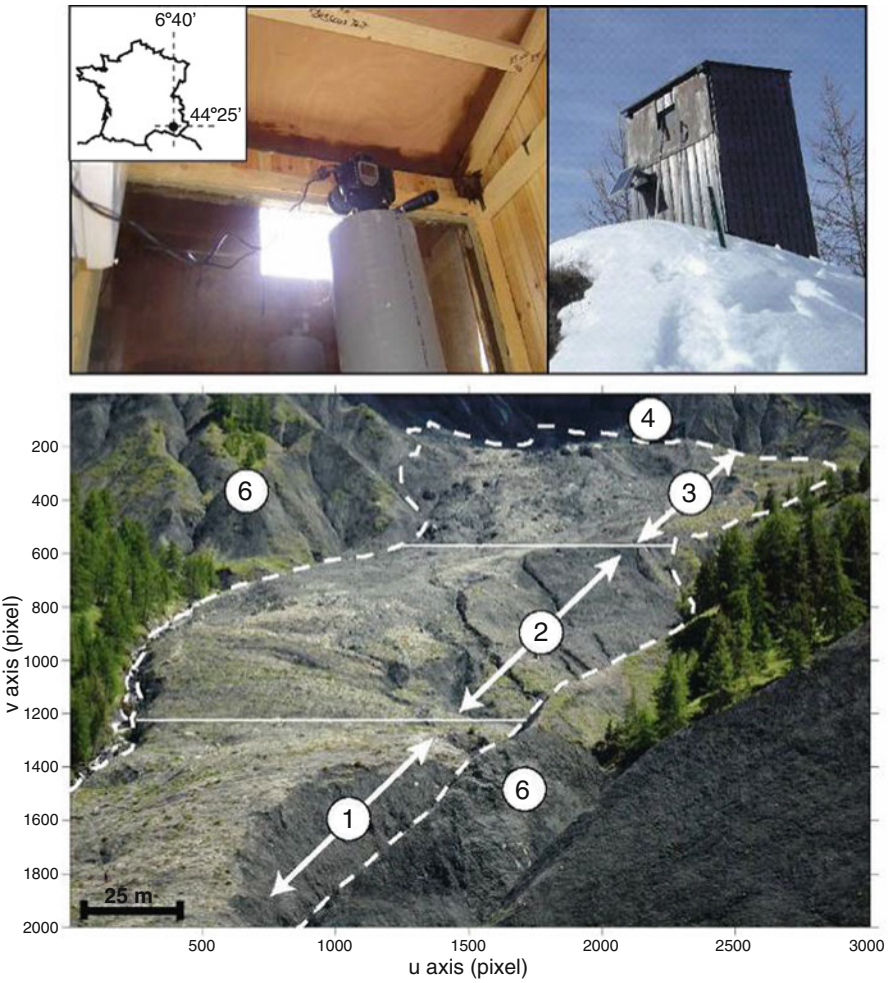

Fig. 2.6 Monitoring system with a very-high resolution camera installed in front of the Super-Sauze landslide on a stable crest. *Top*: Monitoring system. *Bottom*: Image acquired by the monitoring system presenting the different parts of the landslide from the camera location. The numbers refers to: (1) lower part (toe) of the landslide, (2) middle part (transition zone), (3) upper part (ablation zone), (4) main scarp (1,980 m), (5) front (1,734 m), (6) stable crests

2.4.3 Image Correlation of Terrestrial Laser Scanner Point Clouds (TLS)

The potential of Terrestrial Laser Scanner (TLS) for the monitoring of geomorphologic processes has been demonstrated in the last years, mainly for defining the structure of rocky slopes susceptible to rockfalls and rockslides (Abellán et al. 2009; Oppikofer et al. 2009) or characterizing the dynamics of ice glaciers

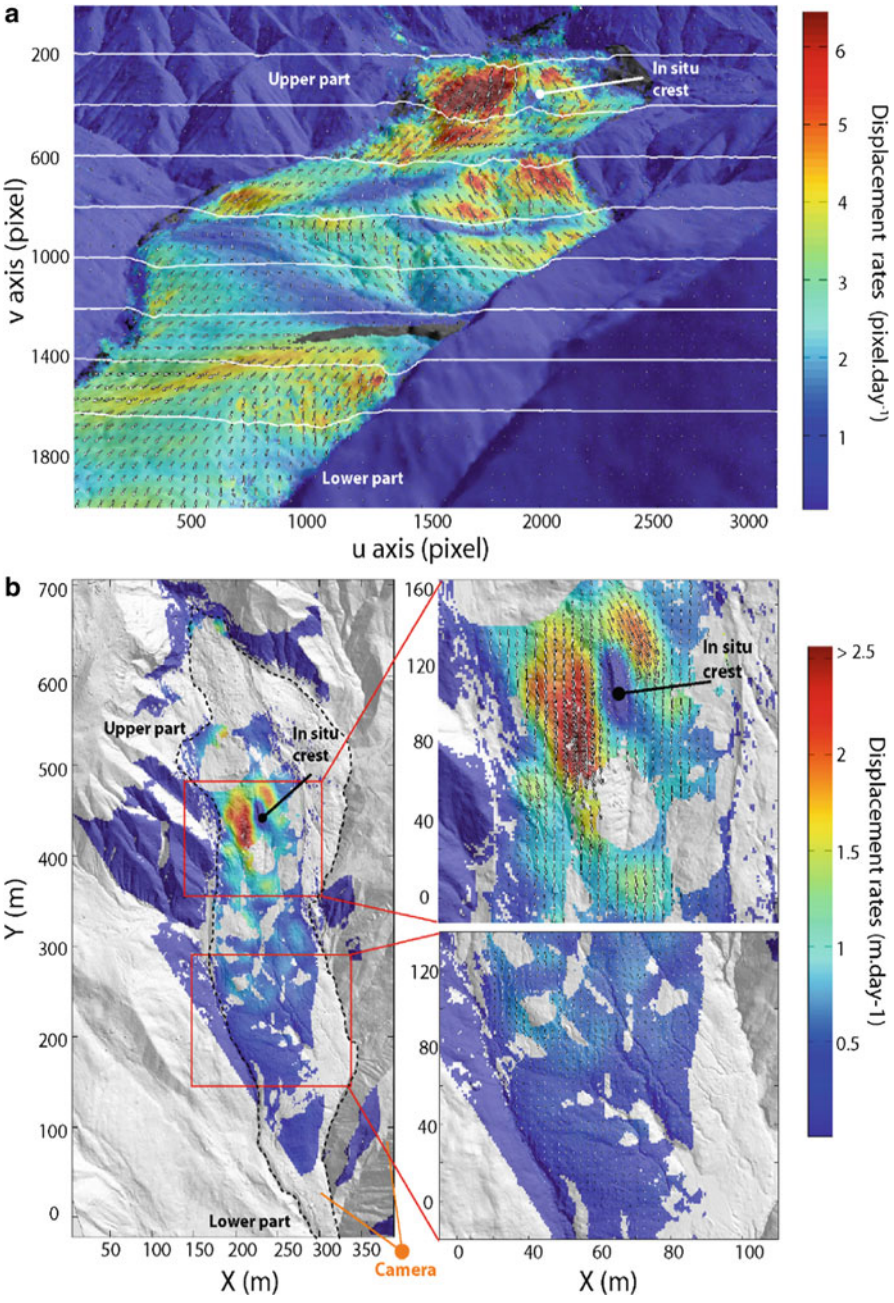

Fig. 2.7 Displacements obtained with Image Correlation for the period 1–4 June 2008: (**a**) Displacement rates amplitude (*color*) and direction (*arrows*) in the image plane and cumulated displacements along eight profiles crossing the landslide, (**b**) Displacement rates map orthorectified in the local geographic coordinate system

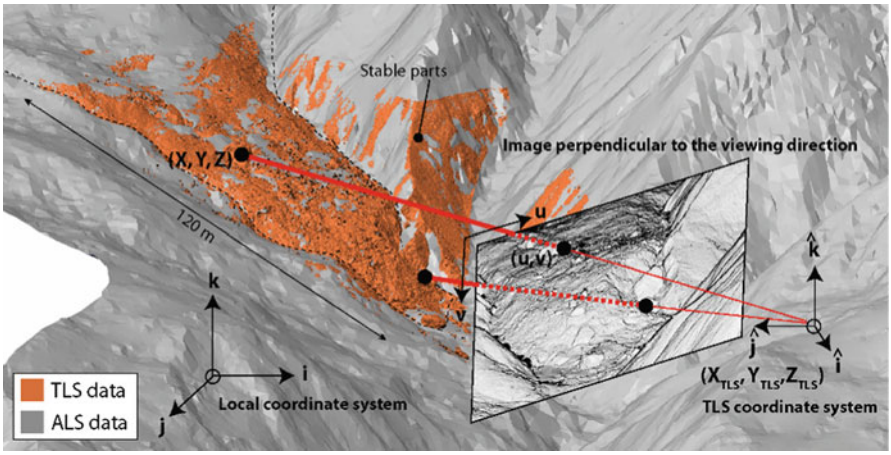

Fig. 2.8 View of the scanned area at the Super-Sauze landslide from the TLS base station, and schematic presentation of the projective projection applied on the TLS point clouds with the different coordinate systems involved in the procedure in order to produce a 2D image converted in *grey-scale* values. The alignment of the *stable parts* of *TLS* point clouds on the *ALS* (Airborne Laser Scanner) point cloud is indicated

(Avian et al. 2009) and landslides (Teza et al. 2008). Automatic matching algorithms applicable to TLS data have started to be developed because of their capability to fully exploit all the geometric information available in the point clouds. The approach is to find correspondences among typical features located in multi-temporal point clouds assuming that the tracked object has a constant geometry in time and/or a perfectly rigid behavior.

Image Correlation techniques can be applied on repeated TLS acquisitions in order to characterize the 3D displacement field. The hypothesis is that for objects scanned from a unique view point, simple 2D correlation functions can be applied on multi-temporal point clouds and yield the same range of accuracy than complex and time-consuming 3D surface matching algorithms (Teza et al. 2008). The performance of the cross-correlation algorithm is tested on datasets acquired at the toe of the Super-Sauze landslide. A long-range terrestrial laser scanner Optech ILRIS-3D has been used for the monitoring.

Ten acquisitions were acquired between October 2007 and May 2010 for the same base station at an average distance of 100 m from the landslide toe. The average point density at the ground surface varies from 153.0 pt·m^{-2} to 234.9 pt·m^{-2} with a standard deviation up to 351.7 pts·m^{-2} and a maximal density of 1,148.3 pts·m^{-2}. A projective transformation is used to represent the entire geometrical information in a plan perpendicular to the viewing direction of the laser scan using the collinearity equations (Kraus and Waldhäusl 1994) (Fig. 2.8). The density varies from 0.78 to 0.94 pt·pixel^{-1} with a relatively low standard deviation of 0.18 pt·pixel^{-1}. The distance between the point clouds to the position of the laser

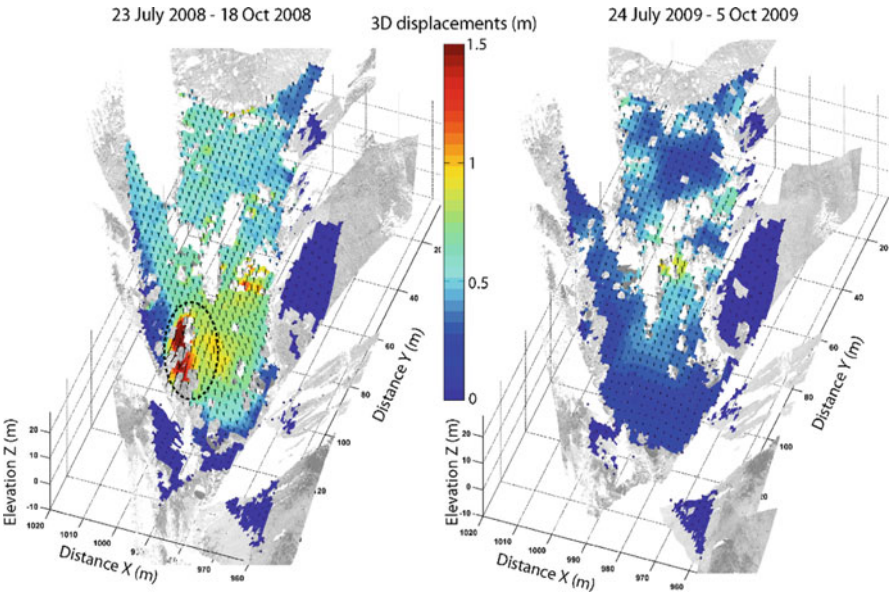

Fig. 2.9 3D displacements field obtained by TLS measurements related to the acquisition periods of July–October of the years 2008 and 2009. The *dashed circle* indicates the detachment of compartment at the front of the toe

scanner is then determined and linearly interpolated in a regular grid. The norm of the 2D gradient in u and v directions of the distance between the point clouds and the TLS station is calculated for emphasizing the morphology of the landslide. The generated images are then converted in grey-scale values (16 bits) and are used as inputs for the image correlation algorithm (Fig. 2.8).

The computed displacements are generally well reproduced for all periods. Two acquisition periods (July–October 2008, July–October 2009) are presented to illustrate the performance of the approach (Fig. 2.9). For the period July–October 2008, displacements between 0.5 and 1.5 m are observed, corresponding to an average displacement rate of 0.6–1.7 cm·day^{-1}. The displacement field displays significant spatial heterogeneities. The largest displacements are detected in the front of the toe where the slope gradient increases. The detachment of a toe compartment is also highlighted in the front.

During the period July–October 2009, the landslide displays a very different kinematics both in terms of magnitude and spatial distribution. Displacements are shorter and range from 0.1 m at the front to 0.6 m in the upper part, corresponding to an average displacement rate of 0.1–0.8 cm·day^{-1}.

The computed displacements are validated by comparing the displacement values to DGPS observations of a series of blocks easily recognizable in the TLS point clouds.

2.5 Conclusion

This section details some of the latest developments of remote-sensing techniques applied for the detection and characterization slow- to moderate-moving landslides. At regional and catchment scales, the landslide hotspot mapping through PSI analysis is an innovative approach for efficiently detecting slow-moving landslides. The approach can automatically detect clustering of PS with locally-high velocity, and a hotspot map indicating where potential mass movements exist. Future work for improvement should focus on short wavelength X-band sensors which largely increases PS density and decreases the revisit time. At the slope scale and for individual landslides, the combination of different monitoring techniques has proven to be very valuable. Since automated total stations require some days to be implemented and points of interest must be preselected, such systems are not rapidly deployable during emergency phases. However, this system is well-suited for long-term autonomous operation and collection of data at active landslides with known elements at risk. The remote sensing approach and rapid deployment of GB-InSAR makes this an ideally suited technology during crisis and rapid intervention. Image Correlation techniques applied to multi-temporal terrestrial photographs or terrestrial Laser Scanner point clouds are of particular interest for monitoring landslides characterized by annual pluri-decimetric displacements.

Considering the increasingly large fleet of remote sensing satellites operated by space agencies and private companies, and the increasing widespread of aerial and terrestrial sensors at constantly decreasing costs, the remote-sensing of landslides and risk related information encounters generally favourable data availability. One exception is currently the segment of L-band spaceborne SAR that has been demonstrated as a valuable tool for the monitoring surfaces that induce a loss of coherence with C- and X-band techniques (Strozzi et al. 2005). It is expected that very high density point clouds derived from ALS and TLS sensors will become a standard tool for landslide investigations. While it can be expected that remaining computational issues arising from large point cloud analyses will be solved as computational time becomes cheaper, many conceptual questions on the integration of high resolution DEMs in hazard and risk assessment remain (Jaboyedoff et al. 2010).

A full exploitation of the daily recorded images will not only depend on the implementation of operational processing systems but also on an easy data access and exchange via European and international networks such as GMES and GEOSS. The ‘International Charter on Space and Major Disasters’ has already demonstrated the advantages of a more liberal data exchange in the aftermath of major disasters. Analogous initiatives to open data archives including comprehensive time-series to a broader group of potential users appear desirable. Similarly to issues concerning easy data access, the availability of high quality software tools for the extraction of the required information is of at least equal importance. Besides proprietary software and in-house algorithms of private companies, many of such tools are also freely available on the web. This includes software for SAR interferometry

(ROI_PAC, StaMPS), open source projects with general GIS and raster processing capabilities (ILWIS, QGIS, OrbGIS). One of the most remarkable examples is probably the ORFEO (Optical and Radar Federated Earth Observation) toolbox which includes wide range of state of the art image processing tools and sensor specifications.

Major challenges for the further development of analysis methods are the integration of multi-modal and multi-temporal remote sensing datasets with existing inventory databases and in-situ measurements. Finally it should also be mentioned that the great success of collaborative mapping projects such as OpenStreetMap has raised a broad public and academic interest in the application of crowd-sourcing for many applications such as the monitoring of transportation networks, the collection of information during disaster response phases or conflict management (Goodchild 2010; Heipke 2010). Examples for the application of such community based platforms during landslide disaster already start to appear on the internet (http://www.gawana.com/peru/ushahidi/). They should be explored as they could yield a valuable information source that may complement "traditional" remote sensing techniques.

References

Abellán A, Jaboyedoff M, Oppikoffer T, Vilaplana JM (2009) Detection of millimetric deformation using a terrestrial laser scanner: experiment and application to a rockfall event. Nat Hazard Earth Syst Sci 9:365–372

Antonello G, Casagli N, Farina P, Leva D, Nico G, Sieber AJ, Tarchi D (2004) Ground-based SAR interferometry for monitoring mass movements. Landslides 1:21–28

Avian M, Kellerer-Pirklbauer A, Bauer A (2009) LiDAR for monitoring mass movements in permafrost environments at the cirque Hinteres Langtal, Austria, between 2000 and 2008. Nat Hazard Earth Syst Sci 9:1087–1094

Berardino P, Fornaro G, Lanari R, Sansosti E (2002) A new algorithm for surface deformation monitoring based on small baseline differential sar interferograms. IEEE Trans Geosci Remote Sens 40:2375–2383

Blanco-Sanchez P, Mallorqui JJ, Duque S, Monells D (2008) The coherent pixels technique (cpt): an advanced dInSAR technique for nonlinear deformation monitoring. Pure Appl Geophys 165(6):1167–1193

Brunner F, Macheiner K, Woschitz H (2007) Monitoring of deep-seated mass movements. In: Proceedings of the 3rd international conference on structural health monitoring of intelligent infra-structure (SHMII-3), Vancouver, 13–16 November, 7p (on CDROM)

Casagli N, Farina P, Leva D, Tarchi D (2004) Application of ground-based radar interferome-try to monitor an active rock slide and implications on the emergency management. In: Evans SG, Scarascia-Mugnozza G, Strom A, Hermanns RL (eds) Landslides from massive rock slope failure, Proceedings of the NATO Advanced Research Workshop on Massive Rock Slope Failure – New Models for Hazard Assessment, Springer, Celano/Berlin, 16–21 June, pp 351–360

Casson B, Baratoux D, Delacourt D, Allemand P (2003) "La Clapière" landslide motion observed from aerial differential high resolution DEM. Eng Geol 68:123–139

Casson B, Delacourt C, Allemand P (2005) Contribution of multi-temporal sensing images to characterize landslide slip surface – application to the La Clapière landslide (France). Nat Hazard Earth Syst Sci 5:425–437

Casu F, Manzo M, Lanari R (2006) A quantitative assessment of the SBAS algorithm performance for surface deformation retrieval from DInSAR data. Remote Sens Environ 102:195–210

Catani F, Casagli N, Ermini L, Righini G, Menduni G (2005) Landslide hazard and risk mapping at catchment scale in the Arno River basin. Landslides 2:329–342

Colesanti C, Ferretti A, Prati C, Rocca F (2003) Monitoring landslides and tectonic motions with the Permanent Scatterers Technique. Eng Geol 68:3–14

Corsini A, Farina P, Antonello G, Barbieri M, Casagli N, Coren F, Guerri L, Ronchetti F, Sterzai P, Tarchi D (2006) Space-borne and ground-based SAR interferometry as tools for landslide hazard management in civil protection. Int J Remote Sens 27:2351–2369

Corsini A, Borgatti L, Cervi F, Daehne A, Ronchetti F, Sterzai P (2009) Estimating mass-wasting processes in active earth slides–earth flows with time-series of High-Resolution DEMs from photogrammetry and airborne LiDAR. Nat Hazard Earth Syst Sci 9:433–439

Crosetto M, Monserrat O, Iglesias R, Crippa B (2010) Persistent scatterer interferometry: potential, limits and initial c- and x-band comparison. Photogramm Eng Remote Sens 76(9):1061–1069

Debella-Gilo M, Kääb A (2010) Sub-pixel precision image matching for measuring surface displacements on mass movements using normalized cross-correlation. Remote Sens Environ 115:130–142

Delacourt C, Allemand P, Casson B, Vadon H (2004) Velocity field of the "La Clapière" landslide measured by the correlation of aerial and Quick-Bird satellite images. Geophys Res Lett 31:1–5

Delacourt C, Allemand P, Berthier E, Raucoules D, Casson B, Grandjean P, Pambrun C, Varel E (2007) Remote-sensing techniques for analysing landslide kinematics: a review. Bull Soc Géologique Fr 178(2):89–100

Duro J, Inglada J, Closa J, Adam N, Arnaud A (2003) High resolution differential interferometry using times series of ers and envisat sar data. In: Proceedings of the FRINGE 2003, ESRIN, Frascati, 1–5 December 2003

Farina P, Colombo D, Fumagalli A, Marks F, Moretti S (2006) Permanent Scatterers for landslide investigations: outcomes from the ESA-SLAM project. Eng Geol 88:200–217

Ferretti A, Prati C, Rocca F (2001) Permanent scatterers in SAR interferometry. IEEE Trans Geosci Remote Sens 39:8–20

Foppe K, Barth W, Preis S (2006) Autonomous permanent automatic monitoring system with robot-tacheometers. In: Proceedings of the XXIII international FIG congress 'Shaping the Change' (FIG-2006), Münich, 8–13 October, 12 p (on CDROM)

Fruneau B, Achache J, Delacourt C (1996) Observation and modelling of the Saint-Etienne-de-Tinée landslide using SAR Interferometry. Tectonophysics 265:181–190

Gens R, Van Genderen JL (1996) SAR interferometry – issues, techniques, applications. Int J Remote Sens 17(10):1803–1835

Getis A, Ord JK (1996) Local spatial statistics: an overview. In: Longley P, Batty M (eds) Spatial analysis: modeling in a GIS environment. Wiley, New York, p 261

Goodchild MF (2010) Crowdsourcing geographic information for disaster response: a research frontier. Int J Digital Earth 3(3):231–241

Heipke C (2010) Crowdsourcing geospatial data. ISPRS J Photogramm Remote Sens 65(6): 550–557

Hervás J, Bobrowsky P (2009) Mapping: inventories, susceptibility, hazard and risk. In: Sassa K, Canuti P (eds) Landslides – disaster risk reduction. Springer, Berlin/Heidelberg

Hooper A, Zebker H, Segall P, Kampes B (2004) A new method for measuring deformation on volcanoes and other natural terrains using InSAR persistent scatterers. Geophys Res Lett 31:L23611

Hooper A, Segall P, Zebker H (2007) Persistent Scatterer InSAR for crustal deformation analysis, with application to Volcan Alcedo. Galapagos J Geophys Res 112:B07407

Jaboyedoff M, Ornstein P, Rouiller JD (2004) Design of a geodetic database and associated tools for monitoring rock-slope movements: the example of the top of Randa rockfall scar. Nat Hazard Earth Syst Sci 4:187–196

Jaboyedoff M, Oppikofer T, Abellan A, Derron MH, Loye A, Metzger R, Pedrazzini A (2010) Use of LiDAR in landslide investigations: a review. Nat Hazard 2010:1–24. doi:10.1007/s11069-010-9634-2

Kraus K, Waldhäusl P (1994) Photogrammetry, fundamentals and standard processes, vol 1. Hermès (ed), Paris

Lanari R, Mora O, Manunta M, Mallorqui JJ, Berardino P, Sansosti E (2004) A small-baseline approach for investigating deformations on full-resolution differential sar interferograms. IEEE Trans Geosci Remote Sens 42:1377–1386

LePrince S, Berthier E, Ayoub F, Delacourt C, Avouac JP (2008) Monitoring earth surface dynamics with optical imagery. Eos Trans Am Geophys Union 89:1–5

Lewis JP (1995) Fast normalized cross-correlation. Vis Interface 95:120–123

Lu P, Casagli N, Catani F (2010) PSI-HSR: a new approach for representing Persistent Scatterer Interferometry (PSI) point targets using the hue and saturation scale. Int J Remote Sens 31(8):2189–2196

Lu P, Stumpf A, Kerle N, Casagli N (2011) Object-oriented change detection for landslide rapid mapping. IEEE Geosci Remote Sens Lett 8(4):701–705

Lu P, Casagli N, Catani F, Tofani V (2012) Persistent Scatterers Interferometry Hotspot and Cluster Analysis (PSI-HCA) for detection of extremely slow-moving landslides. Int J Remote Sens 33(2):466–489

Malet JP, Maquaire O, Calais E (2002) The use of Global Positioning System techniques for the continuous monitoring of landslides: application to the Super-Sauze earthflow (Alpes-de-Haute-Provence, France). Geomorphology 43(1–2):33–54

Massonnet D, Feigl KL (1998) Radar interferometry and its application to changes in the earth's surface. Rev Geophys 36(4):441–500

Mora O, Mallorqui JJ, Broquetas A (2003) Linear and nonlinear terrain deformation maps from a reduced set of interferometric SAR images. IEEE Trans Geosci Remote Sens 41:2243–2253

Naterop D, Yeatman R (1995) Automatic measuring system for permanent monitoring: Solexperts Geomonitor. In: Proceedings of the 4th international symposium on field measurements in geomechanics (FMGM-1995), Bergamo, 18–23 April, pp 417–424

Oppikofer T, Jaboyedoff M, Kreusen HR (2008) Collapse at the eastern Eiger flank in the Swiss Alps. Nat Geosci 1(8):531–535

Oppikofer T, Jaboyedoff M, Blikra LH, Derron MH, Metzger R (2009) Characterization and monitoring of the Aknes rockslide using terrestrial laser scanning. Nat Hazard Earth Syst Sci 9:1003–1019

Petley DN (2004) The evolution of slope failures: mechanisms of rupture propagation. Nat Hazard Earth Syst Sci 4:147–152

Petley DN, Higuchi T, Petley DJ, Bulmer MH, Carey J (2005a) Development of progressive landslide failure in cohesive materials. Geology 33:201

Petley DN, Mantovani F, Bulmer MH, Zannoni A (2005b) The use of surface monitoring data for the interpretation of landslide movement patterns. Geomorphology 66:133–147

Ronchetti F, Borgatti L, Cervi F, Lucente C, Veneziano M, Corsini A (2007) The Valoria landslide reactivation in 2005–2006 (Northern Apennines, Italy). Landslides 4:189–195

Rosen PA, Hensley S, Joughin IR, Li K, Madsen SN, Rodriguez E, Goldstein RM (2000) Synthetic aperture radar interferometry. Proc IEEE 88(3):333–382

Silverman BW(1986) Density estimation for statistics and data analysis. In: Monographs on Statistics and Applied Probability 26. Chapman & Hall/CRC, London. ISBN 0412246201, 9780412246203

Singhroy V, Mattar KE, Gray L (1998) Landslide characterisation in Canada using interferometric SAR and combined SAR and TM images. Adv Space Res 21:465–476

Squarzoni C, Delacourt C, Allemand P (2005) Differential single-frequency GPS monitoring of the La Valette landslide (French Alps). Eng Geol 79(3–4):215–229

Strozzi T, Farina P, Corsini A, Ambrosi C, Thüring M, Zilger J, Wiesmann A, Wegmüller U, Werner C (2005) Survey and monitoring of landslide displacements by means of L-band satellite SAR interferometry. Landslides 2:193–201

Strozzi T, Wegnuller U, Keusen HR, Graf K, Wiesmann A (2006) Analysis of the terrain displacement along a funicular by SAR interferometry. IEEE Geosci Remote Sens Lett 3:15–18

Tarchi D, Casagli N, Fanti R, Leva DD, Luzi G, Pasuto A, Pieraccini M, Silvano S (2003) Landslide monitoring by using ground-based SAR interferometry: an example of application to the Tessina landslide in Italy. Eng Geol 68:15–30

Teza G, Pesci A, Genevois R, Galgaro A (2008) Characterization of landslide ground surface kinematics from terrestrial laser scanning and strain field computation. Geomorphology 97(3–4):424–437

Travelletti J, Malet JP, Delacourt C (in review) Multi-date correlation of terrestrial laser scanning data for the characterization of landslide kinematics. Submitted to Geomorphology

Travelletti J, Delacourt C, Allemand P, Malet JP, Schmittbuhl J, Toussaint R, Bastard M (2012) Correlation of multi-temporal ground-based images for landslide monitoring: application, potential and limitations. ISPRS J Photogramm Remote Sens 70:39–55

Tucker GE, Catani F, Rinaldo A, Bras RL (2005) Statistical analysis of drainage density from digital terrain data. Geomorphology 36:187–202

Werner C, Wegmuller U, Strozzi T, Wiesmann A (2003) Interferometric point target analysis for deformation mapping. In: Proceedings of the IGARSS 2003, Toulouse, 21–25 July 2003, pp 4362–4364

Xia Y, Kaufmann H, Guo XF (2004) Landslide monitoring in the Three Gorges area using D-InSAR and corner reflectors. Photogramm Eng Remote Sens 70:1167–1172

Chapter 3
Innovative Techniques for the Characterization of the Morphology, Geometry and Hydrological Features of Slow-Moving Landslides

Ulrich Kniess, Julien Travelletti, Alexander Daehne, Dominika Krzeminska, Grégory Bièvre, Denis Jongmans, Alessandro Corsini, Thom Bogaard, and Jean-Philippe Malet

Abstract In the last 10 years, landslide characterization has benefited from numerous developments in remote sensing, near surface geophysics, instrumentation and data processing. This section highlights various advances and innovative techniques or processing methods to characterize the morphology, structure and hydrological features of landslides. Airborne Laser Scanner (ALS) technique has emerged as a promising tool for characterizing slope morphology, with the perspective of automatic detection of landslide-affected areas. Combining ALS-data DTM with geophysical and geotechnical information has allowed to reconstruct the 3D landslide geometry considering data uncertainty and resolution. This is a significant forward step in landslide investigation. Of major importance is also

U. Kniess • G. Bièvre • D. Jongmans (✉)
Institut des Sciences de la Terre, CNRS UMR 5275, Observatoire des Sciences de l'Univers, Université Joseph Fourier, BP 53, FR-38041, Grenoble Cedex 09, France
e-mail: denis.jongmans@ujf-grenoble.fr

J. Travelletti • J.-P. Malet
Institut de Physique du Globe de Strasbourg, CNRS UMR 7516, Université de Strasbourg/EOST, 5 rue René Descartes, F-67084 Strasbourg Cedex, France

BEG, Bureau d'Etudes Géologiques SA, Rue de la Printse 4, CH-1994 Aproz, Switzerland

A. Daehne • A. Corsini
Department of Earth Sciences, University of Modena and Reggio Emilia University, Largo Sant' Eufemia 19, IT-41100 Modena, Italy

Department of Geosciences, University of Missouri – Kansas City, 5110 Rockhill Road, Kansas City, MO 64110 , USA

D. Krzeminska • T. Bogaard
Water Resources Section, Faculty of Civil Engineering and Geosciences, Delft University of Technology, Stevinweg 1, 2628 CN Delft, The Netherlands

T. van Asch et al. (eds.), *Mountain Risks: From Prediction to Management and Governance*, Advances in Natural and Technological Hazards Research 34,
DOI 10.1007/978-94-007-6769-0_3,

the detection and monitoring of water infiltration in the sliding masses, using indirect prospecting techniques such as ERT and distributed temperature sensing (DTS) using fibre-optic cables. These new techniques could be a major help in understanding the water paths and in designing appropriate remediation systems. Finally, although most of these results have been obtained in clayey landslides, the applied methods can be extended to other landslide types, with some technical adaptations.

Abbreviations

ALS	Airborne Laser Scanner
DEM	Digital Elevation Model
DTM	Digital Terrain Model
ERT	Electrical Resistivity Tomography
RMSE	Root Mean Square Error
DGPS	Differential Global Positioning System
DTS	Distributed Temperature Sensing
GPR	Ground Penetrating Radar

3.1 Introduction

During the last decade, techniques for landslide investigation and monitoring have undergone rapid development. Innovative methods include remote sensing imaging of the surface, geophysical imaging of the landslide structures and easy-to-deploy point measurements in the landslide mass. This section discusses advanced methods to characterize the morphology of areas affected by active landslides from the processing of airborne laser scanner point clouds (ALS). In particular, the possibility to automatically distinguish sliding zones from stable areas is discussed by characterizing the terrain roughness. Shallow geophysical prospecting has also considerably evolved with the emergence of 3D spatial imaging and 4D time and space imaging, allowing the spatial and temporal variations of landslides to be determined (Jongmans and Garambois 2007). The combination of remote sensing methods and near surface geophysical techniques offers the possibility to image the landslide surface and the structure at depth. ALS data and seismic noise measurements have been used to investigate the 3D geological structure below two large clayey landslides in the Trièves Plateau (France). It is shown that the bedrock topography had, and still has, a major influence on the kinematics of the two landslides. Because multi-source data have different spatial resolution and characteristics, data interpretation and integration for building a 3D geometrical model can turn out to be a difficult task (Bichler et al. 2004; Caumon et al. 2009).

A new methodology for building 3D structure has been proposed for landslides exhibiting a continuous basal shear surface. Finally, rainfall and its consequences (erosion, infiltration, water level rise, pore water pressure built up) have a major influence on the triggering or reactivation of mass movements in clay slopes. The relation between rainfall, water infiltration and sliding activity is however complex, and innovative field investigation is necessary to understand how water infiltrates in cohesive material. The section discusses an attempt to monitor water infiltration and subsurface flow within a clay-shale landslide using time-lapse electrical resistivity tomography (ERT). This electrical survey took place during an artificial rainfall experiment at the Laval landslide (South French Alps). An alternative for soil moisture monitoring is to perform high-resolution temperature measurements using fiber-optic cable. Temperature is used as a tracer to detect spatial and temporal variation in soil moisture conditions through the monitoring of soil thermal properties. The geological, morphological and kinematic settings of the main landslides quoted in this paper – Avignonet and Harmalière (Trièves Plateau, France), Super-Sauze (Barcelonette basin, France), Laval (Draix, France) and Valoria (Northern Apennines, Italy), can be found in Bièvre et al. (2011, 2012), Malet et al. (2003), Travelletti and Malet (2012) and Daehne (2011).

3.2 Characterization of Landslide Morphology from ALS Data Processing

3.2.1 Influence of Vegetation Filtering

In order to obtain a DTM (Digital Terrain Model or bare earth model), which will hold the relevant geomorphological information on a landslide, every point in the point-cloud has to be classified (e.g. as ground, building, low/mid/high vegetation), assigning a tag with the reflecting material to every cloud point. Many filtering methods have been proposed to filter vegetation (Sithole and Vosselman 2001; Zhang and Whitman 2005). For the Trièves Plateau (Avignonet and Harmalière landslides), a "Hierarchical robust filtering" method (Briese et al. 2002) has been applied to such highly vegetated slopes, as shown by the comparison between unfiltered and filtered 2006 ALS point-clouds at Avignonet (Fig. 3.1). In order to derive an equally spaced bare-earth DTM for further morphological analysis, the ALS point cloud at Avignonet and Harmalière landslides was classified and filtered using 'Hierarchical robust filtering' with the software SCOP++. The average density for both scans is therefore about 3 pts·m^{-2}. The comparison of the point cloud densities before and after the filtering (Fig. 3.1) shows that the decrease is higher in vegetated areas.

In order to evaluate the quality of the vegetation filtering, two test-areas of 100 × 100 m characterized by rough terrains are filtered manually using

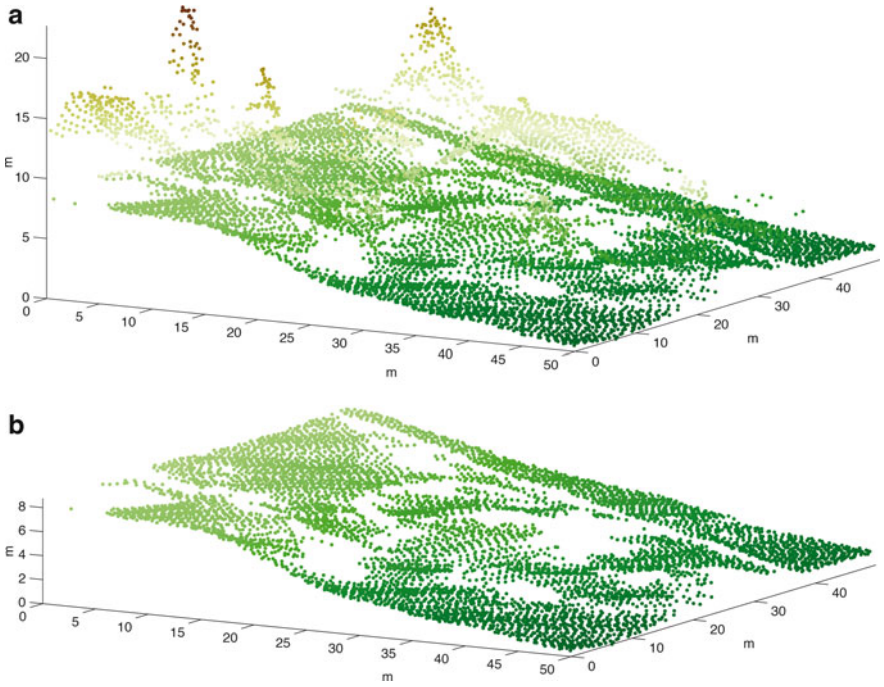

Fig. 3.1 Vegetation filtering on a data subset of the 2006 ALS point-cloud showing the unfiltered (**a**) and filtered point-cloud (**b**). The unfiltered raw point-cloud also includes points resulting from reflections on houses and trees, whereas the filtered point-cloud contains only the points classified as ground

a 3D-Viewer for point clouds with some advanced point selection tools Point Cloud Mapper (PCM). Figure 3.2a shows the unfiltered and filtered DEM (Digital Elevation Model) with the location of the two test-areas. The manual filtered point-cloud and the automatic filtered point-cloud are gridded (2×2 m) and the difference is shown in Fig. 3.2b. Test-area 1 is situated in dense forest with steep slopes (>25°) including a drainage channel. Automatic filtering seems to throw out too many points of the bare-earth as the DTM is too low in average (−0.85 m). The maximal errors are about 3 m and the standard deviation of 0.70 m shows a quite high variation. The second test-area is located in a village on just a minor slope (<10°) including some houses and trees. Results from the automatic filtering are better than for test-area 1, but still below the reference in average (−0.34 m). The standard deviation of 0.37 m indicates that the maximal errors of −2.41 and 1.01 m are mainly outliers. The graphical representation of the two areas (Fig. 3.2b) shows that main difficulties are connected with lineaments, the drainage channel in test-area 1 and tree/bush-chains in test-area 2. These two test-areas are extreme cases and more isolated houses or/and trees have been filtered with less error.

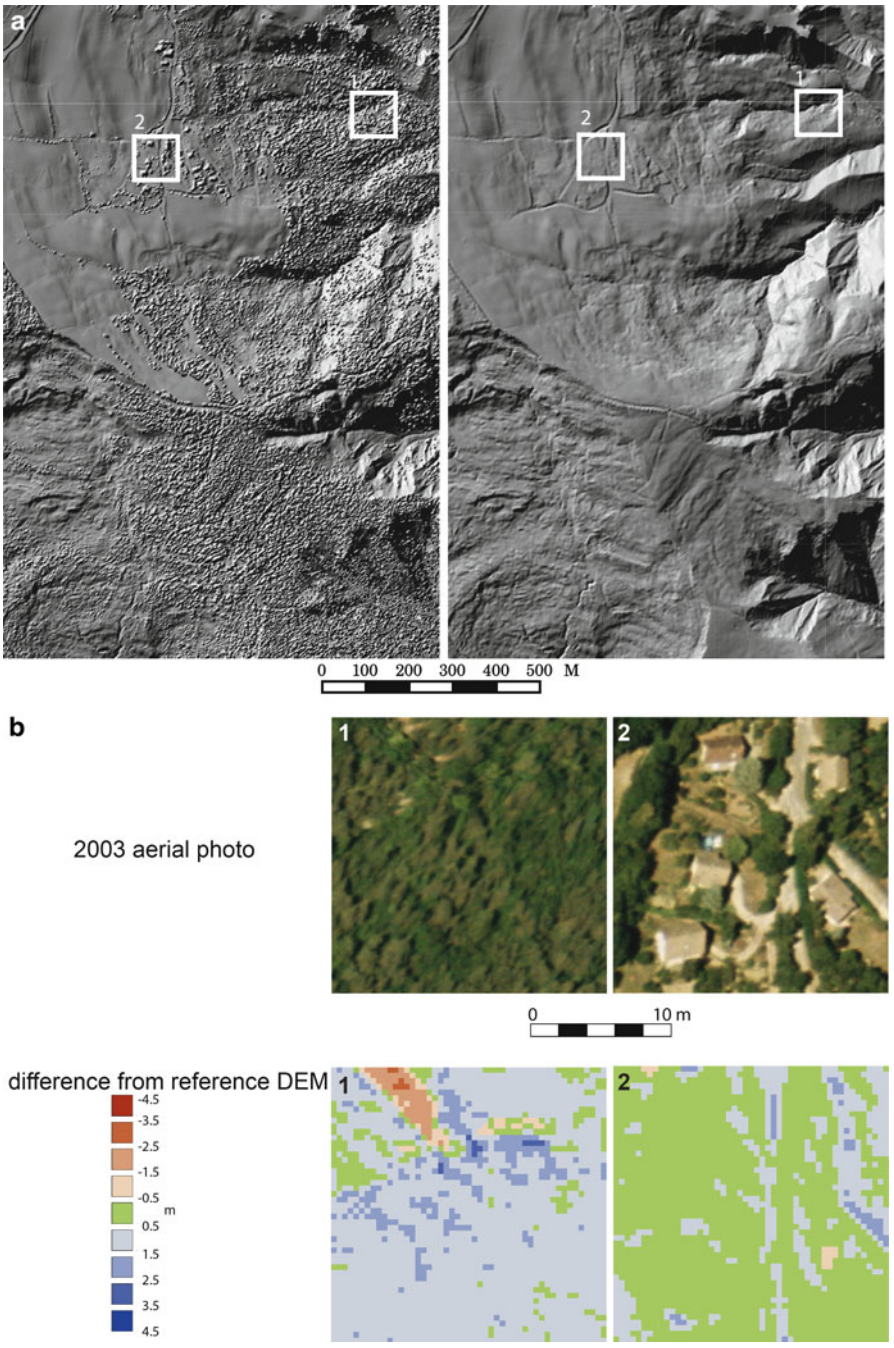

Fig. 3.2 Analysis of the upper part of Harmalière landslide. (**a**) Comparison between the shaded reliefs from the unfiltered (*left*) and filtered (*right*) DEMs, (**b**) aerial photographs (*top*) and difference between manual and automatic filtered DTMs (*bottom*) of the two test-areas

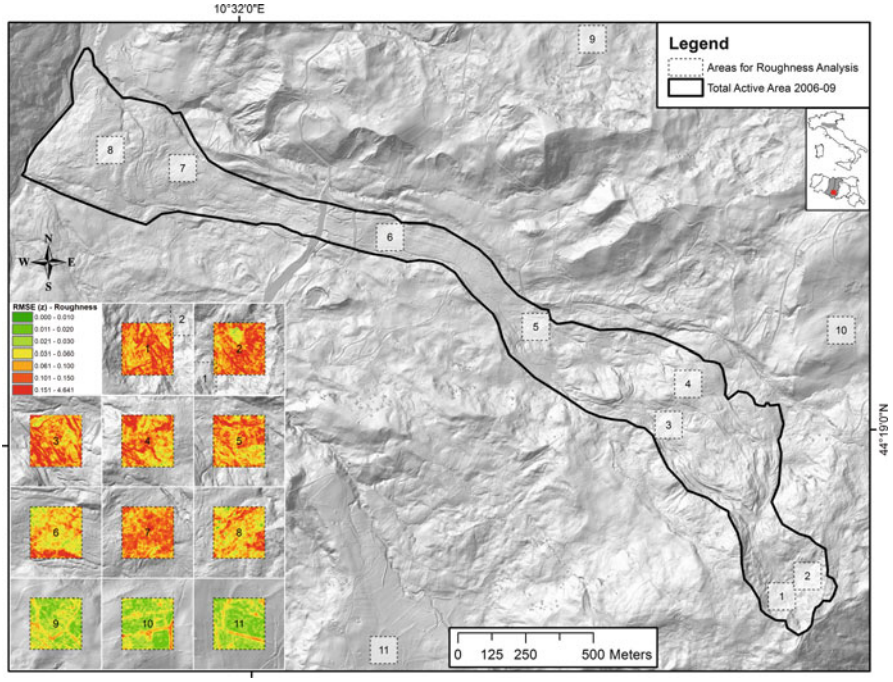

Fig. 3.3 Map situation of the Valoria landslide showing the location of the 11 zones with different slope activity, as well as the RMSE images obtained in these zones. The frequency distributions for each zone are given in Fig. 3.4

3.2.2 Estimation of Surface Roughness

A valuable derivative of a DTM is the surface roughness. Different parameters quantifying roughness have been proposed in the literature, including RMSE (Root mean Square Error on height) and RMS-deviation (see Shepard et al. 2001). Two applications of roughness are shown in this paper. For the Valoria landslide (Italy), the RMSE of the surface elevation is calculated using a moving kernel, with the goal to define characteristic signatures allowing discrimination between active and stable areas. For the Avignonet and Harmallière landslides (Trièves area, French Alps), roughness has been estimated using the RMSD along profiles with two step-sizes.

The Valoria landslide is a complex and composite mass movement, associated with rotational and translational slides in the source area and subsequent earthflows in the track and accumulation zones (Fig. 3.3, Daehne 2011). A Lidar-based DEM, with a 1 m pixel size, was analyzed to compute roughness on specific zones with different slope activity. Point cloud filtering was applied to remove vegetation and scan line effects. Characteristic roughness signatures were calculated for eleven 100 × 100 m zones with known slope activity, ranging from very disturbed areas to flat stable terrain. The locations of the 11 zones are shown in Fig. 3.3. The RMSE values

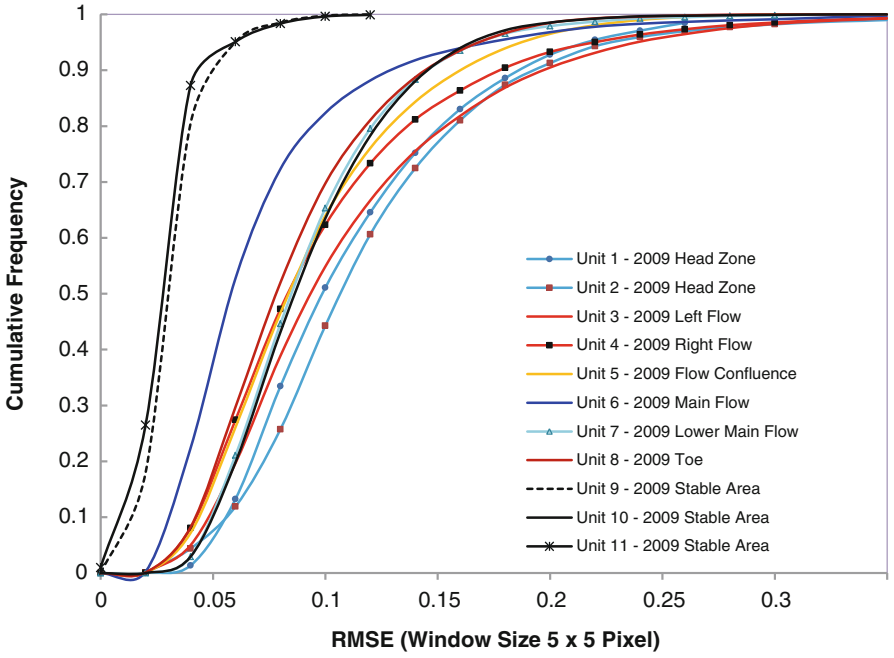

Fig. 3.4 Cumulative frequencies of RMSE values of elevations computed for different landslide units using a 5 × 5 moving window. Clearly distinguishable are stable units (*black*) with the major contributions below RMSE 0.05 with the exception of unit 10 which is slightly biased due to road embankments contained in the sample area. Head zone (*light blue*) and left flow (*red*) have a large percentage of RMSE values above 0.1. Difficulties exist to differentiate right flow, toe, flow confluence and the lower main flow. The main flow (*dark blue*) has a peak contribution from values between 0.04 and 0.08 indicating smooth terrain

of DEM elevations were computed for the different zones using a 5 × 5 m moving window. A de-trending surface representing average slope conditions was applied to the background of surface roughness. The calculated RMS subsets are included in Fig. 3.3. For each zone the corresponding RMSE cumulative frequency curves are shown in Fig. 3.4. Stable areas (zones 9, 11) have RMSE values prevalently lower than 0.04, while the source and the upper track areas (zones 1–4) are characterized by a wide distribution of RMSE between 0.07 to about 0.18, with a prevalence of values above 0.06. The RMSE distributions in zones located in the lower landslide body are very similar. The smooth surface morphology of the main flow stands somewhat out (Fig. 3.4) in that RMSE values are mainly below 0.07. In conclusions, RMSE values lower than 0.04 are capable to unequivocally constrain stable areas, particularly with low vegetating coverage. Conversely, the limit of RMSE equal to 0.05 or 0.1 can be considered as a reasonable boundary for detecting rough or very rough areas, respectively, unequivocally associated to active earth slides or earth flows. In between, no definite conclusion can be drawn.

For the Avignonet and Harmalière landslides, exhibiting major differences in morphology and displacement rates (Bièvre et al. 2011), the spatial roughness distribution was calculated along profiles 10 m apart from the 2 m-resolution 2006 ALS-based DTM. Slope orientation was averaged at small-scale (SSc: 20 × 20 m) and large-scale (LSc: 200 × 200 m), and two height-profiles were extracted, down-slope (UD = up-down) and parallel to the slope (LR = left-right). Roughness (RMSD) was calculated along the profiles with a step-size of 2 and 20 m, at small and large scales, respectively. The four images are shown in Fig. 3.5a, b, d, e. The UD-roughness is low (dark blue) on the plateau and relatively high (red) in Harmalière, the lower part of Avignonet and the terrain along the lake. On the contrary, LR-roughness appears to be low everywhere, except along the lake. Map of Fig. 3.5c shows the difference between the UD and LR roughness maps; it reveals yellow-red areas with predominant UD-roughness and blue areas with predominant LR-roughness. Three zones are distinguished: (1) the plateau and upper part of Avignonet with no specific roughness, (2) Harmalière and lower parts of Avignonet with UD-dominated roughness and (3) the terrain below the Avignonet landslide and E of Harmalière along the lake with LR-dominated roughness. The directional roughness then appears to be a good indicator for landslide activity, revealed by down-slope roughness (created by perpendicular-to-slope scarps), while erosion, generating drainage downslope paths, is shown by roughness along contour lines. Several parts of Harmalière, as well as some regions along the lake, exhibit unpronounced (green color) directional roughness and are not easily classified.

The same maps are presented for the large-scale roughness (20 m) in the lower row of Fig. 3.5d–f. These maps are simpler, owing to the averaging effect of the large profiles (200 m) relatively to the grid-spacing of 10 m. Overall, they show the same trend as the small-scale maps, with however some differences. UD-roughness (Fig. 3.5e) includes larger areas of the upper part of Avignonet, in opposite to the small-scale case. This matches the lower activity in the upper part of Avignonet, which leads to undulated morphology with longer wavelengths. In addition, the directional roughness (Fig. 3.5f) shows LR-dominated (blue) areas along the ridges bordering the landslides. Conclusively, the directional roughness seems to be a promising parameter to classify morphology, especially for discriminating between landslide and erosion morphological patterns. Further investigation on different landslides would be needed to draw definite conclusions.

3.3 Combination of Ground and Airborne Data for 3D Geometry Analysis

Remote sensing techniques and geophysical prospecting methods are increasingly used to image landslide structures at the surface and at depth, respectively. Recently, ALS data were successfully used to map recent and historical landslides in gentle slope areas (Schulz 2007; van den Eeckhaut et al. 2007). Major advantages of ALS

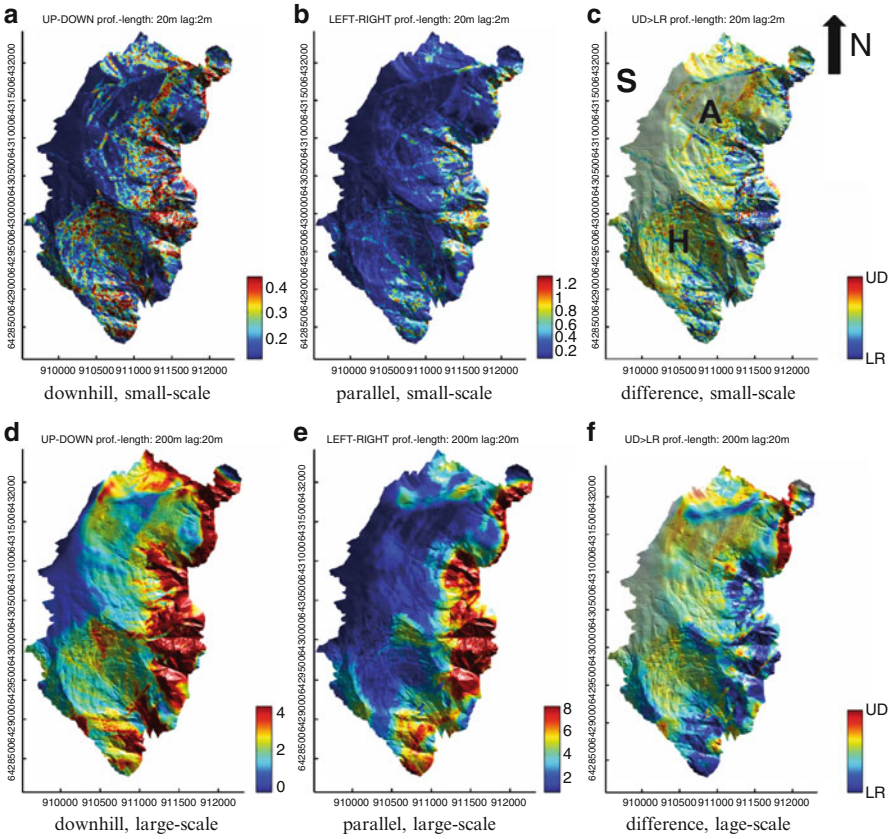

Fig. 3.5 Small-scale (**a**–**c**) and large-scale (**d**–**f**) directional roughness calculated at locations equally distributed at every 10 m. The roughness is shown in downhill direction (**a**, **d**) and parallel to the slope (**b**, **e**). (**c**) and (**f**) present the difference between the downhill (*UD*) and slope-parallel (*LR*) roughness, meaning red areas are more rough downhill than slope-parallel and vice versa. This is meant to show the primary force of morphology alteration, landslide (*red*) vs. erosion (*blue*). The intensity of the colors in (**c**), (**f**) is the sum of the downhill and slope-parallel roughness (general roughness) in order to highlight areas with higher roughness (independent of the direction). The roughness is computed as RMSE-deviation. For small-scales the profile length is 20 m and the lag is 2 m. For large-scales, the profile-length is 200 m and the lag is 20 m. (*A*) Extent of the Avignonet landslide, (*B*) Extent of the Harmalière landslide

point cloud analysis are the flexibility and the quickness of acquisition as well as the relatively simple data processing, allowing multi-temporal Digital Elevation Models (DEM) to be generated (Oppikofer et al. 2008). In parallel, shallow geophysics has also considerably evolved with the emergence of 2D and 3D spatial imaging, allowing the study of the spatial and temporal variations inside landslides (Jongmans and Garambois 2007). Although remote sensing and geophysical techniques are

complementary for landslide imaging purposes, they have been rarely associated. Roch et al. (2006) and Deparis et al. (2008) combined remote and ground imaging techniques for determining the geometry and the 3D fracture pattern of potentially unstable cliff sites. A dense digital surface model of the rock face was measured from ALS and/or photogrammetry, while the GPR performed on the cliff allowed the discontinuity pattern inside rock mass to be obtained.

Two applications of the combination of ground and airborne data are presented. The first investigates the influence of the 3D paleotopography on the activity of two adjacent landslides in glaciolacustrine sediments located in the Trièves area (French western Alps). The second presents a data integration methodology for building 3D landslide geometry, with application to the Super-Sauze and La Valette landslides (Barcelonette Basin, France)

3.3.1 Influence of Bedrock Topography on Landslide Characteristics at Large Scales

In the Trièves Plateau, the two adjacent landslides of Avignonet and Harmalière presents major differences in morphology, displacement direction and displacement rates. GPS measurements and digital photographs reveal that the difference in kinematics between the two landslides can be tracked back to 60 years ago at least (Bièvre et al. 2011).

The Avignonet landslide is directed towards the East (N 100 E) while the Harmalière landslide is mainly oriented towards SE (Fig. 3.6a). The Harmalière landslide, which has failed catastrophically in the 1980s, is still much more active than the Avignonet landslide. A ground geophysical prospecting based on ambient noise measurements (H/V method) was performed to record the resonance frequencies at 104 locations (Fig. 3.6). The H/V technique is a single station method consisting in calculating the horizontal to vertical spectral ratios (H/V) of seismic noise records. For a single homogeneous soil horizontal layer (1D geometry) overlying bedrock, the H/V curve exhibits a peak at the resonance frequency of the soft layer (Bard 1998). Knowing the soil shear-wave velocity, the layer thickness can be calculated. The 104 measured resonance frequencies were turned into clay thicknesses. From these data and using a ALS DEM (Fig. 3.6a), a 3D map depicting the base of the clays is proposed (Fig. 3.6b). It indicates that the basement is very irregularly shaped with strong lateral E-W variations over 150 m. This map reveals the presence of a N-S ridge of hard sediments (Jurassic bedrock and/or compact alluvial layers) on the eastern side of the Avignonet landslide. This ridge disappears when approaching the Harmalière landslide and makes place to what can be interpreted like a NW-SE oriented paleo-valley of the river Drac. This ridge could act as a buttress that could mechanically prevent the Avignonet landslide from evolving as fast as the Harmalière one. Furthermore, the NW-SE paleo-valley located under the Harmalière landslide corresponds to the sliding motion direction.

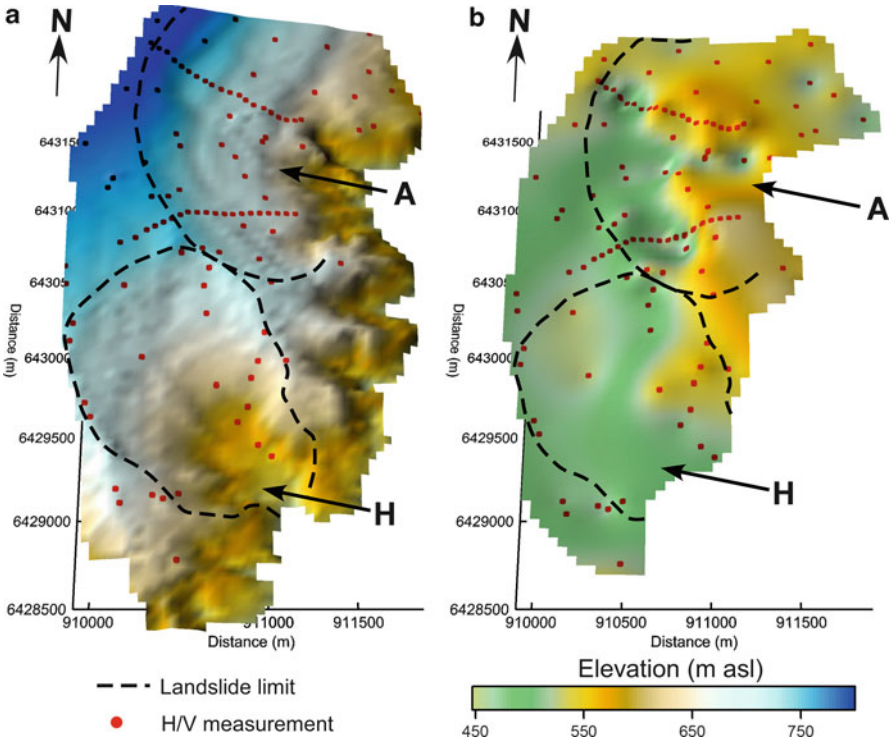

Fig. 3.6 Avignonet and Harmalière landslides: (**a**) ALS-based DEM with the location of the H/V measurements, (**b**) Paleo-topography of the former lake Trièves in the study area. *Dashed lines* stand for Avignonet (*A*) and Harmalière (*H*) landslide boundaries

It is then proposed that the different kinematic behaviours of the landslide are partly controlled by the paleo-topographic setting of the former Trièves lake.

3.3.2 Methodology for 3D Geometrical Modeling at Slope Scales

The data used for landslide analysis and modeling are often numerous and acquired using different techniques, either ground-based or airborne-based. They are thus heterogeneous in terms of physical parameters, accuracy and resolutions. Therefore, a major difficulty in 3D geometrical modeling of landslide consists in the extraction of relevant information on the internal layering and on its integration in a coherent framework (Bichler et al. 2004; Regli et al. 2004; Caumon et al. 2009).

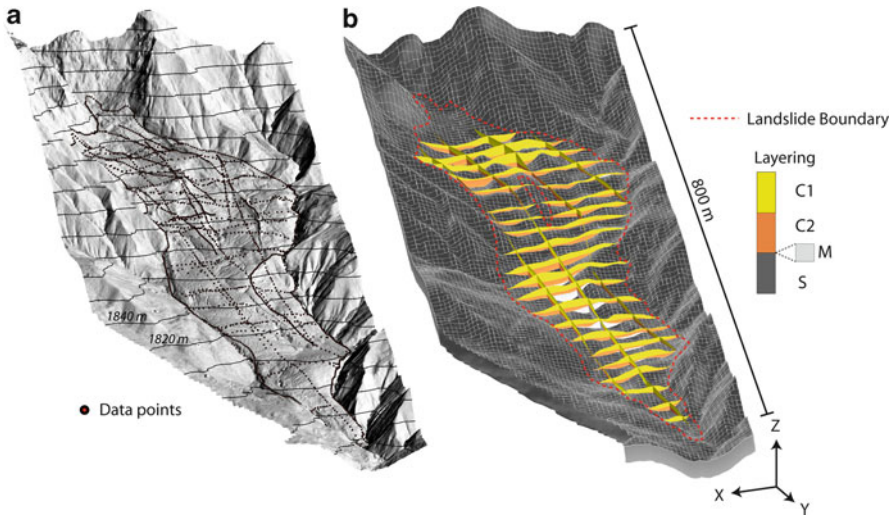

Fig. 3.7 3D geometrical model of the Super-Sauze landslide: (**a**) Location of the data points extracted from the geotechnical, geophysical and geomorphologic data, (**b**) 3D geometrical model illustrated through stratigraphic cross-sections interpolated with Universal Kriging. The landslide material is composed of two geotechnical layers C1 and C2 overlying the stable substratum S with some intercalation of moraine formation and torrential deposits M. (RMSE of the interfaces between C1 and C2 of 1.7 m and RMSE of the interfaces C2 and S of 2.1 m). The layers C1 and C2 have a mean thickness of 5.4 and 3.3 m. The volume of the landslide material is estimated at 560.000 m^3. About 66 % of the volume corresponds to the most active layer C1

Consequently, before incorporating the data in a 3D geometrical model, several pre-processing steps are necessary: (1) to georeference the data in a common reference coordinate system, (2) to define their quality for the purpose of the modeling, and (3) to interpret (or re-interpret) the data. The problem is that, in most cases, typical data for 3D geometrical modeling are already in an interpretive digital or numerical form (e.g. maps, cross-sections) for which the uncertainty is very difficult to assess without access to the raw data.

Travelletti et al. (2011) developed a very flexible methodology applicable to any kinds of digitized data. This methodology has been successfully applied on two landslides located in the Southern French Alps: the Super-Sauze landslide developed in black marls (Fig. 3.7a) and the La Valette landslide developed in flysch formations and black marls (Fig. 3.8a). On both landslides, extensive datasets of geophysical, geotechnical and geomorphological observations are available.

In order to evaluate the quality of the data, the methodology is based on the concept of "hard data" and "soft data" initially defined by Poeter and Mckenna (1995) and Clarke (2004). "Hard data" are characterized by a high degree of reliability (e.g. explicit properties and very low uncertainties) while "soft data" are characterized by a low degree of reliability (e.g. implicit properties and higher uncertainties; Regli et al. 2004; Gallerini and De Donatis 2009). The reliability

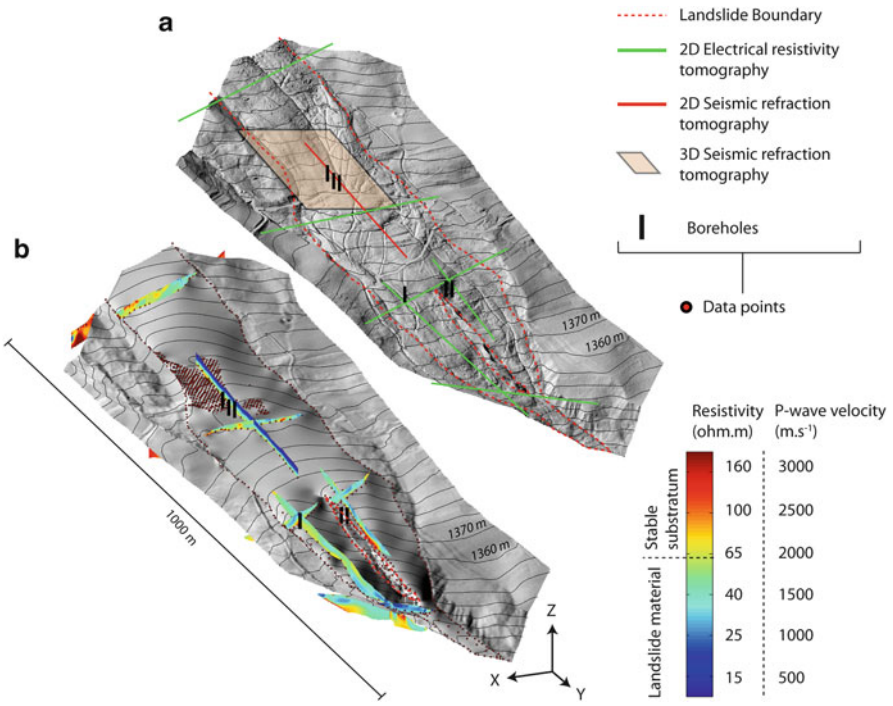

Fig. 3.8 3D geometrical model of the zones of transit and accumulation of the La Valette landslide. (**a**) Location of the geotechnical and geophysical acquisitions, (**b**) 3D geometrical model of the substratum topography interpolated with Universal Kriging (RMSE of 0.6 m). The data points extracted from the geophysical tomographies and from the landslide boundary are also indicated. In the zones of transit and accumulation, the depth of the landslide can reach 35 m. It represents a volume of 2.2 10^6 m^3 equivalent to 62 % of the total volume of the La Valette landslide

index depends on (i) the quality of the original data source and (ii) the number of processing steps needed to extract useful information. Travelletti et al. (2011) defined a scale of reliability index between 1 (very soft) and 4 (very hard) as follows:

1. Very soft data: The original data are noisy, inaccurate for the purpose of the analysis and with a high degree of subjectivity in the interpretation. The original data do not have accurate spatial information. They are already in an interpretative format or are derived from inaccessible raw data.
2. Soft data: The original data need several steps of processing to extract an useful geometrical information. This is usually the case for indirect data such as petrophysical properties determined with geophysical techniques at the ground surface or in boreholes. The non-uniqueness of the inverted solution and the possible decreasing resolution with depth are some drawbacks affecting the accuracy of geophysical methods (Sharma 1997; Jongmans and Garambois 2007).

3. Hard data: The original data represents generally well the geometry of the landslide, even if some ambiguities in the interpretation remain. The data have to be combined with other sources (generally geotechnical tests and geological observations) to reduce the uncertainty in the interpretation.
4. Very hard data: The original data are sufficiently accurate and allow a straightforward interpretation of the geometry without any ambiguity. The data sources are generally direct geomorphological or geological observations, borehole cores and kinematic measurements.

The coordinates of the data points used in the 3D geometrical modeling are extracted from georeferenced cross-sections and from the landslide limits in such manner that the sub-surface topography is fully preserved (Figs. 3.7a and 3.8a). A reliability index is attributed to each data point in order to associate a confidence map to the final geometrical model. This method allows one to set priority for the interpolation to the most reliable input data points. With this procedure, a null value for the reliability index is attributed to the areas unconstrained with data points. A frequent problem in data integration is caused by spatial and temporal inconsistencies among interpretive data (cross-sections or stratigraphic logs) that can be controlled and corrected with hard data located in the vicinity of the acquisition using 3D visualization tools. Temporal inconsistencies (e.g. time-dependent geometrical changes) are more difficult to detect without repetitive data acquisitions at the same location. In theory, the data should be acquired in a time short enough to avoid significant changes in the 3D geometry. In reality, these conditions are hardly ever realized because of temporal, financial and site configuration constraints. Therefore, recent data should have priority on older data. According to the quantity of available data, additional exploration might be necessary. The quality of the 3D geometrical modeling is defined by applying different interpolation techniques (Triangular Irregular Network, Inverse Distance with a weighting factor, Ordinary Kriging and Universal Kriging) and the analysis of the Root Mean Square Error (RMSE) and expert analysis (visualization of the sub-surface topography; Aguilar et al. 2005; Fisher and Tate 2006). In order to compute the RMSE, a subset of data points with a high degree of reliability is withheld from the interpolation by applying a random split-sample method (Declercq 1996). Finally, in order to obtain a geometrical model in agreement with the geological information, Travelletti et al. (2011) defined simple stratigraphic rules to avoid interferences between stratigraphic layers to provide realistic 3D geometrical models (Figs. 3.7b and 3.8b).

The 3D geometrical models of the Super-Sauze and La Valette landslides are based essentially on geophysical surveys (refraction seismic tomography, electrical resistivity tomography) and geotechnical investigations. These spatially distributed techniques were shown to be very efficient for preliminary field investigations because they provide a continuous imaging of the subsurface. However, geophysical tomographies generally display a smooth image of the sub-surface (Figs. 3.7b and 3.8b). The sub-surface appears excessively smoothed compared to the reality.

In such conditions or if no data point is available in a specific area, it is necessary to force the model to produce realistic results by adding data points coming from expert knowledge.

3.4 Characterization of Water Infiltration Using ERT and Temperature Monitoring

Water infiltration plays a crucial role in landslide mechanics (Maquaire et al. 2003). Rainwater or snow melt infiltrates into the soil and recharges the groundwater system. An increase in pore water pressure reduces the internal strength of slopes and can generate instability of soil masses. However, when dealing with shale slopes, material heterogeneity strongly affects the infiltration and moisture pattern. Therefore, moisture monitoring in the shallow soil layer is of prime importance for understanding the spatial and temporal behaviour of landslides. Two applications of monitoring methods are presented here: Electrical Resistivity imaging (ERT) and high-resolution distributed sensing (DTS) using fibre-optic cables.

3.4.1 Time-Lapse Electrical Resistivity Tomography (ERT)

Electrical resistivity of the subsoil is very sensitive to changes in water saturation and pore water salinity. Monitoring Electrical Resistivity through Tomographies (ERT) is potentially able to provide a spatial characterization of water flows within a slope (Daily et al. 1992; Binley et al. 1996; Slater et al. 2000; French and Binley 2004). Therefore, this technique is widely used to complement classical hydrological methods (Robinson et al. 2008). In complement, ERT is also particularly interesting for estimating bedrock geometry in landslide investigations when a resistivity contrast between the bedrock and the mobilized mass exists (Jongmans and Garambois 2007; Marescot et al. 2008).

In order to characterize the dynamics of water infiltration in the subsoil of heterogeneous marly landslides, rainfall experiments were carried out in 2007 and 2008 at the Laval landslide (Laval catchment, Draix, France) and at the Super-Sauze landslide (Barcelonnette Basin, France). In both study cases, the landslide material is composed of weathered Callovo-Oxfordian black marls characterized by a heterogeneous fabric of flakes and centimetric to decimetric blocks encased in a sandy-silty matrix. A multi-technique approach was set up to monitor soil deformation and soil hydrology (e.g. groundwater level measurements, soil water content monitoring, chemical tracer analysis, seismic tomography and ERT; Debieche et al. 2011).

At the Laval landslide, Travelletti et al. (2011) present an analysis of water movement based on the interpretation of ERT monitoring using a time-lapse inversion approach. The main objectives of this study were: (i) to characterize the spatial and temporal development of the water infiltration front and the subsurface flow in the soil and, (ii) to identify the time when the conditions of steady-state flow (e.g. constant water flow rate) is reached.

Six inverted models of time-lapse inversion are used to estimate the uncertainties of the resistivity values and to select the most appropriate inverted model for the hydrological interpretation. The best model has been chosen according to the RMSE of the inversion and the stability of the resistivity values in a test area where no change in resistivity is expected. The noise level due to temperature changes in the inversion process is estimated. A method for determining the time of steady-state flow conditions is proposed and this time is compared to hydrological measurements.

The experimental rain plot is located in the accumulation zone of the Laval landslide on a moderate slope gradient (ca. 20°); the zone is characterized by macro-fissures at the surface which may act as possible preferential water pathways (Garel et al. 2012). The simulated rainfall was applied on an area of 100 m^2 with an average intensity of 11 $mm{\cdot}h^{-1}$ during 67 h and simulated using a water pump and six sprinklers located along the borders of the experimental plot. Chemical tracers (chlorure, bromure) were added to the rain water to characterize the water pathways and flow velocity. The electrical resistivity of the rain was kept constant (18 $\Omega{\cdot}m \pm 4\ \Omega{\cdot}m$) during all the experiment. A network of shallow piezometers (with varying depths of 1–4 m) was installed for water sampling and groundwater level observations. The rain experiment started with unsaturated hydrological condition in the slope material (initial saturation degree of ca. 27 %). The resistivity of the pre-event water present in the slope has an average resistivity of $5\ \Omega{\cdot}m \pm 3\ \Omega{\cdot}m$.

The ERT tomography is located in the central part of the experimental plot in the direction of the main slope gradient. The upstream part of the ERT line is located outside of the artificial rain in an area called ‘dry plot’. The system features an internal switch-system board for 48 electrodes with 1-m inter-electrode spacing. Data acquisition lasted approximately 15 min; an acquisition was conducted every 1–3 h. A Dipole-Dipole configuration was selected. A filtering was applied to remove all data with a measured potential lower than 5 mV. After filtering, 87 % of the original dataset was kept for the analysis. The electrical potential, the input current electrode geometry and the ERT line topography are used to compute apparent resistivity value as input to the inversion process.

To determine the effects of soil temperature on the resistivity values, soil temperature was monitored near the experimental plot along a vertical profile at different depths (−0.13, −0.30, −0.50, −0.85 m). In addition, two temperature sensors were installed inside the rain plot at−1.90 and−2.90 m in piezometers. By using the model of Campbell et al. (2002), this study shows that inverted resistivity values above 0.5 m can be very noisy due to temperature changes. However correction of temperature effects will not significantly improve the results because

the very shallow layers are generally poorly resolved in term of inverted resistivity values. Consequently inverted resistivity values above 0.5 m depth are removed from the inverted models and the consequent analysis. The apparent resistivity values were inverted using the time-lapse approach based on cross-models implemented in the RES2DINV inversion software (Loke 2006). The basic of a cross model is the use of an inverted model from a base dataset as the reference model for later datasets. Changes in subsurface resistivity are computed by using the apparent resistivity changes to ensure that changes of inverted resistivity values are only due to changes in apparent resistivity values (Loke 1999; Miller et al. 2008). Three types of cross-models were compared. The best inverted model exhibits RMSE of less than 2.2 %.

The results show a decrease of resistivity (e.g. negative anomaly) with time following directly the onset of the rain (Fig. 3.9a). The observation coincides with the development of a wetting front progressing mainly vertically during the first 10 h of the experiment. The area located downstream and outside of the rain plot is then affected by a negative anomaly showing that a lateral subsurface flow is developing. After 30 h of rain, this lateral subsurface flow may have reached the Laval stream. The evolution below the weathered clay-shales/bedrock interface is not indicated because the sensitivity is too low below it. Consequently, infiltration inside the bedrock cannot be depicted from the ERT dataset. However, regarding the lateral development of the subsurface water flow at about 20 h after the beginning of the rain, an important permeability contrast between the weathered clay-shales and the bedrock can be suspected.

Despite the difficulty of finding a reliable relationship between resistivity values and soil moisture due to the uncertainty of the inverted resistivity models (non uniqueness of the inversion, 3D effects and the insufficient range of resistivity value at the location of the soil moisture measurements), Travelletti et al. (2011) succeeded in determining the time of steady-state flows based on a noise estimation approach validated with hydrological measurements (Fig. 3.9b). On average, times of steady-state flows conditions are reached 21 h after the start of the rain. The topsoil is characterized by relatively short times varying between 5 and 15 ± 1 h while deeper locations mostly reached steady-state flow conditions after 20–28 ± 1 h. More time is needed for locations downstream outside the rain plot (30–35 ± 5 h) to reach steady-state conditions. This time difference between area outside and inside the rain plot strongly suggests the development of subsurface lateral flow during the rain experiment. Two preferential flow paths could be detected near the abrupt change of slope delimiting the landslide toe from the other part of the landslide body. These flow paths induce fast water infiltration until the weathered clay-shales/bedrock interface thus leading to steady-state conditions after a short time of rain experiment (ca. 15 ± 2 h). These preferential flows are probably connected through the weathered clay-shales/bedrock interface. The inverse of the gradient of steady-state times is used to estimate an apparent saturated hydraulic conductivity of 1.7×10^{-4} m·s^{-1}. This value demonstrates the potential of the weathered soil to rapidly drain the infiltrated water. The ERT interpretations cannot explain complex hydrological behavior underlined by discrete information from direct hydrological and hydrochemical methods (e.g. isolated water at small scale

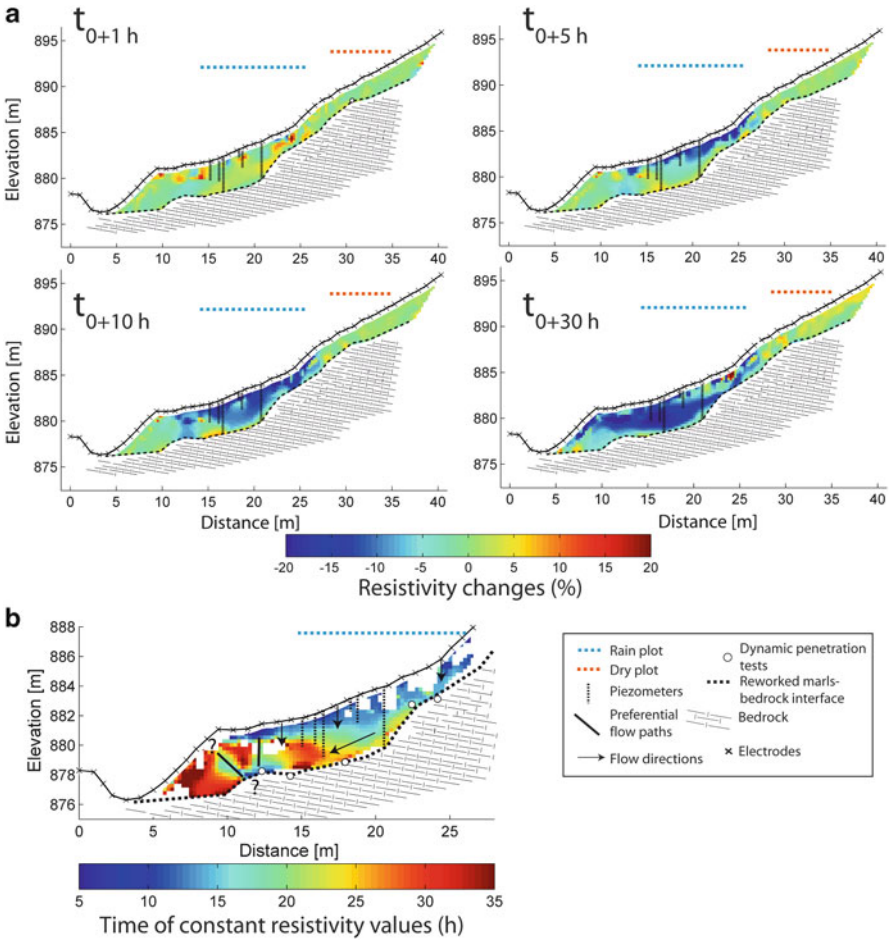

Fig. 3.9 Results of the ERT monitoring during a rainfall experiment at the Laval landslide: (**a**) Resistivity changes relative to a reference inverted resistivity model before the start of the rain experiment, (**b**) time of constant resistivity value indicated hydrologic steady state conditions. The presence of fissure in the landslide toe allowing a rapid infiltration in depth is highlighted

with no connection with the surrounding; Garel et al. 2012). However, the main processes occurring at larger scale are highlighted. The good contrast in resistivity observed is mainly explained by the unsaturated conditions of the slope at the beginning of the experiment.

At the Super-Sauze landslide, similar experiments were realized at larger scales (rain plot areas of 1 m^2) at the Super-Sauze landslide (Fig. 3.10a). In areas characterized by high density of sub-surface fissures, changes in resistivity occurred quite fast after the beginning of the rain at shallow depths and progress very slowly

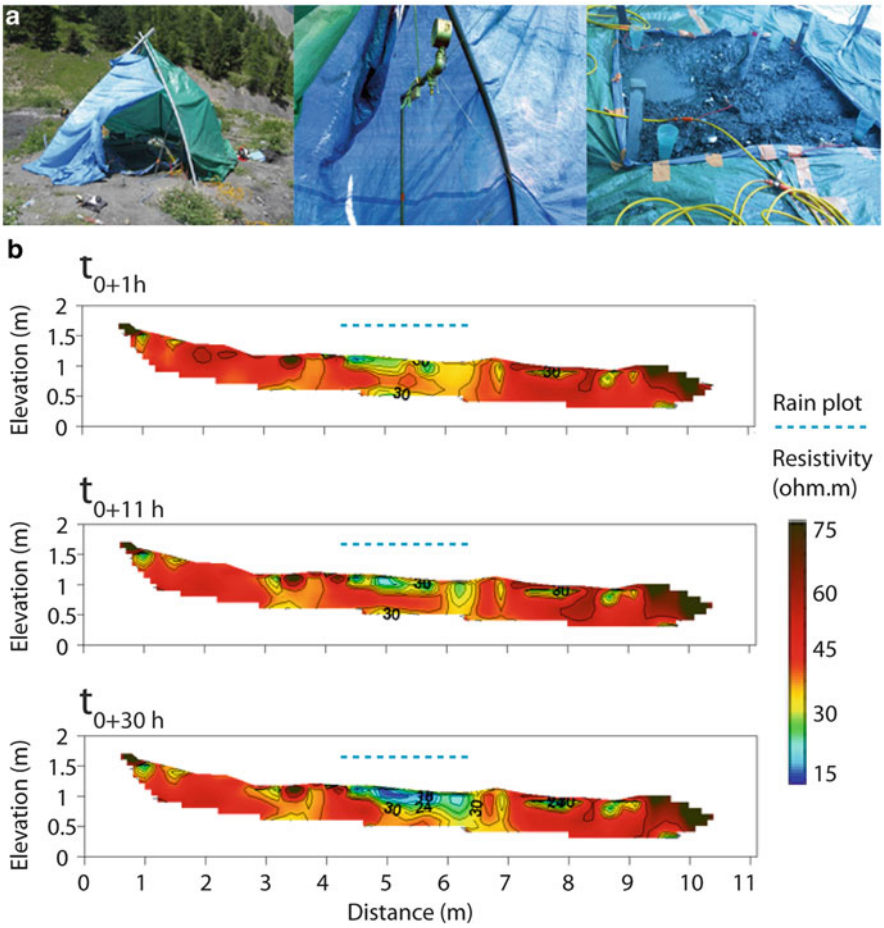

Fig. 3.10 Large-scale rain experiment in the Super-Sauze landslide (**a**) presentation of the experiment rain plot: the shelter, the sprinkler and the ERT line crossing the 1-m^2 rain plot (**b**) time lapse inverted resistivity models (RMSE less than 3 %)

to greater depths (Fig. 3.10b). These observations highlight the important role of preferential flow in clayey landslide for potentially supplying in a short time surficial water to the water table.

Coupling 3D ERT at the ground surface and crossholes ERT measurements with short acquisition time would help for providing 3D interpretation of subsurface water flows and minimizing possible 3D effects. Reproducing similar rainfall experiences with different intensities and slope conditions could provide complementary and valuable information on subsurface flow development in weathered clay-shale slopes.

3.4.2 High-Resolution Distributed Temperature Sensing (DTS) in the Shallow Soil

Temperature measurements are often used in soil science to recover soil properties, including soil thermal diffusivity, which is a good indicator of changes in soil moisture conditions in time and space (Johansen 1975). Recently, high-resolution temperature measurements using fibre-optic cable have been applied in a broad range of hydrological research (Johansson and Farhadiroushan 1999; Selker et al. 2006). Distributed temperature sensing (DTS) offers the opportunity to monitor temporal and spatial temperature patterns in the soil, which is a big advantage over point temperature measurements. The method is based on the observation of back scattering and light travel time in a fibre-optic cable (for detailed description of the method and examples of hydrological applications, Selker et al. 2006). The commercially available DTS systems (e.g.: Sentinel DTS-LR® or Sensa DTS 800®) provide continuous high resolution observation (up to 1 m spatial resolution and a 60 s integration time depending on the laser configuration) over large areas (cables up to 10 km long).

One way to estimate soil thermal diffusivity from set of temperature information is the analysis of its amplitude changes within soil profile. The amplitude method (Horton et al. 1983) assumes temperature fluctuation in the soil to be sinusoidal function of time with constant period of the thermal wave in the soil and exponential decrease of its amplitude with depth. However, in the field scale measurements, application of this method gives only raw estimation of soil thermal diffusivity due to assumed simplifications. Behaegel et al. (2007) showed the capacity to estimate apparent soil thermal diffusivity by solving the heat equation for a homogenous half-space:

$$\frac{\partial T}{\partial t} = D(\theta) \cdot \frac{\partial^2 T}{\partial z^2} \tag{3.1}$$

where T is the soil temperature (K), t is the time (s), D is the apparent thermal diffusivity ($m^2\ s^{-1}$) and is function of soil moisture content (θ), and z is the depth of the soil column (m). The input data set for this estimation is air and ground temperature monitoring performed with the use of two thermistor temperature sensors installed in single soil profile. This methodology was applied to the high resolution temperature data coming from the fibre-optic cable measurements. Steele-Dunne et al. (2010) presented a feasibility study to obtain soil moisture information from passive soil DTS in a sand dune in the Netherlands. The fibre-optic cables were installed at two depths (5 and 10 cm) in a vertical profile to monitor propagation of temperature changes due to the diurnal cycle. Following Behaegel et al. (2007), Steele-Dunne et al. (2010) proposed solving Eq. 3.1 with an implicit finite difference scheme in order to optimize the apparent thermal diffusivity value to obtain the best fit between simulated and observed soil temperature within the

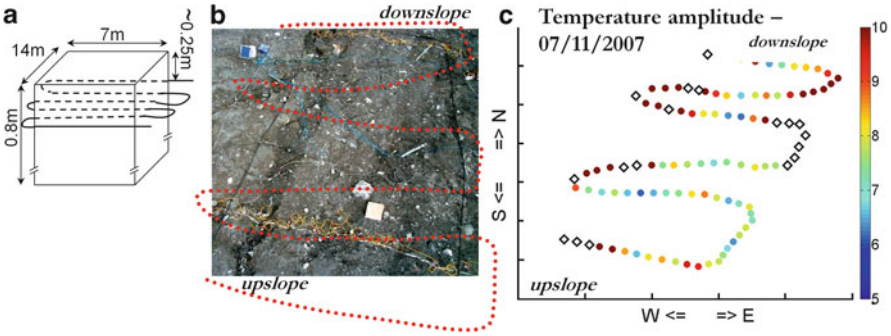

Fig. 3.11 Setup of tje high resolution Distributed Temperature Sensing: (**a**) Schematisation of 1st experimental set up, (**b**) location of the fibre-cable within experimental area, (**c**) example of daily soil temperature amplitude distribution within the experiment area; the rhombuses indicated the area where the cable was surfacing and measuring soil surface temperature (daily amplitude higher than 15 °C)

24-h time window. For detailed information about experimental setup, description of the optimization algorithm and results reader is referred to Steele-Dunne et al. (2010).

Based on the concepts of Steele-Dunne et al. (2010) the high resolution temperature measurements were used to test temperature as a tracer to detect spatial and temporal variation in soil thermal properties, and thus soil moisture conditions, for a clay shale material that is especially prone to landslide (Krzeminska et al. 2011). The soil temperature data were collected during two field campaigns in the black marls mudslide of Super-Sauze (France) with the use of high resolution DTS measurements. Two experimental sets were tested: 1st – using 130 m of fibre-optic cable installed at approximately 0.20 m depth, in the spiral-like shape, covering an area of approximately 100 m^2 (Fig. 3.11a, b), and 2nd – using two fibre-optic cables of 60 m length, installed at two depths as a straight lines, crossing three morphologically diversified sub-areas (Fig. 3.12a, b).

Figures 3.11c and 3.12c, d illustrate the qualitative analysis of observed temperature information. The differences in daily temperature amplitudes allow distinguishing between wet and dry areas at particular time (Fig. 3.11c) as low amplitude value is good indicator of the areas that might be potential wet spots. On the other hand, when looking at temperature variation in time and space (Fig. 3.12c) it is possible to get an impression about wetting and drying periods based on differences in observed temperature amplitude attenuation in time. The example of quantitative analysis of soil DTS measurements are shown in the Fig. 3.12d, e. General, higher values of apparent thermal diffusivity coincided with increases in observed soil moisture content in time and space, giving evidence for wet areas identified during cables installation, and increasing soil wetness at the end of the cables (Fig. 3.12d). Moreover, when accounting for spatial heterogeneity of soil characteristics (e.g. morphological sub-areas; Fig. 3.12b), the apparent thermal diffusivity correlated quite well with the measured soil moisture data (Fig. 3.12e).

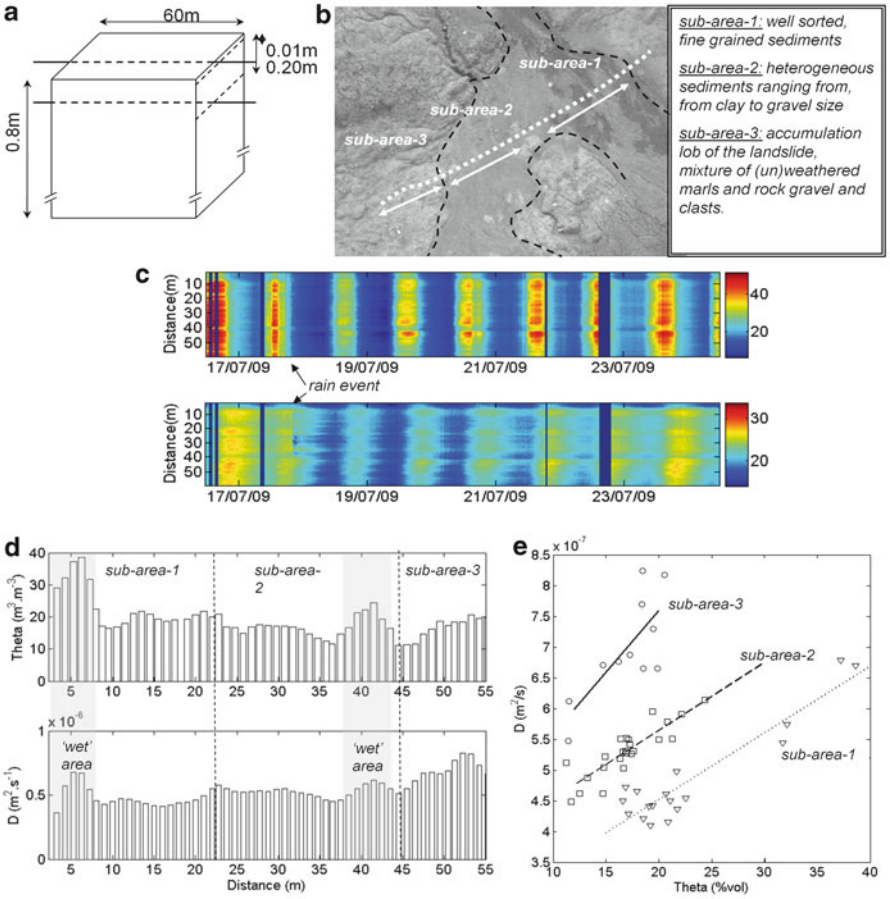

Fig. 3.12 (**a**) Schematisation of 2nd experimental set up (**b**) location of fibre-optic cable within experimental area: the punctuate line shows the location of the fibre-optic cable and the arrows indicate morphological sub-areas.(**c**) Example of DTS measurements: soil surface temperature measured at 0.01 m depth (*upper bar*) and soil temperature measured at 0.20 m depth (*lower bar*), (**d**) Soil moisture measurements along the fibre-optic cables (*upper bar*) and estimated apparent thermal diffusivity (*lower bar*), (e) Relationship between apparent thermal diffusivity values and measured soil moisture content per sub-area

The results of Krzeminska et al. (2011) are coherent with the one presented by Steele-Dunne et al. (2010). The overall trends in estimated diffusivity values were in agreement with observed variation in soil moisture content, in spite of the fact that absolute values for thermal diffusivity were often overestimated. Moreover, both studies show that better control of the depth of sensors installation and additional measurements of the soil surface temperature resulted in a significant improvement of the calculated apparent thermal diffusivity. However, deriving soil moisture information is complicated by the uncertainty and non-uniqueness in the relationship

between thermal conductivity and soil moisture. As a stand-alone technique soil DTS and inversion method is not yet mature to give timely and effective information about soil moisture. Therefore it should be seen more as support measurements to be combined with other spatially distributed survey technique. However, giving further research attention to solve both technical and analytical complications (listed and discussed by Steele-Dunne et al. 2010) seems worthwhile since, once robust, DTS technique can provide spatial and temporal information about soil moisture stage over landslide hotspots with relatively low cost demands. In this way they could become a valuable tool to improve hazard identification, monitoring of landslide behaviour and prediction of their (re-)activation.

3.5 Conclusion

In the last years, landslide characterization has widely benefited from numerous and impressive developments in remote sensing, geophysics, instrumentation and data processing. The possibility of acquiring terrain information (height, displacement, depth, etc.) with high accuracy and high spatial resolution is currently opening up new ways of visualizing, modelling and interpreting these processes. These new sensors can be mounted on terrestrial, aerial and/or satellite platforms or at the ground, covering a full spectra of accuracies, resolutions, and monitoring parameters. Geophysical and geotechnical investigations can also bring additional information on subsurface processes and movements, which are essential for monitoring and early-warning systems.

In this section, recent advances for the characterization of slope morphology, structure and hydrological features are presented. Results have shown the value of complement the different techniques for a better characterization of landslide mechanisms. ALS data acquisition and processing have turned out to be promising tools for the automatic characterization of slope morphology, with the perspective of automatic detection of landslide-affected areas. Combining ALS-based DTM with ground near surface geophysical and geotechnical data allows 3D geometry of the landslide to be constructed considering data uncertainty and resolution. This is a major forward step in landslide investigation. Of major importance is also the detection of water infiltration pathways in the sliding mass, using indirect geophysical techniques such as ERT or DTS with fibre-optic cables.

References

Aguilar FJ, Agüera F, Aguilar MA, Carvajal F (2005) Effects of terrain morphology, sampling density and interpolation methods on grid DEM accuracy. Photogramm Eng Remote Sens 71:805–816

Bard PY (1998) Microtremor measurements: a tool for site effect estimation? In: Irikura K, Kudo K, Okada H, Sasatani T (eds) The effects of surface geology on seismic motion. Balkema, Rotterdam, pp 1251–1279

Behaegel M, Sailhac P, Marquis G (2007) On the use of surface and ground temperature data to recover soil water content information. J Appl Geophys 62:234–243
Bichler A, Bobrowsky P, Best M, Douma M, Hunter J, Calvert T, Bunrs R (2004) Three-dimensional mapping of a landslide using a multi-geophysical approach: the Quesnel Forks landslide. Landslides 1(1):29–40
Bièvre G, Kniess U, Jongmans D, Pathier E, Schwartz S, van Westen C, Villemin T, Zumbo V (2011) Paleotopographic control of landslides in lacustrine deposits (Trièves plateau, French Western Alps). Geomorphology 125:214–224
Biévre G, Jongmans D, Winiarski T, Zumbo V (2012) Application of geophysical measurements for characterizing fissures in clay landslides and understanding their role in water infiltration (Trièves area, French Alps). Hydrol Process 26:2128–2142
Binley A, Henry-Poulter S, Shaw B (1996) Examination of solute transport in an undisturbed soil column using electrical resistance tomography. Water Resour Res 32:763–769
Briese C, Pfeifer N, Dorninger P (2002) Applications of the robust interpolation for DTM determination. IAPSIS XXXIV 3A:55–61
Campbell DI, Laybourne CE, Blair IJ (2002) Measuring peat moisture content using the dual-probe heat pulse technique. Austr J Soil Res 40:177–190
Caumon G, Collon-Drouaillet P, Carlier L, de Veslud C, Sausse J, Visuer S (2009) Teacher's aide: 3D modeling of geological structures. Math Geosci 41(9):927–945
Clarke SM (2004) Confidence in geological interpretation. A methodology for evaluating uncertainty in common two and three-dimensional representations of sub-surface geology. British geological survey internal report, Nottingham, IR/04/164, 29 pp
Daehne A (2011) Innovative techniques for hazard analysis in slow-moving active earthslides-earthflows: applications to the Valoria landslide (Northern Apennines, Italy). Dissertation, Università degli Studi di Modena e Reggio Emilia, Modena
Daily W, Ramirez A, Labrecque D, Nitao J (1992) Electrical Resistivity Tomography of vadose water movement. Water Resour Res 28(5):1429–1442
Debieche TH, Bogaard TA, Marc V, Emblanch C, Krzeminska DM, Malet JP (2011) Hydrological and hydrochemical processes observed during a large-scale infiltration experiment at the Super-Sauze mudslide, France. Hydrol Process 26(14):2157–2170. doi:10.1002/hyp.7843
Declercq F (1996) Interpolation methods for scattered sample data: accuracy, spatial patterns, processing time. Cartogr Geogr Inf Syst 23(3):128–144
Deparis J, Fricourt B, Jongmans D, Villemin T, Effendiantz L, Mathy A (2008) Combined use of geophysical methods and remote techniques for characterizing the fracture network of a potential unstable cliff site (the 'Roche du midi', Vercors massif, France). J Geophys Eng 5:147–157
Fisher PF, Tate NJ (2006) Causes and consequences of error in digital elevation models. Prog Phys Geogr 30(4):467–489
French H, Binley A (2004) Snowmelt infiltration: monitoring temporal and spatial variability using time-lapse electrical resistivity. J Hydrol 297:174–186
Gallerini G, De Donatis M (2009) 3D modeling using geognostic data: the case of the low valley of Foglia river (Italy). Comput Geosci 35:146–164
Garel E, Marc V, Ruy S, Cognard-Plancq AL, Klotz S, Emblanch C, Simler R (2012) Large scale rainfall simulation to investigate infiltration processes in a small landslide under dry initial conditions: the Draix hillslope experiment. Hydrol Process 26(14):2171–2186. doi:10.1002/hyp.9273
Horton R, Wierenga PJ, Nielsen DR (1983) Evaluation of methods for determining the apparent thermal diffusivity of soil near the surface. Soil Sci Soc Am J 47:25–32
Johansen O (1975) Thermal conductivity of soils. Dissertation, University of Trondheim, Trondheim
Johansson S, Farhadiroushan M (1999) Fibre-Optic system for temperature measurements at the Lovon dam. Elforsk Rapport 99:36, Stockholm, 25p

Jongmans D, Garambois S (2007) Geophysical investigation of landslides: a review. Bull Soc Géol France 178(2):101–112

Krzeminska DM, Steele-Dunne SC, Bogaard TA, Rutten MM, Sailhac P, Géraud Y (2011) High-resolution temperature observations to monitor soil thermal properties as a proxy for soil moisture condition in clay-shale landslide. Hydrol Process 26(14):2143–2156. doi:10.1002/hyp.7980

Loke MH (1999) Time-lapse resistivity imaging inversion. In: Proceedings of the 5th meeting of the environmental and engineering geophysical society European section, European section, Em1, Budapest

Loke MH (2006) RES2DINV ver. 3.55, Rapid 2D resistivity and IP inversion using the least-squares method. Software Manual, p 139

Malet JP, Auzet AV, Maquaire O, Ambroise B, Descroix L, Esteves M, Vandervaere JP, Truchet E (2003) Investigating the influence of soil surface features on infiltration on marly hillslopes. Application to callovo-oxfordian black marls slopes in the Barcelonnette basin (Alpes-de-Haute-Provence, France). Earth Surf Proc Land 28(5):547–564

Maquaire O, Malet JP, Remaıtre A, Locat J, Klotz S, Guillon J (2003) Instability conditions of marly hillslopes: towards landsliding or gullying? The case of the Barcelonnette Basin, South East France. Eng Geol 70:109–130

Marescot L, Monnet R, Chapellier D (2008) Resistivity and induced polarization surveys for slope instability studies in the Swiss Alps. Eng Geol 98:18–28

Miller CR, Routh PS, Broster TR, McNamara JP (2008) Application of time-lapse ERT imaging to watershed characterization. Geophysics 73:3–17

Oppikofer T, Jaboyedoff M, Keusen HR (2008) Collapse at the eastern Eiger flank in the Swiss Alps. Nat Geosci 1:531–535

Poeter EP, Mckenna SA (1995) Reducing uncertainty associated with groundwater-flow and transport predictions. Ground Water 33(6):899–904

Regli C, Rosenthaler L, Huggenberger P (2004) GEOSSAV: a simulation tool for sub-surface applications. Comput Geosci 30:221–238

Robinson DA, Binley A, Crook N, Day-Lewis FD, Ferré TPA, Grauch VJS, Knight R, Knoll M, Lakshmi V, Miller R, Nyquist J, Pellerin L, Singha K, Slater L (2008) Advancing process-based watershed hydrological research using near-surface geophysics: a vision for, and review of, electrical and magnetic geophysical methods. Hydrol Process 22:3604–3635

Roch KH, Chwatal E, Brückl E (2006) Potential of monitoring rock fall hazards by GPR: considering as example of the results of Salzburg. Landslides 3:87–94

Schulz WH (2007) Landslide susceptibility revealed by LiDAR imagery and historical records, Seattle, Washington. Eng Geol 89:67–87

Selker JS, Thevenaz L, Huwald H, Mallet A, Luxemburg W, van de Giesen N, Stejskal M, Zeman J, Westhoff M, Parlange MB (2006) Distributed fiber – optic temperature sensing for hydrologic systems. Water Resour Res 42:W12202. doi:10.1029/2006WR005326

Sharma PV (1997) Environmental and engineering geophysics. Cambridge University Press, New York

Shepard MK, Campbell BA, Bulmer MH, Farr TG, Gaddis LR, Plaut JJ (2001) The roughness of natural terrain: a planetary and remote sensing perspective. J Geophys Res 106:32777–32795

Sithole G, Vosselman G (2001) Filtering of laser altimetry data using a slope adaptive filter. Int Arch Photogramm Remote Sens Spat Info Sci 34(3/W4):203–210

Slater L, Binley A, Daily W, Johnson R (2000) Cross-hole electrical imaging of a controlled saline tracer injection. J Appl Geophys 44:85–102

Steele-Dunne SC, Rutten MM, Krzeminska DM, Hausner M, Tyler SW, Selker JS, Bogaard TA, van de Giesen NC (2010) Feasibility of soil moisture estimation using passive distributed temperature sensing. Water Resour Res 46:W03534. doi:10.1029/2009WR008272

Travelletti J, Malet JP (2012) Characterization of the 3D geometry of flow-like landslides: a methodology based on the integration of multi-source data. Eng Geol 128:30–48

Travelletti J, Sailhac P, Malet JP, Grandjean G, Ponton J (2011) Hydrological response of weathered clay-shale slopes: water infiltration monitoring with time-lapse electrical resistivity tomography. Hydrol Process 26(14):2106–2119. doi:10.1002/hyp.7983

van den Eeckhaut M, Poesen J, Verstraeten G, Vanacker V, Moeyersons J, Nyssen J, Van Beek LPH, Vandekerckhove L (2007) Use of LIDAR-derived images for mapping old landslides under forest. Earth Surf Proc Land 32:754–769

Zhang K, Whitman D (2005) Comparison of three algorithms for filtering airborne lidar data. Photogramm Eng Remote Sens 71(3):313–324

Chapter 4
Techniques for the Modelling of the Process Systems in Slow and Fast-Moving Landslides

Alessio Ferrari, Byron Quan Luna, Anke Spickermann, Julien Travelletti, Dominika Krzeminska, John Eichenberger, Theo van Asch, Rens van Beek, Thom Bogaard, Jean-Philippe Malet, and Lyesse Laloui

Abstract This chapter reviews some of the current strategies for landslide modelling. Main physical processes in landslides are first recalled. Numerical tools are then introduced for the analysis of the behaviour of slow- and fast-moving landslides. Representative case studies are introduced through the chapter to highlight how different modelling strategies can be used depending on the physical processes that the modeller wants to take into account.

A. Ferrari (✉) • J. Eichenberger • L. Laloui
Laboratory for Soil Mechanics (LMS), Ecole Polytechnique Fédérale de Lausanne (EPFL), Lausanne, Switzerland
e-mail: alessio.ferrari@epfl.ch

B. Quan Luna
Faculty of Geo-Information Science and Earth Observation (ITC), University of Twente, Enschede, The Netherlands

Department of Natural Hazards (Norwegian Geotechnical Institute – NGI) – International Centre for Geohazards (ICG), Oslo, Norway

A. Spickermann
School and Observatory of Earth Sciences (EOST), Institut de Physique du Globe de Strasbourg (IPGS), Strasbourg, France

J. Travelletti • J.-P. Malet
Institut de Physique du Globe de Strasbourg, CNRS UMR 7516, Université de Strasbourg/EOST, 5 rue René Descartes, F-67084 Strasbourg Cedex, France

BEG, Bureau d'Etudes Géologiques SA, Rue de la Printse 4, CH-1994 Aproz, Switzerland

D. Krzeminska • T. Bogaard
Faculty of Civil Engineering and Geoscience, Water Resources Section, Delft University of Technology, Delft, The Netherlands

T. van Asch • R. van Beek
Faculty of Geosciences, Department of Physical Geography, Utrecht University, Heidelberglaan 2, 3584 CS, The Netherlands
e-mail: aschtheo@gmail.com

T. van Asch et al. (eds.), *Mountain Risks: From Prediction to Management and Governance*, Advances in Natural and Technological Hazards Research 34,
DOI 10.1007/978-94-007-6769-0_4, © Springer Science+Business Media Dordrecht 2014

Abbreviations

H Hydraulic
H-M Hydro-Mechanical
CL Silty clay

4.1 Introduction

As different as the landslide types are, as different are the numerical models, which have been developed to answer some of the common questions arising in landslide hazard assessment: Which are the locations susceptible to climate-induced landslides? Which are the predominant controlling factors for failure? Which are the critical combinations of antecedent and precursor rainfall events? Which is the released volume at failure? When is failure most likely to occur? Of which type is the post-failure behaviour? Which is the probable movement pattern after failure initiation? The variety of landslide types ranging from slow moving (cm/year) to fast-moving landslides (m/s), of landslide volumes varying between a couple to several million cubic meters, their distinct time history and the various involved geomaterials can only be dealt with by means of landslide-specific numerical modelling solutions. Nevertheless, the numerical models mostly share common mathematical frameworks and basic physical concepts. Geomechanical models can be basically categorised in models for the analysis of slope failure initiation and models for post-failure landslide analysis. Both types of models aim at gaining insights in the complex physical mechanisms and controlling factors for the behaviour of instable or potentially instable slopes and to present that information in understandable form. The kinematics of both, shallow and deep-seated landslides is most often governed by climatic conditions influencing the hydraulic regime and the mechanical response of the slope. Consequently, the numerical codes have the common objective of simulating the slope or landslide behaviour due to external hydraulic and/or mechanical perturbations. They are not only useful tools for evaluating the stability of potentially instable slopes, but also for predicting future slope behaviour for different climate scenarios. In consulting expertise, they are often used to assess the effectiveness of planed constructive remedial measures or the likelihood for mass acceleration and subsequent damaging effects on infrastructures.

The numerical modelling of landslides is part of a multidisciplinary process, starting from in-situ investigations and continuous measurements to identify the landslide and its behaviour as a function of external, climatic factors and its geological and hydrogeological structure (Fig. 4.1). Laboratory tests are conducted to determine in more detail the behaviour of the geomaterials composing the landslide. A geological model is built based on the available field data which allows

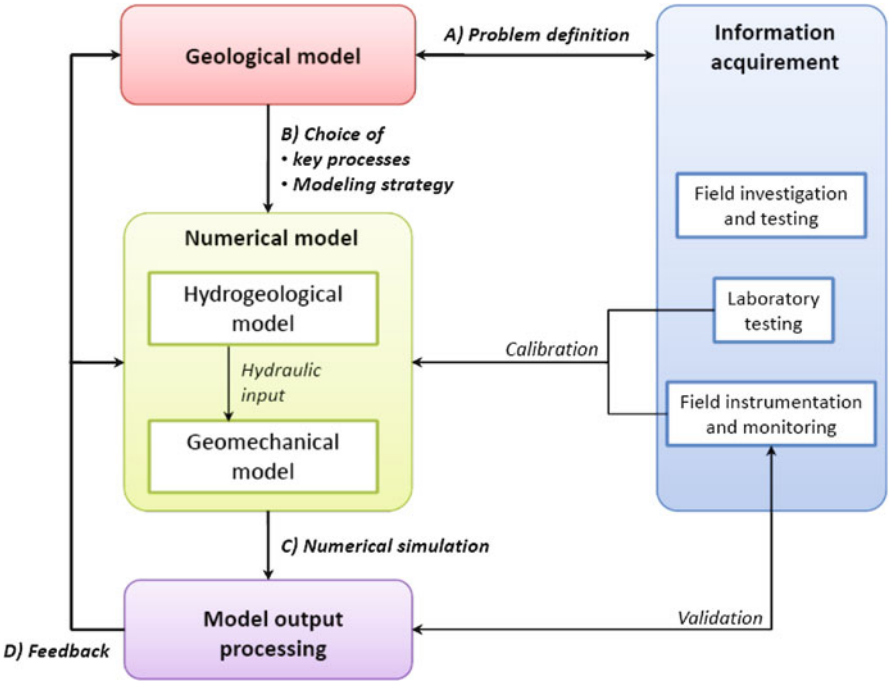

Fig. 4.1 Interdisciplinary, iterative process of landslide modelling

characterising the landslide in more detail. Governing mechanisms are identified or at least hypotheses on possible mechanisms are formulated. In some cases, eventually the cause of the instability is determined. The geological and geotechnical characterisation of the landslide is important for the following modelling steps. The choice of an adequate constitutive model for the numerical simulation of geomaterial behaviour depends on the knowledge and lessons gained from the geological model and the field- and laboratory tests conducted on the different geomaterials. The actual process of numerical modelling itself is subject of technical issues related to the codes and calculation methods, the translation of geological and geotechnical input data into the model and the assumptions made based on geological and engineering expertise. Finally, the results from the numerical model can help in understanding the role of different complex physical processes in the specific case study under consideration. They complete or revise the first output of the geological expertise. In some cases, they identify critical issues which result in further, more detailed and precise site investigations. The complete modelling process is subsequently reiterated. The results from a numerical model need to be subjected to critical evaluation and the model needs to be validated with data from field instrumentation if it is supposed to be further used as a predictive tool for landslide behaviour under variable environmental conditions.

With reference to the described process of landslide modelling, this chapter presents different modelling strategies, which can be applied to landslide problems. In Sect. 4.2, an overview is provided of the main landslide features and key physical processes in slow and fast moving climate-induced landslides, which need to be considered in numerical models to correctly reproduce or predict landslide activity. Although numerical models are often built specifically for a given landslide problem, common modelling strategies are recognised and model classes can be identified, which depend above all on the landslide type under analysis. In this regard, Sects. 4.3 and 4.4 present the modelling frameworks for slow and fast moving landslides, respectively. Applications of different types of numerical models to example case studies from the FP7 Mountain Risks project are presented to elucidate in more detail, which type of information can be gained from different types of numerical models and which conclusions can be drawn for hazard assessment. Finally, Sect. 4.5 provides a summary and recommendations for the use of the results.

4.2 Main Physical Processes Involved in Climate Induced Slow and Fast-Moving Landslides

Numerical models solve the landslide boundary value problem via integration of the discretized physical time and space problem. The construction of the mathematical framework including geomaterial constitutive models is a process of conceptualisation of the real physical problem. It consists of idealisations and simplifications and therefore contains always limitations. This section presents a synthesis of the physical processes that have been identified for shallow slips and flow-type failures and deep-seated, generally slow-moving landslides.

4.2.1 Shallow Slips and Flow-Type Failures

Shallow slips and flow-type failures are the most frequently triggered landslides. The majority is triggered during or shortly after heavy rainfall events of short duration or in combination with episodes of strong snow melting (e.g. Moser and Hohensinn 1983; Harr 1981). In many cases, shallow landslides are triggered over large areas corresponding to the spatial extent of rainfall events (e.g. Crozier 2005; Dai et al. 1999). The following list of points gives an overview of common characteristic slope features and key elements of soil behaviour, which possibly need to be considered in a physically-based analysis of shallow, rainfall-induced landslides:

- **Majority of first-time failures**: Shallow, rainfall-induced landslides are mostly first-time failures preceded by slow, downward slope movements and a sudden

acceleration phase caused by stress changes due to pore water pressure variations. Pre-failure deformations localise in some cases to form narrow bands of high shear deformations.

- **Shallow, translational failure**: Failure occurs most often in 1–3 m depth as a direct consequence of rain infiltration in shallow soil covers overlaying a more consistent substratum (e.g. Dai et al. 1999). Commonly, the depth to length ratio of the slide is less than 15 % and the failure can be characterised as a translational slide (Abramson et al. 2002).
- **Steep slopes**: Shallow slope failures are commonly encountered in steep slopes with angles higher than 25° (Iverson et al. 1997). The slope angle is one of the factors determining the type of slope failure: localised slip failures may occur at various slope angles, while fluid-like landslides in granular soils are observed in slopes with angles close to or lower than the friction angle of the soil (Olivares and Damiano 2007).
- **Partial saturation**: Shallow slips occur mostly in steep slopes where a water table is absent and the slope angle exceeds the friction angle of the soil. The stability prior to a catastrophic event is mainly sustained due to the positive capillary effects in partially saturated conditions (e.g. Fredlund and Rahardjo 1993; Fourie et al. 1999; Godt et al. 2009). The soil water retention behaviour in partially saturated conditions governs the water relative permeability and hydraulic gradients in the soil cover.
- **Soil type, initial stress state and stress history**: Colluvial soils, eolian deposits (e.g. loess, volcanic ashes) and residual soils are particularly prone to shallow failures due to, amongst others, a collapsible soil structure, susceptibility to weathering processes and vertical soil layering from depositional processes favouring the build-up of pore water pressures compromising slope stability (e.g. Springman et al. 2003; Crosta and Dal Negro 2003; Rahardjo et al. 2004). Due to their genesis and shallow depths, stresses are generally low in the shallow soil covers and the soils are in a loose or medium dense state. These soils show high losses of volume due to slight perturbations of the stress state and are prone to flow-type failures in fully or close to fully saturated conditions (e.g. Eckersley 1990; Spence and Guymer 1997; Wang and Sassa 2001). Soils in dense configurations dilate upon wetting-induced shearing and often develop into slip failures presenting a distinct sliding surface (e.g. Picarelli et al. 2008).
- **Strong local material heterogeneities**: Shallow failures involve mostly small volumes of soil (couple of tens to hundreds of cubic meters). Site-related factors often play an important role for the predisposition of a slope to fail. These factors include, amongst others, the stabilising action of soil roots, geometrical irregularities of the slope leading to stress concentrations and concentrations of water flow paths and the presence of multiple soil layers leading to preferential failure zones due to contrasts in mechanical and hydraulic soil properties, which create preferential flow paths and govern the evolution of pore pressures (Johnson and Sitar 1990).
- **Strong relation between hydrological surface and hydrogeological subsurface processes**: Shallow failures are directly related to external climate factors

(e.g. rainfall, snowmelt). Hydrological processes at the soil surface are the first link in the chain of processes leading to failure. These processes include water ingress at the soil surface, evaporation/evapotranspiration and run-off generation.

- **Hydrogeological role of the bedrock**: Soil covers in steep slopes are generally shallow and the bedrock influences greatly the pore pressure response in the soil cover during rain infiltration as it can either act as a sink or source for water in the presence of fractures or impede vertical infiltration and lead to build-up of perched groundwater tables (e.g. Anderson et al. 1997; Cascini et al. 2010).
- **Post-failure kinematics**: Shallow slope failures can either be localised along a slip-surface and the failed mass moves in a block-like manner (i.e. slip) or in a diffuse, fluid-like manner due to partial or complete liquefaction of the soil slope (i.e. debris flow, flowslide). In some cases, the movement of instable soil masses ceases quickly after failure, in others they evolve into flow-type failures with longer run-out distances. Flow-type failures such as debris flows and flowslides result most often from shallow slips (e.g. Dai et al. 1999).

4.2.2 Deep-Seated Landslides

Large landslides present typically a volume of more than 1 million cubic meters. Due to their large extent (several km^2), they possess very often significant hydraulic and mechanical heterogeneities leading to different movement patterns within the sliding body. Large landslides are gravity-driven processes, which are typically in a state of more or less constant movement with possible reactivation phases. They display however considerable differences among each other with respect to their velocities. Slow-moving landslides may reach velocities up to 1.6 m/year and rapid-moving landslides reach velocities higher than 1.8 m/h (Cruden and Varnes 1996; WP-WLI 1995). The following list presents some relevant features and processes in deep-seated landslides:

- **Majority of post-glacial slides with reactivation phases**: Slow-moving landslides are mostly encountered in regions which have been subjected to a relatively fast deglaciation period. Most large landslides have been moving for thousands of years. In most cases, movement takes place along pre-existing slip surfaces. The movement pattern is generally regular, but longer wet periods can lead to acceleration phases. In the case of first-time failures, exceptional climate conditions are often the cause of instability.
- **Groundwater fluctuations**: Large landslides present commonly a groundwater table displaying seasonal fluctuations. Climatic conditions are the principle factor for changing movement activity, even if the variations of the hydrogeological and climatic conditions are in most cases not very marked (Castelli et al. 2009).
- **Pre-existing sliding surface**: Sliding masses move along single or multiple shear surfaces, which are characterised by their limited thickness and reduced (residual) shear strength with respect to the sliding mass (e.g. Alonso et al. 1993; Ferrari et al. 2009).

- **Preferential flow paths**: Fracture flow can play an important role in the hydrogeological system of the landslide. In this case, precipitation itself has limited predictive value for groundwater level fluctuations (e.g. Bogaard 2001; Bogaard and Van Asch 2002). This is especially true when dealing with active landslides, where infiltration processes are strongly affected by presence of a dynamically changing fissure network providing preferential flow paths. On one hand, fissures may provide direct access to the lower groundwater and increase the groundwater recharge. On the other hand, they may increase the rate of natural soil drainage (e.g. McDonnell 1990; Van Asch et al. 1996; Uchida et al. 2001).
- **Kinematic features**: Slow-moving landslides are slides which have either experienced progressive displacements over long time periods and are still active or went through a fast episode of movement in the past and now are only affected by residual movements. Such creeping behaviour (2–5 mm/year) is in some cases associated to displacements due to seasonal groundwater table fluctuations (Alonso et al. 2003; Picarelli et al. 2004) and in other cases is told to be little affected by external climate events (Macfarlane 2009). For cases of first time failure, rapid movements may arise for example from a sudden decrease in shear strength, as encountered in brittle materials such as fractured rock slopes or overconsolidated clays. In stiff clays, the progressive development of the failure surface decreases the average strength of the soil mass at collapse (Skempton 1964; Bjerrum 1967; Potts et al. 1997).
- **Changes in geometry and boundary conditions**: Very often, large landslides are affected by changes in geometry caused for example by toe erosion from a river (Ledesma et al. 2009; Ferrari et al. 2011).

4.3 Behaviour of Slow-Moving Landslides

4.3.1 Modelling Strategies and Hydro-mechanical Couplings

Slow-moving slides are quite frequent in mountainous or hilly areas and do not represent a major challenge for land planning. However, they may display occasional short term crises, generally as a consequence of exceptional climatic conditions, which can damage infrastructure assets and buildings. These situations represent a potential serious hazard that cannot be analysed in terms of probability analysis, as the number of recorded past events is generally very small and climate changes could significantly modify the environmental setting. Quantitative relationships relating climatic condition fluctuations and sliding area velocity must then be pursued by taking into account the most relevant physical processes involved in the landslide behaviours. Conventional slope stability analyses are unable to deal with such questions because they do not allow the velocity fields to be determined. Numerical modelling has been developed to predict landslide displacement patterns

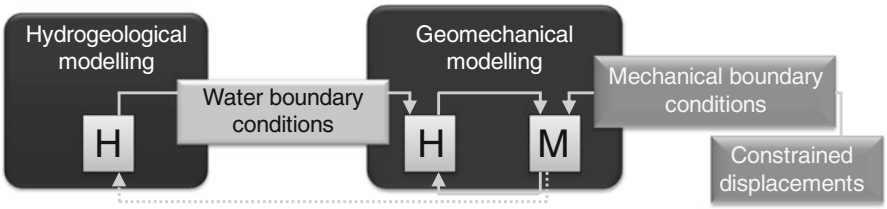

Fig. 4.2 Outline of the coupling between hydrogeological and geomechanical models

over time in order to deal with specific issues such as strain localisations and the development of shear zones (e.g. Dounias et al. 1988), viscous behaviours (e.g. Vulliet 2000) and weathering processes (e.g. Eberhardt et al. 2005). In general, a comprehensive analysis of slow-moving landslides requires a hydrogeological and a geomechanical model. The evolution of pore water pressures within the landslide body is often recognized as the main cause for the occurrence of displacement accelerations. In this sense, the interaction among the hydraulic and the mechanical processes must be considered in order to establish the quantitative relationship between pore water pressure variations and slope movements.

Various levels of coupling between the hydrogeological and the mechanical modelling can be established (Fig. 4.2). The hydraulic response is often analysed first. To this end, a hydrogeological model is set up for the case study under consideration based on the information collected during the monitoring campaign. Rainfall, lateral flows, permeability, non-homogeneity, preferential flow paths and vegetation should be duly considered. Hydrogeological modelling considers the mass conservation of the fluid. In this sense, a purely hydraulic formulation (H) is usually used. The resulting model can be a complex 3D transient finite element model (e.g. Tacher et al. 2005) or a simplified column infiltration model, depending mainly on the complexity and the involved physical processes which are relevant for the analysed case. The hydrogeological model is usually calibrated on the values of pore water pressures registered at several points of the slope for a reference time span. As an outcome, the model provides the evolution of the pore water pressures in time in the slope as a function of the boundary conditions and their fluctuations.

In the general case, geomechanical models include a hydraulic and a mechanical component. Water mass and momentum conservations are usually implemented in the codes. The two sets of equations can be solved simultaneously (fully coupled approach, like in the case of the consolidation analysis) or separately (e.g. seepage calculation coupled with limit equilibrium analyses); in the latter case, the hydraulic part is solved first and the computed pore water pressures are used to drive the mechanical component of the model. The geomechanical model is often calibrated by comparing computed and measured displacements in relevant points of the slope.

The level of coupling between the hydrogeological model and the geomechanical model must be defined. The computed groundwater pressures resulting from the hydrogeological simulations can be introduced in the geomechanical model as boundary conditions and they may evolve with time. In this case, a “one way”

coupling is established between the hydrogeological and the geomechanical model. When appropriate, the outcomes from the geomechanical model can be used in an iterative way to update the hydrogeological model settings. In this way it is possible to simulate the evolution of relevant factors (such as permeability or retention properties of the involved materials) associated to the cumulated displacements. In this case, a "two-way" coupling is established between the two model frameworks.

In the following sections, examples of numerical modelling of case studies are reported with the aim to highlight the different coupling levels that can be established. It will appear that this choice is fundamentally dictated by the physical phenomena that are believed to play an important role for the case under analysis. The mathematical formulation of the couplings (within the geomechanical model, or between the hydrological and geomechanical modelling frameworks) are also presented.

4.3.2 Coupled Hydro-mechanical Approaches

4.3.2.1 The Steinernase Case Study

The Steinernase case study represents an example of how the general methodology for the hydromechanical coupling presented in the previous section can be adapted in order to take into account the specifics of a given case study. Following the outline in Fig. 4.2, pore water pressure evolutions with time and within space were computed by a 3D finite element hydrogeological model and they were inserted as nodal forces in a finite element geomechanical model, which uses the coupled hydro-mechanical formulation (H-M) briefly recalled hereafter (Ferrari et al. 2009). Changes in pore water pressures cause variations in stress, which in turn induce displacements. Once calibrated, the coupled models could be used to assess the landslide behaviour under different scenarios, including modified climatic conditions (i.e. different rainfall patterns) and to implement mitigation measures. This methodology has been successfully applied in other relevant case studies such as the Triesenberg landslide in Liechtenstein (François et al. 2007).

The Case Study

The Steinernase landslide affects a natural slope on the bank of the Rhine between the towns of Stein and Mumpf in the canton of Aargau in Switzerland (Fig. 4.3). Three major infrastructure assets are located at the slope toe, namely a railway, a highway and a cantonal road connecting Zurich and Basel. Due to the strategic importance of the potentially involved infrastructure, systematic monitoring of the landslide started in 1995. Inclinometers, piezometers and topographic control points were installed. A general plan of the slope is shown in Fig. 4.3, showing the active zone, which extends from the mountain road to the upper limit of the railway,

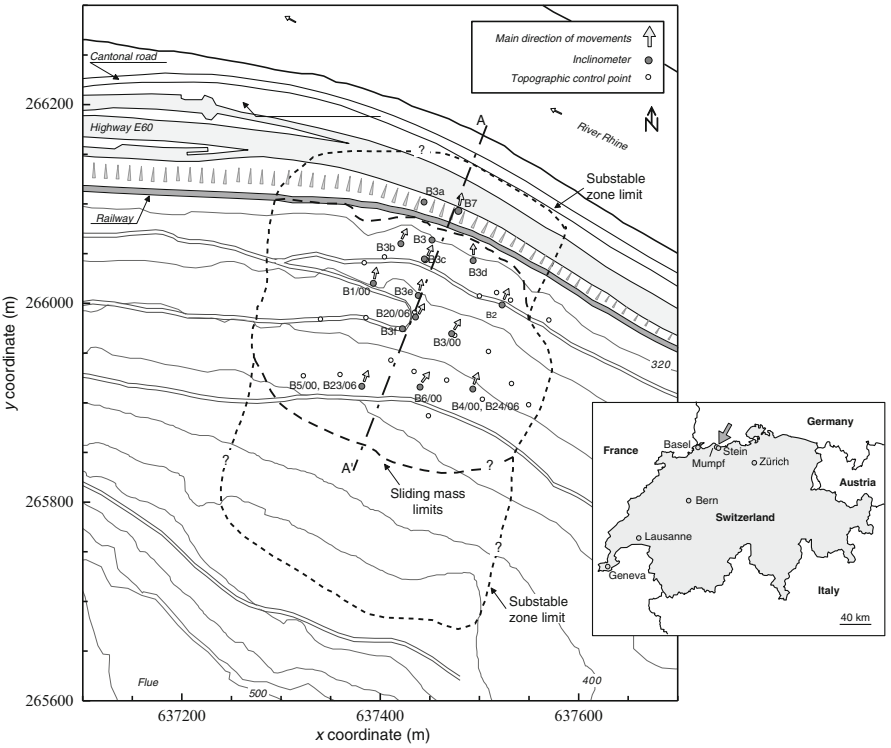

Fig. 4.3 General plan of the Steinernase landslide showing the position of inclinometers and topographic control points (Ferrari et al. 2009)

approximately 300 m in width and 230 m in length. The more active zone seems to be part of a wider substable zone that extends longitudinally from the beginning of the slope main scarp to the cantonal road. Inclinometer profiles clearly showed the presence of a multiple surface failure mechanism: a unique slip surface, present in the upper part of the slope, develops into a multi-surface system in the toe zone. A schematic of the multi-surface system is depicted in Fig. 4.4 (profile A-A' in Fig. 4.3). Three main materials have been identified from the analysis of the boreholes: (i) the soil composing the landslide body, (ii) the bedrock and (iii) the Rhine Alluvium. In spite of some heterogeneity in index properties at a local scale, soil of the landslide body is homogenous at the scale of the landslide and it was classified as CL.

Pore water pressure variation within the slope was recognized as the main cause for accelerations. Even if displacement data are not continuous because of inclinometer reading delays and the assessment of the exact instants in which movements start and end is not possible, it is worthwhile to note that accelerations coincided with total head peaks. The groundwater table does not seem to reach the topographic surface.

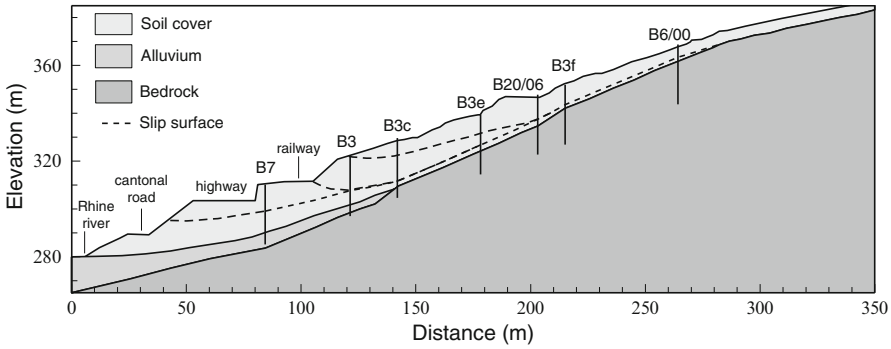

Fig. 4.4 Cross-section along the centre of the landslide, indicating the multiple slip surface system as interpreted from inclinometer readings (Ferrari et al. 2009)

Modelling Strategy

The interaction between the pore fluid pressure and the mechanical behaviour of the solid skeleton is obtained with a Biot-type formulation (Biot 1956), in which the mass and momentum of the fluid and solid phases are conserved. A thermodynamic description of the general form of the field equations is given in Laloui et al. (2003). When the failure mechanism of the slope is located above the piezometric line, it is likely that movement accelerations can occur as a consequence of the changes in the degree of saturation of the materials at the slip surface, due to the fluctuation of the groundwater level. In such a case, the transition from a partially saturated to a fully saturated state of the soil must be taken into account. In this sense, the behaviour of the solid matrix is assumed to be governed by the generalised effective stress equation (Nuth and Laloui 2008; Laloui and Nuth 2009) given by:

$$\boldsymbol{\sigma}' = \boldsymbol{\sigma} - S_r\, p \boldsymbol{\delta} \tag{4.1}$$

where $\boldsymbol{\sigma}'$ is the generalised effective stress tensor, $\boldsymbol{\sigma}$ is the total (Cauchy) stress tensor (compression stresses taken as positive), S_r is the degree of saturation, p is the pore fluid pressure (compression pressure taken as positive) and $\boldsymbol{\delta}$ is the Kronecker's delta. The generalized effective stress definition ensures a smooth transition between partially and fully saturated conditions. Terzaghi's effective stress is recovered when S_r becomes equal to 1. An unsaturated soil is a three-phase porous medium composed of solid, liquid and gaseous phases. The Biot-type formulation uses an equivalent two-phase porous medium with a compressible liquid phase, in which air bubbles are trapped within water. The solid grains are treated as incompressible. A detailed description of the procedure to derive the following equations can be found in Ferrari et al. (2009). The mass conservation equation of the soil is described by:

$$S_r\, div\, \partial_t\, \mathbf{u}_s = div\left[k_r \mathbf{K} \cdot \mathbf{grad}\left(p + \rho_f \mathbf{g} \cdot \mathbf{x}\right)\right] - n\left(\beta_f S_r + \frac{dS_r}{dp}\right)\partial_t\, p \tag{4.2}$$

where $\partial_t \mathbf{u}_s$ is solid skeleton velocity, k_r is a scalar function of the degree of saturation, $\mathbf{K}$ is the tensor of the saturated soil permeability, ρ_f is the volumetric mass of the fluid, $\mathbf{g}$ is the vector of gravity acceleration, $\mathbf{x}$ is the position vector, n is the porosity and β_f is the compressibility of water. Equation (4.2) expresses how the temporal variation of the solid displacement (left side term) may be modified by the Darcy's flow (first right side term) and/or by the pore fluid pressure variation (second right term). The evolution of permeability with the degree of saturation is given by the expression proposed by Van Genuchten (1980):

$$k_r = \left(\frac{S_r - S_{r,res}}{1 - S_{r,res}} \right)^3 \tag{4.3}$$

where $S_{r,res}$ is the residual degree of saturation. Retention curves relate the degree of saturation to the pore fluid pressure; the following expression is used (Van Genuchten 1980):

$$S_r = S_{r,res} + (1 - S_{r,res}) / \left[1 + \left(\alpha \frac{p}{\rho_f g} \right)^2 \right]^{\frac{1}{2}} \text{ if } p < 0; \quad S_r = 1 \text{ if } p \geq 0 \tag{4.4}$$

where α is a material parameter.

The momentum conservation equation can be written as:

$$div\{\mathbf{C} : \boldsymbol{\varepsilon}(\mathbf{u}_s)\} = \rho \mathbf{g} - S_r \mathbf{grad}\, p \tag{4.5}$$

where $\mathbf{C}$ is the constitutive tensor, $\boldsymbol{\varepsilon}$ is the strain tensor which is a function of solid skeleton displacements and ρ is the total average mass density $\rho = \rho_d + n\, S_r\, \rho_f$, with ρ_d being the mass density of the solid skeleton. The choice of the constitutive tensor depends on the behavioural features of the involved materials (e.g. elasto-plastic or visco-plastic). As an example, two different constitutive models (elastic and elasto-plastic with isotropic hardening) are used in the case study described in the following. Two field equations are then obtained with two unknowns ($\mathbf{u}_s$, p).

A hydrogeological model for the entire area was developed by the Laboratory of Engineering and Environmental Geology (GEOLEP) at the EPFL (EPFL 2008). An extensive analysis of the hydrogeological features of the slope pointed out the role of several key factors on the evolution of pore water pressure within the slope, such as infiltration, preferential flows and vegetation. A 3D finite element hydrogeological model was calibrated and validated in order to predict the pore water pressure evolution in the area of interest for the years 2000, 2001 and 2006.

The two-dimensional mesh used for the model was created on the cross-section A-A' in Fig. 4.4. The unstructured mesh includes 1,694 nodes and 1,554 isoparametric 4-node elements (Fig. 4.5). The multiple slip surface failure mechanism was considered an important feature to be explicitly taken into account in the model. Three independent slip surfaces were introduced; their positions were carefully reconstructed taking into account the inclinometer profiles for the instrumented

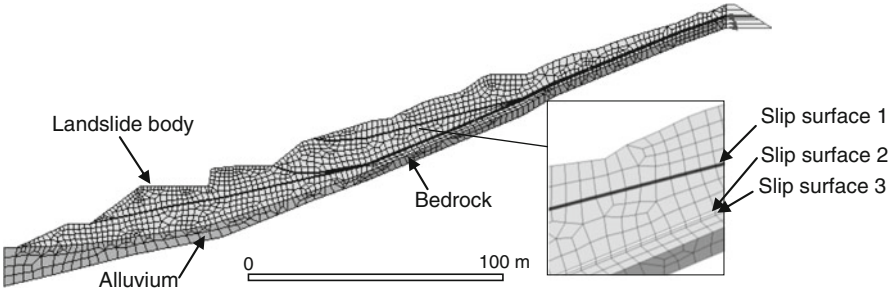

Fig. 4.5 Finite element mesh for the geomechanical model

boreholes close to the cross-section. A Cam-Clay constitutive law was adopted for the materials at the slip surface, while the rest of the landslide body was assumed to behave as a high–rigidity elastic material. The choice of an elasto-plastic constitutive model with isotropic hardening does not allow considering creep effects; even if some creep component of the displacement were observed when ground water fluctuations were small, it has been considered of limited importance for the present analysis, where the focus is on the movements associated to the pore water pressure increase. Fixed nodes were assumed at the bottom of the domain. Horizontal displacements were prevented for the bedrock nodes of the left edge while equivalent loading forces were applied at the right edge of the mesh. The initial state of stress is that induced by the soil weight at rest. This assumption is corroborated by the normal consolidated condition of the soils within the slope, pointed out by the available oedometric tests.

Computed groundwater pressures resulting from the hydrogeological simulation were introduced as nodal forces. They varied over time at selected nodes of the model. Seepage elements were introduced for the superior edges of the domain allowing simulation of the superficial runoff of the infiltrating rain when the superficial layers become fully saturated; in this case, a zero pore water pressure value is automatically imposed in these nodes. The model was calibrated for the period between 1 January, 2000 and 31 December, 2001, during which two acceleration phases were registered. The calibration was performed selecting the values of the constitutive model parameters by matching computed and measured displacement at several points of the domain. Available laboratory tests results were used as guidelines for the selection of material parameters. Table 4.1 reports the obtained parameter values. Further details on the geomechanical model can be found in Ferrari et al. (2009).

Model Results

As a result of the calibration, Fig. 4.6 shows observed and computed displacements for borehole B3e at two different depths (3 and 9 m). The plot shows that

Table 4.1 Material parameters for the slip surfaces

	Slip surface		
Parameter	*1*	*2*	*3*
Slope of the virgin compression line	0.1	0.1	0.1
Slope of the swelling line	0.05	0.05	0.05
Poisson's ratio	0.3	0.3	0.3
Slope of the critical state line	0.90	0.95	1.00
Initial void ratio	0.65	0.65	0.65

accelerations that occurred during crisis periods are reproduced well, both in terms of durations and accumulated displacements. In accordance with measurements in the field, larger displacements are computed for the more superficial part of the slope. Computed pore water pressures for the same nodes are also represented in the figure. The plots allow the appreciation of the quantitative correlation between the evolution of displacement and the evolution of pore water pressure, which constitutes the key point of the coupled hydro-mechanical model. These plots also indicate that displacements in the more superficial part of the slope can be initiated by a reduction (in absolute value) of the negative pore water pressure (suction). The prediction capabilities of the model could be used in order to simulate the behaviour of the slope when subjected to pore water pressure distributions induced by different rainfall patterns and to assess possible stabilisation strategies. As an example of the second case, displacement trends for year 2000-2001 were predicted for the case in which a system of sub-horizontal drains at the slope toe was installed. This analysis considered 50 m long drains drilled from the cantonal road. The presence of the drains was introduced as a boundary condition in the hydro-geological model, and a new distribution of pore water pressure was obtained for the period in question. Predicted displacements are reported in Fig. 4.7 for borehole B3e at different depths. Comparison with the original scenario shows that the drainage system, even if realized at the slope toe, would have a positive effect in terms of movement reduction, including the upper part of the slope.

The agreement between measured and predicted displacements was good in several points of the domain. Moreover, the model sheds light on the physical processes involved in the landslide; in particular, it appears that the transition from partial to full saturation plays a major role in the accelerations in the movement of the superficial material in the landslide in the slide, even though the total displacements are quite small.

4.3.2.2 The Super-Sauze Case Study

The Super-Sauze case study is presented here to highlight how different modelling strategies can be used to analyse a given landslide, depending mainly on the physical processes which are included into the analysis. Different levels of H-M coupling will be required for the different strategies. This section first presents a coupled

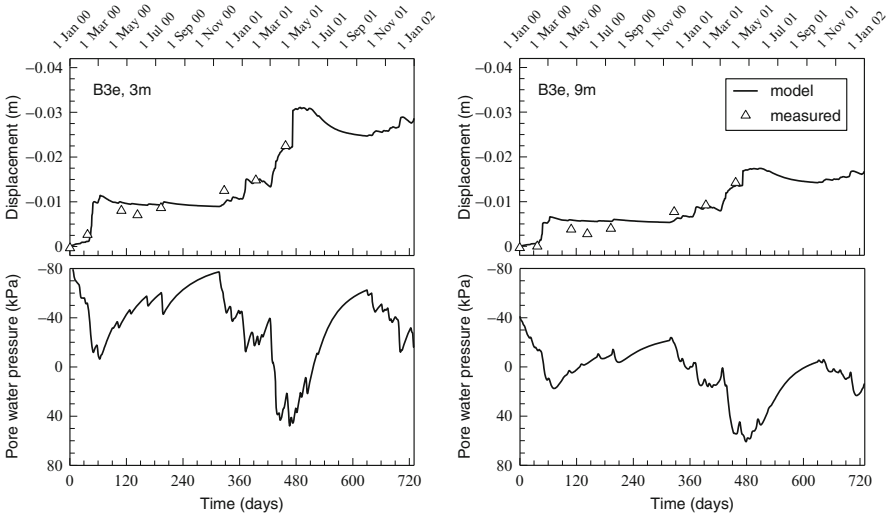

Fig. 4.6 Computed and measured horizontal displacements and evolution of the computed pore water pressures at borehole B3e for the period 1/01/2000–31/12/2001 (negative sign refers to downhill displacements) (Ferrari et al. 2009)

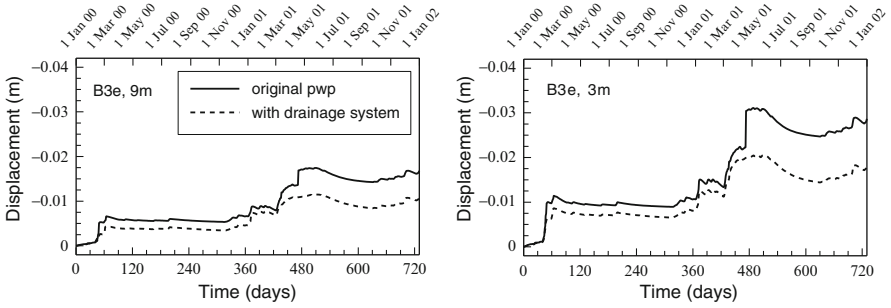

Fig. 4.7 Predicted horizontal displacements at borehole B3e for the scenario with sub-horizontal drains (Ferrari et al. 2009)

hydro-mechanical modelling that was formulated with the main aim to reproduce the short term behaviour of the Super-Sauze mudslide over 1 year and to quantify the influence of the pore water pressure on the general acceleration of the mudslide during the spring seasons of 2008 and 2009. In Sect. 4.3.3, a single phase approach for the geomechanical model is presented in which the effect of the pore water pressure variation is considered via the reduction of the available shear strength; in this latter case, pore water pressures are introduced as a boundary condition into the geomechanical model so that a “one way” coupling is established. It will appear clear that this simplified approach makes the model simpler from a

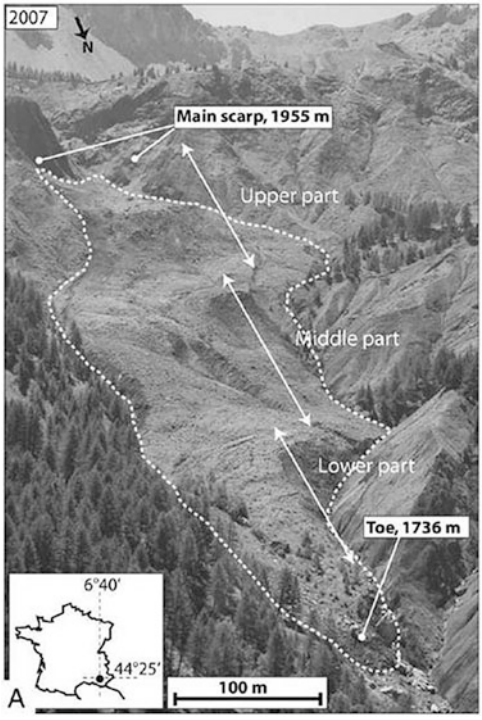

Fig. 4.8 Photograph of the Super-Sauze landslide (Travelletti and Malet 2012)

computational point of view and gives the possibility to have a spatial representation of the results – for example for GIS applications – hardly obtainable with a more elaborates fully coupled FE model. Finally, a hydrological model is presented with the aim to highlight the role of preferential flows on groundwater level changes (Sect. 4.3.4).

The Super-Sauze mudslide (Fig. 4.8) located in the upper part of the catchments basin of the Sauze torrent in the Barcelonnette Basin is a well-documented landslide (Malet 2003; Maquaire et al. 2003; Travelletti and Malet 2012). Geomorphologic, geologic, geophysical, geotechnical and displacement monitoring studies have been conducted over 15 years in order to monitor the landslide dynamics (Fig. 4.9). The vertical structure of the study case can be described by a superficial unit (C1) with a thickness ranging between 5 and 9 m (velocity > 1 cm/day) including a shear surface identified at a depth between 5 and 8 m, a deep unit (C2) with a thickness ranging between 5 and 10 m overlying a stable substratum (S) composed of intact black marls. The C2-unit is considered as impermeable and very compact, with very low to null displacement rates and comparable to a "dead body". Velocities at the slope surface vary temporally and spatially with a typical range of 1–3 cm/d and acceleration peaks until 40 cm/day in the spring season during snowmelt.

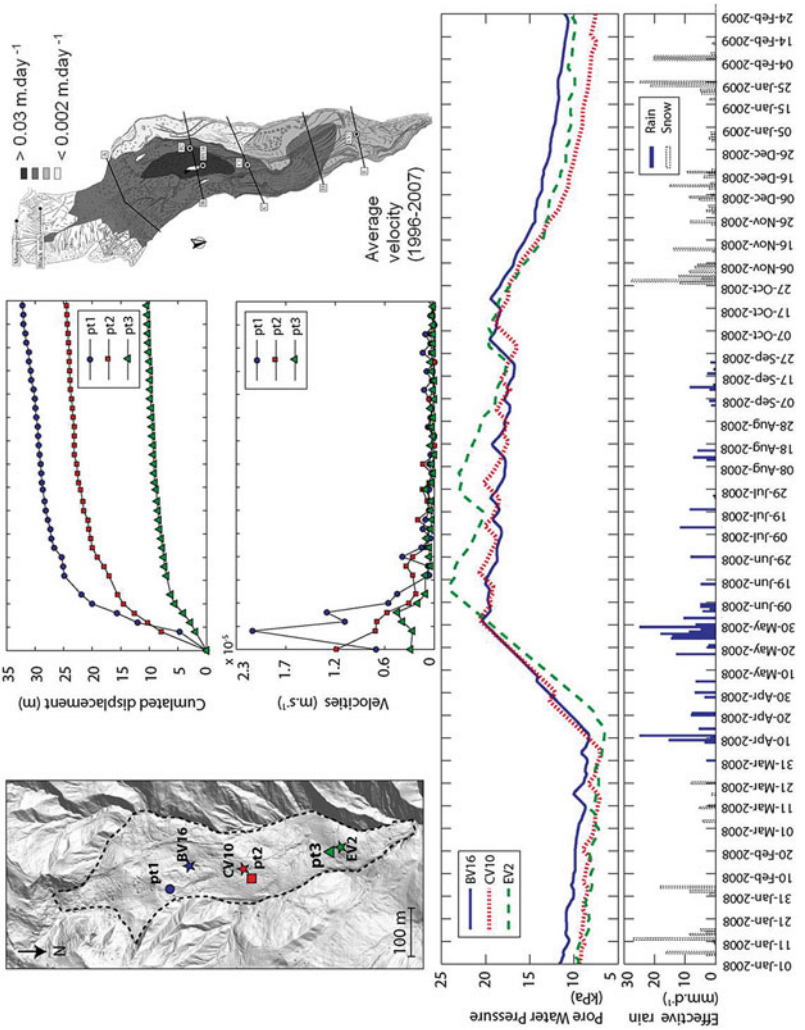

Fig. 4.9 Monitored displacements, velocities, pore water pressures at three different locations at the Super-Sauze landslide and recorded rain and snowfall data from January 2008 until February 2009; *top right*: spatial varying velocity pattern

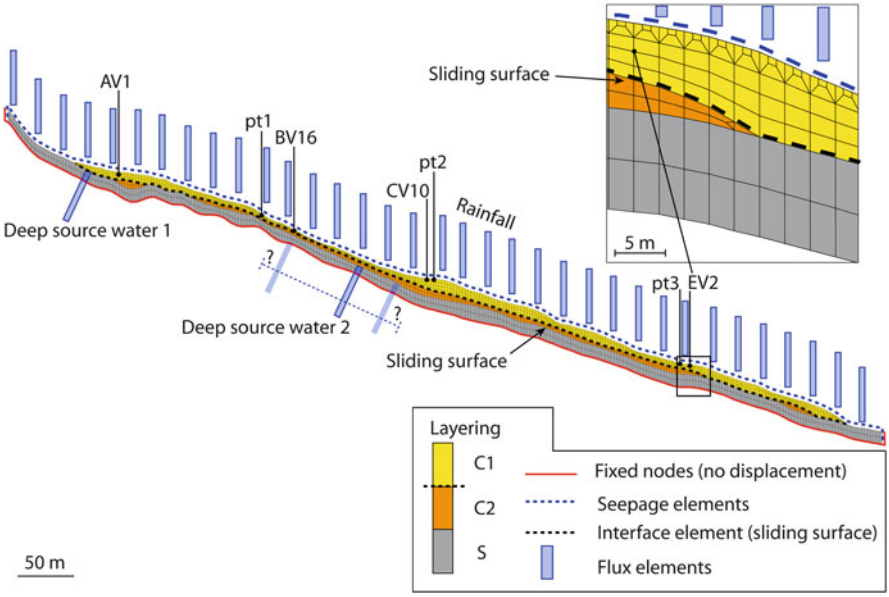

Fig. 4.10 Finite element mesh and boundary conditions for the hydro-mechanical model. The location of the piezometers AV1, BV16, CV10, EV2 and the location of the pt1, pt2 and pt3 where displacements of the ground surface were monitored are also indicated

Modeling Strategy

A 2D hydrological model is first established to reproduce the pore water pressure variations observed in selected piezometers for the years 2008 and 2009 (AV1, BV16, CV10 and EV2 in Fig. 4.10). Then, at each time increment, the solution of the hydrological model is introduced as nodal force in the hydro-mechanical model. A two-dimensional structured mesh composed of 3,955 nodes and 2,854 isoparametric 4-node elements is realized from a cross section of the 3D geometrical model of the Super-Sauze mudslide (Travelletti and Malet 2012) (Fig. 4.9).

The hydrological boundary conditions are defined according to the observations of Malet (2003) and de Montety et al. (2007) who demonstrated the influence of the rain infiltration and the presence of deep water sources on the pore water pressure within the mudslide body. The deep water sources are assumed to maintain a constant basal pore water pressure within the mudslide. The rainfall infiltration is assumed to be the main cause of the variations in pore water pressure. First, flux boundary conditions and seepage elements are assigned along the topography to simulate the rain infiltration in fully drained conditions. Second, two flux boundary conditions are defined between the C2 layer and the stable substratum S to simulate the deep water sources (Fig. 4.9). The stable substratum is considered as impermeable. The effective rainfall recorded by a meteorological station installed on the mudslide is used as input for the rain infiltration fluxes. The hydrological

Table 4.2 Hydrological parameters of the mudslide body

	C1	C2	Substratum	Slip surface
Void ratio	0.7	0.7	0.1	–
K_x ($m \cdot s^{-1}$)	9.6×10^{-7}	2.3×10^{-8}	Impermeable	Fully permeable
K_y ($m \cdot s^{1}$)	1.9×10^{-6}	2.3×10^{-8}	Impermeable	Fully permeable
$S_{r,res}$ (−) (Eq. 4.4)	0.6	0.5	1	–
α (−) (Eq. 4.4)	140	150	–	–

Table 4.3 Mechanical parameters of the mudslide body

	C1	C2	Substratum	Slip surface
Constitutive law	Elastic	Elastic	Elastic	Mohr-Coulomb
E (kPa)	1,500	1,500	200,000	1,500
v (−)	0.4	0.4	0.3	0.4
c′ (kPa)	–	–	–	0
φ′ (°)	–	–	–	26–33[a]
γ ($kN \cdot m^{-3}$)	17	17	26	–

[a]26° in the upper part and 33° in the lower part of the mudslide (Fig. 4.10)

parameters were determined through laboratory tests (Malet 2003) and adjusted in the calibration procedure (Table 4.2). The locations of the deep water sources are also adjusted in the calibration and their fluxes are assumed constant in time. The hydrological calibration was realized over the year 2008 and the validation over the year 2009.

Once the pore water pressure variations are correctly reproduced within the mudslide, the mechanical response of the mudslide is simulated using a "one way" hydro-mechanical coupling. The mechanical boundary conditions were defined according to the interpretation of the geophysical and geotechnical investigations realized in the mudslide between 1996 and 2009 (Travelletti and Malet 2012). A slip surface introduced between the layers C1 and C2 is represented with an interface element in order to reproduce large displacements in the same way as Comegna et al. (2007) (Fig. 4.10). A Mohr-Coulomb constitutive law is attributed to the interface while the rest of the mudslide body is considered as an elastic material. This assumption is justified by the fact that the largest fraction of the observed plastic deformations is concentrated in a relatively thin shear zone (0.20–0.30 m; Malet 2003). The model was calibrated for the period from 1 January 2008 to 29 August 2008. The calibration was done by adjusting the effective friction angle of the slip surface in order to obtain comparable computed and observed displacements at three points of the mudslide obtained from the correlation of ground-based optical images (Travelletti et al. 2012). Results from laboratory tests were used to assign the initial parameters of the slip surface properties (Malet 2003) (Table 4.3). The validation of the hydro-mechanical model was done for the period from 1 January 2009 to 29 August 2009.

Model Results

The results of the calibration of the hydrological model show a good agreement between the observed and computed pore water pressure at each piezometer location (Fig. 4.11a). It was necessary to introduce a permeability anisotropy in the model, which can be explained by the presence of fissures (vertical preferential flow) observed in the mudslide body (Malet 2003). The variations of the pore water pressure are particularly well reproduced during the water-table recharge in spring and the drainage period in summer. As soon as the first rainfall occurred in spring, the upper part of the mudslide rapidly becomes saturated. Water sources observed in this area corroborate this model prediction. The agreement between the observed and computed displacements of the hydro-mechanical model is quite good and the acceleration period in spring 2008 and 2009 are well reproduced (Fig. 4.11b). The spatial distribution of the displacements is presented in Fig. 4.12. The largest displacements are located in the upper part where the mudslide body is the thinnest, which is in accordance with the field observations. The slip surface strength was necessary to increase in the lower part of the mudslide (artificial increase of the effective friction angle) to compensate the narrowing of the valley, which impedes the natural progression of the mudslide downstream (3D geometrical effects) (Fig. 4.12). Possible multiple discontinuous sliding surfaces can also partly explain the increase of the sliding surface strength.

From a hydrological point of view, the good adequacy of the hydrological model with the reality corroborates the presence of deep water sources within the stable substratum. The hydro-mechanical model confirms that the majority of the deformations can indeed be concentrated in a slip surface solicited by pore water pressure variations at the mudslide scale. These variations play a major role in the mudslide kinematics during the acceleration in the spring season (short term behaviour). However, in order to represent more accurately the observed displacements and to model the long term internal deformations of the mudslide (several years), the time-dependent behaviour (viscous component) of the material should be also taken into account in a next step of analysis (Picarelli et al. 2004; Ledesma et al. 2009).

4.3.3 Single Phase and Incompressible Fluid Modelling Approach

The continuum model used to study the slow movements of the Super-Sauze landslide is based on the conservation of momentum given by the common approach of the depth-integrated form of the Navier–Stokes equation of motion considering an incompressible flow (e.g. Savage and Hutter 1989; Hungr 1995; Iverson and Denlinger 2001; Mangeney et al. 2007; Begueria et al. 2009; Hungr and McDougall 2009). It applies the concept of introducing a shear zone and a viscous component

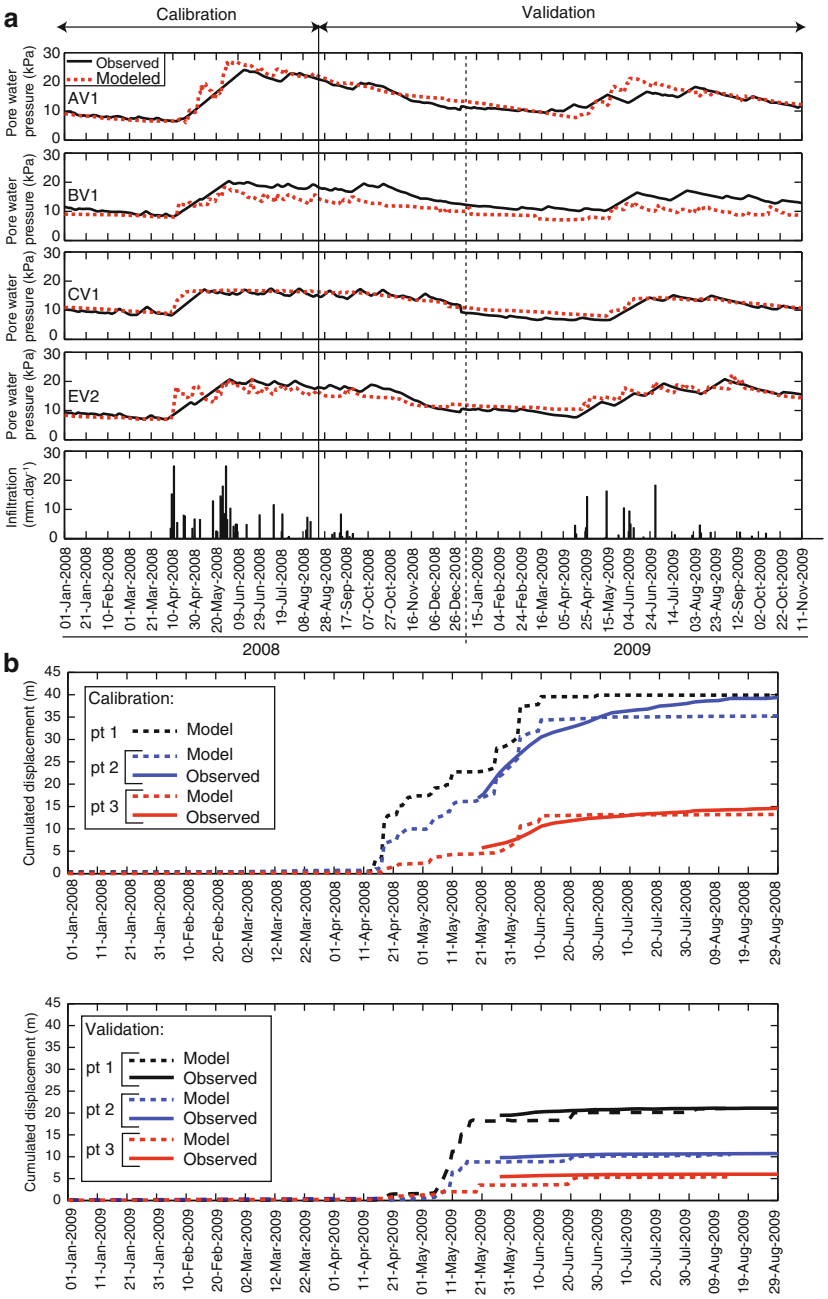

Fig. 4.11 Results of the calibration and the validation (**a**) of the hydrological model, (**b**) of the hydro-mechanical model. The location of the piezometers AV1, BV16, CV10, EV2 and the location of the pt1, pt2 and pt3, where displacements of the ground surface were monitored, are indicated in Fig. 4.10

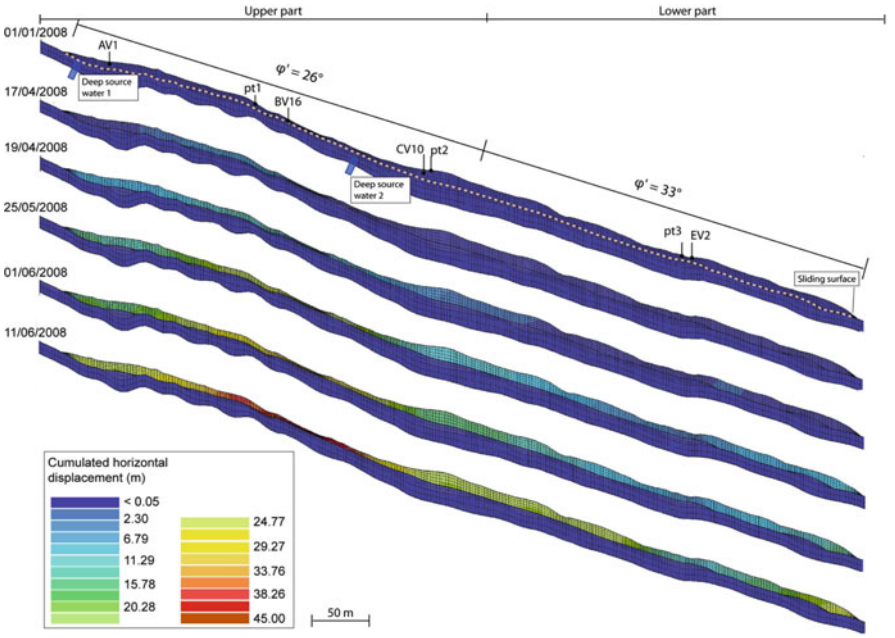

Fig. 4.12 Results of the hydro-mechanical model for the period from 1 January 2008 to 11 June 2008

that is usually dependent on the velocities in the shear zone (Van Asch and Van Genuchten 1990; Van Asch et al. 2006, 2007a, b; Corominas et al. 2005; Ledesma et al. 2009; Ranalli et al. 2010; Ferrari et al. 2011). The assumption of incompressibility is justified since volumetric strains are only very small and landslide kinematics is primarily determined by shear strains. One considerable simplification is the usage of a single phase, i.e. of a completely saturated material within the landslide body.

On the basis of the monitoring data the main factors and mechanisms (besides gravity and shear resistance of the material) determining the motion pattern of the Super-Sauze landslide are assumed to be:

a. the topography of the landslide body, bedrock and shear zone,
b. the rate dependent behaviour of the material in the shear zone, and
c. changes in pore water pressures.

In the following it is described how these factors are taken into account in the numerical approach. With respect to factor (a), the model is implemented in the GIS scripting language PCRaster (Karssenberg et al. 2001) which facilitate the utilization of complex 3D topographies through digital elevation models (DEMs). The geometrical model is assembled by introducing the DEMs as grid (e.g. raster) maps.

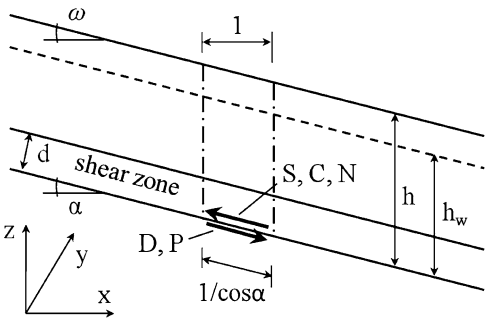

Fig. 4.13 Scheme of the driving and resisting forces calculated in infinite slope conditions

Adopting the theory of infinite slope mechanism, factor (b), is considered by introducing the Mohr-Coulomb instability criterion together with a viscous component into the equation of motion (Eulerian coordinates):

$$\rho h \left(\frac{\partial \mathbf{v}}{\partial t} + \mathbf{v} \nabla \cdot \mathbf{v} \right) = \mathbf{D} + \mathbf{P} - \mathbf{S} - \mathbf{C} - \mathbf{N} \tag{4.6}$$

with $\nabla = \partial/\partial x + \partial/\partial y$ the Nabla operator, $\mathbf{v}$ the velocity, ρ the density, h the height of the moving mass referred to the bedrock topography (Fig. 4.13). $\mathbf{D}$ (M L^{-1} T^{-2}) is the driving shear stress component resulting from the own weight $\mathbf{W} = g\rho h$ (M L^{-1} T^{-2}) of a slice with thickness one, in which g is the gravity constant:

$$\mathbf{D} = \frac{\mathbf{W} \sin \alpha}{1/\cos \alpha} = \mathbf{W} \sin \alpha \cos \alpha. \tag{4.7}$$

The second driving stress component is the earth pressure component $\mathbf{P}$ (M L T^{-2}) limited by a minimum and maximum value according to Rankine's theory (Hungr 1995):

$$\mathbf{P}_{\min / \max} = K_{a/p} \frac{\mathbf{W} \cos \alpha}{1/\cos \alpha} \nabla h = K_{a/p} \mathbf{W} \cos^2 \alpha \nabla h \tag{4.8}$$

The earth pressure coefficient K is the ratio between the tangential and normal stress and differs for the active (extension) and for the passive (compression) case. Resisting stresses are $\mathbf{S}$ (M L^{-1} T^{-2}), the frictional component defined by:

$$\mathbf{S} = \frac{\mathbf{W} \cos \alpha}{1/\cos \alpha} \tan \varphi_{app} = \mathbf{W} \cos^2 \alpha \tan \varphi_{app} \tag{4.9}$$

$\mathbf{C}$ the cohesion, that is set to zero and $\mathbf{N}$ (M L^{-1} T^{-2}) the viscous component. The influence of pore water pressures, factor (c), is taken into account by reducing the shear resistance, e.g. the frictional stress by introducing an 'apparent' friction angle:

$$\tan \varphi_{app} = (1 - r_p) \tan \varphi \tag{4.10}$$

in which r_p is the pore water pressure ratio (Duncan and Wright 2005) that is defined e.g. for flow parallel to the bedrock surface as:

$$r_p = \frac{\gamma_w h_w \cos^2\alpha}{\rho g h} \tag{4.11}$$

with γ_w the specific weight of water, h_w the height of the water level referred to the bedrock and $cos\alpha$ the direction cosine of the bed.

In Malet (2003) viscosity tests on black marls are recalculated and compared using the Bingham, a bi-linear and the Herschel Bulkley model. The comparison and 1D analyses of selected mudflow events at Super-Sauze (Malet 2003) have shown that the Herschel-Bulkley model gives the best results. Nevertheless in a first modeling stage the relationship between viscous stresses and velocity (strain rate) is expressed by the linear Bingham model:

$$\mathbf{N} = \eta\left(\frac{\partial \mathbf{v}}{\partial z}\right) = \eta\left(\frac{\mathbf{v}}{d}\right) \tag{4.12}$$

where η (M L^{-1} T^{-1}) is the viscosity parameter and d (L) is the shear zone thickness because it simplifies the integration scheme solving the differential equations. In this study the change in velocity due to change of position is assumed to be zero, leading to:

$$\rho h\left(\frac{\partial \mathbf{v}}{\partial t}\right) = \mathbf{D} + \mathbf{P} - \mathbf{S} - \mathbf{N} \tag{4.13}$$

Together with the continuity equation of the conservation of mass:

$$\frac{\partial h}{\partial t} + \nabla \cdot (h\mathbf{v}) = 0 \tag{4.14}$$

the momentum Eq. (4.6) is solved using the method of finite differences. Integration of the differential equations is conducted in x- and y-direction.

The height of the landslide is assumed to be equal to the active C1 unit overlying the non-active unit C2 (Fig. 4.9), e.g. the DEM of C2 forms the lower fixed boundary. The time period that is considered in the dynamic modeling coincides with the acceleration period in spring 2008 (Fig. 4.9), e.g. from the 10/04/2008 the start of pore water pressure increase until the 15/07/2008 when movements decelerated and continuous slow motion has been restarted. The DEM (interpolated from elevation data of an airborne laser scanner survey, LiDAR) used as the initial landslide topography is in conformity with the landslide topography in March 2008. The size of one quadratic cell in the x-y-plane is equal to 5 × 5 m. Whereas the topographies of the bedrock and the surface are given the thickness of the shear zone d referred to the bedrock has to be presumed. The shear zone thickness is assumed to be constant (if $d < h$ cosα, else $d = h\,cos\alpha$). According to the monitored

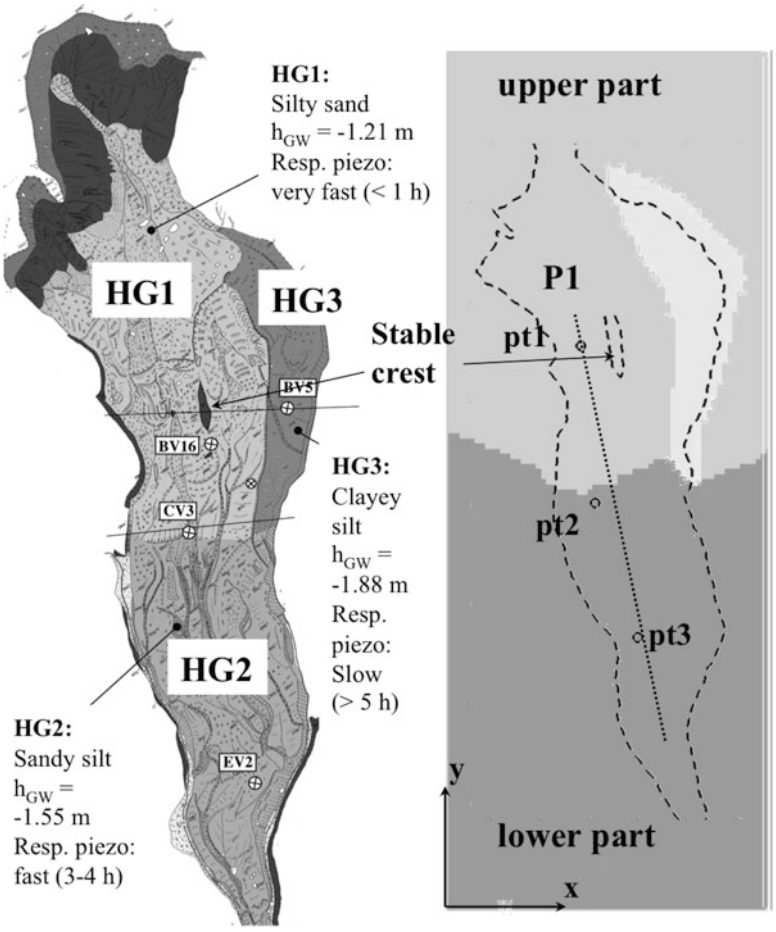

Fig. 4.14 Division of the Super-Sauze landslide into three zones (HG1-3) according to its hydro-geomorphological context (Malet 2003) and corresponding viscosity parameters used in the dynamic model (h_{GW}: average ground water level below landslide surface, Resp. piezo: piezometric response)

spatial velocity pattern (Fig. 4.9) and hydro-geomorphological units (HG, Fig. 4.14) different viscosity parameters are defined for the upper and lower landslide part obtained by calibration. The viscosity of HG1 is set equal to the one of HG3. Calculated velocities in the region of HG3 that is characterized to be dormant are always very small even if the lower viscosity parameter of HG1 is used. The rise in pore water pressures is introduced as a boundary condition (Fig. 4.15). It is pointed to the fact, that the assumption of a constant r_p after the 28th of May 2008 might be more realistic according to the piezometer measurements in Fig. 4.9 (BV16, CV10). Decreasing pore water pressures are introduced to reduce the calculated deceleration time (Fig. 4.16).

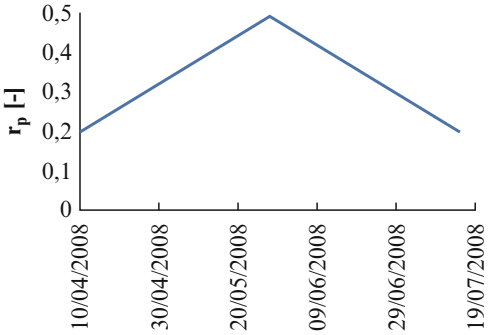

d [m]	1.0
ρ [kg/m^3]	2000
γ_w [kN/m^3][1]	10
φ_{ini} [°]	28

Fig. 4.15 Development of pore water pressure in time induced in the model and input parameters

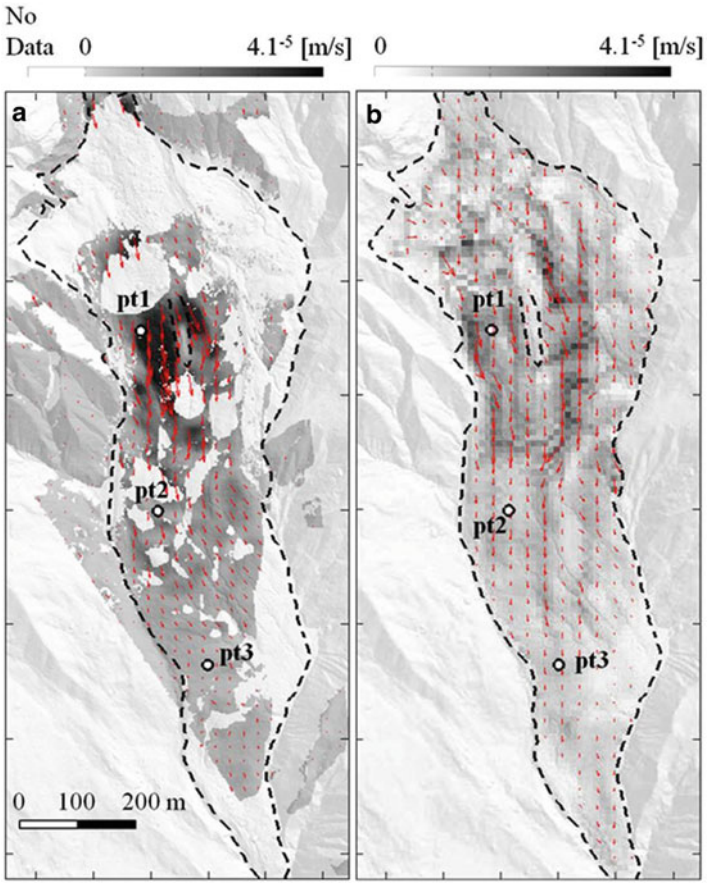

Fig. 4.16 Dynamic analysis of the Super-Sauze landslide; (**a**) monitored and (**b**) calculated peak velocities (magnitude and direction) on the 28/05/2008 with observation points pt1 – pt3

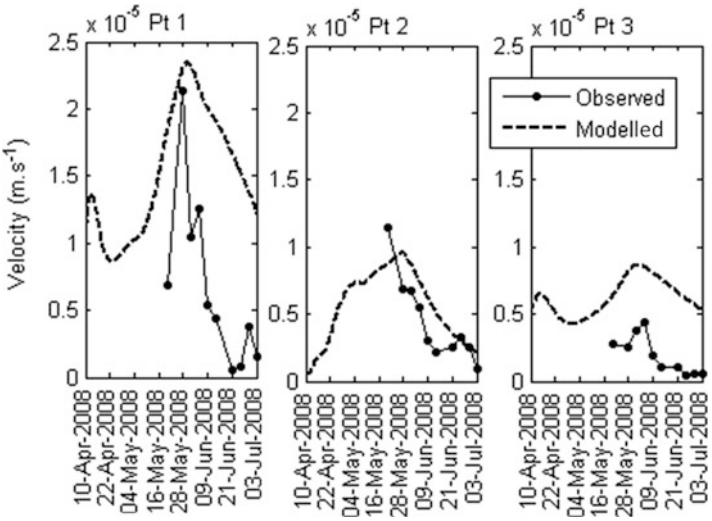

Fig. 4.17 Monitored and calculated development of velocity magnitudes of observation points pt1 – pt3 in the time period from 10/04/2008 to 15/07/2008

In Fig. 4.16 calculated vectors and magnitudes of maximum velocities of the 28th of May 2008 are compared to the monitored ones. Maximum velocities have been observed (by e.g. digital image correlation) to take place around the stable crest in the upper part of the landslide (Fig. 4.14). The directions of the measured velocity vectors (see also Fig. 4.9, top right) is in a good agreement with the results of the dynamic analysis. But there exist local differences in the magnitudes of calculated and measured velocity vectors presented in the time velocity plots (Fig. 4.17) by means of three observation points, pt1 (in HG1), pt2 (near the boundary between HG1 and HG2) and pt3 (in HG2). Whereas peak velocities of pt1 and pt 2 are in a relatively good agreement calculated velocities of pt3 at the lower part of the landslide are too high. The viscous resistance seems to increase in direction to the toe. Another explanation for the decreasing velocities in direction of the toe might be the spatial variation of the hydrological features of units HG1 to HG3 (Fig. 4.14). The average groundwater level of HG1 is higher than the one of HG2. Consequently the shear resistance **S** of HG2 should be larger in HG2 which is not taken into account in the numerical modelling. Differences in the acceleration and deceleration paths are due to the linear relation between viscous resistance and velocity imposed by the Bingham model.

The objective of developing a simple GIS-based model was to reproduce the monitored complex spatial and temporal varying velocity pattern of the Super-Sauze landslide and doing so to understand the main mechanisms controlling the sliding process. On the basis of the field data, it is hypothesized that the main controlling factors and mechanisms (besides gravity and shear resistance of the material) are (a) the topography of the landslide body, bedrock and shear zone, (b) the rate dependent

behavior of the material in the shear zone, and (c) changes in pore water pressures. The known are the 3D structure of the bedrock and surface and the evolution of pore water pressures. The unknown are the rate-dependent material behaviour, i.e. the viscosity, and the geometry of the shear zone.

The differences in calculated and measured velocities result from the simplicity of the numerical formulation. In order to model the velocity pattern varying in space viscosity parameters are defined dependent on the location in the *x*-*y*-plane. With respect to the temporal variation of velocities it is shown that the simple linear Bingham model can be used as a rough assumption, not least because of its convenience in the numerical implementation of partial differential equations. However it is neither sufficient to model the sharp increase and decrease in velocities in acceleration events nor the decrease of velocities directed to the toe. Therefore in the next stage of modelling the numerical formulation has to be extended with respect to a solid and a water phase to cover the strong influence of the pore water pressure increase. The evolution of pore water pressures has to be defined more in detail varying in space. Another key issue in the modelling of the Super-Sauze landslide is the rate-dependent behaviour of the landslide material. In the next stage the non-linear Herschel-Bulkley model has to be introduced.

4.3.4 A Hydrological Model Considering Preferential Water Flows

Van Beek and Van Asch (1999) proposed a conceptual model that explain observed shallow landslide responses to rainfall events combining low matrix permeability with fast, by-passing preferential flow through distinct sets of fissures. Additionally, the use of meta-language of PCRaster GIS package allowed including the spatial variation of the hydrological and geotechnical parameters. A further extension of this concept is used to model complex landslides with dynamic fissure systems and to investigate the interaction between slope stability and spatial and temporal variations in fissure patterns.

A complete mathematical description of the model is given by Van Beek (2002). Herein, only the specific issues directly related to fissure flow and fissures – matrix interaction are described. The explicit inclusion of fissures in STARWARS required an adaptation of the existing model concept (Fig. 4.18). The new concept assumes (after Van Beek and Van Asch 1999) that fissures are distinct from the matrix, however, they are considered to be field with reworked material (no open spaces) and they retain their own water level and soil moisture content. They are characterised by mean aperture (a_{fis} [m]) or the total number of fissures per cell (N_{fis}) and the fraction of cell they cover (f_{fis} [$m^2 \cdot m^{-2}$]) (Fig. 4.18c). They are assumed to be evenly distributed throughout the cell and extend vertically over the full depth of the layer. Connectivity between the fissure networks in adjacent cells (C_{fis}) is prescribed fractionally in the x- and y-directions and represents the chance for fissures to be connected laterally between the soil columns.

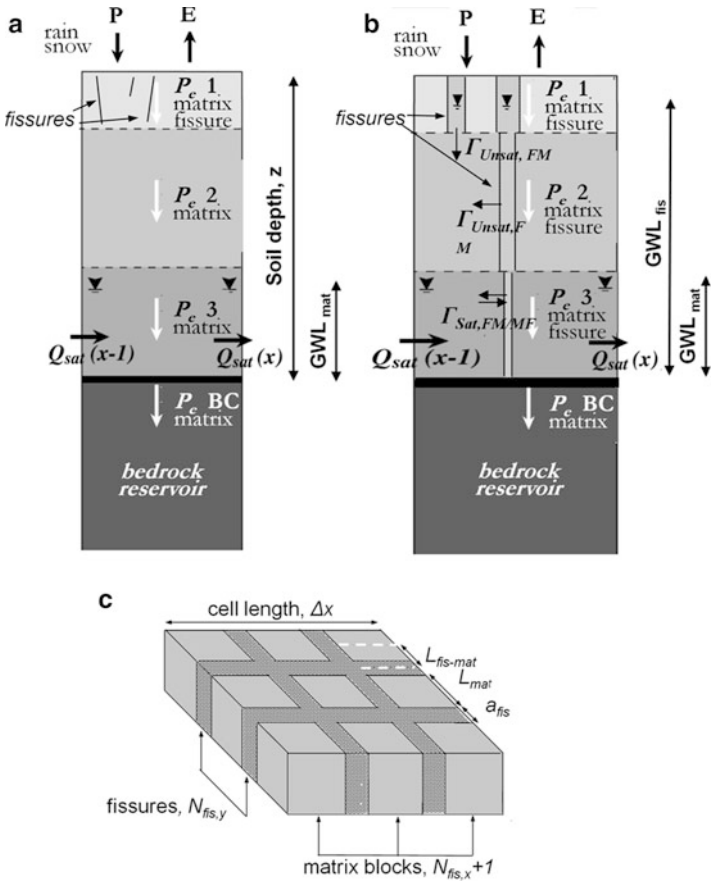

Fig. 4.18 Schematisation of (**a**) the hydrological model (Malet et al. 2005; after Van Beek 2002), (**b**) the hydrological model implemented with this research and (**c**) fissure representation in the single layer of the soil column

Surface fluxes (infiltration and evaporation) are partitioned on the basis of the respective surface area A [m^2]. The available storage capacity of a single cell is the combination of available matrix capacity (a ratio of the saturated hydraulic conductivity of the upper layer) and fissures capacity (potential unlimited; any water that cannot infiltrate into the matrix is passed on to the fissure network). Fissures can be recharged directly by rain or snowmelt or indirectly by overland flow. They maintain their own moisture content and water tables. When the amount of water exceeds the total available storage capacity of the fissure network with the cell, the exfiltration to the surface occurs.

Following the basic assumption of the STARWARS model (Van Beek 2002), the unsaturated flow, both in matrix and fissures, is gravitational and vertical only. However, fissures can drain vertically into the soil when they terminate above the

lithic contact. The unsaturated fluxes within soil column are calculated following the original process description of STARWARS based on the initial degree of saturation in matrix and fissures. Lateral exchange (Γ) within the cell is only possible between the saturated zones of matrix and fissures and unsaturated zone of matrix and saturated zone of fissures (only when the water level in the fissures exceeds that in the matrix). Later flow (Q_{sat}) between cells is a bulk flow across the saturated zone that arises from the gradient in the total piezometric head and is subsequently divided over the matrix and fissure network on the basis of local transmissivity and connectivity of the fissure network. The approximate mean distance from the centre of a fissure to the centre of each matrix block that defines the different gradients is given by:

$$\begin{aligned} L_{mat-fis} &= \frac{1}{2}\left(L_{mat} + a_{fis}\right) \\ L_{mat} &= \left(1 - \sqrt{F_{fis}}\right) \cdot \frac{\Delta x}{N_{fis,x} + 1} \\ N_{fis,x} = N_{fis,y} &= \left(1 - \sqrt{1 - F_{fis}}\right) \cdot \frac{\Delta x}{a_{fis}} \end{aligned} \tag{4.15}$$

where: $N_{fis,x}$ (=$N_{fis,y}$) is number of fissures in x (=y) direction [−] calculated as rounded down to the nearest whole number with a minimum value of 1 when $a_{fis} > 0$ and Δx is the cell length [m]. L_{mat} is width of matrix block, assuming that all fissures are contained by matrix and, therefore, there are $N_{fis,x} + 1$ (looking at x-direction) matrix blocks.

Model development and evaluation of the proof-of-concept are carried out using a simple landslide representation based on the geometry of Super-Sauze (Malet et al. 2005). The digital elevation model (DEM) extends between 1,736 m a.s.l. (toe of the landslide) and 1,955 m a.s.l. (crown of the landslide) with the grid size of 5 × 5 m. This corresponds to a planar slope of 25.1°. The landslide body is delineated by an ellipse-like shape with a length of 800 m and a breadth of 90 m. The maximum depth of the landslide is set to 8 m and decreases towards the borders (Fig. 4.19).

The values for the soil parameters of each layer are defined from field measurements on the Super-Sauze mudslide (Malet et al. 2005). The only exception is the saturated hydraulic conductivity (K_{sat}), which was optimised in order to give best mimic of the range of water level fluctuations (about 2.5 m in average) observed within the Super-Sauze mudslide.

Three scenarios are evaluated:

- scenario 1 – *no fissure* – represents the landslide without consideration of fissures;
- scenarios 2 and 3 – *connected* and *disconnected fissures* – with constant fissures properties over the simulation period, except for fissure connectivity which is set to 10 % (minimum) or 90 % (maximum) for disconnected fissures and connected fissures scenario, respectively.

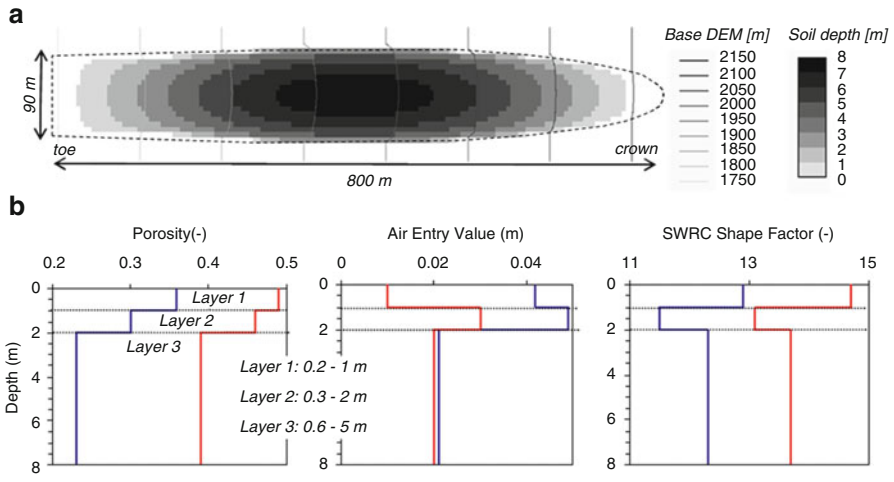

Fig. 4.19 (**a**) Geometry of the simple landslide representation, (**b**) hydrological parameters of the soil layers; *blue* are matrix fraction characteristics and *red lines* fissures fraction characteristics

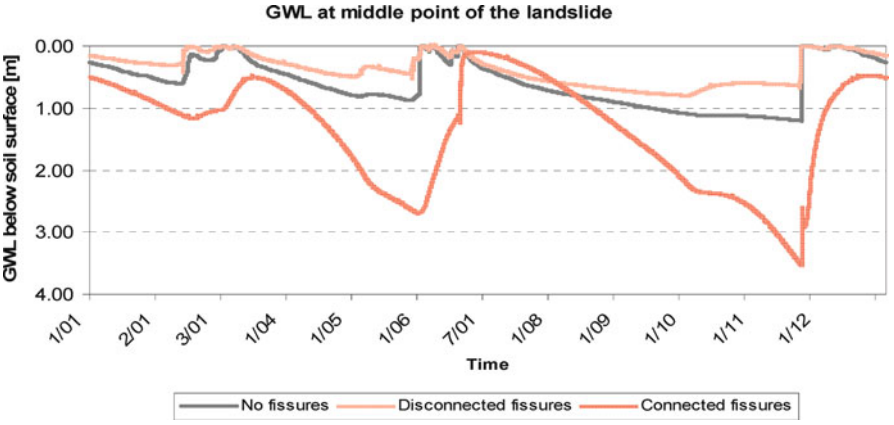

Fig. 4.20 Groundwater level (*GWL*) fluctuations simulated with three scenarios. Example for the middle point of simple landslide representation

The initial conditions (distributed water level, soil moisture and snow thickness) were determined by pre-runs of the model. For connected and disconnected fissures scenarios, an equal distribution of fissures is assumed over the whole landslide. An average fissure fraction was set equal to $F_{dens,max}$ for each of the soil layers and an average fissures aperture was defined equal to 0.20, 0.10 and 0.05 m for the first, second and third layer, respectively.

Figure 4.20 shows groundwater level fluctuations and their dynamics resulting from model simulations for the three scenarios (example for middle point of simple landslide representation). The average groundwater level (GWL_{av}) for *no fissure*

scenario is 0.59 m below the surface and its variance (GWL_{var}) is 0.14 m. The draining effect of *connected fissures* is clear. The water entering the fissures network is drained out of the landslide by the continuous areas of high transitivity. As a consequence, general lowering of the groundwater level is observed ($GWL_{av} = 1.33$ m) but it displays a more dynamic behaviour ($GWL_{var} = 0.73$ m). On the contrary, the model configuration with *disconnected fissures* creates the areas with very high storage capacities but with limited horizontal outflow possibilities. In this way, the groundwater table sustains at a relatively high level ($GWL_{av} = 0.36$ m and $GWL_{var} = 0.06$) compared to the *no fissures* and *connected fissures* scenario. Significant differences between the *connected* and *disconnected fissures* scenarios are visible in water storage capacities of the landslide. Observed water storage capacity of *disconnected fissures* scenario is always higher than the two others: 13–15 % higher compared to the *no fissure* scenario and 3–10 % higher than the *connected fissure* scenario.

It is very important to place an emphasis on the time of appearance and the duration of the period during which full saturation of the soil is observed. During a 1 year simulation period, three sub-periods with high groundwater can be observed for each scenario: early spring (March–April), summer (June–July) and beginning of winter (November–December). There are significant differences in the timing and duration of periods with maximal groundwater level. The full saturation is always first observed for the "disconnected fissures" scenario, then the "no fissures" scenario, and the "connected fissures" scenario. The duration of the period with maximal observed groundwater levels is always the longest for the "disconnected fissures" scenario.

The objective of the presented conceptual model approach was to show the importance of preferential fissures flow for landslide hydrology, and thus slope stability at the field scale. The simulation results show that appearance of fissures and their connectivity have a strong influence on hydrological responses of the landslide and on the timing and the duration of the periods when the landslide body is fully saturated. In saturated conditions, the probability of mass (re-) activation is high (Krzeminska et al. 2012).

Ongoing research aims at linking shifts and hysteresis in landslide activity to feedback mechanisms of hydrological behaviour, differential movement and fissure formations (Krzeminska et al. 2013). The objective is to introduce these dynamics into the STARWARS model. In slow-moving landslides, constant movement of the sliding material and its heterogeneity create the spatially dynamic nature of preferential flow paths system. The connectivity and density of the fissures are among the most important dynamically changing characteristics of fissure systems. In order to mimic dynamic feedback between fissures characteristics, slope stability and hydrology, two relationships have to be established: a dependency of fissures connectivity upon relative degree of saturation of the matrix (e.g.: Tsuboyama et al. 1994; Sidle et al. 2002; Nieber and Sidle 2010) and relationship between potential movement of the landslide and density of the fissures network. Since in STARWARS material deformations are not considered, it was attempted to correlate fissure density, and thus fissure volume, with factor of safety, which is a deterministic measure of slope stability.

4.4 Modelling Fast Moving Landslides

4.4.1 Modelling Strategies

In order to model fast-moving landslides and to assess their characteristics, intensities and run-out, several approaches have been developed. These approaches vary within the needed scope of the assessment and the extent of the outputs required. The array of the approaches goes from empirical-statistical methods to physically-based methods.

Empirical-statistical methods assess the interactions between the characterizing factors of the source area, the travel path (topography and morphology), the mass volume, and the travelled distance. Based on the gathered information via field observation or image interpretation, statistical analyses are performed. These analyses results in statistical functions that express directly or indirectly the mobility of the moving mass. Although a rough estimate of run-outs and travelled distances can be estimated through these methods, they are not able to estimate velocities and impact pressures (important outputs for a Quantitative Risk Assessment). Another disadvantage of the empirical-statistical methods is the demand of reliable data with cumbersome information like: release source point; toe deposition point; and starting and final volume. The collected analyzed data can display a large scattering for developing accurate functions and usually these methods are very dependent of the characteristics of the location of the analysis (site-specific).

To avoid the short comings of the empirical-statistical methods, physical dynamic run-out models have been developed and improved during the last decades. These models have the possibility to have more detailed outputs regarding the intensities of the movements (heights, velocities, pressures) and the outputs can be displayed at different time steps and at different locations during the simulation. Another advantage of physically based modelling is the possibility to add other types of processes that happen during the event like: entrainment, deposition, fluidization, and layering.

A number of dynamic run-out models for fast-moving landslides have been developed and applied for hazard evaluation, risk assessments and the design of mitigation measures (Van Westen et al. 2006). These physically-based models are solved numerically and can simulate the movement of the flow using constitutive laws of granular and fluid mechanics in one (1-D) or two (2-D) dimensions. The 1-D models are lumped-mass models and can be used in case of debris flows which are confined in gullies. In this case the 1-D flow path is well known. The 2-D models are able to simulate unconfined debris flows and to predict the 2D extension on alluvial fans. The 2-D models can route the flow over irregular topographic terrains. They need however an accurate and detailed digital elevation model (DEM) (Hürlimann et al. 2007)

Most numerical models are based on a “continuum approach” that considers the heterogeneous and multiphase moving mass of a debris flow as a continuum. A continuum approach enhances the possibility to model the dynamics of debris

flows using an "equivalent" fluid, whose rheological properties are such that the bulk behaviour of the numerically simulated flowing mass can approximate the expected bulk behaviour of the real mixture of the solid and fluid phases (Hungr and McDougall 2009). Continuum models solve the conservation equations of mass and momentum and are often applied through a depth-averaged approach that integrates the internal stresses in either vertical or bed-normal direction to obtain a form of Saint-Venant or Navier–Stokes equations (shallow water assumption) (Van Asch et al. 2007b), which can be solved either in an Eulerian or Lagrangian form. The internal stresses of the flow are functions of the internal shear strains and are bounded by active and passive states (Rankine's theory). Depth averaging allows representing the rheology of the flow as a single term that expresses the frictional forces that interact at the interface between the flow and the bed path. The conservation equations of mass and momentum are given by Eqs. 4.16 and 4.17 respectively:

$$\frac{\partial h}{\partial t} + \frac{\partial (hu)}{\partial x} + \frac{\partial (hv)}{\partial y} = 0 \tag{4.16}$$

$$\frac{\partial u}{\partial t} + u\frac{\partial u}{\partial x} + v\frac{\partial u}{\partial y} = -g\left(S_x + k\,\frac{\partial h}{\partial x} + S_f q_x\right)$$

$$\frac{\partial v}{\partial t} + v\frac{\partial v}{\partial x} + u\frac{\partial v}{\partial y} = -g\left(S_y + k\,\frac{\partial h}{\partial y} + S_f q_y\right) \tag{4.17}$$

where h is the flow thickness; (u, v) are the x and y components of the depth average velocities (L T − 1). The momentum equation (Eq. 4.17) is expressed in terms of acceleration (L T − 2), where g is the acceleration due to gravity. The second and third terms on the left side of the equation represents the convective acceleration, i.e. the time rate of change due to change in position in the spatial field. The right side of the equation represents the local or time acceleration, expressing the time rate of change at a fixed position. The first term between the brackets represents the acceleration due to gravity, and $S_x = tan\alpha_x$ and $S_y = tan\alpha_y$ are the bed slope gradient in the x and y directions (L L − 1), respectively. The spatial derivative in the second term is the pressure acceleration, i.e. the time rate of change due to pressure differences within the flow. S_f is the flow resistance gradient (L L − 1), which accounts for momentum dissipation within the flow due to frictional stress with the bed. The terms q_x and q_y are coefficients (Eq. 4.18)

$$q_x = \frac{-u}{\sqrt{u^2 + v^2}}$$

$$q_y = \frac{-v}{\sqrt{u^2 + v^2}} \tag{4.18}$$

where the minus sign before u and v ensures that S_f opposes the direction of the velocity. The term k is the earth pressure coefficient, i.e. the ratio between the tangential and normal stresses. It ranges between two extreme values corresponding to the active and passive states in the Rankine's theory, i.e. $k_a \leq 1 \leq k_p$ (Eq. 4.19). These values depend on the internal friction angle of the mixture (Begueria et al. 2009).

$$K_a = \frac{1 - \sin\varphi}{1 + \sin\varphi}$$
$$K_p = \frac{1 + \sin\varphi}{1 - \sin\varphi} \tag{4.19}$$

The most common rheologies used in the dynamic models for the calculation of the basal friction are:

(i) The "Frictional" (or "Coulomb") resistance based on the relation of the effective bed and normal stress at the base and the pore fluid pressure (Hungr and McDougall 2009) (Eq. 4.20);

$$S_f = \tan\varphi'$$
$$\tan\varphi' = (1 - r_u)\tan\varphi \tag{4.20}$$

where, S_f is the unit base resistance, r_u is the pore-pressure ratio which is equal to the bed pore water pressure divided by the bed normal total stress; and φ is the dynamic basal friction angle.

(ii) The frictional-turbulent "Voellmy" resistance proposed initially for snow avalanches (Voellmy 1955) and used for granular cohesionless material with or without the presence of a pore fluid. This model features a velocity-squared resistance term (turbulent coefficient ξ) similar to the Chezy resistance for turbulent water flow in open channels and a Coulomb-like friction (apparent friction coefficient μ). The model assumptions are incompressibility of the flow along the whole path; constant discharge and small variations of flow height along the track; and non-steady quasi-rigid body movement both in the starting and the run-out zone. Voellmy (1955) established this model using a fundamental hydraulic theory with two resistive force contributions, one in which the shear force is proportional to the normal force and the other of viscous type, in which the drag is assumed proportional to the velocity squared. The basal shear stress is calculated as (Eq. 4.21):

$$Sf = \left[\tan\varphi' + \frac{u^2}{\xi h}\right] \tag{4.21}$$

where S_f is the unit base resistance, $tan\,\varphi'$ is the friction coefficient, u is the flow velocity (L T − 1) and ξ is the turbulent coefficient (L T − 2). The parameters μ and ξ are constants whose magnitudes depend, respectively, on the flow properties and the roughness of the flow surface (Christen et al. 2010). Various authors have used the run-out from granular avalanches to estimate the friction coefficients of the Voellmy model (Hungr and McDougall 2009; McDougall and Hungr 2005).

iii. The visco-plastic "Bingham" resistance relationship applicable for plastic clay-rich material (Malet et al. 2005). The Bingham model is a function of flow depth, velocity, constant yield strength (τ_c) and dynamic viscosity (η) (Eq. 4.22). A linear stress–strain rate relationship is assumed once the yield strength is exceeded. The mean flow velocity is derived from the linear increase of shear stress with depth (Coussot 1997). According to Rickenmann et al. (2006), a clay fraction (particle size less than 40 μm) greater than 10 % is necessary so that a flow material may be assumed to behave like a Bingham fluid. The basal shear stress is calculated as (Eq. 4.22):

$$Sf = \frac{1}{\rho g h}\left(\frac{3}{2}\tau_c + \frac{3\eta}{h}u\right) \tag{4.22}$$

where, S_f is the unit base resistance, τ_c is a constant yield strength due to cohesion, ρ is the density of the flow, and η is the viscosity parameter (Begueria et al. 2009). The yield stress and the viscosity of the flow are closely related to the concentration of solids.

iv. The "Quadratic" resistance that incorporates a turbulent contribution to the yield and the viscous term already defined in the Bingham equation (O'Brien et al. 1993). The basal shear stress is calculated as (Eq. 4.23):

$$Sf = \frac{\tau_c}{\rho g h} + \frac{K\eta}{8\rho g (h)^2}u + \frac{n^2(u)^2}{(h)^{\frac{4}{3}}} \tag{4.23}$$

where, S_f is the unit base resistance, τ_c is the resisting shear stress; u is the depth-averaged velocity; h is the flow depth; η is the viscosity of the fluid, which is a function of the sediment concentration by volume; K is a dimensionless resistance parameter that equals 24 for laminar flow in smooth, wide, rectangular channels, but increases with roughness and irregular cross section geometry; and n is the Manning coefficient value that takes into account the turbulent and dispersive components of flow.

A more thorough description of rheologies that are commonly used for simulating debris flows can be found in Naef et al. (2006) and Hungr and McDougall (2009).

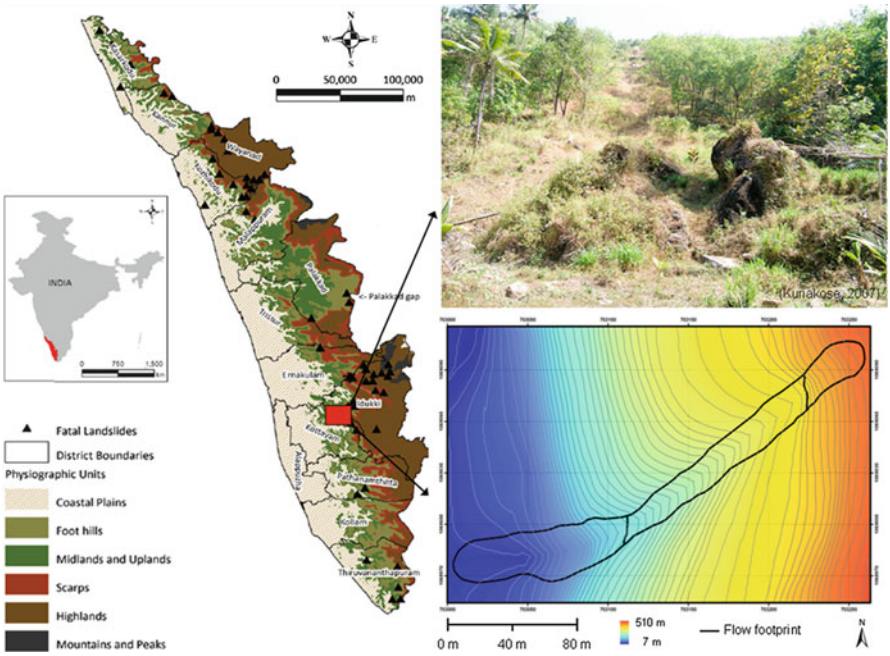

Fig. 4.21 Location of the Peringalam debris flow, in the upper Meenachil river basin, Kerala (Kuriakose 2010)

4.4.2 Back-Analysis and Sensitivity of the Run-Out Models

In order to evaluate the models methods, a back-calibration of a past debris flow that occurred in Peringalam, India was performed with two different dynamic debris-flow models (MassMov2D and DAN3D) that uses different numerical scheme and solution. To make a fair assessment between the two models, only the Voellmy rheology was applied. As described in the previous section, the Voellmy rheology consists of two parameters: a Coulomb frictional term and a turbulent term. The trubulent term ξ, covers all the velocity-dependent factors including the turbulence and the drag in top of the surface of the avalanche.

4.4.2.1 Peringalam, Kerala, India

The Peringalam test site, located near a small village in the upper catchment basin of the Meenachil river in the Kottayam district in the state of Kerala, India. This region has experienced various types of landslides of which the debris flows are the most common. The Peringalam debris flow event occurred in a topographic depression upstream of a first order non perennial stream on 14th of October of 2004 at 5:00 pm (Fig. 4.21). The event caused considerable damage to cultivated land and blocking

the road that connects the village of Peringalam to the nearest major town, Poonjar. The landslide originated at an altitude of 500 m a.s.l. and had a total run-out distance of 290.5 m. Measurements of the landslide where carefully done via fieldwork and aerial imagery. The calculated initial volume of the debris flow was 437 m^3 with a deposited final volume of 1,533 m^3. The area of the landslide body at the initiation zone is 784 m^2, the run-out zone is 2,336 m^2 and the area of the deposition zone is 2,680 m^2.

4.4.2.2 Back-Analysis of the DAN3D with Reference of the Peringalam Event

Besides the information of the release volume and the rheology model parameters, the numerical parameters for DAN3D are: the number of particles, the time step, the particle smoothing coefficient, the velocity smoothing coefficient and the stiffness coefficient. The values of the parameters of the particle smoothing coefficient and the stiffness coefficient were set equal to 4 and 200, respectively as suggested in the applications presented by McDougall and Hungr (2004, 2005) and McDougall (2006). The initially released volume is discretised in particles with equal initial volumes. The number of particles, *N*, should be large enough to ensure the accurate simulation with respect to flow spreading, junctioning and branching. The volumes to be simulated in the back-analysis with the number of particles were set to 2,000 for all the simulations.

It should be noted that the time step should be sufficiently small as not to influence the results of the simulation. A time step equal to 0.05 s was selected as the time step for all simulations. The velocity smoothing coefficient, *C*, increases numerical stability and improves the behaviour of the model in channelized reaches by reducing the tendency for particles to line up. However, it introduces some numerical damping and hence it is not appropriate to use high values. McDougall (2006) suggests a value up to about $C = 0.01$ to be probably appropriate and was selected for the simulations in order to minimise the consequences of this numerical instabilities.

4.4.2.3 Back-Analysis Using MassMov2D with Reference of the Peringalam Event

In the case of MassMov2D the chosen time step was 1 s, although internally the model used fractional time steps which vary depending on the flow characteristics, based on the Courant-Friedrichs-Levy condition (CFL). In order to have numerical stability control the CFL upper limit was set to 0.5 and the lower limit was 0.3.

Five different maps in raster form were used to describe the computational domain. The first map contained information before the debris flow event (pre-event) about elevation and topographical features of the terrain. This map also defines the mesh size where the computations take place. The second map was produced to

Table 4.4 Parameters used for simulating the debris flow in DAN3D and MassMov2D

Software	Rheological model	Model parameters	Entrainment rate
MassMov2D	Voellmy	Apparent friction angle: 34° Turbulent coefficient: 250 m/s^2	0.035 m/s
DAN3D	Voellmy	Apparent friction angle: 34° Turbulent coefficient: 250 m/s^2	0.035 m/s

define the initiation thickness, shape and area of the released mass. A third map was created with a binary form to display an outlet cell for the flow (open boundary). A fourth map was used to define the distance of the whole domain to the toe of the initiation area. And a fifth map was created with the soil depths to identify the amount of eroded material that the flow can entrain.

MassMov2D has also implemented a fluidization term which describes the pace of the transition between the solid release mass and how it fluidizes once the mass is set in motion. This fluidization rate is described as a velocity and it only takes place during the initiation of the movement. In both simulated cases, the fluidization rate chosen was 10 m/s.

The simulation of the Peringalam debris flow event was performed via back-analysis. The input parameters of the rheological models were modified by trial and error until the characteristics of the modelled debris flows were approximately close to the real event debris flows. The criteria that were chosen to compare the simulation results with the real event were deposit depth, volume, area and entrainment volume. Table 4.4 shows the combinations of model parameters that produced the best predictions. Both models use bed entrainment by defining an entrainment zone, a maximum depth of supply material and the average growth or erosion rate, originally implemented in DAN3D.

Both models were calibrated based on the rheological parameters: apparent friction and turbulent coefficients. In terms of the internal pressures (passive and active), both of the models were adjusted to the assumption that the flow was hydrostatic. In both models the same entrainment rate was used as they are implemented with the same entrainment scheme. A time step of 100 s were set in both model and in all the simulations the density of the flow was considered at 2,000 kg/m^3. It was noted during the process of calibration, that the friction angle was the parameter that have a greater impact in the extent of the deposits and the length of the run-out. The turbulent coefficient was the parameter that influenced mostly the velocity and the height of the flow.

DAN3D and MassMov2D were able to predict the run-out of the debris flow event reasonably well, in terms of maximum extension and flow height. The results of both models had some differences in terms of deposition during the course of the flow and in the deposit area. In terms of maximum velocities both models were quite similar but differences arise when comparing it during the course of the flow. In the case of the calculated entrained material, both of the models were consistent with the real event (Table 4.5).

Table 4.5 Comparison of observed and predicted properties of the debris flow

	Observed	DAN3D	MassMov2D
Initial volume (m^3)	1,435	1,435	1,435
Entrained volume (m^3)	593	619	614
Max velocity (m/s)	20	21	24
Mean deposit thickness (m)	1.6	2.2	1.7
Max deposit thickness (m)	4.1	6.9	3.5

In the debris flow event that was simulated, DAN3D estimated the shape of the deposition and the deposits left behind by the flow during its course in a good manner. The maximum and mean thickness was overestimated in accordance to the observations. The final deposition showed a spreading of the material in a more consistent way that is closely to the real event. On the other hand, MassMov2D also was able to predict in a good way the extension of the deposits but it slightly underestimated the deposited area. MassMov2D was able to represent the flow thickness in a closer way to the observations.

Regarding the computational efforts, in a general way a Lagrangian code is more efficient than an Eularian code which requires a structured mesh and high computational power. This was not noticeable in both cases of the simulated event. The computational time was nearly the same and no extra effort was noticed when using the two different models. The simulations of the Peringalam debris flow are presented in Fig. 4.22, which shows selective images of the calculated sequences at time steps 0, 10, 20, 35, 50 and 100 s. The combination of parameters that best corresponds to the field observations was characterised by an apparent angle of friction of 34° and a turbulent coefficient of 250 m/s^2.

Small differences, though, can be observed between the two models regarding the simulation of the behaviour of the flow. With DAN3D, after the mass is released, it accelerates downwards rapidly following the channelled slope until reaching the deposition area. In the deposition area, the flow spread laterally evenly and as the flow starts to come to a rest it can be observed that the tail pushes forward and the deposit takes the shape of a drop. In MassMov2D, the flow is slower at the beginning mainly because of the fluidization rate but when the whole mass is released the flow reaches higher velocities during the course. MassMov2D deposits and spreads the flow in a more even way in the depositional area. However, in both cases the final deposit and velocities correlates well with the field measurements.

4.4.2.4 Sensitivity Analysis of the DAN3D Model and MASSMOV2D Model with Constant Defined Entrainment Rate Value

To evaluate the influence of the variations in the input parameters to the final results, a sensitivity analysis of the models was carried out in order to quantify this impact. This was achieved by evaluating how the variation in the output of a model can

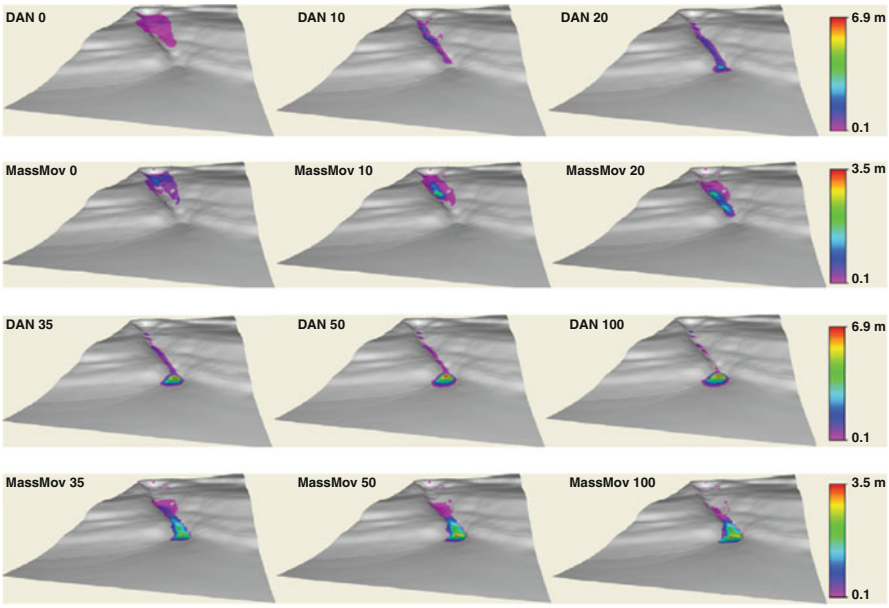

Fig. 4.22 Comparison of the temporal evolution of debris flow height as modelled by MassMov2D and DAN3D

be apportioned, qualitatively or quantitatively, among model inputs. This analysis helped assess how the uncertainty in the output of a model can be allocated to different sources of uncertainty in the model input.

A sensitivity analysis was conducted as a parametric study and was applied to the model to provide insight regarding which model inputs contribute the most to the variability of the model output. This analysis was carried out for the rheological parameters of the Voellmy model. The apparent friction angle was varied as a 10 % of the calibrated value 34°. The values started from 3.4° and ended in 53.2°. The turbulent coefficient was varied in ranges of 25 units, starting from values of 25 to 1,000 m/s^2. In order to compare the results of the sensitivity, the back calibration simulation was used as a reference to control the variation of the parameters. For all the simulations, a total of 47 runs, all the starting parameters were kept constant except the parameter selected for the sensitivity.

The apparent friction angle parameter consists of a term that is independent of the flow velocity but depends on the slope angle with the Coulomb friction coefficient, and a turbulent coefficient parameter is dependent on the square of the flow velocity obtained in imitation of the turbulent friction in fluid mechanics. These parameters are usually are taken as constant during the avalanche event. Some requirements are needed regarding both parameters: – the apparent friction angle must be less than the starting-zone slope, otherwise the flow cannot start moving; – the apparent friction angle cannot be zero; otherwise the flow would not come to rest on a horizontal plane within a finite time; and – both apparent friction angle and turbulent coefficient must be positive or else the friction would not be dissipative.

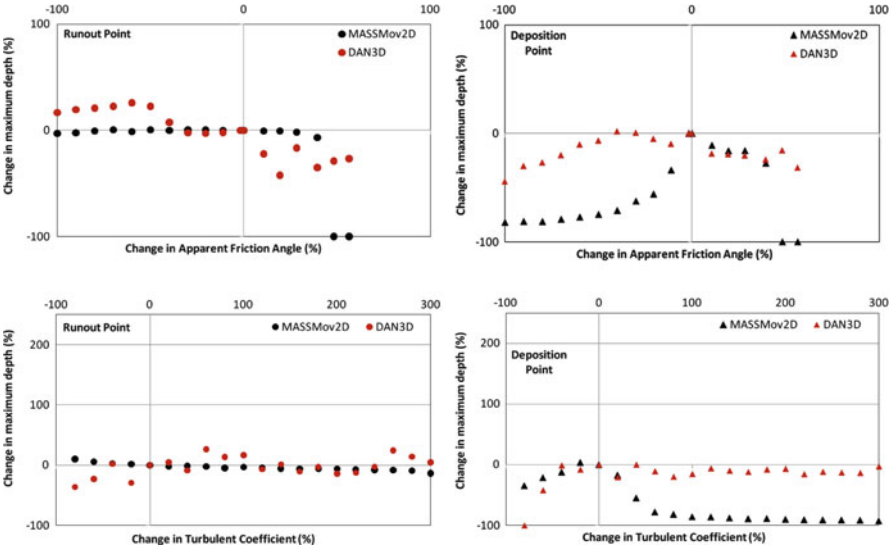

Fig. 4.23 Percentage of change in the flow depth in accordance to the percentage of change in the input parameters of the Voellmy model

Two different locations inside the flow path were used to measure the variation of flow depth and velocity according to the variation of the parameters: the "R" point that was located in the run-out area and the "D" point that was located in the depositional zone.

As expected, the apparent friction angle was the parameter that influenced the most on the run-out distance. This parameter increased the deposits on the channel because the flow spreading as it slows down. The apparent friction angle has a small but visible influence in the final and maximum velocity reached by the flow. It is also observed that lower apparent friction coefficient generates lower deposits heights in the run-out zone and there are fewer deposits (although higher spreading) in the depositional zone. The turbulent coefficient is directly linked to the velocity of the flow. This parameter controls the drag forces of the flow in the topography and influence the speed of the run-out. This makes the deposits spread more evenly during the whole simulations.

The percentage of change regarding depth and velocity of the flow was also assessed based on the percentage variation of the input parameter. As it can be seen in Fig. 4.23, the flow depths remain almost constant in the run-out zone with both models and both parameters. This can be seen as the influence of the morphology of the terrain in the simulations. Once the flow has reached the deposition zone, the changes becomes more visible.

Changes in velocities are more drastic and a slight change in the parameters can cause a significant change in the velocity of the flow. Once the turbulent coefficient is increased to very high quantities, the Voellmy model becomes close to have

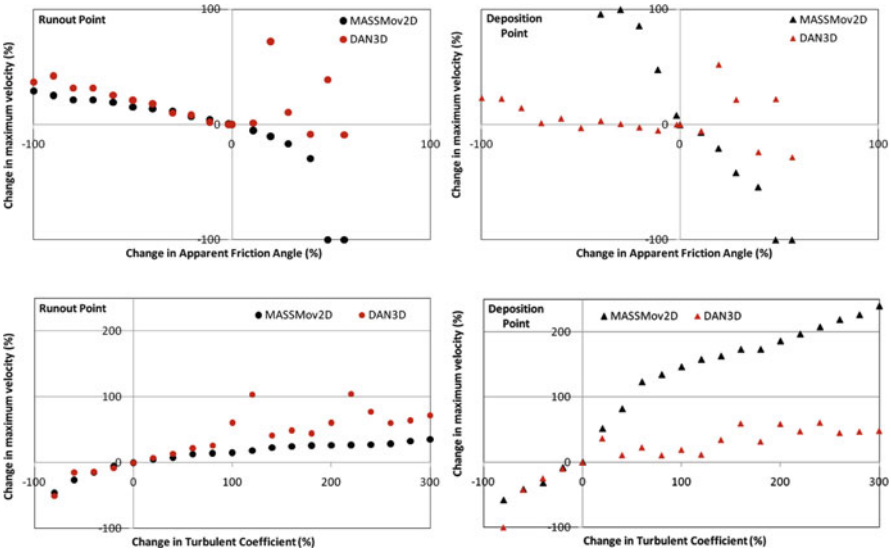

Fig. 4.24 Percentage of change in the flow depth in accordance to the percentage of change in the input parameters of the Voellmy model

frictional behaviour and the only parameter that influences the flow is the apparent friction angle (Fig. 4.24). This makes the flow have higher velocities and a bulkier final deposit. The turbulent coefficient behaves as a drag force in the energy line; this gives closer results of the velocity of the flow when compared to the past event. This effect makes the Voellmy model in comparison to other models (Bingham or pure frictional) to have a more even deposition during the course and deposition of the flow.

4.5 Conclusions

Geomechanical modelling of landslides involves a handful of challenges. These challenges are related to the multidisciplinary process of landslide modelling to which the geomechanical part belongs. The problem of landslides itself is highly complex for it involves different types of materials and their loading histories, geological configurations and complex environmental conditions. A geomechanical model aims at giving an appropriate idealisation of a certain landslide problem. Appropriate means that the model is able to capture the key physical mechanisms in a given landslide problem and possesses predictive capacities so that it can reproduce qualitatively and quantitatively the observed behaviour in nature and further be used to predict the slope behaviour for other environmental configurations.

This chapter has addressed in a synthesised form the different key physical mechanisms in landslides and presented some modelling strategies (and their mathematical frameworks) which imply different levels of coupling between the hydrogeological and the geomechanical responses. Applications of the presented modelling strategies to selected case studies were described with the aim to elucidate, which type of information can be gained from different types of numerical models and which conclusions can be drawn for hazard assessment.

References

Abramson LW, Lee TS, Sharma S, Boyce GM (2002) Slope stability and stabilisation methods, 2nd edn. Wiley, New York

Alonso EE, Gens A, Lloret A (1993) The landslide of Cortes de Pallas, Spain. Géotechnique 43(4):507–521

Alonso EE, Gens A, Delahaye CH (2003) Influence of rainfall on the deformation and stability of a slope in over consolidated clays: a case study. Hydrogeol J 11:174–192

Anderson SP, Dietrich WE, Montgomery DR (1997) Subsurface flow paths in steep, unchanneled catchments. Water Resour Res 33(12):2637–2653

Begueria S, van Asch TWJ, Malet J-P, Grondahl S (2009) A GIS-based numerical model for simulating the kinematics of mud and debris flows over complex terrain. Nat Hazard Earth Syst Sci 9:1897–1909

Biot MA (1956) General solution of the equations of elasticity and consolidation for a porous material. J Appl Mech 19:91–96

Bjerrum L (1967) Progressive failure in slopes in over consolidated plastic clay and clay shales. ASCE J Soil Mech Found Div 93(5):3–49

Bogaard TA (2001) Analysis of hydrological processes in unstable clayey slopes. PhD thesis, University of Utrecht, Utrecht

Bogaard TA, van Asch TWJ (2002) The role of the soil moisture balance in the unsaturated zone on movement and stability of the Beline landslide, France. Earth Surf Process Landf 27:1177–1188

Cascini L, Cuomo S, Pastor M, Sorbino G (2010) Modeling of rainfall-induced shallow landslides of the flow-type. ASCE J Geotech Geoenviron Eng 136(1):85–98

Castelli M, Scavia C, Bonnard C, Laloui L (2009) Mechanics and velocity of large landslides, preface. Eng Geol 109(1–2):1–4

Christen M, Kowalski J, Bartelt P (2010) RAMMS: numerical simulation of dense snow avalanches in three-dimensional terrain. Cold Reg Sci Technol 63:1–14

Comegna L, Picarelli L, Urciuoli G (2007) The mechanics of mudslides as a cyclic undrained-drained process. Landslides 4(3):217–232

Corominas J, Moya J, Ledesma A, Lloret A, Gili JA (2005) Prediction of ground displacements and velocities from groundwater level changes at the Vallcebre landslide (Eastern Pyrenees, Spain). Landslides 2:83–96. doi:10.1007/s10346-005-0049-1

Coussot P (1997) Mudflow rheology and dynamics. IAHR monograph. Balkema, Rotterdam

Crosta GB, Dal Negro P (2003) Observations and modeling of soil slip-debris flow initiation processes in pyroclastic deposits: the Sarno 1998 event. Nat Hazard Earth Syst Sci 3:53–69

Crozier MJ (2005) Multiple-occurrence regional landslide events in New Zealand: hazard management issues. Landslides 2:247–256

Cruden DM, Varnes DJ (1996) Landslide types and processes. In: Turner AK, Schuster RL (eds) Landslides: investigation and mitigation. National Academy Press, Washington, DC

Dai FC, Lee CF, Sijing W (1999) Analysis of rainstorm-induced slide-debris flows on a natural terrain of Lantau Island, Hong Kong. Eng Geol 51:279–290

De Montety V, Marc V, Emblanch C, Malet J-P, Bertrand C, Maquaire O, Bogaard TA (2007) Identifying the origin of groundwater and flow processes in complex landslides affecting black marls: insights from a hydrochemical survey. Earth Surf Process Landf 32:32–48

Dounias GT, Potts DM, Vaughan PR (1988) Finite element analyses of progressive failure: two case studies. Comput Geotech 6:155–175

Duncan JM, Wright SG (2005) Soil strength and slope stability. Wiley, Chichester

Eberhardt E, Thuro K, Luginbuehl M (2005) Slope instability mechanisms in dipping interbedded conglomerates and weathered marls—the 1999 Rufi landslide, Switzerland. Eng Geol 77(1):35–56

Eckersley JD (1990) Instrumented laboratory flowslides. Géotechnique 40:489–502

Ferrari A, Laloui L, Bonnard C (2009) Hydro-mechanical modelling of a natural slope affected by a multiple slip surface failure mechanism. Comput Model Eng Sci 52(3):217–235

Ferrari A, Ledesma A, González D, Corominas J (2011) Effects of the foot evolution on the behaviour of slow-moving landslides. Eng Geol 117:217–228

Fourie AB, Rowe D, Blight GE (1999) The effect of infiltration on the stability of the slopes of a dry ash dump. Géotechnique 49(1):1–13

François B, Tacher L, Bonnard C, Laloui L, Triguero V (2007) Numerical modelling of the hydrogeological and geomechanical behaviour of a large slope movement: the Triesenberg landslide (Liechtenstein). Can Geotech J 44:840–857

Fredlund DG, Rahardjo H (1993) Soil mechanics for unsaturated soils. Wiley, Chichester

Godt JW, Baum RL, Lu N (2009) Landsliding in partially saturated materials. Geophys Res Lett 36(L02403):1–5

Harr RD (1981) Some characteristics and consequences of snowmelt during rainfall in Western Oregon. J Hydrol 53:277–304

Hungr O (1995) A model for the run-out analysis of rapid flow slides, debris flows and avalanches. Can Geotech J 32:610–623

Hungr O, McDougall S (2009) Two numerical models for landslide dynamic analysis. Comput Geosci 35:978–992

Hürlimann M, Medina V, Bateman A, Copons R, Altimir J (2007) Comparison of different techniques to analyse the mobility of debris flows during hazard assessment. Case study in La Comella catchment, Andorra. In: Chen C-l, Major JJ (eds) Debris-flow hazard mitigation: mechanics, prediction and assessment. Mill Press, Rotterdam

Iverson RM, Denlinger RP (2001) Flow of variably fluidized granular masses across three-dimensional terrain. 1. Numerical predictions and experimental tests. J Geophys Res 106:553–566

Iverson RM, Reid ME, LaHusen RG (1997) Debris-flow mobilization from landslides. Annu Rev Earth Planet Sci 25:85–138

Johnson KA, Sitar N (1990) Hydrologic conditions leading to debris-flow initiation. Can Geotech J 27:789–801

Karssenberg D, Burrough PA, Sluiter R, de Jong K (2001) The PCRaster software and course materials for teaching numerical modelling in the environmental sciences. Trans GIS 5(2): 99–110

Krzeminska DM, Bogaard TA, Van Asch TWJ, Van Beek LPH (2012) A conceptual model of the hydrological influence of fissures on landslide activity. Hydrol Earth Syst Sci 16:1–16

Krzeminska DM, Bogaard TA, Malet J-P, Van Beek LPH (2013) A model of hydrological and mechanical feedbacks of preferential fissure flow in a slow-moving landslide. Hydrol Earth Syst Sci 17(3):947–959

Kuriakose SL (2010) Physically-based dynamic modelling of the effect of land use changes on shallow landslide initiation in the Western Ghats of Kerala. PhD thesis, University of Twente, Faculty of Geo-Information and Earth Observation ITC, Enschede, ITC dissertation 178, ISBN: 978-90-6164-298-5

Laloui L, Klubertanz G, Vulliet L (2003) Solid–liquid-air coupling in multiphase porous media. Int J Numer Anal Methods Geomech 27(3):183–206

Laloui L, Nuth M (2009) On the use of the generalised effective stress in the constitutive modelling of unsaturated soils. Comput Geotech 36(1–2):20–23

Ledesma A, Corominas J, González A, Ferrari A (2009) Modelling slow moving landslides controlled by rainfall. In: Picarelli L, Tommasi P, Urciuoli G, Versace P (eds) The first Italian Workshop on Landslides (IWL), rainfall-induced landslides – mechanisms, monitoring techniques and nowcasting models for early warning systems, vol 1. Naples

Macfarlane DF (2009) Observations and predictions of the behaviour of large, slow-moving landslides in schist, Clyde Dam reservoir, New Zealand. Eng Geol 109(1–2):5–15

Malet J-P (2003) Les glissements de type ecoulement dans les marnes noires des Alpes du Sud. Morphologie, fonctionnement et modélisation hydromécanique. PhD thesis in Earth Sciences, Université Louis Pasteur, Strasbourg

Malet J-P, Van Asch TWJ, Van Beek LPH, Maquaire O (2005) Forecasting the behaviour of complex landslides with a spatially distributed hydrological model. Nat Hazard Earth Syst Sci 5:71–85

Mangeney A, Bouchut F, Thomas N, Vilotte JP, Bristeau MO (2007) Numerical modeling of self-channeling granular flows and of their levee-channel deposits. J Geophys Res 112:F02017. doi:10.1029/2006JF000469

Maquaire O, Malet JP, Remaître A, Locat J, Klotz S, Guillon J (2003) Instability conditions of marly hillslopes: towards landsliding or gullying? The case of the Barcelonnette Basin, South East France. Eng Geol 70:109–130

McDonnell JJ (1990) The influence of macropores on debris flow initiation. Q J Eng Geol Hydrogeol 23:325–331. doi:10.1144/GSL.QJEG.1990.023.04.06

McDougall S (2006) A new continuum dynamic model for the analysis of extremely rapid landslide motion across complex 3D terrain. PhD thesis, The University of British Columbia, Vancouver

McDougall S, Hungr O (2004) A model for the analysis of rapid landslide motion across three-dimensional terrain. Can Geotech J 41(12):1084–1097

McDougall S, Hungr O (2005) Dynamic modelling of entrainment in rapid landslides. Can Geotech J 42:1437–1448

Moser M, Hohensinn F (1983) Geotechnical aspects of soil slips in alpine regions. Eng Geol 19:185–211

Naef D, Rickenmann D, Rutschmann P, McArdell BW (2006) Comparison of flow resistance relations for debris flows using a one-dimensional finite element simulation model. Nat Hazard Earth Syst Sci 6:155–165

Nieber JL, Sidle RC (2010) How do disconnected macropores in sloping soils facilitate preferential flow. Hydrol Process 24:1582–1594. doi:10.1002/hyp.7633

Nuth M, Laloui L (2008) Effective stress concept in unsaturated soils: clarification and validation of a unified framework. Int J Numer Anal Methods Geomech 32:771–801

O'Brien JS, Julien PY, Fullerton WT (1993) Two-dimensional water flood and mudflow simulation. J Hydraul Eng 119(2):244–261

Olivares L, Damiano E (2007) Postfailure mechanics of landslides: laboratory investigation of flowslides in pyroclastic soils. J Geotech Geoenviron Eng 133(1):51–62

Picarelli L, Urciuoli G, Russo C (2004) Effect of groundwater regime on the behaviour of clayey slopes. Can Geotech J 41:467–484

Picarelli L, Olivares L, Comegna L, Damiano E (2008) Mechanical aspects of flow-like movements in granular and fine grained soils. Rock Mech Rock Eng 41(1):179–197

Potts DM, Kovacevic N, Vaughen PR (1997) Delayed collapse of cut slopes in stiff clay. Géotechnique 47(5):953–982

Rahardjo H, Aung KK, Leong EC, Rezaur RB (2004) Characteristics of residual soils in Singapore as formed by weathering. Eng Geol 73:157–169

Ranalli M, Gottardi G, Medina-Cetina Z, Nadim F (2010) Uncertainty quantification in the calibration of a dynamic viscoplastic model of slow slope movements. Landslides 41:31–41

Rickenmann D, Laigle D, McArdell BW, Hübl J (2006) Comparison of 2D debris-flow simulation models with field events. Comput Geosci 10:241–264

Savage SB, Hutter K (1989) The motion of a finite mass of granular material down a rough incline. J Fluid Mech 199:177–215

Sidle RC, Tsuboyama Y, Noguchi S, Hosada I, Fujieda M, Shimizu T (2002) Stormflow generation in steep forested headwaters: a linked hydrogeomorphic paradigm. Hydrol Process 14:369–385

Skempton AW (1964) 4th Rankine Lecture: long term stability of clay slopes. Géotechnique 14(2):77–101

Spence KJ, Guymer I (1997) Small-scale laboratory flowslides. Géotechnique 47:915–922

Springman SM, Jommi C, Teysseire P (2003) Instabilities on moraine slopes induced by loss of suction: a case history. Géotechnique 53(1):3–10

Tacher L, Bonnard C, Laloui L, Parriaux A (2005) Modelling the behaviour of a large landslide with respect to hydrogeological and geomechanical parameter heterogeneity. Landslides J 2(1):3–14

Travelletti, J., Malet, J.-P. (2012). Characterization of the 3D geometry of flow-like land slides: a methodology based on the integration of multi-source data. Eng Geol 128:30–48, http://dx.doi.org/10.1016/j.enggeo.2011.05.003

Travelletti J, Delacourt C, Allemand P, Malet J-P, Schmittbuhl J, Toussaint R, Bastard M (2012) Correlation of multi-temporal ground-based optical images for landslide monitoring: application, potential and limitations. ISPRS J Photogramm Remote Sens 70:39–55. doi:10.1016/j.isprsjprs.2012.03.007

Tsuboyama Y, Sidle RC, Noguchi S, Hosada I (1994) Flow and transport through the soil matrix and macropores of a hillslope segment. Water Resour Res 30(4):879–890

Uchida T, Kosugi K, Mizuyama T (2001) Effects of pipe flow on he hydrological process and its relation to landslides: a review of pipe flow studies in forested headwater catchments. Hydrol Process 15:2151–2174

Van Asch TWJ, Van Genuchten PMB (1990) A comparison between theoretical and measured creep profiles of landslides. Geomorphology 3:45–55

Van Asch TWJ, Hendriks MR, Hessel R, Rappange FE (1996) Hydrological triggering conditions of landslides in varved clays in the French Alps. Eng Geol 42:239–251

Van Asch TWJ, Malet J-P, Van Beek LPH (2006) Influence of landslide geometry and kinematic deformation to describe the liquefaction of landslides: some theoretical considerations. Eng Geol 88:59–69. doi:10.1016/j.enggeo.2006.08.002

Van Asch TWJ, Van Beek LPH, Bogaard TA (2007a) Problems in predicting the mobility of slow-moving landslides. Eng Geol 91(1):46–55

Van Asch TWJ, Malet J-P, Van Beek LPH, Amitrano D (2007b) Techniques, issues and advances in numerical modelling of landslide hazard. Bull Soc Géol Fr 178(2):65–88

Van Beek LPH (2002) Assessment of the influence of changes in land use and climate on landslide activity in a Mediterranean environment. PhD thesis, University of Utrecht, Utrecht

Van Beek LPH, Van Asch TWJ (1999) A combined conceptual model for the effects of fissure-induced infiltration on slope stability. In: Process modelling and landform evolution. Lecture Notes Earth Sci 78:147–167. doi:10.1007/BFb0009716

Van Genuchten MT (1980) A closed form equation for predicting the hydraulic conductivity of unsaturated soils. Soil Sci Soc Am J 44:892–898

Van Westen CJ, Van Asch TWJ, Soeters R (2006) Landslide hazard and risk zonation – why is it still so difficult? Bull Eng Geol Environ 65:167–184

Voellmy A (1955) Uber die Zerstorunskraft von Lawinen (On breaking force of avalanches). Schweiz Bauztg 73:212–285

Vulliet L (2000) Natural slopes in slow movement. In: Zaman G, Gioda G, Booker J (eds) Modeling in geomechanics. Wiley, Chichester

Wang G, Sassa K (2001) Factors affecting rainfall-induced landslides in laboratory flume tests. Géotechnique 51(7):587–599

WP-WLI (1995) A suggested method for describing the rate of movement of a landslide. Bull Int Assoc Eng Geol 52(1):75–78

Part II
Methodologies to Assess the Impact of the Natural Hazards on the Society in Terms of Risks

Chapter 5
Methods for Debris Flow Hazard and Risk Assessment

Byron Quan Luna, Jan Blahut, Mélanie Kappes, Sami Oguzhan Akbas, Jean-Philippe Malet, Alexandre Remaître, Theo van Asch, and Michel Jaboyedoff

Abstract Debris flow events yield a threat to different components of mountainous environments not only as the result of the process evolution but of the interaction with human systems and their coupled vulnerabilities. A variety of models exists

B. Quan Luna
Faculty of Geo-Information Science and Earth Observation (ITC), University of Twente, Hengelosestraat 99, NL-7514 AE Enschede, The Netherlands

NGI, Norwegian Geotechnical Institute – ICG, International Centre for Geohazards, Sognsveien 72, NO-0855 Oslo, Norway

J. Blahut • S.O. Akbas
Department of Environmental and Territorial Sciences, University of Milano-Bicocca, Piazza della Scienza 1, IT-20126 Milan, Italy

Department of Engineering Geology, Institute of Rock Structure and Mechanics, Academy of Sciences of the Czech Republic, V Holešovičkách, CZ-4118209 Prague, Czech Republic

Department of Civil Engineering, Gazi University, Maltepe, TR-06570 Ankara, Turkey

M. Kappes
Department of Geography and Regional Research, Geomorphic Systems and Risk Research Unit, University of Vienna, Austria Universitätsstraße 7, AU-1010 Vienna, Austria

The World Bank, Urban, Water and Sanitation/Disaster Risk Management Unit, 1818 H St. NW, Washington, DC 20433, USA

J.-P. Malet (✉) • A. Remaître
Institut de Physique du Globe de Strasbourg, CNRS UMR 7516, Université de Strasbourg/EOST, 5 rue René Descartes, F-67084 Strasbourg Cedex, France
e-mail: jeanphilippe.malet@unistra.fr

T. van Asch
Faculty of Geosciences, Department of Physical Geography, Utrecht University, Heidelberglaan 2, 3584 CS, The Netherlands
e-mail: aschtheo@gmail.com

M. Jaboyedoff
Institute of Geomatics and Risk Analysis, University of Lausanne, Amphipôle, CH-1015 Lausanne, Switzerland

T. van Asch et al. (eds.), *Mountain Risks: From Prediction to Management and Governance*, Advances in Natural and Technological Hazards Research 34,
DOI 10.1007/978-94-007-6769-0_5,

for characterising the hazard that the different mass-flow phenomena present. In the case of dynamic run-out models, they are able to forecast the propagation of material after the initial failure and to delineate the zone where the elements at risk will suffer an impact with a certain level of intensity. The results of these models are an appropriate input for vulnerability and risk assessments. An important feature of using run-out models is the possibility to perform forward analyses and forecast changes in hazards. However, still most of the work using these models is based on the calibration of parameters doing a back calculation of past events. Given the number of unknown parameters and the fact that most of the rheological parameters cannot be measured in the laboratory or in the field, it is very difficult to parameterize the run-out models. For this reason the application of run-out models is mostly used for back analysis of past events and very few studies attempts to achieve a forward modelling with the available run-out models. A reason for this is the substantial degree of uncertainty that still characterizes the definition of the run-out model parameters. Since a variety of models exists for simulating mass-flows and for identifying the intensity of the hazardous phenomena, it is important to assess these models, perform a parameterization and reduce their uncertainties. This will enable to improve the understanding to assess the hazard and will provide the link with vulnerability curves that will lead eventually to generate risk curves and quantify the risk.

This chapter describes the state of the art in dynamic run-out modelling focusing on continuum depth-average models and includes a quantitative risk assessment using run-out models in a specific study sites. The methodology used in the analysis consisted of several components, such as a detailed analysis of rainfall return periods (10, 50, 100 years return period), modelling of rainfall-runoff, modelling of the run-out of the debris flows, and application of debris flow height and impact pressure vulnerability curves and the generation of risk curves based on the economic losses. A special consideration was given to the entrainment mechanism. The increase of volume once a failed mass is in movement due to entrainment enhances the mobility of the flow and can significantly influence the size of the potential impact area.

Abbreviations

QRA	Quantitative Risk Assessment
1-D	One dimension
2-D	Two dimensions
PDF	Probability density function
DEM	Digital elevation model

5.1 Introduction

Run-out analysis can be defined as the forecast of mass-movement displacements whatever the type of deformation mechanism (slow-moving landslides which deformation pattern is mostly located at the shear bands, fast-moving debris flows and mudflows which deformation pattern is mostly located over the entire moving profile, or rockfalls which deformation is mainly controlled by the rolling or falling of individual blocks).

In recent times, numerical simulation models for assessing run-out has been increasingly used for the development of risk and hazard maps. The goals of computer modelling should be to assess the possible spatial extension and the temporal occurrence in advance with a range of potential scenarios to inform local populations so they can respond in reasonable ways and to design proper strategies for mitigation. A variety of models exist for simulating mass-flows and for characterizing the hazard. Defining the spatial extent of the endangered area is very important for Quantitative Risk Assessment (QRA). It requires accurate forecast of the run-out behaviour (e.g. how far and how fast will the mass travel?) expressed through quantitative spatially distributed parameters that include the run-out distance, the run-out width in the spreading zone, the displacement rate (e.g. velocity), the thickness of the moving mass and the impact pressure (Hungr et al. 2005).

However, run-out modelling is rather complicated because of the various physical processes that happen during an event. These processes depend on the characteristics of the source area, on the type of triggering process, on the characteristics of the path and on the type and volume of material incorporated or deposited during the travel. Some of these complex processes are erosion, entrainment and deposition, changes in the rheology during one event, layering and formation of pulses and damming and breaching inside the channels.

This section focuses on the hazard and risk assessment methods developed recently for characterizing the danger caused by one type of fast-moving mass-movements (e.g. debris flows). The current approaches for debris flow run-out modelling are first presented while describing the state of the art in and focusing on continuum depth-average models. Special attention is given to the new developments and difficulties inside the modelling of debris flows at a local and medium scale; while assessing the deterministic characteristics of these models and the possibility to obtain direct intensity values make the run-out models an interesting tool to be used in this type of analyses.

5.2 Current Approaches in Debris Flow Run-Out Modelling for QRA

A very important part of any hazard risk assessment is a quantitative estimate of post-failure motion defining distance, material spreading and velocity through run-out modelling. The methods and tools used in run-out analyses are very different in scale of applications: empirical or statistical techniques are generally applied to predict susceptibility at the regional scale with the purpose of hazard mapping, while process-based approaches are applied at the local scale with the purpose of designing engineered mitigation works and early-warning systems.

5.2.1 Empirical Run-Out Models

Empirical methods for assessing landslide run-out are usually based on extensive amounts of field observations and on the analysis of the relationships between the run-out distance and different landslide mechanisms, their morphometric parameters, the volume of the landslide mass, and the characteristics of the terrain. Empirical approaches are based on simplified assumptions, and although they lead to generalized results they are relatively easy to apply over larger areas. Empirical methods can be subdivided into: heuristic methods, the mass-change method and the angle of reach method.

- Heuristic methods involve the identification and mapping of landslide deposits that provides a direct measurement of the distance travelled in the past. The extent of both ancient and recent landslide deposits is the basis for defining future travel distances. Field work and photo interpretation are classical procedures used to define the spatial distribution and extent of past landslides. The margin of the landslide deposits give an indication of the maximum reach that a landslide is able to reach in the present landscape (Hungr et al. 2005).
- The mass-change method is based on the phenomenon that, as the landslide debris moves down slope, the initial volume/mass of the landslide is being modified through loss or deposition of materials, and that the landslide debris halts when the volume of the actively moving debris becomes negligible (Cannon and Savage 1988). The average mass/volume-change rate of landslide debris was established by dividing the volume of mobilized material from the landslide by the length of the debris trail.
- The angle of reach method is based on the angle of the line connecting the crest of the landslide source to the distal margin of the displaced mass also called the fahrböschung angle (Heim 1932). This angle is also used as an index of efficiency for the dissipation of energy. Once the release source, volume and direction of the flow are known, these methods can estimate the length of the run-out. It is the most commonly used method in assessing the run-out of landslides due to its simplicity and straightforward results. One of the most well-known

examples of the application of this method is done by Corominas (1996) who conducted a detailed study on the influence of various factors that affect the angle of reach using landslide records. He showed a linear correlation between volume and angle of reach for all types of failures. Regression equations for calculating the angle of reach of each landslide type were developed by Corominas (1996), Rickenmann (1999) and Devoli et al. (2009).

The spreading pattern of flow, entrainment and deposition can also be estimated. This requires more detailed morphological parameters accounting exclusively for site-specific conditions. Similar to the volume-angle of reach approach, statistical correlations between volume and deposit area have also been proposed by Iverson et al. (1998). These methods provide estimates of aerial extent for accumulation zones. Other correlations have been developed for estimating certain intensity parameters, including debris flow velocity and discharge (Rickenmann 1999).

A common problem with the empirical methods is that the scatter of the data is too large for anything but very preliminary predictions of the travel distance. The flexibility of the empirical methods allows them to be applied in local to medium-scale landslide susceptibility and hazard maps but as they do not provide kinematic parameters (velocity, kinetic energy) of the landslides these approaches can be hardly applied to site-specific analyses and in QRA.

5.2.2 Physically-Based Dynamic Run-Out Models

The analytical models are based on hydro-mechanics and solve the equations of mass and momentum in a close-form or numerically way. Analytical models are also called dynamic models and perform a time-step solution for a unique geometry and a described material. Dynamic models are physically-based and simulate the movement of the flow using the constitutive laws of fluid mechanics in one (1-D) or two dimensions (2-D). Most models are based on a continuum approach that considers the loose unsorted material and multiphase moving mass of a debris flow as a continuum. A continuum approach enhances the possibility to model the dynamics of debris flows using an 'equivalent' fluid, whose rheological properties are such that the bulk behavior of the numerically simulated flowing mass can approximate the expected bulk behavior of the real mixture of the solid and fluid phases (Hungr and McDougall 2009). Savage and Hutter (1989) developed a continuum mechanical theory (known also as the Savage and Hutter model) capable of describing the evolving geometry of a finite mass of a granular material and the velocity distribution as it slides down an inclined plane (Pudasaini and Hutter 2007). In the Savage and Hutter model, the mass and momentum are averaged over the depth and a scaling analysis is performed with respect to the aspect ratio of the flowing mass, considered to be small. This allows modeling the flow by the Saint-Venant approximation of the shallow water equations derived in a reference frame linked to an inclined plane (Bouchut et al. 2008). The depth-averaged shallow water

equation approach using different solvers has been applied commonly for numerical simulations of rapid mass movements over complex topographies (Chen and Lee 2000; Iverson and Denlinger 2001; Pouliquen and Forterre 2002; Crosta et al. 2003; Mangeney-Castelnau et al. 2005; Pitman and Le 2005; Pudasaini and Hutter 2007; Mangeney et al. 2007a, b; Pastor et al. 2009; Hungr and McDougall 2009; Medina et al. 2008; Begueria et al. 2009; Christen et al. 2010). Depth averaging allows representing the rheology of the flow as a single term that expresses the frictional forces that interact at the interface between the flow and the bed path. The most common rheologies used in the dynamic models are the 'Coulomb' or frictional resistance (Hungr and McDougall 2009); the 'Voellmy' or frictional-turbulent resistance (Voellmy 1955); the 'Bingham' (or 'Herschel-Bulkey') or visco-plastic resistance (Coussot 1997; Malet et al. 2004) and the 'Quadratic' resistance (O'Brien et al. 1993).

A common classification of the physically-based dynamic run-out models distinguishes: (1) models based on the solution dimension simulating motion on 2D/3D topography; (2) models based on the solution reference frame that can be formulated in Eulerian vs. Lagrangian reference coordinate systems; and (3) models based on the basal rheology.

5.2.2.1 Models Based on the Solution Dimension (1D or 2D)

Dynamic models use an approach known as depth-averaging, in which the governing mass and momentum balance equations are integrated with respect to the flow depth. Stresses are assumed to increase linearly with depth below the top surface of the flow, which is assumed to be stress free, and shear stresses in the depth-wise direction are neglected (Savage and Hutter 1989). This is based on the assumption that the depth varies gradually and is small relative to the length and width of the landslide. Depth-averaging combined with the shallow flow assumption essentially eliminates one dimension, the depth-wise dimension, from the governing mass and momentum balances. One dimensional models analyze the movement considering the topography as a cross-section of a single pre-defined width while two dimensional models makes the analysis considering the topography in plan and cross section.

5.2.2.2 Models Based on the Solution Reference Frame (Eulerian or Lagrangian)

The equations of motion can be formulated in two different frames of reference: Eulerian or Lagrangian. A Eulerian reference frame is fixed in space, analogous to an observer standing still as a landslide passes. Models formulated in an Eulerian framework require the solution of a more complex form of the governing equations using a dense, fixed computational grid. The Eulerian approach is the conventional method in computational fluid dynamics. A Lagrangian reference frame moves with

the local velocity, analogous to an observer riding on top of a landslide. This method simplifies the governing equations and does not sacrifice computational resources in void zones. When using the Lagrangian reference (also called material reference), the material velocity and acceleration are expressed by Eqs. 5.1 and 5.2 respectively:

$$V(X,t) = \frac{D\zeta(X,t)}{Dt} \tag{5.1}$$

and

$$A(X,t) = \frac{DV(X,t)}{Dt} = \frac{D^2\zeta(X,t)}{Dt} \tag{5.2}$$

where V is the velocity; A is the acceleration; X is the referential position; ζ is the motion that can be viewed as a transport of points from the reference configuration to the current configuration during a specific time interval [0, t]. Then, the displacement of a particle located at "X" is expressed with Eq. 5.3:

$$U(X,t) = \zeta(X,t) - X \tag{5.3}$$

It is cumbersome to pinpoint the particle reference position X at $t = 0$ and recognize its exact trajectory. For this reason, the Eularian reference (also known as spatial reference) is commonly applied. In the Eularian reference, the attention is given to a certain region in space and the material motion is observed within this region as time proceeds. The quantities of interest are expressed in terms of the current position x (or spatial coordinates) and time t. The spatial velocity and acceleration can be described with Eqs. 5.4 and 5.5 respectively:

$$v = v(x,t) \tag{5.4}$$

and

$$a = a(x,t) \tag{5.5}$$

The displacement u can then be expressed with Eq. 5.6:

$$u(x,t) = x - \zeta^{-1}(x,t) \tag{5.6}$$

5.2.2.3 Models Based on the Basal Rheology

The rheology of the flow is expressed as the resistance force (S_f) that interact inside the flow and at the interface between the flow and the bed path. The most common rheologies used in the dynamic models are: the "Frictional" (or "Coulomb") resistance (Hungr and McDougall 2009), the frictional-turbulent "Voellmy" resistance

Table 5.1 Most common flow resistance terms used in dynamic run-out models

Rheology (basal)	Description	Flow resistance term "Sf"
Frictional (Coulomb)	Resistance based on the relation of the effective bed and normal stress at the base and the pore fluid pressure (Hungr and McDougall 2009)	$Sf = \tan\varphi'$ $\tan\varphi' = (1 - r_u)\tan\varphi$ – Sf is the unit base resistance; – r_u is the pore-fluid pressure ratio; – φ is the dynamic basal friction angle.
Voellmy	Resistance that features a velocity-squared resistance term (turbulent coefficient ξ) similar to the square value of the Chezy resistance for turbulent water flow in open channels and a Coulomb-like friction (apparent friction coefficient μ) (Voellmy 1955).	$Sf = \left[\tan\varphi' + \frac{u^2}{\xi h}\right]$ – Sf is the unit base resistance; – $\tan\varphi' = \mu$ is the apparent friction coefficient; – u is the flow velocity (m/s); – ξ is the turbulent coefficient (m/s^2).
Bingham	Resistance that is a function of flow depth, velocity, constant yield strength (τ_c) and dynamic viscosity (η) (Coussot 1997).	$Sf = \frac{1}{\rho g h}\left(\frac{3}{2}\tau_c + \frac{3\eta}{h}u\right)$ – Sf is the unit base resistance; – τ_c is a constant yield strength due to cohesion; – ρ is the density of the flow; – η is the viscosity parameter
Quadratic	Resistance that incorporates a turbulent contribution to the yield and the viscous term already defined in the Bingham equation (O'Brien et al. 1993).	$Sf = \frac{\tau_c}{\rho g h} + \frac{K\eta}{8\rho g(h)^2}u + \frac{n^2(u)^2}{(h)^{4/3}}$ – Sf is the unit base resistance; – τ_c is the resisting shear stress; – u is the depth-averaged velocity; – h is the flow depth; – η is the viscosity of the fluid, – *K* is a resistance parameter that equals 24 for laminar flow in smooth, wide, rectangular channels, but increases with roughness and irregular cross sections; – n is the Manning coefficient value that takes into account the turbulent and dispersive components of flow.

(Voellmy 1955), the visco-plastic "Bingham" (or "Herschel-Bulkey") resistance (Coussot 1997; Malet et al. 2004), the "Quadratic" resistance (O'Brien et al. 1993) (Table 5.1) A thorough description of rheologies can be found in Naef et al. (2006).

5.2.2.4 Existing Dynamic Run-Out Models

Several dynamic run-out models have been developed in the past. These models have evolved from simple hydrodynamic models to more complex models that include various methods accounting for internal strength, entrainment and rheology variations. Table 5.2 classifies some commonly used run-out dynamic models. Some

Table 5.2 An overview of several 2D dynamic numerical run-out models

Model	Rheology	Solution approach	Reference frame	Change of rheology	Entrainment rate
MADFLOW (Chen and Lee 2000)	Frictional, Voellmy and Bingham	Continuum integrated	Lagrangian with mesh	No	Defined
TOCHNOG (Crosta et al.2003)	Frictional (elastoplastic model)	Continuum differential	Differential (adaptive mesh)	Yes	Process based
RAMMS (Christen et al.2010)	Voellmy	Continuum integrated	Eularian	Yes	Process based and defined
DAN3D (Hungr and McDougall 2009)	Frictional, Voellmy and Bingham	Continuum integrated	Lagrangian meshless	Yes	Defined
FLATMODEL (Medina et al.2008)	Frictional and Voellmy	Continuum integrated	Eulerian	No	Process based
SCIDDICA S3-hex (D'Ambrosio et al. 2003)	Energy based	Cellular automata	Eulerian	No	Process based
3dDMM (Kwan and Sun 2006)	Frictional and Voellmy	Continuum integrated	Eulerian	Yes	Defined
PASTOR model, (Pastor et al.2009)	Frictional, Voellmy and Bingham	Continuum integrated	Lagrangian meshless	Yes	Defined
MassMov2D (Begueria et al.2009)	Voellmy and Bignham	Continuum integrated	Eulerian	Yes	Defined
RASH3D (Pirulli and Mangeney 2008)	Frictional, Voellmy, Quadratic	Continuum integrated	Eularian	No	No entrainment rate is used
FLO-2D (O'Brien et al.1993)	Quadratic	Continuum integrated	Eularian	No	No entrainment rate is used
TITAN2D (Pitman and Le 2005)	Frictional	Continuum integrated	Lagrangian with mesh	No	No entrainment rate is used
PFC (Poisel et al. 2008)	Inter-particle and particle wall interaction	Solution of motion of particles by a distinct element method	Distinct element method	No	No entrainment rate is used
VolcFlow (Kelfoun and Druitt 2005)	Frictional and Voellmy	Continuum integrated	Eulerian	No	No entrainment rate is used

of these models include entrainment rates in their calculations and others neglect this process. The ordering of the models was based on the implementation and scheme of the entrainment rates inside the models: in the 'pre-defined entrainment rate', the amount of entrained material is specified by the user while in the 'process-based entrainment rate', the amount is calculated by a prescribed algorithm that considers the material properties. Other characteristics of the models are also summarized such as the possible rheology, the solution approach, the reference frame and the possibility of variable rheology along the flow path.

Most of the above mentioned models were applied in an important benchmarking exercise on landslide debris run-out and mobility modelling that was carried out in 2007 at the International Forum on Landslide Disaster Management. The main goal of this exercise was to assess whether the field of run-out modelling was on its way towards establishing some degree of commonality among different methods used by various parties and to highlight the main progresses in that topic. In that exercise, 13 research groups that work on the topic of run-out analysis participated in performing simulations of 12 different case studies. The participants were able to select which model and case study was most convenient based on their resources. The main results were presented in the forum and also discussed in a round table. The main key points during that discussion were that:

- Run-out modelling is very sensitive to the topography and the resolution of the computational domain. Mesh refinements methods will help to improve the modelling results.
- Run-out models should be computationally efficient.
- The momentum-based formulation in continuum models is still the most reliable approach for run-out modelling.
- The presented models are consistent in the use of Eulerian and Lagrangian approaches. Although both methods have their advantages and disadvantages, they are viable to use and promising.
- Run-out models can be accurate when used for a back calibration of a well documented event but inconsistencies are evident when performing a forward analysis.
- More data from real landslides is needed to refine the models and their parameterization.
- It is needed to gain more confidence in the selection of suitable rheological models and their parameters for different types of landslides.

5.2.3 Recent Applications of Debris Flow Run-Out Models for QRA

Different approaches have been implemented for QRA using dynamic run-out models. Bell and Glade (2004) performed a quantitative risk analysis (risks to life) in NW-Iceland where the hazards were based on empirical and process modelling

that resulted in specific run-out maps. The hazard zones were determined based on the recurrence interval of the respective processes (e.g. debris flows, rockfalls). Different vulnerability levels were incorporated into a consequence analysis that included elements at risk; spatial and temporal probabilities of impact and the occurrence of the event. Calvo and Savi (2008) proposed a method for a risk analysis in a debris flow-prone area in Ardenno (Italian Alps), utilizing a Monte Carlo procedure to obtain synthetic samples of debris flows. To simulate the propagation of the debris flow on the alluvial fan, the FLO-2D model (O'Brien et al. 1993) was applied and Probability Density Functions (PDFs) of the outputs of a model (forces) were obtained. Three different vulnerability functions were adopted to examine their effect on risk maps. Muir et al. (2006) presented a case study of QRA to a site-specific natural terrain in Hong Kong, where various scenarios were generated with different source volumes and sets of rheological parameters derived from the back analyses of natural terrain landslides in Hong Kong. Run-out modelling was performed using the Debris Mobility Model (DMM) software developed by the Geotechnical Engineering Office (Kwan and Sun 2006), which is an extension of the DAN model developed by Hungr et al. (2005). They derived probability distributions from past events run-outs and calculated the probability distribution of debris mobility for each volume class. The vulnerability was derived from the landslide volume, location of the elements at risk and the protection a facility can offer. Individual risk was calculated as the summation of the product of the frequency of a flow affecting the facility and the vulnerability of the most vulnerable individuals for each of the scenarios. Castellanos (2008) performed a local risk assessment based on historical data of landslides in Cuba. Run-out simulations were carried out with the MassMov2D model (Begueria et al. 2009) for 12 potential hazard zones. Vulnerability curves based on the depth of the flow and the conditions of the buildings were generated using detailed building typology characteristics. Economic risk values were computed for three scenarios. Zimmerman (2005) described the Switzerland's approach for risk management using the Sörenberg debris flow as an example. For the Sörenberg event, hazard maps were prepared according to three probability classes scenarios. Debris-flow run-out was simulated using a random walk approach (Gamma 2000) and applying a simple model that assumes that the motion is mainly governed by two frictional components: a sliding friction coefficient and a turbulent friction coefficient that is determined by a Chezy-type relation (Rickenmann 1999). Results of the modelling were displayed as intensity maps. Federal recommendations provide definite criteria for the intensity classes which are based on the height and the velocity of the flow. Jakob and Weatherly (2005) quantified debris flow hazard and risk on the Jonas Creek fan in Washington, USA constructing frequency-magnitude graphs to build different return period scenarios as an input to a debris flow run-out model. The FLO-2D model was used to calculate maximum flow depths and velocities in order to assess the hazard. Intensity maps were developed based on the outputs of each modeled scenario. Potential deaths were calculated assuming that in the high intensity areas the vulnerability is equal to 1, while the vulnerability is equal to 0

in the medium and low intensity zones. In terms of risk management, Crosta et al. (2005) carried out a cost-benefit analysis for the village of Bindo in the Valsassina valley (Central Pre-alps, Italy). They identified different mitigation plans such as a defensive structure, monitoring and a combination of both. The run-out was simulated with the quasi-three-dimensional finite element method of Chen and Lee (2000) in the Lagrangian frame of reference. The different scenarios were compared with a scenario where no mitigation action was introduced. A cost-benefit analysis of each scenario was performed considering the direct effect on human life, houses and lifelines.

Dynamic run-out models can be of practical assistance to quantify the hazard and its consequences. These models outputs can be used in a hazard analysis to estimate the spatial probability of the flow affecting a certain place with detail, such as the travel distances, the velocities and impact pressures and the deposition patterns. Even though, quantitative information for landslides is difficult to obtain and uncertainties arise due to the large variability in landslide types, to the difficulty in quantifying landslide magnitudes and to the lack of substantial historical damage databases (van Westen et al. 2006).

5.3 Empirical Estimates of Debris Flow Run-Out Parameters for Regional-Scale Susceptibility and Hazard Assessments

Regional-scale analysis which includes scales in the range from 1:10.000 to 1:50.000 can provide an initial overview of the hazard in a specific area. The goal of a medium scale analysis is to identify all the potentially unstable areas as accurate as possible and the down-slope regions probably affected by the flow. This analysis should be used as a first assessment for the potential impact zones and to give an indication where further local studies should be carried out with more detail (van Westen et al. 2006).

5.3.1 The Flow-R Model: Description

A well-known simple method for an empirical determination of the run-out is the Fahrböschung model (Heim 1932), later on translated as angle of reach model (Corominas 1996). It is the angle between an imaginary line connecting the source area with the furthest point of the run-out and the horizontal plane. The angle correlates with the volume: the higher the volume the lower the angle and thus the longer the run-out distance. As a relationship exists between the volume and the frequency of occurrence (high magnitude events with high volumes are less frequent than low magnitude events), the angle of reach is indirectly linked to

the temporal frequency of occurrence (Corominas and Moya 2008). By means of statistical analyses of past events (e.g. rockfalls in the case of Heim 1932), the angles for events of certain volumes can be determined and used for run-out assessments of future mass movements if the potential source areas are known. Schreve (1968) called this angle the 'equivalent coefficient of friction' (Corominas 1996).

This simple approach is used in the recently developed Flow-R model that allows rockfalls and debris flow analyses at regional scales (Horton et al. 2008). The method consists in (1) the identification of the source areas, and (2) the run-out modeling. The source identification is based on the topographical assumption that from a concave slope located below a sufficiently large catchment area and exhibiting a certain slope angle, debris flows will potentially initiate (Horton et al. 2008). The run-out modeling is based on then use of a spreading algorithms (O'Callaghan and Mark 1984; Tarboton 1997; Quinn et al. 1991; Holmgren 1994). For the determination of the run-out distances, the angle of reach principle is implemented to serve as a measure for the friction loss ('constant friction loss angle'). It is included as a parameter describing the constant energy loss in the computation of the kinetic energy of the flow in each pixel (Eq. 5.7):

$$E_{kin}^{i} = E_{kin}^{i-1} - \Delta E_{pot}^{i} - E_{loss}^{i} \tag{5.7}$$

where E_{kin} is the kinetic energy, E_{pot} is the change in potential energy, E_{loss} is the constant loss and i is the time step. Hereby, the constant friction loss angle is subtracted from the actual angle between the source pixel and the pixel towards which the mass is moving. The maximum kinetic energy of the flow can be limited to a realistic velocity of around 15 $m{\cdot}s^{-1}$ for debris flows (Horton et al. 2008). The flow stops as soon as the kinetic energy drops below zero. Finally, the spreading algorithm is complemented by considering the inertia of the flow, e.g. the way a flow reacts on changes in the flow direction. For each single pixel, the run-out is computed and the maximal spatial probability of being affected is outputted.

5.3.2 *Use of the Flow-R Model for Characterizing Debris Flow Susceptibility: The Barcelonnette Case Study*

A first application of the Flow-R consisted in a debris flow susceptibility analysis of the Barcelonnette Basin (Southeast France) which is heavily prone to debris flows with ca. 100 events between 1850 and 2004. However, the complete information including source area and run-out as well as an assessment of the initial and the final volume is only available for one debris flow event. This refers to the 2003 event in the Faucon catchment where 4,000–5,000 m^3 were mobilized in the source areas, while after scouring about 8,500 m^3 were deposited on the debris fan (Remaître and Malet 2010); the angle of reach accounts to 14° (Kappes et al. 2011). The high threat indicates the need for a spatial analysis of the debris flow distribution.

Since statistical analyses for the determination of the angle of reach is obviously not possible due to a lack of data, scenarios of high, medium and low frequency were adjusted in an empirical way as described in the following.

First, potential source areas were identified. Second, three qualitative run out scenarios (high, medium and low frequency scenarios) were established based on the following information and assumptions (Kappes et al. 2011): (1) an inventory derived from the mapping of debris flows in consecutive aerial photographs of the time step 1956, 1974, 1982, 1995, 2000 and 2004 (Stummer 2009); the number of events mapped per time step indicates a high frequency (several incidences per year) at low magnitudes; (2) the interpretation of largely documented debris flow events in 2003 at Faucon, and in 1996 and 2002 at Faucon, Sanières and Bourget. Obviously, the first inventory comprises small and very frequent events (several per year) and the second inventory bigger events of an intermediate frequency (an event every several years). To assess the extent of low frequent but high magnitude events the existence of large debris cones was used as an indicator. An adjustment of the angle of reach to the complete longitudinal coverage of especially the Riou Bourdoux torrent (a torrent described as especially dangerous in the literature; Delsigne et al. 2001) was used for this purpose. The iterative adjustment of the angle of reach led to the following three angles for the three scenarios: 11° for the high frequency scenario, 14° for the intermediate frequency scenario and 30° for the low frequency scenario (Fig. 5.1). Although information on the spatial and temporal probability is available, the result is not, strictly speaking, a full hazard assessment but only a susceptibility assessment since no indication is given on the hazard intensity.

5.3.3 Use of the Flow-R Model for Characterizing Debris Flow Hazard: The Valtellina Case Study

The area of Valtellina di Tirano (Italy) is also prone to damaging debris flow events having caused deaths in some recent cases (years 1983 and 1987). For the construction of a regional debris flow hazard map, the susceptibility map of Blahut et al. (2010a) was used as a basis for the calculation. For each susceptibility class, a spatial and temporal probability of debris flow initiation was computed. The spatial probability was expressed as a density of pixels corresponding to debris flow source areas from available inventories in each susceptibility class. To calculate the temporal probability of debris flow initiation, two sets of aerial photographs and related debris flow inventories were compared (1981, 2001). Only the source areas where new debris flow activity was observed between these two periods were introduced in the calculation. An initiation probability map was then calculated by multiplying spatial and temporal probabilities, and this map served as principal input for the Flow-R run-out modelling.

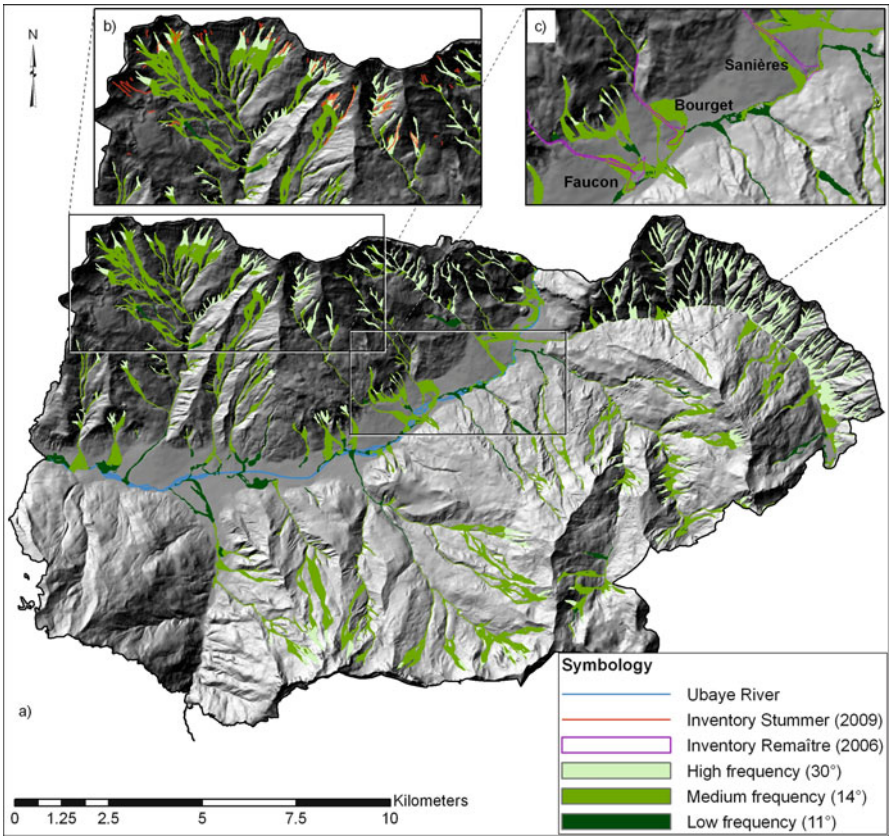

Fig. 5.1 Qualitative debris flow susceptibility scenarios for the Barcelonnette basin (South East France). (**a**) Debris flow susceptibility assessment for the mid-course of the Ubaye River catchment; (**b**) Excerpt of the debris flow susceptibility assessment for the Riou-Bourdoux and La Valette sub-catchments; (**c**) Excerpt of the debris flow susceptibility assessment for the Faucon, Bourget and Sanières sub-catchments

To calibrate the maximum probable debris flow run-out, a well delimited large event from July 1987 was used together with aerial photographs using the edge of alluvial fans where former debris flow activity has been observed. From the calibration phase, the following run-out characteristics were selected: a maximum run-out (shadow) angle of 10°, a maximum limit velocity of debris flow of 15 $m \cdot s^{-1}$ and a Holmgren exponent of 5. Afterwards, a run-out map was calculated for the four highest debris flow hazard initiation classes. A main drawback of a region-scale analysis is that magnitude of particular debris flow remains impossible to calculate. To overpass this problem and to better discriminate the possible different magnitudes (volumes) of debris flows, a qualitative component was added to the hazard map. Three subclasses of spreading direction probabilities were made

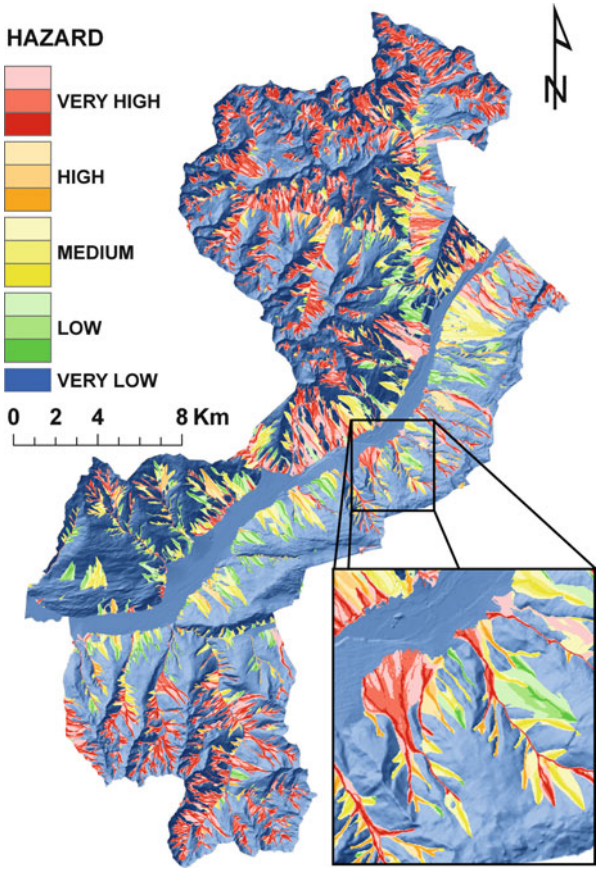

Fig. 5.2 Qualitative debris flow hazard map for the region of Valtellina di Tirano (Central Alps, Italy)

for each run-out class using geometric intervals in order to have a better idea about different run-out of debris flows of different magnitudes. This resulted in a 13-classes hazard map (Fig. 5.2) where higher probabilities of spreading are represented by more vivid colours of each class (Blahut et al. 2010b).

There are many difficulties and uncertainties connected with preparation of a debris flow hazard map on at a region scale. Probably the most important uncertainty arises from the temporal probability analysis. As only two temporal slices are compared, many debris flows source areas could be missed or not recognized. This problem can be over passed by comparing aerial photographs datasets taken with higher frequency and by longer temporal coverage (e.g. 5 datasets in 50 years). As a consequence, less debris flows would be missed and lower error will be connected to the temporal probability. However, no other temporal aerial photographs were available at the time of this analysis, so these errors had to be assumed. Although

the presented approach allows preparation of a hazard map on medium scale, the problem of local controlling factors has to be mentioned. Unlikely, for a study on local/site specific scale, where deterministic modelling and precise calculation of return periods can be performed, on medium scale not enough geotechnical information is available and more assumptions have to be made. Major limitations in the model happen in case of misinterpretation of the reality in the DEM; as a consequence, the spreading areas will contain errors. The multiple flow direction has no physical basis and, as it is regional model, it does not take into account the debris flow volume. However, as it was shown, the magnitude representation can be approximated by reclassification of the spreading direction probabilities.

5.4 Quantitative Estimates of Debris Flow Run-Out Parameters for Site-Scale Susceptibility and Hazard Assessments

Numerical methods for modelling run-out behaviour of landslide debris mainly include fluid mechanical models and distinct element methods. The most common and used approach for this methods is based on continuum mechanics. Continuum fluid mechanics models utilize the conservation equations of mass, momentum and energy that describe the dynamic motion of debris, and a rheological model to describe the material behaviour of the debris. By solving a set of governing equations with a selected rheological model describing the flow properties of the debris, the velocity, acceleration and run-out distance of debris can be predicted (Chen and Lee 2000).

However, most dynamic run-out models assume a constant volume during the motion of the flow, ignoring the important role of material entrained along its path. Consequently, they neglect that the increase of volume can enhance or reduce the mobility of the flow and can significantly influence the size of the potential impact area. Limited work has been done to quantify the entrainment process and only a few have proposed physical explanations for it. One of the reasons is that material entrainment is a complex process and an adequate understanding of the phenomenon is needed to facilitate the development of appropriate dynamic models. A proper erosion mechanism needs to be established in the analyses of debris flows that will improve the results of dynamic modelling and consequently the quantitative evaluation of risk.

This section presents and evaluates the performance of a 1D debris flow model with a material entrainment concept based on limit equilibrium considerations and the generation of excess pore water pressure through undrained loading of the in-situ bed material. The flow is treated as a laminar one-phase material, in which behaviour is controlled by a visco-plastic Coulomb–Bingham rheology. The purpose of developing a 1-D debris flow model that takes into account an entrainment concept was to identify and state the advantages of including entrainment in the calculation of practical debris flow dynamics for hazard analysis.

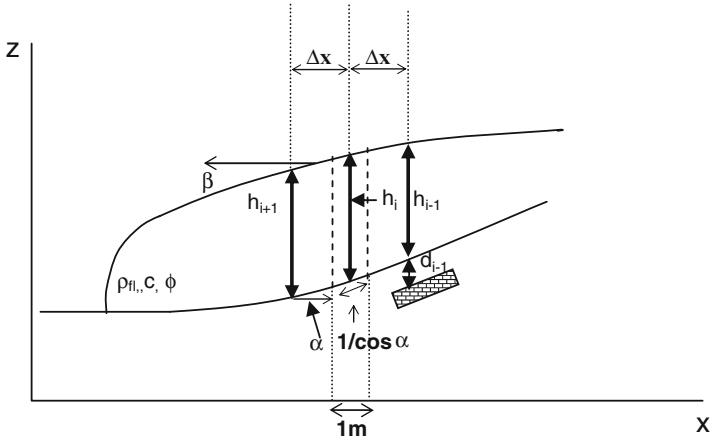

Fig. 5.3 Schematic diagram for the simplified method of limiting equilibrium used in the model and representation of the model parameters

5.4.1 A Dynamic 1D Run-Out Model with Entrainment: Description and Field Application at Faucon

The model proposed here is based on earlier work of van Asch et al. (2004). The proposed approach is a 1D dynamic debris flow model that takes into account entrainment of material from the torrent bed using the concept of undrained loading of the in-situ material. The flow is treated as a laminar one phase, incompressible continuum material. Based on the Savage-Hutter model, the flow can be simulated by numerically solving the system of depth-averaged governing equations composed of the mass balance equation (Eq. 5.8), the momentum conservation equation (Eq. 5.9), and the friction resistance (e.g. Coulomb-Bingham rheological equation; Coussot 1997) (Eq. 5.11). Depth integration is based on the shallow water assumption, which applies where the length of the flowing mass is much greater than the thickness of the flowing mass. In these conditions the vertical velocity of the fluid is small, so that the vertical pressure gradient is nearly hydrostatic (Begueria et al. 2009). The flow is then modelled by a Saint-Venant type system derived in a reference frame linked to an inclined plane (Fig. 5.3).

The mass and momentum can be described with Eqs. 5.8 and 5.9 respectively:

$$\frac{\partial h}{\partial t} + c_x \frac{\partial (hu)}{\partial x} - \frac{\partial d_{sc}}{\partial t} = 0 \tag{5.8}$$

$$\frac{\partial u}{\partial t} + c_x u \frac{\partial u}{\partial x} = g c_x \left[S_x - K \frac{\partial h}{\partial x} - S_f \right] - \frac{\partial u}{\partial t} \frac{\rho_s d_{sc}}{\rho h} \tag{5.9}$$

where h is the flow height in the direction normal to the bed, u is the x component of the velocity, d_{sc} is the scour depth, $c_x = \cos\alpha_x$ is the direction cosine of the bed and α_x is the slope bed angle, which is taken positive when it dips downward in the (positive) x-direction. The momentum equation (Eq. 5.9) is expressed in terms of acceleration (LT^{-2}). The second term on the left side of Eq. 5.9 represents the convective acceleration. The first term on the right side of Eq. 5.9 represents the acceleration due to gravity where S_x is the bed slope gradient. The second term on the right side is the pressure acceleration where K is the earth pressure coefficient, corresponding to the active and passive states in the Rankine's theory. K can have a value of 1 for a perfect fluid, but can vary greatly for plastic materials and ranges between two extreme values corresponding to the active and passive states: $K_a \leq 1 \leq K_p$ (Eq. 5.10).

$$K_a = \frac{1 - \sin\varphi}{1 + \sin\varphi}$$
$$K_p = \frac{1 + \sin\varphi}{1 - \sin\varphi} \tag{5.10}$$

where φ is the internal friction angle of the mixture. The third term on the right side of Eq. 5.9, S_f is the flow resistance due to frictional stress with the bed. The fourth and last term on the right side of Eq. 5.9 is the entrainment rate.

The resisting forces S_f (Eq. 5.9) are dependent on the rheology of the material which controls the flow behavior and represents the bed shear stress of the flow. One-phase, depth-integrated models commonly assumes homogeneous and constant flow properties. A Coulomb-Bingham rheology model (Eq. 5.11) is applied to determine a solution to the resisting force. The model assumes a linear stress–strain rate relationship once the yield strength is exceeded. Other types of rheologies can be integrated to the model giving the possibility to simulate other types of flows.

Mud and muddy debris flows (characterized by clay-shale materials with >10 % clay in the grain size) have often been modeled as viscoplastic materials, e.g. as Bingham rheology with constant yield strength and viscosity (Begueria et al. 2009). The Coulomb-Bingham rheology can be described as:

$$S_f = \tan\varphi' + \frac{1}{\rho g h}\left(\frac{3}{2}\tau_c + \frac{3\eta}{h}u\right) \tag{5.11}$$

where φ' is an apparent or basal of the flow friction angle, η is the dynamic viscosity (closely related to the percent concentration of solids) and τc is a constant yield strength due to cohesion (kPa). Mangeney et al. (2007a, b) introduced a curvature radius, R_x, which describes local convexities or concavities in the slope profile and which influences the flow friction (Eq. 5.12).

$$\frac{1}{R_x} = \frac{\partial^2 h}{\partial x^2} \tag{5.12}$$

The curvature radius is incorporated in Eq. 5.11 and can be replaced in the term gS_f (Eq. 5.9) as follows in Eq. 5.13:

$$gS_f \Rightarrow \left(g - \frac{u^2}{R_x}\right)\tan\varphi' + \frac{1}{\rho h}\left(\frac{3}{2}\tau_c + \frac{3\eta}{h}u\right) \tag{5.13}$$

The internal pore fluid pressure is a transient property that is coupled to the normal stress and can dissipate during motion, making it extremely difficult to model (Begueria et al. 2009). Although some depth-averaged models have been developed that take into account the temporal evolution and spatial variation of pore fluid pressures (Iverson and Denlinger 2001; Pitman and Le 2005), in the presented model the pore pressure ratio (ratio pore water pressure/normal stress) is assumed to be constant. This allows coupling the pressure dissipation into only one term: $\tan\varphi'$ (tangent of the apparent friction angle).

A loading of the bed deposits is generated when the moving mass flows on top. The model calculates this applied loading of the in-situ soil (Fig. 5.3) through the changes of vertical normal stress (Eq. 5.14) and the shear strength (Eq. 5.15) caused by the flow:

$$\Delta\sigma = \rho_{fl} gh \cos^2\alpha \tag{5.14}$$

$$\Delta\tau = \rho_{fl} gh \sin\alpha \cos\alpha \tag{5.15}$$

where ρ_{fl} is the density of the flow material, g is the gravity force, h is the height of the flow and α is the slope angle. Because of this loading, volume reduction and an increase in pore water pressure takes place. This increase in pore water pressure (Eq. 5.16) is calculated based on the Skempton (1954) equation that expresses pore water pressure in an undrained triaxial test and modified by Sassa (1988) for an undrained direct shear test. Assuming that the soils along the shear zone inside the channel deposits are subjected to an undrained direct shear, Eq. 5.16 can then be applied:

$$\Delta p = B_D(\Delta\sigma + A_D\Delta\tau) \tag{5.16}$$

where A_D and B_D are the pore water pressure parameters in the direct shear state.

Based on laboratory compressibility tests and assuming that the soils are not anisotropic, Sassa et al. (1985) proposed that the pore fluid pressure parameter B_D is approximately the same with the B pore fluid pressure parameter proposed by Skempton. B_D value is affected by the loaded stress level and its values are very sensitive to the degree of saturation. In saturated soils, the compressibility of the soil skeleton is almost infinitely greater than that of the pore fluid and essentially all of a stress increment applied to a saturated soil is carried by the pore fluid; $B_D = 1$. In dry soils, the compressibility of the pore air is almost infinitely greater than the compressibility of the soil skeleton, and thus essentially all of the increment in total

stress applied to the dry soil element is carried by the soil skeleton; $B_D = 0$. The pore fluid pressure parameter A_D value changes with strain and probably the A_D value may increase after failure due to the crushing of grains, but dissipation of pore fluid pressure may take place because shear zone is not as great as the compressed zone by the loaded normal stress. In general soft, loose soils have high values of A_D and the higher the shear strain the higher the value of A_D. It is assumed that during an intense rain event, a ground water table may develop in the surface bed layer, and thus because water may flow perpendicular to the in-situ soil, pore fluid pressure is calculated by Eq. 5.17:

$$p_{ini} = \rho_w g d_w \cos^2\alpha \tag{5.17}$$

The total pore fluid pressure is then calculated by Eq. 5.18:

$$p_{tot} = p_{ini} + \Delta p \tag{5.18}$$

New stresses at the bottom of the in-situ soil are then computed by Eqs. 5.19 and 5.20:

$$\sigma_{tot} = (\rho_{fl} g h + \rho_{bot} g d) \cos^2\alpha \tag{5.19}$$

$$\tau_{tot} = (\rho_{fl} g h + \rho_{bot} g d) \sin\alpha \cos\alpha \tag{5.20}$$

where ρ_{bot} is the density of the in-situ soil and d is the depth of the erodible layer. The safety factors at the bottom (Eq. 5.21) and at the top (Eq. 5.22) of the in-situ soil are calculated as follows:

$$F_{bot} = \frac{c_{bot} + (\sigma_{tot} - p_{tot}) \tan\delta_{bot}}{\tau_{tot}} \tag{5.21}$$

$$F_{top} = \frac{c_{bot} + (\Delta\sigma - \Delta p) \tan\delta_{bot}}{\Delta\tau} \tag{5.22}$$

where c_{bot} is the cohesion and δ_{bot} is the friction angle of the in-situ soil. In the case where F_{top} and $F_{bot} < 1$, then d_{sc}, which is the thickness of the failed layer, equals the total thickness of the in-situ material d. In the case where $F_{bot} < 1$ and $F_{top} > 1$, then d_{sc} is again total thickness of in-situ material d and in the case where $F_{bot} > 1$ and $F_{top} < 1$, a portion of d will fail and can be calculated with Eq. 5.23:

$$d_{sc} = \frac{1 - F_{top}}{F_{bot} - F_{top}} d \tag{5.23}$$

This computed failed mass is then incorporated to the flow enlarging its volume and changing its momentum.

The criteria chosen to compare the simulation results with the observational data of the 2003 debris flow event at Faucon were (1) the flow velocity, (2) the deposit heights and (3) the run-out distances. In our case, the calibration was completed through back analysis and was based on a trial and error adjustment of the input parameters defining the flow resistance and entrainment process. The inputs were adjusted until the computed criteria patterns matched as close as possible the real event. The initiation area was distributed in uniform columns of 10 m and a total released volume of 8,443 m^3 was introduced. A Bingham rheology was used to model the event. The parameters that best fitted the event were $\tau_y = 210$ Pa and $\eta = 63$ Pa·s., which matches with a 52–53 % of solid concentration by volume measured for the event (Remaître and Malet 2010). A constant Rankine's earth pressure parameter of one assuming hydrostatic pressure and a density of the flow of 1,850 $kg.m^{-3}$ were used for the simulation. The in-situ soil parameters found to match the entrainment amount were a friction of $\varphi = 15°$ and a cohesion of $c = 0.1$ kPa. The density of the in-situ soil used was 1,600 $kg{\cdot}m^{-3}$. The pore fluid pressure parameter used were $A_D = 0.6$ and $B_D = 0.9$. These values correspond to an in-situ soil that has a high degree of saturation. The surface flow occurs in standard time and no air is entrapped under the water table. A homogeneous erodible in-situ soil depth of 3.5 m was found to be the value that agrees best with the quantity of entrained material by the original event. A calculation time step of 0.05 s was set up and the simulation had a time elapsed of 453.60 s.

The model predicted high velocities and higher amounts of entrainment when the slope is predominantly inclined and lower velocities and entrainment when it reaches the gentler slope in the lower section of the torrent. Figure 5.4 shows the plots for maximum heights and velocities during the course of the flow. The final deposition volume is around 58,338 m^3 (553 % of increase in mass balance) with an average velocity during the whole event of 8.8 $m{\cdot}s^{-1}$. The application to the event gave reasonable results in comparison to the field observations mainly based on the geometry of the deposits. Relative higher deposits were simulated with an average height of approximately 3.2 m and a maximum height of 4.9 m. The difference between the heights and velocities calculated with the model and the real event measured in the field, can be explained by the fact that other processes are involved in the entrainment processes (e.g. abrasion) and due to the application of a 1D-model to a 3D-phenomenon. Figure 5.5 indicates the distribution of the entrained volume during the course of the flow and the accumulated final volume.

5.4.2 A Dynamic 2D Run-Out Model with Entrainment: Description and Field Application at Selvetta

A debris flow, which occurred on 13th July 2008 in the Valtellina Valley (Italy) was analysed through field observations and simulated with the FLO-2D mass flow model incorporating information on rainfall-runoff with empirical parameters,

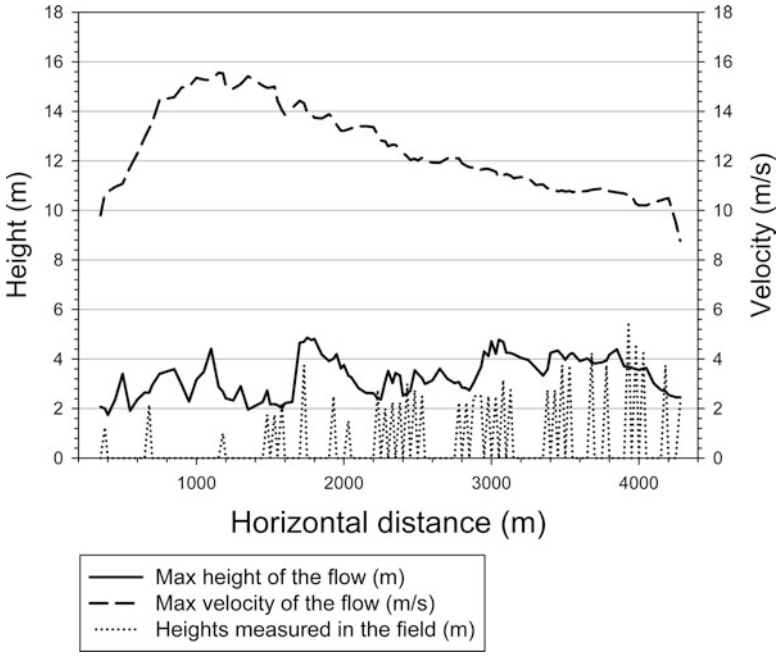

Fig. 5.4 Maximum modelled velocity and height of the debris flow event of 2003 at Faucon during the flow course. The velocity distribution shows that the maximum velocity takes place when the debris is rushing down in the steepest part of the slope

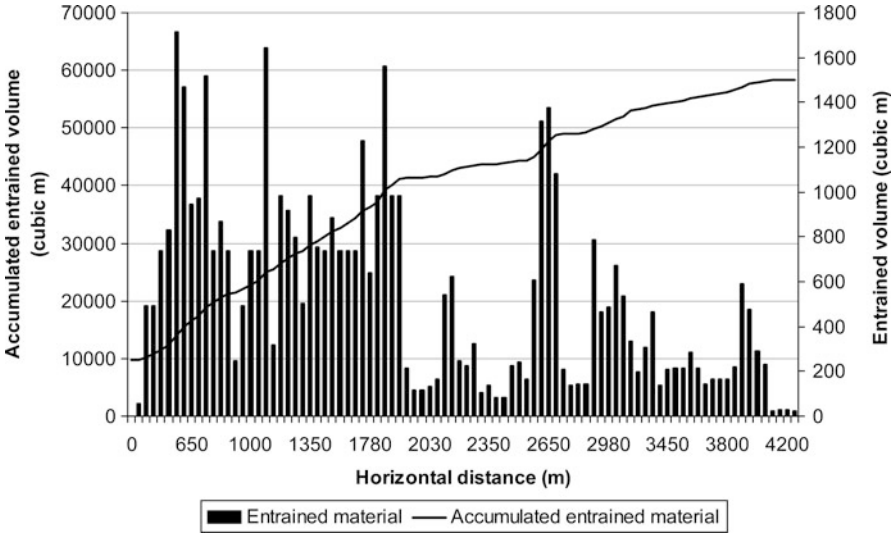

Fig. 5.5 Cumulative volumes of the deposits during the entrainment process and the entrained volume during the course of the flow

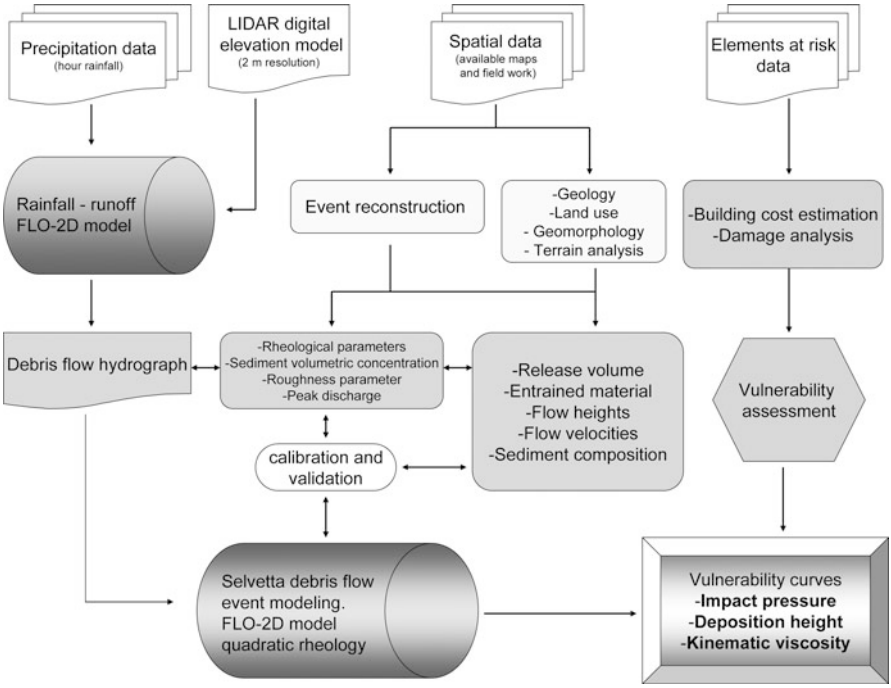

Fig. 5.6 Methodological flowchart applied in the back-calculation of the Selvetta debris flow

including entrainment capacity and sediment composition. The modelling of the Selvetta debris flow was divided in three steps (Fig. 5.6). The first step consisted in a simulation of the rainfall in the area to calculate a discharge hydrograph and the effect of the rainfall intensity on the flow; the second step consisted in the modelling of the entrainment of the channel bed caused by the flow, the third step consisted in a simulation of the debris flow that included the results of modelling of the rainfall and the entrained material. All simulations were based on a 2 m grid DEM obtained form a airborne laser scanning survey.

5.4.2.1 FLO-2D Model

The FLO-2D model (2009) is an Eulerian two-dimensional finite difference model that is able to route non-Newtonian flows in a complex topography based on a volume-conservation model, and is also able to simulate the rainfall-runoff. The flood volume is moved around on a series of tiles to simulate overland flow (2D flow), or through line segments for channel routing (1D flow). Both topography and resistance to flow control flood wave progression over the flow domain. Flow in two dimensions is accomplished through a numerical integration of the equations of

motion and the conservation of fluid volume. The model simulates the shear stress as a summation of five shear stress components: the cohesive yield stress, the Mohr-Coulomb shear, the viscous shear stress, the turbulent shear stress and the dispersive shear stress.

The governing equations, originally presented by O'Brien et al. (1993), are the continuity equation (Eq. 5.24) and the equation of motion (Eqs. 5.25 and 5.26):

$$\frac{\partial h}{\partial t} + \frac{\partial h\, V_x}{\partial x} + \frac{\partial h\, V_y}{\partial y} = i \tag{5.24}$$

$$S_{fx} = S_{ox} - \frac{\partial h}{\partial x} - \frac{V_x}{g}\frac{\partial V_x}{\partial x} - \frac{V_y}{g}\frac{\partial V_x}{\partial y} - \frac{1}{g}\frac{\partial V_x}{\partial t} \tag{5.25}$$

$$S_{fy} = S_{oy} - \frac{\partial h}{\partial y} - \frac{V_y}{g}\frac{\partial V_y}{\partial y} - \frac{V_x}{g}\frac{\partial V_y}{\partial x} - \frac{1}{g}\frac{\partial V_y}{\partial t} \tag{5.26}$$

where h is the flow depth and V_x and V_y are the depth-averaged velocity components along the horizontal x- and y-coordinates. The excess rainfall intensity (i) may be nonzero on the flow surface. The friction slope components S_{fx} and S_{fy} are written as function of bed slope S_{ox} and S_{oy}, pressure gradient and convective and local acceleration terms.

The depth-integrated rheology is expressed (after dividing the shear stresses by the hydrostatic pressure at the bottom of the flow $\gamma_m h$) as (Eq. 5.27):

$$S_f = \frac{\tau_y}{\gamma_m\, h} + \frac{K\, \eta\, V}{8\, \gamma_m\, h^2} + \frac{n t d^2\, V^2}{h^{4/3}} \tag{5.27}$$

where S_f is the friction slope (equal to the shear stress divided by $\gamma_m h$); V is the depth-averaged velocity; τ_y and η are the yield stress and viscosity of the fluid, respectively, which are both a function of the sediment concentration by volume; γ_m is the specific weight of the fluid matrix; K is a dimensionless resistance parameter that equals 24 for laminar flow in smooth, wide, rectangular channels, but increases with roughness and irregular cross section geometry; and n_{td} is an empirically modified Manning n value that takes into account the turbulent and dispersive components of flow resistance (the calculation of n_{td} is hardwired in the model).

The yield stress (Eq. 5.28), the viscosity (Eq. 5.29), and the empirically modified Manning n value (Eq. 5.30) are calculated as follows:

$$\tau_y = \alpha_1\ e^{\beta_1\ C_v} \tag{5.28}$$

$$\eta = \alpha_2\ e^{\beta_2\ C_v} \tag{5.29}$$

$$n_{td} = n_t\ b\ e^{mC_v} \tag{5.30}$$

where α_1, β_1, α_2, and β_2 are empirical constants, C_v is the fine sediment concentration (silt- and clay-size particles) by volume of the fluid matrix, n_t is the turbulent n-value, b is a coefficient (0.0538) and m is an exponent (6.0896). The latter (b and m) are fixed in the model, and cannot be modified.

5.4.2.2 Runout Modelling of the Selvetta Debris Flow Event

The hourly accumulated rainfall preceding the debris flow release in the period of 11th and 13th July 2008 was used as an input of the simulation. The result was a discharge hydrograph incorporating outflow from (1) the source area and (2) the debris flow path channel, where the amount of rain influenced the mobility of the flow and where the contribution of the water added to the flow was canalized. The estimation of the peak discharge is of vital importance as it determines the maximum velocity and flow depth, momentum, impact forces, ability to overrun channel walls, as well as the run-out distances.

Based on the calculated release hydrograph and the rainfall that converge into the channel path, the entrained material was estimated by assuming that the flow travelling on the channel bed deposits causes an undrained loading that generates a high pore fluid pressure. This concept has been described in detail by Sassa (1988), Remaître et al. (2008) and Quan Luna et al. (2011) explaining the long travelling motion of some debris flow saturated with water. A loading of the bed deposits is generated when the sliding mass flows on top. The applied loading of the channel soil was calculated by the change of vertical normal stress and the shear strength caused by the flow. The increase in pore fluid pressure is calculated based on the equation proposed by Sassa (1988) for an undrained direct shear test.

In relation to the slope gradient of the torrent path, the amount of material that could be entrained varied from 1.2 to 2.3 m. A value of the internal friction angle of $\varphi = 30°$ and a cohesion of $c = 0.3$ kPa were selected. The pore fluid pressure parameters used were $A_D = 0.6$ and $B_D = 0.9$. These values correspond to an in-situ soil that has a high degree of saturation and rich in water discharge. The surface flow occurs in usual time and no air is entrapped under the water table. An estimated released volume (rain + failed mass) of 2,337 m^3 was computed. The final calculated deposition volume is 15.324 m^3 (554 % of increase in mass balance), which corresponds to the volume estimates obtained in the field.

Parameterization of the FLO-2D model has been done by calibration, since no independent estimates of the model friction parameters were available. The calibration of the model was based on a trial-and-error selection of rheological models and parameters, and the adjustment of the input parameters which define the flow resistance. Parameters were adjusted until good agreement between the simulated and observed characteristics were accomplished with the following criteria: (1) the velocity and height of the debris flow along the channel, (2) the final observed run-out and (3) the accumulation pattern in the deposition area. The parameters that fit reasonably the calibration criteria and had the best results

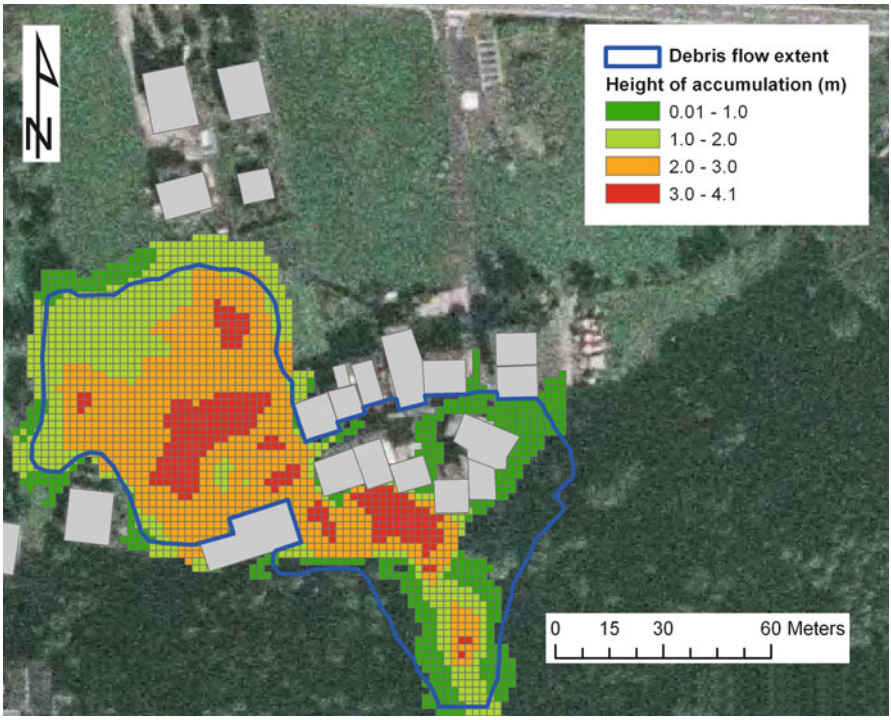

Fig. 5.7 Comparison of observed and modelled debris flow run-out extents. The maximum heights of the debris heights simulated by the FLO-2D model are indicated

were $\tau_y = 1{,}950$ Pa and $\eta = 5{,}000$ Pa. These rheological parameters were calculated according to the sediment concentration inside the hydrograph and appropriate values of α and β were selected from O'Brien and Julien (1988). The chosen Manning n-value that characterizes the roughness of the terrain was 0.04 $sm^{-1/3}$ where the flow was channelled and 0.15 $sm^{-1/3}$ in the deposition zone. A value of K (laminar flow resistance parameter for overland flow) of 24 was used in the channelled section and of 2,350 for the rough surface on the deposition zone. The Manning n-value and K-value were selected based on field evidences of the flow pattern.

A time-stage of sediment concentration was produced based on the shape of the hydrograph. This was done to agree with observations that the peaks in debris flow hydrographs correspond to high sediment concentrations, while the raising and final parts of the hydrograph have a more diluted composition. The procedure also reproduced the distribution of sediment concentration influenced by a dilution in the rising and falling tails of the hydrograph. The maximum and minimum concentrations were 0.55 and 0.25, respectively.

The FLO-2D software can display for each part of the flow, the impact force, velocity, discharge and flow height during all time steps of the simulation. Figure 5.7

shows the simulated maximum run-out and deposition and the field observed extent of the event. The ability of the model to account for the shadow effect created by the houses can be noted. The simulated debris heights are in good agreement with the observations. The highest debris heights are reached upslope from the destroyed and heavily damaged houses. Afterwards, they decrease to the edges of the deposition area. It has to be noted that in some cases the flow did not reach some of the lightly damaged houses. This is caused by the fact that the model does not simulate the destruction of the house and thus it remains as an obstacle causing a shadow effect. Apparent increase of debris deposits in the distal parts of the flow is most probably caused by some imprecision in the used DEM (Quan Luna et al. 2012).

5.5 Probabilistic Assessment of Debris Flow Hazard: Possible Approaches for Dynamic Run-Out Models

Because of the complexity and the difficulty to model all the phenomena that take place in a debris flow event, the use of simplified rheological models that represent the flow behaviour is a common approach. Models based on the rheological characteristics of the flow with three or less adjustable parameters have been used extensively and calibrated as precisely as possible based on back analysis of past events. The calibration of these parameters makes it possible to use the same model for different types of events in different locations. There is a large range of these rheological parameters reported in the literature, and some of them do not have a precise physical meaning which makes a forward analysis very difficult to assess. Often there is not enough information available about the range of rheological parameters for the estimation of hazard at a specific location. To indicate the uncertainty of these input parameters and thus the uncertainty of the run-out hazard analysis it is useful to combine the scarce local information with the range in values obtained by many case studies over similar areas.

5.5.1 Database Description and Compilation

As a first step towards a stochastic analysis of ranges and uncertainties of parameters and their effects on run-out modelling, a database was compiled from past-analyzed events reported in the literature. The database included the rheological parameters (Voellmy and Bingham rheologies) and volumes from many previously back-calibrated events that have been described by many authors. The database included information of 301 run-out events, characterized by the type of landslide, volume, run-out behaviour and rheological parameters derived from model back-calibration (Table 5.3).

Table 5.3 Example of a case analyzed inside the database created showing the different fields of classification

Case study: Panabaj, Guatemala (2005)	Debris flow characteristics
Volume (m^3)	65.000
Run-out length (m)	4,900
Angle of reach (°)	16.3
Max velocity ($m \cdot s^{-1}$)	15
Rheology	Voellmy
Apparent friction coefficient	0.04
Turbulent coefficient ($m \cdot s^{-2}$)	450
Viscosity (Pa·s)	–
Yield stress (Pa)	–
Author and year	–
Method	Back-calibration
Post-failure behaviour	Channeled
Environment	Volcanic
Source sediment	Pyroclastic material

The database was compiled from peer-reviewed literature and unpublished reports. In total 75 % of the cases in the database are debris flows and landslides and 25 % are rock avalanches. The Voellmy rheology is used in 169 events and 132 events use the Bingham rheology.

5.5.2 Design of Probability Density Functions

Uncertainty could be the result of measurement errors, sampling errors, model uncertainty (uncertainty due to simplification of real-world processes, incorrect model structure, misuse of models, and use of inappropriate assumptions), descriptive errors, aggregation errors, errors in professional judgment and uncertainty of the variability. Variability, usually measured as standard deviation or variance, represents natural random processes. The variability for a parameter can be represented as a probability density function (PDF), also referred as a probability function, frequency function, or frequency distribution. For a continuous variable (a variable that can assume any value within some defined range) the probability density function expresses the likelihood that the value for a random sample will fall within a particular very small interval.

Within the database, the variability for a parameter was represented as a probability density function (PDF). Figures 5.8 and 5.9 show different types of curves that were used to fit the distributions of the parameters for the Voellmy and Bingham models, using the values derived from the whole database. A curve fit of the parameters was done using different types of distributions: normal distribution; a kernel distribution, and a Lognormal distribution. A kernel distribution is a

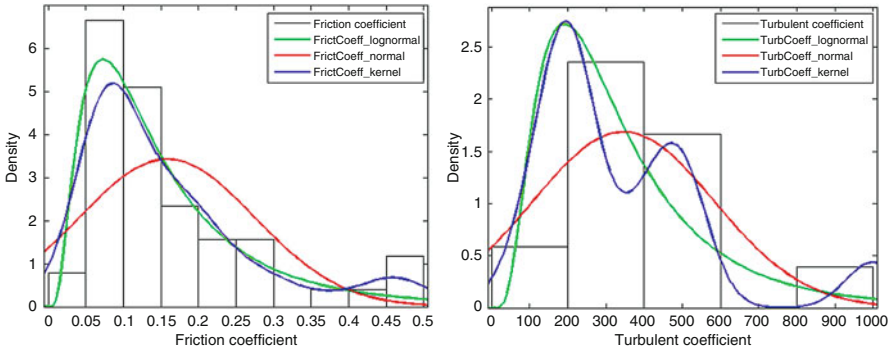

Fig. 5.8 Curves used to fit the probability density function of the apparent friction coefficient (μ) and the turbulent coefficient (ξ) (m/s^2) inside the Voellmy model

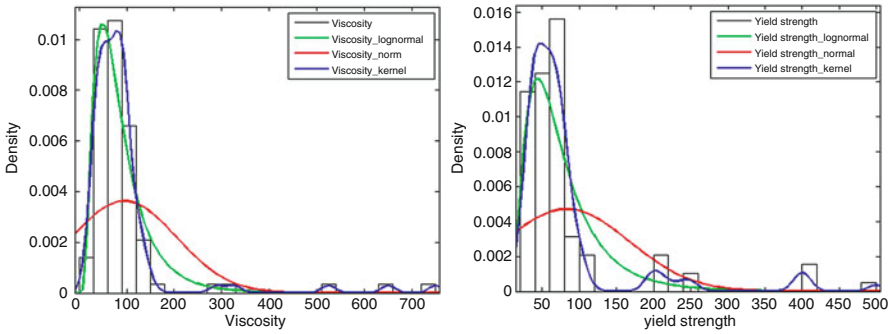

Fig. 5.9 Curves used to fit the probability density function of the viscosity (η) (Pa·s) and the yield stress (τ) (Pa) inside Bingham model

non-parametric way of estimating the probability density function of a random variable. The kernel density estimation is a fundamental data smoothing problem where inferences about the population are made, based on a finite data sample. In the case of the resistance parameters, a Lognormal distribution was found as the one that best fitted the data. The proper selection of the PDF's is essential for a good assessment of the uncertainties associated with the choice of rheological parameters.

The arithmetic and geometric moments for the Lognormal distribution of the Voellmy and Bingham rheology can be seen in Table 5.4. These values can indicate a parameter range for forward modelling using the analyzed rheologies.

The recommended functions of the resistance parameters can also provide a context for the resistance parameters arrangement and can contribute to the fine tuning of the usual iterative process for parameter selection in the construction of a more detailed back analysis. Besides this, the creation of a probability density function is a first step for a stochastic approach to be implemented for dynamic run-out models in order to assess hazard and risk at a specific locality.

Table 5.4 Moments for the fitted lognormal distributions to the resistance parameters

	Lognormal parameters		Arithmetic moments		Geometric moments	
	Mu	Sigma	Mean	Standard deviation	Mean	Standard deviation
Bingham model viscosity	4.2882	0.6240	88.4970	61.0690	72.8378	1.8665
Bingham model yield strength	4.1577	0.6204	77.4994	53.1063	63.9294	1.8597
Voellmy model friction coefficient	−2.0882	0.7310	0.1618	0.1360	0.1239	2.0773
Voellmy model turbulent coefficient	5.6486	0.6302	346.2624	241.7950	283.8959	1.8780

5.5.3 Application of a Monte Carlo Method to Debris Flow Run-Out Modeling

In order to analyze the effect of the uncertainty of input parameters a probabilistic framework based on a Monte Carlo simulation for run-out modelling is considered a useful approach. Monte Carlo analysis is a method that uses statistical sampling techniques to derive the probabilities of possible solutions for mathematical equations or models. Monte Carlo analysis was initially developed in the 1940s and it has been applied to all sorts of problems dealing with the uncertainty of data and models (Metropolis and Ulam 1949; Metropolis 1987).

The framework presented in this chapter is based on a dynamic model, which is combined with an explicit representation of the different parameter uncertainties. The probability distributions of these parameters were determined from the analyzed database described earlier. The uncertainty in these inputs can be simulated and used to quantify the probability of run-out distances and intensities. In a Monte Carlo procedure the input parameters of the numerical model are randomly selected. Many model runs are performed using the randomly generated input values. This allows estimating the probability of the output variables characterizing the intensity of debris flows (for instance depth, velocities and impact pressures) at any point along the path. To demonstrate the implementation of this method, the MassMov2D model was used. The main goal is to present a framework to obtain potentially expected run-out extents and intensities of debris flows in areas where it is not possible to determine the rheological parameters on the basis of back-analysis. In many situations past events have not been well documented, and information is lacking on the exact distribution of the debris flow. Even if this is available it is also difficult to reconstruct information on the released volume, and the height and velocity distribution of the debris flow materials.

One of the reasons to use a Monte-Carlo analysis is to examine the effect of uncertainty regarding the variability of the rheological parameters on the estimation of debris flow run-out. This statistical sampling-analysis method allows evaluating the probability distribution of the relevant parameters (intensity parameters) for

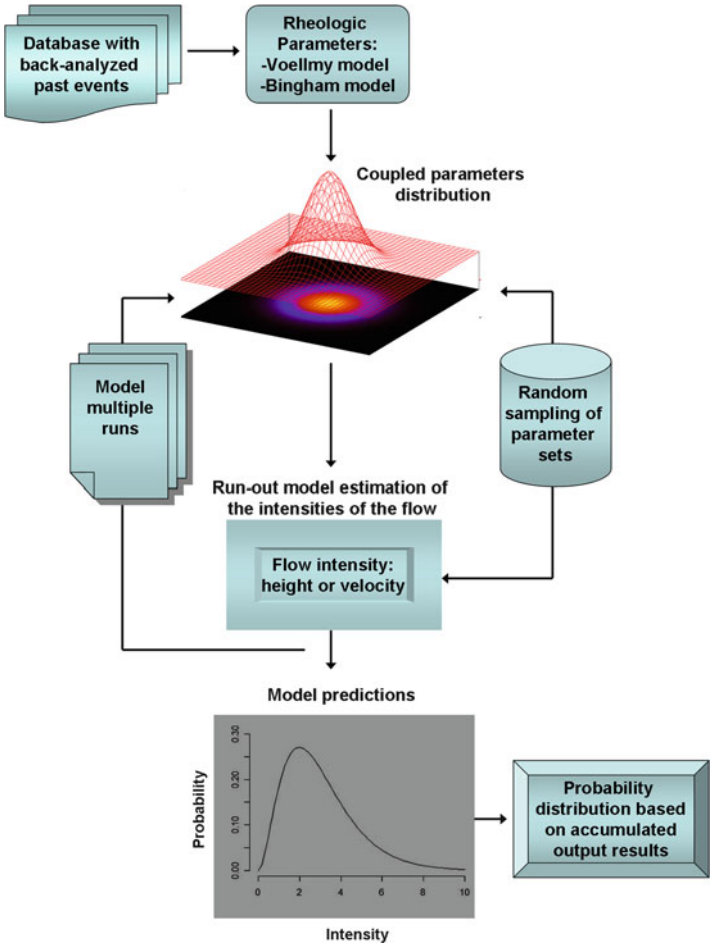

Fig. 5.10 Flow chart of the application of a Monte-Carlo method for debris flow hazard assessment

a hazards assessment once the proper probability distributions for the friction coefficients have been defined. By this way it is possible to account explicitly and objectively for uncertainties in the model inputs definition and in the mapping results. To conduct probabilistic modelling using Monte Carlo analysis each of the input parameters is assigned a distribution. The output from the model is calculated many times, randomly selecting a new value from the probability distributions for each of the input parameters each time. The outputs from each run of the model are saved and a probability distribution for the output values is generated. This allows the probability of the occurrence of any particular value or range of values for the output to be calculated. Figure 5.10 presents a representation of how Monte Carlo analysis is conducted.

The shape of the probability distribution can greatly affect the outcome of the Monte Carlo analysis and it is extremely important that an appropriate distribution is selected. It should be mentioned that a Monte-Carlo analysis does not require PDFs for all input parameters. In multiple-parameter models where there is no basis for assigning a PDF to particular parameters, it is acceptable to keep a fixed value for those parameters while assigning PDFs to parameters where sufficient information is available. In this study, the released volume is considered to be independent from the frictional coefficient terms and was taken constant. The reason for this was that when analyzing the database, similar released volumes in different setting conditions produced significantly different flow dynamics and behaviour (run-out and intensities). Another reason for this is that the variation in volumes is defined by a specific return period which is beyond the scope of this study. The uncertainty resulting from the physical process that is difficult to describe (variability inherent to the phenomenon) is expressed inside the probability density functions of the frictional parameters. The Monte Carlo method involves deliberate use of random numbers in a calculation that has the structure of a stochastic process. Monte Carlo works by using random numbers to sample the "solution space" of the problem to be solved. In our case, we sample randomly with a "random number generator" each distribution (Voellmy and Bingham rheologies) with a number of 5,000 values. Once the PDFs of the input parameters have been defined and used to generate random sets of parameters, a routine was used to repeatedly run the run-out model as many times as the generated sets (5,000 times). After each run of the model was completed, the output values were saved for specific points on the accumulation area. After all the simulations were completed, the frequency of particular output values at these points was analyzed. The resulting set of output values was evaluated to determine descriptive statistics such as the mean, range, standard deviation, etc. In addition, the probability that the outcome will exceed a particular value or will fall within a certain range of values was calculated.

5.6 Estimation of Debris Flow Risk Scenarios

Another aspect of the use of run-out models is the possibility to estimate risk scenarios for QRA. A variety of methods have been developed for the estimation of debris flow risk scenarios. One method is the use of f-N curves, which express the frequency of events with different numbers of casualties (or magnitude of losses expressed in some other way). Such relationships always show aggregated losses for a large region and period of time. They do not help to identify the geographical distribution of damage, for which risk mapping is needed. Risk maps attempt to show the spatial or geographical distribution of expected losses from a natural hazard. Because of the way natural hazards occur, the presentation of annual risk, as defined above, is not necessarily the most useful, and several different ways of presenting losses are commonly used including:

- scenario mapping, where potential losses (e.g. the number of people killed and injured and the damage to buildings and infrastructure) are estimated within pre-defined hazard and vulnerability scenarios. This method is often applied to evaluate the necessary resources to face an emergency quickly and effectively and, in so doing, to reduce disruption, accommodate expected homeless, and minimize the recovery period.
- potential loss mapping, where the effects of expected impacts are mapped, and the locations of communities likely to suffer heavy losses are shown. The communities most at risk, should be prioritized for loss-reduction programs and strategies, and will need more aid or rescue assistance in case of a major disaster.
- annualised risk mapping, where the probability of each damaging event occurring over a period of time is combined with the consequences of that event to generate prospective losses within that time. Summing up the losses for all occurrences gives the total losses expected for the period.

The risk assessment presented hereafter has been carried out in the area of Tresenda (Valtellina Valley, Italy), where three quantitative debris flow hazard scenarios for different return periods were prepared using available rainfall and geotechnical data.

5.6.1 Methodological Framework for the Construction of Risk Scenarios for Tresenda

It was assumed that three potential debris flows occurring in the study site will be triggered in areas of high slope and high flow accumulation rate. Based on extensive field surveys and DEM analyses, three potential sources were identified and modelled by the dynamic numerical model FLO-2D to assess the run-out intensity (Fig. 5.11). To quantify the hazard of these debris flows, several steps were implemented in order to be modelled: (1) a detailed analysis and estimation of rainfall return periods for the study area and a modelling of the rainfall-runoff process based on the different return period scenarios, (2) an analysis of the terrain features, (3) laboratory tests of soil samples and determination of the debris flow rheology, and (4) modelling of the debris flows run-out distances. The modelled hazard scenarios were consequently overlaid with the elements at risk.

111 buildings have been mapped in the immediate vicinity of the Tresenda scenario, 57 of them within the delimited hypothetical scenario area. The majority of them are two to three-story buildings constructed with brick masonry and concrete structures. Value of each building was estimated using the construction prices provided by Engineers and Architects of Milan. According to them, a construction cost of 801 €·m^{-2} corresponds to single standing house with 2–3 storeys. The value of the buildings was calculated by multiplying their area from the DB2000 (2003) database by the number of floors and by the reconstruction value per square meter. Total value of the buildings within the scenario area is reaching 14.895.500 € with

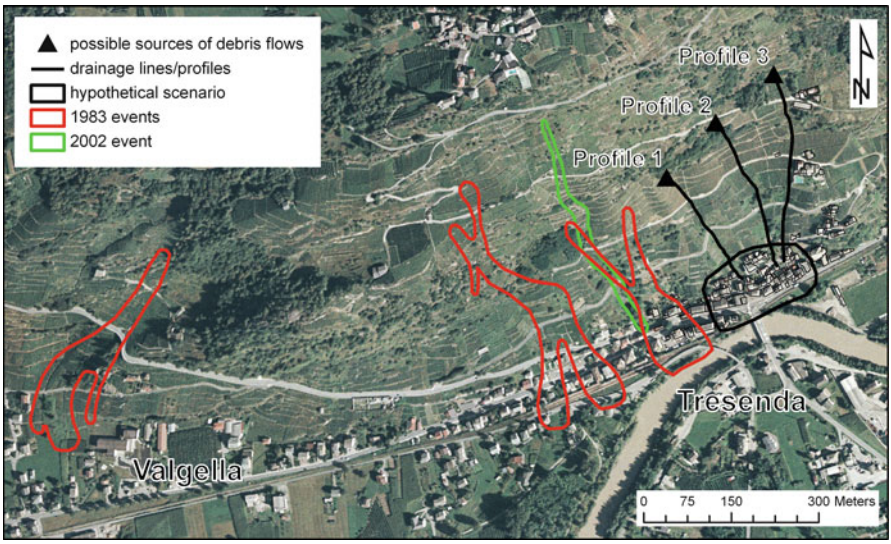

Fig. 5.11 Delimitation of the 1983 and 2002 debris flow according to GeoIFFI and Consortium of Mountain Municipalities of Valtellina di Tirano database. Possible sources and drainage lines/profiles of new debris flows are shown (*in black*) and area of a hypothetical risk scenario is delimited

a range from 34.360€ to € 1.079.000 € for a single building, and with an average reconstruction cost of 261.324 € per building. Besides the buildings, a state road (S.S.38) is located between the buildings and the Adda River and minor paved roads are present. A principal railway line is running along the state road, connecting province capital Sondrio with Tirano and Switzerland upstream of the Adda River. According to the database of Registry Office, 173 people are living in the houses within the delimited scenario. In this approach, only economic risk to buildings is quantified, neglecting the damage to other infrastructure and to the people living in the area. Quantification of damage to buildings in the case study area was done by examination of the results from the hazard modelling to the respective building. Debris heights and high impact pressures near the walls were extracted for each interested building. The results were used to calculate risk maps for the three return periods by using two different fragility curves. The fragility curve proposed by Fuchs et al. (2007) based on the height of the debris flow as an intensity parameter, and the proposed fragility curve by Barbolini et al. (2004) for impact pressure of snow avalanches were used for the analysis. Direct losses to the buildings were calculated by multiplying the calculated vulnerability by the building value (Fig. 5.12). The prospective damage to the houses was estimated using proposed fragility functions (flow height and impact pressure). Direct economic losses to the buildings were estimated depending on the hazard scenario and fragility curve used.

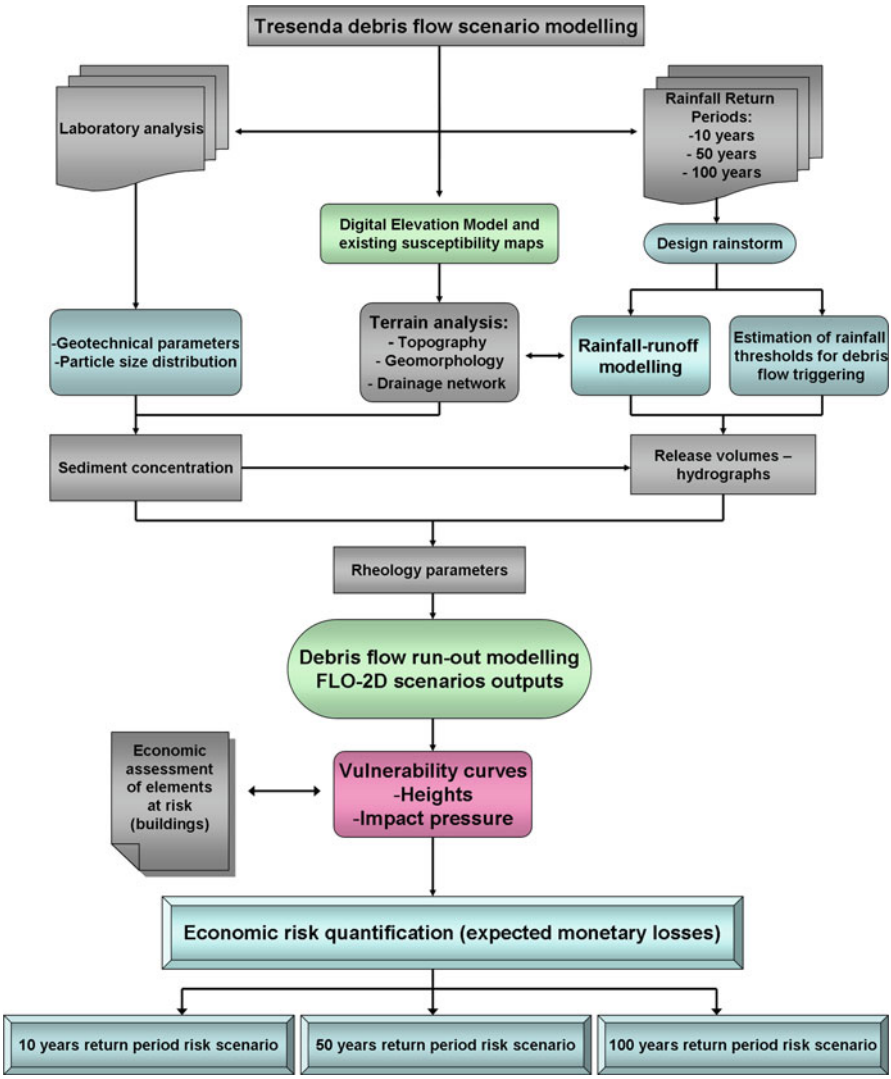

Fig. 5.12 Flowchart of the methodological framework for the estimation of debris flow risk scenarios

5.6.2 Characterization of the Hazard Scenarios and Damage to Buildings

Firstly, available hourly-rainfall records were used to calculate rainfall return periods of 10, 50, and 100-years using data from the Castelvetro rain gauge. A 48-h rainfall, which may trigger a debris flow, was simulated in the study area and

Table 5.5 Rainfall thresholds for debris flow initiation using a 48-h rainfall in Castelvetro rain gauge

Author	Type	Value
Govi et al. (1984)	I-D	2.74 $mm \cdot h^{-1}$
Cancelli and Nova (1985)	I-D	2.18 $mm \cdot h^{-1}$
Ceriani et al. (1992)	I-D	2.38 $mm \cdot h^{-1}$
Agostoni et al. (1997)	IMAP-D	2.51 $mm \cdot h^{-1}$
Luino (2005)	IMAP-D	1.74 $mm \cdot h^{-1}$

the time of exceedance of rainfall threshold was investigated for different return periods based on historical information (Crosta et al. 2003) of past debris flow events. The storm rainfall was discretized as a cumulative percentage of the total. This discretization of the storm distribution was established through local rainfall data that defines storm duration and intensity. The storm was modelled spatially over the grid system. Several rainfall thresholds available for the study area were calculated in the past. Debris flow initiation thresholds were calculated for the 48-h rainfall (Table 5.5).

The simulated rainfall was then used to specify the time when rainfall threshold was exceeded and a debris flow triggered. The rainfall-runoff modelling allowed specifying nine input hydrographs for the three potential debris flow sources and three return periods. Soil samples were collected in the field and detailed geotechnical analyses were performed. Two representative samples were selected based on the criteria of the proximity location to the possible initiation and run-out zones. Geotechnical parameters and particle size distribution for each sample were obtained and used to infer the rheological parameters to be used in the dynamic run-out model.

The slope materials are mixed loose deposits mostly composed of gravel and sand with a consistent percentage of silt and almost absent clay. According to the Unified Soil Classification System (USCS), chosen by the American Society for Testing and Materials (ASTM) as standard, they are GM (silty gravel with sand) or SM (silty sand with gravel), with a uniformity coefficient (CU) between 20 and 157. The mean sample has the following composition: gravel (36 %), sand (44 %), silt (19 %) and clay (1 %). All the samples are very superficial so they are particularly rich of organic matter (3.3–7.3 %). The natural water content (W_0) is strictly dependent on the climatic condition during sampling, and its value range from 0.5 to 14.5 %. The bulk unit weight (γ_0), measured in place by the sand-cone method, ranges between 13.8 and 16.1 $kN \cdot m^{-3}$ while the calculated γ_{dry} ranges between 12.8 and 15.7 $kN \cdot m^{-3}$. With an estimated specific gravity of the soil solids (G_s) equal to 27.2 $kN \cdot m^{-3}$, the calculated porosity (n) is 42–53 % and the sediment volumetric concentration varies between 0.47 and 0.58 $m^3 \cdot m^{-3}$. Atterberg limit results are not determinable because of the almost total lack of clay: this means that the studied material pass from the semi-solid to the liquid state. Direct shear tests were performed to obtain the peak and residual values of the shear strength parameters ($c_p = 3.4–18.5$ kPa; $\varphi_p = 28–36°$; $c_r = 0–17$ kPa; $\varphi_r = 26–35°$). The time where the rain storm exceeded the threshold was registered. The threshold used for the

Table 5.6 Release volumes (in cubic meters) and peak discharges (in cubic meters per second) for the three scenario profiles and return periods

	10 years	50 years	100 years
Profile 1	$V = 390\ m^3$, $Q = 4.8\ m^3 \cdot s^{-1}$	$V = 1{,}162\ m^3$, $Q = 11.4\ m^3 \cdot s^{-1}$	$V = 1{,}424\ m^3$, $Q = 13.4\ m^3 \cdot s^{-1}$
Profile 2	$V = 330\ m^3$, $Q = 4.2\ m^3 \cdot s^{-1}$	$V = 1{,}142\ m^3$, $Q = 11.2\ m^3 \cdot s^{-1}$	$V = 1{,}410\ m^3$, $Q = 13.3\ m^3 \cdot s^{-1}$
Profile 3	$V = 425\ m^3$, $Q = 5.1\ m^3 \cdot s^{-1}$	$V = 1{,}251\ m^3$, $Q = 12.1\ m^3 \cdot s^{-1}$	$V = 1{,}518\ m^3$, $Q = 14.1\ m^3 \cdot s^{-1}$

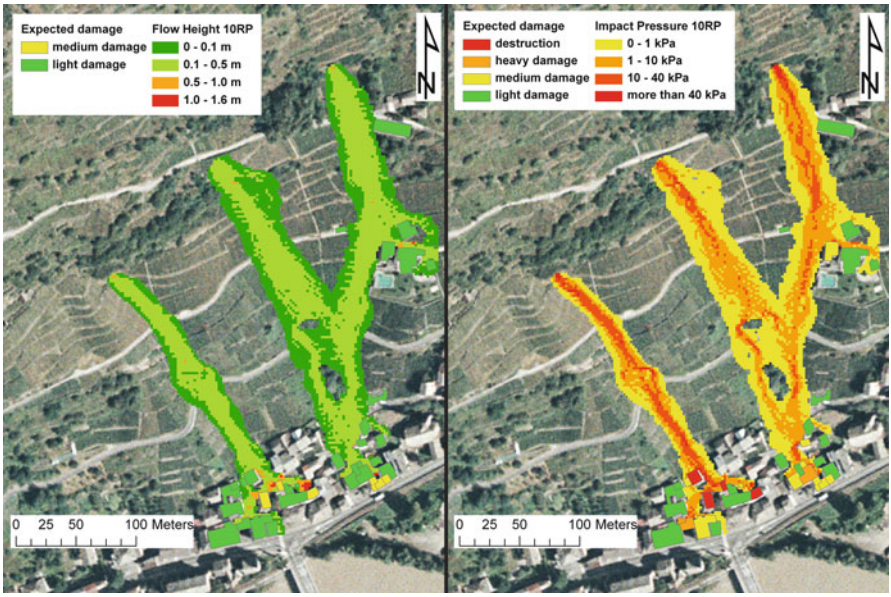

Fig. 5.13 Results of the hazard modelling for the 10-year return period showing the calculated degree of damage to the buildings. On the *left* height of accumulation, on the *right* impact pressures

assessment was the one defined by Luino (2005) assuming a worst-case scenario. Discharge hydrographs were produced from the previous rainfall-runoff modelling. Volumes were calculated from the peak discharge hydrographs (Table 5.6).

Several debris flows run-outs were then simulated with the FLO-2D model. The rheological properties of the flow were estimated based on the results of the laboratory analysis. The final parameters used in the modelling were $\tau_y = 1{,}500$ Pa and $\eta = 2{,}800$ Pa. The Manning n-value that characterises the roughness of the terrain was selected as $0.04\ sm^{1/3}$.

In total, six hazard scenarios were prepared for each return period and for accumulation heights and impact pressures, respectively. The results are presented in Figs. 5.13, 5.14, and 5.15, showing the difference in the magnitude of the hazard. Moreover, information about the possible damage to the houses is shown,

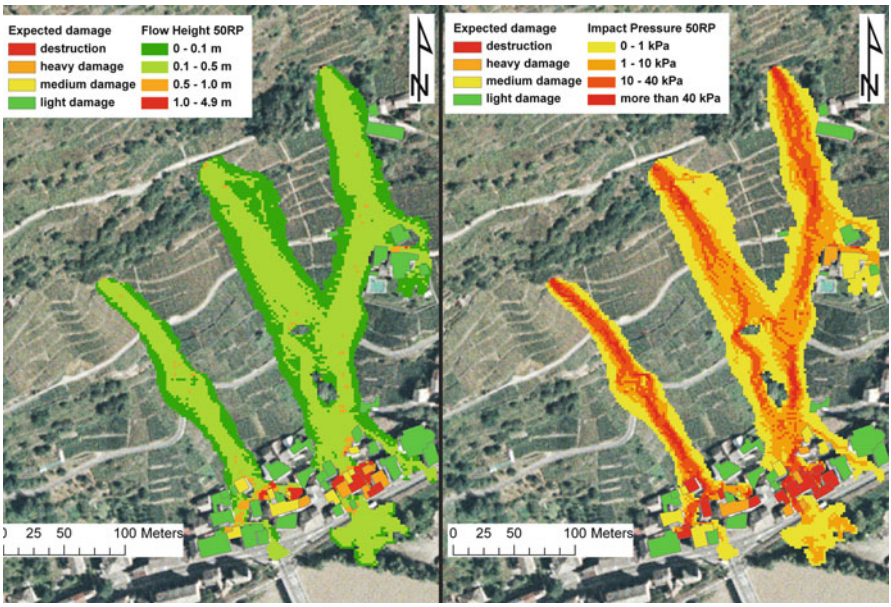

Fig. 5.14 Results of the hazard modelling for the 50-year return period showing the calculated degree of damage to the buildings. On the *left* height of accumulation, on the *right* impact pressures

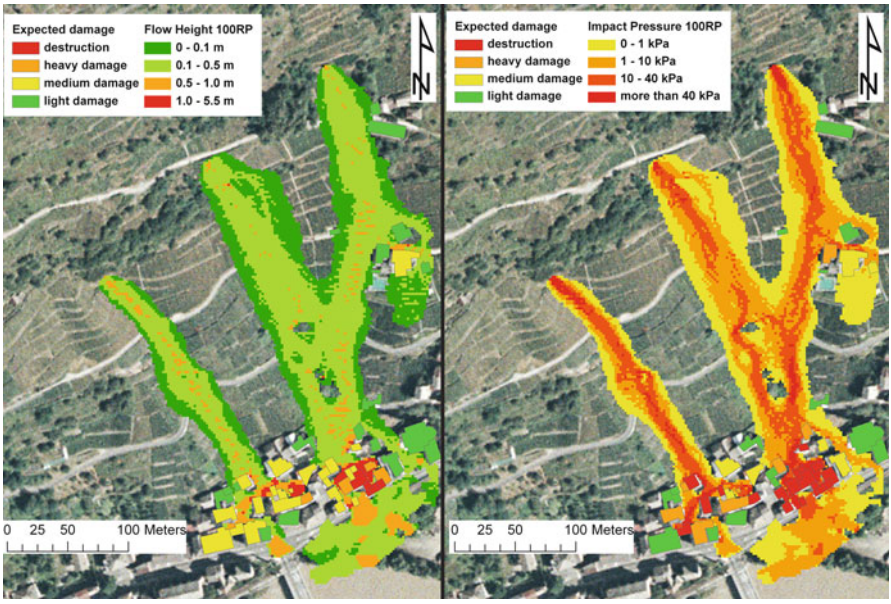

Fig. 5.15 Results of the hazard modelling for the 100-year return period showing the calculated degree of damage to the buildings. On the *left* height of accumulation, on the *right* impact pressures

resulting from the calculated vulnerability using the respective fragility function. Light damage means vulnerability between 0 and 0.1, medium damage represents vulnerability 0.1–0.5 and heavy damage relates to vulnerabilities between 0.5 and 1. Destruction means that vulnerability of 1 was reached.

In the debris flow hazard scenario considering to the 10-year return period (0.1 probability), 35 buildings are likely to be impacted. The total direct damage to houses is considerably affected by the use of different fragility functions. Considering the flow height fragility function, the direct damage reaches 610.088 €. In the case of impact pressure fragility function, the total direct monetary loss to the buildings is estimated to 2.059.321 € (337 % of the first damage estimate). Risk levels span from 0 (no risk) to 8,271 €·year^{-1} for a single building in case of the height of accumulation fragility function and from 0 to 27.780 €·year^{-1} for a single building in case of the use of impact pressure fragility function (Fig. 5.13).

In the debris flow hazard scenario considering to the 50-year return period (0.02 probability), 49 buildings are likely to be impacted. After the application of the fragility function using as an intensity parameter the flow height, 32 buildings will suffer light damage, 9 buildings medium damage, and 5 buildings high damage. Three buildings will be completely destroyed. After application of the impact pressure fragility function, different results were obtained: 21 buildings will suffer light damage, 8 buildings will have medium damage and 6 buildings will have heavy damage. Fourteen buildings will be probably destroyed. Considering the flow height fragility function, the direct damage reaches 2.311.219 €. In the case of impact pressure fragility function, it reaches 5.059.011 €. Risk reaches 7,644 €·year^{-1} for a single building in both cases of risk calculation (Fig. 5.14).

In the debris flow hazard scenario considering to the 100-year return period (0.01 probability), 49 buildings are likely to be impacted as in the case of the 50-year scenario. After the application of the fragility function using as an intensity parameter the flow height, 19 buildings will suffer light damage, 22 buildings medium damage, and four buildings high damage. Four buildings will be completely destroyed. After application of the impact pressure fragility function, higher damage pattern was obtained: 16 buildings will suffer light damage, Seven buildings will have medium damage and eight buildings will have heavy damage. Eighteen buildings will be probably destroyed. These results show the same pattern as in the case of 10 and 50-year return periods. The number of affected houses is similar to the previous scenario. Expected damage is, however, much higher. The total direct damage to houses is considerably affected by the used of the different fragility functions as in the case of the previous scenarios. Considering the height of accumulation fragility function, the direct damage reaches € 3,151,675. In the case of impact pressure fragility function application, the total direct monetary loss to the buildings is estimated to 6.453.366 €. Risk reaches 3.822 €·year^{-1} for a single building in case of the flow height vulnerability calculation and 6,127 €·year^{-1} for a single building in case of the impact pressure use (Fig. 5.15).

Six risk scenarios were compared (for the three return periods and for the two vulnerability functions each). It can be noted that the total damage estimate is increasing with the debris flows magnitude. There are, still, considerable differences

between the estimates for the same return periods. However, the scenario approach proposed in this section may assist local decision makers in determining the nature and magnitude of the expected losses due to a dangerous event. Besides, a preventive knowledge of the prospective physical effects and economic consequences may help to properly allocate financial resources for disaster prevention and for mitigation measures. Nevertheless, beside its limitations, it increases the knowledge about prospective outcomes of future hazards and thus contributes to the protection of the people and their assets.

5.7 Conclusion

This research analyzed different approaches, developments and difficulties regarding the application of dynamic run-out modelling of debris flows, mud flows and landslide hazard at a local and medium scale with a focus on physically-based approaches. Emphasis was given to the problems involved in parameterization of such models, focusing on rheological parameters and entrainment. The main objective of this research was to apply, improve and optimize the use of dynamic run-out models in quantitative risk assessment. The deterministic characteristics of these models and the possibility to obtain direct intensity values make the run-out models an interesting tool to be used in these types of analyses.

The current practice of landslide risk assessments procedures are still performed with a great deal of empiricism and personal judgment needs to be introduced in the definition of important inputs. Consequently, the results are strongly sensitive and influenced by the "knowledge" of the individual that produces the assessment. This work addresses the urgent demand for methods in quantifying the uncertainties in the definition of the various input variables and the resulting effect in a hazard assessment. Applying, evaluating and introducing a probabilistic method to dynamic run-out models were regarded in this research as the main point to address these problems. In addition, while evaluating the application of dynamic run-out models to past events and back calibrating the rheological parameters, it was observed that the inclusion of the entrainment process in the simulations improved their quality, Entrainment is a key feature mechanism that is able to change significantly the mobility of the flow, the flow volume and its rheology.

It is important to bear in mind that run-out models are conceptual representations of a complex phenomenon. Good models explain the past, make predictions about the future, are cost effective, and easy to use. All models are limited by the assumptions made in constructing them, as the number of assumptions increases, the accuracy and relevance of the model for exploring the phenomenon decreases. Models are also limited by the extent and quality of the input data: with poor quality input, the predictions will be equally unreliable. For this reason it is relevant to assess the uncertainties involved in the parameters used in the run-out models.

The aim of run-out modelling in practice is to determine the hazard at a given location in order to take protective measures. It has to be noted that nowadays

there is not a single model that is able to assess all the aspects of the hazard. Determination of realistic conditions is a serious problem in practical applications that has not received sufficient attention in the past. A practical implementation of the different elements of this research was done to support the validity of the described methodologies and to give encouraging hints for further work.

References

Agostoni S, Laffi R, Sciesa E (1997) Centri abitati instabili della provincia di Sondrio. CNR-GNDCI, Milano, 59 pp + annexes

Barbolini M, Cappabianca F, Sailer R (2004) Empirical estimate of vulnerability relations for use in snow avalanche risk assessment. In: Brebbia C (ed) Risk analysis IV. WIT Press, Southampton

Begueria S, van Asch TWJ, Malet JP, Grondahl S (2009) A GIS-based numerical model for simulating the kinematics of mud and debris flows over complex terrain. Nat Hazard Earth Syst Sci 9:1897–1909

Bell R, Glade T (2004) Quantitative risk analysis for landslides – examples from Bíldudalur, NW-Iceland. Nat Hazard Earth Syst Sci 4:117–131

Blahut J, van Westen CJ, Sterlacchini S (2010a) Analysis of landslide inventories for accurate prediction of debris-flow source areas. Geomorphology 119(1–2):36–51

Blahut J, Horton P, Sterlacchini S, Jaboyedoff M (2010b) Debris flow hazard modelling on medium scale: Valtellina di Tirano, Italy. Nat Hazard Earth Syst Sci 10(11):2379–2390

Bouchut F, Fernandez-Nieto ED, Mangeney A, Lagree PY (2008) On new erosion models of Savage-Hutter type for avalanches. Acta Mech 199:181–208

Calvo B, Savi F (2008) A real-world application of Monte Carlo procedure for debris flow risk assessment. Comput Geosci 35(5):967–977

Cancelli A, Nova R (1985) Landslides in soil debris cover triggered by rainstorms in Valtellina (Central Alps – Italy). In: Proceedings of 4th international conference and field workshop on land-slides. The Japan Geological Society, Tokyo, pp 267–272

Cannon SH, Savage WZ (1988) A mass change model for debris flow. J Geol 96:221–227

Castellanos Abella EA (2008) Local landslide risk assessment. In: Castellanos Abella EA (ed) Multi-scale landslide risk assessment in Cuba. ITC dissertation, Utrecht University, Utrecht

Ceriani M, Lauzi S, Padovan N (1992) Rainfall and landslides in the Alpine area of Lombardia Region, Central Alps, Italy. In: Proceedings of the Internationales Symposium Interpraevent, vol 2, Bern, pp 9–20

Chen H, Lee CF (2000) Numerical simulation of debris flows. Can Geotech J 37:146–160

Christen M, Kowalski J, Bartelt P (2010) RAMMS: numerical simulation of dense snow avalanches in three-dimensional terrain. Cold Reg Sci Technol 63:1–14

Corominas J (1996) The angle of reach as a mobility index for small and large landslides. Can Geotech J 33:260–271

Corominas J, Moya J (2008) A review of assessing landslide frequency for hazard zoning purposes. Eng Geol 102:193–213

Coussot P (1997) Mudflow rheology and dynamics. Balkema, Rotterdam

Crosta GB, Fratinni P, Fugazza F, Caluzzi L, Chen J (2005) Cost-benefit analysis for debris avalanche risk management. In: Hungr O, Fell R, Couture R, Eberhardt E (eds) Landslide risk management. Taylor & Francis, London, pp 533–541

Crosta GB, Imposimato S, Roddeman D (2003) Numerical modelling of large landslides stability and run-out. Nat Hazard Earth Syst Sci 3(6):523–538

Delsigne F, Lahousse P, Flez C, Guiter G (2001) Le riou bourdoux: un “monstre” alpin sous haute surveillance. Revue forestère française LIII:527–540

D'Ambrosio D, Di Gregorio S, Iovine G (2003) Simulating debris flows through a hexagonal cellular automata model: SCIDDICA S3-hex. Nat Haz Earth Syst Sci 3:545–559
Devoli G, De Blasio F, Elverhøi A, Høeg K (2009) Statistical analysis of landslide events in Central America and their run-out distance. Geotech Geol Eng 27(1):23–42
FLO-2D (2009) Reference manual 2009. FLO-2D Software Inc., 73 p. Available at http://www.flo-2d.com/wp-content/uploads/FLO-2D-Reference-Manual-2009.pdf
Fuchs S, Heiss K, Hübl J (2007) Towards an empirical vulnerability function for use in debris flow risk assessment. Nat Haz Earth Syst Sci 7:495–506
Gamma P (2000) DF-Walk: Ein Murgang-Simulationsprogramm zur Gefahrenzonierung (Geographica Bernensia, G66). University of Bern, Bern (in German)
Govi M, Mortara G, Sorzana P (1984) Eventi idrologici e frane. Geologia Applicata e Idrogeologia XCVIII: 3 p
Heim A (1932) Bergsturz und Menschenleben. Beiblatt zur Vierteljahresschrift der Naturforschenden Gesellschaft in Zurich 77:1–218
Holmgren P (1994) Multiple flow direction algorithms for runoff modelling in grid based elevation models: an empirical evaluation. Hydrol Process 8:327–334
Horton P, Jaboyedoff M, Bardou E (2008) Debris flow susceptibility mapping at a regional scale. In: 4th Canadian conference on geohazards, Université Laval, Québec
Hungr O, McDougall S (2009) Two numerical models for landslide dynamic analysis. Comput Geosci 35:978–992
Hungr O, Corominas J, Eberhardt E (2005) Estimating landslide motion mechanism, travel distance and velocity. In: Proceedings of the international conference on landslide risk management. Balkema, Leiden, Vancouver
Iverson RM, Denlinger RP (2001) Flow of variably fluidized granular masses across three-dimensional terrain. 1. Coulomb mixture theory. J Geophys Res 106:537–552
Iverson RM, Schilling SP, Vallance JW (1998) Objective delineation of lahar-inundation hazard zones. Geol Soc Am Bull 100:972–984
Jakob M, Weatherly H (2005) Debris flow hazard and risk assessment, Jones Creek, Washington. In: Hungr O, Fell R, Couture R, Eberhardt E (eds) Landslide risk management. Taylor & Francis, London
Kappes M, Malet JP, Remaître A, Horton P, Jaboyedoff M, Bell R (2011) Assessment of debris flow susceptibility at medium-scale in the Barcelonnette Basin, France. Nat Hazard Earth Syst Sci 11:627–641
Kelfoun K, Druitt TH (2005) Numerical modeling of the emplacement of Socompa rock avalanche, Chile. J Geophys Res 110:B12202
Kwan JSH, Sun HW (2006) An improved landslide mobility model. Can Geotech J 43:531–539
Luino F (2005) Sequence of instability processes triggered by heavy rain-fall in the northern Italy. Geomorphology 66(1–4):13–39
Malet JP, Remaître A, Maquaire O (2004) Run-out modeling and extension of the threatened area associated with muddy debris flows. Geomorphologie 3:195–210
Mangeney A, Bouchut F, Thomas N, Vilotte JP, Bristeau MO (2007a) Numerical modeling of self-channeling granular flows and of their levee-channel deposits. J Geophys Res 112:F02017. doi:10.1029/2006JF000469
Mangeney A, Tsimring LS, Volfson D, Aranson IS, Bouchut F (2007b) Avalanche mobility induced by the presence of an erodible bed and associated entrainment. Geophys Res Lett 34:L22401. doi:10.1029/2007GL031348
Mangeney-Castelnau A, Bouchut F, Vilotte JP, Lajeunesse E, Aubertin A, Pirulli M (2005) On the use of Saint-Venant eqations for simulating the spreading of a granular mass. J Geophys Res 110:B09103. doi:10.1029/2004JB003161
Medina V, Hürlimann M, Bateman A (2008) Application of FLATModel, a 2D finite volume code, to debris flows in the northeastern part of the Iberian Peninsula. Landslides 5:127–142
Metropolis N (1987) The beginning of the Monte Carlo method. Los Alamos Sci 15(Special Issue dedicated to Stanisław Ulam):125–130

Metropolis N, Ulam S (1949) The Monte Carlo method. J Am Stat Assoc 44(247):335–341. doi:10.2307/2280232

Muir I, Ho KSS, Sun HW, Hui THH, Koo YC (2006) Quantitative risk assessment as applied to natural terrain landslide hazard management in a mid-levels catchment, Hong Kong. In: Nadim F, Pöttler R, Einstein H, Klapperich H, Kramer S (eds) Geohazards. ECI symposium series, vol P07, Engineering Conferences International, New-York

Naef D, Rickenmann D, Rutschmann P, McArdell BW (2006) Comparison of flow resistance relations for debris flows using a one-dimensional finite element simulation model. Nat Hazard Earth Syst Sci 6:155–165

O'Brien JS, Julien PY (1988) Laboratory analysis of mudflow properties. J Hydraul Eng 114(8):877–887

O'Brien JS, Julien PY, Fullerton WT (1993) Two-dimensional water flood and mudflow simulation. J Hydrol Eng 119(2):244–261

O'Callaghan J, Mark D (1984) The extraction of drainage networks from digital elevation data. Comput Vis Graph 28:328–344

Pastor M, Haddad B, Sorbino G, Cuomo S, Drempetic V (2009) A depth-intergrated, coupled SPH model for flow-like landslides and related phenomena. Int J Num Anal Meth 33:143–172

Pirulli M, Mangeney A (2008) Results of back-analysis of the propagation of rock avalanches as a function of the assumed rheology. Rock Mech Rock Eng 41(1):59–84

Pitman BE, Le L (2005) A two-fluid model for avalanche and debris flow. Philos Trans R Soc A 363:1573–1601

Poisel R, Preh A, Hungr O (2008) Runout of landslides – continuum mechanics versus discontinuum mechanics models. Geomech Tunn 1:358–366

Pouliquen O, Forterre Y (2002) Friction law for dense granular flows: application to the motion of a mass down a rough inclined plane. J Fluid Mech 453:133–151

Pudasaini SP, Hutter K (2007) Avalanche dynamics dynamics of rapid flows of dense granular avalanches. Springer, Berlin

Quan Luna B, Blahut J, van Westen CJ, Sterlacchini S, van Asch TWJ, Akbas SO (2011) The application of numerical debris flow modelling for the generation of physical vulnerability curves. Nat Hazard Earth Syst Sci 11:2047–2060. doi:10.5194/nhess-11-2047-2011

Quan Luna B, Remaitre A, van Asch TWJ, Malet JP, van Westen CJ (2012) Analysis of debris flow behavior with a one dimensional run – out model incorporating entrainment. Eng Geol 128:63–75

Quinn P, Beven K, Chevallier P, Planchon O (1991) The prediction of hillslope flow paths for distributed hydrological modelling using digital terrain models. Hydrol Process 5:59–979

Remaître A, Malet JP (2010) The effectiveness of torrent check dams to control channel instability: example of debris-flow events in clay shales. In: Garcia CC, Lenzi MA (eds) Check dams, morphological adjustments and erosion control in torrential streams. Nova Science Publishers Inc., New York

Remaître A, van Asch TWJ, Malet JP, Maquaire O (2008) Influence of check dams on debris flow run-out intensity. Nat Hazard Earth Syst Sci 8:1403–1416

Remaître A, Malet JP, Maquaire O (2009) Sediment budget and morphology of the 2003 Faucon debris flow (South French Alps): scouring and channel-shaping processes. In: Malet JP, Remaître A, Boogard TA (eds) Proceedings of the international conference 'Landslide Processes: from geomorphologic mapping to dynamic modelling', CERG Editions, Strasbourg pp 75–80

Rickenmann D (1999) Empirical relationships for debris flows. Nat Hazard 19(1):47–77

Sassa K (1988) Geotechnical model for the motion of landslides. In: Proceedings of the 5th international symposium on landslides. Balkema, Rotterdam

Sassa K, Kaibori M, Kitera N (1985) Liquefaction and undrained shear of torrent deposits as the cause of debris flows. In: Proceedings of the international symposium on erosion, debris flows and disasters prevention. Tsukuba, pp 231–241

Savage SB, Hutter K (1989) The motion of a finite mass of granular material down a rough incline. J Fluid Mech 199:177–215

Schreve RL (1968) The Black Hawk landslide. Geological Society of America, Special Paper, 108, Boulder, 47 p

Skempton AW (1954) The pore-pressure coefficients A and B. Geotechnique 4:143–147

Stummer R (2009) Räumliche und zeitliche variabilität von murereignissen. MSc dissertation, University of Vienna, Vienna

Tarboton DG (1997) A new method for the determination of flow directions and upslope areas in grid digital elevation models. Water Resour Res 33:309–319

Van Asch TWJ, Malet JP, Remaître A, Maquaire O (2004) Numerical modelling of the run-out of a muddy debris-flow. The effect of rheology on velocity and deposit thickness along the run-out track. In: Lacerda W (ed) Proceedings of the 9th international symposium on landslides, Rio de Janeiro

Van Westen CJ, van Asch TWJ, Soeters R (2006) Landslide hazard and risk zonation—why is it still so difficult? Bull Eng Geol Environ 65:167–184

Voellmy A (1955) Uber die Zerstorunskraft von Lawinen (on breaking force of avalanches). Schweizerische Bauzeitung 7:212–285

Zimmerman MN (2005) Analysis and management of debris-flow risks at Sörenberg, Switzerland. In: Jakob M, Hungr O (eds) Debris-flow hazards and related phenomena. Praxis/Springer, Berlin/Heidelberg

Chapter 6
Review and Advances in Methodologies for Rockfall Hazard and Risk Assessment

Olga-Christina Mavrouli, Jacoppo Abbruzzese, Jordi Corominas, and Vincent Labiouse

Abstract This section reviews the current methodologies that are used for the assessment of the rockfall susceptibility, hazard and risk. Emphasis is given on quantitative methods although qualitative ones are also discussed. The different methodologies are presented with respect to their application scales (regional, local or site-specific). Highlight is given to recent advances, especially involving the consideration of the magnitude of the events and the intensity of the phenomena at selected locations as well as the incorporation of a quantitative vulnerability into the risk equation.

Abbreviations

RHV	Rockfall Hazard Vector
RHAP	Rockfall Hazard Assessment Procedure
QRA	Quantitative Risk Assessment

O.-C. Mavrouli (✉) • J. Corominas
Department of Geotechnical Engineering and Geosciences, Technical University of Catalonia, BarcelonaTech, Jordi Girona 1-3, SP-08034 Barcelona, Spain
e-mail: olga-christina.mavrouli@upc.edu

J. Abbruzzese • V. Labiouse
Ecole Polytechnique Fédérale de Lausanne (EPFL), Laboratory for Rock Mechanics (LMR), Station 18, CH-1015 Lausanne, Switzerland

T. van Asch et al. (eds.), *Mountain Risks: From Prediction to Management and Governance*, Advances in Natural and Technological Hazards Research 34,
DOI 10.1007/978-94-007-6769-0_6, © Springer Science+Business Media Dordrecht 2014

6.1 Introduction

Risk assessment is increasingly becoming an important tool for the decision-taking in rockfall threatened areas, with regard to the urban or rural zoning and the application of protection measures for the protection of people and infrastructures. For the risk assessment, both hazard and vulnerability components are involved and have to be evaluated. The expression of the hazard and vulnerability of the exposed elements and their superposition in order to yield risk results, as well as the terms in which the risk is expressed define whether the assessment is qualitative or quantitative. Distinct methodologies apply to each case. On one hand, the use of qualitative methods is based on the evaluation of the hazard and vulnerability components using descriptive rankings (for example low, moderate, high), weighted indexes and numerical classification systems leading, accordingly, to descriptive and ordinal risk expressions. On the other hand, quantitative methods use numerical scales or ranges of values that incorporate and express the annual probability of occurrence of a given magnitude rockfall event, or the probability of an expected level of loss, either it refers to economical loss (e.g. risk expressed in €·year^{-1}) or to injury and death of people (expressed in fatalities·year^{-1}).

Qualitative and quantitative methods may be simultaneously or alternatively used, depending on the scale and the objective of the analysis as well as the quality of the input data. Depending on the scale of the analysis more or less sophisticated empirical and analytical models may be used to simulate realistically the rockfall phenomenon during all its stages. These stages mainly include the rockfall detachment from slope face, the possible fragmentation of the detached rock mass upon impact with the ground, the propagation of the rock blocks down the slope and the spatial distribution of their intensity, the potential reach up of the blocks to the exposed elements and impact on them, and, last but not least, the potential loss (property damage or fatality) in case of impact.

To incorporate all the afore-mentioned stages into the risk assessment, the effect of each one of these processes has to be, separately, measured and expressed. To this purpose some key-components of risk, which present a complexity in their measurement and expression have to be investigated. These components mainly are: (i) the rockfall frequency-magnitude (volume) relation that provides results on the number of given rockfall volumes, (ii) the fragmentation effect, which is expressed by the frequency-size distribution of the rockfall mass on its impact with the ground and its separation into blocks that follow independent trajectories, (iii) the spatial distribution of the rockfall intensity, (iv) the vulnerability of the exposed elements and especially of the buildings, considering that it depends on the magnitude (volume) and intensity (velocity) of the rockfalls and incorporating uncertainties relevant to the impact location of the rock on the building, that have a crucial influence on the level of damage.

This section is organized so as to distinguish between hazard and risk assessment methodologies at different scales, respectively. An emphasis is given on the methodologies for the quantitative assessment and the relevant achievements in the framework of the Mountain Risks project are explained.

6.2 Methodologies for Rockfall Hazard Assessment and Zoning

Many different approaches to rock fall hazard assessment and zoning are currently available, and the choice of the most appropriate methodology to be used depends on the purpose (susceptibility, hazard, risk), the scale (regional, local, site specific) and the intended level of detail (preliminary, detailed, advanced) required for the study. In addition, other factors such as time, funds and amount/quality of data may play an important role when deciding which methodology should be applied.

Despite the variety of possible approaches for hazard assessment and zoning, current procedures are not fully satisfying, due to the several uncertainties affecting hazard analyses, particularly for what concerns detailed studies at the local scale. These uncertainties do have an influence on the results, and further work is therefore necessary in order to achieve more objective and reliable hazard zoning.

The following Sections give an overview on both methodologies suitable to regional scale studies and methodologies which can be used at the local scale – the interested reader can find more detailed descriptions of these methodologies in Labiouse and Abbruzzese (2011). Then, uncertainties affecting current procedures are briefly outlined, and finally some new developments towards a more objective and rigorous methodology for rock fall hazard zoning are introduced.

6.2.1 Methods for Rockfall Susceptibility Assessment and Zoning at the Regional Scale

Regional scale zoning is obtained starting from rough input data, and provides a quick yet effective detection of possible conflicts between the rock fall run-out zone and the current or future land use over a given territory, allowing the establishment of which areas must be given priority for detailed zoning at the local scale.

The most common approaches usually allow at first for identifying potential unstable areas, according to quick criteria (e.g. slopes defined as unstable if steeper than 45°, as computed from DEMs). Then, the potential run-out of the process can be evaluated using simplified propagation models (Jaboyedoff and Labiouse 2003; Ruff and Rohn 2008), which can be easily implemented in Geographic Information Systems. One of the most common approaches for evaluating rock fall run-out and performing zoning is the 'energy line' method (Heim 1932). According to this method, the maximum predicted run-out distance travelled by a block along a 2D slope profile is given by the intersection of the topography with a line starting either from the location of the rock fall source (Fahrböschung method – Heim 1932), or from the highest point of the talus slope (shadow angle method – Evans and Hungr 1993), and inclined at an angle φ with respect to the horizontal (marked in Fig. 6.1 as φ_F for the former model and φ_S for the latter). The method can also be extended to 3D analyses, e.g. the 'cone method' (Jaboyedoff and Labiouse 2003, 2011). In this

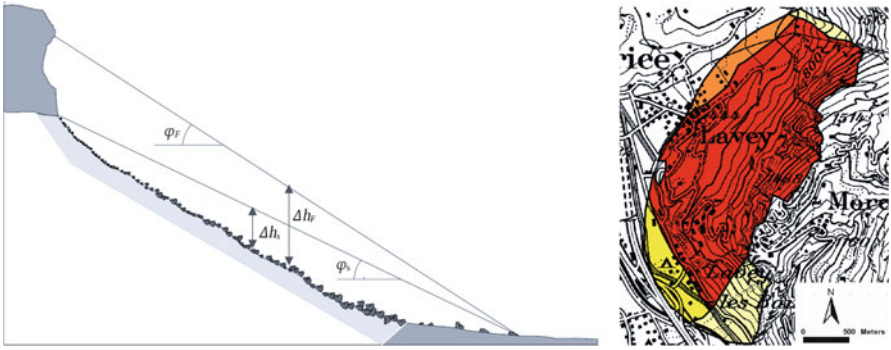

Fig. 6.1 Energy line method. *Left*: 2D definition of the Fahrböschung φ_F and of the shadow angle φ_S (from Abbruzzese 2011). *Right*: example of zoning performed in 3D with the 'cone method' (from Jaboyedoff and Labiouse 2003)

case, the energy line becomes a cone (the location of the cone apex depends on which model is adopted, Fahrböschung or shadow angle) and the areas potentially affected by rock fall trajectories are delineated by the intersection of the cone surface with the 3D topography.

Based on this method, maps representing the degree of run-out susceptibility (rather than hazard, as the failure frequency is not taken into account) can be derived. The obtained maps somewhat differ depending on the variant considered for the run-out model (e.g. Fahrböschung or shadow angle method), and/or because several energy lines may be used, associated to different block volumes (APB 2008) or to different values of probability of reach (Copons 2007). A match between modelled and observed run-out can also be considered, for determining 'proved', 'inferred' and 'potential' run-out zones (Jaboyedoff and Labiouse 2003, 2011).

6.2.2 *Methods for Rockfall Hazard Assessment and Zoning at the Local Scale*

In those areas where conflicts exist between the potential rockfall run-out and the location of human settlements, as a result of regional scale susceptibility analyses, more detailed hazard analyses are required, for an appropriate land use planning aiming at preserving human lives and properties.

Also at the local scale, a variety of approaches is available for tackling this objective. These approaches can be mostly divided into qualitative and quantitative methods, and some can be used for regulating land use planning for urban development (OFAT/OFEE/OFEFP 1997; MATE/METL 1999; Altimir et al. 2001; Raetzo et al. 2002; Copons 2007), while others are better suited to assessing hazard and/or risk along infrastructures (Pierson and Van Vickle 1993; Hoek 2007; Sasaki et al. 2002).

Qualitative methods mainly rely on expert's advices and/or on semi-quantitative rating-based analyses, while quantitative methods may be based on magnitude-frequency relationships (when more oriented to the characterisation of the hazard at the source area), and/or on trajectory modelling, for describing in detail the potential run-out of the process and its intensity. However, only a few approaches combine frequency and intensity (expressed for rock falls in terms of kinetic energy), as hazard analyses should in fact foresee, according to current definitions of hazard discussed at the international level (IUGS 1997; Fell et al. 2005, 2008; MR 2010). Among all the approaches presented in this Section, therefore, particular attention is paid to quantitative hazard assessment methodologies based on trajectory modelling, that combine rock fall intensity and frequency, and that are used for regulating urban development.

6.2.2.1 Qualitative Approaches

'Expert evaluation approaches' can be divided in two types (Aleotti and Chowdhury 1999): methods based on field geomorphological analyses and methods overlapping several index maps (with or without weighting) in GIS environment.

The LPC method (Interreg IIc 2001; LCPC 2004) provides a purely qualitative, expert's advice-based description of potentially unstable cliffs and associated hazards. At first, potential sources of instabilities are identified according to geological, geometric, geomechanical, topographic and environmental features of the cliff. Based on this information, the hazard is then defined as a function of the volume of the unit block after fragmentation and as a function of the likelihood with which an event producing this block volume occurs within a given reference time. Finally, a qualitative estimate of the run-out determines the likelihood of a given point to be reached by one block.

The Rock Engineering System (RES) method (Mazzoccola and Hudson 1996; Interreg IIc 2001) is based on the General System Theory, which is made for solving numerous high complexity problems in rock mechanics. This approach foresees the definition of the relevant parameters for rock fall hazard assessment and the study of cause-effect relationships between them, as well as of the relative importance of each parameter on hazard.

The R3S2 method (Mölk et al. 2008), proposed in Austria for a preliminary detection of conflicts between rockfall run-out and urban settlements, uses a combination of rating system and empirical run-out model. Once field investigations have been carried out for identifying potential rock fall sources, the shadow angle method is applied in order to delineate the rock fall run-out zone. If run-out zone and areas of urban settlements overlap, a rating system is used for determining the severity of the risk potentially affecting the settlements, based on the scores assigned to factors and parameters influencing rock fall probability of occurrence and potential damages. In particular, on the basis of a 'Frequency/Consequence' diagram, the study area can be characterised by a tolerable risk, or be classified as 'rock fall indication zone' (e.g. a zone requiring more detailed hazard analyses) or be characterised by an unacceptable risk.

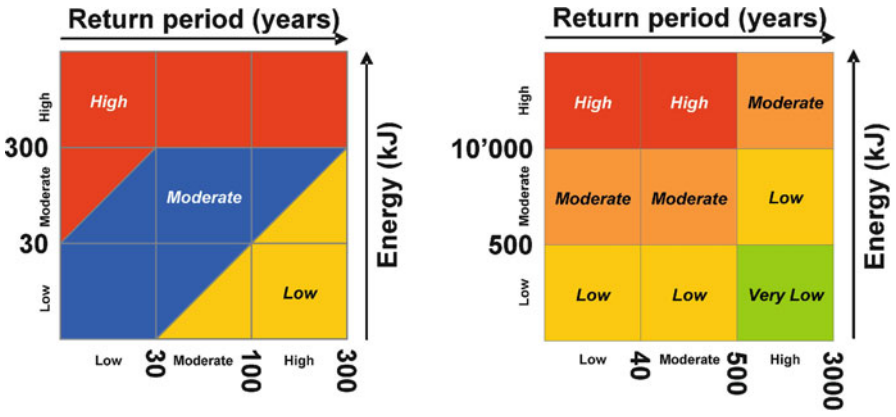

Fig. 6.2 Intensity-frequency diagrams for rock fall hazard zoning. *Left*: Swiss diagram (OFAT/OFEE/OFEFP 1997). *Right*: diagram used in the Principality of Andorra (Copons 2007)

6.2.2.2 Quantitative Approaches

Quantitative approaches are mostly based on rockfall trajectory modelling. Some of them combine intensity and frequency of occurrence according to the definition of hazard (Rouiller et al. 1998; Jaboyedoff et al. 2005; Copons 2007), while others do not really account for one of these parameters (frequency or energy), but may account for others, such as the cliff activity (Mazzoccola and Sciesa 2000) or the height of rebound of the boulders (Crosta and Agliardi 2003; Lan et al. 2007). Examples of procedures combining intensity and frequency are the Matterock and Cadanav methodologies, developed in Switzerland, and a methodology called 'Eurobloc', proposed in the Principality of Andorra.

The Matterock methodology (Rouiller et al. 1998), applied in the Canton of Valais in Switzerland according to the Swiss Codes for hazard zoning (OFAT, OFEE, OFEFP 1997), combines a detailed characterisation of the rockfall departure zone with 2D trajectory simulations. The study of the cliff aims at qualitatively determining a likelihood of mobilisation of the rock mass, depending on factors influencing the stability of the cliff. The propagation is studied on the other hand by means of rockfall trajectory modelling, which allows for determining the probability of reach of the blocks each point of the 2D slope profile, and their kinetic energy. The probability of reach and the likelihood of mobilisation are then combined, in order to obtain a likelihood of occurrence of the event, classified into three categories (low, moderate, high). The rockfall energy is given at each point of the profile by the 90th percentile of the energy distribution values computed at that abscissa with respect to the total number of simulated trajectories. The energy is also classified as low, moderate and high, according to the threshold values reported in the Swiss intensity-frequency diagram (Fig. 6.2). This diagram is finally used for superposing the information on energy and frequency (e.g. inverse of the return period, expressed

in this methodology as a likelihood of occurrence) and for determining therefore the corresponding hazard degree, classified as low, moderate or high.

The Eurobloc methodology (Copons 2007), complying with the guidelines proposed in the Principality of Andorra for hazard zoning (Altimir et al. 2001; Copons 2007), combines frequency of the events and energy as follows. The frequency is determined from the analysis of historical data and from field investigations, which allow for estimating return periods associated to specific rockfall volume classes. This frequency, characterising the source area, is classified as low, moderate or high according to threshold values contained in the Andorran intensity-frequency diagram (Fig. 6.2). The class of frequency defined for the source area is then assigned to all the points of the slope located uphill with respect to a 'limit abscissa', which is the point reached by a specific percentage of blocks (with respect to the total number of simulations), whose value is fixed as a function of the volume class. Beyond the limit abscissa, the frequency is considered as low up to the maximum observed run-out, regardless of its classification before this abscissa. The energy at every point of the slope is computed from the envelope of the maximum values obtained from the cumulative energy distribution determined at each abscissa, based on all the computer runs performed. It is classified as low, moderate or high according to the thresholds in the intensity-frequency diagram. The diagram is finally used for obtaining the hazard (classified in four degrees), determined by the combination of frequency and energy.

The Cadanav methodology (Jaboyedoff and Labiouse 2002; Jaboyedoff et al. 2005), developed at the École Polytechnique Fédérale de Lausanne (EPFL) according to the Swiss Guidelines, expresses the hazard in terms of temporal frequency $\lambda(E, x)$ of blocks reaching a given point of the slope x with a given energy E (Eq. 6.1):

$$\lambda(E, x) = \lambda_f x N_{blocks} \times P_r(E, x) \tag{6.1}$$

The rock fall frequency λ_f and the number of released blocks per event N_{blocks} are estimated from field investigations and, particularly concerning the frequency, from available historical data about past events. The probability of reach $P_r(E, x)$ associated to a given energy is obtained defining probability curves for each energy threshold of the Swiss diagram (0, 30 and 300 kJ). These curves represent the percentage of blocks travelling beyond a specific abscissa with an energy equal or higher than the considered threshold. They are built starting from a modification of the energy profiles obtained from the rockfall simulations, e.g. for each trajectory, the raw energy profile is reduced to a step diagram characterised by three energy values only, each corresponding to one of the thresholds in the Swiss diagram. Once the failure frequency and the probability curves yielding the $P_r(E, x)$ values are known, energy and frequency are coupled (Fig. 6.3) according to seven combinations of energy and return period in the Swiss diagram. These combinations are associated to a change in hazard level and, thanks to the $P_r(E, x)$ curves, provide

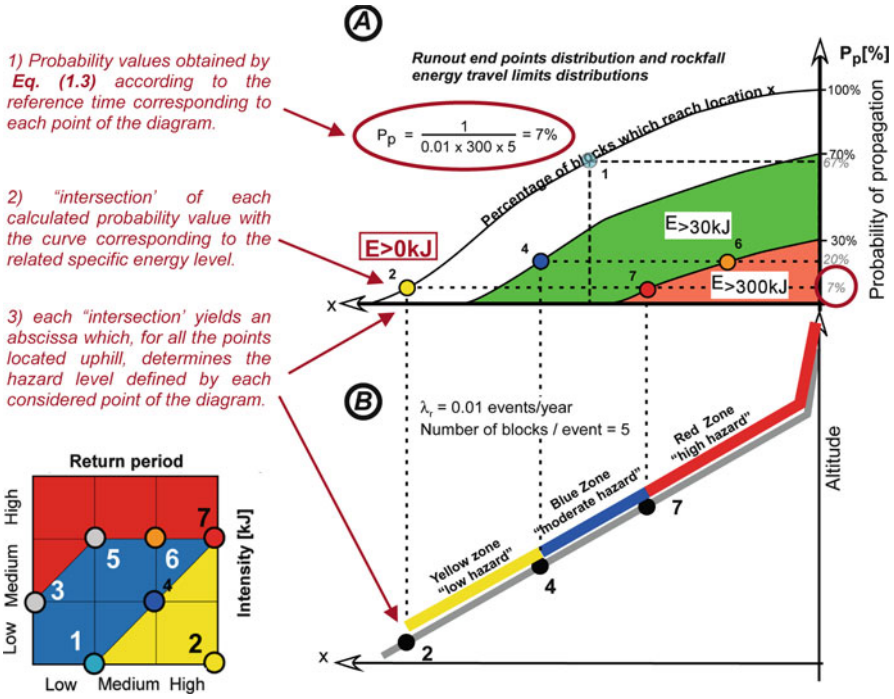

Fig. 6.3 Cadanav methodology, determination of the hazard zone limits (Jaboyedoff et al. 2005). In the example, events releasing five blocks with a failure frequency of one event over 100 years are considered

the extent of the respective hazard zones: low, moderate, high. In particular, when several points may provide the extent of the same hazard zone, the one giving the most downhill limit is considered.

Other examples of methodologies using trajectory modelling, but not coupling intensity and frequency, are the A.D.R.G.T. method (Desvarreux 2002, 2007), developed in the Rhone-Alpes Region in France, the R.H.A.P. (Mazzoccola and Sciesa 2000) and the RHV (Crosta and Agliardi 2003) methodologies, developed in the Lombardia Region in Italy, and the procedure based on the Rockfall Analyst code (Lan et al. 2007), developed in Canada.

The A.D.R.G.T. method only provides a zoning of probabilities of reach, classified as low, moderate or high based on specific probability threshold values. The hazard is classified accordingly, as low, moderate and high, without accounting for energy and frequency of the rockfall events.

The Rockfall Hazard Assessment Procedure (R.H.A.P) accounts for probability of reach and rockfall activity (which gives a qualitative information on the failure likelihood), but not for energy. Based on the combination of these two parameters, it yields zoning maps constituted by five degrees of hazard.

The Rockfall Hazard Vector (RHV) methodology is based on 3D rockfall simulations and provides maps featuring 3 levels of hazard, obtained by combining the frequency of reach, the maximum energy and the maximum height of rebound at each cell of a DEM by means of a three-dimensional matrix diagram.

The Rockfall Analyst code, developed as a GIS extension, allows the performance of 3D rockfall simulations, by means of which rockfall frequency of reach, maximum energies and heights of rebound are determined at each DEM cell. The raw results provided by the computations are then processed using various interpolation techniques (e.g. Kriging), and finally combined at every cell of the topographic model (given by a DEM) by means of a weighted sum yielding the hazard, which can be classified into a given number of degrees (e.g. five).

6.2.3 Quantitative Approaches for Hazard Assessment: Uncertainties and Challenges

Quantitative approaches for hazard assessment should in principle provide a more rigorous and reliable hazard zoning compared to qualitative methods, as they are less dependent on subjective procedures and expert's advice. However, as mentioned in the introduction, several uncertainties characterise as well these techniques, in relation to the assumptions behind each methodology. Consequently, the variety of possible approaches proposed so far yield zoning results which vary a lot, according to the used methodology, as well as to the national guidelines based on which these procedures were developed (Abbruzzese and Labiouse 2010a, b). Differences in hazard zoning related to assessment techniques may constitute a questionable result, since the obtained maps are meant to be basic documents for land use planning (Labiouse and Abbruzzese 2011; Abbruzzese 2011). More precisely, uncertainties affect at first the estimation of the failure frequency (Corominas and Moya 2008). Methods for estimating the temporal frequency of failure are usually based on magnitude-frequency relationships, but most of the times the main problem of these procedures is the lack of historical data used for calibrating the chosen mathematical model (e.g. power law) at a given site. Consequently, it is common in the current practice to estimate rock fall likelihood of failure using qualitative methods (as in the Matterock methodology), even though such types of approaches involve a lot of subjectivity and experts' judgement with respect to quantitative methods.

Another source of uncertainties is linked to the calibration of trajectory simulation codes and to the post-processing of their results. On one hand, attention should be paid to the calibration of the codes, which should be carefully done based on field data, in order for the trajectory results (and then zoning maps) to be reasonably representative of the situation observed on site. On the other hand, also the processing of the raw trajectory results does have an influence on zoning, as the values obtained for energy and probability of reach depend on the adopted processing method. In addition, the number of runs computed in a simulation and

the presence of possible outliers in the modelling results may also condition zoning (Abbruzzese et al. 2009).

Finally, the techniques for combining energy and frequency may differ substantially and be more or less rigorous from one approach to the other, e.g. some procedures are semi-quantitative, and account only qualitatively for the failure frequency, or some others combine intensity and frequency by simply superposing this information instead of fully coupling the two parameters (Abbruzzese et al. 2009). Further work is therefore undoubtedly necessary for improving rigour and reliability of hazard assessment and zoning practices.

6.2.4 New Cadanav Methodology for Rockfall Hazard Zoning at the Local Scale

Among the presented procedures based on trajectory modelling, the Cadanav methodology proposes a more objective, reproducible and fully quantitative technique for assessing rockfall hazards with respect to the others, and it really allows for combining failure frequency, propagation of the process and intensity.

Despite these advantages, some points certainly need to be further improved for this methodology, with particular regards to the consequences on zoning of the energy profiles modification and of the limited number of energy-return period couples considered for hazard assessment (seven couples only). For this purpose, a new version of Cadanav was developed (Abbruzzese 2011; Abbruzzese and Labiouse 2013), which allows to remove these simplifications and extend the applicability of the previous version, by improving the way trajectory modelling results are used for hazard zoning and by proposing a new method for coupling rockfall energy and frequency.

The new Cadanav methodology evaluates the hazard degree by means of 'hazard curves'. They are built starting from the cumulative distribution of the energy values at each point of the slope, as obtained from the rock fall simulation results, and by combining these cumulative probabilities with the failure frequency at the source area, in order to obtain the frequency of occurrence of an event of a given intensity at a given point of the slope.

The hazard curves are described at each slope unit by energy-return period couples, to be superimpose to an intensity frequency diagram in order to determine which hazardous condition prevails at that point of the slope. In particular, when a hazard curve is superimposed to an intensity-frequency diagram:

- if the curve is entirely located inside one single domain of the diagram, corresponding to a given hazard level, the considered point of the slope is assigned that hazard level;
- if the curve crosses more than one hazard domain, the hazard degree is established based on the most unfavourable condition (e.g. higher hazard degree).

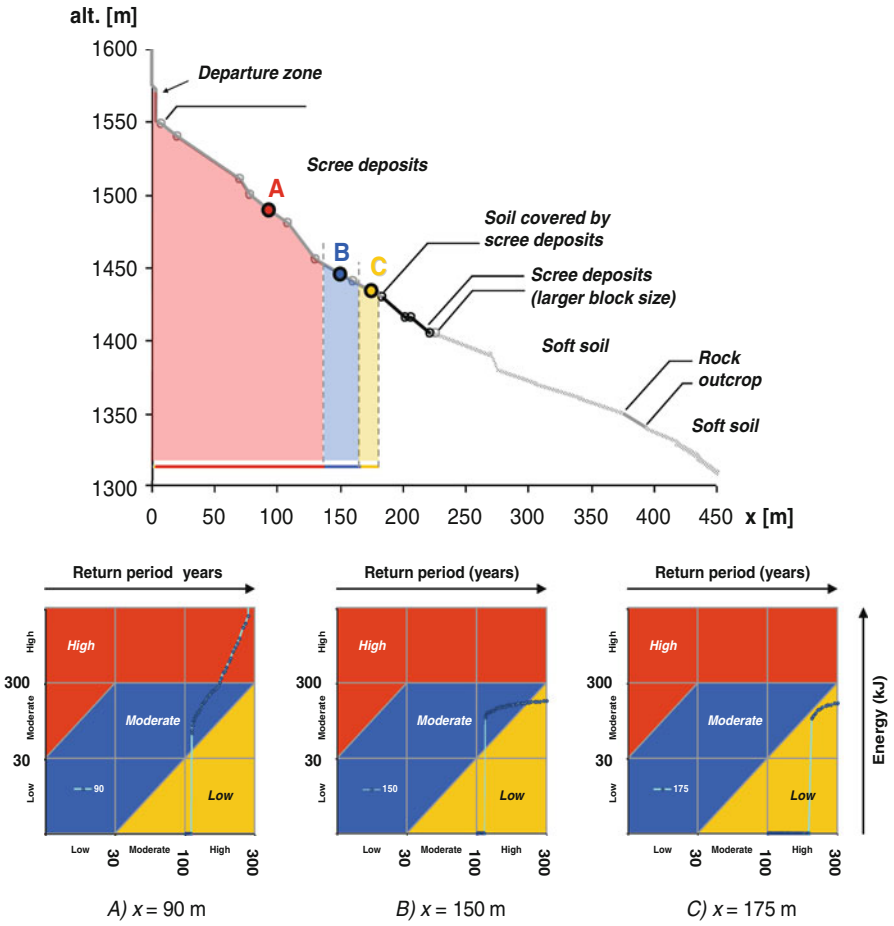

Fig. 6.4 New Cadanav methodology: hazard zoning along a 2D slope profile, performed according to the Swiss guidelines. The hazard curves reported for points A, B and C show the application of the criterion for assigning the degree of hazard at a given abscissa, and how the hazard evolves down-slope

Figure 6.4 illustrates an example of hazard zoning performed along a 2D slope profile characterising a Swiss site. The zoning was obtained from a 2D simulation run for a 10 m^3 block volume, assuming a failure frequency of 1 block failing on average every 200 years per unit length of cliff, and a block size of 2 m. Together with the extent of the hazard zones along the profile, hazard curves are reported for 3 abscissas (Points A, B and C), in order to show the way the hazard degree is determined, based on the superposition of the curve with the Swiss intensity-frequency diagram. The curves also allow the quick visualisation of the hazardous conditions potentially affecting each location of the study site.

Compared to the original Cadanav, the new methodology provides a sounder and more rigorous zoning, and, even though it was here applied based on rockfall simulations on a 2D slope profile, it can be easily used as well for hazard zoning starting from trajectory modelling on a 3D topography. In addition, as the construction of the hazard curves does not depend on the diagram they are then superimposed to, the new Cadanav methodology can be easily applied with any intensity-frequency matrix.

6.3 Approaches for Rockfall Risk Assessment

6.3.1 Methods for Rockfall Risk Assessment and Mapping at the Regional Scale

At regional scale, both qualitative and quantitative risk analyses can be performed (Remondo et al. 2005) but usually, for regional scale analyses the quality and quantity of available data are poorer and of lower precision and accuracy in comparison with those that can be collected for site-specific and local analysis. Thus in order to avoid inconsistencies, qualitative analysis is usually preferable and empirical models are most often implemented (Corominas and Mavrouli 2011a).

Qualitative risk analysis is simpler and quicker to perform than quantitative. It requires knowledge of the hazards, the elements at risk and their vulnerabilities, expressed in qualitative (or semi-quantitative) terms, typically as ranked attributes (IUGS Working Group on Landslides, Committee on Risk Assessment 1997) e.g. risk rating systems, risk scoring schemes and risk ranking matrices. The qualitative expression of risk serves in providing a relative comparison of risks for different sites and in facilitating prioritization of follow-up actions, at regional scale. Official qualitative landslide risk assessment systems exist in USA, Canada, China, Italy and Spain. A review of them is presented by Pantelidis (2011), amongst which is the Rockfall Hazard Rating System (Pierson et al. 1993). Most of these systems use the concept of detailed rating to numerically differentiate the risks at the identified sites. The detailed rating includes a number of factors on which basis slopes are evaluated and assigned a score referring to both hazard and consequences.

In many cases, geographical information systems can also be used for the elaboration and the superposition of factors that are involved in risk evaluation (van Westen 2010). The procedure concerns the organization of information for every component of the hazard, exposure and vulnerability into different levels and the models used are in most cases deterministic.

For regional analysis, the exposure and vulnerability of the elements at risk are often considered as a single term. This means that buildings inside the zones of possible rockfall reach have a deterministic vulnerability value depending on their typology and no consideration is made on the potential location of the rockfall impact on the building, which is crucial for the resulting damage.

6.3.2 Methods for Rockfall Risk Assessment and Mapping at the Local/Site Specific Scale

In comparison with regional scale, for local and site-specific scales the acquisition of more precise and accurate data is feasible, thus permitting the use of more precise and sophisticated empirical and analytical models.

For local and site-specific scales, risk assessment can be as well both qualitative and quantitative. Risk in that case can be calculated as the product of the probability of the rockfall occurrence, the probability of encounter with the exposed elements and their vulnerability. The output is the probability of loss (e.g. annual), and is expressed by Eq. 6.2:

$$R = H \times E \times V \tag{6.2}$$

where, H is the probability of the occurrence of a rockfall of a given magnitude, E is the probability of the encounter with the element or set of elements at risk (property, persons), and V is the vulnerability of the exposed element(s).

The risk calculation takes place by assessing each of these components and combining them. For site-specific and local scales, the hazard may include information on the exact location of the rockfall source and the rockfall run-out by propagation analysis, taking into consideration the local topographical characteristics. The reach distance of the rockfall is calculated probabilistically rather than deterministically.

The vulnerability of the exposed buildings may be calculated probabilistically as well, considering the uncertainty of the impact location, on which their final damage level depends (see Sect. 6.3.3.2).

6.3.3 Quantitative Risk Assessment (QRA)

The QRA practices for landslides, including rockfalls, that are applied all over the world present a large variability, which in turn results from the variety of procedures applied for the determination of each parameter involved in the risk assessment. Besides the rich investigation in this scientific field, which is accompanied by numerous reports and published articles, in the last decades an effort has been done for the establishment of official guidelines or even practices, to be applied by national or local authorities and practitioners, for the quantification of the risk related to landslides, including rockfalls. Such examples are the Hong-Kong guidelines (ERM 1998), and the Australian Guidelines for the landslide management (AGS 2007). Other important contributions are those by Hungr (1997) and Fell et al. (2005), among others.

The general framework for rockfall quantitative risk analysis is multidisciplinary, and consists of the following activities:

- Hazard analysis, including the assessment of the size, probability, velocity and reach of the potential rockfall.

- Identification of the number and characteristics of the elements at risk and their spatio-temporal probability.
- Vulnerability analysis of the elements at risk.
- Calculation of the risk from the hazard analysis, elements at risk and the vulnerability.

The hazard level is usually associated with the probability of having a rockfall magnitude (volume) and/or intensity (velocity) as discussed in Sect. 6.2. The investigation of the elements at risk involves their identification (e.g. persons, buildings, vehicles, infrastructures, other types of property . . .), the temporal-spatial probability of them being affected by a rockfall event, and their vulnerability, which refers to the potential of loss in case that they are hit by a rockfall of a certain magnitude and intensity. The value of the exposed elements might be expressed in absolute terms (e.g. euros) or in relative (e.g. ratio of repair cost to the value of the building).

The rockfall phenomenon is characterized by a lot of uncertainties, which should be incorporated at all the aforementioned stages depending on the scale and the desired level of detail. Thus the risk evaluation requires the use of probabilistic approaches.

Methodologies used worldwide for QRA due to landslides vary according to the type of mechanism, the applied scale, and the available input data. For what concerns rockfall risk, several important contributions to the field of QRA were made by Hungr et al. (1999), Bell and Glade (2004), Roberds (2005), Corominas et al. (2005), Agliardi et al. (2009), Li et al. (2009).

Corominas and Mavrouli (2011a) give details for the expressions that are used to quantify the risk for elements located on a slope potentially affected by rockfall trajectories. The expression formatted in Eq. 6.3 can be used:

$$\mathrm{R} = \mathrm{P(R_i)xP(D : R_i)xP(S : T)xVxC} \tag{6.3}$$

where R is the expected loss due to rockfall $\mathrm{R_i}$, $P(R_i)$ is the probability of a rockfall of magnitude i, $P(D{:}R_i)$ is the probability of a rockfall reaching a location at a distance D from the source, $P(S{:}T)$ is the spatio (S) and temporal (T) probability of the element at risk (probability of encounter with the rockfall), V is the vulnerability of the exposed element impact of a rockfall and C is the value of the element at risk.

The component $P(R_i)$ refers to either the temporal probability or the frequency, depending on the expected outcome from the risk equation. For example, if the objective is the calculation of the probability over a given time span of either the partial or total loss for an exposed element due to a potential rock impact then the temporal probability is used. If the objective is to estimate the cumulative damage (e.g. in euros) due to all potential rock impacts over a given period of time, then frequency may be used instead (Hungr et al. 2005; Agliardi et al. 2009). The parameters $P(R_i)$ and $P(D{:}R_i)$ refer to the hazard, P(S:T) to the exposure and V to the vulnerability.

For a detailed analysis, $P(D{:}R_i)$ may be substituted by the probability of a rockfall reaching a location with a given kinetic energy, $P(E_j{:}R_i)$. On the other hand, for the same rockfall magnitude (i) and intensity (j), depending on the type of the element at risk, the vulnerability $V(R_{ij})$ is different; so to calculate the risk, for every type of element the risk has to be calculated separately and summed-up. To obtain the risk for each exposed element, Eq. 6.3 becomes:

$$R(P) = \sum_{i=1}^{i} \sum_{j=1}^{j} \left[P(R_i) x P(E_j : R_i) x P(S : T) x V(R_{ij})\right] x C \tag{6.4}$$

where, $R(P)$ is the expected loss to the property due to rockfall, $P(R_i)$ is the probability of a rockfall with a magnitude i, $P(E_j{:}R_i)$ is the probability of the rockfall reaching the exposed element(s) with a certain kinetic energy Ej, given that a rockfall has occurred, $P(S{:}T)$ is the temporal-spatial probability of the element at risk, $V(R_{ij})$ is the vulnerability of the exposed element for a rockfall of magnitude i and kinetic energy E_j and C is the value of the exposed element.

Small size and mid-size rockfalls usually begin by the detachment of a more or less coherent rock mass that after the first impact with the slope face splits into several pieces. The latter is the case of a fragmental rockfall which is characterized by the independent movement of individual rock fragments after detachment from a rock face (Evans and Hungr 1993).

For taking fragmentation into account, $P(R_i)$ can be substituted by $\lambda(R_s)$, which is the frequency of rockfalls of a defined block size 's', and it is given by the Eq. 6.5 (Corominas and Mavrouli 2011b):

$$\lambda(R_s) = \sum_{i=1}^{i} [\lambda(R_i) \cdot \times \cdot N_s(R_i)] \tag{6.5}$$

where $\lambda(R_s)$ is the frequency of blocks of 's' volume, $\lambda(R_i)$ is the frequency of rockfalls of 'i' volume and $N_s(R_i)$ is the number of blocks of 's' volume due to rockfall of 'i' volume.

6.3.3.1 Exposure and Vulnerability

The exposure of an element to rockfalls is expressed by the inherent temporal-spatial impact probability of it being affected during or after an event. Rockfalls present the peculiarity of the punctual effect of their impact on specific exposed elements and key-locations on them, instead of the areal distribution of landslides, rock slides and rock avalanches. For fragmental rockfalls usually only buildings at the first row next to a slope and people inside, are affected. Analytical expressions for the calculation of exposure of buildings, vehicles and people, can be found in Corominas and Mavrouli (2011a). For small scales, considering of the impact probability on specific exposed elements is not permitted by the resolution of the analysis. Conversely, for

local and site-specific scales the impact probability is a basic component of the consequences analysis that could be incorporated into the vulnerability assessment. Impact probability may be calculated for structures (spatial), vehicles (spatial and temporal) and people (spatial and temporal).

6.3.3.2 Risk to Buildings – Infrastructures

To assess the performance of a structure struck by a rockfall, both the intensity and impact location must be considered (Mavrouli and Corominas 2010a). These two parameters determine whether there will be initial damage to load-bearing structural elements (e.g. columns) and whether this will affect the overall structural stability. With reference to the impact location, there are, in general, three possibilities: (1) a free-fall rock dropping on the roof, (2) a rock moving along a trajectory path and hitting the exposed façade, and (3) a rock passing through the façade and perforating a floor slab on a downward movement. In terms of impact effects, damage can be categorized into the following groups: primary structural damage (of primary structural elements such as columns, beams, etc.) that determines the overall stability of the building; secondary structural damage (of secondary load-bearing elements such as slabs, etc.); primary nonstructural damage that may cause injuries (e.g., infill walls,ceilings, etc.); secondary nonstructural damage (e.g., furniture, fixtures, etc.); and damage to services (electrical and mechanical equipment, etc.).

For reinforced concrete structures, the location of the impact on the exposed façade is fundamental (Fig. 6.5). Damage to a nonstructural element (e.g., an infill wall) is not critical to building stability, but collapse of a structural element, such as a column or a beam, may initiate progressive collapse. So, in a nonstructural impact, the damage is restricted to the nonstructural element itself, but in a structural impact, the final damage may vary from slight to total.

Details on the quantitative evaluation of the vulnerability of buildings for incorporating this aspect into the risk equation are given in Chap. 8 of this book. A vulnerability index to be used directly for the risk quantification is given by Mavrouli and Corominas (2010b). It considers the variation of the damage according to the impact location of rockfalls, and is calculated as a function of the rockfall magnitude and velocity:

$$\mathrm{V}(\mathrm{R_{ij}}) = \sum_{K=1}^{k} (P_{ek} X\ RRC_k) \leq 1 \tag{6.6}$$

where $V(R_{ij})$ is the vulnerability for a rock block with a magnitude 'i' and intensity (velocity) 'j', $P_{e,k}$: is the encountered probability of a rock with a possible structural and nonstructural element of the building 'k' that may be struck by a rock block of magnitude 'i' and RRC_k is the relative recovery cost that corresponds to the strike of a possible structural and nonstructural element of the building 'k' by a rock block of magnitude 'i' and velocity 'j'.

Fig. 6.5 Nonstructural damage at a workshop in Santa Coloma (Principality of Andorra) due to rockfall in April, 2008. No further damage was produced because none of the columns were impacted and broken by the block

6.3.3.3 Risk to Persons

People are vulnerable to rockfalls depending on their location with respect to the rockfall path. In many cases different vulnerabilities have been considered for people of different ages and particular conditions (for example people in hospitals). Conservatively, it can be considered that when a person is hit by a rock block, he/she will die, but in many real events, slight injuries instead of fatalities have been observed. Thus the vulnerability of persons due to rockfalls should consider the magnitude of the event as well (Bunce et al. 1997).

The risk to persons can be expressed either for an individual or for a group of people (societal). In the latter case the societal risk is expressed through a F-N (frequency-mortality) chart. For the F-N chart, the annual probabilities of 1, 2, ... and up to n persons being injured or killed due to rockfalls in a given region are calculated and then summed up. For this, the density of the population in a building is considered, depending on its use (e.g. school, workshop, residential).

6.3.4 Forthcoming Improvements in Risk Assessment: Integrating Vulnerability in the Risk Equation

Within the Mountain Risks project the main improvement achieved for the quantitative risk assessment is the incorporation of the vulnerability into the risk equation, particularly with regard to fragmental rockfalls. To this end, an analytical approach was followed. The advantages of such approach are the objectivity and the incorporation of the uncertainty of the impact location on key structural elements, as well as the response of the whole structural system. This provides a realistic evaluation of the response of the buildings. This procedure requires the analysis of a representative set of cases and different building typologies.

6.4 Conclusion

The methodologies for the QRA vary significantly depending on the landslide type, the scale of the analysis, the considered exposed elements and the techniques used for collecting input data. Quantitative estimates provide more objective and comparable hazard and risk results than the qualitative ones.

The cases presented in this chapter summarise the progress experienced in rockfall hazard and risk assessment during the last few years. The advance has been evident in the consideration of the magnitude of the events, the intensity of the phenomena at selected locations and in the vulnerability assessment. One of the main challenges in quantitative rockfall hazard zoning at both local and regional scales is the spatial distribution of the hazard levels which are better described by the kinetic energy rather than by the magnitude (size) of the event. To this end, rockfall hazard curves have become extremely helpful. They are built based on the cumulative distribution of the energy values at each point of the slope obtained by trajectographic analyses and combining them with the failure frequency at the source area. This yields the frequency of occurrence of an event of a given intensity at a given point of the slope.

The risk analysis has benefited from the progress produced in the evaluation of the vulnerability of the exposed elements. The analytical approaches are more objective and incorporate the uncertainty of the impact location on key structural elements and the response of the whole structural system. The vulnerability obtained can be directly integrated in the risk equation. However, these approaches require the consideration of a large variety of structural typologies and arrays which analyses are not yet available.

Despite this progress, further research is still required before QRA could become a routine. Determining the size of the potential rockfalls is still a challenge. Magnitude-frequency relations are fundamental input data for quantitative hazard and risk analysis, however the scarcity of good quality geological and historical data in many regions restricts its construction. On the other hand, magnitude-frequency analyses assume the existence of steady conditions for both triggers and slopes. This assumption is, however, arguable in some geological contexts, particularly in alpine mountainous regions which were glaciated during Pleistocene times. The conditions responsible for the rockfall frequency after the glacial retreat, which is often the observed frequency, might no longer exist (Wieczorek and Jager 1996).

An additional difficulty is the fact that small size and mid-size rockfalls usually begin by the detachment of a more or less coherent rock mass that after the first impact produces fragmental rockfalls. The fragmentation mechanism is not currently included in trajectographic models and may strongly affect the reliability and validity of the results. The detachment of such type of rockfalls without considering their fragmentation will give unrealistic travel distances and impact energies in excess of what should be expected.

Segregating the risk equation has highlighted the role of the exposure of the elements at risk (spatio-temporal probability of the elements at risk) which has

received little attention so far. Traditional approaches used in risk analysis tend to simplify risk in two main components: hazard and vulnerability. Nevertheless, practical application of QRA has shown that exposure, particularly for mobile elements at risk (cars, trains, persons) has a strong influence in risk results and on the probability of loss of life. The consideration of exposure within vulnerability is not an appropriate way to address this issue because vulnerability is an intrinsic property of the element at risk while exposure may be a transient attribute even for buildings which exposure to landslide hazards is conditioned by the presence of other (future) buildings within the landslide track. Simplified approaches are often required for evaluating the exposure, such as for instance, assuming the same exposure for all buildings in a neighbourhood. This type of approaches may be acceptable for small scale analyses but must be refined when working at either local or site specific scale.

References

Abbruzzese JM (2011) Improved methodology for rock fall hazard zoning at the local scale. PhD dissertation N°5082, Rock Mechanics Laboratory of the Swiss Federal Institute of Technology of Lausanne (École Polytechnique Fédérale de Lausanne, EPFL)

Abbruzzese JM, Labiouse V (2010a) Comparison of two rock fall hazard mapping methodologies based on the French and Swiss guidelines. In: Proceedings of the Rock Slope Stability RSS 2010 symposium, Paris, France, 24–25 November

Abbruzzese JM, Labiouse V (2010b) Challenges in achieving European-wide methodologies for rock fall hazard mapping. In: Malet JP, Glade T, Casagli N (eds) Mountain risks – bringing science to society. CERG, Strasbourg

Abbruzzese JM, Labiouse V (2013) New Cadanav methodology for quantitative rock fall hazard assessment and zoning at the local scale. Landslides. doi:10.1007/s10346-013-0411-7

Abbruzzese JM, Sauthier C, Labiouse V (2009) Considerations on Swiss methodologies for rock fall hazard mapping based on trajectory modelling. Nat Hazard Earth Syst 9:1095–1109

Agliardi F, Crosta GB, Frattini P (2009) Integrating rockfall risk assessment and countermeasure design by 3D modelling techniques. Nat Hazard Earth Syst 9:1059–1073

AGS (2007) Guideline for landslide susceptibility, hazard and risk zoning for land use planning. Aust Geomech Soc Aust Geomech 42(1):13–36

Aleotti P, Chowdhury R (1999) Landslide hazard assessment: summary review and new perspectives. Bull Eng Geol Environ 58(1):21–44

Altimir J, Copons R, Amigó J, Corominas J, Torrebadella J, Vilaplana JM (2001) Zonificació del territori segons el grau de perillositat d'esllavissades al Principat d'Andorra, La Gestió dels Riscos Naturals, 1es Jornades del CRECIT (Centre de Recerca en Ciencies de la Terra), Andorra la Vella, 13–14 September 2001, pp 119–132

APB Provincia Autonoma di Bolzano (2008) Sistema informativo sui rischi idrogeologici (IHR), Relazione metodologica conclusiva. Provincia Autonoma di Bolzano – Alto Adige Ripartizione provinciale Opere idrauliche (eds), Bolzano

Bell R, Glade T (2004) Quantitative risk analysis for landslides – examples from Bνldudalur, NW-Iceland. Nat Hazard Earth Syst 4(1):117–131

Bunce CM, Cruden DM, Morgenstern NR (1997) Assessment of the hazard from rockfall on a highway. Can Geotech J 34:344–356

Copons R (2007) Avaluació de la perillositat de caigudes de blocs rocosos al Solà d'Andorra la Vella. CENMAm Institut d'Estudis Andorrans (ed), 213 pp

Corominas J, Mavrouli O (2011a) Rockfall quantitative risk assessment. In: Stéphane L, François N (eds) Rockfall engineering. Wiley, London, pp 255–296
Corominas J, Mavrouli O (2011b) Estimation quantitative du risque (QRA) pour les bâtiments induit par des éboulements rocheux : état des lieux. Journée de rencontre sur les dangers naturels 2011. Institut de Géomatique et d'Analyse du Risque, Unil Lausanne, February 17–18, Lausanne, Switzerland
Corominas J, Moya J (2008) A review of assessing landslide frequency for hazard zoning purposes. Eng Geol 102:193–213
Corominas J, Copons R, Moya J, Vilaplana JM, Altimir J, Amigó J (2005) Quantitative assessment of the residual risk in a rock fall protected area. Landslides 2:343–357
Crosta GB, Agliardi F (2003) A methodology for physically based rockfall hazard assessment. Nat Hazard Earth Syst 3:407–422
Desvarreux P (2002) Considérations sur le zonage en France, Lecture notes from the course 'Université Européenne d'été sur les risques naturels 2002: glissements de terrain et instabilités de falaise', Sion, September 2002
Desvarreux P (2007) Problèmes posés par le zonage, Lecture notes from the course 'Université Européenne d'été 2007: éboulements, chutes de blocs – rôle de la forêt', Courmayeur, September 2007
ERM (1998) Landslides and boulder falls from natural terrain: interim risk guidelines. GEO Report No. 75
Evans SG, Hungr O (1993) The assessment of rockfall hazard at the base of talus slopes. Can Geotech J 30:620–636
Fell R, Ho KKS, Lacasse S, Leroi E (2005) A framework for landslide risk assessment and management. In: Hungr O, Fell R, Couture R, Eberhardt E (eds) Landslide risk management. Taylor & Francis Group, London
Fell R, Corominas J, Bonnard C, Cascini L, Leroi E, Savage WZ on behalf of the JTC-1 Joint Technical Committee on Landslides and Engineered Slopes (2008) Guidelines for landslide susceptibility, hazard and risk zoning for land use planning. Eng Geol 102:85–98
Heim A (1932) Bergsturz und Menschenleben. Beiblatt zur Vierteljahrschrift der Naturforschenden Gesellschaft in Zürich 77:218
Hoek E (2007) Practical rock engineering, course notes in rock engineering at the University of Toronto. http://download.rocscience.com/hoek/pdf/Practical_Rock_Engineering.pdf
Hungr O (1997) Some methods of landslide hazard intensity mapping. In: Fell R, Cruden DM (eds) Proceedings of the Landslide risk workshop. Balkema, Rotterdam
Hungr O, Evans SG, Hazzard J (1999) Magnitude and frequency of rock falls and rock slides along the main transportation corridors of southwestern British Columbia. Can Geotech J 36(2):224–238
Hungr O, McDougall S, Bovis M (2005) Entrainment of material by debris flows. In: Jakob M, Hungr O (eds) Debris-flow hazards and related phenomena. Springer, Berlin/Heidelberg
Interreg IIc (2001) Prévention des mouvements de versants et des instabilités de falaises: confrontation des méthodes d'étude d'éboulements rocheux dans l'arc Alpin, Interreg Communauté européenne
IUGS (1997) Quantitative risk assessment for slopes and landslides – the state-of-the-art. In: Cruden D, Fell R (eds) Landslide risk assessment. Balkema, Rotterdam
Jaboyedoff M, Labiouse V (2002) Etablissement d'une méthodologie de mise en œuvre des cartes de dangers naturels du Canton de Vaud Cadanav – Méthodologie instabilités rocheuses, Rapport pour le Canton de Vaud. LMR – EPFL, Lausanne
Jaboyedoff M, Labiouse V (2003) Preliminary assessment of rockfall hazard based on GIS data. ISRM 2003–Technology roadmap for rock mechanics. South Afr Inst Min Metall 1:575–578
Jaboyedoff M, Labiouse V (2011) Technical note: preliminary estimation of rockfall runout zones. Nat Hazard Earth Syst 11:819–828
Jaboyedoff M, Dudt JP, Labiouse V (2005) An attempt to refine rockfall hazard zoning based on the kinetic energy, frequency and fragmentation degree. Nat Hazard Earth Syst 5:621–632

Labiouse V, Abbruzzese JM (2011) Rockfall hazard zoning for land use planning. In: Stéphane Lambert, François Nicot (eds) Rockfall engineering. Wiley/ISTE ltd, New York/London

Lan H, Derek Martin C, Lim HC (2007) RockFall analyst: a GIS extension for three-dimensional and spatially distributed rockfall hazard modeling. Comput Geosci 33:262–279

Laboratoire Central des Ponts et Chaussées (LCPC) (2004) Les études spécifiques d'aléa lié aux éboulements rocheux – Guide technique, Collection Environment: Les Risques Naturels, 86 pp

Li ZH, Huang HW, Xue YD, Yin J (2009) Risk assessment of rockfall hazards on highways. Georisk 3(3):147–154

MATE/METL (1999) Plans de Prévention des Risques Naturels (PPR), Risques de Mouvements de Terrain, Guide Méthodologique. La Documentation Française (ed).

Mavrouli O, Corominas J (2010a) Vulnerability of simple reinforced concrete buildings in front of the rockfall impact. Landslides 7:169–180

Mavrouli O, Corominas J (2010b) Rockfall vulnerability assessment for reinforced concrete buildings. Nat Hazard Earth Syst 10(10):2055–2066

Mazzoccola D, Hudson J (1996) A comprehensive method of rock mass characterization for indicating natural slope instability. Q J Eng Geol Hydroge 29:37–56

Mazzoccola D, Sciesa E (2000) Implementation and comparison of different methods for rock fall hazard assessment in the Italian Alps. In: 8th international symposium on landslides, Cardiff, UK, pp 1035–1040

Mölk M, Poisel R, Weilbold J, Angerer H (2008) Rockfall rating systems: is there a comprehensive method for hazard zoning in populated areas? In: Proceedings of the 11th INTERPRAEVENT 2008 congress, vol 2, 26–30 May 2008, Dornbirn (Vorarlberg), Austria

MR (Mountain Risks Research Training Network). Glossary: http://www.unicaen.fr/mountainrisks/spip/spip.php?page=presentation_article&id_article=51#1. Accessed 15 Sept 2010.

OFAT/OFEE/OFEFP (1997) Prise en compte des dangers dus aux mouvements de terrain dans le cadre des activités de l'aménagement du territoire, edited by OFAT/OFEE/OFEFP (1997), Bern. http://www.planat.ch/ressources/planat_product_fr_1032.pdf

Pantelidis L (2011) A critical review of highway slope instability risk assessment systems. Bull Eng Geol Environ 70:395–400

Pierson LA, Van Vickle R (1993) Rockfall hazard rating system. Publication No. FHWA SA-93-057

Raetzo H, Lateltin O, Bollinger D, Tripet JP (2002) Hazard assessment in Switzerland – codes of practice for mass movements. Bull Eng Geol Environ 61:263–268

Remondo J, Bonachea J, Cendrero A (2005) A statistical approach to landslide risk modelling at basin scale: from landslide susceptibility to quantitative risk assessment. Landslides 2:321–328

Roberds W (2005) Estimating temporal and spatial variability and vulnerability. In: Eberthardt E, Hungr O, Fell R, Couture R (eds) Landslide risk management. Taylor & Francis, London

Rouiller JD, Jaboyedoff M, Marro C, Phillippossian F, Mamin M (1998) Pentes instables dans le Pennique valaisan, Rapport final PNR 31, VDF (ed), Zürich

Ruff M, Rohn J (2008) Susceptibility analysis for slides and rockfall: an example from the Northern Calcareous Alps (Vorarlberg, Austria). Environ Geol 55:441–452

Sasaki Y, Dobrev N, Wakizaka Y (2002) The detailed hazard map of road slopes in Japan. In: Instability – planning and management, Thomas Telford, London, pp 381–388

van Westen CJ (2010) GIS for the assessment of risk from geomorphological hazards. In: Alcantara-Ayala I, Goudie A (eds) Geomorphological hazards and disaster prevention. Cambridge University Press, Cambridge

Wieczorek GF, Jager S (1996) Triggering mechanisms and depositional rates of in the Yosemite Valley, California. Geomorphology 5:17–31

Chapter 7
Medium-Scale Multi-hazard Risk Assessment of Gravitational Processes

Cees van Westen, Melanie S. Kappes, Byron Quan Luna, Simone Frigerio, Thomas Glade, and Jean-Philippe Malet

Abstract This section discusses the analysis of multi-hazards in a mountainous environment at a medium scale (1:25,000) using Geographic Information Systems. Although the term 'multi-hazards' has been used extensively in literature there are still very limited approaches to analyze the effects of more than one hazard in the same area, especially related to their interaction. The section starts with an overview of the problem of multi-hazard risk assessment, and indicates the various types of multi-hazard interactions, such as coupled events, concatenated events, and events changing the predisposing factors for other ones. An illustration is given of multi-hazards in a mountainous environment, and their interrelationships,

C. van Westen (✉)
Faculty of Geo-Information Science and Earth Observation (ITC), University of Twente, Hengelosestraat 99, NL-7514 AE Enschede, The Netherlands
e-mail: c.j.vanwesten@utwente.nl

M.S. Kappes
Geomorphic Systems and Risk Research Unit, Department of Geography and Regional Research, University of Vienna, Austria Universitätsstraße 7, AU-1010 Vienna, Austria

The World Bank, Urban, Water and Sanitation, Sustainable Development Department, 1818 H St. NW, Washington, DC 20433, USA

B. Quan Luna
Det Norske Veritas, Veritasveien 1, Høvik, Norway

S. Frigerio
Italian National Research Council – Research Institute for Geo-Hydrological Protection (CNR – IRPI), C.so Stati Uniti 4, IT-35127 Padova, Italy

T. Glade
Geomorphic Systems and Risk Research Unit, Department of Geography and Regional Research, University of Vienna, Austria Universitätsstraße 7, AU-1010 Vienna, Austria

J.-P. Malet
Institut de Physique du Globe de Strasbourg, CNRS UMR 7516, Université de Strasbourg/EOST, 5 rue René Descartes, F-67084 Strasbourg Cedex, France

T. van Asch et al. (eds.), *Mountain Risks: From Prediction to Management and Governance*, Advances in Natural and Technological Hazards Research 34,
DOI 10.1007/978-94-007-6769-0_7,

showing triggering factors (earthquakes, meteorological extremes), contributing factors, and various multi-hazard relationships. The second part of the section gives an example of a medium scale multi-hazard risk assessment for the Barcelonnette Basin (French Alps), taking into account the hazards for landslides, debris flows, rockfalls, snow avalanches and floods. Input data requirements are discussed, as well as the limitations in relation to the use of this data for initiation modeling at a catchment scale. Simple run-out modeling is used based on the energy-line approach. Problems related to the estimation of temporal and spatial probability are presented and discussed, and methods are shown for estimating the exposure, vulnerability and risk, using risk curves that expressed the range of expected losses for different return periods. The last part presents a software tool (Multi-Risk) developed for the analysis of multi-hazard risk at a medium scale.

Abbreviations

DTM Digital Terrain Model
DSM Digital Surface Model
GIS Geographic Information Systems
DSS Decision Support System

7.1 Introduction

A generally accepted definition of multi-hazard still does not exist. In practice, this term is often used to indicate all relevant hazards that are present in a specific area, while in the scientific context it frequently refers to "more than one hazard". Likewise, the terminology that is used to indicate the relations between hazards is unclear. Many authors speak of interactions (Tarvainen et al. 2006; de Pippo et al. 2008; Marzocchi et al. 2009; Zuccaro and Leone 2011; European Commission 2011), while others call them chains (Shi 2002), cascades (Delmonaco et al. 2006a; Carpignano et al. 2009; Zuccaro and Leone 2011; European Commission 2011), domino effects (Luino 2005; Delmonaco et al. 2006a; Perles Roselló and Cantarero Prados 2010; van Westen 2010; European Commission 2011), compound hazards (Alexander 2001) or coupled events (Marzocchi et al. 2009).

There are many factors that contribute to the occurrence of hazardous phenomena, which are either related to the environmental setting (topography, geomorphology, geology, soils etc.) or to anthropogenic activities (e.g. deforestation, road construction, tourism). Although these factors contribute to the occurrence of the hazardous phenomena and therefore should be taken into account in the hazard and risk assessment, they are not directly triggering the events. For these we need triggering phenomena, which can be of meteorological or geophysical origin (earthquakes, or volcanic eruptions). Figure 7.1 illustrates the complex interrelationships

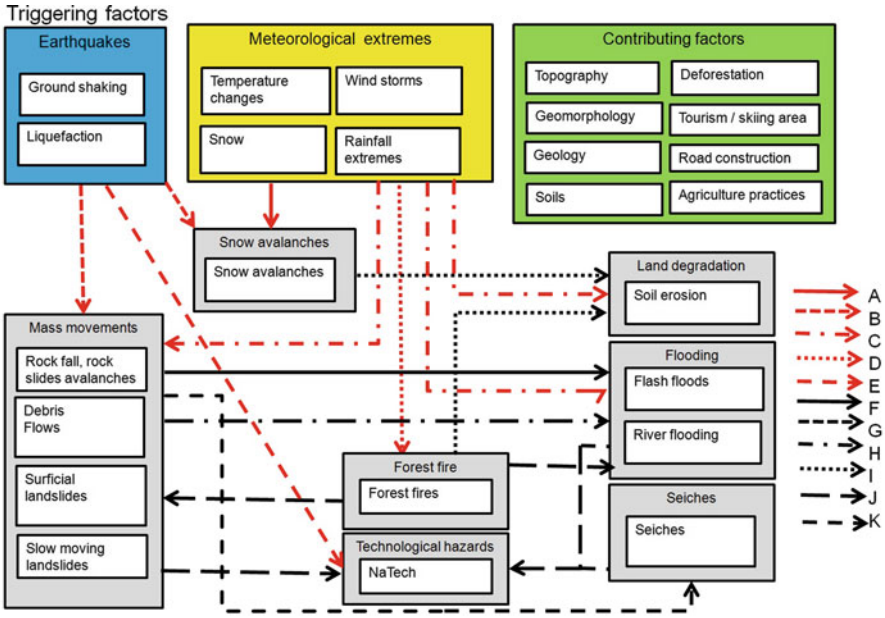

Fig. 7.1 Multi-hazard in a mountainous environment, and their interrelationships. Above the triggering factors are indicated (earthquakes, meteorological extremes), and the contributing factors. The *red arrows* indicate the hazards triggered simultaneously (coupled hazards). The *black arrows* indicate the concatenated hazards: one hazard causing another hazard over time. (**a**) Snow accumulation causing snow avalanches, (**b**) Earthquakes triggering landslides and snow avalanches simultaneously, (**c**) extreme precipitation causing landslides, debris flows, flooding and soil erosion, (**d**) drought and/or lightning causing forest fires, (**e**) earthquakes causing technological hazards, (**f**) landslides and debris flows damming rivers and causing dam break floods, (**g**) large rapid landslides or rockfalls in reservoirs causing water floods, (**h**) debris flows turning into floods in the downstream torrent section; (**i**) snow avalanches or forest fires leading to soil erosion, (**j**) forest fires leading to surficial landslides, debris flows and flash floods, (**k**) landslides, debris flows or floods leading to technological hazards

between multi-hazards potentially affecting the same mountainous environment. This graphic indicates that a multitude of different types of interrelations exists:

The first multi-hazard relationship is therefore between different hazard types that are triggered by the same triggering event. These are what we would call coupled events (Marzocchi et al. 2009). The temporal probability of occurrence of such coupled events is the same as it is linked to the probability of occurrence of the triggering mechanism. For analyzing the spatial extent of the hazard, one should take into account that when such coupled events occur in the same area and the hazard footprints overlap, the processes will interact, and therefore the hazard modeling for these events should be done simultaneously, which is still very complicated. In order to assess the risk for these multi-hazards, the consequence modeling should therefore be done using the combined hazard footprint areas, but differentiating between the intensities of the various types of hazards and using

different vulnerability-intensity relationships. When the hazard analyses are carried out separately, the consequences of the modeled scenarios cannot be simply added up, as the intensity of combined hazards may be higher than the sum of both or the same areas might be affected by both hazard types, leading to overrepresentation of the losses, and double counting. Examples of such types of coupled events is the effect of an earthquake on a snow-covered building (Lee and Rosowsky 2006) and the triggering of landslides by earthquakes occurring simultaneously with ground shaking and liquefaction (Delmonaco et al. 2006b; Marzocchi et al. 2009).

Another, frequently occurring combination are landslides, debris flows and flash-floods caused by the same extreme rainfall event. The consideration of these effects is fundamental since chains "expand the scope of affected area and exaggerate the severity of disaster" (Shi et al. 2010).

A second type of interrelations is the influence one hazard exerts on the disposition of a second peril, though without triggering it (Kappes et al. 2010). An example is the "fire-flood cycle" (Cannon and De Graff 2009): forest fires alter the susceptibility to debris flows and flash floods due to their effect on the vegetation and soil properties.

The third type of hazard relationships consists of those that occur in chains: one hazard causes the next. These are also called domino effects, or concatenated hazards. These are the most problematic types to analyze in a multi-hazard risk assessment. The temporal probability of each hazard in a chain is dependent on the temporal probability of the other hazard causing it. For example a landslide might block a river, leading to the formation of a lake, which might subsequently result in a dam break flood or debris flow. The probability of the occurrence of the flood is depending on the probability of the landslide occurring in that location with a sufficiently large volume to block the valley. The occurrence of the landslide in turn is related to the temporal probability of the triggering event. The only viable solution to approach the temporal probability of these concatenated hazards is to analyze them using Event Trees (Egli 1996; Marzocchi et al. 2009) a tool which is applied extensively in technological hazard assessment, but is still relatively new in natural hazard risk assessment. Apart from analyzing the temporal probability of concatenated events, the spatial probability is often also a challenge, as the secondary effect of one hazard (e.g. the location of damming of a river) is very site specific and difficult to predict. Therefore a number of simplified scenarios are taking into account, often using expert judgment.

7.2 Approaches for Multi-hazard Risk Assessment

Risk can be described in its simplest way as the probability of losses. The classical expression for calculating risk (R) was proposed by Varnes (1984) considered risk as the multiplication of H (Hazard probability), E (the quantification of the exposed elements at risk, and V (the vulnerability of the exposed elements at risk as the degree of loss caused by a certain intensity of the hazard).

As illustrated in Fig. 7.1 there are three important components in risk analysis: hazards, vulnerability and elements-at-risk (Van Westen et al. 2008). They are characterized by both non-spatial and spatial attributes. Hazards are characterized by their temporal probability and intensity derived from frequency magnitude analysis. Intensity expresses the severity of the hazard. The hazard component in the equation actually refers to the probability of occurrence of a hazardous phenomenon with a given intensity within a specified period of time (e.g. annual probability). Hazards also have an important spatial component, both related to the initiation of the hazard and the spreading of the hazardous phenomena (e.g. the areas affected by landslide run-out or flooding).

Elements-at-risk or 'assets' also have non-spatial and spatial characteristics (e.g. material type and number of floors for buildings). The way in which the amount of elements-at-risk is characterized (e.g. as number of buildings, number of people, economic value or the area of qualitative classes of importance) also defines the way in which the risk is presented.

The spatial interaction of elements-at-risk and hazard defines the exposure and the vulnerability of the elements-at-risk. Exposure indicates the degree to which the elements-at-risk are actually located in the path of a particular hazardous event. The spatial interaction between the elements-at-risk and the hazard footprints are depicted in a GIS by map overlaying of the hazard map with the elements-at-risk map. Physical vulnerability is evaluated as the interaction between the intensity of the hazard and the type of element-at-risk, making use of so-called vulnerability curves. For further explanations on hazard and risk assessment the reader is referred to textbooks such as Smith and Petley (2008), van Westen et al. (2009), and Alcantara-Ayala and Goudie (2010).

Loss estimation has been carried out in the insurance sector since the late 1980s using geographic information systems (GIS; Grossi et al. 2005). Since the end of the 1980s risk modelling has been developed by private companies (such as AIR Worldwide, Risk Management Solutions, EQECAT), resulting in a range of proprietary software models for catastrophe modelling for different types of hazards.

One of the first loss estimation methods that was publicly available was the RADIUS method (Risk Assessment Tools for Diagnosis of Urban Areas against Seismic Disasters), a simple tool to perform an aggregated seismic loss estimation using a simple GIS (RADIUS 1999).

The best initiative for publicly available loss estimation thus far has been HAZUS (which stands for 'Hazards U.S.') developed by the Federal Emergency Management Agency (FEMA) together with the National Institute of Building Sciences (NIBS, Buriks et al. 2004). The first version of HAZUS was released in 1997 with a seismic loss estimation focus, and was extended to multi-hazard losses in 2004, incorporating also losses from floods and windstorms (FEMA 2004). HAZUS was developed as a software tool under ArcGIS. HAZUS is considered a tool for multi-hazard risk assessment, but the losses for individual hazards are analyzed separately for earthquakes, windstorms and floods. Secondary hazards (e.g. earthquakes triggered landslides) are considered to some degree using a basic approach. Although the HAZUS methodology has been very well documented, the tool was

primarily developed for the US, and the data formats, building types, fragility curves and empirical relationships cannot be exported easily to other countries. Several other countries have adapted the HAZUS methodology to their own situation, e.g. in Taiwan (Yeh et al. 2006) and Bangladesh (Sarkar et al. 2010). The HAZUS methodology has also been the basis for the development of several other software tools for loss estimation. One of these is called SELENA (SEimic Loss EstimatioN using a logic tree Approach), developed by the International Centre for Geohazards (ICG), NORSAR (Norway) and the University of Alicante (Molina et al. 2010).

Whereas most of the above mentioned GIS-based loss estimation tools focus on the analysis of risk using a deterministic approach, the Central American Probabilistic Risk Assessment Initiative (CAPRA 2012) has a true probabilistic multi-hazard risk focus. The aim of CAPRA is to develop a system which utilizes Geographic Information Systems, Web-GIS and catastrophe models in an open platform for disaster risk assessment, which allows users from the Central American countries to analyze the risk in their areas, and be able to take informed decisions on disaster risk reduction. The methodology focuses on the development of probabilistic hazard assessment modules, for earthquakes, hurricanes, extreme rainfall, and volcanic hazards, and the hazards triggered by them, such as flooding, windstorms, landslides and tsunamis. These are based on event databases with historical and simulated events. This information is combined with elements-at-risk data focusing on buildings and population. For the classes of elements-at-risk, vulnerability data can be generated using a vulnerability module. The main product of CAPRA is a software tool, called CAPRA-SIG, which combines the hazard scenarios, elements-at-risk and vulnerability data to calculate Loss Exceedance Curves.

In New Zealand, a comparable effort is made by developing the RiskScape methodology for multi-hazard risk assessment (Reese et al. 2007; Schmidt et al. 2011). This approach aims at the provision of a generic software framework which is based on a set of standards for the relevant components of risk assessment. Another good example of multi-hazard risk assessment is the Cities project in Australia, which is coordinated by Geoscience Australia. Studies have been made for six cities of which the Perth study is the latest (Durham 2003; Jones et al. 2005). Also in Europe, several projects have developed multi-hazard loss estimations systems and approaches, such as the ARMAGEDOM system in France (Sedan and Mirgon 2003) and in Germany (Grünthal et al. 2006).

In the areas of industrial risk assessment, a number of methods have been developed using GIS-based DSSs (Decision Support Systems). One of these is the ARIPAR system (Analysis and Control of the Industrial and Harbour Risk in the Ravenna Area, Analisi e controllo dei Rischi Industriali e Portuali dell'Area di Ravenna, Egidi et al. 1995; Spadoni et al. 2000). The ARIPAR methodology is composed of three main parts: the databases, the risk calculation modules and the geographical user interface based on the Arc-View GIS environment. Currently the system is converted to ArcGIS, and also natural hazards are included in the analysis.

For risk assessment for mountainous areas, there are up to date no tools that analyze multi-hazard risk for combined processes, such as snow avalanches, rockfall, debris flows, floods and landslides. Studies on the assessment of landslide

risk or flood risk separately have been carried out, at different scales and using different methods (Bell and Glade 2004; Remondo et al. 2008; Alkema 2007; Zezere et al. 2008; Cassidy et al. 2008). However, multi-hazard risk examples are still scarce. Van Westen et al. (2002) present a case study of the city of Turrialba (Costa Rica), subjected to landslide, earthquake and flood risk, and propose three different schemes to assess hazard and vulnerability and integrate the losses afterwards. Lacasse et al. (2008) carried out a multi-hazard risk assessment related to the potential collapse of the Aknes rock slide in Norway, using an event tree, for the different scenarios which include the triggering of tsunamis. Event trees were also used by Carboni et al. (2002) to analyze the probabilities of different event scenarios of a single which might lead to the partial damming of a nearby river and the followed dambreak flooding.

When evaluating the existing methods for multi-hazard risk assessment applicable in mountainous areas, the following aspects can be mentioned:

- As many areas are exposed to more than one type of hazard, in the hazard identification phase of the risk assessment, all hazards have to be taken into account as risk analyses are spatially oriented (Greiving et al. 2006) to enable overall risk reduction.
- The models (heuristic, statistical, physically based) required for analysis of hazard for different processes vary considerably. They depend on hazard type, scale, data typology and resolution (Delmonaco et al. 2006b) and complicate the comparison of the very different results (units of the outcome, quality, uncertainty, resolution etc.) even further. A main problem is the comparability of hazards since they vary in "nature, intensity, return periods, and [. . .] effects they may have on exposed elements" (Carpignano et al. 2009).
- Also for vulnerability models a very similar situation exists. For some hazards a variety of analytical methods exist while for other processes none or only very few are established and the approaches vary widely between hazards (Hollenstein 2005).
- The way in which coupled and cascading events are evaluated. Natural hazards are not independent from each other. Instead, they are highly connected and interlinked in the natural geosystem (Kappes et al. 2010).
- The availability and quality of data are important since the model choice, the information value of the results as well as the detail of the analysis depends on these prerequisites. Each of the hazard types has different requirements with respect to the input data. The historical information on past events is crucial for most types of hazards, but the availability of historical records differs greatly among the hazard types, also depending whether these are derived from measured records (flood discharge, earthquake catalogues), archives, image interpretation, or interview (van Westen et al. 2008).
- Uncertainty plays a major role in hazard and risk assessment. The uncertainties may be due to inherent natural variability, model uncertainties and statistical uncertainties. This leads to different uncertainty levels for the various hazards. The inclusion of uncertainty is actually a necessity in probabilistic risk assessment,

and methods should still be developed to better represent these for mountain hazards and risks.

- Difficulties concerning the administrative issues as different organizations are normally involved for analyzing the hazard and risk for individual hazard types, which may make the comparison and standardization of the results difficult (Marzocchi et al. 2009). Young (2003) describes an example in the framework of environmental resources management and called this phenomenon the 'problem of interplay'.
- The natural and the administrative system are in most cases neither sharing the same spatial nor temporal framework conditions. Hazards are not restricted to administrative boundaries (e.g. river floods or earthquakes). However, hazard and risk management is mostly operating on administrative units. Therefore, a larger coordination is required between the two affected administrative units. In these cases hazard analyses should not be limited to the administrative unit, since the cause of a damaging event might be far away from the area of impact. In the case of earthquakes, for example, the impact might be far away from the epicentre. Some hazards exhibit very long return periods, therefore preventive measures will probably not show any effect during one or few legislative periods. Young (2002) entitled this phenomenon as 'problem of fit'.
- Not only the stakeholders involved in the elaboration of the analysis request detailed analysis and information. For example, the needs of emergency managers and civil protection are surely different from those of spatial planners.
- Hazard and risk assessment requires a multitude of data, coming from different data sources. Therefore it is important to have a strategy on how to make data available for risk management. Since data is coming from different organizations it is important to look at aspects such as data quality, metadata, multi-user databases, etc. Spatial risk information requires the organization of a Spatial Data Infrastructure, where through internet basic GIS data can be shared among different technical and scientific organizations involved in hazard and risk assessment.

To illustrate some of these aspects a case study is presented of medium scale multi-hazard risk assessment in the Barcelonnette area, one of the test sites within the Mountain Risk project. The Barcelonnette area is one of the best studied areas in the Alps, and a large amount of data has been collected over the years by different research teams and in different (EU funded) projects, coordinated by CNRS (Flageollet et al. 1999; Maquaire et al. 2003; Remaître 2006; Thierry et al. 2007; Malet 2010). The case study presents the results of hazard and risk assessment for floods, landslides, rockfall, snow avalanches and debris flows, based on a number of previous works (Kappes and Glade 2011; Kappes et al. 2010, 2011, 2012a, b; Bhattacharya et al. 2010a, b; Ramesh et al. 2010; van Westen et al. 2010; Hussin et al. 2012). The aim of the case study is not so much to show the actual values, as the complete multi-hazard risk analysis requires more detailed work, but more to illustrate the procedure and to show the problems involved and the levels of uncertainty.

7.3 Case Study: Medium Scale Multi-hazard and Risk Assessment in the Barcelonnette Area

The method followed in this case study closely follows the framework for multi-hazard risk assessment, presented in Fig. 7.1, with the following steps: input data collection, susceptibility assessment, hazard assessment, exposure analysis, vulnerability assessment and risk analysis. The aim of the exercise was to show the steps required for a risk assessment at the medium scale (1:25,000 to 1:50,000), and to outline the level of uncertainty associated with each of the components. Whereas risk assessment at a local scale, e.g. for a single debris flow torrent or landslide, can be done with a lower level of uncertainty, as more detailed data is available (e.g. Remaitre 2006; Hussin et al. 2012) the challenge is to do such an analysis for different types of hazards at a catchment level.

7.3.1 Input Data

The input data for the hazard and risk assessment was derived mainly from Malet (2010), and additional field investigations. A GIS database was generated, containing information on the following components: image data, topographic data, elements at risk data, environmental factors, triggering factors, and hazard inventory data (see Table 7.1). Of these factors the hazard inventory data is the most important, as it gives vital information on the dates, location, characteristics and damage caused by past occurrences.

Data from past flood events were based on technical reports, newspapers, and information from the local municipality and the RTM (Service de Restauration des Terrains de Montage– Mountain Land Restoration Service) and previous studies (Lecarpentier 1963). Data was available for one discharge station and two rainfall stations for a considerable time period (1904–2009). An inventory of active and relict landslides has been compiled by Thierry et al. (2007) at 1:10,000 scale using aerial photo-interpretation (API), fieldwork and analysis of archives. To characterize uncertainty in the mapping process, different levels of confidence were defined during the photo-interpretation and field survey (Thierry et al. 2007). A collection of historical data in archives, newspapers, monographs, technical reports, bulletins and scientific papers for the period between 1850 and 2009 has been carried out. Detailed descriptions on the type and quality of information collected and the methodologies used to analyze the data can be found in Flageollet et al. (1999) and Remaître (2006).

Over the period 1451–2010, about 600 references with exact date and location of landslide triggering have been recorded by the group of Malet (2010). For each soil slide and debris flow event, information is available on the date and location,

Table 7.1 Input data for multi-hazard risk assessment in the Barcelonnette area (OMIV 2013)

Type	Data	Characteristics
Image data	Satellite image	Downloaded from Google Earth, orthorectified, and resampled to 1.5 m pixel size
	3-D image	Anaglyph made by combining Google Earth image and DEM
	Airphotos	A set of panchromatic airphotos from different years
Topographic data	Contour lines	Digitized from topographic map, with 5 m contour interval
	DEM	Interpolated from contour lines
	Slope angle	Slope steepness made from DEM
	Slope aspect	Slope direction made from DEM
	Hillshading	Artificial illuminated made from DEM
	Openness	Visualization of DEM
	Plan curvature	Concavity-convexity made from DEM
	Flow accumulation	Contributing area made from DEM
Elements at risk data	Communes	Adm. units with population data
	Building footprints	Individual buildings & characteristics
	Cadastral map	Individual land parcels with ownership
	Roads/powerlines	Linear structures
	Bridges	Point file with bridge characteristics
	Lithology	Lithological units
Environmental factors	Materials	Unconsolidated materials
	Soils	Soil types and average depths
	Landuse 2007	Land use map of 2007
	Landuse 1980	Land use map of 1980
Triggering factors	Rainfall data	Daily rainfall for two stations from 1904 to 2009
	Discharge data	Discharge data for one station from 1904 to 2009
Hazard inventory data	Flood scenarios	Flood extend, water depth and velocity modelled for different return periods (100, 150, 250 and 500 years)
	Streams	Drainage network
	Flood events	Historical flood events from 1957 to 2008
	Avalanche field	Catalogue of avalanches mapped in field
	Avalanche photo	Catalogue mapped from airphotos
	Landslide inventory	Mapped from photos and field
	Landslide dates	Table with known landslide dates
	Heuristic hazard	Hazard map: direct mapped by experts
	Statistical hazard	Hazard map through statistical analysis by Thierry et al. (2007)
	Debris flow dates	Table with known events
	Debris flow zones	Map of catchments with DF frequency
	Rockfall area	Inventory of rockfall areas

although many of them are by approximation only. After reviewing the data, a catalogue remained of 106 mass-movement events (53 debris flows and 53 soil slides; Remaître and Malet 2011).

Information on the location of snow avalanches and rockfalls was obtained from a snow avalanche inventory made by field inventory and photo interpretation. Although a number of individual dates of occurrence could be obtained from reports, it was not possible to link the individual polygons of snow avalanches and rockfall to specific dates.

The official existing hazard map of the area is the PPR (Plan des Prévention des Risques Naturels Prévisibles, MATE/MATL 1999), which subdivides the area in three risk zones: high risk in red zones, medium risk in blue zones and low or no risk in white zones. In the red zone no permission to develop any kind of new infrastructure is allowed, whereas in the blue zone it requires a special permission.

7.3.2 Gravitational Processes Source Area Characterization

Susceptibility maps indicating the relative likelihood for the initiation of gravitational processes were generated for the various processes: snow avalanches, shallow landslides and rockfalls. Two different approaches were used: heuristic and statistical methods. The heuristic methods partly followed the methodology of the PPR (MATE/MATL 1999) by identifying sectors with homogeneous environmental characteristics, taking into account the possibility of landslide development (up- and downhill) for a 100 years period, based on a set of expert rules (Thierry et al. 2008). Shallow landslide initiation susceptibility maps for a part of the study area were also prepared using weights of evidence modelling (Thierry et al. 2007) and using fuzzy logic approach (Thiery et al. 2006) for rotational and translational landslides. In the rest of the area expert rules were used to classify specific combinations of environmental factors such as slope steepness, lithology, surface deposits, and land use. Avalanche source areas were outlined according to the methodology proposed by Maggioni (2004). Potential rock fall sources were mapped by means of a threshold slope angle and the exclusion of certain rock types as for example outcropping clays (Corominas et al. 2003). The input maps for each analysis were combined in GIS using joint-frequency tables, in which the expected susceptibility class (high, moderate, low or not susceptible) was indicated for each specific combination of the input maps. The susceptibility maps were tested using the existing inventories, and the decision rules were improved using an iterative procedure until a good agreement was reached. In order to be able to use the initiation susceptibility maps for the run-out susceptibility assessment, and given the lack of sufficient data on the dates and locations of the individual events, an assumption was introduced to indicate in which zones events were likely

Table 7.2 Assumption used in analyzing the susceptibility maps

	Triggering event		
Susceptibility class	Major event	Moderate event	Minor event
High	1	1	1
Moderate	1	1	0
Low	1	0	0
Not	0	0	0

The value of 1 indicates that gravitational processes may occur

to be initiated in three different triggering events. Table 7.2 indicates that, during a major triggering event, gravitational processes might initiate in all three zones (high, moderate and low susceptible areas). During a moderate triggering event, only gravitational processes are expected to be initiated in the moderate and high susceptible zone, and during a minor triggering event only in the high susceptible zones. Given the lack of temporal information this was the best option available. It is however, one of the major sources of uncertainty in the entire process leading to the risk assessment.

The analysis resulted in a series of 12 binary maps, indicating the presence or absence of source areas for major, moderate and minor triggering events for all types of gravitational processes.

7.3.3 Gravitational Hazard Assessment: Run-Out Modelling

The source areas defined in the previous section were subsequently used for run-out modelling on a medium (1:25,000) scale using the routing-spreading model Flow-R (Horton et al. 2008; Kappes et al. 2011). The model takes the results of the source area identification and calculates the spreading zone for each source. The choice of spreading algorithms is made by the user. This run-out modelling approach does not consider the volume of the source mass, which is another major source of uncertainty in the risk analysis. The run-out distance calculation is based on a unit energy balance, a constant loss function and a velocity threshold (Horton et al. 2008).

For each of the types of processes (debris flows, snow avalanches, rockfalls, shallow landslides) reach angles were obtained from literature (Corominas 1996). The calculation of the probable maximum run-out is based on the definition of an average slope angle between the starting and end point, considering a constant friction loss. The friction loss angles selected were between 5° and 30° and the velocity thresholds between 5 and 30 m/s depending on the type of process and the severity of the event. In the analysis a Holmgren routing algorithm was chosen for debris flows and snow avalanches because it fits reasonable with convergent flows, and the so-called D8 algorithm was used for rockfalls. The results of this analysis

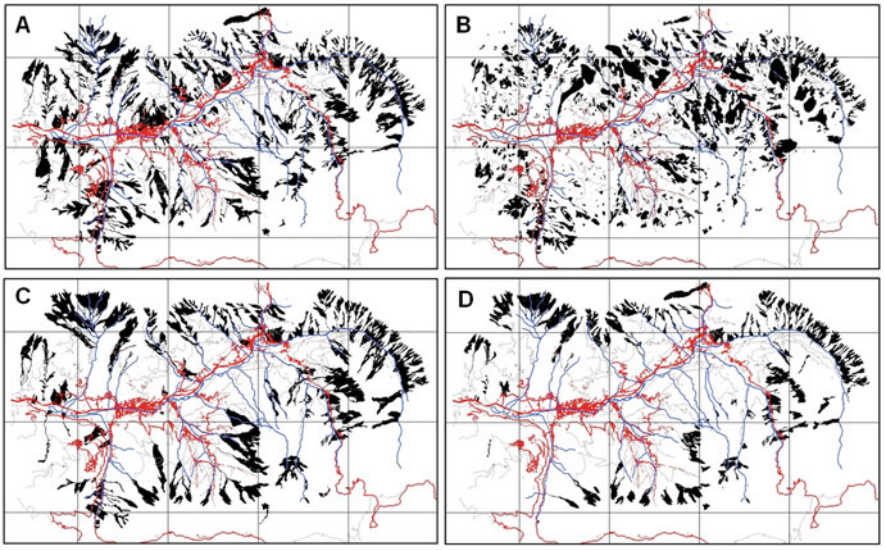

Fig. 7.2 Examples of run-out maps for major events. (**A**) Debris flow, (**B**) landslide, (**C**) rockfall and (**D**) snow avalanche

are actually more an indication rather than an accurate prediction of run-out distance and energy. Nevertheless they do give a fairly good indication as shown by Blahut (2009). Figure 7.2 shows some example of the results of the run-out assessment.

The resulting maps of Kinetic Energy were converted into impact pressure maps using average values for bulk densities of run-out materials. The maps were also classified into three susceptibility classes for run-out. It is evident from Fig. 7.4 that the determination of the source areas, and the selection of the average run-out angles may lead to an overestimation of the areas potentially affected. This process was done iteratively and the results were compared with the inventories, until a reasonable result was obtained.

7.3.4 Estimating Temporal and Spatial Probabilities of Gravitational Processes

The susceptibility assessment for gravitational processes resulted in a total of 24 susceptibility maps: three maps representing the severity classes of the triggering events (major, moderate and minor) for four hazard types (landslide, rockfall, debris flow and snow avalanche) for initiation susceptibility and a also 12 maps for the run-out susceptibility. These should be converted in hazard maps, not by changing of the actual boundaries of the susceptibility maps, but by characterizing them in terms of

Table 7.3 Summary of the information available to assess temporal, spatial and magnitude probabilities of gravitational hazards

	Spatial occurrence	Temporal information	Intensity
Snow avalanche	Only snow avalanche accumulation areas are available without dates of occurrence	Attribute tables have dates but not reliable. Return periods were estimated.	Simple estimation of impact pressure from FLOW-R Frequency-size distribution of events
Rockfall	Only rockfall accumulation areas are available without dates of occurrence	Only a few dates are known of rockfalls. Return periods were estimated	Simple estimation of impact pressure from FLOW-R
Debris flow	Only for a few of debris flows the areas are known	Debris flow dates are know for 53 events. Analysis based on antecedent rainfall analysis	Simple estimation of impact pressure from FLOW-R
Landslide	A complete landslide inventory was available for part of the area (Thierry et al. 2007). Used to calculate landslide density.	Landslide dates are known for 53 events. Analysis based on antecedent rainfall analysis	Simple estimation of impact pressure from FLOW-R Frequency-size distribution of events
Flood	Only 2 historic flood maps, and modelled flood maps for 150, 250, 500 and 1,000 year return period	Discharge information from 1905 to 2009 were analyzed using Gumbel frequency analysis	Flood depth and velocity maps are available for each return period resulting from flood modelling.

their spatial and temporal probability and intensity. The following information for each class should be indicated:

- Temporal probability: the probability that a triggering event with a severity level (major, moderate or minor) will take place within a given time period.
- Spatial probability: the probability that a pixel located within one of the susceptibility classes for the initiation and run-out susceptibility maps will actually experience a damaging gravitational process during a triggering event.
- Intensity: a measure of the intensity of the gravitational processes at a certain location, within one of the initiation or run-out susceptibility classes for the three classes of triggering events.

Ideally this process should be carried out using event-based landslide inventories, which are inventories caused by the same triggering event, for which the return period is know. Unfortunately no such event-based inventories are available for the Barcelonnette area. So the estimation was mostly based on expert opinion. Table 7.3 lists the main criteria used in the estimation of these values for the four types of gravitational processes and for flooding.

Table 7.4 Estimated return periods and uncertainties for major, moderate and minor triggering events for the four types of gravitational hazards

	Triggering event					
	Major		Moderate		Minor	
	Return period	Uncertainty estimate	Return period	Uncertainty estimate	Return period	Uncertainty estimate
Snow avalanche	150	±50	70	±25	25	±8
Rockfall	500	±200	200	±100	50	±20
Debris flow	180	±40	90	±20	30	±10
Landslide	200	±50	100	±30	40	±10

For the assessment of the temporal probability of shallow landslides and debris flows, Remaître and Malet (2011) carried out an extensive analysis of rainfall thresholds using a number of different models, such as the antecedent precipitation analysis, Intensity-Duration (I-D) model (Guzzetti et al. 2008), I-A-D model (Cepeda et al. 2009), and FLaIR (Sirangelo and Versace 2002). Based on their analysis they concluded that debris flows are triggered by storms lasting between 1 and 9 h, and are adequately predicted using an Intensity-Duration threshold, and soil slides are triggered by storms with durations between 3 and 17 h. Based on these values, an estimation could be made of the number of the return periods for triggering rainfall for debris flows and shallow landslides. For rockfalls we do not have enough known dates of occurrence to make a good frequency analysis. Based on the scarce information that we had on the occurrence of historical events, we made an estimation of the return periods, and associated levels of uncertainty of the three severity classes of triggering events for the hazard types (Table 7.4). Note that due to the lack of event-based inventories there is a very high level of uncertainty in these values. The spatial probability gives an indication of the probability that if a triggering event occurs (Major, Moderate or Minor), and an element at risk is located in the modelled run-out area, of the probability that this particular element at risk would be hit.

Since the run-out maps cover quite a large area, it is not to be expected that all the modelled areas will be affected. By analyzing the distribution of the past events, we estimated how many individual gravitational processes were initiated during a triggering event, and what their size was. We divided the modelled area of the run-out in each class by the area that was covered by gravitational processes during a similar event, to get an estimation of the spatial probability. The results are indicated in Tables 7.5 and 7.6.

Also this estimation has a considerable degree of uncertainty, as we do not have event-based landslide maps, which would allow us to directly calculate the number of gravitational processes and their average size for particular triggering events. The results also show that run-out modelling resulted in a considerable overestimation of the potentially affected areas. The better it is possible to limit the modelled run-out areas to those zones that will actually get affected, the higher the spatial probability values will be.

Table 7.5 Estimated number of gravitational processes and average sizes for major, moderate and minor triggering events for the four types of gravitational hazards

	Triggering event					
	Major		Moderate		Minor	
	Number of events	Average size (m^2)	Number of events	Average size (m^2)	Number of events	Average size (m^2)
Snow avalanche	20 ± 6	$40{,}000 \pm 10{,}000$	10 ± 3	$20{,}000 \pm 6{,}000$	5 ± 2	$10{,}000 \pm 2{,}000$
Rockfall	7 ± 4	$10{,}000 \pm 5{,}000$	5 ± 2	$5{,}000 \pm 1{,}500$	2 ± 1	$2{,}500 \pm 500$
Debris flows	15 ± 8	$40{,}000 \pm 20{,}000$	10 ± 4	$20{,}000 \pm 10{,}000$	5 ± 2	$10{,}000 \pm 2{,}000$
Landslide	50 ± 20	$10{,}000 \pm 5{,}000$	20 ± 5	$5{,}000 \pm 1{,}000$	5 ± 2	$2{,}500 \pm 500$

Table 7.6 Estimated spatial probabilities of gravitational processes for major, moderate and minor triggering events for the four types of gravitational hazards

	Triggering event		
	Major	Moderate	Minor
	Spatial probability	Spatial probability	Spatial probability
Snow avalanche	0.0305 ± 0.0168	0.0163 ± 0.0098	0.0114 ± 0.0069
Rockfall	0.0017 ± 0.0018	0.0011 ± 0.0008	0.0005 ± 0.0004
Debris flow	0.0123 ± 0.0127	0.0070 ± 0.0063	0.0069 ± 0.0041
Landslide	0.0166 ± 0.0671	0.0085 ± 0.0038	0.0025 ± 0.0015

7.3.5 Flood Hazard Assessment

The procedure for flood hazard assessment is described separately because it follows a different procedure than for gravitational processes. For analyzing the temporal probability of flood events, the flood discharge data for the period 1904–2009 was used in a statistical analysis using the Gumbel and Pearsons models to derive the relationship between discharge and return period (Bhattacharya et al. 2010a). Based on that, discharges were defined for return periods of 100, 150, 250 and 500 years. Hydraulic simulation software, in this case SOBEK and HEC-RAS, was used to analyze the flow of water in greater detail (Bhattacharya et al. 2010a; Ramesh et al. 2010). For this analysis a detailed Digital Surface Model had to be generated that incorporates all obstructions, including embankments and main buildings. This was done by interpolating the available 5 m contour lines with the incorporation of the stream network by eliminating the morphologic features within the river bed to have an un-braided structure. The building foot print layer has been used for the addition of the heights of physical elements, taking into account that there were important changes during the two historical flood events of 1957 and 2008. The changes have been incorporated and two DSM's were generated. The dyke and the embankment were included with respective heights and included in the final DSM. The land use maps from two periods were used to generate two maps of Manning's surface roughness values. For hydraulic modelling the combined 1D and 2D flood model of SOBEK was used to characterize flood events over complex topography, in both time periods, representing the situation during 1957 and during the present situation. The output data of the model consists of a series of water depth and flow velocity maps at different time steps. In this case, the maps were generated at 1 h intervals. The model also created a set of maps that summarize the simulation, which include a maximum water depth map (representing the highest water depth value that was reached at some point during the simulation), a maximum flow velocity map (representing the highest flow velocity value that was reached at some point during the simulation), and two maps that indicate the time at which the maximum water depth and the maximum flow velocity were reached and a map that shows the time at which a pixel started being inundated. To validate the flood models, the two historical flood events of 1957 and 2008 were reconstructed using the SOBEK

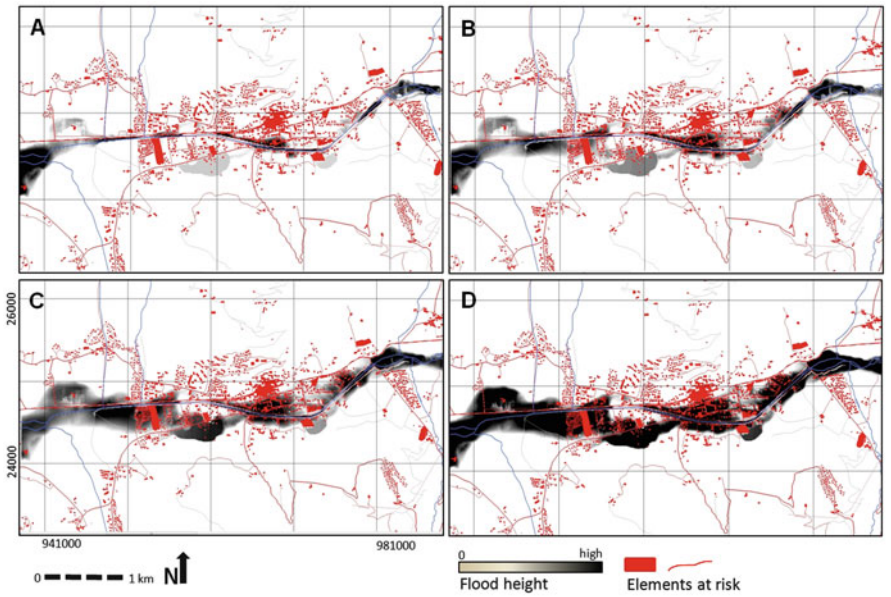

Fig. 7.3 Examples of flood maps resulting from the flood modeling for different return periods. (**A**) 150 year, (**B**) 250 year, (**C**) 500 year, (**D**) 1,000 year (Bhattacharya et al. 2010a)

modelling. The 1957 flood corresponds to a flood with a return period of 200 years. For the modelling the Digital Surface Model and the roughness map representing the 1957 situation were used (see Fig. 7.3). The analysis resulted in eight maps: maximum water height and flow velocity maps for four return periods, which can be combined in impact maps.

7.3.6 Exposure and Vulnerability Assessment

In the exposure analysis, the 24 hazard maps for the gravitational processes and the 8 maps for flood hazards were subsequently combined in GIS with the elements at risk. The building map contains information on all the buildings in the study area, where each building has its own attributes, related to building type, number of floors, occupancy type, and number of inhabitants for a daytime and night-time scenario. The exposure analysis identifies the exposed number of buildings (Table 7.7) which can also be classified according to the attributes mentioned above. The characteristics of the number of inhabitant can also be used to calculate the number of exposed people in different temporal scenarios. In this analysis also the time of the year should be incorporated, given the fact that the Barcelonnette area is a touristic destination, with a very different population distribution in winter (chalets, hotels, and ski areas), summer (camping sites, hotels and chalets) and the off season period.

Table 7.7 Summary of the number of buildings exposed to the various hazard types and severity of triggering events

	Major event	Moderate event	Minor event
Debris flow	396	171	10
Landslide	49	4	1
Rockfall	140	13	1
Snow avalanche	55	10	5
Flooding	565	364	233

Table 7.8 Exposed areas of main land use types to debris flow (in km^2)

	Major event	Moderate event	Minor event
Forest	24	4.40	3.10
Arable land	2	0.70	0.05
Pastures	12.10	4.40	0.45
Urban fabric	0.58	0.11	0.02

Table 7.9 Exposed length of main linear features to debris flows (in km)

Length affected (km)	Major event	Moderate event	Minor event
Main road	3.71	1.29	0.18
Secondary road	55.27	18.24	2.21
Unpaved road	150.41	49.01	2.91
Ski chair lift	0.12	0	0
Skilift	0.23	0	0
Electric powerline	2.33	0	0

Exposure was also calculated for land use types, by combining the recent land use maps with the 32 hazard scenarios, and representing the exposed areas of different land use types in km^2. For example, Table 7.8 shows the results for debris flows.

A similar analysis was carried out for the transportation infrastructure, and lifelines. Table 7.9 shows an example for the length of these linear features exposed to debris flows.

Minor triggering events occur mostly in uninhabited areas, and would mostly affect forested areas (e.g. debris flows, snow avalanches and rockfall). The level of uncertainty of the exposed elements at risk depends partly on the completeness (spatially and temporally) of the elements at risk map, but much more on the modeled susceptible areas. As mentioned in the previous section, the modeled run-out areas are an overrepresentation of the areas that would be actually affected in the case of a triggering event, and the variation in the spatial probability is therefore an indication of the uncertainty in the exposure.

The last component required for analyzing the risk is the physical vulnerability of the exposed elements at risk, which requires the application of vulnerability curves, giving the relation between hazard intensity and degree of damage for

different types of elements at risk. For flood vulnerability several stage-damage curves that related water height to damage were used from the UK (Pennin-Rowsell et al. 2003), Germany (Buck and Merkel 1999) and France. For the gravitational processes, several vulnerability curves and matrices were used (Bell and Glade 2004; Fuchs et al. 2007; Quan Luna et al. 2011). It should be noted here that these vulnerability curves and matrices are general approximations, and show substantial differences. For the run-out hazard maps, we use the curves derived by Quan Luna et al. (2011) that relate impact pressure to degree of damage. Given the large uncertainty of the modeled intensity of the various processes at a medium scale, and the uncertainty associated with the use of empirically derived curves, which show the average damage of a group of similar buildings exposed to the same hazard intensity, the results of the vulnerability assessment also have a very high degree of uncertainty. Furthermore, only the vulnerability of the structures was evaluated using vulnerability curves. The vulnerability in terms of building contents was evaluated by assuming a standard set of assets per building occupancy type and unit floor space, and assuming total destruction of building contents when debris flows or floods entered the ground floor.

7.3.7 Risk Assessment

The results from the previous analyses (initiation and run-out susceptibility analysis, temporal and spatial probability assessment, exposure and vulnerability analysis) were integrated in order to estimate the expected losses. The expected losses can be calculated by integrating the temporal probability of occurrence of the different scenarios and the consequences, which are calculated as the multiplication of the spatial probability, amount of exposed elements at risk and their vulnerability. The expression used for analyzing the multi-hazard risk is given by Eq. 7.1:

$$\text{Risk} = \sum_{\text{All hazards}} \left(\int_{P_T=0}^{P_T=1} P_{(T|HS)} * \left(P_{(S|HS)} * \sum \left(A_{(ER|HS)} * V_{(ER|HS)} \right) \right) \right) \tag{7.1}$$

where $P_{(T|HS)}$ is the temporal probability of a certain hazard scenario (HS); $P_{(S|HS)}$ is the spatial probability that a particular pixel in the susceptible areas is affected given a certain hazard scenario; $A_{(ER|HS)}$ is the quantification of the amount of exposed elements at risk, given a certain hazard scenario (e.g. expressed as the number or economic values) and $V_{(ER|HS)}$ is the vulnerability of elements at risk given the hazard intensity under the specific hazard scenario.

The multiplication of exposed amounts and vulnerability should be done for all elements at risk for the same hazard scenario. If the modelled hazard scenario is not expected to be producing the hazard phenomena, as is the case in most of

the gravitational processes hazard maps, the results should be multiplied with the spatial probability of hazard events $P_{(S|HS)}$. The resulting value represents the losses, which are plotted against the temporal probability of occurrence for the same hazard scenario in a so-called risk curve. This is repeated for all available hazard scenarios. At least three individual scenarios should be used, although it is preferred to use at least six events with different return periods (FEMA 2004) to better represent the risk curve. The area under the curve is then calculated by integrating all losses with their respective annual probabilities. Multi-hazard risk is calculated by adding the average annual losses for the different types of hazard. The risk analysis can be done for different spatial units. It is possible to create risk curves for the entire study area, or for administrative units (communes, census tracts) or for manually drawn homogeneous units with respect to land use.

In this study we only focused on analyzing building losses for the five different hazard types as mentioned earlier. For each hazard type we only used three hazard scenarios (major, moderate and minor) which have different return periods for each of the hazard types. We also expressed the uncertainty of each of the components of the risk assessment procedure. The results are shown in Table 7.10 and in Fig. 7.4.

The variation between the calculated losses depending on the uncertainty of the temporal probability of the identified hazard scenarios is shown in the right side of Fig. 7.4. It is clear from this figure that flood risk is much higher than any of the other four types, because it directly affects the urban center of Barcelonnette, whereas the other hazards occur more in the mountainous part of the area, where much less buildings are exposed. Debris flows follow as second important hazard type, although the expected losses are much less. When the uncertainty in terms of hazard modelling is included by incorporating also the component of spatial probability (Ps) it is clear that the expected losses for the gravitational hazards decrease considerably. The spatial probability of the modelled flood scenarios is considered one because each of the areas under the hazard footprint is expected to experience flooding, be it of different intensity. For the gravitational processes, this uncertainty is much higher, and the inclusion of the spatial probability decreases the expected losses with a factor of 100, purely based on the uncertainty of modelling the areas where actual gravitational processes are likely to happen. The better the run-out models are able to narrow down to the future sites of events, the higher the $P_{(S|HS)}$ will be. Low accuracies in modelling will therefore result in lower risks.

7.4 MultiRISK, a Platform for Multi-hazard Risk Modeling and Visualization

The calculation of multi-hazard risk requires a large number of calculation steps which could be integrated in a spatial DSS. In the framework of the Mountain Risks project a prototype software for multi-hazard risk analyses has been developed.

Table 7.10 Result of the quantitative risk assessment for the four gravitational hazards and for flood hazard

		Annual probability (P_T)		Spatial probability (P_S)		Exposed	Losses if	Expected losses (million)	
	Scenario	min	max	min	max	buildings	$P_S = 1$	min	max
Debris flow	Major	0.007	0.005	0.003	0.028	496	24.8	0.0744	1.3888
	Moderate	0.014	0.009	0.002	0.015	171	8.55	0.0171	0.2565
	Minor	0.050	0.025	0.003	0.012	10	0.50	0.0015	0.0120
Landslide	Major	0.007	0.004	0.005	0.139	49	2.45	0.0123	0.6811
	Moderate	0.014	0.008	0.005	0.013	4	0.20	0.0010	0.0052
	Minor	0.033	0.020	0.001	0.004	1	0.05	0.0001	0.0004
Rock fall	Major	0.003	0.001	0.001	0.004	240	12	0.0120	0.0960
	Moderate	0.010	0.003	0.001	0.002	13	0.65	0.0007	0.0026
	Minor	0.033	0.014	0.001	0.002	1	0.05	0.0001	0.0002
Snow avalanche	Major	0.010	0.005	0.016	0.050	55	2.75	0.0440	0.2750
	Moderate	0.022	0.011	0.008	0.027	10	0.50	0.0040	0.0270
	Minor	0.059	0.031	0.005	0.019	5	0.25	0.0013	0.0095
Flood	Major	0.001	0.001	1	1	389	100	100	160
	Moderate	0.003	0.002	1	1	357	17	17	30
	Minor	0.005	0.004	1	1	322	5	5	9

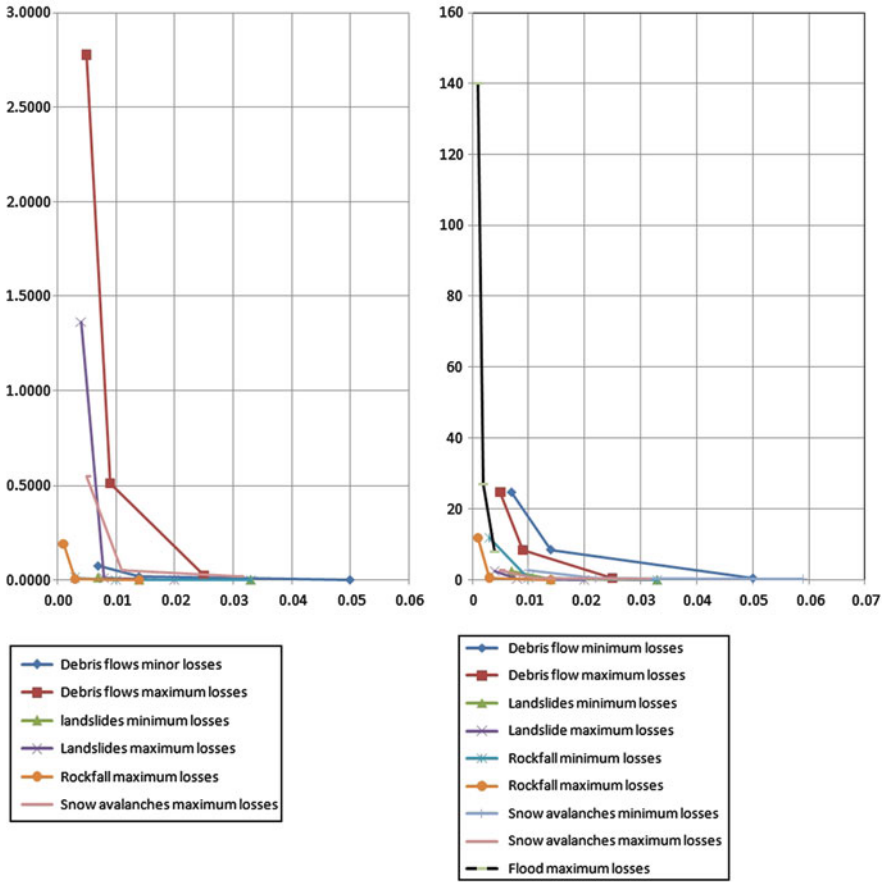

Fig. 7.4 Risk curves of the five hazard types, displaying the variation of losses (shown on X-Axis in M€) against temporal probability (annual probability shown on Y-axis). The *left graph* shows the results taking into account both temporal and spatial probability (note that the flood losses are excluded). The *right graph* shows the variation only in terms of temporal probability

This tool is designed to offer a user-friendly, fast and combined examination of multiple mountain hazards (e.g. debris flows, rock falls, shallow landslides, avalanches and river floods). Since multi-hazard studies suffer from high data requirements a top-down approach is recommendable within which, by means of a regional study, areas of potential risk and hazard interactions are identified to be subsequently analyzed in detail in local studies. The MultiRISK Modeling Tool is designed according to a top-down concept. It consists of at least two scales at which analyses are carried out – first an overview analysis and secondly detailed studies (possible extension by a third even more detailed scale for e.g. specific engineering purposes). In its current version MultiRISK consists still exclusively of the regional overview analysis (∼1:10,000–1:50,000) but will be extended in the future by

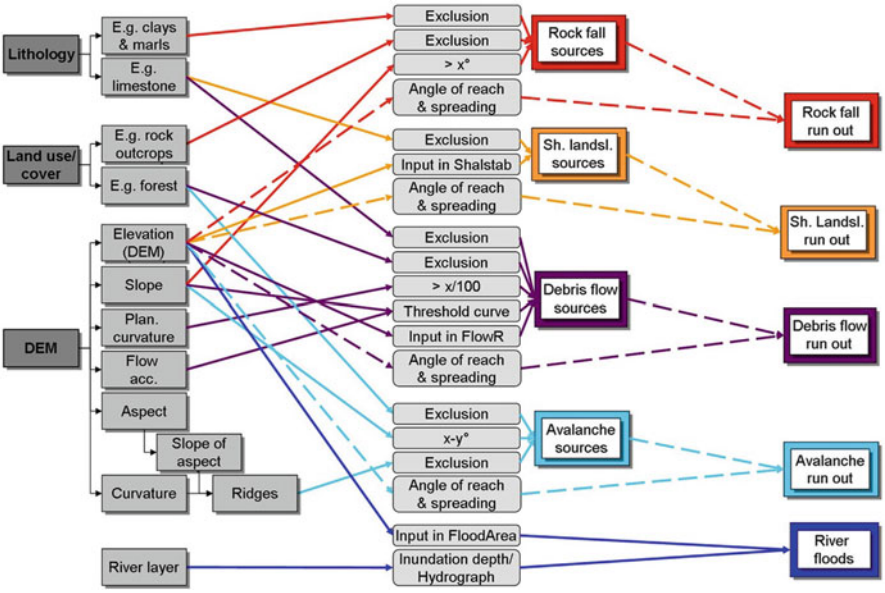

Fig. 7.5 Analysis scheme for the MultiRISK Modeling Tool (Kappes et al. 2012a, b)

local models and methods. In this section, the regional analysis scheme behind the analysis software as well as the structure of the software itself is presented shortly (for a more detailed presentation, refer to Kappes et al. 2011, 2012a, b).

For the regional analysis simple empirical models with low data-requirements were chosen. For the identification of potential rock fall sources a method was used which employs a threshold slope angle and the exclusion of certain rock types as for example outcropping clays (Corominas et al. 2003). For the flood analysis a method was selected which extrapolates the inundation over a DSM based on a fixed inundation depth (Geomer 2008). Shallow landslide source areas are modeled with Shalstab (Montgomery and Dietrich 1994), avalanche source areas are modeled according to the methodology proposed by (Maggioni 2004) and debris flow sources with Flow-R after (Horton et al. 2008). The run out of rock falls, shallow landslides, avalanches and debris flows is computed with Flow-R as described in Horton et al. (2008). The spatial input data needed for all these models is composed of a DEM and derivatives, land use/cover and lithological information. Figure 7.5 gives an indication of the decision rules used in the multi-hazard analysis.

The complexity of the analysis scheme indicates the effort necessary and the time-consumption for the step-by-step performance of the whole procedure in GIS software. Hence, an automation was undertaken to relief the modelers of the intermediate steps (Fig. 7.5), simplify the structure to the important decisions and facilitate a fast and reproducible computation and re-computation of a multi-hazard analysis (Fig. 7.6).

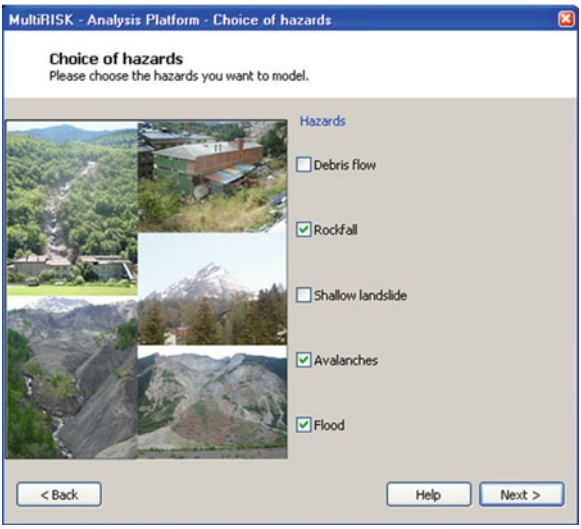

Fig. 7.6 Interface of the MultiRISK Modeling Tool

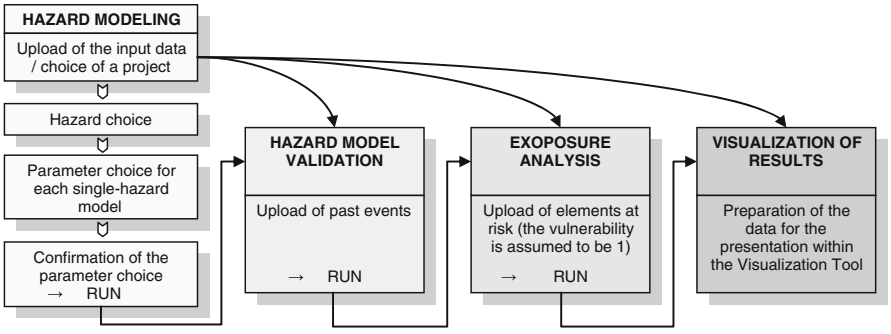

Fig. 7.7 Flow chart of the MultiRISK Modeling Tool (Kappes et al. 2012a, b)

Table 7.11 Confusion matrix (from Beguería 2006)

	Modeled	Not-modeled
Recorded	True positives	False negatives
Not-recorded	False positives	True negatives

Additionally to the hazard modeling, a model validation step as well as an exposure analysis are included (Fig. 7.7).

The validation is carried out according to Begueria (2006) by means of an overlay of the modeling result with recorded events and the area falling into the resulting four categories (Table 7.11) quantified in a confusion matrix.

The exposure analysis offered in MultiRISK is carried out by means of an overlay of the elements at risk and the single-hazard zones. The number of buildings, length of infrastructure or proportion of settled area exposed is calculated.

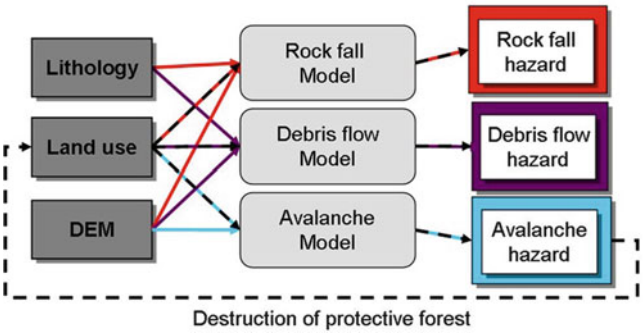

Fig. 7.8 Proposed feedback loop (From Kappes et al. 2010)

The effect of interactions is not yet implemented in the structure of the software tool but conceptual considerations how to account for them do already exist. First, it refers to the alteration of the disposition one hazard by another. Within the analysis procedure this refers to the alteration of factors which serve as input data as e.g. the impact of avalanche events on the land use (the destruction of forest) and subsequently the modification of future rock fall, debris flow and avalanche hazard this entails. By means of feedback-loops this phenomenon can be included (Fig. 7.8). The manual creation of an updated land use file for the re-upload as input file and the re-computation of the three affected hazards already allow carrying out this feedback-loop. Second, the triggering of one hazard by another resulting in so-called hazard chains has to be regarded. At a regional scale, only the identification of places potentially prone to such chains can be identified whereas their detailed examination by means of e.g. event trees is restricted to local analyses (Delmonaco et al. 2006a). Potential chains arising within the set of hazard currently included in MultiRISK are especially the undercutting of slopes during flood events and the damming of rivers and torrents due to landsliding. By an overlay of the respective hazard layers the zones can be identified.

The MultiRISK Modelling Tool is linked to the MultiRISK Visualization Tool to facilitate the display of the analysis results and together they form the MultiRISK Platform. The MultiRISK Visualization Tool is presented in Sect. 15.4.

7.5 Conclusion

This chapter outlines a number of aspects dealing with the assessment of multi-hazard risk assessment at a medium scale (1:25,000 to 1:50,000) for mountainous areas in Europe. The procedure outlined in this chapter is not intended to focus on the actual calculated risk values, as much more work needs to be done in better defining the temporal probability, in modelling the run-out areas related to hazard

events with a specific return period, in quantifying the physical vulnerability to gravitational processes, and representing the replacement costs. The main aim of this chapter was to show the procedure for quantitative multi-hazard risk assessment and to illustrate the large degree of uncertainty involved if event-based inventories are not available.

The modelling of the temporal probability of triggering events for different hazard types will remain problematic, given the limited available historical information on gravitational processes occurrences. Although this is improving nowadays as more countries are implementing national landslide inventories, often with a web-GIS interface. Also for large triggering events there are more possibilities to collect the event-based landslide inventories due to the available of more frequent and more detailed satellite data. However, the conclusion that quantitative multi-hazard risk assessment in mountainous areas can only be carried out if more detailed historic inventories are available, is too obvious. Many areas will continue to suffer from this problem, yet solutions must be found and estimations of loss should be given to improve disaster risk reduction planning. Therefore the use of tools such as the Multi-Risk platform outlined in this chapter, should be promoted, allowing for simple but efficient methods for estimating the risk of different hazards in the same area, and comparing their expected losses.

In the risk assessment a number of challenges remain. One of them is the modelling of hazard initiation points for different hazards (e.g. flooding and gravitational processes) based on the same meteorological trigger. These initiation points, which will vary with respect to the temporal probability of the triggering rainfall, should be used for modelling runout with quantifiable intensity measures. The modelling of uncertainty in this process is another major challenge, as well as the generation of vulnerability relations that incorporate uncertainties. And finally also the link with non-quantifiable aspects should be made using indicators for social, economic and environmental vulnerability.

Hazard, vulnerability and risk are dynamic, as changes occur in the hazard processes, human activities and land use/landcover patterns in mountainous areas, due to global changes. The analysis of changes in risk is therefore a very relevant topic for further study. This is the research topic of the CHANGES network (Changing Hydro-meteorological Risks – as Analyzed by a New Generation of European Scientists) funded by the EU FP7 Marie Curie Initial Training Network (ITN) Action. The project will develop an advanced understanding of how global changes (related to environmental and climate change as well as socio-economical change) will affect the temporal and spatial patterns of hydro-meteorological hazards and associated risks in Europe; how these changes can be assessed, modelled, and incorporated in sustainable risk management strategies, focusing on spatial planning, emergency preparedness and risk communication. The CHANGES network hopes to contribute to the Topical Action numbers 2 and 3 of the Hyogo Framework for Action of the UN-ISDR, as risk assessment and management, combined with innovation and education are considered essential to confront the impacts of future environmental changes (ISDR 2009). The network consists of 11

full partners and 6 associate partners of which 5 private companies, representing 10 European countries, and 12 ESR's (PhD researchers) and 3 ER's (Postdocs) are hired. The project has a duration of 4 years and has started in January 2011 (www.changes-itn.eu).

References

Alcantara-Ayala I, Goudie AS (2010) Geomorphological hazards and disaster prevention. Cambridge University Press, Cambridge

Alexander D (2001) Natural hazards. In: Encyclopedia of environmental science. Kluwer Academic Publishers, Dordrecht

Alkema D (2007) Simulating floods: on the application of a 2D-hydraullic model for flood risk assessment. International Institute for Geo-information Science and Earth Observation, Enschede

Beguería S (2006) Validation and evaluation of predictive models in hazard assessment and risk management. Nat Hazards 37:315–329

Bell R, Glade T (2004) Quantitative risk analysis for landslides – examples from Bνldudalur, NW-Iceland. Nat Hazard Earth Syst 4(1):117–131

Bhattacharya N, Kingma NC, Alkema D (2010a) Flood risk assessment of Barcelonnette for estimation of economic impact on the physical elements at risk in the area. In: Malet JP, Glade T, Casagli N (eds) Mountain risks – bringing science to society. CERG, Strasbourg

Bhattacharya N, Alkema D, Kingma NC (2010b) Integrated flood modeling for hazard assessment of the Barcelonnette municipality, South French Alps. In: Malet JP, Glade T, Casagli N (eds) Mountain risks – bringing science to society. CERG, Strasbourg

Blahut J (2009) Debris flow hazard and risk analysis at medium and local scale. PhD dissertation. University of Milan Bicocca, Faculty of Mathematical, Physical and Natural Sciences. Department of Environmental and Territorial Sciences, pp230

Buck W, Merkel U (1999) Auswertung der HOWAS – Datenbank, Institut fur Wasserwirtschaft und Kulturtechnik (IWK) der Universitat Karlsruhe, Karlsruhe, Report Nr. HY 98/15

Buriks C, Bohn W, Kennett M, Scola L, Srdanovic B (2004) Using HAZUS-MH for risk assessment: how-to guide. Technical Report 433, FEMA

Cannon S, DeGraff J (2009) The increasing wildfire and post-fire debris-flow threat in western USA, and implications for consequences of climate change. In: Sassa K, Canuti P (eds) Landslides – disaster risk reduction. Springer, Heidelberg

CAPRA (2012) Central American Probabilistic Risk Assessment (CAPRA). World Bank. www.ecapra.org

Carboni R, Catani F, Iotti A, Monti L (2002) The Marano landslide (Gaggio Montano, Appennino Bolognese) of February 1996. Quaderni Geol Appl 8(1):123–136

Carpignano A, Golia E, Di Mauro C, Bouchon S, Nordvik J-P (2009) A methodological approach for the definition of multi-risk maps at regional level: first application. J Risk Res 12:513–534

Cassidy MJ, Uzielli M, Lacasse S (2008) Probability risk assessment of landslides: a case study at Finneidfjord. Can Geotech J 45:1250–1267

Cepeda J, Díaz MR, Nadim F, Høeg K, Elverhøi A (2009) An empirical threshold model for rainfall-induced landslides: application to the Metropolitan Area of San Salvador, El Salvador

Corominas J (1996) The angle of reach as a mobility index for small and large landslides. Can Geotech J 33:260–271

Corominas J, Copons R, Vilaplana J, Altimir J, Amigó J (2003) Integrated landslide susceptibility analysis and hazard assessment in the principality of Andorra. Nat Hazards 30:421–435

de Pippo T, Donadio C, Pennetta M, Petrosino C, Terlizzi F, Valente A (2008) Coastal hazard assessment and mapping in Northern Campania, Italy. Geomorphology 97:451–466

Delmonaco G, Margottini C, Spizzichino D (2006a) ARMONIA methodology for multi-risk assessment and the harmonisation of different natural risk maps. Deliverable 3.1.1, ARMONIA
Delmonaco G, Margottini C, Spizzichino D (2006b) Report on new methodology for multi-risk assessment and the harmonisation of different natural risk maps. Deliverable 3.1, ARMONIA
Durham K (2003) Treating the risks in cairns. Nat Hazards 30(2):251–261
Egidi D, Foraboschi FP, Spadoni G, Amendola A (1995) The ARIPAR project: analysis of the major accident risks connected with industrial and transportation activities in the Ravenna area. Reliab Eng Syst Safe 49(1):75–89
Egli T (1996) Hochwasserschutz und Raumplanung. Schutz vor Naturgefahren mit Instrumenten der Raumplanung – dargestellt am Beispiel von Hochwasser und Murgängen. vdf Hochschulverlag AG, ETH Zürich
European Commission (2011) Risk assessment and mapping guidelines for disaster management. Commission staff working paper, European Union
FEMA (2004) HAZUS-MH. FEMA's methodology for estimating potential losses from disasters. US Federal Emergency Management Agency. http://www.fema.gov/plan/prevent/hazus/index.shtm
Flageollet JC, Maquaire O, Martin B, Weber D (1999) Landslides and climatic conditions in the Barcelonnette and Vars basins (Southern French Alps, France). Geomorphology 30(1–2):65–78
Fuchs S, Heiss K, Hóbl J (2007) Towards an empirical vulnerability function for use in debris flow risk assessment. Nat Hazard Earth Syst 7:495–506
Geomer (2008) FloodArea – ArcGIS extension for calculating flooded areas: user manual. Geomer GmbH and Ingenieurgemeinschaft
Greiving S, Fleischhauer M, Lückenkötter J (2006) A methodology for an integrated risk assessment of spatially relevant hazards. J Environ Plann Man 49(1):1–19
Grossi P, Kunreuther H, Patel CC (2005) Catastrophe modeling: a new approach to managing risk. Springer, New York
Grünthal G, Thieken AH, Schwarz J, Radtke KS, Smolka A, Merz B (2006) Comparative risk assessments for the City of Cologne – storms, floods, earthquakes. Nat Hazards 38(1–2):21–44
Guzzetti F, Peruccacci S, Rossi M, Stark CP (2008) The rainfall intensity-duration control of shallow landslides and debris flows: an update. Landslides 5(1):3–17
Hollenstein K (2005) Reconsidering the risk assessment concept: standardizing the impact description as a building block for vulnerability assessment. Nat Hazard Earth Syst 5:301–307
Horton P, Jaboyedoff M, Bardou E (2008) Debris flow susceptibility mapping at a regional scale. In: 4th Canadian Conference on Geohazards, Québec, Canada. Université Laval
Hussin HY, Quan Luna B, van Westen CJ, Christen M, Malet JP, van Asch TWJ (2012) Parameterization of a numerical 2-D debris flow model with entrainment: a case study of the Faucon catchment, Southern French Alps. Nat Haz Earth Syst Sci (NHESS) 12(10):3075–3090
Jones T, Middelmann M, Corby N (2005) Natural hazard risk in Perth, Western Australia. The cities project, Geosci Aus. http://www.ga.gov.au/hazards/reports/perth/
Kappes M, Glade T (2011) Landslides considered in a multi-hazard context. In: Proceedings of the second world landslide forum, Rome
Kappes M, Keiler M, Glade T (2010) From single– to multi-hazard risk analyses: a concept addressing emerging challenges. In: Malet JP, Glade T, Casagli N (eds) Mountain risks – bringing science to society. CERG, Strasbourg
Kappes MS, Malet JP, Remaitre A, Horton P, Jaboyedoff M, Bell R (2011) Assessment of debris-flow susceptibility at medium-scale in the Barcelonnette Basin, France. Nat Hazard Earth Syst 11:627–641
Kappes M, Gruber KSF, Bell R, Keiler M, Glade T (2012a) A medium/regional-scale multi-hazard risk analysis tool: the multirisk platform. Geomorphology 151–152:139–155
Kappes M, Gruber K, Glade T (2012b) Multi-hazard risk analyses with MultiRISK – tools for a user-friendly performance. In: 12th congress INTERPRAEVENT, Grenoble

Lacasse S, Eidsvik U, Nadim F, Hoeg K, Blikra LH (2008) Event tree analysis of Aknes rock slide hazard. In: Locat J, Perret D, Turmel D, Demers D, Leroueil S (eds) Proceedings of the IVth Canadian conference on geohazards: from causes to management. Presse de l'Université Laval, Québec, pp 551–557

Lecarpentier MC (1963) La Crue de Juin 1957 en Ubaye et ses consequences morphodynamiques. PhD dissertation, University of Strasbourg

Lee K, Rosowsky D (2006) Fragility analysis of woodframe buildings considering combined snow and earthquake loading. Struct Safe 28:289–303

Luino F (2005) Sequence of instability processes triggered by heavy rainfall in the northern Italy. Geomorphology 66:13–39

Maggioni M (2004) Avalanche release areas and their influence on uncertainty in avalanche hazard mapping. PhD dissertation, Universität Zürich

Malet JP, Remaitre A (2011) Statistical and empirical models for prediction of precipitation-induced landslides. Barcelonnette case study. Safeland deliverable. EU Safeland project

Maquaire O, Malet JP, Remaître A, Locat J, Klotz S, Guillon J (2003) Instability conditions of marly hillslopes: towards landsliding or gullying? The case of the Barcelonnette basin, south east France. Eng Geol 70(1–2):109–130

Marzocchi W, Mastellone M, Di Ruocco A (2009) Principles of multi-risk assessment: interactions amongst natural and man-induced risks. European Commission

MATE/MATL (1999) Plan de prévention des risques (PPR): risques de mouvements de terrain, ministère de l'Aménagement du territoire et de l'Environnement (MATE), ministère de l'Equipement des transports et du logement (METL). La Documentation Française, Paris, 72p

Molina S, Lang DH, Lindholm CD (2010) SELENA – an open-source tool for seismic risk and loss assessment using a logic tree computation procedure. Comput Geosci 36(3):257–269

Montgomery D, Dietrich W (1994) A physically based model for the topographic control on shallow landsliding. Water Resour Res 30:1153–1171

OMIV – Barcelonnette area. http://eost.u-strasbg.fr/omiv/data.php. Accessed Apr 2013

Penning-Rowsell EC, Johnson C, Tunstall S, Morris J, Chatterton J, Cokera A, Green C (2003) The benefits of flood and coastal defence techniques and data for 2003. Flood hazard Research Centre, Middlesex University, Middlesex

Perles Roselló M, Cantarero Prados F (2010) Problems and challenges in analyzing multiple territorial risks: methodological proposals for multi-hazard mapping. Boletín de la Asociación de Geógrafos Espanoles 52:399–404

Quan Luna B, Blahut J, van Westen CJ, Sterlacchini S, van Asch TWJ, Akbas SO (2011) The application of numerical debris flow modelling for the generation of physical vulnerability curves. Nat Hazard Earth Syst 11:2047–2060

RADIUS (1999) RADIUS method (Risk Assessment Tools for Diagnosis of Urban Areas against Seismic Disasters). http://www.geohaz.org/news/images/publications/RADIUS_RiskAssessment.pdf

Ramesh A, Glade T, Alkema D, Krol BGCM, Malet JP (2010) Model performance analysis for flood hazard assessment in Ubaye river, Barcelonnette, France. In: Malet JP, Glade T, Casagli N (eds) Mountain risks – bringing science to society. CERG, Strasbourg

Reese S, Bell R, King A (2007) RiskScape: a new tool for comparing risk from natural hazards. Water Atmos 15:24–25

Remaître A (2006) Morphologie et dynamique des laves torrentielles : application aux torrents des Terres Noires du bassin de Barcelonnette (Alpes du Sud). PhD dissertation, University of Caen Basse-Normandie, Caen

Remondo J, Bonachea J, Cendrero A (2008) Quantitative landslide risk assessment and mapping on the basis of recent occurrences. Geomorphology 94:496–507

Sarker JK, Ansary MA, Rahman MS, Safiullah MM (2010) Seismic hazard assessment for Mymensingh, Bangladesh. Environ Earth Sci 60:643–653

Schmidt J, Matcham I, Reese S, King A, Bell R, Henderson R, Smart G, Cousins J, Smith W, Heron D (2011) Quantitative multi-risk analysis for natural hazards: a framework for multi-risk modeling. Nat Hazards 58(3):1169–1192

Sedan O, Mirgon C (2003) Application ARMAGEDOM Notice utilisateur, BRGM open file BRGM/RP-52759-FR

Shi P (2002) Theory on disaster science and disaster dynamics. J Natural Disaster 11:1–9

Shi P, Shuai J, Chen W, Lu L (2010) Study on the risk assessment and risk transfer mode of large scale disasters. In: The 3rd international disaster and risk conference *IDRC*, Davos

Sirangelo B, Versace P (2002) Un modello probabilistico per la predizione in tempo reale delle altezze di precipitazione a scala oraria. Proceedings 'XXVIII Convegno di Idraulica e Costruzioni Idrauliche', Potenza, 2:395–414

Smith K, Petley DN (2008) Environmental hazards. Assessing risk and reducing disaster. Taylor & Francis, London

Spadoni G, Egidi D, Contini S (2000) Through ARIPAR-GIS the quantified area risk analysis supports land-use planning activities. J Hazard Mater 71(1–3):423–437

Tarvainen T, Jarva J, Greiving S (2006) Spatial pattern of hazards and hazard interactions in Europe. In: Schmidt-Thomé P (ed) Natural and technological hazards and risks affecting the spatial development of European regions. Geological survey of Finland, special paper 42. Geological Survey of Finland, Espoo, pp 83–91, 2 tables, 3 maps

Thiery Y, Malet J-P, Maquaire O (2006) Test of Fuzzy logic rules for landslide susceptibility assessment. In: Weber C, Gancarski P (eds) SAGEO 2006, Proceedings international conference on spatial analysis and geomatics, Strasbourg, France, CD-Rom Support Proceedings, 18 p

Thiery Y, Malet JP, Sterlacchini S, Puissant A, Maquaire O (2007) Landslide susceptibility assessment by bivariate methods at large scales: application to a complex mountainous environment. Geomorphology 9(1–2):8–59

Thierry P, Stieltjes L, Kouokam E, Nguéya P, Salley PM (2008) Multi-hazard risk mapping and assessment on an active volcano: the GRINP project at Mount Cameroon. Nat Haz 45:429–456

Van Westen CJ (2009) Multi-hazard risk assessment, guide book. Distance education course, Faculty of Geo-Information Science and Earth Observation (ITC), University of Twente

Van Westen CJ (2010) GIS for the assessment of risk from geomorphological hazards. In: Geomorphological hazards and disaster prevention. Cambridge University Press, Cambridge

Van Westen CJ, Montoya L, Boerhoom L, Coto EB (2002) Multi-hazard Risk Assessment using GIS in Urban areas: a case study for the city of Turrialba, Costa Rica. Proceedings of Regional Workshop on Best Practices in Disaster Mitigation, Lessons learned from the Asian Urban Disaster Mitigation Program and other initiatives, 24–26 September, Bali, pp 53–72

Van Westen CJ, Castellanos Abella, E.A. and Sekhar, L.K. (2008) Spatial data for landslide susceptibility, hazards and vulnerability assessment: an overview. Eng Geol 102(3–4):112–131

Van Westen CJ, Castellanos Abella EA, Sekhar LK (2008) Spatial data for landslide susceptibility, hazards and vulnerability assessment: an overview. Eng Geol 102 (3–4):112–131

Varnes DJ (1984) Landslide hazard zonation: a review of principles and practice. Commission on landslides of the IAEG, UNESCO. Nat Hazards 3:61

Yeh CH, Loh CH, Tsai KC (2006) Overview of Taiwan earthquake loss estimation system. Nat Hazards 37(1–2):23–37

Young OR (2002) The institutional dimension of environmental change: fit, interplay, and scale. MIT Press, Cambridge

Young OR (2003) Environmental governance: the role of institutions in causing and confronting environmental problems. Int Environ Agreements Polit Law Econ 3(4):377–393

Zêzere JL, Garcia RAC, Oliveira SC, Reis E (2008) Probabilistic landslide risk analysis considering direct costs in the area north of Lisbon (Portugal). Geomorphology 94:467–495

Zuccaro G, Leone M (2011) Volcanic crisis management and mitigation strategies: a multi-risk framework case study. Earthzine 4

Chapter 8
Methods for the Characterization of the Vulnerability of Elements at Risk

Simone Sterlacchini, Sami Oguzhan Akbas, Jan Blahut, Olga-Christina Mavrouli, Carolina Garcia, Byron Quan Luna, and Jordi Corominas

Abstract Risk assessment is the process of determining the likelihood or threat of a damage, injury, liability, loss, or other negative occurrence that is caused by external or internal vulnerabilities and that may be neutralized through preventive action. More precisely, risk assessment is the systematic prospective analysis aimed at defining, as quantitatively as possible, the potential loss of life, personal injury,

S. Sterlacchini (✉)
Italian National Research Council, Institute for the Dynamic of Environmental Processes (CNR – IDPA), Piazza della Scienza 1, IT-20126 Milan, Italy
e-mail: simone.sterlacchini@unimib.it; simone.sterlacchini@idpa.cnr.it

S.O. Akbas
Department of Environmental and Territorial Sciences, University of Milano-Bicocca, Piazza della Scienza 1, IT-20126 Milan, Italy

Department of Civil Engineering, Gazi University, Maltepe, TR-06570 Ankara, Turkey

J. Blahut
Department of Environmental and Territorial Sciences, University of Milano-Bicocca, Piazza della Scienza 1, IT-20126 Milan, Italy

Department of Engineering Geology, Academy of Sciences of the Czech Republic, Institute of Rock Structure and Mechanics, V Holešovičkách, CZ-4118209 Prague, Czech Republic

O.-C. Mavrouli • J. Corominas
Department of Geotechnical Engineering and Geosciences, Technical University of Catalonia, BarcelonaTech, Jordi Girona 1-3, SP-08034 Barcelona, Spain

C. Garcia
Department of Environmental and Territorial Sciences, University of Milano-Bicocca, Piazza della Scienza 1, IT-20126 Milan, Italy

Regional Independent Corporation of the Centre of Antioquia (CORANTIOQUIA), Cr 65 No. 44A – 32, Medellin, Colombia

B.Q. Luna
Faculty of Geo-Information Science and Earth Observation (ITC), University of Twente, Hengelosestraat 99, NL-7514 AE Enschede, The Netherlands

T. van Asch et al. (eds.), *Mountain Risks: From Prediction to Management and Governance*, Advances in Natural and Technological Hazards Research 34,
DOI 10.1007/978-94-007-6769-0_8,

economic loss, and property damage resulting from natural and/or anthropogenic hazards, by assessing the exposure and vulnerability of people and property to those hazards. The risk assessment procedure, developed in the Mountain Risks project, is based on the following five steps: (1) Identification and analysis of the specific types of hazards that could affect a territory and its community; (2) Definition of the spatial and temporal likelihood of the damaging events considered in the analysis as well as their magnitude; (3) Inventory of the assets and study of the social and economic features of the study areas; (4) Assessment of vulnerability, evaluating all the hazard consequences for each dimension composing the systems at risk (physical/functional, economic, socio-cultural, ecological/environmental and; political/institutional); (5) Evaluation of the prospective cost of damage or costs avoided through mitigation strategies. Vulnerability assessment plays a crucial role both in 'translating' the assessed level of hazard into an estimated level of risk and in providing leading information in mitigation planning processes and emergency management strategies. Under this perspective, it is really difficult, or even impossible, to address risk assessment without assessing vulnerability first and it appears unquestionable that a multi-disciplinary approach is required in vulnerability assessment studies. In this section, the different components (dimensions) of vulnerability are analyzed, both theoretically and practically, and then different methodological approaches, applications and solutions are provided.

Abbreviations

C3L	Concrete frame with unreinforced masonry infill walls
C1L	Concrete moment frame
DBMS	Database Management Systems
DI	Damage Index
DHA	Department of Humanitarian Affairs
DMTP	Disaster Management Training Programme
ESPON	European Spatial Planning Observation Network
FEMA	Federal Emergency Management Agency
FOSM	First-Order Second Moment
GIS	Geographic Information Systems
HAZUS	Hazards United States
IPCC	Intergovernmental Panel on Climate Change
IUGS	International Union of Geological Sciences
ISTAT	Italian Institute of Statistics
OMI	Osservatorio del Mercato Immobiliare
PGA	Peak Ground Acceleration
PGD	Permanent Ground Deformation
PC2L	Precast concrete frames with concrete shear walls
PC1	Precast concrete tilt-up walls
QRA	Quantitative Risk Assessment

RC	Reinforced Concrete
C1	Reinforced Concrete Moment Resisting Frames
RM2L	Reinforced masonry retaining walls with precast concrete diaphragms
RM1L	Reinforced masonry retaining walls with wood or metal deck diaphragms
RRC	Relative recovery cost
SDOF	Single Degree of Freedom
CapHaz-Net	Social Capacity Building for Natural Hazards
SL	Specific loss
S2L	Steel braced frame
S5L	Steel frame with unreinforced masonry infill walls
UNDP	United Nations Development Programme
URML	Unreinforced masonry bearing walls
W2	Wood commercial and industrial
W1	Wood light frame

8.1 Introduction

Vulnerability is a term that seems to defy consensus usage (Few 2003) showing many different connotations depending on the research orientation, overview and educational background. The review of current vulnerability definitions demonstrates that, at least, two main different perspectives exist: one related to an engineering and natural science overview; a second one related to a social science approach. Both of them are mainly depending on the components (dimensions) of vulnerability that each school of thought takes into account and privileges, such as:

- the physical/functional dimension, related to the predisposition of a structure, infrastructure or service, to be damaged due to the occurrence of a specific hazardous event;
- the socio-cultural dimension, related to the exposure of human beings (individually or aggregated in communities) to certain hazards and their coping capacities in the event of disaster. It encompasses issues related to social and health status, gender, age, religion, cast, etc. Blaikie et al. (1994) classify such coping strategies as preventive, impact-minimizing or post-event coping actions;
- the economic dimension, related to the economic stability of a region that could be endangered by a decrease in income due to a decline in production, distribution and consumption of goods. The economic dimension of vulnerability offers an interesting approach to regional vulnerability, especially from the insurance company point-of-view of damage potential (Kumpulainen 2006);
- the ecological/environmental dimension, related to the interrelation between different natural ecosystems/environments and their ability to cope with and recover from different hazardous events (Kumpulainen 2006) and to tolerate stresses over time and space (Williams and Kaputska 2000);

– the political/institutional dimension, related to the issues targeted to prevent the damaging consequences of a harmful event and to reduce the negative effects through political/institutional actions (livelihood diversification, relocation of belongings, distribution of emergency drug supplies, etc).

In short term, when a disaster strikes, the potential losses due to casualties (deaths, missing persons and injured people), physical/functional consequences on buildings, services, and infrastructure and direct economic losses are of primary concern. In the long term, indirect economic losses, social disruption, political/institutional instability, and environmental degradation may become of greater importance.

From an engineering and natural science perspective and according to the definition proposed by Varnes and the IAEG Commission on Landslides and other Mass-Movements (1984), 'vulnerability is the degree of loss to a given element or set of elements at risk resulting from the occurrence of a hazard of a given magnitude in a given area'. Ten years later, the United Nations Development Programme (UNDP 1994) took up Varnes' definition adding something more about the possibility to describe/define/measure the damage state: 'vulnerability depends upon the degree of loss to a given element at risk at a certain severity level. Generally, it is expressed as the percentage of loss (between 0: no damage, to 1: total damage) caused by given hazards'. Some other definitions of vulnerability include: '. . . the potential to experience adverse impacts' (Alexander 1999); '. . . a measure of the damage suffered by an element at risk when affected by a hazardous process' (DHA 1992; Dooge 2004); '. . . a measure of the robustness or the fragility of an element' (Vandine et al. 2004); '. . . a measure of the exposure to or protection from the expected potentially damaging event' (Vandine et al. 2004), and '. . . the ability of an element to withstand hazards of a given type or size' (Alexander 2005). In general terms, the definitions from the engineering and natural sciences relate vulnerability to the consequences of hazard impacts, able to cause damage and losses to a given element or set of elements at risk, expressed as the percentage of loss, between 0 (no damage) to 1 (total damage).

Among social scientists, there is a convergence of opinions among those that define vulnerability in terms of variations in exposure to hazards (Wisner and Luce 1993; Wisner et al. 2005) and those defining it in terms of variation in people's capacity to cope with hazards (Few 2003). For example, Blaikie et al. (1994) define vulnerability as 'characteristics of a person or group in terms of their capacity to anticipate, cope with, resist against, and recover from the impact of natural hazards'. Adger (2000) provides an alternative definition closer to this sense: 'the presence or lack of ability to withstand shocks and stresses to livelihood'. Cannon et al. (2003) define social vulnerability as a complex set of characteristics that includes a person's initial wellbeing, livelihood and resilience, self-protection, social protection and social and political networks and institutions. Cutter et al. (2003) define social vulnerability as 'a multidimensional concept that helps to identify those characteristics and experiences of communities (and individuals) that enable them to respond to and recover from natural hazards'.

In summary, definitions of vulnerability tend to fall into two broad categories that deal with vulnerability in terms of damage caused to a system by a particular hazard or climate-related event (hazards and hazard impacts approach) or in terms of 'inherent vulnerability' ('social vulnerability' for people, Adger et al. 2004) that is an intrinsic property of a system (community) before encountering an external hazardous event. In the former perspective, the role of the system in mediating the outcomes of hazards is downplayed or even neglected; in the latter, it is the interaction of hazard with an existing system state that produces an outcome (Brooks 2003).

The Hurricane Katrina and the city of New Orleans may probably help to understand better this apparent dualism. The history of disaster in New Orleans is well-known (Comfort 2006): the city is about 7 ft below the sea level and is surrounded by the Mississippi River in one side and Lake Pontchartrain in the other side. For this reason, the city was protected by a levee system built up by Engineers of the U.S. Army Corps between the 1920s and the 1930s. The building code used was design to allow the city to withstand category 3 hurricanes on the Saffir-Simpson scale. Nonetheless, the levee system had not been adequately maintained and reinforced during the last decades due to lack of funds. Katrina was a category 4 hurricane (5 in some places far from the city) and did not affect New Orleans directly when it first stroke the city. However, at 2:00 p.m. on August 29, 2005, due to the intense rainfall, part of the levee system failed, allowing the waters of Lake Pontchartrain to flood the city. Therefore, the disaster took place due to a lethal mix of internal city vulnerabilities which, according to Comfort (2006), included:

- the low level of maintenance and reinforcement of the levee system during the years due to the denial of Federal financing (physical/functional and political/institutional dimension);
- the decrease in the economic activities due to the weakening in the petroleum industry in Louisiana (economic dimension);
- the increase in unemployment rate given that approximately 25 % of the city's inhabitants were living in poverty (socio-economic dimension);
- the lack of efficient transportation facilities to evacuate the city (socio-economic dimension);
- the lack of public knowledge on the possible consequences of severe hurricanes and floodings (socio-cultural dimension).

Many scientists underline that it is extremely rare to lose an entire city as occurred in New Orleans (Comfort 2006). Even in the San Francisco earthquake of April 18, 1906, sections of the city remained intact and operational. In the Great Chicago Fire of October 9, 1871, whole neighbourhoods remained functional. But this was not the case for New Orleans where the system was not able to anticipate, cope with, resist against and recover fast from the impact of the hazard. The amount of disturbance the system was able to absorb, and still remaining operational, was very low. Very low or even negligible was its self-organisation capability and its capacity to learn from past disasters (such as the flooding of 1965) and to adapt to the new situation.

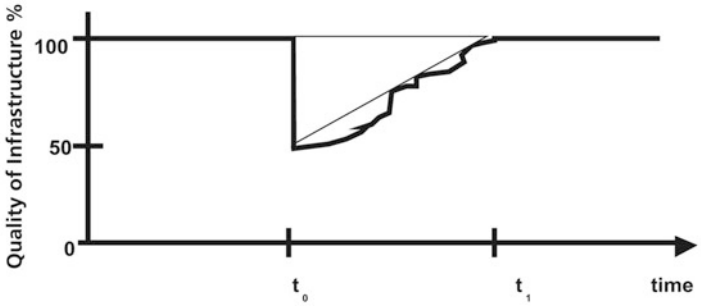

Fig. 8.1 The resilience triangle. On the X-axis, proactive resilience is represented, on the Y-axis, reactive resilience is expressed. Smaller the triangle, more resilient the system is (Tierney and Bruneau 2007)

The self-organisation capacity is known in literature as reactive resilience; while the capacity to learn from past disasters and to adapt is known as proactive resilience. The proactive resilience includes the ability to plan, prepare for, facilitate and implement preparedness and response activities against hazards. This is achieved by linking the analysis of present and future hazardous conditions with the evaluation of specific strategies for enhancing the capacity for disaster prevention and preparedness. In Fig. 8.1 the resilience triangle represents the loss of functionality from damage and disruption, as well as the pattern of restoration and recovery over time (Tierney and Bruneau 2007). A comprehensive review of concepts and definitions concerning the different perspectives of vulnerability can be found in Cutter (1996), Weichselgartner (2001), Klein et al. (2003), Glade (2003), Adger (2004) and Fuchs et al. (2007).

After analyzing vulnerability from different perspectives, some authors tried to 'merge' all the above mentioned definitions into an exhaustive and comprehensive one. From a theoretical point of view, a first attempt was made by the ESPON Hazards project (2005) that defined vulnerability as 'the degree of fragility of a person, a group, a community or an area towards defined hazards'. Vulnerability is then defined as a set of conditions and processes resulting from physical, social, economic and environmental factors that increase the susceptibility of a community to the impact of hazards. It also encompasses the idea of response and coping, since it is determined by the potential of a community to react and withstand a disaster. Moreover, the IPCC in its Third and Fourth Assessment Report (IPCC 2001, 2007) aimed to systematise the approach of vulnerability: 'vulnerability is a function of the character, magnitude, and rate of climate variation and it also depends on system's exposure, its sensitivity, and its adaptive capacity'. In this way, both hazards and hazard impacts approach and system state approach are addressed.

At last, vulnerability is a function of the objective of the study (which establish the number of dimensions to be included) and the temporal and spatial scale of analysis. Systematic vulnerability assessments have to meet the needs of the potential end-users, including public administrators (responsible for urban planning

and development), economists, managers (dealing with services, buildings or other vulnerable facilities), insurance companies, lawmakers and policy makers (drafting building regulations or codes of practise for construction), people responsible for civil protection, relief and emergency services (whose job is to prepare contingency plans).

Thus, the previous reflects why vulnerability assessment represents an important step in a general risk assessment framework, why vulnerability is so complex and difficult to assess, who is really interested in and which scientists are assessing each component. Vulnerability assessment is a crucial step because it allows to 'translate' the assessed level of hazard into an estimated level of risk and provide leading information in mitigation planning processes and emergency management strategies. It is really difficult, or even impossible, to address risk assessment without assessing vulnerability first. And, in the peculiar case of Quantitative Risk Assessment (QRA), scientists have also to be able to (1) assess hazard, as quantitatively as possible, and (2) assess vulnerability, from a qualitative and quantitative point of view, evaluating all possible undesirable consequences of hazard impacts for each dimension composing a system (physical/functional; economic; socio-cultural; ecological/environmental; political/institutional).

As a consequence, vulnerability is often hard to assess because of:

- the common lack of observational data concerning past hazardous events and related damage state;
- the difficulty in collecting data of the inherent characteristics of the elements at risk and of their spatial and temporal exposure to the hazards;
- the number of dimensions to be explored;
- the complexity of the damage state mechanism of each dimension concerning the system under study. The scientists have to know how the system, as a whole, reacts when stressed by an event; that is, how each component of a system reacts when disturbed by an event and how it can 'influence' other dimensions (conjoint and cascade effects).

Therefore, it is unquestionable that a multi-disciplinary approach is requested in vulnerability assessment studies.

8.2 Inventory of Elements at Risk

Identification and mapping of elements at risk are essential tasks for vulnerability assessment studies, providing one of the main spatial data layer required for a total risk calculation (van Westen et al. 2008). In general terms, elements at risk comprise the population, properties, economic activities, private and public services potentially threatened by a harmful event in a territory, either directly or indirectly (Alexander 2005; van Westen and Montoya 2009). Elements at risk are defined as objects which possess the potential to be adversely affected (Hufschmidt et al. 2005). Depending on the aim of the project and the working scale adopted, different levels of detail and accuracy have to be pursued during the data collection and

storage phases. An exhaustive list of elements at risk and related spatial and non spatial characteristics for physical vulnerability assessment has been compiled by literature review and presented in Table 8.1.

All buildings and structures, belonging to each of the categories listed above, together with the communities exploiting these facilities, have to be characterized by a series of data (Table. 8.2).

8.3 Brief Review of Concepts and Methods on Vulnerability Assessment

Physical vulnerability can be measured and/or quantified either on a metric scale (in terms of a given currency) or on a non-numerical scale (based on social values or perceptions and evaluations; Glade 2003). The type of scale is strictly related to the type of damage, referred to tangible losses or intangible losses. The former relates to the physical/functional and economic dimensions of vulnerability; the latter refers to the other dimensions previously described (socio-cultural, ecological/environmental and political/institutional). Regarding to tangible losses, different methodological approaches can be applied, known in literature as heuristic, economic, empirical, analytical and probabilistic approaches.

The heuristic approach expresses vulnerability of structures and infrastructure in qualitative (descriptive) terms and describes the level of damage as aesthetic, functional and structural. For aesthetic (minor) damage, it is assumed that the functionality of the elements at risk is not compromised at all and the damage can be repaired rapidly at low cost. For functional (medium) damage, the functionality of the affected elements is compromised, and the damage takes time and large resources to be fixed. Finally, for structural (total) damage, the elements at risk are severely or completely damaged and extensive works, long time and large resources are required to fix the damage; demolition and reconstruction may be required (Cardinali et al. 2002; Reichenbach et al. 2005). In the framework of a heuristic approach, people's vulnerability can be described by a qualitative description of expected casualties (e.g., none, few, numerous, very numerous).

Disaster consequences can also be expressed through other parameters, such as the economic cost of damage. This approach allows dealing with a wide range of effects. On this regard, Alexander (2000, 2005), Galli and Guzzetti (2007) stated that, when expressed economically, the degree of loss of the elements at risk can be defined in terms of:

- monetary value, defined as the price or current value of the asset, or the cost to reconstruct or replace it with a similar or identical asset, if totally destroyed or written off;
- intrinsic value, defined as the extent to which an asset is considered important and irreplaceable, and;
- utilitarian value, defined as the usefulness of a given asset or the monetary value of its usage averaged over a specified time span.

Table 8.1 Classes of elements at risk to be collected for a physical vulnerability assessment (from literature review)

Essential facilities	Industrial and high potential loss facilities	Transportation lifelines	Utility lifelines	Facilities containing hazardous materials
Recreational/tourist facilities (hotels, resorts, parks, public gardens, camping grounds, sporting areas, etc.)	Dams and ponds	Highway segments, bridges and tunnels	Potable water facilities, pipeline segments and distribution lines	Nuclear power plants
Educational facilities (schools, universities, etc.)	Nuclear power plants	Railway track segments, bridges and tunnels	Waste water facilities, pipeline segments and distribution lines	Military installations
Medical and healthcare facilities (hospital, ambulatory, etc.)	Military installations	Light rail track segments, bridges and tunnels	Oil systems facilities and pipeline segments	Fuel reservoirs, pipelines and pumps
Emergency response facilities (fire station, police station, shelters, etc.)	Fuel reservoirs, pipelines and pumps	Bus facilities	Natural gas facilities, pipeline segments and distribution lines	Gas power plants, storage and pipelines
Offices (government, post, town halls, law courts, banks and financial centres)	Gas power plant, storage and pipelines	Ports and harbors	Electric power facilities and distribution lines	
Markets and shopping centres	Power (electric) generating plants and lines	Airports facilities and runways	Communication facilities (stations) and distribution lines (cables, networks)	
Worship facilities (churches, cathedral, ccemeteries, etc.)	Water and hydroelectric power plants, tanks and lines			
Waste management sites	Timber processing facilities			

Table 8.2 List of parameters to be collected for physical and social vulnerability assessment (from literature review)

Geocoding data	Function data	General information data
Street	Residential	Evacuation plans available
Street number	Industrial	Past disasters experience
Zip code	Commercial	
City	Tourist	
Nation	Educational	
Geometrical data	**Structural features data**	**Demographic data**
Height	Building technique	Rate of occupancy or number of residents
Area	National/local building codes	Number of people
Volume	Construction material (concrete, pre-stressed concrete, masonry, metal-aluminum, wrought iron or cast iron-, steel, timber, other)	Distribution (address, street number, etc.) and type (ethnic minorities, immigrants, people with disabilities, homeless, etc.) of vulnerable populations
Presence of gardens and trees	Structural components (beams, columns, walls–thickness-, foundations, roof frame, anchoring structures, straps, rafters, door type-wood, metal-, window type, roof system)	Gender, age, and income distribution (data from Local Registry Offices)
	Number of floors	
	Maintenance works (methods of repair and reconstruction)	

Potential 'vulnerable populations'
Aboriginal or indigenous people
Alcohol/drug dependent individuals
Children (especially those of pre-school age), when isolated from parents during impact; when gathered in large groups (e.g., schools); when the ratio of children to adults is significantly high (e.g., daycares, day homes)
Ethnic minorities
Families of emergency service personnel
Homeless or 'street people'
Immigrants (especially those from 'visible' cultures, or cultures that are diverse from the local 'mainstream')
Incarcerated individuals
Language-limited (e.g., those who do not speak the mainstay language)
Large and high-density households
Livestock owners
Marginalized groups (e.g., by society or the community)
Medication dependent individuals (e.g., diabetics, schizophrenics)
Migrant workers
People depending on public transport (versus car owners)
People living below the poverty line
People on social assistance
Renters (especially in low-rental areas)
Seniors with limited mobility, isolated or confined, medically fragile, heavily dependent on medication or on life-support systems(s)
Single-parent families, especially those who are on public 'assistance or unable to take time off (e.g., during the response or recovery period)
Socially isolated people
Tourists
Unemployed
Women, especially those who are single, single parents or unemployed

Tangible losses can be classified into direct and indirect economic costs. The direct costs can be considered as the 'most visible' economic consequence, and may be quantified in terms of cost of recovering and/or restoring the original conditions (for aesthetic and/or functional damage) or in terms of cost of partial or complete reconstruction (for structural damage). The indirect costs are generally related to the loss of revenue and income, increase in unemployment, and other economic aspects related to the interruption or the reduction of production, distribution and consumption of goods (economic activity).

Regarding the empirical approach, the interaction between hazardous event(s) and elements at risk can be analyzed using empirical damage or fragility curves for several types of hazards. This approach is mainly based on data derived from well-documented case studies. By using this method, the degree of loss is expressed in the form of a damage probability matrix or in economic terms. In the former case, the probability that a building of a certain type will experience a particular level of damage, as a result of particular event intensity, is calculated. In the latter case, vulnerability is calculated using an economic approach and is defined as the ratio between the loss and the restoration/reconstruction value of the assets under study.

Fuchs et al. (2007) obtained an empirical vulnerability function analyzing data from a well-documented debris flow event in 1997 in the Austrian Alps, linking process intensities to object vulnerability values. The elements at risk were represented by brick masonry and concrete buildings located on the fan of the torrent. Vulnerability was calculated in terms of damage ratio (that describes the amount of loss related to the overall potential damage of the structure) and the debris flow intensity (Fig. 8.2). This vulnerability function can be used as a proxy for structural resistance of buildings with respect to dynamic debris flow impacts.

Akbas et al. (2009) developed an empirical vulnerability function based on observations of a debris flow that occurred on July 13, 2008, in the village of Selvetta, in the Valtellina Valley (Northern Italy). In this study (Fig. 8.3), vulnerability was calculated using an economic approach and defined as the ratio between the loss and the individual reconstruction value for each of the 13 buildings that were affected by the debris flow event. Damage-related data were obtained from official documents and an approximate reconstruction value for each building was extracted from the Housing Price Book, prepared by the Engineers and Architects of Lombardy Region (DEI 2006), according to the building type and size. The obtained ratios were coupled with the corresponding deposition height to compare the results and to perform a critical assessment of vulnerability functions developed for debris flows by different authors. Differences in the estimated vulnerabilities suggest that there is a need for further studies with additional data to construct empirical curves that can be used with a higher level of confidence. Barbolini et al. (2004) derived vulnerability curves relating damage state with the avalanche dynamic parameters, such as velocity and flow depth. The elements at risk were alpine buildings, as well as the people inside them and people directly exposed to avalanches (Fig. 8.4). The vulnerability of buildings was defined as the ratio between the cost of repair and the

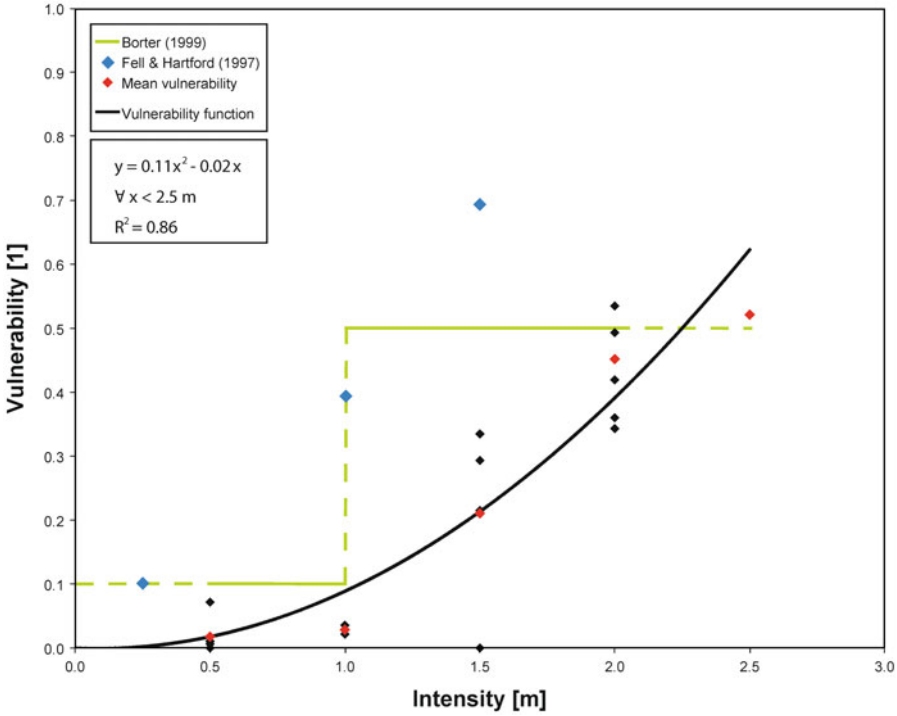

Fig. 8.2 Relationship between debris flow intensity and vulnerability expressed by a second order polynomial function for an event intensity (e.g. debris height) <2.5 m (Fuchs et al. 2007)

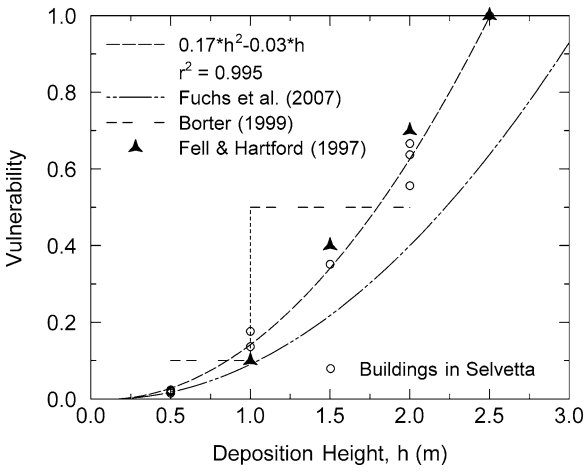

Fig. 8.3 Example of fragility curve and function (*dashed line*) between debris flow height and vulnerability (Akbas et al. 2009)

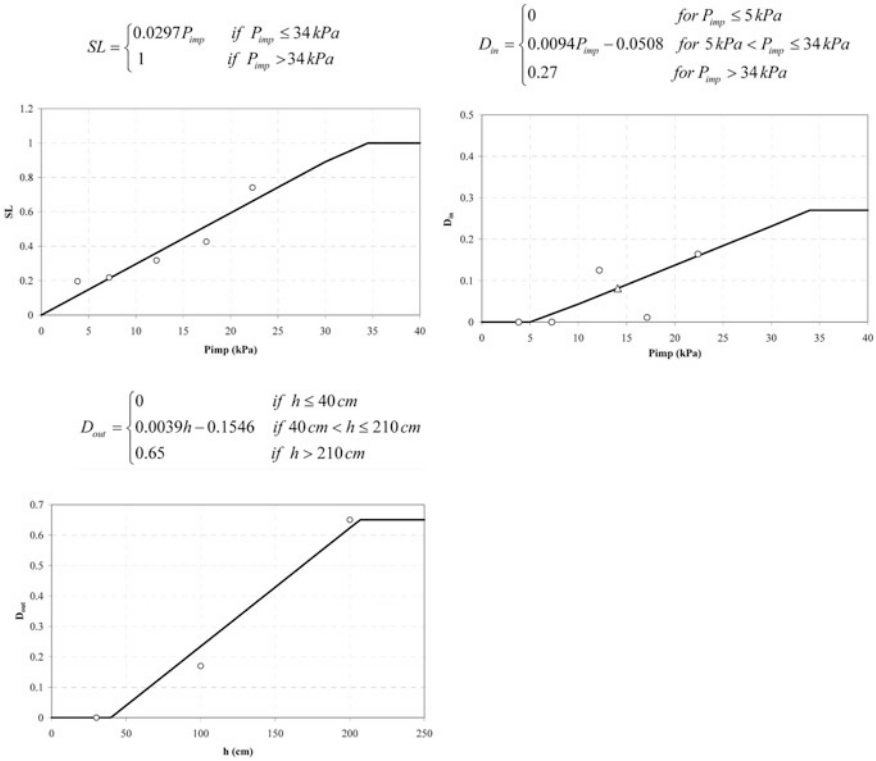

Fig. 8.4 Fragility curves and functions relating damage state with avalanche dynamic parameters. *Top-left*: vulnerability of buildings. *Top-right*: vulnerability for people inside buildings (D_{in}). *Bottom-left*: vulnerability for people outside buildings (D_{out})

building value (referred as specific loss, SL). The buildings have been divided in five classes according to five pressure ranges and an average value of vulnerability was calculated for each class. The vulnerability for people inside buildings (D_{in}), was defined as the probability of being killed by an avalanche if one stays inside a building when the event occurs. D_{in} was calculated for each building dividing the number of victims by the number of people inside it. The average impact pressure and the average D_{in} for each class were plotted and the points obtained were fitted by a linear least square regression. To obtain a vulnerability relation for people outside buildings the idea was to relate the probability of being killed to the degree of burial. The degree of burial was then tentatively related to flow depth of the avalanche (h). Using available data, the death probability outside buildings (D_{out}) was calculated for each degree of burial class as the ratio between the number of death and the number of people involved in the accidents with a flow depth equal to 2 m in the case of complete burial of people, a flow depth equal to 1 m for people partially

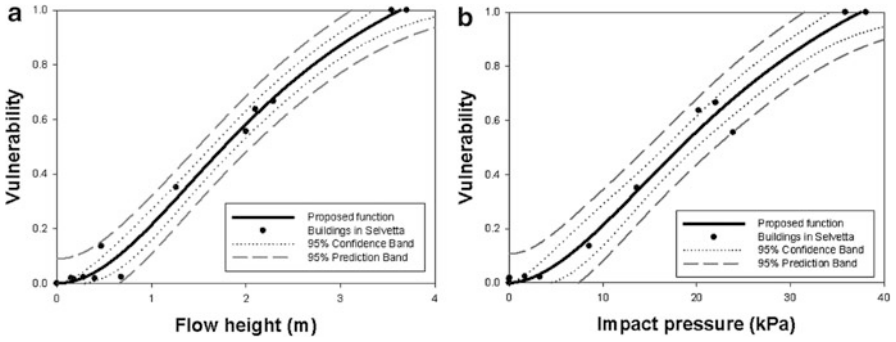

Fig. 8.5 Proposed synthetic fragility function for debris flow deposit heights (*left*) and impact pressures (*right*)

buried and a flow depth of 30 cm for people not buried. Quan Luna et al. (2011, submitted) derived synthetic physical vulnerability curves (Fig. 8.5) that related the outputs of numerical dynamic run-out models (flow depth and impact pressures) with economic values of physical damage to the elements at risk (buildings). The elements at risk were represented by single to three-storey brick masonry and concrete buildings (Quan Luna et al. 2011). Vulnerability was defined as the ratio between the loss and the restoration/reconstruction value of the 13 buildings affected by the debris flow event in Selvetta, previously described. As a general comment concerning the empirical approach, although the observational source is the most realistic, the data are often problematic to collect due to inaccuracy, incoherence and subjectivity associated with building types, damage states and intensity descriptors (flow accumulation heights, impact pressures, etc.). These problems lead to substantial scatter of data, especially for low damage states.

On regard to the analytical approaches, they are usually applied for the assessment of damage predictions to buildings, casualties and economic losses due to structural damage. The procedure to create these analytical fragility curves is to define the elements at risk and the intensity by which the hazard will affect them. Then, an analysis of the elements at risk is carried out using statistical relations. The use of analytical methods presents the following advantages: (1) it is independent of the existence of a past event inventory; (2) it permits the development of fragility curves and functions for a range of event magnitudes without any interpolation or extrapolation assumptions; (3) it takes into account the peculiarities of the threaten buildings for the study site; and (4) it offers objectivity of the results. Its application is suggested for site-specific or local scale.

By using a probabilistic approach, the interaction between the hazardous event(s) and the elements at risk can be expressed by damage or fragility curves for several types of hazards. Fragility curves describe the probability of reaching or exceeding different damage states for different model building/structure types due to the building/structure response to the intensity of the external stressing event. The extent and severity of damage to structural and nonstructural components of a

given building type can be described by one of five damage states: none, slight, moderate, extensive, and complete. Large work was carried out in USA by FEMA on fragility functions for earthquakes, floods and hurricanes. These functions were used to quantitatively estimate the losses in terms of direct costs, regional economic impacts, and casualties (HAZUS 2003, 2010). Fragility functions have also been created for landslides and debris flows, calculating the damage ratio and the event intensity. Kaynia et al. (2008) applied to a real event a probabilistic methodology to estimate the physical vulnerability of building structures and the population to landslides. They defined quantitatively the vulnerability as the product of landslide intensity and the susceptibility to damage of elements at risk. The uncertainties are considered by a First-Order Second Moment approach (FOSM). Li et al. (2010) proposed new functions for the vulnerability of structures and persons based on the landslide intensity and the resistance of the elements at risk. For assessing the physical vulnerability to a debris flow, Haugen and Kaynia (2008) make use of damage state probability functions. This was done by using the principles of dynamic response of simple structures to earthquake excitation and fragility curves (HAZUS 2003).

Akbas et al. (2013) developed a theory-based generalized methodology for estimating the damage on buildings due to debris flow impact along with the associated uncertainties. The methodology was based on the construction of fragility curves which express the 'probable damage state' to an element at risk for a 'given level of hazard' that was specified as a result of hazard assessment. For a given hazard scenario, damage to different types of elements at risk were probabilistically estimated using corresponding fragility curves. This approach has strong similarities with that employed in earthquake, as the debris flow impact will lead to structural vibrations and will damage the structure approximately in the same way as an earthquake.

However, many other consequences, equally or even more important than tangible losses, should be accounted for, although they cannot be measured/quantified easily or converted into a monetary equivalent (DMTP 1994). These are referred to as intangible losses: environmental degradation, social and cultural disruption, political/institutional instability, and psychological consequences resulting from disasters. The differences between tangible and intangible losses make their aggregation into a single indicator of disaster impact practically impossible. Moreover, the same system may be accounted for tangible and intangible losses. A building collapse (tangible) can cause deaths and injuries among people (tangible); this may produce the interruption or the reduction to a lower level of the economic activities (tangible) but also social and psychological effects on remaining community affected by the threat (intangible). Environmental degradation may be partially solved by cleaning and repairing operations, but the consequences due to the sudden impoverishment of the natural environment, health risks, and increment of risk to future disasters cannot be quantified in terms of economic cost. Moreover, the occurrence of a threat may generate changes in human behaviour and actions, e.g. people may avoid affected areas on the basis of internal rules that judge the event

to be more frequent and dramatic than actually is (Starmer 1996). In addition, the same hazard may be perceived differently by individuals and groups.

Human life represents a special case since its intrinsic value when threatened by a hazard is incalculable (Galli and Guzzetti 2007). However, in some cases, attempts to quantify human life in monetary terms have been performed (Linneroth 1979), especially in life insurance calculations, arising many ethical questions.

Finally, evaluating prospective losses requires the ability of 'reading' potential damage from a physical, economic, social, cultural, environmental and political point of view. It is important to predict how the territory (as a whole) may 'react' to the impact, both in a short-term and in a long-term view perspective.

8.4 Methods to Assess the Physical Dimension of Vulnerability

Although different approaches exist to describe the physical dimension of vulnerability, it is possible to make a distinction between two groups: (1) vulnerability models, developed to explain vulnerability and its dynamics, and (2) vulnerability indicators, developed to allow the vulnerability to be retraced and compared to locations and societies. The ultimate goal of vulnerability assessment should be to measure/quantify it as quantitatively as possible, so that subsequent evaluations can be carried out to determine if it is being reduced or not. The physical vulnerability is a representation of the expected level of damage and its assessment requires an understanding of the interaction between the hazardous event(s) and the elements at risk. It is quantified on a scale ranging from 0 (no loss or damage) to 1 (total loss or damage) (UNDP 1994; Fell et al. 2005).

8.4.1 Empirical Approaches

Most of the published works on QRA of debris flows analyzes the hazard separately from the vulnerability of the elements at risk. In the Mountain Risks project, it was decided to use the outputs of the numerical dynamic run-out models to quantify physical vulnerability by means of the flow height and impact pressure outputs. An integrated approach was applied using rainfall data and dynamic modelling to calculate the intensity and run-out zone of the 2008 Selvetta debris flow. The debris flow event was reconstructed and back-analyzed (Quan Luna et al. 2010). Geomorphologic investigations were carried out to study the behaviour of the flow and intensity aspects, such as run-out distances, velocities and depths, resulting in synthetic physical fragility curves that were prepared based on the flow depth and impact pressures. These curves relate the physical outputs of the hazard modelling with the economic values of physical damage to the elements at risk (buildings).

The physical fragility functions were calculated using data obtained from the official documents of damage assessment coupled with the information from the modelling outputs. For each building, the approximate restoration/reconstruction value was calculated according to the building type and size, using the data given in the Housing Prices Index prepared by the Engineers and Architects of Lombardy Region (DEI 2006). All of the buildings are single to three-storey brick masonry and concrete structures (Quan Luna et al. 2011). Physical vulnerability was then defined as the fraction between the loss and the individual restoration/reconstruction value and was calculated for each of the 13 building structures affected by the debris flow event. The obtained results were coupled with the modelling results (height of accumulation, impact pressures), allowing to develop fragility curves that relate the building vulnerability values with the process intensity.

8.4.1.1 Definition of Fragility Curves Using Debris Heights

Quan Luna et al. (2011) extracted the height of debris deposits for each affected building. An average height near building walls, oriented towards the flow direction, was considered. Figure 8.5a (on the left) shows the relationship between vulnerability and deposition height values and indicates that the vulnerability increases with increasing deposition height. The authors propose to use a logistic function (Eq. 8.1) with a coefficient of determination (r^2) equal to 0.99, for debris flow intensities between 0 and 3.63 m:

$$\begin{aligned} v &= \frac{1.49^{*}|h/2.513|^{|-1.938|}}{1+|h/2.513|^{|-1.938|}} && \text{for h} \leq 3.63\,\text{m} \\ v &= 1 && \text{for h} \leq 3.63\,\text{m} \end{aligned} \tag{8.1}$$

where V is the vulnerability and h is the modelled debris height. From its definition, the vulnerability cannot exceed 1; thus for flow accumulation heights greater than 3.63 m, the vulnerability is equal to 1.

8.4.1.2 Definition of Fragility Curve Using Impact Pressures

Impact pressure values were extracted in the same way as the debris heights, considering the values near building walls oriented towards the flow direction. Maximum modelled impact pressures were used to calculate the fragility function (Fig. 8.5b). The authors propose to use a logistic function (Eq. 8.2) with a coefficient of determination (r^2) equal to 0.98, for debris flow impact pressures up to 37.5 kPa:

$$\begin{aligned} v &= \frac{1.596^{*}|P/28.16|^{|-1.808|}}{1+|P/28.16|^{|-1.808|}} && \text{for } P \leq 37.5\,\text{kPa} \\ v &= 1 && \text{for } P \leq 37.5\,\text{kPa} \end{aligned} \tag{8.2}$$

where V is vulnerability and P is the modelled impact pressure. As vulnerability cannot exceed 1, for pressures higher than 37.5 kPa, the vulnerability is equal to 1.

Dynamic numerical modelling of debris flows can present an advantage in the generation of fragility curves since the intensity outputs are straightforward and can be spatially visualized. Intensity factors of the hazard were analyzed in conjunction with the physical vulnerability of the elements at risk, making it possible to quantify the physical consequences due to the occurrence of a damaging event. The proposed functions can be assumed as an approximation of a building resistance to endure a debris flow and the opportunity to present different types of fragility curves can help the decision makers to decide which type of intensity description fits best to their needs and affected area.

8.4.2 Probabilistic Approaches

As discussed previously, many of the proposed fragility functions for debris flows are empirical in nature. Although these are very useful, especially for sites with similar hydrological, geological and building stock characteristics, it should be mentioned that, due to the nature of the hazard event, many existing vulnerability models are based on limited local event data which undermine their universal applicability. Therefore, vulnerability values that are determined through sound analytical or theoretical criteria are required for realistic estimations of risk.

Within the framework of considerations mentioned above, an attempt was made to develop a theory-based generalized methodology for estimating the damage to buildings due to debris flow impact along with the associated uncertainties (Akbas et al. 2013). This probabilistic approach is based on the idea presented by Haugen and Kaynia (2008). The method is based on the construction of fragility curves which express the 'probable damage' to an element at risk for a 'given level of hazard' that is specified as a result of hazard assessment. For a given hazard scenario, damage to different types of elements at risk are probabilistically estimated using corresponding fragility curves and then the results are combined to estimate the level of risk. This approach has already been successfully employed in earthquake and hurricane risk assessments (Shinozuka et al. 2001; Li and Ellingwood 2006). Unless fragility curves can be developed from comprehensive sets of coupled damage and hazard data, which is highly unlikely for landslides or debris flows, the use of fragility curves is the most versatile approach for the estimation of quantitative risk.

For the methodology proposed herein, consider a given structural type subjected to a debris flow impact P(t) with intensity ξ. This impact will lead to structural vibrations and will damage the structure approximately in the same way as an earthquake. Next, assume that the 'engineering demand parameter', e.g. the limit state of this structure is denoted as z for a specific damage level, e.g. moderate damage, high damage, etc. Many engineering demand parameters have been suggested in the literature: spectral displacement, spectral acceleration, inter-storey drift ratio, PGA (Peak Ground Acceleration) and PGD (Permanent Ground Deformation) has

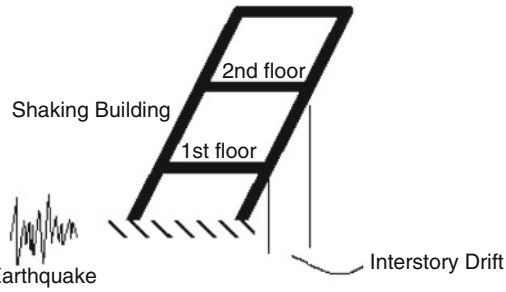

Fig. 8.6 Inter-story drift in a shaking building (HAZUS 2003)

frequently been used for earthquakes; peak gust wind speed is the most commonly used for hurricanes and cyclones. Except for a few brittle structural systems, building damage is primarily a function of building displacement, rather than force. Therefore, the drift ratio (Fig. 8.6), which is defined as the difference in lateral displacements in between two consecutive floors normalized by the storey height, is proposed as a relevant parameter.

The debris flow impact pressure is composed of two main components: the hydrodynamic overpressure due to frontal impact, which is a function of the square of the debris flow velocity (v), and the hydrostatic pressure, which is mainly a function of debris flow depth (d). Note that, in general, for debris flow velocities higher than 4–5 $m \cdot s^{-1}$, the hydrodynamic component dominates. Thus, both d and v are effective as intensity measures (ξ) of debris flow. Therefore, the energy of the debris flow, which is denoted as (v^2*d) is selected as the intensity parameter characterizing the debris flow.

It is clear that many uncertainties exist in the estimation of impact pressure and/or the impact energy. These uncertainties arise from many sources including the unknown shape of the impulse curve and the ratio of the impulse duration to the natural period of the structure, as well as errors in the assessment of velocity due to strong randomness inherent within flow dynamics, homogeneity and flow constituents. Drift ratio thresholds are functions of structural system type and damage state (e.g., slight, moderate, extensive, complete). An example from HAZUS (2003) is given in Tables 8.3 and 8.4.

Considering the existing building inventory in the Valtellina Valley (Italy), a basic classification in three classes has been performed: (1) the oldest buildings (constructed at the beginning of the last century or even older with 40–60 cm thick stone walls, wood frame for 1st floor and roof, mansard roof), (2) the pre 1970s buildings (constructed in brick columns and with un-reinforced masonry), and (3) the post 1970s buildings (constructed in reinforced concrete and masonry).

Uncertainties also exist in the engineering demand parameter. These consist of uncertainty in the limiting drift ratio for a given type of structure (experimental results from RC-Reinforced Concrete frames suggest a lognormal distribution of drift ratio threshold with a covariance of 31 %) and the variability in the capacity (response) properties of the building type of interest (due mainly to varying qualities

Table 8.3 Typical drift ratios used to define median values of concrete structures (HAZUS 2003)

		Drift ratio threshold of structural damage			
Seismic design level	Building type (low-rise)	Slight	Moderate	Extensive	Complete
High-code	W1/W2	0.004	0.012	0.040	0.100
	C1L, S2L	0.005	0.010	0.030	0.080
	RM1L/RM2L, PC1/PC2L	0.004	0.008	0.024	0.070
Moderate-code	W1/W2	0.004	0.010	0.031	0.075
	C1L, S2L	0.005	0.009	0.023	0.060
	RM1L/RM2L, PC1/PC2L	0.004	0.007	0.019	0.053
Low-code	W1/W2	0.004	0.010	0.031	0.075
	C1L, S2L	0.005	0.008	0.020	0.050
	RM1L/RM2L, PC1/PC2L	0.004	0.006	0.016	0.044
	URML, C3L, S5L	0.003	0.006	0.015	0.035
Pre-code	W1/W2	0.003	0.008	0.025	0.060
	C1L, S2L	0.004	0.006	0.016	0.040
	RM1L/RM2L, PC1/PC2L	0.003	0.005	0.013	0.035
	URML, C3L, S5L	0.002	0.005	0.012	0.028

W1 wood, light frame, *W2* wood, commercial and industrial, *C1L* concrete moment frame, *S2L* steel braced frame, *RM1L* reinforced masonry retaining walls with wood or metal deck diaphragms, *RM2L* reinforced masonry retaining walls with precast concrete diaphragms, *PC1* precast concrete tilt-up walls, *PC2L* precast concrete frames with concrete shear walls, *URML* unreinforced masonry bearing walls, *C3L* concrete frame with unreinforced masonry infill walls, *S5L* steel frame with unreinforced masonry infill walls

Table 8.4 Extent and severity of damage to structural and nonstructural components of a given building type (Reinforced Concrete Moment Resisting Frames – C1) described by one of five damage states: none, slight, moderate, extensive, and complete (HAZUS 2003)

Reinforced concrete moment resisting frames (C1)
Slight Structural Damage: Flexural or shear type hairline cracks in some beams and columns near joints or within joints.
Moderate Structural Damage: Most beams and columns exhibit hairline cracks. In ductile frames some of the frame elements have reached yield capacity indicated by larger flexural cracks and some concrete spalling. Non-ductile frames may exhibit larger shear cracks and spalling.
Extensive Structural Damage: Some of the frame elements have reached their ultimate capacity indicated in ductile frames by large flexural cracks, spalled concrete and buckled main reinforcement; non-ductile frame elements may have suffered shear failures or bond failures at reinforcement splices, or broken ties or buckled main reinforcement in columns which may result in partial collapse.
Complete Structural Damage: Structure is collapsed or in imminent danger of collapse due to brittle failure of non-ductile frame elements or loss of frame stability.
Approximately 13 % (low-rise), 10 % (mid-rise) or 5 % (high-rise) of the total area of C1 buildings with Complete damage is expected to be collapsed.

of workmanship and materials). After the selection and characterization of intensity and engineering demand parameters, the methodology proposed for the generation of fragility curves can be summarized as follows:

- obtain equivalent Single Degree of Freedom (SDOF) structural parameters through dynamic or equivalent static analysis, (e.g. SAP 2000® – Computers and Structures, Inc. and/or empirical formulas), along with their statistical descriptors (from literature review) for the three proposed building classes;
- establish limiting value of engineering demand parameter and its uncertainty for each damage state;
- conduct (n times) non-linear time history analyses (Monte Carlo Simulation) of generated SDOF models using a specifically developed program such as Nonlin® (Advanced Structural Concepts Inc. 2003) in order to take uncertainties into account by considering the structural input parameters, impact pressure parameters and engineering demand parameter as random variables;
- estimate the probability of attainment or exceedance of engineering demand parameter at a specific intensity (P_f) as the output of simulations (Eq. 8.3):

$$P_f(z;\xi) = \frac{\#\{z_i(\xi) > z\}}{n} \tag{8.3}$$

  where ξ is the intensity of the debris flow impact, z is the engineering demand parameter (e.g. the limit state of a given structure for a specific damage level) and n is the number of times the non-linear time history analysis is performed.
- repeat the last two steps by changing the intensity level ξ to obtain the fragility curve for a given damage state;
- repeat the procedure for different damage states to obtain the complete set of fragility curves;
- transfer the information from fragility curves to vulnerability.

A sample output (e.g. fragility curves for 1 to 2-storey reinforced concrete structures typical of the Valtellina Valley) is given in Fig. 8.7.

It is not possible to directly compare the expected vulnerabilities represented in Fig. 8.7 with those represented in Fig. 8.5 because the intensity parameters do not have one to one correspondence. However, a basic analysis conducted using typical velocity and depth parameters indicates that empirically obtained synthetic fragility functions are significantly less conservative than the curves given above.

8.4.3 Analytical Approaches

The use of analytical methods for the quantitative evaluation of vulnerability of buildings presents the following advantages: (a) independence of the necessity of past event inventories; (b) possibility of development of fragility functions for a range of harmful event magnitudes without any interpolation or extrapolation assumptions; (c) possibility to integrate the peculiarities of the threaten buildings for the study site; and (d) objectivity of the results. Its application is suggested for site-specific or local scale.

For buildings, as observed from historical rockfalls and debris flows, the impact due to rock boulders may lead to damage of disperse severity, from slight non-

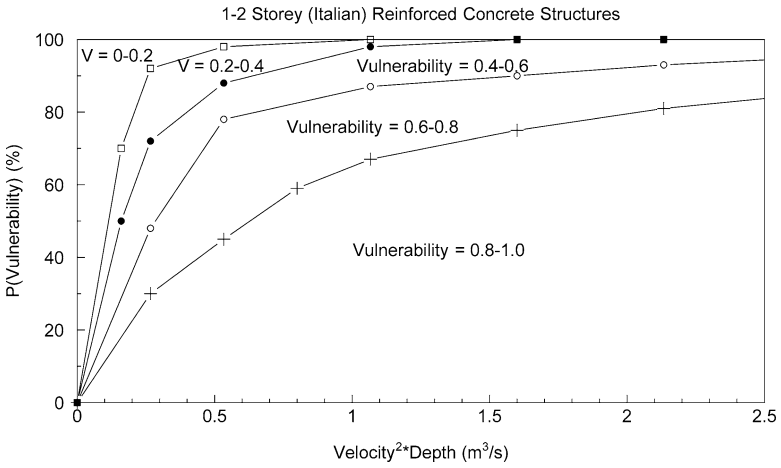

Fig. 8.7 Proposed fragility curves for 1 to 2-storey reinforced concrete structures observed in the Valtellina Valley, Italy (Akbas et al. 2013)

structural damage (destruction of infill walls, doors, windows and furniture) (Bell and Glade 2004) to destruction of roofs and slabs due to vertical impacts (Corominas et al. 2005), to partial collapse (Lopez-Garcia 2005), to extensive damage or complete collapse of buildings (Agliardi et al. 2009). Empirical methodologies usually assume that damaging events of similar magnitude produce similar level of damage. However, this assumption is not strictly true, especially for rockfalls because, for instance, the damage caused by a rockfall of a given magnitude depends on both the location and the energy of the impact, which may change from one event to the other. The importance of the impact location especially applies for frame structures (reinforced concrete, steel or timber) where the extensive damage of a key-element may lead to general instability and progressive collapse. For masonry structures the damage is usually local because, given the hyper-static load-bearing system, alternative load paths may be easily found (Corominas and Mavrouli 2011).

An analytical procedure that takes into account the impact location for the evaluation of the structural response of a building impacted by rockfalls should include two phases: firstly, the evaluation of the structural damage caused by impacts on primary structural key-elements and, then, the analysis of the response of the whole structural system (Fig. 8.8).

The proposed methodology (Mavrouli and Corominas 2010a, b) includes four main steps: (a) calculation of the encounter probability of a rock with a key-element; (b) evaluation of the response of one or more structural key-elements to the hit based on their capacity; (c) assessment of the robustness of the whole structural system calculating the potential for progressive collapse, in case of failure of one or more key-elements in the previous step; and (d) calculation of the damage using a damage index (DI), equivalent to the proportion of failed structural elements to the total elements. A vulnerability index to be used directly for the risk quantification that considers the variation of the damage, according to the impact location of rockfalls

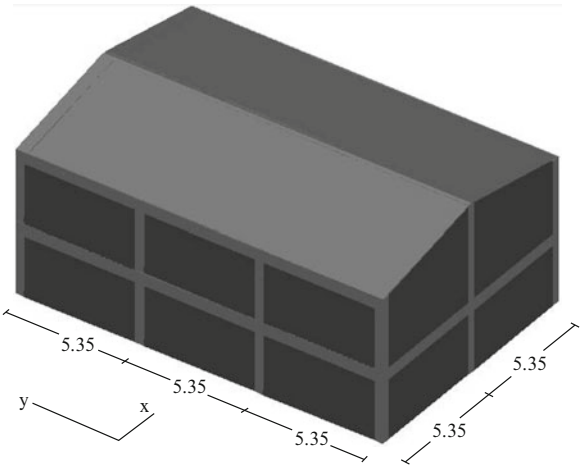

Fig. 8.8 Considered structural typology for the vulnerability evaluation (Mavrouli and Corominas 2010b)

and calculated as a function of the rockfall magnitude and velocity, is given by Mavrouli and Corominas (2010b):

$$V\left(R_{ij}\right) = \sum_{k=1}^{k} \left(P_{e,k} x\, RRC_k\right) \leq 1 \tag{8.4}$$

where $V(R_{ij})$ is vulnerability for a rock block with a magnitude i and intensity velocity j; $P_{e,k}$ is the encounter probability of a rock with a possible structural and nonstructural element of the building k that may be struck by a rock block of magnitude i and RRC_k is the relative recovery cost that corresponds to the struck of a possible structural and nonstructural element of the building k by a rock block of magnitude i and velocity j.

Details for the calculation of the probability of each impact location are given in Mavrouli and Corominas (2010b) where the RRC expresses the cost of the repair in relation to the value of the building. The RRC is calculated as a function of the physical structural (expressed by the DI) and nonstructural damage, translated into economical cost, for every potential location of the impact.

The vulnerability of structures to rockfalls may be associated, as well, with their expected performance when subjected to a rockfall impact of a certain magnitude. This can be performed through the definition of a correlation function between the intensity of the impact and the probability of exceeding a certain response level accounting, at the same time, for the uncertainty of the impact location. This function may be expressed using sets of fragility curves. Families of fragility curves for different intensities (velocities) can be developed in function of the magnitude (diameter), taking into consideration the uncertainty of the impact location.

A step-by-step procedure for the calculation of rockfall fragility curves has been proposed and described in detail by Mavrouli and Corominas (2010b). It consists in the calculation of the cumulative probability of low, moderate, high and very high

Table 8.5 Damage levels and respective impact energies, DI and damage description

Damage level	E_k (kJ)	Conditions	Impact location	Damage description
Low	$E_k \leq E_c$	$m \geq 250$ kg	Infill wall or column	Nonstructural
Moderate	$E_c < E_k \leq 2E_c$	$0.0 < DI \leq 0.05$	One central column	Local structural
High	$E_c < E_k \leq 2E_c$	$0.05 < DI \leq 0.3$	One corner column	Partial collapse
Very high	$E_k > 2E_c$	$DI \geq 0.3$	More than one central/ corner column	Extensive or total collapse

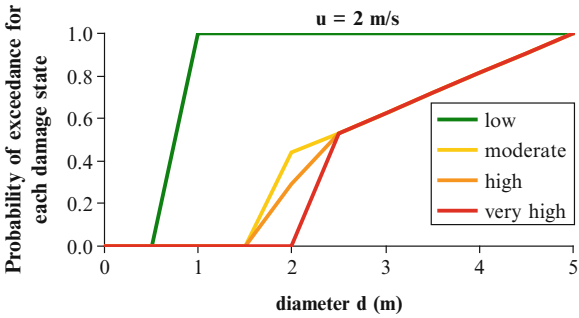

Fig. 8.9 Indicative fragility curves for a building and a given velocity

damage. The value of the cumulative probability depends on the block magnitude and the building geometry (the width of the columns and infill wall dimensions on the exposed façade) and it is calculated as the probability of impact on a structural element (one or more columns, key-element(s) for the stability of the building) or a nonstructural one (an infill wall). If E_c is the level of energy sufficient to cause the destruction of one column on a block impact, the potential damage levels are proposed to be as shown in Table 8.5.

Low damage corresponds either to impact and destruction of an infill wall for a minimum rock block mass (here, a mass of 250 kg is approximately considered to cause important damage of an adobe wall) or to impact of a rock block on a column but with energy (E_k) which is not sufficient to cause its destruction ($E_k \leq E_c$). Moderate damage is caused in the given building when a central column is impacted by a block with energy sufficient to cause its destruction, given that for this building, beams form a bridge across the destructed column and extensive collapse is avoided.

High damage is due to destruction of a corner column, with the same energy as previously; but, in this case, a cascade of failures may initiate and a partial collapse of the building across its height be observed. At the end, very high damage refers to extensive collapse of the building which is ought to a cascade of failures, initiated by the destruction of two or more columns.

The fragility curves diagram of Fig. 8.9 provides the cumulative probability P of each damage level (from low to very high), for increasing block diameters. It can be observed that for $d > 1$ m low damage is certain ($P = 1$). For $d = 2$ m, the probability of moderate and high damage is slightly higher than 0.4 and 0.3, respectively, and for $d = 5$ m very high damage is strongly expected ($P = 1$).

The presented approach for generating fragility curves are mainly focused in terms of the intensity parameters which can be spatially displayed and computed by numerical modelling at a local scale. This can be assumed as a rough estimation of a building resistance to a damaging external event. The main goal is to link the results of numerical models which calculate the intensity of the hazard with the physical vulnerability of the elements at risk, making it possible to quantify the suffered consequences. The estimated functions do not and should not conflict with the damage state probability functions that plot probabilities of the different damage states of a structure; and, although many uncertainties are involved in the computation process, the presented approach attempts to propose a quantitative method to estimate the vulnerability of an exposed element to a damage that can be independent on the temporal occurrence of the hazardous event.

8.5 Methods to Assess the Economic Dimension of Vulnerability

As previously discussed, physical effects expressed in terms of economic costs are known as tangible losses and are classified into direct and indirect losses. This paragraph will essentially focus on problems arising from estimation of economic value of assets. For the elements at risk which can be quantified in monetary terms, the economic estimation of their value is rather straightforward. However, economic value of an asset can be quantified using at least two main approaches: (1) construction value (e.g. cost of material, work, and other related expenses needed to build the asset); (2) market value (e.g. cost of the asset on the local real estate market).

Both approaches have advantages and disadvantages. Main advantage of the use of construction values for prospective damage estimation is that these values slightly suffer from the speculative conditions in the aftermath of a damaging event. Construction values are also usually used for insurance purposes. Main disadvantage is that the construction values are uniformly distributed over the analyzed area and particular disparities between economically different zones cannot be distinguished. On the other side, the main advantage of using market values to estimate risk and prospective losses is that areas of higher economic importance can be effectively discriminated from economically marginal areas. For example, buildings in a renowned tourist resort will have higher market values than buildings in rural areas. The market values will be different because the real estate market conditions are different. Location plays an important part in establishing market value: distance from schools and commercial facilities, quality of surrounding properties, and neighborhood amenities are examples of factors that could cause a purchaser to pay more for a home in one neighborhood than in another. In that case, the construction values could be very similar, while market values will be highly different. As a consequence, the market values will more realistically depict the real estate market

condition. However, the main disadvantage of using market values is that these values are subject to larger changes during time, mostly due to speculative reasons. As a consequence, all risk and loss estimations have to be considered 'static' in the sense that they are relevant only for the date of the analysis. In the peculiar case of public properties (roads, railways, etc.), these have to be handled using construction values as they cannot be quantified using market prices.

Medium scale (1:25,000–1:50,000) economic risk studies have been performed in Valtellina Valley handling both types of values (construction and market values). To estimate the direct economic risk, values of all classes of elements at risk were collected from available sources:

- values of real properties in urbanized areas, estimated from house market values of the second half of 2008, available from the webpage of the Italian National Territorial Agency (OMI 2009);
- values of the agricultural land in Sondrio Province in 2008 (Valori Agricoli Medi 2009);
- costs of road construction, issued by the Engineers and Architects of Lombardy Region (DEI 2006).

Market values were preferred in the analysis as they describe better the actual distribution of economic activities and prices. Urbanized areas in the land use map (1:10,000) lack a good delimitation of each house or building. As a consequence, it was assumed that houses cover 25 % of each urban area polygon of the land use map. This is also in accordance to calculations and comparisons made between the land use map and database DB2000 (2003). DB2000 is a database of assets in the study area at 1:2,000 scale, originally used by local planners and civil protection authorities, mapping assets allocated on the floodplain only. Values of real properties in urbanized areas were estimated from house market values of the second half of 2008, available from the webpage of the Italian National Territorial Agency (OMI 2009). On this webpage, a minimum and maximum price per m^2 of different building types in different polygons, defining urban areas according to the market value of the houses, are available. As the working scale (1:25,000–1:50,000) and data availability do not permit to fully distinguish between different types and usage of houses (private, public, commercial, etc.), an average value for each polygon for normal state of private building was calculated. Private buildings constitute more than 90 % of the buildings in the study area and, according to fieldwork observations, an average building in the study area presents two storeys. Consequently, to obtain an average value of urban areas per cell (10×10 m), the average price per m^2 of house was divided by 4 (1/4 of the urban area is covered by houses) and multiplied by 2 (number of storeys in an average house type).

Prices per pixel of the non-urban areas were estimated using information about average market values of agricultural land in the Sondrio Province in 2008 (Valori Agricoli Medi 2009). Highest values per hectare are located on apple orchards (90,500 €/ha) and vineyards (59,200 €/ha), while the lowest values represent the forested areas (4,000 €/ha) and grassland/pastures (2,400 €/ha). It has to be noted that low values of forested areas are caused by the system of calculation. In this cost

Table 8.6 Values of the elements at risk used in the analysis of direct economic damage

Elements at risk	2008 value	€ pixel^{-1}
Urban area	640–2.375 €·m^{-2}	32.000–118.750
Primary road	20 €·m^{-2}	2.000
Secondary road	15 €·m^{-2}	1.500
Railway	N.A.	N.A.
Orchard	90.500 €·ha^{-1}	905
Vineyard	59.200 €·ha^{-1}	592
Permanent crop	50.400 €·ha^{-1}	504
Pasture (intensive)	49.200 €·ha^{-1}	492
Swamp/peat-bog	7.700 €·ha^{-1}	77
Forest (without timber)	4.000 €·ha^{-1}	40
Pasture/grassland (high altitudes)	2.400 €·ha^{-1}	24
Junkyard	N.A.	N.A.
Quarry	N.A.	N.A.
Degraded land	N.A.	N.A.
Shrubs and bushes	N.A.	N.A.
Vegetation on rocks	N.A.	N.A.
Scarce vegetation	N.A.	N.A.
Glacier/river/water	N.A.	N.A.
Bare land	N.A.	N.A.

N.A. information not available (from literature review)

estimation, only value of land is considered without taking into account the value of the timber. The estimation of the price of timber is very difficult. However, majority of the forests have protective function and are not considered as market goods; only the value of the land is considered in this analysis.

Public roads do not represent a private property, so only construction costs (and not market values) were estimated per square meter of primary and secondary roads using information available from the construction costs of roads (DEI 2006). Unfortunately, it was not possible to acquire any information about construction costs of railways in the study area, not even nationally for Italy, so no values were assigned to primary and secondary railways in the study area. All the values calculated for the elements at risk are summarized in Table 8.6.

Importance of the assessment of indirect economic costs has been proofed several times in recent years by showing that indirect economic losses can easily exceed direct ones (Giacomelli 2005; Sterlacchini et al. 2007). For that reason, estimation of economic flows and trends should be an integral part of any risk analysis. Moreover, assessment of the indirect economic consequences has to be made not only within the hazardous area but also on a broader-regional basis. However, most indirect costs are difficult to evaluate and thus are often ignored or, when estimated, are too conservative (Schuster 1996). Indirect losses represent mostly disruptions of economic activities and can affect much larger areas; they include losses from interruption of transportation routes, tourist revenues, reduced real estate values,

or costs of mitigation measures. In particular, the interruption of transportation can have serious outcomes in costs arising from (1) blockage of the services (transport of people and goods); (2) increased traffic and fuel consumption in case of availability of alternative routes, and (3) secondary costs for the economy arising from blocked or longer alternative routes (non-availability of goods, longer travel time, etc.). In the case of landslides, the estimation of indirect losses is a relatively new scientific field. Unlike other hazards (e.g. earthquakes, floods, windstorms), loss estimation models and approaches almost do not exist for landslide hazards (van Westen et al. 2005). This situation is partly caused by the limited extent of landslides compared to other natural hazards and by the scarcity of historical data. However, for the purposes of land use planning and mitigation measure design, information about possible indirect economic damage is of high relevance, especially when the cost-benefit analysis is performed.

At last, there are many classes of elements at risk that do not have any specified economic value set by the official resources. However, it has to be noted that many of them have intangible values associated with their environmental importance as natural resources (glaciers, rivers, lakes) or linked with their public importance (junkyards, quarries). These values are hardly definable even to environmental economists. As a consequence, the value of these assets is usually neglected in scientific studies. Future studies related to the economic dimension of vulnerability should be more focused to estimate indirect costs and, if possible, to analyze in detail the intangible damage.

8.6 Methods to Assess the Social Dimension of Vulnerability and Translate the Risk Perception into QRA

Social vulnerability is a dynamic and challenging area of the academic discourse. Tapsell et al. (2010) in the CapHaz-Net EU project and several authors have extensively worked on its description and definition (Blaikie et al. 1994; Cutter et al. 2003; Dwyer et al. 2004; Birkmann 2007; Van der Veen et al. 2009).

As described previously, in most vulnerability analyses, vulnerability indicators are based on the physical features of the building environment and on general social and economic characteristics of a community (e.g. age, education, employment rate). Conversely, characteristics such as risk perception, preparedness and awareness are still generally neglected although they have been identified as an important resource (Glatron and Beck 2008). This importance is because different levels of risk perception and preparedness can directly influence people's vulnerability and the way they might react in case of an emergency caused by natural hazards (Slovic 1987; Birkmann 2007; Haynes et al. 2008; Paton et al. 2008). Using the spatial relationship of perceived risks and preparedness, local authorities can design better educational activities in order to increase the preparation of particularly vulnerable groups within a community (Leonard et al. 2006; Birkmann 2007). It can also be

Table 8.7 Proposed quantitative vulnerability indexes and indicators based on census data (Garcia 2011)

	Indexes	Indicators
Quantitative social vulnerability	Population fragility	Age dependency radio
		Gender (household masculinity index)
	Population density	Population density
	Response household fragility	Family density index
	Education	Education

useful for emergency personnel in order to optimally direct the actions in case of emergency.

Consequently, the way a particular community may respond to a particular hazard is an important aspect of its social vulnerability (Glatron and Beck 2008). Social vulnerability has emerged as a central concept for understanding which conditions of people enable a hazard to become a disaster. According to Tapsell et al. (2010), information on social vulnerability helps to define where the greatest needs are, to set priorities (e.g. by deriving knowledge about spatial distribution patterns), to determine actions (e.g. by improving intervention tools), to measure effectiveness of mitigation approaches, to inform policymakers and practitioners, to alert the public and raise awareness, to gain funding (e.g. for poverty reduction initiatives) and to represent social responsibility.

A methodology to estimate the social vulnerability at municipal scale was applied in Valtellina Valley by Garcia et al. (2010) and Garcia (2011). Traditional quantitative vulnerability indicators based on information from the Italian Census 2001 were compared to qualitative vulnerability indicators (such as risk perception, preparedness and awareness) obtained with a comprehensive social survey. These qualitative vulnerability indicators are combined to give an idea of the capacity reaction of the exposed population at municipal level. Next, both sets of vulnerability indicators are compared with hazard indicators and visualized with Geographical Information Systems (GIS) techniques. The main objective is to identify the risk hotspots in the areas where vulnerability and hazard are highest by means of maps and to use this tool in a further stage to communicate the results to the stakeholders, including local authorities, emergency technicians and the exposed community.

Using the available information of the Italian Census of 2001 (Italian Institute of Statistics – ISTAT, 2001), quantitative vulnerability indexes were defined for social vulnerability including: population fragility, population density, response household fragility and education (Table 8.7).

Several indicators were selected to evaluate the reaction capacity of the municipalities of the study zone considered as an important aspect of social vulnerability. Since the results are based on the answers of the questionnaires applied in the study area, the indicators derived from the questionnaire are called 'qualitative social vulnerability', and include: population capacity, risk perception, sense of community, self efficacy and self preparedness (Table 8.8).

Table 8.8 Proposed qualitative vulnerability indexes and indicators based on psychological surveys (Garcia 2011)

	Indexes	Indicators
Qualitative social vulnerability: reaction capacity	Population capacity	Educational level
		Previous hazard experience/knowledge
	Risk perception	Risk perception
		Initial level of concern
	Sense of community	Number of generations living on the community
		Participation in voluntary groups
		Previous hazard experience/knowledge
		Willingness to participate on future meetings
	Self efficacy	Willingness to receive/to look for new information
		Personal mitigation measures
		Knowledge of the responsible for emergency management
		Knowledge of the emergency plan/emergency procedures
		Level of perceived self preparedness
		Knowledge about NH legislation
	Self preparedness	Personal mitigation measures
		Knowledge of emergency procedures
		Knowledge about mass movements and flooding
		Perceived self preparedness

The results for the quantitative social vulnerability indicate that it is predominantly low, except for the municipality of Tirano, where the high vulnerability results mainly from its high 'population density' and high 'response household fragility' (Fig. 8.10).

Contrastingly, the results for the reaction capacity/qualitative vulnerability present a highly heterogeneous distribution. Two extreme groups of municipalities were distinguished: those with the highest reaction capacity/lowest vulnerability (including Aprica, Bianzone, Mazzo di Valtellina and Villa di Tirano) and those with the lowest reaction capacity/highest vulnerability (including Grosio, Lovero, Sernio and Vervio). These results suggest that in case of a regional event, the population of the former municipalities is better prepared to respond efficiently, while the population of the latter is less prepared to properly respond.

The relationship among vulnerability and hazard, at the municipal scale, was developed in a quantitative framework by normalizing the debris flow hazard assessment of Blahut et al. (2010) and represented spatially in Fig. 8.11.

Results show that the municipality with the highest debris flow hazard level is Vervio, followed by Lovero and Grosotto, while the municipalities with the lowest debris flow hazard level are Aprica, Villa di Tirano and Bianzone. A comparative matrix of social vulnerability, hazard and reaction capacity of the Valtellina di Tirano municipalities is presented in Table 8.9.

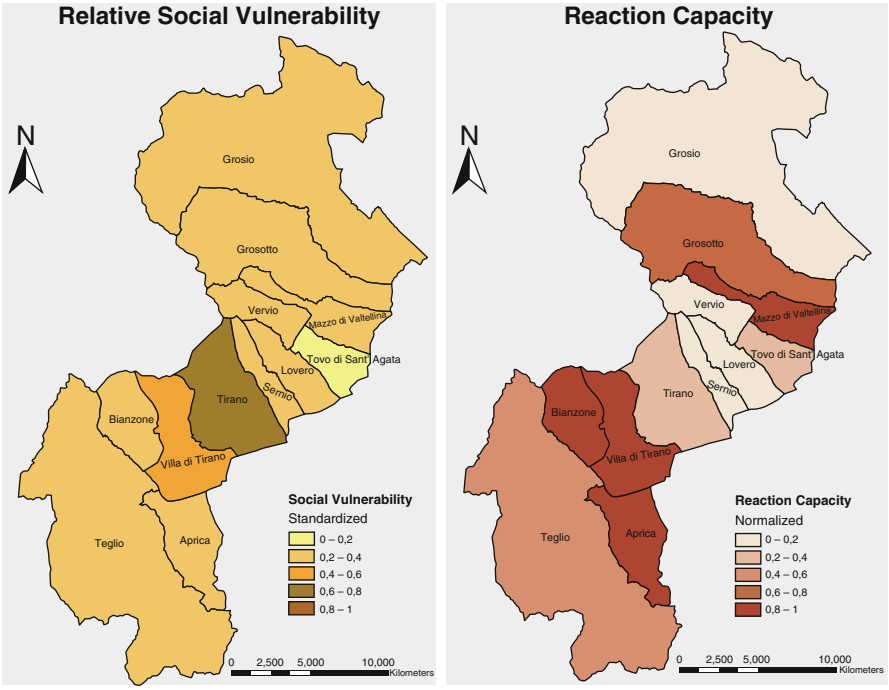

Fig. 8.10 Municipal Social Vulnerability. Quantitative social vulnerability (*on the left*); Reaction capacity – Qualitative social vulnerability (*on the right*) (Garcia 2011). The study area consists of a consortium of 12 mountain municipalities (Comunità Montana Valtellina di Tirano) spread over an area of about 450 km^2 in the Italian Central Alps (Lombardy Region, Northern Italy) with approximately 29,000 inhabitants

The levels were divided in five classes, from Very Low (0–0.2; including the municipalities with the lowest value in each variable) to very high (0.8–1; including the municipalities with the highest value in each variable). The matrix allows observing and comparing the different levels of vulnerability compared to the debris flow hazard, which gives an idea of the levels of risk. It is important to remember that the represented values are not absolute values but more a comparison among the extreme lowest and highest values of the different municipalities.

8.7 Methods to Assess the Political and Institutional Dimension of Vulnerability

Ultimately, decision-making on loss reduction strategies is a political issue on which all sections of the community must be consulted and to which the normal political processes of social decision-making must be harnessed (DMTP 1994). Any

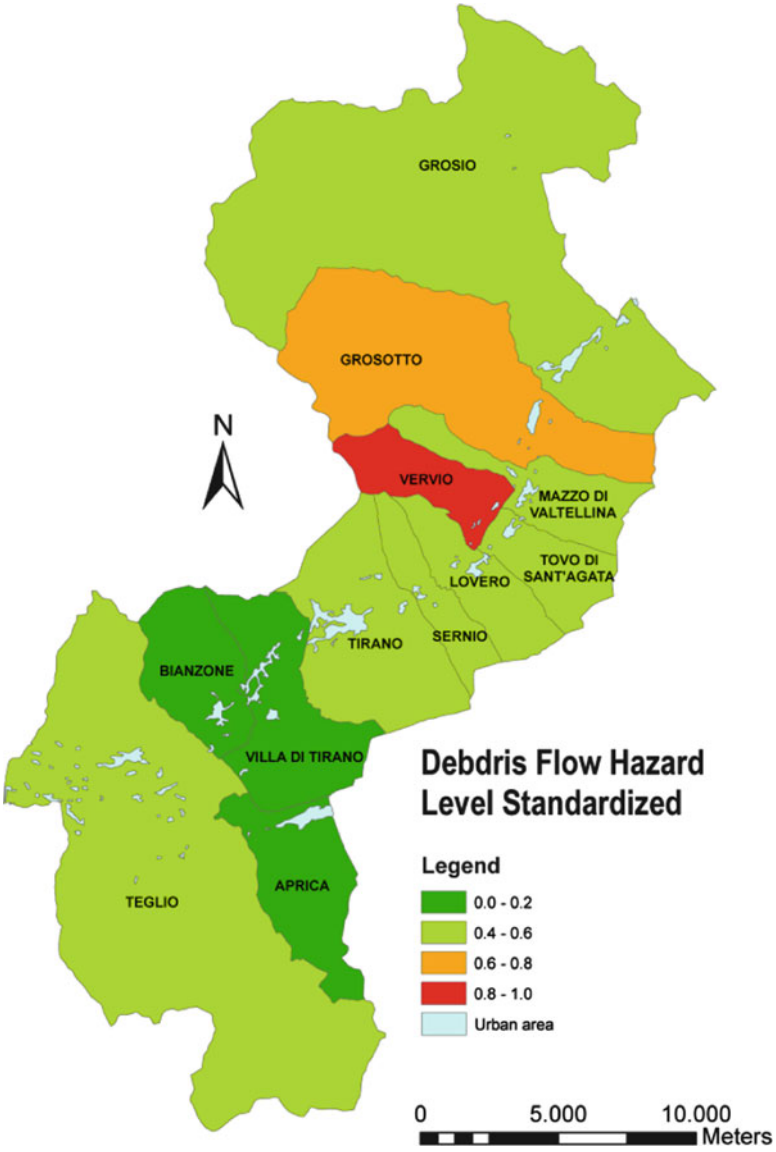

Fig. 8.11 Relative debris flow hazard map at municipal level of the Consortium of Mountain Municipalities of Valtellina di Tirano (Garcia 2011)

strategy must be not only feasible according to the local conditions but also publicly acceptable and institutionally manageable.

Two different time-dependent strategies may be accounted for loss reduction: (1) a long-term strongly political strategy, based on urban and spatial planning, institutional rules and laws to reduce the vulnerability and decrease the consequences of

Table 8.9 Comparative table of quantitative social vulnerability, qualitative social vulnerability and hazard of the Valtellina di Tirano municipalities (Garcia 2011)

Municipality	Quantitative social vulnerability	Qualitative social vulnerability: reaction capacity	Debris flow hazard
Aprica	L	VH	VL
Bianzone	L	VH	VL
Grosio	L	VL	L
Grosotto	L	H	M
Lovero	L	VL	M
Mazzo di Valtellina	L	VH	L
Sernio	L	VL	L
Teglio	L	M	L
Tirano	H	L	L
Tovo di Sant'Agata	VL	L	L
Vervio	L	VL	VH
Villa di Tirano	M	VH	VL

The reaction capacity is inverse since its relation with vulnerability is inverse; e.g. the higher reaction capacity the lower vulnerability is present
VH very high, *H* high, *M* medium, *L* low, *VL* very low

a disaster before it happens, and (2) a short-term strategy, based on response and rescue activities (emergency plans), put immediately in practise in the aftermath of a disaster, targeted to reduce the potential losses due to casualties (deaths, missing persons and injured people) and to recover, in the shortest time, essential facilities, transportation and utility lifelines.

A discussion of these important topics is beyond the scope of this section. Other chapters of the book deal in more detail with the implementation of long-term and short-term disaster mitigation programs (e.g. Sections 10, 11, 12 and 13).

8.8 Methods to Identify and Quantify the Source of Uncertainties in Vulnerability Analyses

For vulnerability assessment, the type, availability and accuracy of the data are crucial aspects strictly related to the focused analysis scale. The objective of the assessment, the extent of the study area and an appropriate cost/benefit analysis closely controls the data collection phase and, in so doing, the outcomes of the vulnerability assessment (Aleotti and Chowdhury 1999). Although data collection and storage phase has been greatly enhanced by the introduction of Geographical Information Systems (GIS) and Database Management Systems (DBMS), it remains undoubtedly one of the most burdensome and costly operations, given that data reliability and accuracy has to be guaranteed through continuous operations of data updating and reviews.

On a regional scale (1:100,000–1:500,000), less accurate but more easily accessible data can be highlighted as the most performing to carry out vulnerability analysis over large areas. Frequently, this type of analysis is a preliminary step targeted to more site-specific studies where the scale should be more detailed (medium scale: 1:25,000–1:50,000).

On a medium scale (1:25,000–1:50,000), several limitations exist and many uncertainties are intrinsic within the results (Table 8.10). As stated by Bell and Glade (2004), due to the uncertainties concerning each input factor of risk analysis, the resulting risk values also encompass a considerable level of uncertainty. One of the main limitations, specifically for susceptibility and hazard mapping, is related to the spatial resolution and reliability of the inputs. However, other uncertainty arises from the computed probabilities of hazard and risk when there is no guarantee that all the information about past events was used in the analysis. Another limitation is related to the 'static' expression of hazard and risk, showing only the situation according to the date of acquisition of the inputs to analyse. IUGS Working Group on Landslides – Committee on Risk Assessment (1997) and Heinimann (1999) recommended that final results should be treated as relative results and not as absolute ones. This is probably the only effective way of using the many valuable tools of hazard and risk analysis in disaster mitigation without losing the trust in the results (Bell and Glade 2004).

Moreover, specific (economic, social, and environmental) risk maps should be used for the calculation of a total quantitative risk map. However, this still seems to be a long journey because of the high-resolution data needs on large areas and the usage of static type of data. Some future developments in remote (near) real-time data acquisition of inputs and automated (but supervised) processing of the results might result in dynamic quantitative risk maps at medium scale, which represent the ultimate goal in QRA at this scale of study.

On a local scale (<1:10,000), the main uncertainties involved in vulnerability assessment are related to the subjective properties of some of the parameters required and the lack of quantitative data regarding the potential damage related to the harmful events on the built environment and the exposure of the elements. The elements assessed should be always linked to the intensity of the hazards whose calculation is often linked to a high degree of uncertainty. For example, in the specific case of vulnerability of buildings to rockfalls, uncertainties are mainly correlated to both the impact phenomenon and the response of the building. Concerning the former, the transmission of energy from the block to the impacted element is affected by many parameters very difficult to quantify (shape and size of the block, rigidity of both block and impacted element, etc.). As result, the phenomenon is characterized by high uncertainty. The same applies for the response of the building which is associated to its geometry, the dimensions of key-elements and the properties of the materials. A measure of the uncertainty in the estimated vulnerability could be obtained using appropriate stochastic techniques such as first-order second moment (FOSM) techniques (Uzielli et al. 2008) or Monte-Carlo simulations.

Table 8.10 Qualitative estimation of uncertainties in diverse steps of the risk analysis on medium scale approach

	Factors	Uncertainty	Reason	Significance	Improvement
Susceptibility analysis	Inventories	Low-medium	Imprecision	High	Increase of data collection
	Digital elevation model	Low	Resolution	Medium	Increase of resolution
	Geo-factors	Low	Resolution	Low-medium	Up-to-date information
	Susceptibility model	Low-medium	Model limitations	Medium-high	Non-linear models
	Map classification	Medium	Subjectivity	Medium-high	–
Hazard analysis	Temporal probability	Medium-high	Average values	High	Increase of data collection
	Digital elevation model	Medium	Imprecision	Very high	Increase of resolution
	Model calibration	Medium-high	Average values	High	Analysis of past events
	Map classification	Low-medium	Subjectivity	High	–
Risk analysis	Value of elements at risk	Low	Data availability	Low-medium	Up-to-date information
	Vulnerability approximation	High	Subjectivity	Very high	Analysis of past events
	Elements at risk classification	Low	Subjectivity	Low-medium	Analysis of past damage
	Map classification	High	Subjectivity	High	Risk perception study

The table structure is adopted from Bell and Glade (2004)

At last, it is very difficult to make a complete and objective calculation of the vulnerability as such. However, it is an important task to present an approach that attempts to propose a quantitative method to estimate the vulnerability of an exposed element to a harmful event that can be independent on the temporal occurrence of the hazardous event.

8.9 Conclusion

In recent years, the assessment of hazard, vulnerability and risk has become a topic of major interest for natural and social scientists and engineering professionals as well as for the community and the local administrations in many parts of the world (Aleotti and Chowdhury 1999). During the same time, potentially mountain hazardous processes (e.g. landslides, debris flows and floods) have increased in frequency and magnitude in hilly and mountainous areas, affecting elements at risk that are continuously growing in number. In doing so, the economic losses due to these harmful events increase as well, showing an over proportional growth in comparison to the frequency and magnitude of the damaging processes. This could be explained by the increased pressure of development and urbanisation on the environment; that is, an increasing demand by population for resources which has given raise to a continuous pressure to settle in places with more exposure and vulnerability.

Vulnerability plays an important role in the hazard-risk cycle. As well as hazard frequency and magnitude, vulnerability needs to be estimated before an event happens as the 'vulnerability of what', the 'vulnerability to what' and at 'what scale'. Vulnerability is often poorly assessed because of the real lack of observational data concerning past hazardous events and related damage state; the difficulty to collect data of the inherent characteristics of the elements at risk in terms of their spatial and temporal exposure to the hazards, the number of dimensions to be explored; the complexity of the damage mechanism of each dimension of the system under study. The scientists have to know how the system, as a whole, reacts when stressed by an event; that is, how each component of a system reacts when disturbed by an event and how it can 'influence' other dimensions.

For this reason, for many years, a qualitative or semi-qualitative evaluation of consequences, mainly based on expert judgment, has been preferred as the more convenient method in terms of application. Subsequently, different techniques and methodologies, mainly based on the interplays of various experts, have been applied. In this chapter, the different components (dimensions) of vulnerability (physical/functional, socio-cultural, economic, ecological/environmental and political/institutional) are firstly analyzed, both theoretically and practically, and then different methodological approaches, applications and solutions provided.

References

Adger WN (2000) Institutional adaptation to environmental risk under the transition in Vietnam. Ann Assoc Am Geogr 90(4):738–758

Adger WN (2004) Vulnerability. In: Forsyth T (ed) Encyclopedia of international development. Routledge, London, pp 742–743

Adger WN, Brooks N, Bentham G, Agnew M, Eriksen S (2004) New indicators of vulnerability and adaptive capacity. Tyndall Centre for Climate Research, Norwich

Advanced Structural Concepts Inc (2003) NONLIN – Computer program for nonlinear dynamic time history analysis of single- and multi-degree-of-freedom systems. User's manual. Advanced Structural Concepts Inc., Blacksburg

Agliardi F, Crosta GB, Frattini P (2009) Integrating rockfall risk assessment and countermeasure design by 3D modelling techniques. Nat Haz Earth Syst Sci 9:1059–1073. doi:10.5194/nhess-9-1059-2009

Akbas SO, Blahut J, Sterlacchini S (2013) Estimation of a vulnerability function for debris flow risk assessment using a well-documented event in Selvetta, Italy. B Eng Geol Environ

Akbas SO, Blahut J, Sterlacchini S (2009) Critical assessment of existing physical vulnerability functions for debris flows. In: Malet JP, Remaître A, Boogard TA (eds) Landslide processes: from geomorphologic mapping to dynamic modelling. CERG, Strasbourg

Aleotti P, Chowdhury R (1999) Landslide hazard assessment: summary review and new perspectives. Bull Eng Geol Environ 58:21–44

Alexander D (1999) Vulnerability. In: Alexander D, Fairbridge RW (eds) Encyclopedia of environmental science. Kluwer Academic Publishers, Boston

Alexander D (2000) Confronting catastrophe. Terra Publishing, Harpenden

Alexander D (2005) Vulnerability to landslides. In: Glade T, Anderson M, Crozier MJ (eds) Landslide hazard and risk. Wiley, Chichester

Barbolini M, Cappabianca F, Sailer R (2004) Empirical estimate of vulnerability relations for use in snow avalanche risk assessment. In: Brebbia C (ed) Risk analysis. WIT Press, Southampton

Bell R, Glade T (2004) Quantitative risk analysis for landslides. Examples from Bildudalur, NW-Iceland. Nat Hazard Earth Syst Sci 4:117–131

Birkmann J (2007) Risk and vulnerability indicators at different scales: applicability, usefulness and policy implications. Environ Hazards 7:20–31

Blahut J, Horton P, Sterlacchini S, Jaboyedoff M (2010) Debris flow hazard modelling on medium scale: Valtellina di Tirano, Italy. Nat Hazard Earth Syst Sci 10:2379–2390

Blaikie P, Cannon T, Davis I, Wisner B (1994) At risk: natural hazards, people's vulnerability, and disasters. Routledge Publisher, London

Brooks N (2003) Vulnerability, risk and adaptation: a conceptual framework. Tyndall Centre for Climate Research, Norwich

Cannon T, Twigg J, Rowell J (2003) Social vulnerability, sustainable livelihoods and disasters. Report to DFID. Conflict and Humanitarian Assistance Department (CHAD) and Sustainable Livelihoods Support Office. http://www.livelihoods.org/info/docs/vulnerability.doc

Cardinali M, Reichenbach P, Guzzetti F, Ardizzone F, Antonini G, Galli M, Cacciano M, Castellani M, Salvati P (2002) A geomorphological approach to estimate landslide hazard and risk in urban and rural areas in Umbria, central Italy. Nat Hazard Earth Syst Sci 2:57–72

IPCC – Intergovernmental Panel on Climate Change (2001) Third assessment report. Climate change 2001. Working group II: impacts, adaptation and vulnerability. Chapter 1

IPCC – Intergovernmental Panel on Climate Change (2007) Fourth assessment report. Climate change 2007. Working group II: impacts, adaptation and vulnerability. Appendix 1 – Glossary

Comfort LK (2006) Cities at risk: Hurricane Katrina and the drowning of New Orleans. Urb Aff Rev 41(4):501–516

Corominas J, Mavrouli O (2011) Rockfall Quantitative risk assessment. In: Stéphane L, François N (eds) Rockfall engineering. Wiley, London, pp 255–296

Corominas J, Copons R, Moya J, Vilaplana JM, Altimir J, Amigó J (2005) Quantitative assessment of the residual risk in a rock fall protected area. Landslides 2:343–357
Cutter SL (1996) Vulnerability to environmental hazards. Prog Hum Geogr 20(4):529–539
Cutter SL, Boruff BJ, Shirley WL (2003) Social vulnerability to environmental hazards. Soc Sci Q 84(2):242–261
DB2000 (2003) Database of the consortium of mountain municipalities of Valtellina di Tirano mapped at 1:2.000 scale. Consortium of mountain municipalities of Valtellina di Tirano. http://www.cmtirano.so.it/sistemainformativo.php
DEI (2006) Prezzi Tipologie Edilizie 2006. DEI Tipografia del Genio Civile. CD-ROM
DHA – Department of Humanitarian Affairs, United Nations (1992) International agreed glossary of basic terms related to disaster management. United Nations, Geneva
DMTP – Disaster Management Training Programme (1994) Vulnerability and risk assessment. Module prepared by Coburn AW, Sspence RJS, Pomonis A. Cambridge Architectural Research Limited. The Oast House, Malting Lane, Cambridge
Dooge J (2004) Water and ethics. Ethics of water-related disasters. UNESCO, Paris
Dwyer A, Zoppou C, Nielsen O, Day S, Roberts S (2004) Quantifying social vulnerability: a methodology for identifying those at risk to natural hazards. GeoCat No. 61168, Geoscience, Australia
ESPON Hazards project – European Spatial Planning Observation Network (2005) The spatial effects and management of natural and technological hazards in general and in relation to climate change. Final Report, March 2005
Fell R, Ho KKS, Lacasse S, Leroi E (2005) A framework for landslide risk assessment and management. In: Hungr O, Fell R, Couture R, Eberhardt E (eds) Landslide risk management. Taylor & Francis, London
Few R (2003) Flooding, vulnerability and coping strategies: local responses to a global threat. Prog Dev Stud 3(1):43–58
Fuchs S, Heiss K, Hübl J (2007) Towards an empirical vulnerability function for use in debris flow risk assessment. Nat Hazard Earth Syst Sci 7:495–506
Galli M, Guzzetti F (2007) Landslide vulnerability criteria: a case study from Umbria, Central Italy. Environ Manage 40:649–664
Garcia C (2011) Mountain risk management: integrated people centred early warning system as a risk reduction strategy, Northern Italy. PhD dissertation, Università degli Studi di Milano Bicocca
Garcia C, De Amicis M, Sterlacchini S, Pasuto A, Greiving S (2010) Community based early warning system for mountain risks, northern Italy: identifying challenges and proposing disaster risk reduction strategies. In: Malet JP, Glade T, Casagli N (eds) Mountain risks – bringing science to society. CERG, Strasbourg
Giacomelli P (2005) Economic evaluation of risk. The case of a mountain area. Aracne, Roma
Glade T (2003) Vulnerability assessment in landslide risk analysis. Die Erde 134:123–146
Glatron S, Beck E (2008) Evaluation of socio-spatial vulnerability of citydwellers and analysis of risk perception: industrial and seismic risks in Mulhouse. Nat Hazard Earth Syst Sci 8:1029–1040
Haugen ED, Kaynia AM (2008) Vulnerability of structures impacted by debris flow. In: Chen Z et al (eds) Landslides and engineered slopes. Taylor & Francis, London
Haynes K, Barclay J, Pidgeon N (2008) Whose reality counts? Factors affecting the perception of volcanic risk. J Volcanol Geotherm Res 172(3–4):259–272
HAZUS-MH (2003) Multi-hazard loss estimation methodology, earthquake model, technical manual developed by Department of Homeland Security Emergency Preparedness and Response Directorate FEMA Mitigation Division, Washington, DC. http://www.fema.gov/plan/prevent/hazus
HAZUS-MH (2010) FEMA's methodology for estimating potential losses from disasters. http://www.fema.gov/plan/prevent/hazus/index.shtm
Heinimann HR (1999) Risikoanalyse bei gravitativen Naturgefahren – Methode, Umwelt-Materialien, 107/I, Bern, p 115

Hufschmidt G, Crozier M, Glade T (2005) Evolution of natural risk: research framework and perspectives. Nat Hazard Earth Syst Sci 5:375–387

ISTAT – Istituto Nazionale di Statistica (2001) http://www.istat.it/it/censimento-popolazione-e-abitazi/popolazione-2001

IUGS – International Union of Geological Sciences (1997) Quantitative risk assessment for slopes and landslides – The state of the art. In: Cruden DM, Fell R (eds) Landslide risk assessment. IUGS working group on landslides, Committee on Risk Assessment. Balkema, Rotterdam, pp 3–12

Kaynia AM, Papathoma-Köhle M, Neuhäuser B, Ratzinger K, Wenzel H, Medina-Cetina Z (2008) Probabilistic assessment of vulnerability to landslide: application to the village of Lichtenstein, Baden-Württemberg, Germany. Eng Geol 101(1–2):33–48

Klein RJT, Nicholls RJ, Thomalla F (2003) Resilience to natural hazards: how useful is this concept? Environ Hazards 5:35–45

Kumpulainen S (2006) In: Philipp S-T (ed) Natural and technological hazards and risks affecting the spatial development of European Regions, vol 42. Geological Survey of Finland, Espoo, pp 65–74

Leonard GS, Johnston DM, Saunders W, Paton D (2006) Assessment of Auckland Civil Defence and Emergency Management Group warning system options. GNS Science Report 2006/002

Li Y, Ellingwood BR (2006) Hurricane damage to residential construction in the US: importance of uncertainty modeling in risk assessment. Eng Struct 28(7):1009–1018

Li Z, Nadim F, Huang H, Uzielli M, Lacasse S (2010) Quantitative vulnerability estimation for scenario-based landslide hazards. Landslides 7(2):125–134

Linneroth J (1979) The value of human life: a review of the models. Econ Inq 17:52–74

Lopez-Garcia D (2005) Discussion on: critical building separation distance in reducing pounding risk under earthquake excitation. Struct Saf 27(4):393–396

Mavrouli O, Corominas J (2010a) Vulnerability of simple reinforced concrete buildings in front of the rockfall impact. Landslides 7:169–180

Mavrouli O, Corominas J (2010b) Rockfall vulnerability assessment for reinforced concrete buildings. Nat Hazard Earth Syst Sci 10(10):2055–2066

OMI – Osservatorio del Mercato Immobiliare (2009) Agenzia del Territorio. http://www.agenziaterritorio.it/

Paton D, Smith L, Daly M, Johnston D (2008) Risk perception and volcanic hazard mitigation: individual and social perspectives. J Volcanol Geotherm Res 172(3–4):179–188

Quan Luna B, Blahut J, van Westen CJ, Sterlacchini S, van Asch TWJ, Akbas SO (2011) The application of numerical debris flow modelling for the generation of physical vulnerability curves. Nat Haz Earth Syst Sci 11(7):2047–2060. doi:10.5194/nhess-11-2047-011

Quan Luna B, Blahut J, Camera C, van Westen CJ, Apuani T, Jetten V, Sterlacchini S (submitted) Quantitative risk assessment for debris flows and estimation for the economic damage to structures. Natural Hazards, Springer

Reichenbach P, Galli M, Cardinali M, Guzzetti F, Ardizzone F (2005) Geomorphologic mapping to assess landslide risk: concepts, methods and applications in the Umbria Region of Central Italy. In: Glade T, Anderson MG, Crozier MJ (eds) Landslide hazard and risk. Wiley, Chichester

Schuster RL (1996) Socioeconomic significance of landslides. In: Turner AK, Schuster RL (eds) Landslides, investigation and mitigation. Transportation Research Board, Special report. 247, National Academy Press, Washington, D.C., pp 12–35

Shinozuka M, Feng MQ, Kim H, Uzawa T, Ueda T (2001) Statistical analysis of fragility curves. Technical report MCEER, University of Southern California

Slovic P (1987) Perception of risk. Sci New Ser 236(4799):280–285

Starmer CV (1996) Explaining risky choices without assuming preferences. Soc Choice Welf 13:201–213

Sterlacchini S, Frigerio S, Giacomelli P, Brambilla M (2007) Landslide risk analysis: a multi-disciplinary methodological approach. Nat Hazard Earth Syst Sci 7:657–675

Tapsell S, McCarthy S, Faulkner H, Alexander M, Steinführer A, Kuhlicke C, Brown S, Walker G, Pellizzoni L, Scolobig A, De Marchi B, Bianchizza C, Supramaniam M, Kallis G (2010) Social vulnerability to natural hazards. Social vulnerability to natural hazards. Report D 4.1-Version 2.2, CapHaz-Net Project

Tierney K, Bruneau M (2007) Conceptualizing and measuring resilience: a key to disaster loss reduction. TR News, May–June, 250:14–17

UNDP – United Nations Development Programme (1994) Vulnerability and risk assessment. United Nations Development Programme, Cambridge

Uzielli M, Nadim F, Lacasse S, Kaynia AM (2008) A conceptual framework for quantitative estimation of physical vulnerability to landslides. Eng Geol 102(3–4):251–256

Valori Agricoli Medi – Provincia di Sondrio (2009) http://www.asr-lombardia.it/ASR/lombardia-e-province/agricoltura/produzione-agricola-zootecnia-e-risultati-economici/tavole/1097/2009/

Van der Veen A, Dopheide E, Parker D, Tapsell S, Handmer J, Gregg C, Bonadonna C, Ferrara F (2009) State-of-art on vulnerability of socio-economic systems. Del. 1.1.3 of the ENSURE EC FP7. Project: methodologies to assess vulnerability of structural, territorial and economic systems. EC, Brussels

van Westen CJ, Montoya L (2009) Multi-hazard risk assessment: Distance Education Course. Guide Book Enschede, ITC

van Westen CJ, van Asch TWJ, Soeters R (2005) Landslide hazard and risk zonation – why is it still so difficult? Bull Eng Geol Environ 65:167–184

van Westen CJ, Castellanos Abella EA, Sekhar LK (2008) Spatial data for landslide susceptibility, hazards and vulnerability assessment: an overview. Eng geol 102:112–131

Vandine DF, Moore G, Wise M, Vanbuskirk C, Gerath R (2004) Technical terms and methods. In: Wise M, Moore G, Vandine D (eds) Landslide risk case studies in forest development planning and operations. B.C., Ministry of Forests, Forest Science Program, abstract of land management handbook

Varnes DJ, IAEG Commission on Landslides and other Mass-Movements (1984) Landslide hazard zonation: a review of principles and practice. The UNESCO Press, Paris

Weichselgartner J (2001) Disaster mitigation: the concept of vulnerability revisited. Disaster Prev Manag 10(2):85–94

Williams L, Kaputska L (2000) Ecosystem vulnerability: a complex interface with technical components. Environ Toxicol Chem 19(4):1055–1058

Wisner B, Luce HR (1993) Disaster vulnerability: scale, power and daily life. GeoJournal 30: 127–140

Wisner B, Blaikie PM, Cannon T (2005) At risk: natural hazards, people vulnerability and disasters, 2nd edn. Routledge Publisher, London

Chapter 9
The Importance of the Lessons Learnt from Past Disasters for Risk Assessment

Carolina Garcia, Jan Blahut, Marjory Angignard, and Alessandro Pasuto

Abstract Within the Mountain Risk Project, the study area of the Consortium of Municipalities of Valtellina di Tirano (Italian Alps), has been selected in order to collect both kinds of knowledge, scientific and local, and to correlate it to the levels of preparedness and perceived risk of the population. A quantitative survey was performed using a comprehensive questionnaire to evaluate several aspects related to the response capacity. In the meantime available historical information about natural hazards (landslides and floods) and consequent disasters have been collected and organized in a comprehensive database designed with the aim of using such data for hazard estimation and definition of risk scenarios as a basis for Civil Protection planning and emergency management purposes.

The results show that even if: (a) there have been multiple damaging events in the past, as show in the database, and (b) most of the population is aware of the

C. Garcia
Department of Environmental and Territorial Sciences, University of Milano-Bicocca, Piazza della Scienza 1, IT-20126, Milan, Italy

Regional Independent Corporation of the Centre of Antioquia (CORANTIOQUIA), Cr 65 No.44A – 32, Medellin, Colombia

J. Blahut
Department of Environmental and Territorial Sciences, University of Milano-Bicocca, Piazza della Scienza 1, IT-20126, Milan, Italy

Department of Engineering Geology, Institute of Rock Structure and Mechanics, Academy of Sciences of the Czech Republic, V Holešovičkách, CZ-4118209, Prague, Czech Republic

M. Angignard
Institute of Spatial Planning, Dortmund University of Technology, August-Schmidt-Straße 10, D-44227, Dortmund, Germany

A. Pasuto (✉)
Italian National Research Council – Research Institute for Geo-Hydrological Protection (CNR – IRPI), C.so Stati Uniti 4, IT-35127 Padova, Italy
e-mail: alessandro.pasuto@irpi.cnr.it

T. van Asch et al. (eds.), *Mountain Risks: From Prediction to Management and Governance*, Advances in Natural and Technological Hazards Research 34,
DOI 10.1007/978-94-007-6769-0_9, © Springer Science+Business Media Dordrecht 2014

existence of past events, the levels of preparedness are low and the population has low levels of perceived risk, and what is more, population neglect the existence of recurrent small to medium events (which are the most common according to the database) and remember mostly the large events, as the one of (Alexander 1988). This means that in the study are a gap between the occurred disasters and the possible lessons to be learnt still exist and an effective method to share and disseminate knowledge is missing.

Additionally, when the information is collected and available, it is necessary to communicate it to the local authorities so they can adapt the existent governance framework not only to the physical situation but also to the perception, awareness and risk knowledge of the population. According to Wanczura (2006), the aim of providing people with information is to broaden their view of hazards and risks, because only those hazards and risks that are known and understood can be mitigated. Lessons learnt from local knowledge of previous events are not sufficient to manage disasters effectively since, even if this knowledge helps reduce risk, it is sometimes inadequate to cope with new disasters. Similarly, scientific knowledge, technology and data are not enough to assure an effective risk reduction since they lack of a holistic picture and deeper analysis of the local vulnerability context. What is fundamental is the ability to combine them and to put them into practice being this the real reflex of learning from previous experiences. Combining both types of knowledge is crucial to reduce uncertainty, thus proving more precise information for the decision-making, key element of any risk governance process.

Abbreviations

UNISDR	United Nations International Strategy for Disaster Reduction
AAR	After Action Review
EWS	Early-Warning Systems

9.1 Introduction

Hydro-geological hazard is a serious problem worldwide causing frequent loss of life and damage to infrastructures. Therefore it is of paramount importance to mitigate its effects in order to enhance the performance of structures, infrastructure elements and institutions in reducing losses from such phenomena.

Landslides can be triggered by a wide range of factors like earthquakes, typhoons, intense or prolonged rainfalls, rapid snow melt etc. Moreover, climate change could influence on the number and magnitude of possible natural hazards, including landslides which are one of the most dangerous phenomena, due to the difficulty of a temporal prediction and the high energy and velocity involved in the process. It has been estimated that every year about 225,000 lives are lost because of natural events among which several mass movements causing many

casualties. Actually, besides high-magnitude landslides which occur quite seldom, there is a huge number of medium to small size mass movements which are so widespread that the related cost for the human society is even higher than that of catastrophic events. The losses due to low-magnitude, high-frequency events is generally increasing, especially in developing countries, because of human activity and above all, increasing in the frequency of some triggering factors like intense rainfalls or typhoons.

In this framework, the risk reduction can be achieved on one hand, by means of structural mitigation measures which contribute to decrease the hazard and, on the other hand, by reducing vulnerability through a comprehensive program of non-structural measures like public awareness and education, event mapping, early warning and monitoring systems (Garcia 2012). Structural measures are generally more expensive and not always effective especially if they are not properly managed and maintained; non-structural measures are strongly encouraged by UNISDR (United Nations International Strategy for Disaster Reduction) in the Hyogo Framework for Action adopted by 168 Member States of the United Nations in 2005 at the World Disaster Reduction Conference held in Kobe (Japan).

Among these measures, the sharing of knowledge and experiences derived from lessons learnt from past disaster can be powerful to increase awareness and education among the people potentially at risk. Making the best re-use of lessons learned is essential for building up our knowledge and expertise and therefore a resilient community capable to face with the future emergency situations. So we need to develop a culture for systematically doing this.

There are different approaches to better exploit the experiences gained from past disaster response efforts, but what has to be done is to analyse what went well and what went badly in the emergency phase and to establish if some unexpected occurrences took place. In other words, the key point is to turn mistakes and poor performance into learning opportunities.

In this framework, the After Action Review (AAR) is a simple tool mainly consisting in a structured review after the emergency that analyses what happened, why it happened, and how it can be done better. Another technique of gathering lessons learnt is to encourage people to talk about their experiences through stories. It builds and makes full use of this natural way in which we learn from each other and gain understanding about risk situations through storytelling.

9.2 General Concepts

Lessons learnt from past disasters usually involve experiences and local knowledge of the population at risk and scientific analysis of information on past events, which combined and incorporated in practical structures serve to reduce the vulnerability of human systems (De Marchi 2007).

Lessons learnt by the population can either emerge from direct experience of hazardous events or from transfer of this knowledge from generation to generation.

These lessons learnt may increase the level of knowledge, awareness and preparedness, thus contributing to disaster risk reduction (Cashman and Cronin 2008; Gaillard et al. 2010; UN/ISDR et al. 2008). The local knowledge arising from lessons learnt can be incorporated in disaster management strategies and in consequence can lead to a more cost-effective, sustainable, more realistic and site-specific emergency plan (UN/ISDR et al. 2008; Komino 2008; Barszczynska et al. 2006), contributing in this way to the local risk governance. The involvement of local population in the process of sharing experiences and storytelling is also important because this promotes mutual trust, acceptability, common understanding, and improves the community's sense of ownership and self-confidence (Dekens 2007). However, this does not mean that all local knowledge, practices, and beliefs are relevant, sustainable or appropriate for risk governance and disaster risk reduction. It is fundamental to study and analyse the existing local knowledge, to elicit the information relevant for decision-making and to decide how to integrate it into local policy in order to facilitate the risk governance process. This step is challenging, first, due to the general belief in the scholar community that scientific knowledge is 'superior' to local knowledge, and second, due to the fact that to identify, use, assess, validate, generalize and replicate local knowledge is difficult and time consuming (Dekens 2007). Since local knowledge, as well as the level of risks are both dynamic and change over time, preparedness and response strategies should be continuously adapted to the new conditions, updated and rehearsed on a regular basis (Thrupp 1989; UN-ISDR 2005). This is particularly important when a period of 20–30 years has passed since the last significant threat or event (Southern 1995), or when previous emergency crises were successfully managed and their impacts and damages were low. Any of the previous aspects can generate among the authorities and the exposed population an underestimation of the risk and therefore an increment of vulnerability.

According to UN/ISDR et al. (2008), in the last decades, there has been a tendency to not pass the local knowledge from one generation to the next anymore, causing that knowledge and perception are more and more restricted to the personal experiences and no longer to the collective memory. For this reason, it is crucial that academic researchers collect, compile and systematize the diverse range of local knowledge before it disappears.

Regarding scientific research, the collection and analysis of data related to past events are an integral component of hazard assessment, e.g. for calibration or validation of future risk scenarios. The primary step for this analysis is the setting up of comprehensive databases composed by the information available from previous hazardous events. The detailed analysis of the databases gives an indication on which areas could be affected in the future, the expected magnitude and intensity of the events, their temporal frequency and the possible impacts on the territory. Databases generally contain geographical, numerical and alphanumerical information at different geographical and temporal scales, in various digital formats, including: vector and raster maps, terrestrial, aerial and satellite imagery, time series, tabular data, texts, documents and images. Information stored in geo-databases can be compiled at different geographical and temporal scales, using a variety of

methods and technologies (Couture and Guzzetti 2004). However, the geo-databases need to be well designed, compiled and validated. Moreover, the compilation of this kind of database is very time-consuming and, particularly the collection of historical information requires skills in history, linguistic, etc. Additionally, the uncertainties connected with type of harmful processes regarding their temporal and spatial location increase back in time. When these ambiguities are well handled, the database represents a very valuable basis for hazard/risk analysis for civil protection purposes as well for spatial planning and risk governance.

Finally, the scientific analysis of past events combined with the local knowledge of the population is crucial to predict the characteristics of a future event. This information is essential in the operational risk governance and must be communicated to the general public and other stakeholders.

Huge databases related to landslides and floods are already available in different European Countries; they are in charge of regional government, Civil Protection association, scientific institution etc. However the quality of data stored into these databases is not always good and a validation is needed before using them.

9.3 Collecting Local Knowledge and Information on Past Events: A Case Study in the Italian Alps

In order to better explain how important is the lesson learnt from past landslide disasters in increasing the public awareness and to highlight the positive feedback the dissemination and the sharing of information can have on prevention and preparedness as well as on the management of emergency phase, a research activity has been developed in the Consortium of Municipalities of Valtellina di Tirano (Central Italian Alps) in order to integrate Community Based Early Warning systems and emergency plans for disaster risk reduction. Part of this activity was aimed at the evaluation of the level of risk perception among the population potentially affected by landslides and debris flows.

A comprehensive survey among the local population was performed in order to evaluate, among others, the previous experiences of natural hazards, the risk perception of landslides and flooding and the level of preparedness. Results from Garcia (2011) showed that most of the population (88.3 %) either have experienced floods and/or landslides in the past, or know about the occurrence of past events, especially the big event of 1987. Despite of this, the average level of perceived risk is rather low with a mean value of 2.2 based on a Likert Scale (Babbie 2005) of 1–5, with 1 being the lowest perceived risk and 5 the highest.

The Table 9.1 and the Fig. 9.1 illustrate the relationship between the previous experiences and knowledge of past events versus the perceived levels of risk and preparedness levels. Results indicate that the perceived levels of risk, knowledge and preparedness are generally low even in the people previously damaged by the hazard process. Therefore, experiences or awareness of the occurrence of past events, have no significant effect on the perceived levels of risk, knowledge and preparedness.

Table 9.1 Cross tabulation with results of previous experiences versus perceived levels of risk, knowledge and preparedness of the population (Garcia 2011)

Previous experience of natural hazards	I. Yes, but no damage suffered	II. Yes, and directly affected	III. No, but with knowledge of past events	IV. No, without knowledge of past events
Perceived risk	2.2	2.3	2.2	2.1
Individual preparedness	2.4	2.5	2.4	2.4
Population preparedness	2.5	2.5	2.6	2.3
Individual risk knowledge	2.5	2.7	2.5	2.4
Population risk knowledge	2.6	2.9	2.7	2.8

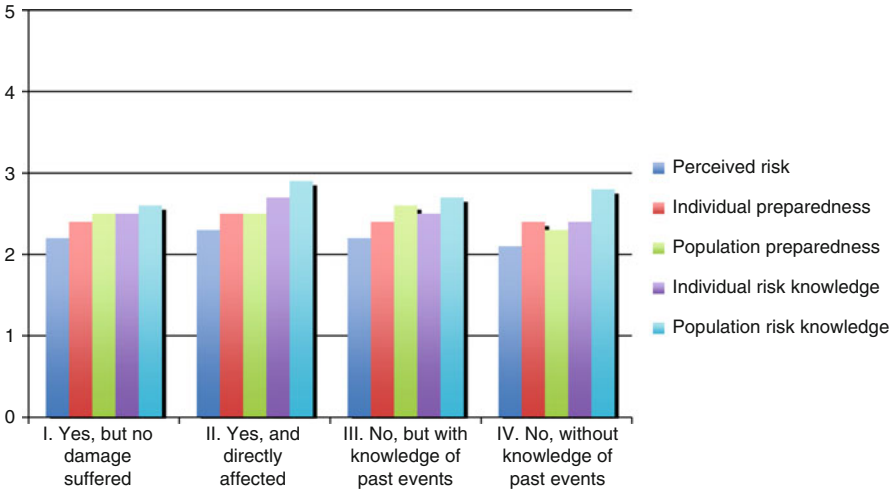

Fig. 9.1 Experiences of past event disasters in terms of perceived levels of risk and knowledge and preparedness of the population (Garcia 2011)

A database of damaging hydro-geological events was prepared for the territory. Original purpose of the database was to collect all possible information about past events which may (1) help to prepare reliable hazard and risk scenarios for civil protection purposes (Blahut et al. 2012), and (2) use the gathered data to identify possible trends in the temporal and spatial patterns of the past damaging events in relation to population distribution (Frigerio et al. 2010).

The database covers a period from 1600 till 2008. Available official sources (Guzzetti et al. 1994; Agostoni et al. 1997; PAI 2001; Lombardy Region 2002; GeoIFFI 2006) were joined with additional information from the Geological Reports for the Municipalities of the study area, books, papers and newspapers. The final database contains 615 records of past destructive events stored as geo-referenced points (Fig. 9.2). However, these points do not always refer to the same part

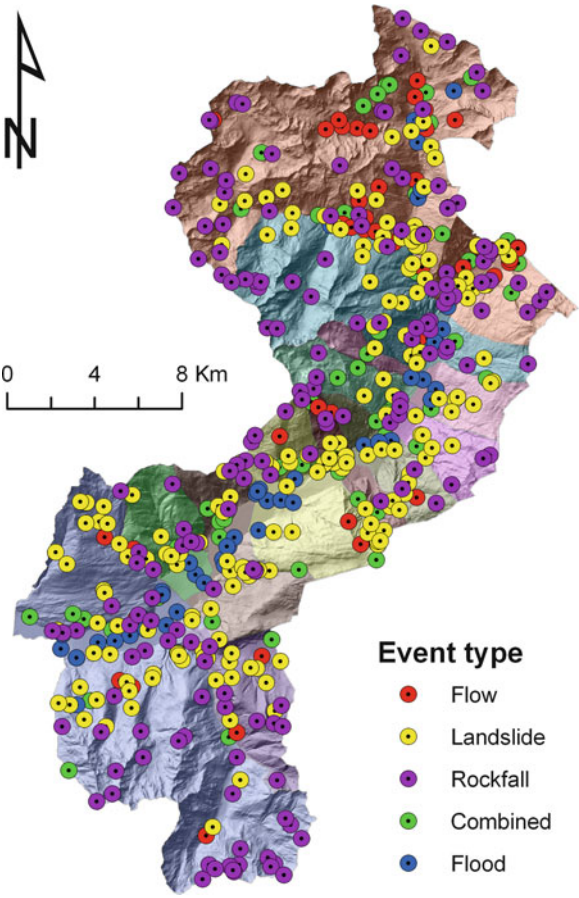

Fig. 9.2 Distribution of five main groups of records of the disaster database of the Consortium of Municipalities of Valtelina di Tirano

of the process as it could represent the source area, the transport area or the impact/deposition area, and it is not always easy to distinguish among them. Additional text information about location is also stored.

The identification of the typology of observed events is not always possible due to a high level of uncertainties and confusion especially in old chronicles and news. The number of landslide events is also underestimated due to low population density and lack of vulnerable elements before the World War II. Nevertheless, the collection of historical information has been useful in order to define possible future scenarios related to landslides and floods as well as evaluate the main threats in the investigated area. Historical knowledge of past disasters allow both authorities and the community to be more aware of the problems related to natural hazards as well as of possible affected areas, expected magnitude, frequency and impacts on vulnerable elements.

9.4 Conclusion

The risk perception among the inhabitants and their willingness to be informed on natural hazards has been studied in a territory affected by multiple natural hazards in the Italian Central Alps, where the culture of dissemination and/or of sharing experiences is not well developed.

Two main ways of transferring lessons learnt are feasible. The first is related to storytelling and it is obviously biased by the perception of the people involved in the event; however this method seems somehow to be weak since the survey carried out among the local population by means of questionnaires revealed that the people tends to remove the memories very quickly and the reports are often inaccurate and incomplete. Nevertheless storytellers are greatly exploited in other countries (Japan, China, Philippines) through thematic museums dealing with past disasters (e.g. Kobe Earthquake Memorial Museum, Wenchuan Earthquake Memorial).

Considering the type of documents collected and implemented in the databases during the project, we can argue that the second method to transfer knowledge is more reliable even if less effective due to the difficulty in sharing documents and related lesson learnt with the population. Most of the available information in the study area has been provided by national and regional authorities as well as research institutions so the main type of collected document is mainly technical reports or validated data. In this framework, we can state the quality of information is quite high but there is still a great difficulty in transforming these "technical" data in easy-to-use inputs for the general public. In other words, for the Consortium of Municipalities of Valtellina di Tirano, a reliable tool to disseminate knowledge is missing. Part of the collected data has been extracted by AVI Database, which was mostly implemented by using newspapers and historical chronicles starting from the nineteenthcentury. In this case, the accuracy of the reported information concerning typology, magnitude, effects and above all location of the landslide was not always satisfactory but this is usual when these sources are used.

Nevertheless the experiences carried out show the usefulness of such type of data in building a comprehensive view of the past disasters occurring in the area and delineating possible lessons to be learnt concerning magnitude and style of activity of occurred landslides and, above all, area involved and problems related to the risk management.

Such kind of lessons can be profitable once transferred to the Civil Protection as well as to Municipalities and the people living at risk but we should make an effort to "translate" technical information into information understandable by the general population, such as behavioral rules to be included in effective civil protection and urban development plans.

Useful lessons from the database analysis and information collected among the population in the study area can be drawn, although they should not be seen as foolproof recipes for handling future events. We have to keep in mind that likelihood of future disasters might differ sharply from previous ones and, even if well prepared, the people will still have to face unexpected developments. But lessons

from past events such as landslides and flooding can provide a framework for facilitating the risk management, mitigating the effects and improving disaster response and recovery.

References

Agostoni S, Laffi R, Sciesa E (1997) Centri abitati instabili della provincia di Sondrio. CNR-GNDCI, Milano

Alexander D (1988) Landslide and flood emergency, Northern Italy, 1987. Disasters 12(3):212–222

Babbie ER (2005) The basics of social research. Thomson Wadsworth, Belmont, CA

Barszczynska M, Bogdanska−Warmuz R, Konieczny R, Madej P, Siudak M (2006) In time for the flood a methodological guide to local flood warning systems. Institute of Meteorology and Water Management, Wroclaw

Blahut J, Poretti I, Sterlacchini S, De Amicis M (2012) Database of Geo-hydrological disasters for civil protection purposes. Nat Hazards 60(3):1065–1083. doi:10.1007_s11069-011-9893-6

Cashman KV, Cronin SJ (2008) Welcoming a monster to the world: myths, oral tradition, and modern societal response to volcanic disasters. J Volcanol Geoth Res 176:407–418

Couture R, Guzzetti F (2004) Preface Geo-databases for natural hazards and risk assessment. Nat Hazard Earth Syst 4:183–185

De Marchi B (2007) Not just a matter of knowledge. The Katrina debacle. Environ Hazards 7:141–149

Dekens J (2007) Local knowledge for disaster preparedness: a literature review. International Centre for Integrated Mountain Development (ICIMOD), Kathmandu

Frigerio S, Blahut J, Sterlacchini S, Poretti I (2010) Landslides historical dataset and population distribution: hystoric@, the experience of the consortium of mountain municipalities of valtellina di tirano, Italy. In: Malet JP, Glade T, Casagli N (eds) Mountain risks – bringing science to society. CERG, Strasbourg

Gaillard JC, Wisner B, Benouar D, Cannon T, Creton-Cazanave L, Dekens J, Fordham M, Gilbert C, Hewitt K, Kelman I, Lavell A, Morin J, N'Diaye A, O'Keefe P, Oliver-Smith A, Quesada C, Revet S, Sudmeier-Rieux K, Texier P, Vallette C (2010) Alternatives pour une réduction durable des risques de catastrophe (Alternatives for sustained disaster risk reduction). Hum Geogr 3(1):66–88

Garcia C (2011) Risk management: integrated people centred early warning system as a risk reduction strategy, Northern Italy. PhD dissertation, Università degli Studi di Milano Bicocca

Garcia C (2012) Designing and implementing more effective integrated early warning systems in mountain areas: a case study from Northern Italy. Revue de géographie alpine/J Alpine Res 100(1). doi: 10.4000/rga.1679

GEOIFFI (2006) The regional inventory (1:10000) of landslides and hydrogeological events, Lombardy Region, Italy. http://www.cartografia.regione.lombardia.it/GeoIFFI. Accessed 10 May 2009

Guzzetti F, Cardinali M, Reichenbach P (1994) The AVI project: a bibliographical and archive inventory of landslides and floods in Italy. Environ Manag 18:623–633

Komino T (2008) Indigenous coping mechanisms for disaster management in Mansehra and Battagram districts, North West Frontier Province (NWFP), Pakistan. In: Indigenous knowledge for disaster risk reduction: good practices and lessons learned from experiences in the Asia-Pacific region

Lombardy Region (2002) Inventario delle frane e dei dissesti idrogeologici della Regione Lombardia. Direzione generale territorio e urbanistica, Struttura rischi idrogeologici, Milan, 2 CD-ROM

PAI (2001) Piano stralcio per l'Assetto Idrogeologico (PAI): Interventi sulla rete idrografica e sui versanti. Linee generali di assetto idraulico e idrogeologico, Adda sopralacuale (Valtellina e Valchiavenna). Autorità di bacino del fiume Po: Parma

Southern RL (1995) Warnings that failed, warnings that worked and a few heroes: stories from Bangladesh and Australia. Stop Disasters 25:9–10

Thrupp LA (1989) Legitimizing local knowledge: from displacement to empowerment for third world people. Agr Hum Value 6(3):3–24

United Nations-International Strategy for Disaster Reduction (UN-ISDR) (2005) United Nations. Bureau for crisis prevention and recovery. Reducing disaster risk: a challenge for development. http://www.undp.org/bcpr/disred/rdr.htm

United Nations-International Strategy for Disaster Reduction (UN-ISDR) & Kyoto University and European Union (2008) Indigenous knowledge for disaster risk reduction: good practices and lessons learned from experiences in the Asia-pacific region. UN/ISDR, Bangkok

Wanczura S (2006) Assessment of the spatial planning approaches to natural hazards in selected EU member states. In: Fleischhauer M, Greiving S, Wanczura S (eds) Natural hazards and spatial planning in Europe. Dortmunder Vertrieb für Bau– und Planungsliteratur, Dortmund

Part III
The Response of the Society Towards the Problems of Hazard and Risk

Chapter 10
Disaster Mitigation by Spatial Planning

Stefan Greiving and Marjory Angignard

Abstract The core element of spatial planning is to prepare and make decisions about future land use. Thus, disaster risks have to be taken into consideration when deciding about the usability of a plot of land. In doing so, planning is able to mitigate risk by e.g. keeping hazard threatened areas free of further development and taking care for the protection of buildings which are exposed to hazards. However, the planning cultures among Europe differ considerably. Thus, the different systems are characterised according to their main functions in order to indicate their effectiveness for disaster risk mitigation. Moreover, the role of spatial planning within disaster risk assessment and management is discussed in detail. The importance of already built-up areas is expressed, because preventive measures taken by spatial planning must fail. Here, more discourse-based approaches are needed due to the given private property rights. Further on, different options for mitigating risk by spatial planning are explained. The role of spatial planning in practise is highlighted by the example of the municipality of Barcelonette, (France).

Abbreviations

CCVU	Communauté de communes de la vallée de l'Ubaye
CLPA	Location Maps of Avalanches
EU	European Union
MDGs	Millennium Development Goals
PACA	Provence-Alpes-Côte d'Azur
PER	Risk Exposure Plan

S. Greiving (✉) • M. Angignard
Institute of Spatial Planning, TU Dortmund University, August-Schmidt-Straße 10,
D-44227 Dortmund, Germany
e-mail: stefan.greiving@tu-dortmund.de

T. van Asch et al. (eds.), *Mountain Risks: From Prediction to Management and Governance*, Advances in Natural and Technological Hazards Research 34,
DOI 10.1007/978-94-007-6769-0_10,

PPR Risk Prevention Plan
POS local land use plans
PSS Plans of Submersible Surfaces

10.1 Introduction: Definition, Role and Families of Spatial Planning in Europe

Spatial planning is defined as the whole comprehensive, co-ordinating spatially-oriented planning at all scales (from national to local), aiming at an efficient and balanced territorial development: 'Spatial planning operates on the presumption that the conscious integration of (particularly public) investment in sectors such as transport, housing, water management, etc. is likely to be more efficient and effective than uncoordinated programmes in the different sectors' (ODPM 2005). Thus, the core element of spatial planning is to prepare and make decisions about future land use. This can be specified for different spatial scales as follows:

- Regional planning/development: The task of settling the spatial or physical structure or development by drawing up either regional plans as an integrated part of a formalised planning system of a state or more programmatic development programmes. Regional planning is required to specify aims of spatial planning, which are drawn up for an upper, overall level and sets a framework for decisions on land use or local investments taken at the local level within land-use planning of the municipalities. Its textual and, if in some member states, cartographic determinations and information typically range on a scale from 1:50,000 to 1:300,000.
- Local land-use planning: Creation of policies at local/municipal level to guide land and resource uses. The main instrument of land-use planning is zoning or zoning ordinances, respectively. Land-use planning normally consists of two stages with specific planning instruments on each of these: first, a general or preparatory land-use plan (scale from 1:5,000 to 1:50,000) for a whole municipality and second, a detailed land-use plan for small part of it, mostly legally binding (scale 1:500 to 1:5,000).

In some of the EU Member States (e.g. Germany), a new development is legally allowed when it is conforming to the land use as laid down in the legally binding regional plan. This so called regulatory function of spatial planning is known under the term "conforming planning" in the international discourse on planning theory (Rivolin 2008; Larsson 2006). In most of the EU Member States however, the so called development function dominates at the regional level which is discussed under the term "performing planning". This planning type is characterized by legally non-binding programmatic and/or strategic statements. Potential projects are then evaluated against the question whether they support the implementation of the programme or strategy. Furthermore, there are – if at all – only partially

binding effects for the subordinated local level. At the local level, in contrast, the similarities between the planning systems between the Member States are much higher compared to the regional level. Throughout Europe – with the well known exception of the United Kingdom – there are two-level planning systems at the local level, consisting of a legally binding zoning of the urban or municipal area ('conforming planning'). It shall be mentioned that also at the European level the development function of territorial development has a much larger importance due to the non-existing legislative competences of the EU in the field of spatial planning (see European Spatial Development Perspective, Territorial Agenda of the EU).

However, the legal frameworks determine how strategies and measures for risk management are designed and by which institutions they are implemented. As an example, the setting of legally binding and spatially specific objectives (e.g. to keep an area free of further settlement development) presumes that there are laws enabling the enactment and enforcement of such spatial objectives. Thus, the differences in the planning systems shall be taken into consideration for deriving management options.

The following Table 10.1 indicates the main characteristics of the planning systems in those member states which are represented by a case study area:

10.2 Relevance of Spatial Planning for Risk Management

A risk is unavoidable whenever a decision is made about whether it has spatial relevance or not. In this context, space can be defined as the area within which human beings and their artefacts may be threatened by spatially relevant hazards. The decision about whether to tolerate a risk or to try to alter it can be understood as an integral part of the existing socio-economic structures and institutions, with spatial planning representing one element in the total equation.

Spatial planning makes decisions for society about whether and how certain spaces will be used. Therefore, spatial planning influences the vulnerability in cases of spatially relevant natural and technological hazards (Greiving 2002).

It is due to authors like Burby (1998) and Godschalk et al. (1999) that the need and the important role spatial planning has to play in the whole disaster management cycle was highlighted. In recent years however, this has not only been accepted by planners and policy makers but corresponds also with latest research initiatives where the potential role of spatial planning in risk management has been stressed (e.g. European Commission 2007).

The spatial character of a hazard can either be defined by spatial effects that might occur if a hazard turns into a disaster, or by the possibility for an appropriate spatial planning response. This dual character also opens up questions about the relevance of different levels of spatial planning as well as the relationship to sectoral planning. Furthermore, the nature of spatial planning requires a multi-risk approach that considers all relevant hazards that threaten a certain area as well as the vulnerability of this area.

Table 10.1 Main characteristics of national planning systems

State	Structure of the state	Spatial planning at the regional level	Co-ordination between regional and local levels	Spatial planning at the local level
France (Fleischhauer 2006)	Central state, consisting of 22 regions and 96 departments	At the regional level there is programmatic development planning which has no direct connection to land use questions	There is a lack of legal settings for the co-ordination between the planning levels. There is no binding effect of regional plans for the local level. In fact, the co-ordination is based on informal agreements	At inter-municipal level a strategic development plan exists that prescribes planning principles and objectives but without any spatially specific regulations for land use. At the local level there is a non-obligatory land use plan (zones of different land use) that is binding for public authorities
Germany (own elaboration)	Federation, consisting of 16 federal states (e.g. Länder) which possess competences for spatial planning	Spatial plans for federal states (scale 1:100,000–1:300,000) and regional plans for parts of a federal state (scale 1:50,000–1:100,000) with graphically designated regulations concerning spatial functions and land use	Principle of countervailing influence Binding effects for sectoral planning of the state and local land-use planning on the one hand and local responsibility or involvement in the design of regional plans, respectively, on the other hand	Land-use planning consisting of a preparatory plan for the whole municipal area (binding for authorities; scale in general 1:10,000–1:20,000) and a detailed plan for parts of the municipal area (binding for everybody; scale usually 1:500–1:1,000)
Italy (Menori/ Galderisi 2006)	Italy is subdivided into 20 Regions and 103 Provinces. Even if a devolution process has been going on since 1944, the country still has a centralised structure	General plans are the regional plan (*piano territoriale regionale*) and the provincial coordination plan (*piano territoriale di coordinamento provinciale*). The regional plans are of a strategic character. Provinces have to work out and adopt provincial co-ordination plan. The main content of the provincial co-ordination plans is the spatial distribution of land-uses. They contains maps	Regional plans provide guidelines and wide perspective strategies for land-use as well as directions for spatial distribution of equipments and infrastructures of regional relevance The provincial plan represents the link between regional development strategies and spatial planning choices of the municipalities.	Comprehensive master plan ("*piano regolatore generale*") legally binding for all parties and citizens Different kind of detailed plans for industrial areas (*piano degli insediamenti produttivi)*; for public housing (*piano di edilizia economica e popolare)* and for historic centres preservation (*piano di recupero*)

Switzerland (own elaboration)	Federation, consisting of 26 federal states ("Kantone")	Regional plan ("Richtplan") with legally-binding designation about land use	The regional plan is binding for the local level.	Local land-use plan ("Nutzungsplan") which differentiates between settlement zones, agricultural zones and protection zones
United-Kingdom (Fay 2006)	Central state, consisting of the entities England, Scotland, Wales and Northern Ireland	Spatial strategy documents at the regional level.	The local development plans in general have to be in line with national policies and regional spatial policy documents.	Local development plans determine programmatic prescriptions for projects which are decided upon in a "planning permission". A legally binding zoning of the municipal area (as known from continental Europe) does not exist in the U.K.

It is a fact that every hazard has a spatial dimension (it takes place somewhere). A spatially oriented risk assessment has three main characteristics: First it is has to be multi-hazard oriented, which means that it is must go beyond sectoral considerations of risks. Second, only those risks are considered that have a spatial relevance. This means that ubiquitous risks like epidemic diseases or traffic accidents are not the focus of the analysis. And third, only collective risks that threaten a community as a whole are relevant and not individual risks like driving in a car or smoking (Greiving et al. 2006). The spatial dimension is also relevant when talking about climate change and adaptation to its unavoidable effects.

One of the most serious problems in context of dealing with natural hazards in land-use planning is represented by the so called external effects: a land-use and temporal inconsistence between chances and risks which are related with every decision making about a future land-use or a concrete investment at a certain location. A classic example for this planning problem is represented by the (intra-generational) conflict between actors which are located upstream and downstream: A municipality located upstream might profit from the chances of a suitable location for an industrial area located in the flood plains of a river and could protect this area by means of a dike. The direct consequence of this action would be among others an increased flood risk for downstream located areas, because of the reduced flood plain capacities in combination with flood waves which would occur faster and with a higher peak.

In terms of sustainable development, this conflict can be described as an intra-generational conflict. Aside from this, inter-generational aspects have to be taken into consideration. Inter-generational justice can be understood as a second prerequisite for reaching a balance of chances and risks. The "Theory of Justice" based the necessity of a consensus about normative regulations on a consensus with the righteous interests of future generations instead of just a consensus of people who are actually alive now. The 'Veil of Ignorance' or the view of short-term chances hinders an appropriate estimation of long-term negative affects that might threaten mainly future generations (Rawls 1971). The greater the persistence of possible harmful effects of an event or decision, the greater the importance and problems related to a decision that accepts consequences from hazardous events (Berg et al. 1995). For example, the Chief Building Inspector had justified a governmental responsibility for building safety standards after the Loma-Pieta-earthquake as follows: 'I represent, in absentia, the unknown future user' (Godschalk et al. 1999). This example indicates that planning related decisions based on a consensus of all stakeholders could fail in relation to the temporal and, as mentioned above, land-use dimensions. The same decision is possibly based on free market transactions. Even if all participants of a transaction of land designated for construction would come to an agreement, they might fail in relation to an unacceptable use of common pool goods.

However, what does this imply for the role spatial planning for both, assessing and managing risks?

Risk management is defined as adjustment policies that intensify efforts to lower the potential for loss from future extreme events, e.g. risk management

is characterised by decisions of stakeholders. Decision-making is a normative, politically influenced strategy about tolerating or altering risks. The authority in charge (democratically legitimised) has to decide the main planning goals to deal with hazards.

When looking at relevant policy documents, it becomes clear that planning and planners are also responsible to reduce vulnerability and to develop mitigation and adaptation capacities against the impacts of climate change, but also natural disasters (Stern 2006; IPCC 2007). Also, the World Bank Report 'The Global Monitoring Report 2008' which deals with climate change and the Millennium Development Goals (MDGs) concludes that the development of adaptive urban development strategies is a fundamental field of action for dealing with the challenges of natural disasters and climate change (World Bank 2008). Additionally, the EU White Paper 'Adapting to climate change: Towards a European framework for action' (European Commission 2009) explicitly relates to spatial planning and territorial development, respectively: "Extreme climate events cause huge economic and social impacts. Infrastructure (buildings, transport, energy and water supply) is affected, posing a specific threat to densely populated areas. The situation could be exacerbated by the rise in sea level. A more strategic and long-term approach to spatial planning will be necessary, both on land and on marine areas, including in transport, regional development, industry, tourism and energy policies." Moreover, the Territorial Agrenda of the European Union explicitly refers with priority 5.1 to the need to promote 'Transeuropean risk management strategies' (European Commission 2007).

As risk assessment and management can be interpreted as an ongoing process, it is often illustrated as the disaster management cycle by which public and private stakeholders plan for and reduce the impact of disasters in the pre-emergency phase (mitigation and preparedness), react in the emergency phase (response) and in the post-emergency phase (recovery).

At all points of the cycle, appropriate actions lead to a reduction of damage potential, reduced vulnerability or a better prevention of disasters. Land-use planning most likely does not play a decisive role in all phases of the disaster management cycle but it has some specific functions in risk management.

The action decided upon is the result of a weighting process between different management option which can be structured along the triangle 'resistance-resilience-retreat' (Greiving 2006);

- Resistance is the protection against (all) hazards by means of structural measures;
- Resilience can be defined as minimization of the risk to life and property when a disaster occurs, and;
- Retreat is the abandonment of risky areas.

Even though spatial planning is considered to be an important instrument to cope with climate change induced impacts, it is limited in its powers and can only solve parts of the problem (Schmidt-Thomé and Greiving 2008). The Table 10.2 indicates, to what extend land-use planning is able to handle natural hazards. It is divided into the main areas assessment and management.

Table 10.2 Strength and weaknesses of spatial planning in the context of dealing with natural hazards

	Milestones	Potential of spatial planning	Description
Risk assessment	Assessment and appraisal of long-term impacts on the human-environmental-system such as climate change	Fair	Possible based on regional impact studies, planning has to have at hand. A strength of comprehensive planning is the traditionally integrated view on different change processes (demography, economy, environment, climate)
	Identification of interaction between land-uses and hazards	Good	Such assessments can easily be integrated in the strategic environmental assessment which is obligatory for any land-use plan or program
	Assessment of frequency and magnitude of extreme events (exposure)	Poor	That is clearly a task for specialised authorities like water management where land-use planning does not have any competence at hand
Risk management	Adaptation of existing land-use structures (settlements, infrastructure)	Poor	Any adaptation of existing structures is hardly possible through regulatory planning due to the given private property rights. Suitable approaches base on incentives and communication to private households
	Avoidance of non-adapted developments	Good	This is in focus of planning which is very much about future developments. The effectiveness of actions depends partly from the existing regulatory framework (zoning instruments)
	Keeping disaster prone areas free of further development	Good	At least conforming planning systems have regulatory zoning instruments at hand. Keeping free of areas prone to extreme events is thereby possible
	Differentiated decisions on land-use: Acceptable land-use types according to the given risk	Fair	Almost possible, but not effective with regard to existing settlement structures
	Relocation/retreat from threatened areas	Poor	Again in conflict with property rights. Full recompensation is normally needed which fails mostly due the lack of financial resources. Possible in areas with shrinking population where the existing building stock will be (partly) deconstructed based on planning strategies (see e.g. Eastern Germany)

Source: own table

Table 10.3 Contribution of land-use planning and supporting instruments to risk management strategies (Greiving and Fleischhauer 2006)

Risk management strategy	Regional planning/ development	Local land-use planning	Supporting instruments
Long-term prevention	Fostering resilience as planning strategy, e.g. by following the robustness principle		Tax system, strategies for reducing greenhouse gas emissions
Mitigation of hazard impacts (non-structural)	Maintenance or reinforcement of protective features that absorb or reduce hazard impacts (mangroves, retention areas etc.)	e.g. local rain water infiltration, adapted land cultivation	Economic incentives, Communication strategies
Mitigation of hazard impacts (structural)	Secure the availability of space for protective infrastructure	Protective infrastructure, Obligations for the design of individual buildings. Retrofitting of existing buildings	Communication strategies,
Vulnerability reduction	Spatial development concepts like decentralised concentration	Keeping hazard prone areas free of further developments	Financial incentives for reallocation of threatened objects
Preparedness, response, recovery	–	Allocation of critical infrastructure outside hazard prone areas and rebuilding planning	Emergency plans and information and training, risk awareness

Risk assessment is a task for sectoral planning authorities. Land-use planning plays a minor role in this context and can be understood as one important end-user of hazard related information, provided by sectoral planning. Hazard maps with a scale of about 1:2,000–1:10,000 are necessary for the enforcement of restrictions of land use at the municipal land use planning level.

Due to its coordinative role and responsibility land-use planning is relevant and responsible for non-structural adaptation measures as part of risk management strategies. There are several possible types of zoning related instruments that might be able to improve non-structural mitigation and some supporting instruments could promote planning initiatives, as explained in Table 10.3:

The assessment of the long-term consequences of climate change calls for an expertise that land-use planning partly lacks (Fleischhauer/Greiving/Wanczura 2006). The field of climate change is important for regions characterized widely by the dominance of existing settlement structures, cultural landscapes and infrastructures which have been developed over centuries. Prevention actions, carried out by land-use planning, are less effective as in countries which are still growing rapidly in terms of population and the built environment where hazard prone areas could be kept free from further development.

The Strategic Environmental Assessment (SEA) which came into force by EU Directive 2001/42/EC in 2001 offers a suitable procedural frame for risk assessment and embedding risk management in decision-making by land-use planning (Greiving 2004). The use of impact assessment methodologies encourages a more informed approach to planning and regional development. The identification of cumulative impacts highlights areas where land-use planning needs to focus on adaptation measures can be highlighted. Adaptation measures need to be designed to deal with several impacts similarly. Planning is mainly able to guide future developments; adapting existing settlement structures can be seen as the main challenge for regulatory land-use planning due to the given private property rights.

10.3 Case Study: Spatial Planning and Natural Hazards in the Barcelonnette Basin

Barcelonnette is a small town of less than 3,000 inhabitants located in the southern French Alps. It is settled on the northern bank of the river Ubaye, in a bowl shaped basin. The mountains around show peaks ranging between 2,800 and 3,100 m, and the town itself occupied slopes between 1,100 and 1,200 m a.s.l. From an administrative point of view, Barcelonnette is situated in the North-East of the Département 'Alpes-de-Haute-Provence', embedded in the Région 'Provence-Alpes-Côte d'Azur' (PACA) (Fig. 10.1). Locally, a community was founded gathering the town and 13 other municipalities in order to join their efforts regarding several aspects of development and local governance. The so-called 'Communauté de Communes de la Vallée de l'Ubaye' (CCVU) is an important actor of local decisions.

The Barcelonnette Basin has been the subject of many scientific activities for more than two decades. Its particular geomorphologic background makes it a very interesting study object. Recently, other disciplines have been involved in field work in the area, giving more space to social sciences.

In France, spatial planning at the local level is not directly connected to regional plans. It consists in strategic development plans, at the municipal or inter-municipal scale, that prescribe planning principles and objectives. As opposed to the regional scale, local plans include a legally binding land use part (Fleischhauer 2006).

Concerning natural hazards, specific plans have been developed in France. At first they were hazard specific, only focusing on one type of phenomenon (e.g. floods for the PSS – Plans of Submersible Surfaces, established in 1935). A systematic mapping of past events was also initiated for some hazards (e.g. avalanches with the CLPA – Location Maps of Avalanches, established in 1970). A consequent corpus of knowledge has been accumulated on natural hazards since the seventeenth century, and in particular on techniques and protection works such as dams and dykes (Pottier et al. 2004). These hazard specific plans were initially joint as annexes to local land use plans (POS), in which they had to be considered.

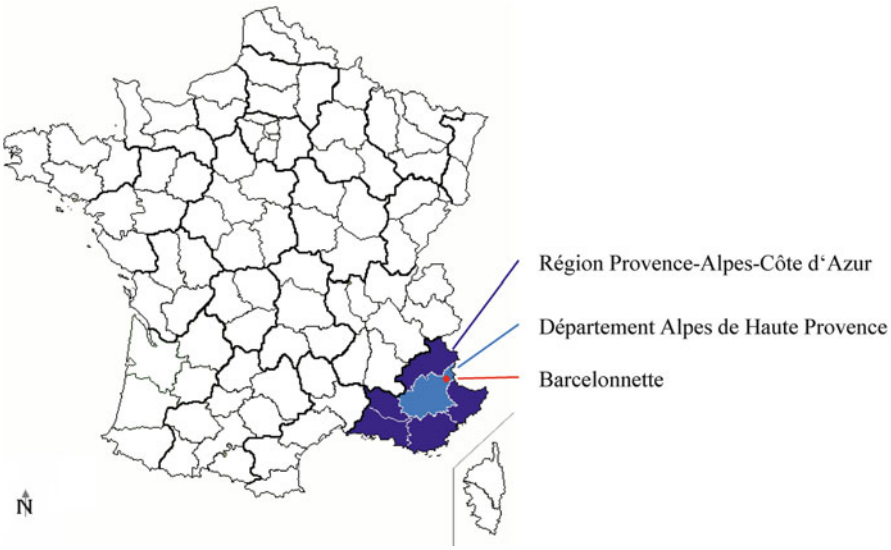

Fig. 10.1 Administrative map of France indicating the location of the municipality of Barcelonnette

In 1982, the legal framework related to natural hazards evolved with the enforcement of a law on insurance and compensation of goods against natural disasters. In addition, a new type of plans was established, the Risk Exposure Plans (PER). Initiated by local authorities, these plans were 'a significant step forward in risk prevention because they united domains that had been separated until then: they enunciated the characteristics of the risks, situated them on the communal territory, regulated land use, and defined [. . .] measures to reduce risks, lower their consequences or make them acceptable [. . .]' (Garry et al. 2004). The different hazards were considered separately. The PER introduced an obligation of retrofitting for buildings located in dangerous areas, if the estimated cost of works did not exceed 10 % of the building's worth.

In 1995, all the documents related to natural hazards management or prevention were abandoned with the creation of an harmonised prevention document, the PPR (Risk Prevention Plan). As opposed to the PER, the PPR is prescribed by the State (through its local representative, the prefect) to communes that are threatened by serious natural risks. The structure of the document is defined by regulation: a summary and map of historical events, a qualification of existing hazards and a hazard map, a qualification of stakes and a stakes map, a land use zoning map differentiating white, blue and red zones, a list of rules applicable to each zone (white zone = no limitation to construction and settlement, blue zone = defined prevention or protection measures necessary for building or settlement, red zone = only certain types of land use allowed). The PPR can be single or multi-hazard. Contrariwise to the PER, PPR do not apply to existing building and settlements.

Fig. 10.2 La Valette landslide, over the municipality of Barcelonnette

The municipality of Barcelonnette, and more largely the entire river basin, is threatened to several hazards. First, floods can be induced by the river Ubaye (especially when the snow melts and adds to the stream) or by the torrents. Second, the slopes are prone to mass movements of different types (landslides, mud flows, etc.). In particular, the large landslide of La Valette is monitored (Fig. 10.2). Finally, the whole region is prone to seismic hazard. In addition to the threat to the population, these natural phenomena could also affect the local tourism industry (the Ubaye valley being both a winter and a summer holiday destination). Moreover, a natural disaster could block the roads. As most of them are unique and not doubled by any other passage, this could isolate entire villages.

The aforementioned hazards already realised themselves into disasters in the past. The main flood event happened in 1957, and was afterwards qualified as 100 years return period. More recently, in 2008, an 'almost flood' event raised the concern of both local authorities and the population when the river threatened to overflow its banks. Other flood events were registered and documented in 1856, 1863, 1868, 1874, 1926, 1951, 1960, 1963, 1970, 1983 and 2003 (Flageollet et al. 1996; Weber 1994). The landslide of La Valette was triggered in 1982 (Fig. 10.3). Although no major earthquake happened in the Ubaye valley, dozens of quakes are measured every year, some of them being felt by inhabitants.

The acknowledgement of these hazards led to an early willingness of prevention and protection in the area. During the second half of the nineteenth century, the

Fig. 10.3 Example of two main types of check dams observed in the Faucon torrent often affected by debris flow events, near Barcelonnette. (**a**) Photograph of a typical masonry check dam; (**b**) Photograph of a typical concrete check dam

large reforestation movement initiated in France gained the region, and slopes were progressively recovered in trees. At the same time, the existing torrents were corrected and secured. A large amount of check dams were built in all of them in order to avoid massive debris flows (Fig. 10.3).

Later on, these hazards were considered in land use plans. In 1986, the implementation of a multi-hazard PER concerning floods, landslides and earthquakes started. The final version of the document was approved in 1991. A revision of this PER started in 1994 and ended up in 1995, with the snow avalanche hazard being added to the document. This version remained valid until the prefect office required by prescription the realisation of a PPR for Barcelonnette, in 2001 (Fig. 10.4). After a long investigation process, including a public consultation, the final version was approved and enforced in 2009.

In particular, a PSS (specific plan for emergency and rescue) has been issued for the La Valette landslide in 1992, revised in 1996, and finally included in the PPR. This plan encompasses practical measures targeted at the population living next to the slide to be taken when an alarm is triggered. A clear chain of command is defined, so that rescue can be organised as fast as possible. In addition, the tenants of houses located in the risky area are advised on the behaviour they should have in case of emergency and a leaflet with all relevant information is distributed regularly.

Although the PPR is a largely acclaimed land use tool when facing natural hazards, it also has drawbacks. The example of Barcelonnette illustrates some of them. If the efficiency of the plan is clear for future settlements, it is not the case on existing ones. No retrofitting measures are imposed. This lowers considerably the efficiency of the whole plan on the area, where most houses and buildings were built before the PPR was enforced.

Although the document is made available to every citizen in the town hall, its existence is not known to everybody. Mostly people who had to consult it for building permit, or to sell or rent a house or a flat (information about existing natural and technological hazards is compulsory in such case in France) know about it.

Fig. 10.4 PPR zoning map of the municipality of Barcelonnette (originally in black and white, colors added by the author)

In Barcelonnette, like in many mountain communities, the lack of space leads to conflicts. Safety of people and goods is in competition with development of activities and settlements. Therefore, the considerable investments required for protection and prevention of natural hazards are seen as a free pass for development: it does not seem legitimate to authorities to keep protected areas free of further settlements. The existence of a residual risk in these zones is sometimes neglected. Some authorities might try to bargain with experts to lower the risk affected to these areas. Barcelonnette and the surrounding river basin have always been prone to several hazards, typical from its mountain situation. Along the years, the local authorities developed various approaches to deal with them, including land use regulation and spatial planning. The recent enforcement of a new PPR creates hope for a better management of natural hazards.

10.4 Conclusion

Spatial planning is theoretically able to mitigate risk to a particular extend. Independently from the planning culture, a country is characterised by, are planning authorities key actors for risk management. However, the quality of planning based response strategies depend from the quality of risk information. The outcome of risk assessments have to be tailor-made to the needs of their users such as planning authorities. They have also to be explained and visualised in way which meets the educational background of the general public as planning process are based on a participation of the public.

The effectiveness of on-paper disaster risk management depends in practice also from the level of trust in public decision-making which differs among Europe. Particularly in the South of Europe are many structures illegally built and do not have a building permission. Any strategy which bases on mandatory decision-making and land-use regulations for hazard zones must fail under these circumstances. As already explained, are many hazard zones (e.g. flood zones) settled since centuries. Both problems call for discourse based strategies and inclusiveness. There is a growing need for involving all stakeholders from the early beginning of the risk assessment and management process in order to improve the effectiveness of disaster risk response. This aspect was discussed in more detail by the introduction of this book.

The case of study of Barcelonette illustrated the wide range of possible contributions of land-use planning and supporting instruments to risk management strategies which were systematised by Table 10.3. Moreover, it underlined the political and normative character of any planning approach, but particularly dealing with disaster risks due to contradicting (economic) interests. This observation is equally important for the whole Europe.

References

Berg M (1995) Was ist ein Schaden? Zur normativen Dimension des Schadensbegriffs in der Risikowissenschaft. Verlag der Fachvereine, Zürich

Burby RJ (1998) Cooperating with nature: confronting natural hazards with land-Use planning for sustainable communities. Joseph Henry Press, Washington, DC

European Commission (2007) Territorial Agenda of the European Union, Brussels

European Commission (2009) White paper adapting to climate change: towards a European framework for action, COM (2009) 147 final, Brussels

Fay H (2006) UK. In: Fleischhauer M, Greiving S, Wanzura S (eds) Natural hazards and spatial planning in Europe. Dortmunder Vertrieb für Bau– und Planungsliteratur, Dortmund

Flageollet JC, Maquaire O, Weber D (1996) The temporal stability and activity of landslides in Europe with respect to climatic change. In: Dikau R (ed) CEC programme. European Commission, Brussels

Fleischhauer M (2006) France. In: Fleischhauer M, Greiving S, Wanzura S (eds) Natural hazards and spatial planning in europe. Dortmunder Vertrieb für Bau– und Planungsliteratur, Dortmund

Fleischhauer M, Greiving S, Wanczura S (2006) Natural hazards and spatial planning in Europe. Dortmunder Vertrieb für Bau– und Planungsliteratur, Dortmund

Garry G, Gaume É, Meschinet de Richemond N (2004) Cartographie et outils de gestion des risques naturels en France. In: Veyret Y, Garry G, Meschinet de Richemond N (eds) Risques naturels et aménagement en Europe. Armand Colin, Paris

Godschalk DR et al (1999) Natural hazard mitigation – recasting disaster policy and planning. Island Press, Washington DC

Greiving S (2002) Räumliche Planung und Risiko. Gerling Akademie Verlag, München

Greiving S (2004) Risk assessment and management as an important tool for the EU strategic environmental assessment. DISP 157:11–17

Greiving S, Fleischhauer M (2006) Spatial planning response towards natural and technological hazards. In: Natural and technological hazards and risks affecting the spatial development of European regions (ed) Schmidt-Thomé P. Geol S Finl 42:109–123

Greiving S, Fleischhauer M, Wanczura S (2006) European management of natural hazards: the role of spatial planning in selected member states. J Environ Plann Man 49(5):739–757

Intergovernmental Panel on Climate Change (IPCC) (2007) Climate Change 2007: synthesis report – an assessment of the Intergovernmental Panel on Climate Change, Geneva

ISDR/World Bank (2008) Mitigating the adverse financial effects of natural hazards on the economies of South Eastern Europe, Geneva

Larsson G (2006) Spatial planning systems in Western Europe: an overview. Ios Press, Delft

Menori S, Galderisi A (2006) Italy. In: Fleischhauer M, Greiving S, Wanzura S (eds) Natural hazards and spatial planning in Europe. Dortmunder Vertrieb für Bau– und Planungsliteratur, Dortmund

ODPM (Office of the Deputy Prime Minister) (2005) Planning policy statement 1: delivering sustainable development. Stationery Office, London

Pottier N, Veyret Y, Meschinet de Richemond N, Hubert G, Reliant C, Dubois-Maury J (2004) Évaluation de la politique publique de prévention des risques naturels. In: Veyret Y, Garry G, Meschinet de Richemond N (eds) Risques naturels et aménagement en Europe. Armand Colin, Paris

Rawls J (1971) A theory of justice. New York. The Belknap Press of Harvard University Press. Cambridge, Massachusetts

Rivolin UJ (2008) Conforming and performing planning systems in Europe: an unbearable cohabitation. Plan Pract Res 23(2):167–186

Schmidt-Thomé P, Greiving S (2008) Response to natural hazards and climate change in Europe. In: Faludi A (ed) European spatial planning and research. Lincoln Institute for Land Policy, Cambridge

Stern M (2006) The economics of climate change – the stern review. Cambridge University Press, Cambridge

Weber D (1994) Research into earth movements in the Barcelonnette Basin. University of Strasbourg, Strasbourg

Chapter 11
Disaster Mitigation by Corrective and Protection Measures

Olga-Christina Mavrouli, Alessandro Corsini, and Jordi Corominas

Abstract This section offers a panorama of the corrective and protection measures that might be applied for the mitigation of landslide risk. Two different strategies may be envisaged depending on whether the aim is at the reduction of the landslide hazard or of the respective consequences. Hazard reduction measures are distinguished into stabilization measures and control measures. The first category includes the stabilization measures that lead to the reduction of the driving forces or to the increase of the resistant ones, while the second one refers to the interception and control measures that diminish the landslide severity (e.g. magnitude, impact energy or pressure) or even the probability of reaching the elements at risk. Consequence avoidance includes measures for the protection of the exposed elements or even the decrease of their vulnerability, although the latter lacks in efficiency in comparison with the rest. Using this classification, a variety of mitigation measures is presented for three different landslide types: rockfalls, debris flows and landslides, the latter embracing a broad range of shallow to deep-seated slope movements, including rock slides, earth slides, earth flows or complex phenomena.

11.1 Introduction

Landslide risk management and mitigation involves a wide range of measures, from precautionary to remedial ones. As discussed in Sect. 1.3, landslide risk mitigation by corrective and protection measures must be considered only if other

O.-C. Mavrouli • J. Corominas (✉)
Department of Geotechnical Engineering and Geosciences, Technical University of Catalonia, BarcelonaTech, Jordi Girona 1-3, SP-08034 Barcelona, Spain
e-mail: jordi.corominas@upc.edu

A. Corsini
Department of Earth Sciences, University of Modena and Reggio Emilia University, Largo Sant' Eufemia 19, IT-41100 Modena, Italy

T. van Asch et al. (eds.), *Mountain Risks: From Prediction to Management and Governance*, Advances in Natural and Technological Hazards Research 34,
DOI 10.1007/978-94-007-6769-0_11,

available options have been disregarded or need to be supplemented. Landslide hazard and risk are best addressed with land-use planning regulations, by restricting the development in dangerous locations because developing landslide prone areas is delicate. The realisation of cuts and fills, loads due to building construction, leakage of either water supply or sewage systems may cause the reactivation of dormant landslides or trigger new failures. Corrective and protective measures should be primarily conceived to reduce risk level in threatened areas already developed.

Two different strategies may be envisaged to mitigate risk (Corominas 2013): (1) reducing the landslide hazard; and (2) reducing consequences. The first strategy aims at diminishing the probability of the landslide occurrence or its reactivation, and/or the probability of reaching the exposed element. The second strategy looks for avoiding or minimizing damages by reducing the exposure and/or the vulnerability of the exposed element. This may be achieved by implementing either active or passive measures. Active measures aim at modifying the slope stability conditions or restricting the landslide progression by any means, which may involve earthworks, the construction of concrete structures (structural measures) or by the implementation of surface protective works including eco-engineering techniques (non-structural measures). Passive measures do not interfere with the occurrence and spatial development of the landslide and are conceived to avoid adverse consequences and include a variety of options such as the early warning systems.

Corrective and protection measures against landslides are designed according to the standards of practice which include the consideration of a suitable factor of safety. The degree of safety to achieve depends on the available funds, risk acceptability, maintenance requirements and on other environmental or social restrictions. Large amount of funds are often required to protect populated areas or critical facilities such as main road networks, dams or industrial plants. The main challenge is to implement an optimal design that could be cost-effective and achieve a reasonable degree of safety. To this end, an appropriate understanding of the landslide mechanisms and the triggering processes is required as well as the assessment of the soil and rock strength parameters and their uncertainties. The analysis is usually performed by a qualified engineer or engineering geologist based on detailed reconnaissance and field sampling, laboratory work and stability calculation of the slope or landslide under different circumstances.

Reduction of the landslide hazard may be performed at the landslide source by means of stabilization works. The probability of slope failure may be prevented by either reducing driving forces in the slope or by increasing resisting forces in the potentially mobilized mass, or by both. Driving forces acting on a slope or on an existing landslide are mainly associated to its geometry and to the occurrence of transient phenomena such as earthquake shaking. Remedial actions are in general more feasible for the changes in geometry. Grading (cut and fill) of slopes may be performed in active or dormant landslides to achieve more stable slope geometry. However, this must be designed with care to ensure that indiscriminate excavation or fill will not destabilize the slope or accelerate the landslide displacements. Little can be done against the occurrence of landslide triggers such as intense rainfall

or earthquakes. The increase of driving forces produced by the triggers may be counteracted by undertaking prevention measures such as surface and subsurface drainage which are considered soft-structural measures. The increase of the resisting forces in the slopes is sought through external reinforcement by increasing the internal strength or by providing support through man-made structures. The overall effect of all these measures will reduce the probability of failure and, subsequently, the hazard level.

Hazard level may also be reduced by interventions along the landslide path in order to diminish the landslide magnitude, its velocity, or both. The goal is to reduce the severity of the event (its mass, kinetic energy or impact pressure) and the probability of reaching an exposed element. To this end, structural works aiming at intercepting and storing the landslide debris or for lessening the velocity and dissipating the energy may be foreseen. Designing this type of structures requires the appropriate assessment of the potential movable volume in order not to overcome the storage capacity of the retention works, and of its dynamics along the path which will facilitate the decision of the location of the structures (e.g. barriers, dissipaters).

Finally, risk may be mitigated by avoiding undesired consequences. This is the goal of protective works that avoid exposure of the elements at risk such as galleries or diversion works which do not interfere with the landslide dynamics. Reinforcement and strengthening of threatened elements to decrease vulnerability must be considered a very last option only. Few structures are able to resist the impact of very rapid landslides. Structural reinforcement of foundations such as slabs may be considered in foundation on slow moving landslides (some mm to few cm·year^{-1}) to prevent their differential displacement and possibility of cracking.

In the following, a description of landslide risk mitigation options for different landslide mechanisms is proposed.

11.2 Mitigation Measures for Rockfall Hazard

The measures which are applied for the mitigation of rockfalls can be classified into two main categories according to whether they aim at the reduction of the hazard, or of the consequences. In the following, some of the strategies which are commonly applied are presented.

11.2.1 Hazard Reduction

Hazard reduction measures can be categorized into stabilization methods and severity reduction methods. Stabilization aims at reducing the rockfall occurrence at the source. On the other hand severity reduction methods are used in order to decelerate the rock block mass, to intercept it or to control its trajectory so as to reduce is destructive potential.

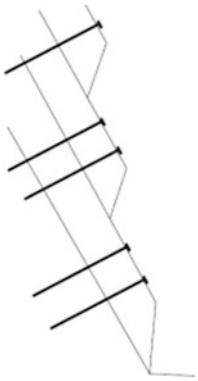

Fig. 11.1 Rock bolts

In the following, a series of techniques referring to both types of measures are briefly presented. A single or a combination of techniques might be used. The selection is based on criteria related to the complexity, effectiveness, durability, constructability, cost, maintenance requirements and aesthetic impacts (Andrew et al. 2011). Further details for the application of these techniques are given in Kliche (1999) and Hoek and Bray (1981).

11.2.1.1 Stabilization Measures

The minimization of the rockfall hazard might be obtained by different types of measures. One of them is the direct intervention at the source of instability, by block removal of potential unstable rocks. Three types of techniques are applied to this purpose: resloping zones of unstable rocks, trim blasting of overhangs and removing loose blocks of rocks. Further details for each one of them and their execution can be found at (Wyllie et al. 2004). Removal should be used on the condition that the new face will be stable and that no risk of undermining the upper part of the slope exists.

The rockfall occurrence can also be diminished by interventions that aim at affecting the probability of rock detachment from the slope face, by improving its stability or, alternatively, by reducing the driving forces that contribute to instability. Stabilization measures refer to reinforcement of the rock mass. The most common in practice are mentioned in the following. Different types of steel rods may be used to stabilise the rock mass. Rock bolts are long anchor bolts used to transfer load from the unstable exterior, to the confined and more resistant interior of the rock mass (Fig. 11.1). They are used in tension. Dowels instead are generally short grouted steel reinforcement bars acting as passive reinforcement elements that require some ground displacement to be activated and subjected to both shear and tensile stresses. Shear pins, which are metal rods designed to shear, break in the case of overload, thus preventing the overload of the rock mass.

Fig. 11.2 Combined use of rock bolts, shotcrete and wire mesh to prevent rockfalls in the road from Zarautz to Getaria, Basque Country, Northern Spain (© J. Corominas)

Alternatively, zones or beds of closely fractured or degradable rock can be protected by applying a layer of shotcrete to the rock face (Fig. 11.2). Shotcrete utilizes pneumatically applied mortar and concrete sprayed onto a slope face to seal it. It controls both the fall of small blocks of rock and progressive raveling that will produce large, unstable overhangs on the face. However it provides little support against sliding of the overall slope (Turner and Schuster 1996). In some cases, injectable resin/epoxy also serves as rock bonding inside the open joints.

Buttresses and beams retain and protect areas of weak rock and supporting overhangs. Buttresses should be designed so that the thrust from the rock to be supported, loads the buttress in compression. In this way bending moments and overturning forces are eliminated and there is no need for heavy reinforcement of the concrete (Turner and Schuster 1996).

On the other hand, reduction of the driving forces in tension cracks and vertical joints can be achieved with drainage. Methods of controlling water pressure include limiting surface infiltration and drilling horizontal drain holes or driving adits at the toe of the slope to create outlets for the water. A variety of techniques and their appropriateness for precipitation due to different rainfall intensities or snow melt is described at Wyllie et al. (2004).

Geotextiles draped over slopes can also be used for the drainage and stabilization of rockfalls. A big variety of materials exists to this purpose (Kliche 1999). Geotextile filters act as graded granular filters and they are designed for soil retention, system permeability and long-term filtration.

11.2.1.2 Interception and Control Measures

Protection measures aim at the reduction of the severity of an event by deceleration, trajectory control or deflection of the rock mass(es). Severity refers to rock block velocity and run-out distance, which are measures of its destructive potential. There exist a variety of rockfall protection measures which can be applied either at the proximity of the rockfall source, or in an intermediate distance between the source and the exposed elements. The most common in practice are mentioned in the following.

Wire mesh and cable nets systems that are used to control rockfall activity are among the most famous protection measures and consist of steel fabric/mesh running over a slope (Fig. 11.3). They might be draped and/or suspended from upslope anchors, thus deriving its support from either the available interface friction between the mesh and the ground or the anchors or a combination of both.

Forest cover on rockfall corridors may have a positive effect on dissipating part of the energy of the rock blocks moving down-slope, amongst other, through their contact with stems and the energy absorption, the contact with ground vegetation and the high surface roughness due to vegetation and dead wood (Brauner et al. 2005).

Barriers and fences aim at the deceleration up to the catchment and stopping of moving rock blocks (Fig. 11.4). They include different types such as earthen berms and gabions to contain the run-out, wooden, steel or concrete walls and other types of fencing.

Hybrid rockfall protection barriers (attenuators) might be as well used, which are a combination of rockfall protection drapes/rockfall nettings and flexible rockfall protection barriers without bottom supporting ropes. The possibility of incorporating sensors that check the maintenance status of the afore-mentioned rockfall protection systems and set off an alarm if limit values are exceeded also exists and can be used for the implementation of early warning systems.

11.2.2 Consequence Reduction

11.2.2.1 Protection Measures

Protection measures are considered to be those that are situated next to the exposed elements and aim at their direct protection from rock impacts.

Rockfall galleries have been proven to be efficient for the rockfall mitigation of highways and railways (Fig. 11.5). A lot of investigation is currently going on, for the incorporation of damper systems, the optimization of the resistance of supporting beams and the use of energy absorption layers of sand or other materials (Schellenberg and Vogel 2007).

Ditches are mostly referred to as catchment areas and they are constructed at the toe of a slope when there is enough space, to prevent rockfalls from reaching the highway. Sand cushions are often used to achieve the block catchment by increasing

Fig. 11.3 General view of the San Juan de la Peña monastery, Central Pyrénées, Spain, built under an overhanging conglomerate cliff and detail of the wire mesh installed to avoid the direct fall of cobbles detached from the rock mass (© J. Corominas)

the energy absorption at the impact of the rock to the ground. Hybrid ditches may also be used which are a combination of a barrier and a ditch. The ditch width depends on the slope height.

At the level of buildings, a variety of barriers exist that can be constructed either to enhance the performance of excavated ditches or to form catchment zones at the toes of the slopes (Turner and Schuster 1996). The required type of barrier and its

Fig. 11.4 Rockfall fence installed at the Canal de l'Alzina to intercept and/or reduce the velocity of the falling blocks before reaching the bottom of the slope where Santa Coloma neighborhood, Principality of Andorra, is built (© J. Corominas)

Fig. 11.5 Gallery and a combination of ditch and barrier to protect against the occurrence of rockfalls in the coastal road of Gipuzkoa, Basque Country, Northern Spain (© J. Corominas)

dimensions depends on the rockfall intensity, the slope geometry and the permitted cost. The goal of the barriers is to trap the falling rocks and they are particularly useful when placed at the toes of slopes. To protect the structures and the people from direct impacts, different types of barriers can be used among which the most common are such reinforced concrete or geo-fabric and soil barriers.

11.2.2.2 Vulnerability Reduction

The efficiency of structural protection measures that are considered for the buildings' design against rockfalls is low in comparison with hazard or consequences reduction measures. Some recommendations for the design of buildings against mountain hazards and progressive collapse have been made by Holub and Hübl (2008), Ellingwood and Dusenberry (2005) and Izzuddin et al. (2008).

11.3 Mitigation Measures for Debris Flow Hazard

Debris flows are one of the most damaging landslide-related phenomena. They often occur in steep slopes covered by unconsolidated layers of colluvium or weathered rocks. The predominant initiation mechanism is a shallow translational or rotational slope failure triggered by intense rainy episodes and sudden collapse of the bank material in torrent beds. Debris is transported down slope normally through pre-existing drainage ways until it is deposited in areas of decreased gradient and confinement where it may spread out to form a fan (Costa 1984). The steepness of the slopes confers a high potential energy to debris flows which may propagate at extremely high velocities (up to some tens of meters per second). Damages produced by the debris flow events are mainly due to their high impact energy and to the burial of the exposed elements by debris. In the last years, a large number of casualties and losses have been reported in different parts of the world due to debris flows. For instance, 161 deaths were reported in the events of Sarno and Quindici in 1998 (Revellino et al. 2004; Zanchetta et al. 2004), around 30,000 people were killed by debris flows and floods in the coastal zone of Vargas, Venezuela in December 1999 (Wieckzorek 2001), or a total of US$ 200 million of property losses and 29 persons lost their life by floods and debris flows during the passage of the Typhoon Mindulle in Taiwan in July 2004 (Chen and Petley 2005), to mention just a few.

11.3.1 Hazard Reduction

Massive debris flow occurrence is associated to extreme rainfall events which affect large areas (over thousands of square kilometers) or to large magnitude earthquake events. In these circumstances is not unusual to report thousands of failures and,

because of that, these events have been named as multiple occurrence of regional landsliding events or MORLES (Crozier 2005).

The large size of the areas affected by MORLES does not facilitate the implementation of measures to systematically stabilize the source areas and minimize the probability of occurrence. Afforestation and reforestation are nonstructural slope reinforcement measures that may restrict the occurrence of the slope failures and the development of debris flows. Vegetation strengthen the surficial formation layer by the anchoring effect of the root system and by improving the hydrological conditions of the slope through pumping groundwater by evapotranspiration which reduces pore water pressures (Sidle et al. 1985). Several studies have demonstrated the beneficial influence of forest on the stability of slopes (Fannin and Rollerson 1993). However, even though it is observed that number and density of slope failures are significantly smaller in forested slopes, the role of the forest cannot prevent from slope failures completely.

In individual basins with well identified debris sources, the stabilization measures may be considered. These measures mainly consist of structures to protect unconsolidated sediments from erosive processes. Biotechnical stabilization techniques combine vegetation and man-made structural elements to bind soil components and reinforce the ground surface (Highland and Bobrowsky 2008). Rock slabs, timber and other natural elements are often used thus allowing an adequate visual integration in the landscape. Light structural elements such as gabions walls and nets are also used to protect sediments from undermining and erosion and provide some support to the bottom of the slope. This type of protection is not usually designed to prevent the slope failure from occurring but to restrict the enlargement of the landslide scar and the availability of sediment. The cost and maintenance of such measures restrict its extensive usage in mountain areas.

The severity of the debris flow events is reduced by means of a variety of structural measures that are usually emplaced along the track. These measures are aimed at protecting torrent banks from erosion, minimize the mobilized debris volume and/or reduce the speed and subsequent kinetic and impact energies.

Check-dams are typical structures of masonry or concrete built in the debris flow tracks with manifold goals (Fig. 11.6). The main effect is the stabilization of the bed and the protection of the banks against torrent erosion. This plays an important role because a debris flow may significantly increase its volume along the track (Cannon 1993). To achieve this goal it is fundamental that dams could be founded in sound bedrock as erosion of the ground around the abutments may lead to the loss of support and to the destruction of the dam (Alcoverro et al. 1999). An additional effect of the check-dams is the energy dissipation through the jumps. The amount of sediment retained by a system of check-dams is, in general, negligible. Dams are often filled immediately with sediments by regular torrent floods. The location of the dams in the steep stretches of the torrents makes the emptying and maintenance unaffordable.

Retention basins are conceived to store debris thus reducing the volume and speed of the debris flow (Fig. 11.7). Openings at the dam are sometimes included to allow the passage of water and the fine sediment fraction. This type of measure is restricted by the availability of the space in the basin. Basins are usually designed to

Fig. 11.6 Series of check dams at the Barranco de Arás, Central Pyrénées, Spain (© J. Corominas)

Fig. 11.7 Retention basin, Bolzano Province, Italy (© J. Corominas)

store some tens of thousands of cubic meters of debris but steep torrent beds allow the storage of small amount of debris only. Flexible ring net barriers capable to withstand high static and dynamic loads may be alternatively used (Fig. 11.8). They can be easily installed with minor earthwork and cost. Their capacity allows trapping up to 1,000 m^3 of debris and, if required several barriers may be installed along

Fig. 11.8 Net at Rumí torrent in Portainé, Eastern Pyrénées. Series of nets are located along the torrent bed, which have been filled with debris (© J. Corominas)

the debris flow track to increase the storability. Basins and nets must be emptied periodically in order to keep their storage capacity and access to machinery must be guaranteed. It is not unusual that some elements of the nets had to be replaced after an event making maintenance costs expensive.

Best performance of retention basins and flexible barriers is obtained in catchments affected by small size and episodic debris flow events that are expected not to overcome the storability of the system. The occurrence of either large or frequent debris flow events may result in saturation of the system and rendering it inefficient.

11.3.2 Consequence Reduction

Protection measures for debris flow may be conceived to confine the flow within the channel by constructing an artificial concrete bed or earth embankments. In this case a critical parameter for the design is the knowledge of the maximum discharge of the potential event in order to avoid overflowing. An alternative or complement to the mentioned measures is the construction of protection dykes or diversion channels (by-pass). These measures aim at avoiding the undesired consequences without interfering on the dynamics of the debris flow. Either man-made or enlarged natural avulsion channels at the fan apex may be used to divert flow from populated areas or critical facilities (Fig. 11.9). Channel banks may be enlarged and/or reinforced with levees and concrete or rip-rap walls (Prochaska et al. 2008). The scarcity

Fig. 11.9 Diversion channel (*right*) at the Biescas debris fan in the Central Pyrenees, Spain. The step-like longitudinal profile will contribute to the energy dissipation of the flow and force debris deposition at the fan apex (© J. Corominas)

of magnitude-frequency data necessary for the proper design of such diversion structures is a main constraint in mountain areas. Calculations of the potential debris flow discharge made based on observation of historical events could be deceptive as shown in recent events in Italy (Arattano et al. 2010). Events larger than expected (the design-event) may have catastrophic consequences for such developed fans.

Mountain roads show numerous crossings with torrents affected with debris flow activity. This is typically made with bridges and less frequently with galleries. Bridges must have a span large enough to allow the discharge of debris. Failure in identification of the potentially of the torrent to generate debris flow may result in inadequate designs that may endanger motorists and cause the interruption of necessary evacuation ways.

11.4 Mitigation Measures for Landslide Hazard

This paragraph deals with corrective and protection measures that can be applied to a broad range of shallow to deep-seated slope movements, including rock slides, earth slides, earth flows or complex phenomena. These types of landslides are affected by changes in resisting and driving forces due to the variously combined effects of slope geometry, groundwater and surface water.

11.4.1 Reduction of Driving Forces by Changing the Surface Geometry of the Slope

The main measure to reduce driving forces in a landslide is changing the surface geometry of the slope in order to reduce the integral of tangential stresses acting on the failure surfaces. Two fundamental approaches can be used to change the surface geometry of the slope: regular reshaping of the slope to a semi-constant new defined inclination, or stepped grading of the slope by creating a series of planar slope surfaces (known as "banks" or "benches") linked by inclined slope intersections.

Regular reshaping is particularly effective in rotational movements. It involves downloading the head portion of the landslide – where the inclination of the sliding surface is expected to be higher – and at the same time loading the toe portion of the slope – where the contrary occurs. The morphology of the intermediate portion of the landslide, in between the so called drained and the undrained "neutral lines" (Hutchinson 1977), is left mostly unchanged. Loading at the toe of the landslide can be done either by using and compacting the landslide material excavated in the head zone, or by using heavy-weight external materials (e.g. boulders, reinforced earth embankments, etc.).

Stepped grading can be applied in rotational or translational movements and is generally carried out in steep scarp or toe zones of the landslide. Its purpose is not only to increase resisting forces, but to provide for erosion control and vegetative establishment. In irregular terrains, grading is generally carried out by mimicking the contours of the slope. Graded slopes that are to be stabilized with grass shall not be steeper than 2:1. However, the max inclination of the angular slopes and of the entire graded slope should be carefully designed on the basis of the geotechnical characteristics of materials. Reverse slope benches are generally used in steep graded slopes. Surface drainage is assured at each individual bench by ditches and shallow drains that convoy runoff to a stable portion of the slope (Fig. 11.10).

11.4.2 Reduction of Driving Forces and Increase of Resisting Forces by Drainage

Groundwater expressed as hydrostatic pore water pressure can reduce the effective stress acting on the sliding surface and inside the landslide mass and it can consequently reduce the resisting forces due to soil shear strength. In some cases, such as in presence of vertical joints in rock slopes or with tension cracks in soil slopes, infilling water pressure can be an extra driving force acting in the slope.

Subsurface and surface drainage systems are the most commonly used structural measures for water drainage. Subsurface systems are designed for draining the larger possible amount of groundwater from inside the slope. Surface systems are designed for controlling surface runoff, therefore reducing groundwater recharge due to infiltration of rainfall or pounding water. At the same time, surface drainage systems are also effective in reducing sheet and rill erosion along the slope.

Fig. 11.10 Example of stepped grading of a landslide head scarp zone (Ca'Lita landslide, northern Apennines, Italy). (**a**) Global view form orthophoto; (**b**) detail view of benches

11.4.2.1 Subsurface Drainage Systems

Subsurface drainage systems include: drainage trenches; sub-horizontal drains, shields of deep drainage wells, large diameter drainage wells. Less frequently, and in particularly large stabilization projects, drainage tunnels and micro-tunnels are also used.

Drainage trenches are trenches filled with free-draining geomaterials (coarse granular fills and geosynthetics). They should be preferably oriented longitudinally or in fish-bone arrays so to minimize the possibility of damages due to slope movements. If excavation and filling is made with conventional methods, their depth is rarely more than 4 m, since higher depths involve large graded trenches, so costs would increase significantly. However, by using clam buckets for excavation and pre-assembled drainage panels of synthetic material for filling the depth can be higher with relatively limited costs.

Sub-horizontal drains are drainage pipes made of special non-rotting casings (made of metal or pvc) of around 10 cm diameter placed in the underground in slightly upward direction by using rotating drilling rigs. The length may be up to 100 m and are generally constructed in series of drains spaced one another from 5 to 10 m. In addition to intercepting and evacuating ground water, sub-horizontal drains are effective because they alter the subsurface flow pattern inducing a stabilizing vertical current pressure. One of the main problems with sub-horizontal drains is their maintenance in the long term, as clogging can reduce their effectiveness in relative short times, and costly unclogging operations might be often required. Another problem is that their relatively small diameter makes them vulnerable to slope movements. It is therefore good practice not to place them across major sliding surfaces. Another good practice is to couple them with retaining structures, so to assure the stability of the outlet end of the drain.

Shields (curtains) of deep drainage wells are series of 1.0–1.5 m diameter wells connected by a 0.1–0.2 m diameter basal drainage collector ensuring gravity discharge (Fig. 11.11). This system was first patented in the early 1980s as "Rodren". Drilling in the ground is done with rotating tapperred buckets or hougers drillers. The hole is then fitted with pre-assembled metal inner casing and the basal drainage collector is drilled from one well toward the adjacent one. Wells can be of two kinds: inspection wells, i.e. wells in which the metal casing is left empty, and drainage wells, e.g. wells that are completely filled with coarse draining material. The spacing between adjacent wells is generally limited to about 5–10 m, a distance limited by the difficulties in creating basal drainage collector. The depth can be significantly high, up to 35 m and more in favorable geological conditions, and it is actually only limited by the operative range of the drilling rig. The basal drainage collector is certainly the most vulnerable component of this drainage system, as it's clogging or rupture can seriously affect the overall efficiency. For this reason, shields of deep drainage wells are often installed upslope retaining structures, so to have a coupled stabilizing effect for both type of consolidation work.

Large diameter drainage wells are drainage wells up to more than 25 m deep and of at least 3.5 m diameter (Fig. 11.12). They are constructed of either steel or reinforced concrete segments, and concrete is used at the well bottoms and the upper portion of the well. Water is drained from the surrounding ground by a series of radial and multilevel positioned sub-horizontal drains. Often, in weak underground materials, their excavation requires the prior creation of a circular set of adjacent caisson piles. The most vulnerable parts of these systems are certainly the sub-horizontal drains that can be cut by slope movements and clogged by hard water or the fine grained fraction of the ground.

11.4.2.2 Surface Drainage Systems

Surface drainage systems usually consists of surface channels and catchpits that are the chambers that collect water from different channels. Surface channels are created by excavation of trapezoidal ditches. Generally, the bottom of the

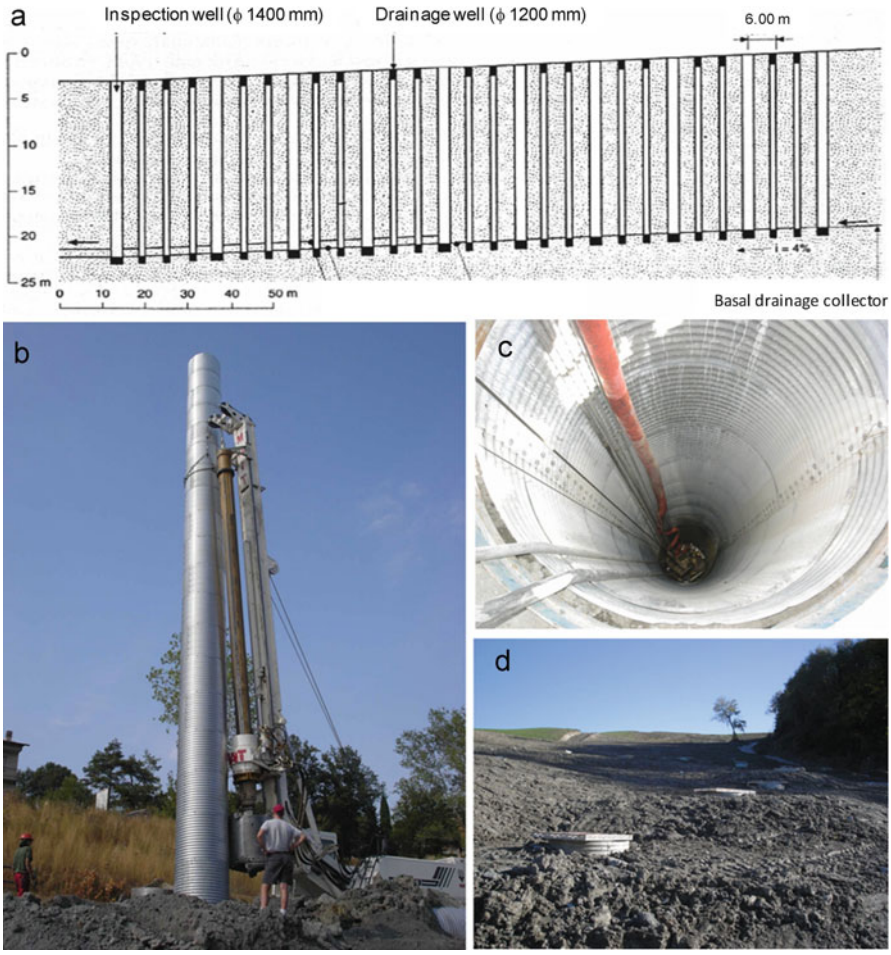

Fig. 11.11 Example of a shield of deep drainage wells (Magliatica landslide, northern Apennines, Italy). (**a**) General construction scheme; (**b**) hole fitting with pre-assembled metal inner casing; (**c**) inner view of drainage well during drilling of the basal drainage collector; (**d**) final setup of the drainage system (© G. Truffelli)

channel is protected from erosion by covering it with rock blocks, wood beams, imbricated pre-constructed concrete elements, metal half-pipes, or geosynthetic matting, geotextiles or erosion matting. Catchpits are made of plastic or concrete materials, and can vary in size, shape, number of inflow points according to the specific requirements of the surface drainage network, and can eventually be filled by draining material. Catchpits can also be used as sampling and flow rate measurement points.

Fig. 11.12 Example of large diameter drainage well (Garfagnolo landslide, northern Apennines, Italy). (**a**) Excavation inside the circular set of adjacent caisson piles; (**b**) drilling of radial subhorizontal drains; (**c**) inner view of the drainage well with water inflow from radial drains; (**d**) final setup of the drainage system (© G. Truffelli)

11.4.3 Increase of Resisting Forces by Retaining Structures

Earth pressure can be counterbalanced by retaining structures. Commonly adopted retaining structures for landslide consolidation are: gabions, retaining gravity/concrete walls, bored caisson piles (coupled to concrete walls), micropiles and reinforced earth structures.

Gabions are rectangular wire mesh baskets filled with rock boulders, that are modularly assembled on site to form a retaining structure (Fig. 11.13). Gabions are generally assembled on top of a superficial foundation shaft slightly dipping upslope, or on deep pile-funded shafts. The main advantages are flexibility and permeability of the resulting structure. They are used in different slope instability situations, to sustain source areas and scarps, to control toe erosion and to stabilize banks.

Gravity and concrete walls are retaining structures made of blocks or reinforced concrete. Typically retaining walls are cantilevered from a footing extending up beyond the grade on one side and retaining a higher level grade on the opposite side. They are among the most commonly used systems in engineering works for sustaining excavation fronts and road cuts. They can also be used for stabilizing

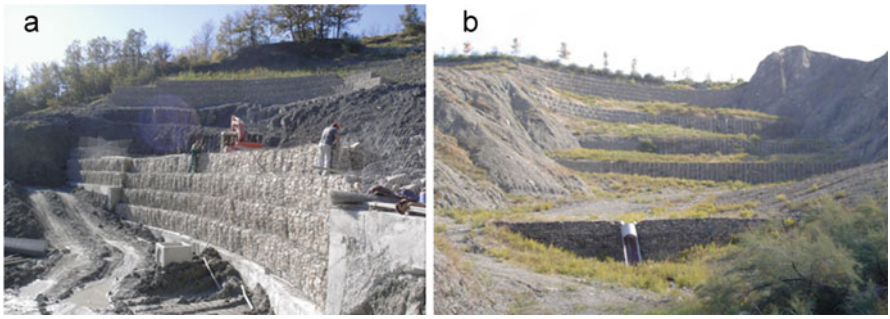

Fig. 11.13 Example of usage of gabions. (**a**) Construction phase at the head zone scarp of a landslide. (**b**) Final gabions setup at the head zone scarp of a landslide (© G. Truffelli)

landslides of limited size and depth, whereas they are generally inefficient for large landslides, unless they are coupled to deep pile foundation. Their efficiency depends on the quality of the rear drainage, as groundwater pressure is among the main causes of base sliding or overturning.

Bored caisson piles (coupled to concrete walls) are among the most resistant retaining structures. The term caisson is normally used to identify large bored concrete piles. Caissons are constructed by drilling a hole in the ground and filling it with concrete. A reinforcement cage is placed prior to concreting. Two types of drilling machines are in use: auger types and bucket types. The diameter of caissons can be as high as 1 m and its length can be up to 35 m or more. Piles can be built equally spaced, intersecting one another or distributed at quincunx. At ground level, a beam of reinforced concrete is constructed to link the upper termination of the piles (Fig. 11.14). The beam acts as connection to the uppermost concrete wall. This type of construction is in most cases completed with anchoring systems dipping into the slope for tens of meters that allows transferring earth pressures from the beam to the deep seated firm ground. This type of retaining structure has been successfully used in several slope consolidation projects of deep earth slides (Fig. 11.15). Good practices require the creation of a good drainage system upslope the piles lineament, by means of drainage trenches or, optimally, deep drainage wells.

11.5 Conclusion

Slope stabilization and protection measures are best recommended in situations where population or infrastructures are subjected to an imminent landslide threat. To stabilize a slope failure requires the appropriate understanding of the landslide geometry and mechanism. This may require time to investigate and while complete stabilization, particularly for large landslides can sometimes be too expensive or impractical. Stabilization measures may reduce the hazard level by either diminishing

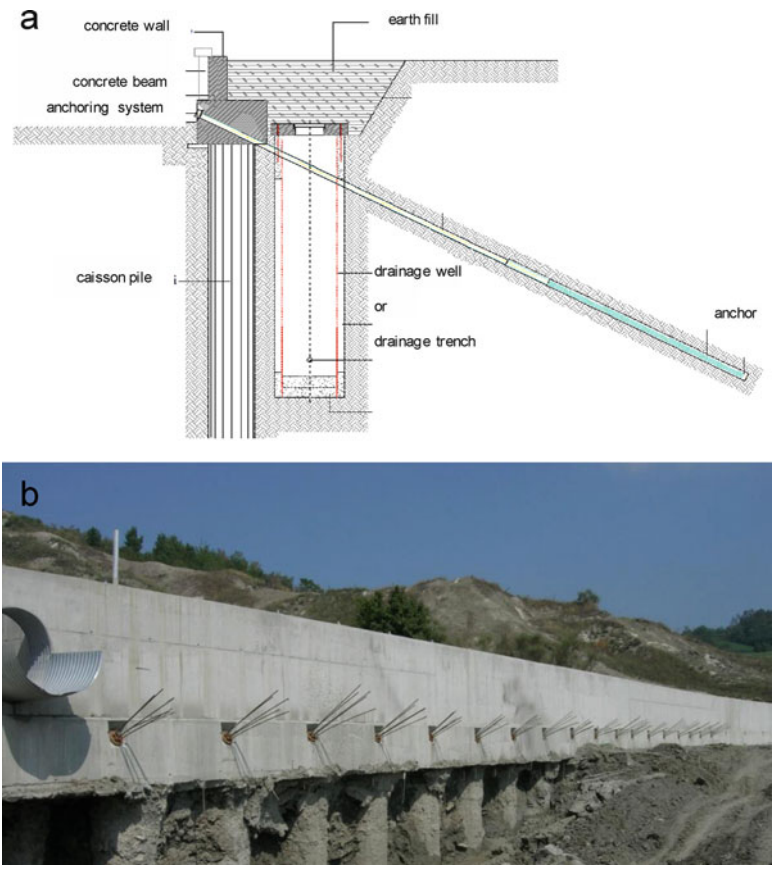

Fig. 11.14 Example of bored caisson piles coupled to concrete walls (Ca'Lita landslide, northern Apennines, Italy). (**a**) General construction scheme; (**b**) exposed caisson piles, reinforced concrete beam and anchoring systems (© G. Truffelli)

the driving forces in the slope (or existing landslide) or by increasing soil and/or rock strength. Hazard level may be also reduced by constraining the progression of the landslide in order to reduce the distance travelled, its velocity (energy) or both. In mountain environments, the remedial measures are intensively implemented in linear infrastructures (roads and railways), particularly when crossing of landslide prone areas is unavoidable. However, it must be taken into account that reduction of hazard might only be a transient solution because maintenance works are usually required. Retention structures may deteriorate with time, especially in aggressive environments. Failure to maintain structural elements such as rock anchors, nets or fences may lead to the loss of their efficacy and to the onset of the instability of the slope. Several administrations have prepared maintenance guides for slopes to promote good risk management practices (GEO 2003). In any case, as an additional

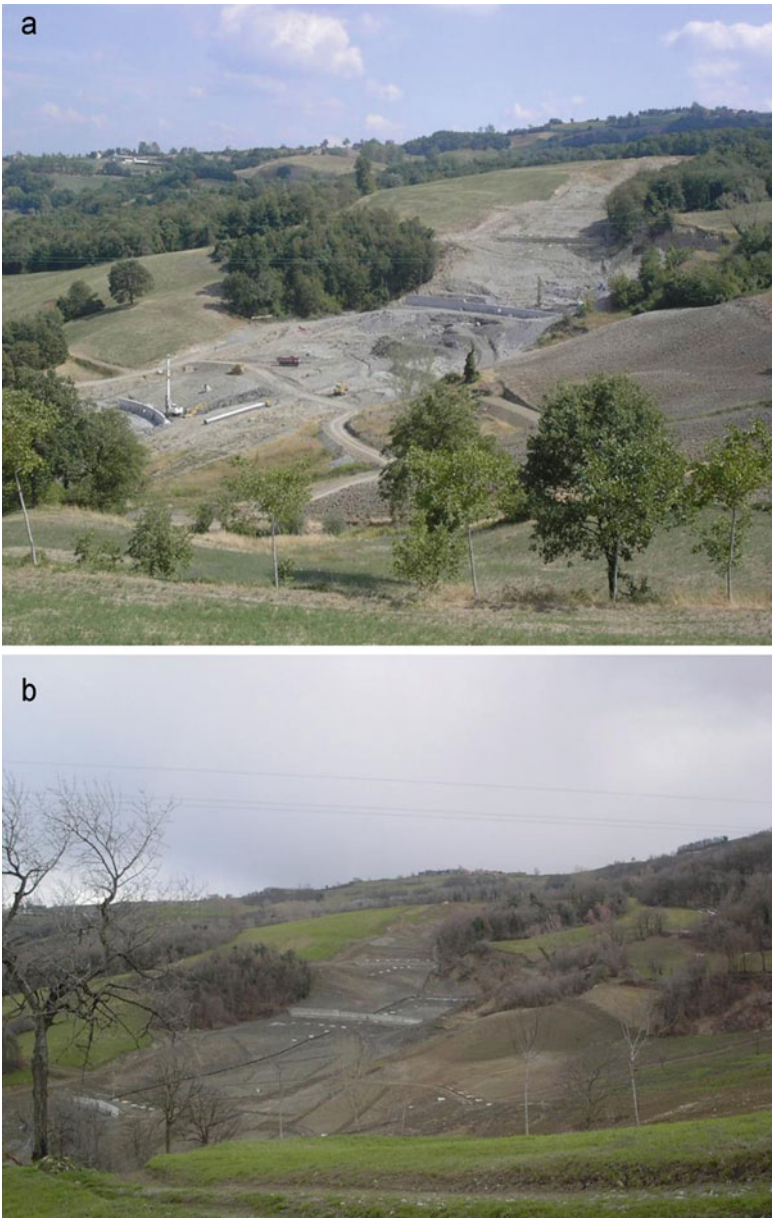

Fig. 11.15 Example of coupled usage of bored caisson piles and shield of deep drainage wells (Magliatica landslide, northern Apennines, Italy). (**a**) During construction; (**b**) finalized consolidation work (© G. Truffelli)

Fig. 11.16 A 2,000 KJ protection fence in Andorra la Vella, Andorra Principality, damaged by a rockfall in April 2008. Replacement of the elements was carried out in a few weeks to immediately restore the protection level of the area (© J. Corominas)

measure, it is recommended the setting up of a monitoring system in the engineered slopes or stabilized landslides to check the performance and level of safety of the whole system (Corominas 2013).

Corrective and protective measures are components of a living with risk management strategy. It is important to avoid false sense of security, particularly in urbanized areas and to inform population properly. Design is normally subjected to a large degree of uncertainty of the input data, particularly of the slope strength parameters or on magnitude-frequency relations of future events. Structural solutions are designed according to standards of practice which may be adequate in front of infrequent events but in some circumstances not for the worst case scenario. Protection against the latter is often unaffordable.

Care must be taken after the occurrence of landslide events that might have compromised the performance of the measures. For instance, a rockfall may destroy a protection fence or a debris flow event may fill the capacity of the retention basins (Fig. 11.16). Events occurring before the replacement of the damaged elements or completion of the maintenance work will produce undesired consequences. Because of these reasons, these types of mitigation measures must be fully integrated within a risk management framework and be continuously monitored.

The use of biotechnical slope stabilization methods using geotextiles, vegetation and foresting is increasing. These “soft” landslide mitigation techniques, if correctly applied can be proved efficient and at the same time, they are presenting the advantages of being environmental “friendly” and aesthetically improved in comparison with steel and concrete structural mitigation measures.

Even though measures implemented may justify the development of threatened areas or the construction of infrastructures, it is recommended that landslide hazard maps reflect in some way the existence of the potential hazard. This is particularly relevant when considering that future changes such as forest fires which may burn protection forest in rockfall prone areas, may facilitate the failure of the unprotected soils in the slope.

References

Alcoverro J, Corominas J, Gómez M (1999) The barranco de arás flood of 7 august, 1996 (biescas, central Pyrenees, Spain). Eng Geol 51:237–255

Andrew R, Bartingale R, Hume H (2011) Context sensitive rock slope design solutions. Publication No. FHWA-CFL/TD-11-002, Federal highway administration of US. http://extra.cflhd.gov/programs/techDevelopment/geotech/css. Accessed July 2011

Arattano M, Conte R, Franzi L, Giordan D, Lazzari A, Luino F (2010) Risk management on an alluvial fan: a case study of the 2008 debris-flow event at Villar Pellice (Piedmont, N-W Italy). Nat Hazard Earth Syst 10:999–1008

Brauner M, Weinmeister Agner P, Vospernik S, Hoesle B (2005) Forest management decision support for evaluating forest protection effects against rockfall. For Ecol Manag 207:75–85

Cannon SH (1993) An empirical model for the volume-change behavior of debris flows. In: Proceedings of Hydraulic Engineering, vol 2, San Francisco, pp 1768–1777

Chen H, Petley DN (2005) The impact of landslides and debris flows triggered by Typhoon Mindulle in Taiwan. Q J Eng Geol Hydrogeol 38:301–304

Corominas J (2013) Avoidance and protection measures. In: Shroder J (Editor in Chief), Marston RA, Stoffel M (eds) Treatise on geomorphology, vol 7, Mountain and hilslope geomorphology. Academic Press, San Diego, pp 259–272

Corominas J, Remondo J, Farias P, Estevao M, Zérere J, Díaz de Terán JR, Dikau R, Schrott L (1996) Debris flows. In: Dikau R, Brunsden D, Schrott L, Ibsen ML (eds) Landslide recognition. Wiley, Chichester/New York

Costa JE (1984) Physical geomorphology of debris flows. In: Costa JE, Fleisher PJ (eds) Developments and applications of geomorphology. Springer, Berlin

Crozier MJ (2005) Multiple occurrence regional landslide events in New Zealand: hazard management issues. Landslides 2:247–256

Ellingwood B, Dusenberry D (2005) Building design for abnormal loads and progressive collapse. Comput Aid Civil Infrastruct Eng 20:194–205

Fannin RJ, Rollerson TP (1993) Debris flows: physical characteristics and behaviour. Can Geotech J 30:71–81

GEO – Geotechnical Engineering Office (2003) Layman's Guide to slope maintenance. The Government of Hong Kong, Hong Kong

Highland LM, Bobrowsky P (2008) The landslide handbook—a guide to understanding landslides, U.S. Geological Survey Circular 1325. U.S. Geological Survey, Reston, 129 p

Hoek E, Bray JW (1981) Rock slope engineering, 3rd edn. Taylor & Francis, London

Holub M, Hübl J (2008) Local protection against mountain hazards – state of the art and future needs. Nat Hazard Earth Syst 8:81–99

Hutchinson JN (1977) The assessment of the effectiveness of corrective measures in relation to geological conditions and types of slope movement. Bull Int Assoc Eng Geol 16:131–155

Izzuddin BA, Vlassis AG, Elghazouli AY, Nethercot DA (2008) Progressive collapse of multi-storey buildings due to sudden column loss – part I: simplified assessment framework. Eng Struct 30(5):1308–1318

Kliche CA (1999) Rock slope stability. Society for Mining, Metallurgy, and Exploration, Inc, Littleton, 253 pp

Prochaska AB, Santi PM, Higgins JD (2008) Debris basin and deflection berm design for fire-related debris-flow mitigation. Environ Eng Geosci 14:297–313

Revellino R, Hungr O, Guadagno FM, Evans F (2004) Velocity and runout simulation of destructive debris flows and debris avalanches in pyroclastic deposits, Campania region, Italy. Environ Geol 45:295–311

Schellenberg K, Vogel T (2007) Tests and analytical model of rockfall impacts on galleries. In: Proceedings of protect 2007, Structures under extreme loading, Aug. 20–22, Whistler

Sidle RC, Pearce JC, O'Loughin CL (1985) Hillslope stability and land use, vol 11, Water resources monograph series. AGU, Washington, DC, 140 pp

Turner A, Schuster R (1996) Landslides. Investigation and mitigation. Special report 247. National Research Council of US

Wieczorek GF, Larsen MC, Eaton LS, Morgan BA, Blair JL (2001) Debris-flow and flooding hazards associated with the December 1999 storm in coastal Venezuela and strategies for mitigation. USGS, Open-file report: ofr-01-0144. http://pubs.usgs.gov/of/2001/ofr-01-0144/

Wyllie D, Mah C, Hoek E (2004) Rock slope engineering: civil and mining, 4th edn. Taylor & Francis, London

Zanchetta G, Sulpizio R, Pareschi MT, Leoni FM, Santacroce R (2004) Characteristics of May 5–6, 1998 volcaniclastic debris fows in the Sarno area (Campania, southern Italy): relationships to structural damage and hazard zonation. J Volcanol Geoth Res 133:377–393

Chapter 12
The Relevance of Legal Aspects, Risk Cultures and Insurance Possibilities for Risk Management

Marjory Angignard, Carolina Garcia, Graciela Peters-Guarin, and Stefan Greiving

Abstract Risk culture expresses a variety of factors such as attitudes, believes, values, goals, and practices, shared by an institution, organization or group that influences the way risk is handled in a particular setting. The cultures of risk vary considerably among Europe and often even between regions within a particular country as well as between different social groups, age groups and gender. The interconnection of factors that determine the perception of risk and the social variables is discussed. However, not all of these factors are addressed by this chapter which concentrates on the relevance of legal frameworks and insurance possibilities. The theoretical implications of risk culture on risk assessment and management in practise are explained by the example of the case study Valtellina, Italy.

Abbreviations

EU	European Union
ISDR	International Strategy for Disaster Reduction
PPR	Plan de Prévention des Risques, Risk Prevention Plan
PRIM	Programme Regionale Integrato di Mitigazione dei Rischi, Integrated Regional Programm of Risk Mitigation

M. Angignard (✉) • G. Peters-Guarin • S. Greiving
Institute of Spatial Planning, TU Dortmund University, August-Schmidt-Straße 10, D-44227 Dortmund, Germany
e-mail: marjory.angignard@tu-dortmund.de

C. Garcia
Department of Environmental and Territorial Sciences, University of Milano-Bicocca, Piazza della Scienza 1, IT-20126 Milan, Italy

Regional Independent Corporation of the Centre of Antioquia (CORANTIOQUIA), Cr 65 No.44A – 32, Medellin, Colombia

T. van Asch et al. (eds.), *Mountain Risks: From Prediction to Management and Governance*, Advances in Natural and Technological Hazards Research 34,
DOI 10.1007/978-94-007-6769-0_12,

RTM Restauration des Terrains de Montagne, Restoration of Mountain Terrains
WBGU Wissenschaftlicher Beirat des Bundesregierung Globale Umweltänderungen, German Advisory Council on Global Change

12.1 Introduction

There is more than one way to deal with natural hazards. Across the world, several approaches have been developed and applied. Even in comparable risk settings (same hazards, same intensity, same expected range of damages) the option chosen can differ largely. This is due to the existence of different risk cultures. Risk culture is the 'collective knowledge' of risk in a given space and time, common to all members of a social group (Glatron 2003). Risk culture is expressed through an ensemble of factors such as attitudes, believes, values, goals, and practices, shared by an institution, organization or group that influences the way risk is handled in a particular setting. It comprises elements as diverse as the disaster history of the area, its economic situation, its demographical evolution, the insurance possibilities, the legal framework in force and the type of administrative organization. As expressed in the definition, risk culture is not static in space (it varies from one setting to another) or time (in the same setting it varies through time). The same factors that build risk culture make it evolve. For instance, the lessons learnt after a disaster become part of the risk culture. They influence the perception of risk, and have an impact on the management decisions taken afterwards.

Importantly, it is the definition of risk that affects risk policy and moreover, defining risk is an exercise in power in view of existing ambiguity. In European Member States, governed according to law, the existing legal framework – which is to a certain extent the outcome of a particular (risk) culture – serves as normative basis for any risk assessment and risk management, to be taken by public as well as private bodies.

12.2 The Role of Risk Culture

An important and interesting aspect of risk perception is the variation in different cultural (regional, national) contexts, a perspective studied within the cultural risk paradigm. Risk perception enters the risk management equation through differing estimations on, for example, how probable an event may be, and how much money is to be spent on preparedness. The following Fig. 12.1 shows the interconnections between the different factors which determine how a risk is perceived and evaluated:

Individual risk perception is also shaped by how the community or a certain socio-cultural milieu generally deals with a special type of risk or risky situations. Estimating how risk is perceived by a particular community may provide a basis

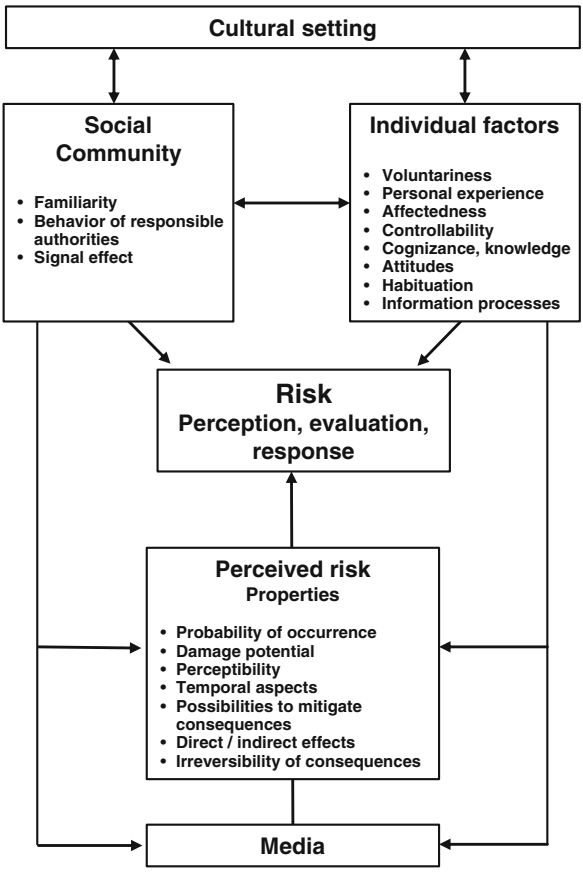

Fig. 12.1 Elements of perceived risk (WBGU 1999)

for understanding and anticipating public responses to hazards (Slovic 1987). This is particularly relevant for governments and emergency personnel because, in many cases, the lack of understanding about how risk is perceived by a particular community may result in well intended policies being ineffective (Slovic 1987). Understanding the way the people of a particular community think about risk is fundamental to correctly address risk reduction efforts, to improve risk communication and to define preparedness strategies, including policies and emergency plans (Slovic 1987; Frattini and Crosta 2006; Haynes et al. 2008; Bird et al. 2009).

Both risk appraisals and behaviour in risk situations are influenced by cultural belief systems, the value systems contained in these and social roles. The cultural belief system determines extensively the collective notions of how the world functions. These collective notions are also termed social representations, as they contain socially constructed 'images' of the world.

Social representations comprise the knowledge of 'facts' and 'events' (e.g. what constitutes an insult, how to resolve conflicts, whether the forest is dying etc.) shared within a group. This knowledge is essential for people to appraise situations,

evaluate them and act. This knowledge is propagated, stabilized and modified by communicative processes (interpersonal communication). To understand the ways in which risks are dealt with, it is essential to take into consideration the socio-cultural setting.

As seen in the previous part, different countries facing similar hazards can develop different strategies to deal with them. Due to the existence of various risk cultures, the panel of possible choices for addressing natural hazards and risks is very large. This is not only due to intrinsic organisational factors such as the legal and administrative contexts or the compensation and insurance system regarding natural hazards. As Veyret & Meschinet de Richemond explain, 'the relation to danger and the construction of risk [depends on] the past events and the cultural diversity that characterise each country' (Veyret and Meschinet de Richemond 2003).

This cultural diversity can be expressed through various aspects of a country's identity. Risk culture is 'transmitted knowledge, forged more or less consciously' (Glatron 2003) and varies in space and time. Some of its constitutive elements are very abstractive and difficult to grasp, because they refer to more or less immaterial objects such as the collective memory of past events, the consequences on peoples' lives of the existence of hazards, economic activities, demography, or the focus of action against natural hazards, but also sociological parameters (gender, age, ethnicity, social level, ...) and cognitive elements such as knowledge and understanding of the risk, familiarity to the risk situation, choice of the risky activity, or previous experience of the phenomenon (Glatron 2003).

Therefore, risk cultures are plural, even in one space or time unit.

Across Europe, many differences can be observed, for instance on the following points (Veyret and Meschinet de Richemond 2003):

- the level in which decision are made: although national, regional and local levels are involved in risk management, usually one of them has a more important role than the others (e.g. in Germany, the regional level with the Länder and in the Netherlands, the local level);
- the focus of action: the policies and strategies against natural hazards can address specific parts of the risk governance framework, sometimes focusing particularly on one of them. This leads to completely different strategic orientations (e.g. prevention and protection in France, crisis management in Portugal);
- the place and role of insurance in the compensation system: in some European countries insurance against natural disasters is compulsory, either state managed (e.g. in France) or completely private, whereas in others it is optional (e.g. in Germany). This influences the relation to risk. If all damages due to natural disasters are covered by insurance, and victims are certain to get a compensation for them, people might tend to accept higher levels of risk and not take any precaution against hazards, and;
- the place of stakeholders and population in the decision making process: although involving the whole society in risk related decision making is nowadays recognised as a positive action and largely encouraged, it is addressed in different

manners across Europe. For instance, the consultation of the public during a decision making process is made compulsory by law in France, whereas in Switzerland a 'culture of public debate' exists and does not require any legal obligation.

It is crucial to recognise and document these differences, not only as social objects, but because of the importance they have when considering a European standardisation. In the general dynamic of European harmonisation of policies on several topics, the question of a harmonisation of risk governance policies can be posed (Angignard 2011). Natural phenomena are not limited to administrative borders. The hazards present in Europe are largely diffused, and large areas are concerned with similar problematic. In order to manage trans-border hazards, for instance earthquakes or floods in large river basins, it is of benefit to install collaboration between countries. This would be highly facilitated by a harmonisation of risk governance methods. Moreover, this could improve the share of information among European countries and regions, reaching for a larger and deeper corpus of knowledge about natural hazards and risk related policies.

12.3 Legal Frameworks and Insurance Possibilities

In the Mountain Risks network, a particular attention was paid to two elements linked with risk culture: the legal framework, and the compensation system. The legal framework and administrative system enforced on a given territory are highly influenced by the existing risk culture, and have an important impact on it. This framework differs considerably among Europe and can be grouped into different administrative families (Fig. 12.2).

The approach and focus chosen depend on the priorities which are defined through the prism of the local risk culture. The construction of risk culture is a cycle. Different directions can be chosen by authorities concerning their risk related legislation, focusing for instance on prevention, protection, reaction to disasters, or several of these steps. The conception of the repartition of responsibilities between authorities and individuals also influences the choice of focus. Historically, some countries were founded on the monopolisation of powers, resulting in centralised organisations (e.g. France, United Kingdom). On the opposite, other countries applied 'negotiated cooperation' between the State and the other levels of authorities (regions), resulting in polycentric organisations (e.g. Germany, Italy). This difference leads to the development of various approaches towards risk management, with a more or less important place of the State. Although the centralised organisation tends to be more efficient regarding security matters, regional authorities can have a better understanding of the local context, and laws emanating from this level can be expected to be more adapted to the actual situation, when national laws could be too general and obliterate local specificities. For the same reasons, polycentric organisation is considered as more adapted to preventive actions. The relation

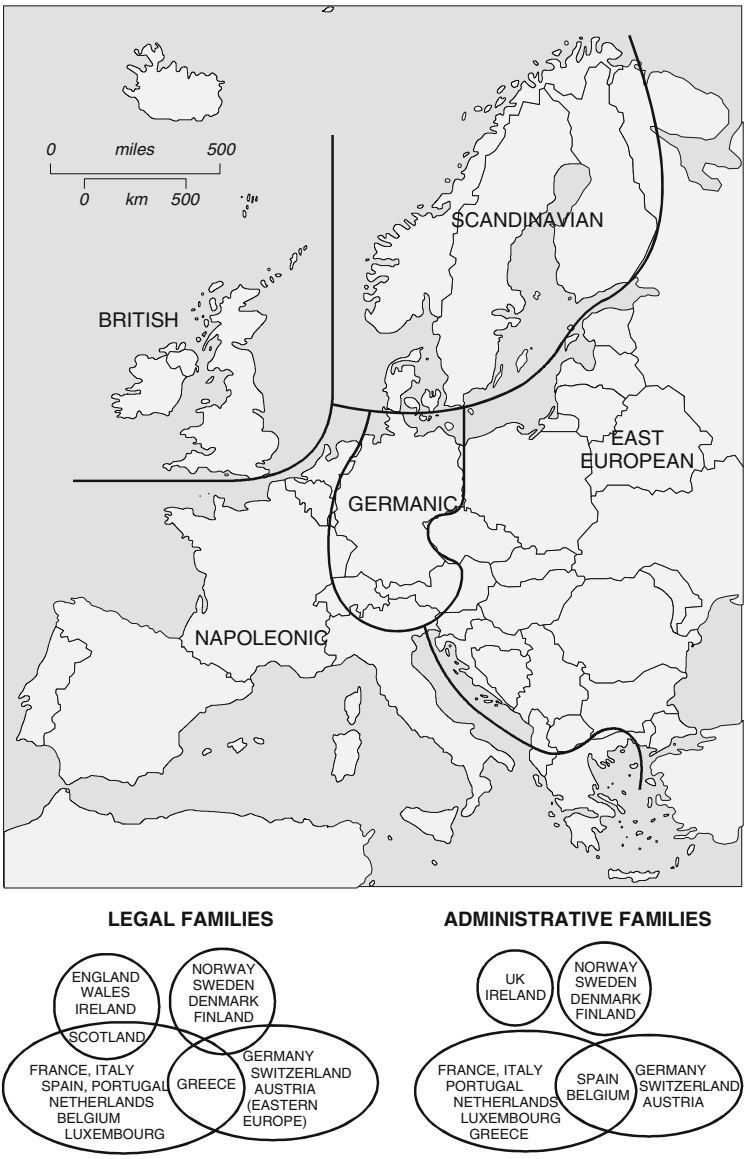

Fig. 12.2 The legal and administrative 'families' of Europe (Newman and Thornley 1996)

between a State and its population also counts in the orientation of a risk-related legal framework. An 'almighty state' in which citizens are used to transfer their responsibilities to the authorities will be responsible for every aspect from hazard assessment to recovery, whereas in a country where individuals carry responsibility

for their own safety the authorities will have fewer duties and leave space for personal action.

Following the same pattern, risk culture is also relevant for explaining the differences of organization of compensation of losses in a particular country (state-based fund, private system of insurances etc.). The insurance against natural hazards is probably the most adopted way how to transfer economic losses from particular risks. In every country (or even a particular region) this risk transfer can be achieved through different possibilities.

In Europe, coverage for disasters caused by the impact of natural hazards by both the insurance industry and the government varies from one country to another (ISDR/World Bank 2008). One can distinguish four main categories:

1. In countries like the Netherlands or Denmark, insurers play a minimal role in the provision of coverage against natural hazards. The State organizes the insurance scheme through the government annual budget or through a tax levied on fire insurance policies (which are managed by a specific fund).
2. In Switzerland, the State does not intervene in the provision of insurance but makes the insurance of chosen risks compulsory, most of the time by means of fire insurance contracts. Without having insurance, no building permission will be granted.
3. In countries like France, Norway and Spain, the solution is compulsory insurance provided by State-backed insurance entities. In France for instance, a fund is fed by a levy on insurance primes. Similar schemes are currently being considered by the Governments of Italy and Romania. The compulsory requirement is typically enforced through the inclusion of disaster insurance coverage in the fire policy, which is the most common product in the market.
4. Finally, the most common solution is the case in which the State's intervention is officially totally absent and most of the coverage relating to natural hazards is optional and granted on a case-to-case basis, by financial aid, proved by the government an a case-to-case basis. In addition, those states (i.e. Germany, Italy, United Kingdom) believe in a commercially structured 'free market solutions'.

It is also interesting to note that the hazards covered are not the same everywhere. Regional specificities lead to the need to insure people against particular hazards (e.g. landslides in the Alps, subsidence in the Mediterranean area) and to ignore others because they are not present in an area (e.g. avalanches in plains, seismic hazard). Some countries decide to cover only events above a given intensity. In France for instance, damages can be covered by the national CatNat fund (Catastrophe Naturelle: Natural Disaster) only if they result from 'the abnormal intensity of a natural hazards, when the usual measures to prevent theses damages could not stop their happening or could not be taken' (Code des Assurances). This definition excludes compensation when mitigation measures failed to be taken or implemented, thus encouraging citizens and local authorities to undertake prevention and protection measures.

Since government aid is not based on formal legislation, it depends on many other factors such as, for instance, media coverage, which makes it difficult for affected persons to rely on this kind of compensation. Due to broad media coverage of disasters and media-driven politics, the extent of damages is often overestimated in the immediate aftermath of a disaster caused by the impact of natural hazards. Government ad hoc relief programmes often reduce the incentive to keep the risk of damage to infrastructure and private property low through private and collective preventive measures. There are many cases where local authorities do not step up their efforts in risk prevention and development planning, because they expect the federal Government to cover the cost of any necessary repairs to public assets.

12.4 Case Study Valtellina Valley, Lombardy Region, North of Italy

This concept is illustrated by the analysis of two case study sites (the Ubaye Valley in France; the Valtellina Valley in Italy). In each of them, a large survey targeted at the population addressed the questions of risk perception and expectations regarding risk governance. In addition, local experts and decision makers were interviewed. The results revealed interesting differences between both sites that can help understand how the different risk cultures existing in these apparently similar areas (similar hazard profile, events history) were shaped. In the following, the case of Valtellina is discussed in more detail.

12.4.1 Italian Legal Framework for Risk Management and Civil Protection

The Civil Protection is the main body for emergency management in Italy. The Department of the Civil Protection of the cabinet is the operative body of the Prime Minister's Office (Presidente del Consiglio dei Ministri, in Italian), regarding the safeguarding of people and assets exposed to particular threats derived by natural or man-made disasters.

Since its origins, the Department of the Civil Protection has been in charge of managing the natural and technological risks. As described in Garcia (2011), after multiple changes in the Italian legal framework (Fig. 12.3), it was established that the Civil Protection is in charge, not only of the emergency management, but also the forecasting, prevention and recovery phases. Nowadays, the legislation establishes that it is fundamental to identify in advance the possible future damaging events, the possible affected zones and the activities which should be performed before, during and after the emergency.

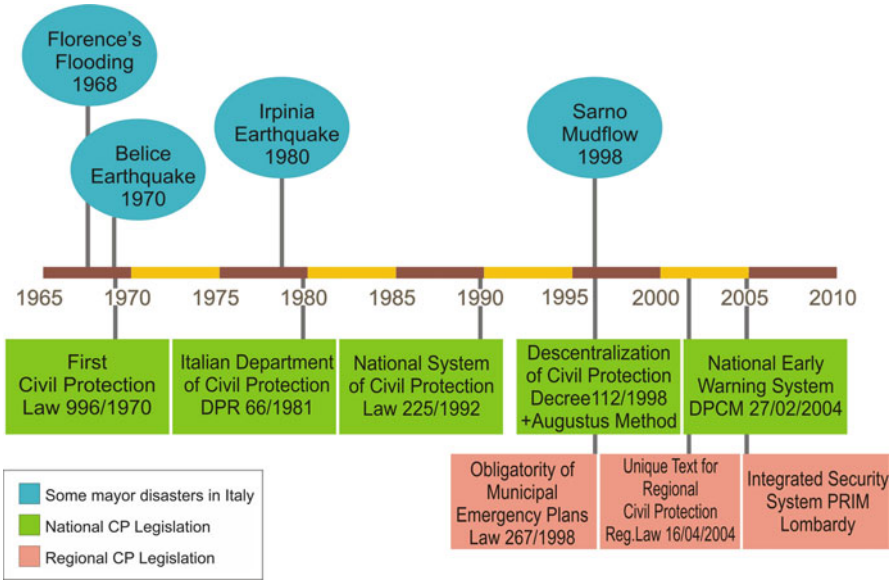

Fig. 12.3 Evolution of the civil protection legislation in Italy (Garcia 2011)

The origins of the Civil Protection in Italy can be traced back to more than 40 years with the creation of the first modern national civil protection law, the Law 996 of 1970. This law, known as the 'Norm about the rescue and assistance of the population affected by a calamity – Civil Protection', institutionalized some of the temporary measures adopted during these events and gave leading responsibility for disaster relief to the fire brigades and the Red Cross. The direction of the disaster management was assigned to a Commissar appointed by the government for every new event.

After the 1980 earthquake in Irpina, that left more than 2,700 people dead, a new civil protection legislation was established, the Decree of the President of the Italian Republic (D.P.R.) 66/1981. This decree gave the local responsibilities to the prefect and the local authorities, promoted the 'self-protection' based on civil protection education and also established a ministerial position for the general direction of major national disasters.

It was not until 1992 that the modern National Civil Protection was instituted with the Law n. 225/1992. This constituted the model for the rest of Europe, as it became the pattern mandated by an EU directive (Alexander 2002). The main innovations of the Law n. 225/1992 were, first, to establish that the Civil Protection System should not be constituted when an event occurs, but that it should be pre-existent to the event. Second, that the mayors are the main local Civil Protection authority, and therefore the primary responsible for disaster planning and management at the local level. And third, that it is necessary to give a high importance to the volunteer organizations.

The Italian Service of Civil Protection is a complex system that involves many different public, scientific/academic and private organizations. According to the Article 6, Law 225/1992, the components of the Italian Service of Civil Protection includes not only governmental bodies at different levels such as ministries, regions, provinces, prefectures, municipalities, mountain consortiums and public institutions, but also scientific research groups, and particularly important, the citizens and the volunteers groups.

In 1998, the Legislative Decree 112, 1998, known as the Bassanini Law No 59, set out the rules for decentralizing the Civil Protection in Italy. The law transferred some responsibilities from the national government to the regions, provinces mountain consortiums and municipalities. The municipalities acquired the whole competence of the Civil Protection at local level while the Regions were responsible for the employment of the volunteers and the Province for the elaboration of the Provincial Emergency Plans.

According to Alexander (2002), the real pillars on which Italian civil protection rests are the municipalities (comuni) and the voluntary organizations. As in many other countries, in Italy the local mayor is the final authority when a disaster strikes. Municipalities have been busy setting up emergency offices and developing plans, reaching, in some cases, high degrees of sophistication and prominence.

The Civil Protection works based on the principle of subsidiarity, which is the idea that a central authority should have a subsidiary function, performing only those tasks which cannot be performed effectively at a more immediate or local level.

At local scale, it was only with occurrence of several disastrous events, such as the landslide of Sarno and Quindicci of 1998, that the necessity of a stronger organization of the local authorities was evident. In this regard, the Law 267/1998 established the obligatory elaboration of a Municipal Emergency Plan in the municipalities with high risk zones (Regione Lombardia 2004).

Lombardy, the largest Italian region, embraces 11 Provinces and 1,546 municipalities and has more than 200 civil protection voluntary units. In 1998, Lombardy Region published the first 'Regional Program for Forecasting and Prevision for Civil Protection' – RPFP 1998 which included the identification and representation, in a general cartographic scale, of the principal risks presented in the region, including geohydrological, seismic, industrial, nuclear and fire risks.

Another important legislative instrument for civil protection of the Lombardy Region is the Regional Law 22nd of May 2004, n. 16, known as the 'Unique text about the regional dispositions in regard of Civil protection' (Testo unico delle disposizioni regionali in materia di Protezione Civile, TUPC, in Italian). This law, based on the principles of subsidiarity, suitability and differentiation, has as main objective to improve the emergency services provided to the citizens through a fluid and more efficient emergency management and to promote the return to 'normality' as fast as possible.

Taking into account the recommendations of the UN– Disaster Reduction meeting Kobe in 2005, Lombardy Region structured the PRIM based on the principles of: priority of action, meaning to select the major risks first; strong institutional base, in particular related to the institutions for risk prevention; need to identify,

evaluate and monitor risks, including appropriate forecasting and early warning systems; promote a culture of resilience; promote emergency preparedness, in both institutions and social networks; and finally, the construction of a global response network on prevention and protection, through the involvement, according to the respective competences, of the national government, the region, the local authorities and the end-user and citizens.

The integral risk vision of the PRIM 2007–2010, promoted the transition from a single risk approach to a multi-risk approach and the integration of informative and technological monitoring infrastructure.

12.4.2 Perception of Risk in the Mountain Consortium of Municipalities Valtellina of Tirano

As described in Garcia (2011), in order to evaluate the perception of mass movements and flooding risks in Valtellina of Tirano several aspects were considered including: (i) levels of worry or concern about natural hazards; (ii) perceived danger of different hazards; (iii) hazard of most concern; (iv) estimation of the likelihood of a set of risky events.

(i) The results of the levels of concern show a medium level of concern, with a mean of 2.46 (using a 5 points Likert scale from 1/not at all to 5/completely) at the beginning of the questionnaire and a mean of 2.70 at the end;

(ii) A list of eight different hazards was provided in order to rate how dangerous each hazard is considered using a Likert scale from 1/without consequences to 5/extremely dangerous. Three different mass movements were included in the list (landslide, debris flow and rock falls), and also were included snow avalanches, floods, forest fires, earthquakes, and 'others'. Results show that the hazards rated as most dangerous are forest fires (mean = 3.32), followed by landslides (mean = 3.00) and floods (mean = 2.97);

(iii) Results show that the hazards that concern the most are floods, followed closely by landslides, and then forest fires, earthquakes and snow avalanches;

(iv) The estimated likelihood of a hazardous event in the next year was low for both mass movement and flooding. Even lower was the perceptions of risk to personal and family safety which was clearly different to the perceptions of risk to property and to the whole population. The perceived risks to transport networks and critical lifelines were really similar and the highest of all parameters. This optimistically perceived risk for personal safety, property and other structural elements is consistent with the results of Perry and Lindell (2008). According to Perry and Lindell (2008) this results may reflect the fact that the individuals sense that the warning systems will allow them to escape personal harm, while the property and structures left behind are exposed to higher risks.

12.4.3 A Comparison of Risk Cultures Between Barcelonnette and Valtellina

The first element of difference between the Ubaye and the Valtellina valleys is the actor of reference. Although in both cases the mayor is responsible for risk management, the municipality works with local experts. This was further expressed through the answers of the population about risk governance actors. In every case, they showed more trust and deemed more qualities to these actors. The choice of these experts reveals different conceptions of risk governance. In the Ubaye Valley, the key actor when dealing with natural hazards is the local RTM service (Reforestation of Mountain Terrains). This body was first funded in the second half of the nineteenth century to re-establish and maintain state-owned forests in mountains. Their role shifted to technical experts, and they are nowadays dealing with protective works (dams, dykes) and risk prevention. In Valtellina, the reference actor is the Civil Protection. This corps, including volunteers, focuses on preparedness and response, providing expertise and help in crisis management. The traditional direction of risk related policies taken in France and in Italy are reflected in this observation: when in France actions are positioned in prevention and protection, in Italy they address preferentially preparedness and response.

A second element was revealed when asking the population about the risk related topics they are interested in. The major topics of concern were similar in both cases and revealed very practical concerns: evacuation procedures and emergency management. After these, the respondents in Valtellina were interested in individual mitigation measures, whereas respondents in Ubaye requested information about the risk zoning. In France, the risk zoning can be included in a legally binding land use plan. It is not the case in Italy. The difference observed in these choices can be seen as ‘an opposition of what people have to do and what people can do against natural hazards’ (Angignard 2011).

Third, the type of media solicited for information about natural hazards and risks was largely differing between the studied sites. In Ubaye, respondents asked for official information by involvement of local authorities (legally responsible for risk management). In Valtellina, mass media were solicited (television). These answers reveal differing expectation regarding the type of information. In Ubaye, directive information based on the local situation are expected, when in Valtellina it is more informative elements on a larger scale.

Moreover, the legal frameworks are in general different but share several aspect. In both cases the mayor is responsible for safety in his commune. In both France and Italy, important laws were emitted in reaction to major events. The Valtellina Law (Legge Valtellina) taken in 1990 after the events of 1987, or the Barnier Law (Loi Barnier) taken in 1995 after the floods of 1992 in south of France are good examples of this reactive legislations. Nevertheless the orientation of risk-related policies is different. In Italy the framework applied to natural hazards encompasses national and regional laws while in France laws are only emitted on the national level.

The actual orientations of these legal and administrative frameworks also differ. The French approach is mainly based on prevention and protection through land use regulation (e.g. risk prevention plans, PPR) and mitigation measures (e.g. dykes, landslide drainage, dam). In Italy the focus lays on alert and reaction, and recovery (for instance, the key actor of risk management is the civil protection).

The different risk cultures are also expressed via different conceptions of the role of insurance regarding natural hazards. In France the insurance of buildings and goods against natural hazards is compulsory and compensation comes from a fund managed by the State. In Italy natural events are not generally insured but private insurance is possible, however, in the case of a major event and declaration of 'natural calamity' the state usually allocates some money to the impacted people. This situation, however, leads in some occasions to an overestimation of the consequences of an event in order to receive more compensation from the state.

12.5 Conclusion

Risk cultures are an essential element of a risk setting. The influence they have on the social construction of risk is important, and they have to be taken into account when considering risk acceptance and deriving management options. It is crucial not to neglect them in risk governance and decision making, as cultural elements might hinder or facilitate the application and implementation of policies and measures. The comparison between the two cases of Valtellina and Barcelonette proved this key finding. Consequently, any risk assessment and management strategy must be designed tailor-made to the risk culture of the respective region. Moreover, the transferability of any 'best practice' from one country to another must take cultural aspects into consideration. Thus, any documentation of best practices for disaster risk assessment or management should contain sufficient information about the cultural context even through a particular best practice may be a pure technical solution. The political culture of the EU which is based on the subsidiarity principles is fully in line with these findings as it gives flexibility to the member states in regard to the way a particular EU directive has to be implemented into national law.

References

Alexander D (2002) The evolution of civil protection in modern Italy. In: Dickie J, Foot J, Snowden FM (eds) Disastro! disasters in Italy since 1860: culture, politics and society, 1st edn. Palgrave, New York

Angignard M (2011) Applying risk governance principles to natural hazards and risks in mountains. PhD dissertation, Dortmund University of Technology

Bird DK, Gisladottir G, Dominey-Howes D (2009) Resident perception of volcanic hazards and evacuation procedures. Nat Hazard Earth Syst 9:251–266

Fleischhauer M, Greiving S, Wanczura S (2006) Natural hazards and spatial planning in Europe. Dortmunder Vertrieb für Bau– und Planungsliteratur, Dortmund

Frattini P, Crosta G (2006) Valutazione dell'accettabilità del rischio da frana e analisi costi-benefici. Giornale di Geologia Applicata 4:49–56. doi:10.1474/GGA.2006-04.0-06.0134

Garcia (2011) Mountain risk management: integrated people centred early warning system as a risk reduction strategy, Northern Italy. PhD dissertation, Università degli Studi di Milano Bicocca

Glatron S (2003) Culture des risques. In: Moriniaux V (ed) Les risques. Éditions du temps, Nantes

WBGU – German Advisory Council on Global Change (1999) World in transition: strategies for managing global environmental risks. Annual report 1998. Springer

Haynes K, Barclay J, Pidgeon N (2008) Whose reality counts? factors affecting the perception of volcanic risk. J Volcanol Geoth Res 172:259–272

ISDR/Wold Bank (2008) Mitigating the adverse financial effects of natural hazards on the economies of South Eastern Europe, Geneva

Newman P, Thornley A (1996) Urban planning in Europe; international competition, national systems and planning projects. Routledge, London

Perry RW, Lindell MK (2008) Volcanic risk perception and adjustment in a multi-hazard environment. J Volcanol Geoth Res 172:170–178

Regione Lombardia (2004) La Pianificazione di emergenza in Lombardia. Guida ai piani di emergenza comunali e provinciali. I quaderni della Protezione Civile 7. Regione Lombardia, Milano

Slovic P (1987) Perception of risk. Science 236:280–285

Veyret Y, Meschinet de Richemond N (2003) Les risques naturels en Europe: la diversité des réponses. In: Veyret Y (ed) Les Risques. Sédes, Paris

Chapter 13
The Relevance of Early-Warning Systems and Evacuations Plans for Risk Management

Carolina Garcia, Simone Frigerio, Alexander Daehne, Alessandro Corsini, and Simone Sterlacchini

Abstract Early-Warning Systems (EWS) include the provision of timely and effective information, through identified institutions, that allows individuals exposed to hazard to take action in order to avoid or reduce risk and prepare for effective response. EWS are extensive frameworks that integrate different components of risk governance and disaster risk reduction policies with the main purpose of minimizing loss of life and reducing the economic and social impact of a threatening event on the physical assets and populations exposed to hazards. This section describes and analyzes different types of EWS with the aim to connect scientific advances in hazard and risk assessment with management (emergency preparedness and

C. Garcia
Department of Environmental and Territorial Sciences, University of Milano-Bicocca, Piazza della Scienza 1, IT-20126 Milan, Italy

Regional Independent Corporation of the Centre of Antioquia (CORANTIOQUIA), Cr 65 No.44A – 32, Medellin, Colombia

S. Frigerio
Italian National Research Council – Research Institute for Geo-Hydrological Protection (CNR – IRPI), C.so Stati Uniti 4, IT-35127 Padova, Italy

A. Daehne
Department of Earth Sciences, University of Modena and Reggio Emilia University, Largo Sant'Eufemia 19, IT-41100 Modena, Italy

Department of Geosciences, University of Missouri – Kansas City, 5110 Rockhill Road, Kansas City, MO 64110, USA

A. Corsini
Department of Earth Sciences, University of Modena and Reggio Emilia University, Largo Sant'Eufemia 19, IT-41100 Modena, Italy

S. Sterlacchini (✉)
Italian National Research Council, Institute for the Dynamic of Environmental Processes (CNR – IDPA), Piazza della Scienza 1, IT-20126 Milan, Italy
e-mail: simone.sterlacchini@idpa.cnr.it

T. van Asch et al. (eds.), *Mountain Risks: From Prediction to Management and Governance*, Advances in Natural and Technological Hazards Research 34,
DOI 10.1007/978-94-007-6769-0_13,

response) strategies and practical demands of stakeholders and end-users. Besides a structural approach, an Integrated People-Centred EWS (IEWS) is also presented. The system is mainly based on prevention as a key element for disaster risk reduction and aims not only to increase the level of awareness and preparedness of the community and decrease its vulnerability, but also to strengthen institutional collaboration, in particular at a local level, in order to assure sustainability of the efforts in the long term and to strength the risk governance process. In this way, the whole disaster cycle can be covered, trying to apply the most advanced technology available and also making the solutions easier to use by people not accustomed to manage these techniques in their daily tasks.

Abbreviations

DSS	Decision Support Systems
DEFRA	Department of Environment Food and Rural Affairs
DKKV	Deutsches Komitee Katastrophenvorsorge e.V.
DMTP	Disaster Management Training Programme
DREAD-ED	Disaster Readiness through Education
DRR	Disaster Risk Reduction
DEWS	Distant Early Warning System
EW	Early-Warning
EWC	Early-Warning Conference
EWS	Early-Warning Systems
EDURISK	Educational Itineraries for Risk Reduction
EPRS	Emergency Preparedness and Response Strategies
EC	European Commission
GPRS	General Packet Radio Service
GIS	Geographical Information Systems
GPS	Global Positioning System
GBInSAR	Ground Based Radar Systems for Movement Monitoring
ICT	Information and Communication Technology
IRASMOS	Integral Risk Management of Extremely Rapid Mass Movements
FLOODSite	Integrated Flood Risk Analysis and Management Methodologies
NEAREST	Integrated observations from near shore sources of Tsunamis
IEWS	Integrated People-Centred Early-Warning System
IRGC	International Risk Governance Council
IREALP	Istituto di Ricerca per l'Ecologia e l'Economia Applicate alle Aree Alpine
LEWIS	Landslide early-warning integrated system
SAFELAND	Living with Landslides Risk in Europe
PPR	Plan de Prévention des Risques
PPEW	Platform for the Promotion of Early Warning
RINAMED	Rischi Naturali nel tratto Mediterraneo Occidentale

RISKRED	Risk Reduction Education for Disaster
SAFER	Seismic Early Warning for Europe
SLEWS	Sensor based Landslide Early Warning System
SMS	Short Message Service
SAR	Synthetic Aperture Radar
TLS	Terrestrial Laser Scanning
TETRA	TErrestrial Trunked RAdio
TRANSFER	Tsunami Risk and Strategies For the European Region
UN/EP	United Nations/Environment Programme
UN/ISDR	United Nations/International Strategy for Disaster Reduction
WMO	World Meteorological Organization

13.1 Introduction

Early Warning (EW) is defined as 'the provision of timely and effective information, through identified institutions, that allows individuals exposed to hazard to take action to avoid or reduce their risk and prepare for effective response' (UN/ISDR 2006). Early Warning Systems (EWS) include not only the warning itself but are extensive frameworks that integrate different components of risk governance and disaster risk reduction (Basher 2006). These components interact long before the crisis may start with the main purpose of minimizing loss of life and reducing the economic and social impact of an event on the physical assets and population exposed to hazards. The International Strategy for Disaster Reduction (UN/ISDR – PPEW 2005) has implemented a permanent platform for the promotion of Early Warning (http://www.unisdr.org/ppew/ppew-index.htm) whose efficacy is defined by four interlinked components (Basher 2006): (1) prior knowledge of the risks, (2) technical monitoring and warning service, (3) dissemination and communication of understandable warnings and (4) knowledge and preparedness to act (response capabilities).

EWS face various challenges associated to the difficulties and problems to integrate multiple components. Regarding the decision-making on EWS, the uncertainties inherent to any predictive process may lead to wrong decisions, even in highly-developed EWS and with well-prepared personnel. Wrong decisions can either lead to missed alarms when the mitigation action is not taken when it should have been; or false alarms when the mitigation action is taken when it should not have been (Grasso et al. 2007). For this reason, the levels of uncertainty of the information must always be communicated to the users, together with the EW, since the lack of clear and honest information can confuse people and undermine their confidence in government (Grasso 2007). Furthermore, it is fundamental that local governments, local institutions and communities are constantly involved in the entire policy-making process of the risk governance and during the elaboration of the EWS in order to increase the awareness and preparedness levels. This involvement implies to decentralize the decision-making process enhancing responsibilities of local governments and communities (EWC-II 2003).

For being effective and assuring a timely warning, EWS must be integrated into policies for disaster mitigation and risk governance. At the same time, governance priorities must include protecting the public from disasters through the implementation of disaster risk reduction policies which are only completed if EWS and the other non-structural countermeasures are included. On this regard, WMO (2010) and EWC-II (2003) propose some key elements for integrating EWS into disaster risk governance policies including:

- strong political commitment from the government, supported by Disaster Risk Reduction (DRR) plans and clear legislation, that allows to strengthen the legal frameworks;
- coordination among national services for sharing information and dissemination of warnings that take exposure and vulnerability of the elements at risk into account;
- promotion of communication and dissemination systems, that ensures warnings are received at all community levels, through clear protocols and procedures regularly tested, evaluated and maintained;
- emergency preparedness, including education to appropriately use of weather-, water- and climate-related information and early warnings;
- implementation of local to national emergency response plans with clear and regularly updated procedures practiced through simulation exercises;
- assignment of clear roles and responsibilities for all organizations and stakeholders at different territorial levels in order to improve efficiency, credibility, trust and cost-effectiveness of the risk management procedure;
- elaboration of feedback mechanisms between national to local governments, national services and the community, to facilitate evaluation and improvement of the warning system;
- in-depth collaboration, by developing institutional networks and participatory strategic plans with multi-disciplinary research and multi-stakeholder participation, and;
- promoting the availability of economic and human resources in order to establish proper priorities to allow their secure allocation.

As pointed out by Chang Seng (2010), the most appropriate governance on EWS is to encourage: (1) a multi-hazard approach; (2) enhanced bilateral and multilateral cooperation among the stakeholders, (3) innovative partnerships, (4) capacity building, (4) sharing and exchange of local experiences and (5) scientific knowledge.

In this section, different types of EWS (structural and non-structural) and emergency preparedness and response strategies developed in Europe are described and analyzed. Then, an Integrated People-Centred EWS (IEWS) is proposed with the aim to increase the level of awareness and preparedness of the community at risk and to decrease its vulnerability, to strengthen institutional collaboration and to assure sustainability of the efforts in the long term. All these topics are expected to contribute to improve risk governance and disaster risk reduction policies and strategies on the base of the practical demands of stakeholders and end-users.

13.2 Status of EWS for Natural Hazards in Europe

The European Commission (EC) has identified in several documents on risk management the need for adaptation as a consequence to climate and environmental changes (EC 2009). Integrated approaches are needed for connecting scientific advances in hazard and risk assessment with management strategies and practical demands of stakeholders and end-users. In many cases, the scientific outcomes remain rooted solely within the scientific community (IRGC 2005). This is mainly due to the complexity of human-environment interactions which are often too complex to be properly recognized, represented, and modelled. This fact generates that the approaches developed by the scientific community are often not easy to be implemented by the stakeholders/end-users community.

Nowadays, in the context of the EU Environmental Assessment Directive in risk prone areas, it is well recognized that shared knowledge is the key element to get to a harmonised decision-making tool structure for hazard and risk management. In this way, the whole disaster cycle can be covered, not only applying the most advanced technology available but also making the solutions easier to use by people not accustomed to manage Decision Support Systems (DSS) and Geographical Information Systems (GIS) techniques in their daily tasks (Muntz et al. 2003). Through the dissemination of knowledge, by specific public education programs, all people who may be threatened by a disaster may learn in advance what to expect and how to react. This will lead citizens to improve their awareness, develop their preparedness and response capabilities, strengthen institutional collaboration and, in so doing, protect themselves more efficiently.

Western European countries have a long experience in dealing with natural hazards and scientists of these countries present a strong understanding of the natural phenomenon. However, there is still a strong tendency to focus most of the efforts in risk assessment and structural mitigation, usually leaving preparedness and prevention widely neglected. There are obviously marked differences among all the Western European countries but there are also strong similarities on the socio-economic and political conditions that constitute the base for this generalization.

For example, in Germany, the Committee for Disaster Reduction (DKKV 2007) acknowledged the critical importance of preparedness as a fundamental element for DRR. DKKV also affirms that if a participatory approach is used, involving responsible bodies and population in all phases of disaster reduction, the likelihood of achieving DRR is greatly improved. Even if this approach is applied in most of the DRR initiatives funded by Germany in developing countries, the application of this strategy in the German territory is generally neglected. A survey on risk perception was developed by Plapp and Werner (2006) in zones affected by flooding and earthquakes in the south of Germany. The survey showed that the population perceived lack of possibilities to protect themselves from a hazard or to create shelter against it, lack of possibilities to prepare for the hazard, and lack of precise, timely or reliable predictions and warnings. Furthermore, responses indicate that research on natural hazards is rather unknown, not noticed or even not memorized

by the public. Despite of considering that one of the main causes of the disasters are inappropriate land use planning, the public assumes that there are too little possibilities to prepare and to response to a hazard event. The previous results show the low perceived self-efficacy and strong lack of preparedness in the population, probing the necessity to develop risk communication strategies that emphasize preparedness and offer information about possible self-preventive measures.

In Iceland, the study of Bird et al. (2009) about an evacuation exercise for volcanic crisis, describes an example of how a population can still have low levels of risk perception regardless of being aware of the multiple hazards they face. This, together with a failure from the emergency personnel in providing adequate information about preparedness and evacuation procedures, generates a low response capability, leading to the failure of the whole warning system.

Italy is one of the most multi-hazard prone countries in Europe. It is characterized by a marked heterogeneity among the regions, both physiographically and culturally, that explains why each region has its own risk management legal framework. In the whole country, the National Civil Protection authorities are the ones in charge of monitoring and managing the largest emergencies in magnitude and consequences, while the development of the local contingency plans is competence of each municipality. The National Law 225/1992 specifically establish the responsibility of the mayors to elaborate the local evacuation plan of the municipality, to manage the emergency and to educate and to keep the citizens informed in order to prepare them for possible crisis. In spite of that, the preparation activities organized by municipalities are present in just few regions and most of the actual educational activities are still isolated efforts (such as EDURISK) of some academic institutions (as the National Civil Protection and the National Institute of Geology and Vulcanology – INGV) to increase awareness and preparedness in case of large future events. Some Italian regions have completely acknowledged the main principles of the National Law 225/1992, tailoring them to their own requirements (for example, the Regional Decrees 'Direttiva Regionale per la Pianificazione di Emergenza degli Enti Locali' and 'Direttiva Regionale per la gestione organizzativa e funzionale del sistema di allerta per i rischi naturali al fine di Protezione Civile' – Regione Lombardia 2007, 2009) while some others did it only partially or not at all.

The location of most of the Netherlands territory below sea level makes it highly susceptible to flooding. For this reason, the Netherlands have develop a flood defence system with the highest safety standards worldwide (Van de Ven 2004). As pointed by Ten Brinke et al. (2008), the result is that Dutch society has come to rely on this defence system to the extent that other possible measures for flood risk management, in terms of spatial planning (pro-action) or contingency planning (preparation, response, recovery) have received little attention. The same authors affirm that 'the population and economic growth in the area protected by mainly preventive measures have increased the country's vulnerability to the extent that a flood would result in massive economic and social disruption'. For the previous reason, it is necessary to invest more on response and recovery in order to broaden the historical flood defence strategy into a true risk policy by taking stronger account of the consequences of possible flooding (Ten Brinke et al. 2008).

United Kingdom (UK) is a model for the evolution to a more participatory and people-centred approach related to risk flood management. This includes the establishment of: (1) resilience forums, in the context of the legal emergency preparedness framework denominated Civil Contingencies Act (UK Cabinet Office 2004), (2) programs for education at schools such as the 'Japan-UK Disaster Risk Reduction Study Programme', (3) flood emergency plans, that take into account the needs of the communities and, (4) education campaigns, to promote self-help and preparedness among the vulnerable residents (DEFRA 2009). Furthermore, the legislation in force since April 2009 imposes a new statutory duty on local authorities 'to inform, consult and involve citizens and communities in the design, delivery and assessment of services' (Filey Flood Working Group 2009). This statute highlights the responsibilities of people to protect themselves and their properties (Ten Brinke et al. 2008). These efforts are mainly focused on flooding while preparation toward other hazards is not so strongly attended. Additionally, it is important to mention that prevention, related to structural works, is generally weak in UK (Ten Brinke et al. 2008).

In France, the municipalities at risk, marked out by the prefect of the 'Département', have to elaborate risk prevention plans (Plans de Prévention des Risques – PPR). The French PPR are often cited as an example of efficient use of spatial planning in risk prevention. They are regulatory hazard-zoning documents that delimit certain hazard zones with restrictions for construction and further development (Fleischhauer 2006). The PPR contain a presentation of the risk setting (it can be single or multi-hazard oriented), maps presenting historical events, existing hazards, stakes and assets, and finally risk zoning maps. The maps portray three types of zones: red (high risk, no further construction allowed and in some cases expropriation can be considered), blue (medium risk, construction allowed under some restrictions, e.g. compliance to codes) and white (low or no risk, no restriction). These documents are not risk maps per se, as they also include the current and planned use of parcels. For example, there can be 'white zones' prone to hazards (e.g. cultivated areas in flood plains). In the French legal framework, the insurance of buildings and goods against natural hazards is compulsory and compensation comes from a fund managed by the State.

Although there is still a general lack of participatory activities and involvement of the community in the EWS in Western Europe, several countries have developed many interactive educational tools of excellent quality, mostly targeted to the school population (Becker et al. 2009). These products have been produced in part by European projects, such as RINAMED (2002–2004), EDURISK (since 2002), OIKOS (since 2007), RiskRED (since 2006), FloodSite (2004–2009), DREAD-ED (2008–2010), Be-Safe-Net (since 2007), among many others. It appears, however, that today there is a lack of strategies to disseminate these products and broadly educate the population.

There is also still a general lack of efforts from the scientific community and researchers to divulgate their studies and results using dissemination media accessible for the public and a simple language that allows the understanding of the message by all the general community. Recent scientific projects funded by the

European Union on EWS do not seem to call for any involvement of the exposed population: SLEWS (2007–2010), SAFER (2006–2009), DEWS (2007–2010), LEWIS (2002–2005); NEAREST (2006–2010). For the risk reduction projects, there are some notable exceptions such as: TRANSFER (2006–2009) which includes, among its objectives, programs to enhance local community awareness and preparedness against the tsunami and marine hazards, as well as other types of hazards, and guidelines for community participation and emergency plans; SAFELAND (2009–2012) which couples a foreseen participation of policy-makers, public administrators, researchers, scientists, educators and other stakeholders with an improved harmonised framework and methodology for the assessment and quantification of landslide risk at a local, regional and European scales but not the public. As pointed by IRASMOS (2005–2008), in several European countries the most important threat regarding natural hazards is the poor knowledge of the people about natural hazards and their missing competence to live with risks. This may lead to a non-adequate behaviour in case of an emergency or to problems in the implementation process of countermeasures and of land-use planning. It is, therefore, fundamental to improve the efforts in preparedness, communication and education initiatives, including elements such as EWS and emergency plans.

13.3 Recommendations for the Setup of Structural EWS

13.3.1 Risk Knowledge Constraints

Risk assessment provides essential information to set priorities for mitigation and prevention strategies and designing EWS. In particular, as indicated by UN/EP (2010) and Kollarits et al. (2010), the distinction between stepwise-onset hazards (also defined as slow-onset or 'creeping' hazards) and sudden-onset hazards (also defined as rapid-onset hazards) is relevant.

Any process that is developing in a time span shorter than the intervention time required must be considered to be 'sudden' from the point of view of EWS. According to Kollarits et al. (2010), stepwise-onset hazards are those whose effects take a long time to produce emergency conditions (such as large river floodings). This natural hazard type is characterized by the fact that: on the one hand, historic data and forecasting information (from gauges, meteorological network and established threshold values) are typically available allowing longer forewarning times and well established warning and alert stages in the hazard management cycle and, on the other hand, the evolution of the scenario/event follows a regular sequence of processes which are usually quite well-known on the basis of the historic knowledge of similar events and that can be foreseen and predicted based on validated models and real-time monitoring data. On the contrary, sudden-onset hazards are characterized by a highly dynamic/composite evolution of

event scenario and by a limited reaction time. In particular, small catchments in mountain areas are very frequently affected by rapidly evolving events. Extreme meteorological conditions, causing torrential rains within a very short time span in a local watershed, can trigger different processes such as landslides, rockslides, rockfalls, debris flows and torrential flash-floods leading to complex multi-hazard scenarios. According to Kollarits et al. (2010), rapid/sudden-onset and slow-onset events can provide different amounts of warning time. Even in the case of existing forewarning systems installed, the warning time is very short in case of rapid-onset hazards. When time allows, after an attention/alert phase, a pre-alarm or a very short alarm phase follows immediately before the impact.

13.3.2 Technical Constraints

Especially for rapid/sudden onset events, the provision of timely and effective information can be most often fulfilled by using structural monitoring systems whose selection should start from a clear statement on (Corsini 2008):

- 'why' the monitoring has to be carried out (e.g. what is the purpose of monitoring);
- 'when' the monitoring has to be performed (e.g. the period of interest for data);
- 'what' has to be monitored (e.g. the object and the observational parameters to monitor);
- 'where' the monitoring must be performed (e.g. the choice of the specific environmental site conditions).

As regards the questions 'why' and 'when' and given the assumptions that, at the occurrence of a damaging event no previous monitoring data are available, the following direct relationships between 'risk management phase' and 'period of interest' exist:

- a response period, defined as the period generally limited to the 1–3 weeks that are needed to control the development of the event and to keep updated the on-going event scenarios;
- a recovery period, defined as the period generally lasting 1–3 months and needed to control the residual development of the event;
- a prevention period, defined as the period generally lasting 1–3 years or even 3–10 years and corresponding to the time needed to analyse the cause-effect relationships, define future possible event scenarios, and put in action the risk prevention strategies;
- a preparedness period, defined as the period generally lasting in the order of 1–10 years or more, and that is the time needed to make cost-effective the set-up and the maintenance of an EWS.

The definition of 'why' and 'when' monitoring must be carried out can lead to the exclusion of specific monitoring systems on the basis of practical constraining factors. The following typical situations, linked to 'what' and 'where' monitoring must be carried out, can be considered:

- accessibility of the site: if, in the period of interest, the site is for any reason inaccessible, then all of the in-place sensing systems are to be excluded and remote sensing is thus the only possible option;
- visibility of the site from a panoramic stable ground position: if, in the period of interest, the site is not visible from a panoramic point, due to topography of the area or vegetation coverage, then all of the terrestrial remote sensing systems are to be excluded;
- visibility of the site from aerial position: if, in the period of interest, due to topography of the area or vegetation coverage, the site is not visible from air, then aerial or satellite remote sensing systems are generally to be excluded;
- value of expected movements: if, in the period of interest, the factor exceeds the range of movement that a given system can cope with/without damage, then that system is to be excluded. This is crucial for systems placed into boreholes, such as inclinometers or piezometers.

Once accounted for such factors, the selection for a specific monitoring system goes forth to the specific characteristics of the systems (range, resolution, installation and maintenance effort, possibility to transfer and process data in real-time or near real-time, etc.). For instance, the effort needed for installing a system, the possibility to reach the location with the needed equipment and the feasibility that in the period of interest the system could operate with the required data acquisition and availability configuration, are certainly to be considered. Besides technical factors, available budget and system costs are important constraints controlling the definitive choice of the structural monitoring system.

The specific technical factors that must be considered for implementing an EWS are:

- data acquisition frequency: in-situ sensors are appropriate for continuous and discontinuous monitoring, while only a few well-tested remote sensing systems (such as, for instance, total stations) are appropriate. In other cases such as, for example, GBInSAR (Ground Based Radar Systems for Movement Monitoring) or TLS (Terrestrial Laser Scanning), continuous data acquisition is still to be considered somehow experimental, even if it is quite likely that it will become routine in a few years from now;
- data availability timing: in-situ sensors are appropriate for near real-time and real-time monitoring, while only a few well-tested remote sensing systems (such as, for instance, total stations) are appropriate. In other cases (such as, for example, TLS), their near real-time usage is rapidly becoming an available option;
- data spatial extent: in-situ sensors provide spatially localised data, while remote sensing systems provide spatially distributed data or, alternatively, multi-point data;

– long term stability and probability of malfunctioning: IREALP (2005) suggested a classification of systems based on four instrument classes with decreasing level of stability and increasing probability of malfunctioning;
– operative conditions: IREALP (2005) suggested a classification based on the duration of monitoring and the accessibility of the instruments after installation and divided instruments in four classes (class 1.0 – long period-non accessible, class 1.1 – long period-accessible, class 2.0 – short period-non accessible, class 2.1 – short period-accessible).

Another key technical issue in EWS is the reliability of data transmission procedures and infrastructure, as monitoring networks designed for EWS deliver data timely and certainly. Therefore, EWS must adopt redundant data transmission systems so to ensure against possible failures. Commonly used data transmission platforms are Radio (e.g. TErrestrial Trunked RAdio – TETRA – that is a digital trunked mobile radio standard used in Civil Protection), General Packet Radio Service (GPRS), Satellite Internet access, W-Lan. Each of these systems has pro and cons related to data band-width, reliability in hostile meteorological conditions and likelihood of blacking out during the emergency situation and so on. The preference for one communication protocol rather than another must be based on a clear layout, on the system design phase and on the operative constraints.

Finally, EWS on a technical level are not all about sensors and data transmission, but are also about data storage and management and real-time data analysis. Data warehousing, via public or commercial facilities, is increasingly used to manage large databases that must be accessed and queried by several clients. This operative procedure will soon take a role on EWS, as more sensors will be deployed and more data will have to be shared. As regards real-time data analysis, it is common standard that the data management software can perform customised data download duties, pre-processing, and graphitising. Essential for EWS is the possibility to define attention, alert and alarm thresholds, based on a specific set or subset of parameters, by using logic, mathematic, statistic and even more complex rules for combination.

13.4 Recommendations for the Setup of Non-structural Integrated People-Centred EWS (IEWS): Examples of the Consortium of Mountain Municipalities of Valtellina di Tirano (Italy) and of the Barcelonnette Basin (France)

A methodology to integrate EWS and emergency plans into a local disaster plan has been elaborated in the Consortium of Mountain Municipalities of Valtellina di Tirano (Central Alps, Northern Italy). Taking into account the actual state of disaster management and risk reduction initiatives in the study area, it was decided that the methodology that fits best with the present conditions would be a non-structural

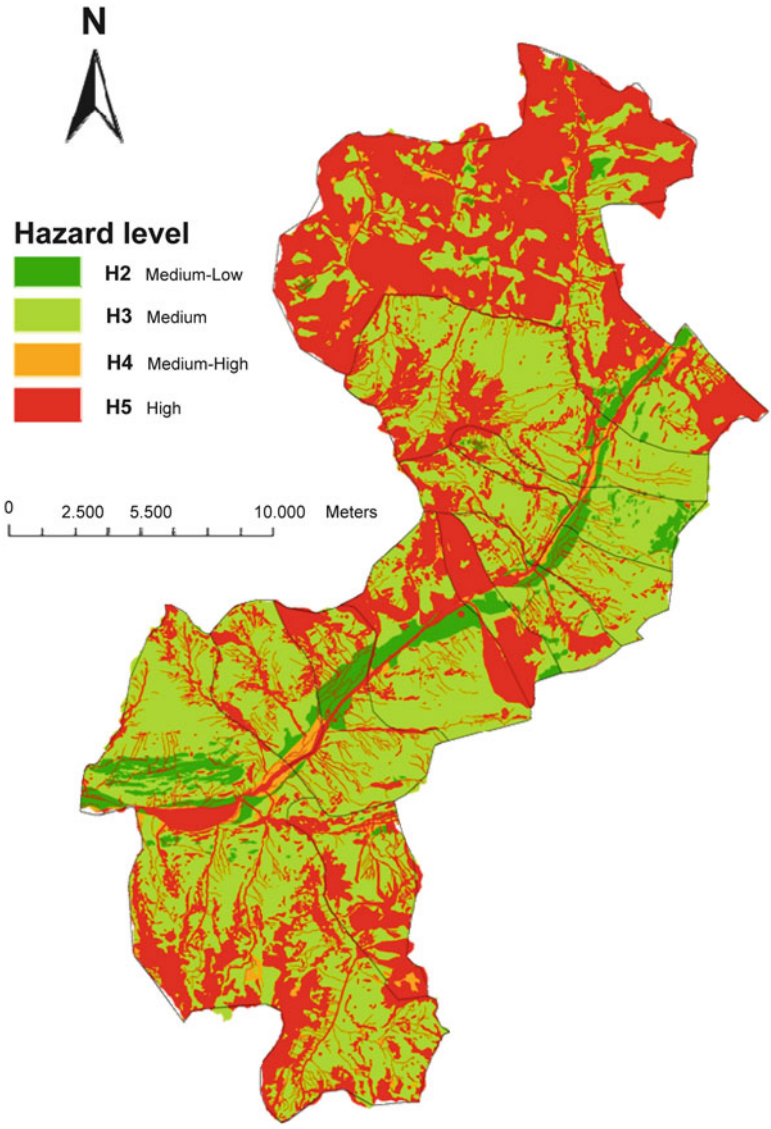

Fig. 13.1 Hazard map of the Consortium of Mountain Municipalities of Valtellina di Tirano (Comunità Montana Valtellina di Tirano). The area spreads over 450 km^2 in the Italian Central Alps (Lombardy Region, Northern Italy) with approximately 29,000 inhabitants. In the detailed box, it is possible to appreciate different hazard levels delimitated by municipal boundaries (Garcia 2011)

approach such as an Integrated People-Centred Early Warning System – IEWS (Garcia 2011). The methodology (Fig. 13.1) focuses on prevention as a key element for disaster risk reduction and aims not only to increase the level of awareness and preparedness of the community and decrease its vulnerability, but also to

strengthen institutional collaboration, in particular at local level, in order to assure sustainability of the efforts in the long term and to strength the risk governance process (Garcia et al. 2010; Garcia 2012).

13.4.1 Characterization of Risk Knowledge

The current regulatory maps for hazard and risk and the risk management present several constraints, some of which related to the fact that there are no legal standardized procedures to produce hazard, risk and vulnerability maps with a sound scientific basis. The current risk maps are derived from spatial planning maps, and the criteria used to produce the maps may differ among municipalities. As result, in the current regional risk map, the risk levels differ among municipalities even in geologically homogeneous areas (Fig. 13.2). The suggested risk assessment should be holistic and integrated and not hazard focused as nowadays. An integrated vulnerability analysis that involves economic, physical and social aspects should be developed. The results of the vulnerability analysis need to be integrated with accurate hazard maps in order to obtain a more reliable risk zoning. The risk maps, instead of being a secondary product of the spatial planning maps (as they currently are), should be used to improve them.

It is essential to put research into practice by disseminating scientific results among decision-makers and local technicians, using a simple and understandable language. The experience in the study area with the emergency response tool shows the importance of performing follow-up activities once the scientific products are handed out to local authorities. Otherwise, the utility of what in principle could be an excellent scientific tool will be reduced due to the lack of continuity on its maintenance, constant updating or underestimation of its full potential. It is fundamental to share responsibilities among different actors in order to improve the current situation, and scientists must team work with local authorities for updating the emergency response tool and communicate it to the population.

13.4.2 Recommendation for Process Monitoring and Warning

Taking into account the extension of the study area and the extreme variability in its morpho-climatic conditions, it seems that the current number of meteorological stations installed in the study zone is not enough to correctly define and analyze the different microclimates presented. Unfortunately, the high cost entailed to increase the amount of stations installed makes it highly difficult. An economic, even if not simple alternative to improve the forecasting and monitoring, would be to create a network of low cost rain gauges monitored by inhabitants of the area that should also be prepared to recognize local changes in the dynamic of the territory. The network

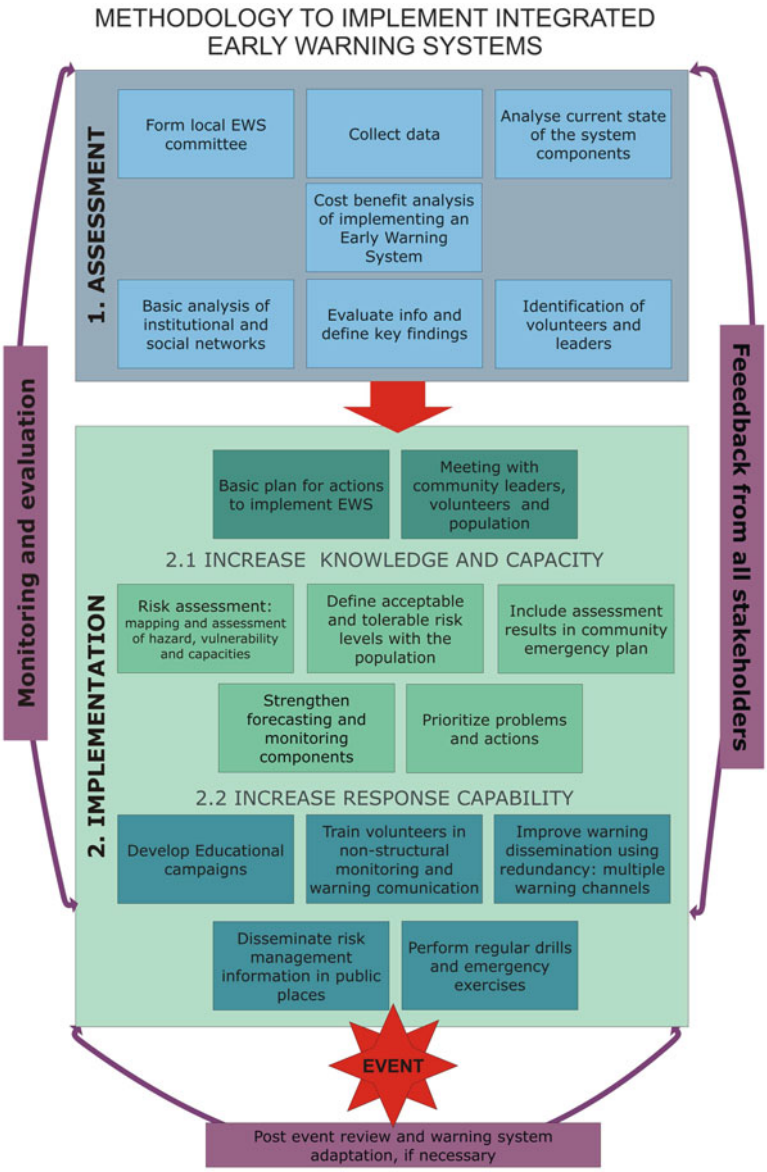

Fig. 13.2 An Integrated Early Warning System (IEWS) (Garcia 2011)

should be coordinated by local authorities and Civil Protection and should be in constant communication with local/regional authorities and scientific bodies.

13.4.3 Recommendation for Risk Knowledge Communication

A survey applied to the population in the study area (Garcia 2011) indicated, among others, to evaluate the preferences of the people regarding the warning communication and dissemination. The survey assessed the practicability and efficiency of the warning methods used until the present, as well as the levels of trust of the population towards the different authorities providing the warning (Garcia 2011). Results show medium levels of trust towards the local authorities who, at the same time, are perceived to be moderately prepared. The preferred media to issue the warning is mainly an acoustic signal followed by television reporting.

In order to improve the communication and dissemination element, it is fundamental to involve the people at risk during the whole process, before and during the emergencies, with constant and widely available briefings. Additionally, in order to assure that the message arrives to the whole population, it is important to use multiple warning methods, including long-range acoustic signals. The message should be disseminated by an institution respected and trusted by the population at risk. Finally, the methods for communication and dissemination should be locally adapted, taking into account not only the technical and legal constraints, but also the preferences of the population expressed on the survey.

13.4.4 Preparedness and Response Capability

On regard to the preparedness and response capability of the population, the survey showed that nearly 90 % of the population knows about the existence of large events in the past. In spite of that, at the present time, the population presents:

- low levels of preparedness and perceived risk;
- lack of general knowledge related to natural hazards and emergency management, and;
- a high transfer of responsibility on risk reduction from the population to the authorities (Garcia 2011).

These combined results indicate that it is fundamental to perform activities to increase preparedness and to improve the response capability of the population exposed to hazards. Therefore, small scale communication and education campaigns have been developed in some schools of the study area in collaboration with several local/regional/national institutions such as the Mountain Consortium authorities, IREALP (www.irealp.it/) and Legambiente (www.legambiente.it/). Considering the answers of the survey and using the scientific products,

an educational and communication campaign with participative workshops was designed by an interdisciplinary group to cover the specific information needs of the population. The education strategies were addressed to the local community and practitioner stakeholders, with the aim to increase the awareness and preparedness for future events. However, these activities are not enough; it is necessary to divulgate the emergency plans (available in each municipality encompassed within the Consortium) among the whole local population and to perform regular large scale campaigns, developed by local authorities with the collaboration of scientific and local institutions.

Recently, the European Commission stressed the importance of co-operation in disaster relief operations by pooling the resources, improving the response techniques and enhancing public awareness. Consequently, the necessity to combine Geographical Information Systems (GIS) and Decision Support System (DSS) became a critical task in EW and emergency management (Chieh et al. 2007; Lazzari and Salvaneschi 1999; Junkhiaw et al. 2004). MacEachren et al. (2005) underlined the necessity of a mutual and dialogue-based frame for data sharing as key factor before and during a crisis phase. The idea of simple, intuitive and easy-to-use instruments deals with their intensive use in the field of Civil Protection for managing and overtaking a crisis phase (Muntz et al. 2003). Additionally, Armstrong and Densham (2008) suggested the importance of multi-participant seminars, public dissemination programmes and workshops to improve citizens' awareness and general knowledge on disasters issues.

User-friendly and visual-based strategies to support the emergency requirements were designed and applied in order to minimize the adverse effects of a harmful event in the study area through effective precautionary, rehabilitation and recovery actions to ensure a timely, appropriate and effective organization and delivery of relief and assistance following a disaster (DMTP 1994).

The co-operation among researchers and local stakeholders has led to the development of contingency plans, drawn up according to the national and regional laws in force, to quickly respond to an emergency applying the most advanced technology available and also making the solutions easier to use by people not accustomed to managing these techniques in their daily tasks. Therefore, the key-action was to integrate the main mapping and analysis tools of GIS with workflow management modules (DSS) and communication tools and positioning devices (ICT) to share information during the emergency and to control the location of squads operating on the field (Fig. 13.3).

These plans are based on a clear sequence of actions to be put in practice before and in the aftermath of a critical event in order to: (1) define in advance a straightforward flow of actions in case an event occurs; (2) identify people in charge to perform each action; (3) prepare them to take actions; (4) keep them aware of resources really available to overcome the crisis phase (Sterlacchini and Frigerio submitted; Frigerio et al. 2011).

As stated before, the mayor of each municipality is responsible for emergency management. Anyway, the Consortium of Mountain Municipalities (acting as a local government entity) has the authority to prepare the Civil Protection plans for

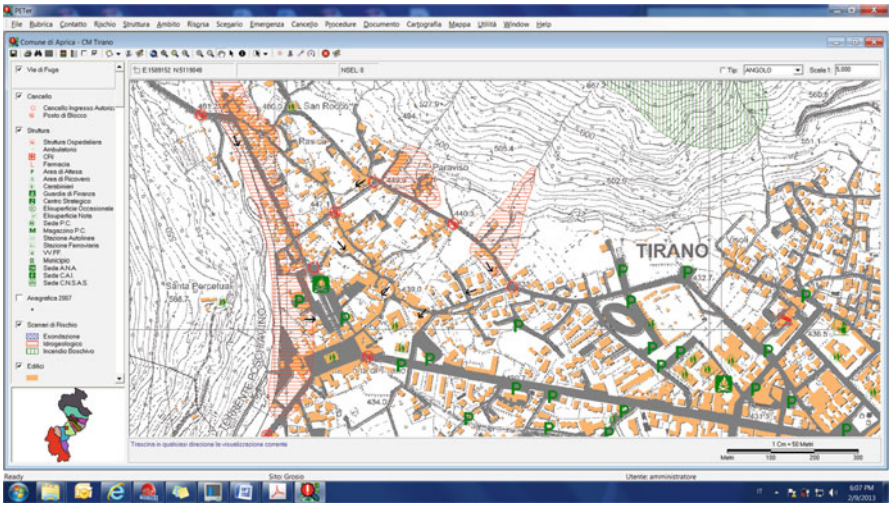

Fig. 13.3 Front view of the tool used for designing preparedness and response activities, represented as a classical GIS template where mapping and analysis tools are available

all the twelve municipalities encompassed within the Consortium (sometimes not properly self-sufficient for budget, resources and structures), although each mayor is the person in charge to manage the emergency and take actions during a crisis phase within his/her own municipality.

In the study area, data were derived from official available databases and on-site surveys (Frigerio et al. 2010), including information on hydrogeological hazard scenarios derived from statistic and/or deterministic analysis, urban spatial planning maps, data from Registry Office concerning the population, historical data on past landslides and floodings, historical data concerning damage and casualties due to past events, repair and reconstruction costs, structural and functional details of buildings and infrastructure and environmental consequences.

More precisely, the system provides tools to cope with emergency preparedness and response activities, taking advantage of data processing capabilities by GIS, workflow management modules by DSS and communication and positioning systems by ICT (Sterlacchini and Frigerio submitted). The system provides solutions to:

– design and manage Civil Protection plans by a GIS and DSS-based architecture to store and analyze spatial and tabular data and manage a step-by-step list of instructions (Fig. 13.4). Emergency managers can handle the features involved, compulsory documents, relations among 'objects' (e.g. facilities, equipments, etc.) and their 'users' (e.g. holders, managers, etc.), workflows. Many documents (e.g. evacuation, occupancy of public area, etc.) are standardized but can also be customized on-demand and every object may be printed out to pose solutions for crisis requirements (e.g. manuals or personnel badges). Therefore, the managers

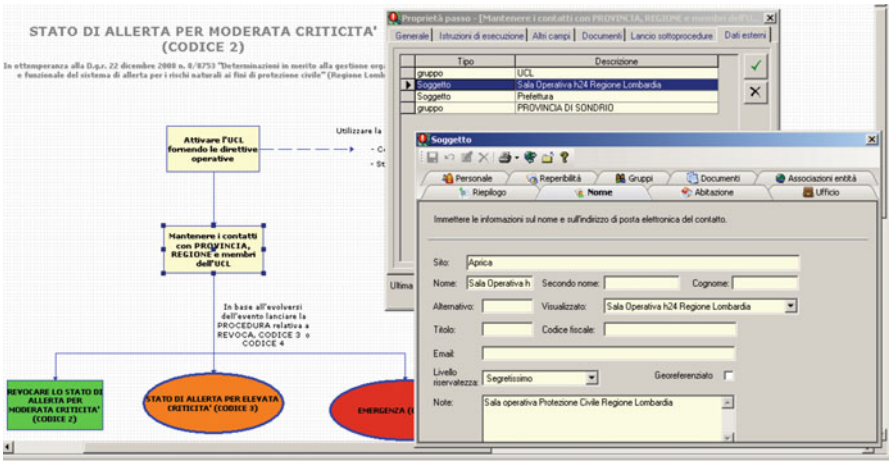

Fig. 13.4 Workflow and graphical charts. The 'Step Property' ('Proprietà Passo' in Italian) related to the action 'Keep the contact with Region, Province and Local Crisis Unit personnel' (workflow in background) includes a list of people in charge to take actions. Each person ('Soggetto') is thoroughly described in a different window (in foreground)

are 'guided' in many activities by a graphical workflow able to suggest them the actions to be sequentially executed and related instructions of execution as well as the identification of people in charge to take actions, the list of documents to be issued during or after each phase of the emergency, the utilization of resources really available to overcome each phase of the emergency. The workflows are designed during peace-time and tested in training exercises. Consequently, uncertainty and hesitation can be reduced, improving the crisis response and coherence of each action.

– transfer knowledge by a web-service module (Fig. 13.5), to allow data access and sharing with different levels of permission. Every emergency plan has been uploaded on Civil Protection Central Office server of the Consortium and periodically updated. The Central Office has read/write permissions on all emergency plans stored, while each municipality has read/write permissions only on its own plan. All the people involved in Civil Protection actions can access both GIS and DSS modules and some training courses and education campaigns on natural risks affecting the territory have been provided by this module.
– sharing information during the emergency by a communication module. This module allows the transfer of information and procedures providing tools to dial phone numbers, posting reports, receive GPS signal, sending SMS and email (Fig. 13.6).

The system is already running in the Consortium of Mountain Municipalities of Valtellina di Tirano, and in advanced stage of development in the Barcelonnette basin. In the French study site, it was fundamental the collaboration among CNR (National research Council of Italy), CNRS (Centre National de la Recherche

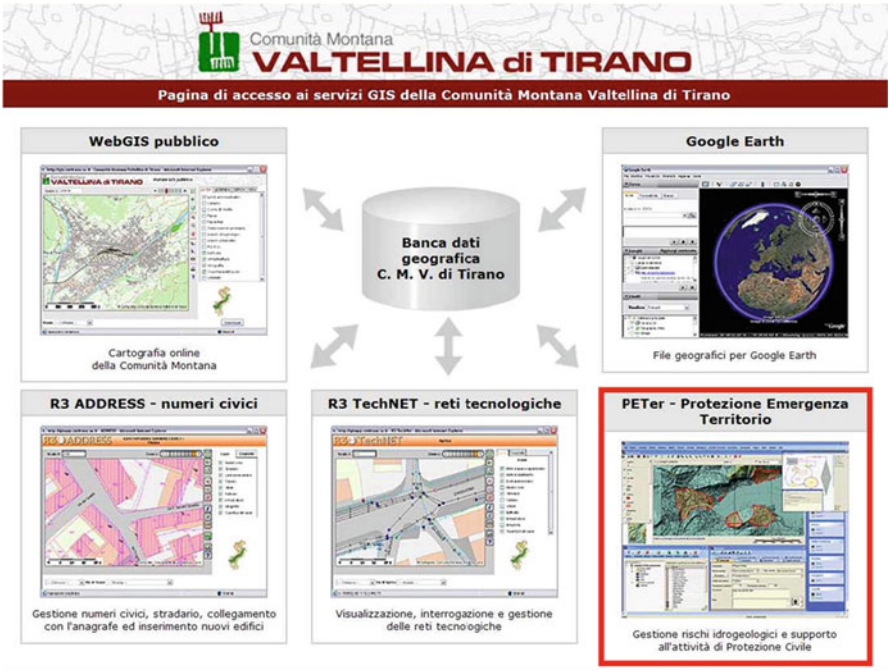

Fig. 13.5 Webpage of the Consortium of Mountain Municipalities of Valtellina di Tirano. *On the bottom right corner* there is the WEB access to the system designed to manage hydrogeological risk scenarios and Civil Protection activities

Scientifique) and the University of Strasbourg from the scientific side and ONF-RTM (Restauration des Terrains en Montagne) and the Préfecture of Alpes de-Haute-Provence (France) from local stakeholders/end-users side. In the study site, the Prefect of the "Département" points out the municipalities at risk that have to set up the risk prevention plan. All the municipalities composing the Barcelonnette basin have to provide a risk prevention plan.

In both study sites, the efforts towards the attention of emergencies or in preventing the disaster have to be balanced. Particularly concerning the Italian study site, although all the elements of EWS are present, they display multiple shortcomings, are independently developed, have no structure and are poorly linked. As a result, it is possible to say that several components of EWS exist as non-coordinated risk management strategies but they have to be brought together and connected in order to establish an EWS. The designed methodology (Fig. 13.2) proposes several actions to integrated the different risk management strategies into a structured IEWS adapted to the necessities of the local population and of the technical and administrative entities.

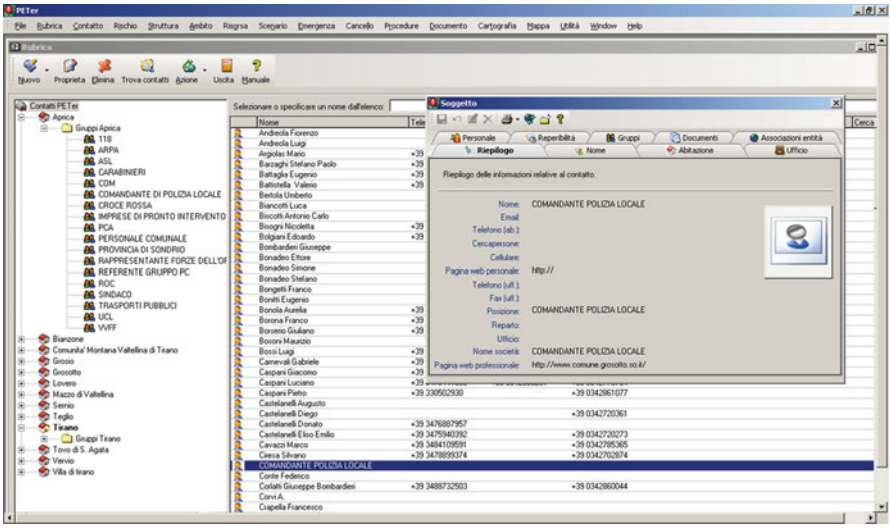

Fig. 13.6 Communication module. Similar to a personal agenda, it manages all the contacts related to the people potentially involved in emergency. A double click on a contact opens a personal chart with all general information and relations with structures, resources, etc.

The methodology has strong legal, social, technical and scientific components, and presents several phases, including:

- hazard, vulnerability (both social, physical and economical) and risk assessment;
- analysis of the legal framework;
- application of a comprehensive survey to evaluate the levels of perceived risk, knowledge, awareness, preparedness and information needs of the community;
- proposal of prevention and monitoring strategies, and;
- development of preparedness activities.

13.5 Conclusion

The failure or success of (structural and not-structural) EWS and emergency preparedness and response strategies (EPRS) is dependent on how well-connected all their components are (Garcia and Fearnley 2012). Regarding the governance and decision-making on EWS and EPRS, whereas the emission of the warning is based on technical information and risk monitoring, it is a political decision the one required to give the order for the warning and to act in a threatening situation. The political decision to act is not only performed by the authorities and institutions at various levels, but is also a responsibility of the local communities. Therefore, in order to increase the effectiveness of EWS and EPRS and to strengthen the risk management and governance process, all stakeholders, including local governments

and communities, must participate in the entire policy making process, so they are fully aware and prepared to respond (Sagala and Okada 2007; Chang Seng 2010; Garcia 2012).

EWS should become a national and local priority for the governments. It is therefore important to show the governments the economical benefits of EWS with a cost-benefit analysis of previous successful EWS backed with very strong governance systems, such as the ones in Japan and United States of America (EWC-III 2008; Chang Seng 2010). As pointed by EWC-II (2003), investing in EWS is neither simple nor inexpensive, but the benefits of doing so, and the costs of failure, are considerable. As stated above in the chapter, the provision of timely and effective information to people, likely affected by a prospective damaging event, is most often fulfilled by using structural EWS, the structure of which has to be as effective as possible from a cost-benefit point of view. For this reason, structural EWS should start after answering the four "W" questions (Corsini 2008) indicated previously.

Considering Integrated People-Centred EWS, it is necessary to assure that this kind of EWS are adapted to the local risk culture and that are fully integrated into the risk governance process, in order to decrease the amount of people directly affected by a disaster. This means to develop institutional, legislative and policy frameworks at national and local level, in order to provide an institutional and legal basis for the implementation and maintenance of effective EWS. The policies developed should help to decentralize disaster management and to encourage community participation.

When advanced warnings are available and the general public is well aware of the multiple hazards they may face, disaster preparedness and response strategies are the following topics of major concern. In this way, the whole disaster cycle can be covered, trying to apply the most advanced technology available and also making the solutions easy to use by people not accustomed to managing these techniques in their daily tasks. As discussed in the chapter, an integrated system to cope with disaster preparedness and response is presented. It couples data processing capabilities by GIS, DSS and ICT tools. Consequently, municipal contingency plans can be to set up, managed, and coordinated in advance, before a crisis phase occurs. The main aim of the system is to identify and prepare people in charge to take actions, define the activities to be performed, be aware of available resources, and optimize the communication system for the transfer of knowledge: co-operation and information available on-demand in case of emergency improves the response to the negative effects of a disaster and increases the effectiveness of rescue, relief and assistance operations.

References

Armstrong MP, Densham PJ (2008) Cartographic support for locational problem-solving by groups. Int J Geogr Inf Sci 22:721–749

Basher R (2006) Global early warning systems for natural hazards: systematic and people-centred. Philos Trans R Soc 364:2167–2182

Becker JS, Johnston DM, Paton D, Ronan K (2009) Community resilience to earthquakes: understanding how individuals make meaning of hazard information, and how this relates to preparing for hazards. New Zealand Society for Earthquake Engineering 2009 Conference, 3–5 April, Christchurch

Be-Safe-Net (since 2007) Protect yourself from hazards. http://www.besafenet.net/

Bird DK, Gisladottir G, Dominey-Howes D (2009) Resident perception of volcanic hazards and evacuation procedures. Nat Hazard Earth Syst Sci 9(1):251–266

Chang Seng D (2010) The role of risk governance, multi-institutional arrangements and polycentric frameworks for a resilient tsunami early warning system in Indonesia. PhD dissertation, Bonn University. http://hss.ulb.unibonn.de:90/2010/2227/2227.pdf

Chieh YF, Yuan CC, Chi LS, Ching LY, Yu WS, Wai CK (2007) A web-based decision support system for slopeland hazard warning. Environ Monit Assess 127:419–428

Corsini A (2008) Monitoring methods: systems behind a safer environment. In: Mayer R, Bohner A, Plank C, Marold B (eds) Results of the international conference monitor/08. Agricultural Research and Education-Centre Raumberg-Gumpenstein, Irdning, pp 47–54. ISBN 978-3-902559-19-7

DEFRA – Department of Environment, Food and Rural Affairs (2009) The Government's response to Sir Michael Pitt's Review of the summer 2007 Floods. Progress report

DMTP – Disaster Management Training Programme (1994) Vulnerability and risk assessment. Module prepared by Coburn AW, Sspence RJS, Pomonis A. Cambridge Architectural Research Limited. The Oast House, Malting Lane, Cambridge

DEWS – Distant Early Warning System (2007–2010) http://www.dews-online.org/

DKKV – Deutsches Komitee Katastrophenvorsorge e.V. – German Committee for Disaster Reduction (2007) Germany's policy on disaster reduction Abroad. http://www.auswaertiges-amt.de/diplo/en/Aussenpolitik/Themen/HumanitaereHilfe/Downloads/PolicyDisasterReduction.pdf

EC – European Commission (2009) Adapting to climate change: towards a European framework for action. White paper, Brussels. http://eur-lex.europa.eu/LexUriServ/LexUriServ.do?uri=COM:2009:0147:FIN:EN:PDF

DREAD-ED – Disaster Readiness through Education (2008–2010) http://www.dread-ed.eu/

EDURISK – Educational Itineraries for Risk Reduction (Since 2002) http://www.form-it.eu/goodpractice/projects/edurisk.shtml

EWC-II (2003) Integrating early warning into relevant policies. Second international conference on early warning. UN/ISDR, Bonn. http://www.unisdr.org/ppew/info-resources/docs/ewcii-Policy_brief.pdf

EWC-III (2008) Developing early systems: a checklist EWC III. Third international conference on early warning, from concept to action. UN/ISDR, Bonn

Filey Flood Working Group (2009) Joint County and district council flood scrutiny group. Final report, June 2009. http://www.floodforum.org.uk/files/Filey%20Flooding%20Final%20Report%20Committee%20Approved%20100809.pdf

Fleischhauer M (2006) Spatial planning and the prevention of natural risks in France. In: Fleischhauer M, Greiving S, Wanczura S (eds) Natural hazards and spatial planning in Europe. Dortmunder Vertrieb für Bau- und Planungsliterartur, Dortmund

Frigerio S, Sterlacchini S, Puissant A, Malet JP, Wehrle M, Guiter G (2010) Integration of a GIS-based decision support system in the context of French civil defence. The La Valette case study in the South Alps. In: Malet JP, Glade T, Casagli N (eds) Mountain risks – bringing science to society. CERG, Strasbourg

Frigerio S, Sterlacchini S, Malet JP, Pasuto A (2011) Emergency management support by geo-information technology. A common methodology in different European contexts. In: Proceedings of GEORISQUE 2011 – 7ème Edition – Plan Communal de Sauvegarde & Outils de Gestion de Crise, University of Montpellier III, Montpellier, 25–26 January 2011

Garcia C (2011) Risk management: integrated people-centred early warning system as a risk reduction strategy, Northern Italy. PhD dissertation, Università degli Studi di Milano Bicocca

Garcia C (2012) Designing and implementing more effective integrated early warning systems in mountain areas: a case study from Northern Italy. Revue de Géographie Alpine 100(1). doi: 10.4000/rga.1679

Garcia C, Fearnley C (2012) Evaluating critical links in Early Warning Systems for natural hazards. Special Publication: Disaster Risk Reduction: Connecting Research and Practice. Environ Hazards 11(2):123–137

Garcia C, De Amicis M, Sterlacchini S, Pasuto A, Greiving S (2010) Community-based early warning system for mountain risks, Northern Italy: identifying challenges and proposing disaster risk reduction strategies. In: Malet JP, Glade T, Casagli N (eds) Mountain risks – bringing science to society. CERG, Strasbourg

Grasso V (2007) Early warning systems: state-of-art analysis and future firections. Draft report for United Nations Environment Programme (UNEP). http://na.unep.net/geas/docs/Early_Warning_System_Report.pdf

Grasso VF, Beck JL, Manfredi G (2007) Automated decision procedure for earthquake early warning. Eng Struct 29(12):3455–3463

IREALP – Istituto di Ricerca per l'Ecologia e l'Economia Applicate alle Aree Alpine (2005) Monitoraggio: linee guida per il controllo dei fenomeni franosi. In: Mannucci G, Notarpietro A (eds) 1:1–127. http://www.irealp.it/84,Pubblicazione.html/

IRGC – International Risk Governance Council (2005) White Paper No 1 "Risk Governance – Towards an Integrative Approach", IRGC, Geneva

IRASMOS – Integral Risk Management of Extremely Rapid Mass Movements (2005–2008) Best practice of integral risk management of snow avalanches, rock avalanches and debris flows in Europe. http://irasmos.slf.ch/

Junkhiaw S, Sivongs W, Sukhapunnaphan T, Tangtham N (2004) Developing flood warning system for upland watersheds of the Chao Phraya basin. In: 6th international study conferences on GEWAX in Asia and GAME, Kyoto International Community House, Kyoto, pp 3–5

Kollarits S, Leber D, Corsini A, Papez J, Preseren T, Schnetzer I, Schwingshandl A, Kreutzer S, Plunger K, Stefani M (2010) Monitor II: new methods for linking hazard mapping and contingency planning. http://www.monitor2.org/

SLEWS – Sensor based Landslide Early Warning System (2007–2010) http://www.slews.de/

Lazzari M, Salvaneschi P (1999) Embedding a geographic information system in a decision support system for landslide hazard monitoring. Nat Hazards 20:185–195

LEWIS – Landslide early-warning integrated system (2002–2005) http://www.silogic.fr/lewis/

MacEachren AM, Cai G, Sharma R, Rauschert I, Brewer I, Bolelli L, Shaparenko B, Fuhrmann S, Wang H (2005) Enabling collaborative geoinformation access and decision-making through a natural, multimodal interface. Int J Geogr Inf Sci 19:293–317

FLOODSite – Integrated Flood Risk Analysis and Management Methodologies (2004–2009) http://www.floodsite.net/

Muntz RR, Barclay T, Dozier J, Faloutsos C, MacEachren AM, Martin JL, Pancake CM, Satyanarayanan M (2003) IT roadmap to a geospatial future, Report of the Committee on Intersections Between Geospatial Information and Information Technology. National Academies Press, Washington, DC

NEAREST – Integrated observations from NEAR shore sourcES of Tsunamis: towards an early warning system (2006–2010) http://nearest.bo.ismar.cnr.it/

OIKOS (since 2007) Students for sustainable economics and management. http://www.oikos-international.org/

Plapp T, Werner U (2006) Understanding risk perception from natural hazards: examples from Germany. In: Amman WA, Dannenmann S, Vulliet L (eds) In: RISK 21 – coping with risks due to natural hazards in the 21st century: proceedings of the CENAT-Workshop 2004. Taylor & Francis, London

Regione Lombardia (2007) Direttiva regionale per la pianificazione di emergenza degli enti locali. Regional Decree n. VIII/4732, 6 May 2007, Milano

Regione Lombardia (2009) Direttiva Regionale per la gestione organizzativa e funzionale del sistema di allerta per i rischi naturali ai fini di Protezione Civile. Regional Decree 27 January 2009. Milano

Repubblica Italiana (1992) Legge 24 Febbraio 1992, n. 225 – Istituzione del Servizio Nazionale della Protezione Civile. http://www.protezionecivile.gov.it/cms/view.php?dir_pk=41&cms_pk=137

RINAMED – Elaboration and application of a common strategy among local actors in the Mediterrean Arc to inform and sensibilise the populations to natural risks (2002–2004) http://www.territorialcooperation.eu/frontpage/show/3191

RISKRED – Risk Reduction Education for Disaster (Since 2006) http://www.riskred.org/

SAFELAND – Living with Landslides in Europe: Assessment Effects of Global Change and Risk Management Strategies (2009–2012) http://www.safeland-fp7.eu/

SAFER – Seismic Early Warning for Europe (2006–2009) http://www.saferproject.net/

Sagala S, Okada N (2007) Managing early warning systems in tsunami prone communities: the need for participatory approach (PRA). Disaster Prevention Institute, Kyoto University, Kyoto, pp 195–204

Sterlacchini S, Frigerio S (submitted) Preparedness and response to disaster-related emergency: an integrated GIS, DSS and ICT-based system. Natural Hazards, Springer

Ten Brinke WBM, Bannink BA, Ligtvoet W (2008) The evaluation of flood risk policy in the Netherlands. J Water Manag 161:181–188

TRANSFER – Tsunami Risk ANd Strategies For the European Region (2006–2009) http://www.transferproject.eu/

UK Cabinet Office (2004) Civil Contingencies Act (2004) A short guide. http://www.cabinetoffice.gov.uk/media/132428/15mayshortguide.pdf

UN/EP – United Nations/Environment Programme (2010) Early-warning systems: state-of-art analysis and future directions. Draft report by Grasso VF, Singh A. http://na.unep.net/geas/docs/Early_Warning_System_Report.pdf

UN/ISDR – United Nations/International Strategy for Disaster Reduction (2005) PPEW – platform for the promotion of early warning. Basics of early warning: the four elements of effective people centered early warning systems, presented at the Virtual Symposium, Public Entity Risk Institute: Early Warning Systems – Interdisciplinary Observations and Policies from a Local Government Perspective. 18–22 April, 2005. http://www.unisdr.org/ppew/whats-ew/basics-ew.htm

UN/ISDR – United Nations/International Strategy for Disaster Reduction (2006) Early warning – from concept to action: the conclusions of the third international conference on early warning (EWC III), 27–29 March 2006, Bonn

Van de Ven GP (2004) Man-made lowlands. History of water management and land reclamation in the Netherlands. Matrijs, Utrecht

WMO – World Meteorological Organization (2010) A framework for disaster risk management derived from HFA. World Meteorological Organization (WMO). Disaster risk reduction (DRR) programme Geneva. http://www.wmo.int/pages/prog/drr/DrmFramework_en.htm

Chapter 14
Risk Assessment: Establishing Practical Thresholds for Acceptable and Tolerable Risks

Graciela Peters-Guarin and Stefan Greiving

Abstract Risk levels or 'thresholds' presents a standard for determining lower and upper thresholds above and below which risks are either negligible and unacceptable respectively. Between these two thresholds there is a region where risks are tolerated.

Nevertheless as people do not necessarily share the same risk perceptions the acceptability thresholds will vary for different sources of hazard and different cultural and social conditions. In disaster related studies, and particularly for phenomena such as mass movements, there are surprisingly few cases where household culture on risk management and risk acceptability thresholds are analysed.

The locality of Tresenda (Sondrio Province, Italy) is considered to be one of the most exposed to significant potential losses due to Debris flows in the area. By making use of people-centred approaches such as surveys and with semi-structured interviews the attitude of households towards risk, and their perception of the maximum damage – in economic terms, they can both manage and tolerate was researched. The case study helped to expose a culture of risk denial and optimistic bias where people tend to reject own risk and hope that dreadful things will never happen to them but rather to 'the others'. The poor risk avoidance culture found, evidences how, despite a widespread knowledge of the risk, people's awareness and concern not necessarily lead to actions such as avoiding or shifting the risk. In terms of damage they would be able to deal with low to moderate levels leaving a great

G. Peters-Guarin (✉)
Anthropology Department, Vanderbilt University, 2301 Vanderbilt Place, 124 Garland Hall, Nashville, TN 37235, USA

Institute of Spatial Planning, Dortmund University of Technology, August-Schmidt-Straße 10, D-44227 Dortmund, Germany
e-mail: graciela.peters.guarin@vanderbilt.edu; gpeters321@gmail.com

S. Greiving
Institute of Spatial Planning, TU Dortmund University, August-Schmidt-Straße 10, D-44227 Dortmund, Germany

T. van Asch et al. (eds.), *Mountain Risks: From Prediction to Management and Governance*, Advances in Natural and Technological Hazards Research 34,
DOI 10.1007/978-94-007-6769-0_14,

percentage of residual risk either uncovered or to be undertaken by the state. In small isolated towns, factors such as the greying' phenomenon where found to decrease the manageability of risk by natural hazards such as debris flows.

Abbreviations

UN-ISDR	United Nations International Strategy for Disaster
ALARP	As Low As Reasonably Practicable
AGS	Agency of Global security
CDRSS	Committee on Disaster Research in the Social Sciences
RASDA	Raccolta Sceda Danni -Damage Assessment Form

14.1 Introduction

The International Strategy for Disaster Reduction (ISDR) has defined Risk as the combination of the probability of an event and its negative consequences. Nevertheless, as Smith (1992), Zezere et al. (2008) and Bell et al. (2005a) stated, the risk concept is not easily transferred to (landslide) risk management, because the concept of risk has different meanings for different people. Moreover any particular interpretation of "Hazard × Vulnerability × Elements at Risk" can be accepted or not by an individual, community or society depending on their view of the environment and their general attitude towards risk in life, and ultimately on the level of probability and degree of damage involved. People do not necessarily share the same perceptions of the significance, consequence and underlying causes of different risks (Slovic 1987; Sjöberg 2000; Wisner et al. 2004; ISDR 2004; Plapp and Werner 2006).

Risk assessment therefore requires a broad understanding of the relevant losses and harm, and their consequences for interested or affected parties, and it must be targeted to determine the acceptability of a given risk for diverse groups or individuals within any society. If certain levels of risk are deemed by people as 'unacceptable', measures for risk reduction need to be implemented (Klinke and Renn 2002). The most widespread taxonomy regarding risk levels or 'thresholds' presents a standard for determining the acceptability of risk based on the ALARP (As Low As Reasonably Practicable) approach (AGS 2007). The approach identifies an upper threshold above which risks are generally unacceptable, and a lower threshold below which risks are generally acceptable and require no action. Between these two thresholds is a region where risks are tolerated only on the basis that they are kept ALARP. This classification is based on the assumption that not only the magnitude of impact, but also its frequency, will determine the acceptability of risk. Nevertheless the acceptability thresholds will vary for different sources of hazard and different cultural and social conditions (AGS 2007; Bell et al. 2005b). The ISDR (2004) complements the definition of acceptable risk as the level that a

given society is prepared to accept without any specifically designated management programme. Risk management may aim to reduce all risk to this level. Tolerable risk on the other hand refers to the level of risk that a society is prepared to live with because there are net benefits in doing so, as long as that risk is monitored and controlled and actions are taken to reduce it (Crozier and Glade 2005).

Most countries in the European Union have a formal approach to risk management based on a culture of avoidance and risk burden-sharing by means of insurance for third parties (Risk transference). Financial consequences of particular risks (natural hazards in this case) are either avoided by legal tools such as restrictions in land use and land use planning or housing design, or by risk shifting from one party to another. In this risk prevention setting, even if the individual is not aware of a pending threat, the state obliges him/her to transfer the risk of their life or property to an insurance company by enforcement of the country's legal regulations. The government and legal institutions are therefore the ones determining what levels of risk are acceptable or tolerable for the society, and individuals should comply with these regulations.

In many other countries however, official approaches are not available or agreements at 'society' level have not been established. Hence the responsibility for managing the potential consequences of natural events and absorbing -or transferring- the risk is laid on the individual or household. In these settings, it is more appropriate to refer to processes of, what has been defined by Alexander (2000) as "internalisation" of risk, and by Bell et al. (2005a) as 'individual acceptance' of risk, where the responsibility for risk is assumed or accepted by the individuals. In some cases it is more pertinent to talk about involuntary risks being taken, because there are no reasonable alternative, and, because the bearer is unable or reluctant to forgo the benefits associated with taking the risk (Alexander 2002).

Risk acceptability and tolerance, therefore, depend greatly on the existing social, economic, political, cultural, technical and environmental conditions present at society and individual level at a given moment in time. In disaster related studies, and particularly for processes such as mass movements, there are surprisingly few cases where household culture on risk management is analysed. People's perception of risk, their response to diverse hazards, adjustments and the range of socioeconomic strategies available (or not) to manage the damage caused by those hazards, and the levels of risk they are prepared or willing to live with, are rarely analysed (CDRSS 2006; Murphy and Gardoni 2006; Lacasse et al. 2010). This neglecting approach to risk cultures and awareness occur despite the fact that, when examined at worldwide level, risk transference and insurance are the exception and not the rule. In settings where risk has not been collectively discussed and agreed, consideration is needed of the individual, social and risk management cultural context in which hazardous phenomena take place (Meacham 2007; Nathan 2008; Lindell and Hwang 2008; Bell et al. 2005b).

An understanding of the risk that individuals or communities are willing to accept requires that analysis of the physical events and their economic consequences go hand in hand with an evaluation of the levels of concern and cost-benefit circumstances existing among exposed individuals and communities (e.g. affordable

housing, facilities etc). Exposure to particular hazards, previous experiences, perceptions of own risk and socio-economic characteristics greatly determine how risk is judged at household level and the willingness of the family or individual to accept living with certain levels (thresholds) of risk or attempt to reduce them. If people exposed to (natural) hazardous phenomena perceive themselves as less exposed than others in their community or, if even they have knowledge or past experiences of the risk, they may fail to use this information for their own protection. Consequently, they may fail to reach consensus on collective thresholds for risk acceptance and the required actions to reduce or mitigate it.

Nevertheless as stated by Fell (1994) and Bell et al. (2005a), a basic issue about risk assessment is that tolerable and acceptable levels are usually defined by scientists, governmental institutions or politicians, and not by the people affected. In the following section, an empirical approach to defining acceptable and tolerable risk thresholds at individual and household level is discussed, based on 'houses and inhabited buildings', which were deemed in this research to be one of the most important economic and social assets of a family. The study was carried out in the Municipality of Teglio, Sondrio Province in the North of Italy.

14.2 Approaching Acceptable and Tolerable Risk Thresholds at Local Level

In Italy, risk transfer by means of insurance is not compulsory; therefore although private insurance is available, the practice is not widespread, especially in small towns and semi-urban environments. Calamities, such as those caused by natural events, are relieved by the state by means of economic aid to the affected people; Nevertheless this assistance has to be preceded by a declaration of 'calamity' issued by the Municipal authorities whose judgement is based on the amount of collective damage. This implies that the occurrence, and impact, of a hazardous event will not always lead to the declaration of a 'state of calamity'. Moreover, depending on the number of people or assets damaged, the individual household may not get the assistance which it requires to completely cover the losses undergone. In that case, and regardless of their economic or social status, they have to rely entirely on their own resources to recover or rebuild their assets.

In this research, the use of formal definitions for risk acceptability and tolerability (e.g. as defined by the UN-ISDR) was not considered to be practical. Formal definitions would imply a negotiated consensus amongst the members of a community on the level of potential acceptable losses and on the measures needed to reduce possible harm. This was not the case for the study area, where the community has to deal with damages from events in the past by assuming losses at individual level, getting relief and assistance from the government, and by reducing future harm by following government-imposed landuse restrictions on plots which were previously occupied by houses that were destroyed or seriously damaged by debris flows.

Therefore it was decided to focus on understanding how individuals or households in the study area bear or assume different risk levels in regard to debris flow and what may be their strategies to cope with different levels of damage. Consequently the analysis was aimed at understanding on the one hand, the attitude of households towards risk, and on the other hand, households' perception of the maximum damage – in economic terms, they can both manage and tolerate. In this case it was deemed appropriate to use the term 'manage' instead of 'accept', as the former term better addresses people's capacity to handle challenging situations depending on their resources and range of coping mechanisms (Peters-Guarin et al. 2011).

By means of an approach that combined people-oriented tools such as mini-surveys and semi-structured interviews, this information was elicited at household level in terms of:

- Risk knowledge regarding experiences with past events;
- Risk perception regarding people's attitudes when they think about debris flows;
- Risk awareness about debris flow probabilities and recurrence by asking how likely they consider that a debris flow will affect both the community and their own property in the coming 1, 5, and 10 years;
- Individual's acceptance of risk by considering the potential damage their property can suffer and how much of the damage they can or cannot afford to repair with resources at hand.

The house or building inhabited by a household is one of the most important tangible and intangible resources of a household. More than any other valuable, damage to a household's dwelling causes emotional distress and potential physical exposure to the elements of both the people and assets if the damage implies the structural elements of the house. Increasing levels of damage to the house will therefore trigger the need for immediate decision-making at family level (e.g. whether to rebuild, abandon, temporarily relocate while considering other options etc.). Consequently this study decided to use the potential damage to household dwelling as a proxy for the estimation of a households' acceptable and tolerable risk thresholds.

Thresholds for risk manageability and tolerability were elicited by asking the household to express the sum (in Euros) they are willing or able to spend in repairing their property in case it is damaged by a debris flow. Regarding this information two assumptions were made: on the one hand, it was assumed that the amount the household is willing to pay/able to pay using immediate resources at hand (e.g. savings, cash, shares or any other valuable asset directly available) represents the risk they are willing to take/accept and therefore represents their risk manageability. On the other hand, risk tolerability was assumed as the amount the household is willing/able to pay by making use of gradual -short to medium term- coping mechanisms such as loans, mortgages, and selling of assets e.g. land plots, buildings, cars and the like.

14.3 Case Study: The Locality of Tresenda (Italy)

The study took place in the locality of Tresenda (Teglio Municipality, Sondrio Province). The geological and geomorphological situation in this small village favours the occurrence of mass movements, creating an extremely hazardous setting in a relatively small area. In fact the population of this locality, approximately 1,242 inhabitants by 2009 (Municipality of Teglio 2009); is considered to be one of the most exposed to significant potential losses in the region. Soil slips, and debris-flows have already occurred on the steep slopes above Tresenda as a result of the collapse of dry-stone terraces or unconsolidated material from unstable and intensely fractured areas (Cancelli and Nova 1985; Ceriani et al. 1992; Crosta et al. 2003; Blahut 2010; Blahut et al. 2010). This small village already suffered disastrous landslides several times in the past, with major events occurring in 1983 and 2002 (Fig. 14.1). On May 23, 1983 two soil-slips occurred on the slope above the village. These slips transformed into debris-flows that affected a large portion of the community and left 18 people dead, levelled buildings, damaged properties and blocked the national road (SS 38) (Giacomelli 1987).

For many centuries, the practice of viticulture has been the main source of livelihood of local populations in the Valtellina region. The grapevine has been a constant feature in Valtellina's agriculture. Its cultivation has played a significant

Fig. 14.1 Photographs of debris flows affecting the locality of Tresenda on 23rd of May 1983 (Source: Archive of CNR-IRPI, Torino)

Table 14.1 Population distribution by age groups in Tresenda

Age group	Male	%	Female	%
0–6 years	31	2.5	41	3.3
7–14 years	41	3.3	48	3.8
15–29 years	88	7.0	93	7.4
30–65	349	27.9	322	25.7
Over 65	108	8.6	131	10.5
TOTAL	617	49.3	635.0	50.7

Source: Municipality of Teglio (2009)

role in the history of the valley throughout the centuries and has modified the agricultural landscape as well as influencing the economic life of its inhabitants. Socio-economic changes that occurred in the last 40 years have induced a partial urbanization of the rural population and, consequently a reduction in attention for the tillage and maintenance of terraced slopes and drainage. This has worsened the lack of maintenance of the whole system, and, in some cases, caused their abandonment. In Tresenda the decay in traditional livelihoods is partially caused by phenomena such as depopulation and ageing, as shown in Table 14.1.

Lack of skills and human power to keep the terracing system working properly brings about an almost immediate decay, indicating that their maintenance is a fundamental issue not only for landscape conservation, but also for slope stability (Frepazz et al. 2007) and for decreasing the risk to the exposed population from debris flows.

14.4 From Risk Perception to Manageability and Tolerability Strategies: Using Surveys to Elicit Risk-Related Knowledge

As mentioned above, the research made use of people-centred approaches. From the several tools available in this methodology we chose to conduct surveys combined with semi-structured interviews. These proved to be extremely useful to understand and elicit local knowledge at individual level, in this case regarding debris flow risk. The number of households in Tresenda by 2009 was about 400, with an average of three persons per family unit (Municipality of Teglio 2009). The research took place mostly on the southeast-facing slope of the locality where 111 families are settled. They are considered to be potentially the most exposed to the occurrence of mass movements. Around 25 households or 22.5 % of this population voluntarily participated in the survey.

Individuals in the interviewed households were 57.5 years old on average which was considered as representative, given the age distribution of this community (Table 14.1). Most of the interviewees (64 %) were born in the locality with an average of 45 years of living in Tresenda. Among the reasons found for being settled in this locality are family and property attachments (52 %), working opportunities

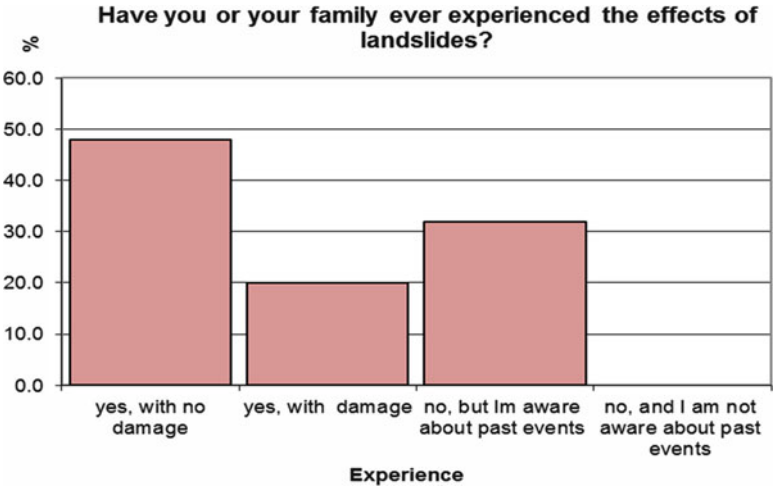

Fig. 14.2 Distribution of interviewees by debris flow risk experience

Table 14.2 Report of feelings regarding the occurrence of debris flows by the interviewees in the locality of Tresenda (Italy)

Scale[a] / Feelings	None (%)	Low (%)	Moderate (%)	High (%)	Very high (%)	No answer (%)
Awareness	4	12	32	40	12	0
Worry	4	32	28	24	8	4
Calm	8	20	32	32	4	4
Indifference	88	0	12	0	0	0

[a]Likert scale

(28 %) affordability of commodities (e.g. housing) and services, or because the cost of living in general is cheaper than in bigger cities nearby (12 %), better quality of life (8 %), or combinations of several reasons.

The survey showed how, with regard to previous experiences of hazardous events, all the interviewees (100 %) acknowledged the occurrence of debris flows in the locality, either because they had witnessed or been affected by past events (68 %) or, as in the case of new settlers, because they have been told about them (32 %), as shown in Fig. 14.2.

Reports about knowledge of debris flows with losses (16 %) included structural damage, external and internal walls (60 %), damage to backyard gardens and damage to house contents (carpets, wall paintings, furniture) caused by the intrusion of mud inside the house (40 %).

Regarding risk perception and feelings engendered when thinking about debris flows, the survey showed how most of the people interviewed have moderate to high levels of awareness (84 %). However despite the fact that they do not consider themselves as indifferent to the problem (88 %) the levels of concern or worry shown, tended to be moderate to low (64 %). The types of feelings engendered when they think about the potential occurrence of a debris flow are shown in Table 14.2.

Table 14.3 Report of the likelihood that a debris flow will affect the community (C) or their own property (OP) in 1, 5 and 10 years as perceived by the interviewees in the locality of Tresenda (Italy)

Recurrence / Scale[a]	1 year		5 years		10 years	
	C	OP	C	OP	C	OP
Highly unlikely (%)	56	72	32	64	8	56
Unlikely (%)	44	20	44	12	40	16
Likely (%)	0	0	24	16	48	20
Highly likely (%)	0	0	0	0	4	0
Extremely likely (%)	0	0	0	0	0	0
No answer (%)	0	8	0	8	0	8

[a]Likert scale

The results in Table 14.2 may initially look ambiguous. On the one hand, most of the households have had direct or indirect experiences with debris flows, and on the other hand they manage relatively moderate to high levels of 'calm' and low to moderate levels of 'worry'. This apparent contradiction however may indicate that people in hazard-prone areas have, at some point, become used to being exposed; in other words, risk has become part of their life-style. The survey shows the households are aware of the risk they are exposed to, however apparently their concern does not necessarily trigger actions towards avoiding or shifting risks. At some level this may explain why despite the known risk, a primary self-protective, non-structural measure such as property insurance against natural hazards was not found in this community.

Table 14.3 shows the results of interviews regarding perceptions about recurrence and the likelihood that a debris flow can affect the community and personal property in the coming 1, 5, and 10 years.

The results from Table 14.3 on the one hand show that people in general consider that it is Very Unlikely that in the short term (1 year) a debris flow will affect their property (72 %) or the community (56 %) in general. However, in the long term (10 years) the probability increases, although not in an even proportion. In their perception, it is Very Likely (48 %) and even Highly Likely (4 %) that in this period of time the community will suffer some damage, but not their own personal properties (56 % Highly unlikely, and 0 % highly likely). In this respect the survey again shows some intriguing results. As can be seen from the three proposed scenarios, the interviewees consider the rest of the community to be more exposed or likely to be affected by a debris flow than their own property (as highlighted by the shadowed cells). This typically positive perception can be seen as an example of what has been called optimistic self-perception and optimistic bias in risk, health and behavioural research (Gierlach et al. 2010; Anderson and Galinsky 2006; Bränström et al. 2005). The results of the survey are typical for cultures of risk 'denial' characterised by the human tendency to reject own risk, the belief that one is more immune to disasters compared to others, and the hope that dreadful things will never happen to oneself, but rather to 'others' (Horlick-Jones and Jones 1993; Gopalakrishnan and Okada 2007; Zaalberg et al. 2009).

Fig. 14.3 Typical stone wall (*left*) and brick masonry (*right*) houses in Tresenda

Table 14.4 Structural and non-structural components of a house used to elicit the damage a debris flow can cause to the property according to the interviewee's own perception

Scale* House / Components	None (%)	Low (%)	Moderate (%)	High (%)	Very high (%)	No answer (%)
Garden and external components	4	4	20	16	20	36
Floor and carpet	4	12	8	40	20	16
Furniture	8	4	8	44	20	16
Internal walls	4	0	20	48	24	4
External walls	4	0	20	40	36	0
Overall structural frame of the house	4	4	8	48	36	0

The last objective of the survey was to try to understand the individual and household level of risk acceptance both in qualitative and quantitative terms (when possible). By individual risk acceptance, or internalisation of risk, we mean the amount of damage that people consider the occurrence of debris flows can cause to their property and how much of that 'perceived' damage they can or cannot afford to repair. The houses in Tresenda are typically three storey buildings made of unreinforced stone walls, brick masonry and concrete structures with piles and cross bars (Fig. 14.3).

In order to facilitate answers from the interviewees, these questions were divided into structural and non-structural components of the property, as shown in Table 14.4.

The answers suggest that, in people's own perception, the damage a debris flow can cause to their own property ranges mostly from High to Very High, with especial concern for structural damage to internal (48 %) and external walls (40 %) and the structural frame of the building (48 %). This perception may be the result of having witnessed the damage and destruction that debris flows caused in the past to similar buildings in the locality or nearby areas, as shown in Fig. 14.1.

People were asked how much of the perceived potential damage they cannot manage or are not willing to repair with their own resources. The results are shown in cumulative percentages in Table 14.5.

On the one hand, up to 20 % of the interviewees are not able to, or are not willing to pay for, any (no) level of damage, even to non-structural constituents of

Table 14.5 Potential damage caused by debris flows on structural and non- structural elements of the house and interviewee's intentions to repair them

Damage scale* / House components	None (%)	Low (%)	Moderate (%)	High (%)	Very high (%)	No answer (%)
Garden and external components	20	44	48	52	72	100
Floor and carpet	16	20	48	52	72	100
Furniture	16	20	24	68	88	100
Internal walls	16	16	20	72	100	100
External walls	16	16	20	72	100	100
Overall structural frame of the house	16	16	20	68	100	100

Table 14.6 The amount people are able to pay using resources at hand and financial coping mechanisms in case of building damage, as stated by the interviewees in the locality of Tresenda (Italy)

Amount in € (by June-2010)	Amount people are able to pay using immediate resources at hand (in %) (threshold for household manageable risk)	Amount people are able to pay using gradual coping mechanisms (in %) (threshold for household tolerable risk)
0–10,000	38.9	14.3
11,000–30,000	33.3	21.4
31,000–50,000	16.7	28.6
51,000–100,000	11.1	21.4
≤200,000	0.0	14.3

the house such as 'Garden and External Components'. On the other hand 72 % of the interviewees are not able, nor are willing, to pay for repairing 'High' structural damage to internal and external walls. In general terms the results displayed on Table 14.5 suggest that once the level of damage overcomes the 'Moderate' threshold most of the households are not willing, and are not capable in economic terms, of repairing or rebuilding their house. Low wages (less than € 2,500/month) or average age older than 70 years were some of the characteristics of the households who consider they cannot afford, nor are willing to repair, the slightest levels of damage to any of the components of the house (16–20 %).

The research however deemed it relevant to figure out the amount of economic resources the individual or household is able or willing to use in case of damage to their house, in other words the manageability and tolerability thresholds at household level as defined in this research. It was assumed this amount will be used, either in the short or medium term, for recovering the previous state of the dwelling.

Table 14.6 presents the household economic capacity to manage the damage in case of a debris flow by using their own resources or with coping strategies at hand.

Table 14.6 shows that in June 2010, the sum the household is able and willing to pay by using immediate resources in order to repair house damage from a debris flow averaged € 30,000 (± € 3,000). It should be noted that in this case the damage perceived as Manageable is more related to destruction of gardens, carpets, floors, furniture and electrical appliances. Tolerable losses were referred to as moderate damage to floors, doors, windows, painting of the house and minor

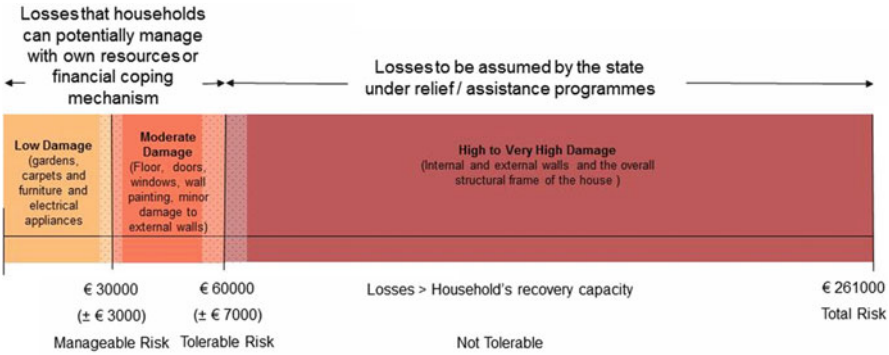

Fig. 14.4 Households' manageable and tolerable risk thresholds to house damage by debris flow using average price of buildings for Tresenda (North Italy)

Table 14.7 Economic losses to private property due to mass movements from 2007 to 2010 as reported by the civil protection of Lombardy (RASDA documents)

Year	Number of events causing losses to private property	Total damage to private property (Million Euros)
2007	3	0.17
2008	12	5.00
2009	4	0.16
2010	9	0.25
Total	28	5.58

structural damage in external walls. In this case the amount able to be paid by the households was an average of € 600,000 (± € 7,000) by making use of medium term mechanisms such as family and bank loans.

Based on the price per m^2 reported by the Association of Engineers and Architects of Milan (DEI 2006) Blahut (2010) established for Tresenda an average value of € 261,000 per building in 2009, each house having an average size of 310 m^2. According to the figures obtained by the survey and presented in Table 14.6, the risk thresholds for debris flows, which the households in Tresenda are able to manage and tolerate, represent around 10 and 20 % of the building value correspondingly (Fig. 14.4).

By comparing these values against some of the losses caused by mass movements in the region some conclusions can be drawn. Table 14.7 shows data provided by the Civil Protection of the Lombardy Region on the damage to private property just for the Sondrio Province during the period 2007–2010. The data on losses were obtained from the official documents called RASDA (Raccolta Scheda Danni or Damage Assessment Form), which by law should be drafted within 48 h after a major event for claim purposes.

The reports made available by the Civil Protection do not offer precise information on the number of households affected per event; nevertheless it can be

reasonably assumed they did not involve numerous buildings as none of them lead to evacuation of people or triggered the declaration of a 'calamity state'. Additionally, the total damage of structures was not reported for any of the events. By using the data on Table 14.7 it was inferred that in the last 4 years an average of 7 events per year have caused losses of around € 1.1 million to private property in the Sondrio region. Assuming an average of two buildings per event the average damage therefore amounts to nearly € 80,000 per household (when affected). Nevertheless this amount seems to include only light to moderate damage and therefore does not involve heavy destruction of the structural components of the house. When compared with the thresholds depicted in Fig. 14.4 it can be seen how even in the most conservative scenarios assumed in this research, the average loss per event almost triples the risk manageability threshold of the interviewees and exceeds their risk Tolerability threshold likewise. Moreover Blahut (2010) found that a debris flow with a 10-year return period will cause direct monetary damage to buildings in the path of the landslide of about € 27,800 per household per year. In risk thresholds terms, this figure implies that under a 10–year return period scenario, there is a 10 % probability every year that the risk manageability threshold of the individual or household will be exceeded.

The quantitative and qualitative components of the survey make it evident, that for this community, the level of damage required for equalling or exceeding both the Manageability and Tolerability risk thresholds is relatively low and mostly related to non-structural elements of the house. Given the fact that probably no calamity state will be declared in such cases the possibility to secure assistance from the government is very low, therefore it remains the individual or household who has to bear the loss and fix the damage. It is therefore necessary to understand what could be the potential strategies to be followed by individuals or households once the damage/loss surpasses their Manageable and Tolerable thresholds. So far the research inquired about the use of 'inherent' immediate and medium term resources. In addition, the existence of coping mechanisms 'external' to the household was considered as well. Economic support from extended family members or credits available from the financial system may enhance the manageable and tolerable risk thresholds of a family. The survey therefore included enquires about potential paths of action once the 'inherent' coping mechanisms were depleted. The options provided were as follows: (1) Sell the property, (2) Mortgage the property, (3) Loan from the bank, (4) Loan from family/friends, (5) Leave it as it is, (6) Abandon the property. Figure 14.5 shows the answers by strategies and age group.

The option of selling or mortgaging the property is not considered as viable for any age group; the explanation being that nobody will buy or pledge a credit on a damaged house. Borrowing either from a bank or family and friends were the strategies preferred by the economically active group (between 30 and 65 years old) which represents nearly 54 % of the population. For those above this age group, borrowing money from financial institutions is not a coping mechanism available anymore. In their case, abandoning the house, moving or renting somewhere nearby would be their preferred option. The fact that they perceive themselves as 'close to pass away' renders the effort of investing in rebuilding or recovering the house

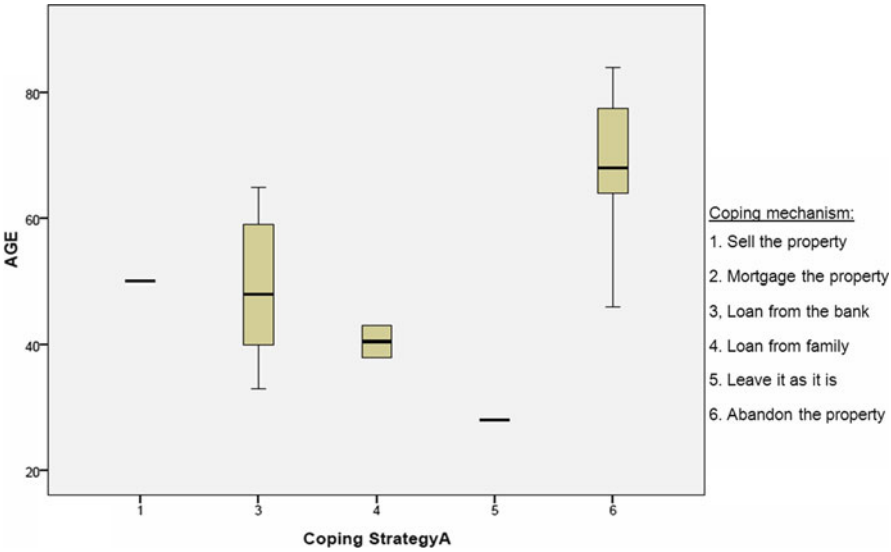

Fig. 14.5 Coping strategies by age group in case the house is seriously damaged by a debris flow (Tresenda)

'useless' in their own words. Beyond the displacement or homelessness of the adult population, this 'ultimate' coping mechanism has economic implications for financial institutions and ultimately for the government. In the case of mortgages, it has to be considered that people will not be able to continue paying the loans. Most probably, as seen from previous events, where plots were damaged or destroyed, the houses still standing will be bought by the state and incorporated in future risk mitigation and prevention plans by means of urban spatial planning.

Finally it should be mentioned that the research found the amount of money reported as the households' Manageable and Tolerable risk thresholds correlates with figures such as Average Income (+0.51), Age (−0.53) and Ownership of the house (+0.72). Again, the group of older people getting their income from a pension (48 %) and living as renters are those less able to allocate resources such as money and time for repairing damages or investing in risk prevention measures.

14.5 Conclusions

In countries were risk prevention and transference is not compulsory the risk of disasters has to be endured by individuals or households based on their own resources. The willingness or capacity to manage or tolerate the potential losses at this level however is influenced by the predominant risk culture and the social and economic context in which natural hazards take place.

The case study in the north Italian locality of Tresenda helped to expose on the one hand a culture of risk denial and optimistic bias where people tend to reject own risk and hope that dreadful things will never happen to them but rather to 'the others'. Under several scenarios for debris flow occurrence (1, 5, and 10 years) interviewees always considered themselves as less exposed or their property less likely to be damaged by a landslide that the rest of the community. On the other hand the poor risk avoidance culture found, evidences how, even if the community has a widespread knowledge of the risk, their awareness and concern not necessarily lead to actions such as avoiding or shifting the risk as so far nor insurance against natural hazards was found among the interviewees. The failure to use this information on a consistent way is crucial for further awareness rising programmes that lead people to better formulate a judgment of their own exposure to harm and, more important, take risk management actions.

Regarding the thresholds for losses that people is in the capacity to manage and tolerate, the research found how they range within the 10–20 % of the house value (for 2009 in Tresenda). In terms of damage they would be able to deal with low to moderate levels of it, corresponding to destruction of backyards, carpets and floors, furniture, wall painting and minor structural components of the house such as windows, doors, and external unreinforced walls. This type of damage has occurred in the past to several households and therefore they are 'familiar' in dealing with it. The residual risk, therefore, which represents nearly 80 % of the house, will have to be undertaken by the state. So far reactive relief and recovery programmes are the Italian state's coping mechanism in place, after getting short in promoting preventive risk transference schemes. Assistance and relief from the state, once the disaster has taken place, seems to provide the ultimate households' coping mechanism against debris flow in these types of hazard-prone and poor risk prevention culture environments.

The survey showed how factors such as occupation, income level but moreover age influence the Manageability or Tolerability of risk. The greying phenomenon is not exclusive of Tresenda; in fact the north part of Italy has one of the highest ratios of elderly to youth population in west Europe. Under a Global warming scenario the increasing life expectancy and potential intensification of mass movement occurrence (triggered by changing hydro-meteorological patterns) ask for policies that avails differentiated risk prevention measures for the diverse groups of a society. Insurance schemes against environmental hazards and other available coping mechanism tailored to the possibilities of the rising older segment of the population need to become available.

Finally it worth mentioning that despite the small size of the survey, the amounts reported equivalent to around 10 and 20 % of the building value (by 2010) can be taken as an initial indicator of the losses that at household level can be managed or tolerated. Stakeholders such as authorities may use them as starting point for further inquiries about risk manageability. Moreover discussions at local level can be fostered in order to look for what exposed people in this locality consider as the risk they as a whole community are able or willing to manage

or tolerate. On the other hand, risk insurance companies would be able to better address programmes (e.g. risk education, risk transference) and insurance policies adequate to those thresholds and the characteristics of the individuals and the community.

References

Alexander DE (2000) Confronting catastrophe: new perspectives on natural disaster. Terra publishing/Oxford University Press, Harpenden/New York

Alexander D (2002) From civil defense to civil protection–and back again. Disaster Prev Manag. 11(3):209–213. http://www.emeraldinsight.com/journals.htm?articleid=871006&show=abstract

Anderson C, Galinsky AD (2006) Power, optimism, and risk-taking. Eur J Soc Psychol 36:511–536

Australian Geomechanics Society – AGS (2007) Guidelines for landslide susceptibility, hazard and risk mapping for land use planning

Bell R, Glade T, Danscheid M (2005a) Risks in defining acceptable risk levels. In: Hungr O, Fell R, Couture R, Eberhardt E (eds) Landslide risk management. Taylor & Francis, London

Bell R, Glade T, Danscheid M (2005b) Challenges in defining acceptable risks. In: CENAT (ed) Coping with risks due to natural hazards in the 21st century – RISK21. Balkema, Rotterdam

Blahut J (2010) Debris flow hazard and risk analysis at medium and local scale. PhD dissertation. University of Milano, Bicocca

Blahut J, Horton P, Sterlacchini S, Jaboyedoff M (2010) Debris flow hazard modelling on medium scale: Valtellina di Tirano, Italy. Nat Hazard Earth Syst Sci 10:2379–2390

Bränström R, Kristjansson S, Ullen H (2005) Risk perception, optimistic bias, and readiness to change sun related behaviour. Eur J Public Health 6(5):492–497

Cancelli A, Nova R (1985) Landslides in Soil debris cover triggered by rainstorms in Valtellina (Central Alps – Italy). In: Proceedings of the 4th international conference and field workshop on lanslides. The Japan Geological Society, Tokyo

Ceriani M, Lauzi S, Padovan N (1992) Rainfall and landslides in the Alpine Area of Lombardia Region, Central Alps, Italy. In: Proceedings of the international symposium interpraevent. Bern

Committee on Disaster Research in the Social Sciences (CDRSS) (2006) Facing hazards and disasters: understanding human dimensions. The National Academies Press, Washington, DC

Crosta GB, Dal Negro P, Frattini P (2003) Soil slips and debris flows on terraced slopes. Nat Hazard Earth Syst Sci 3:31–42

Crozier MJ, Glade T (2005) Landslide hazard and risk issues, concepts and approach. In: Glade T, Anderson M, Crozier MJ (eds) Landslide hazard and risk. Wiley, Chichester

DEI (2006) Prezzi Tipologie Edilizie 2006. DEI Tipografia del Genio Civile. CD-ROM

Fell R (1994) Landslide risk assessment and acceptable risk. Can Geotech J 31(2):261–272

Frepazz M, Agnelli A, Drusi B, Stanchi S, Galliani C, Revel Chion V, Zanini E (2007) Terraced vineyard in alpine Environments (Vallee d'Aoste – NW Italy): an anthropogenic landscape. In: Proceedings of the 5th international congress of the European Society for soil conservation "Changing soils in a Changing World: the soils of tomorrow" Palermo, Italy

Giacomelli L (1987) Speciale valtellina 1987: Cronaca, storia, commenti. Notiziario della Banca Popolare di Sondrio, No 45, Bergamo

Gierlach E, Belsher BE et al (2010) Cross-cultural differences in risk perceptions of disasters. Risk Anal 30(10):1539–1549

Gopalakrishnan C, Okada N (2007) Designing new institutions for implementing integrated disaster risk management: key elements and future directions. Disasters 31(4):353–372

Horlick-Jones T, Jones DKC (1993) Communicating risk to reduce vulnerabilities. In: Merriman PA, Browitt CWA (eds) Natural disasters: protecting vulnerable communities. Thomas Telford, London

Lindell MK, Hwang SN (2008) Households' perceived personal risk and responses in a multihazard environment. Risk Anal 28(2):539–556

Klinke A, Renn O (2002) A new approach to risk evaluation and management: risk-based, precaution-based, and discourse-based strategies. Risk Anal 22(6):1071–1094

Lacasse S, Nadim F, Kalsnes B (2010) Living with landslide risk. Geotech Eng J SEAGS & AGSSEA 41(4):13 p

Meacham BJ (2007) Using risk as a basis for establishing tolerable performance: an approach for building regulation. In: Proceedings of the special workshop on risk acceptance and risk communication, Stanford University, Stanford

Municipality of Teglio (2009) Popolazione residente a Tresenda anno 2009. Written report

Murphy C, Gardoni P (2006) The role of society in engineering risk analysis: a capabilities based approach. Risk Anal 26(4):1085–1095

Nathan F (2008) Risk perception, Risk Management and vulnerability to landslides in the hill slopes in the city of La Paz, Bolivia. A preliminary statement. Disasters 32(3):337–357

Peters-Guarin G, Mc Call M, van Westen C (2011) Coping strategies and risk manageability: using participatory geographical information systems to represent local knowledge. Disasters 36(1):1–27

Plapp T, Werner U (2006) Understanding risk perception from natural hazards: examples from Germany. In: Amman WJ, Dannenmann S, Vulliet L (eds) RISK 21: coping with risks due to natural hazards in the 21st century. Taylor & Francis, London

Sjöberg L (2000) The methodology of risk perception research. Qual Quant 34:407–418

Slovic P (1987) Perception of risk. Science 236:280–285

Smith K (1992) Environmental hazards: assessing risk and reducing disaster, The Routledge physical environmental series. Routledge, London

United Nations International Strategy for Disaster Reduction (UN-ISDR) (2004) Terminology on Disaster Risk Reduction. Geneva. Available online at http://www.unisdr.org/eng/terminology/terminology-2009-eng.html

Wisner B, Blaikie P, Cannon T, Davis I (2004) At risk: natural hazards, people's vulnerability and disasters, 2nd edn. Routledge, London

Zaalberg R, Midden C, Meijnders A, McCalley T (2009) Prevention, adaptation and threat denial: flooding experiences in The Netherlands. Risk Anal 29(12):1759–1778

Zezere JL, Garcia RAC, Oliveira SC, Reis E (2008) Probabilistic landslide risk analysis considering direct costs in the area of north of Lisbon (Portugal). Geomorphology 94:467–495

Chapter 15
The Use of Geo-information and Modern Visualization Tools for Risk Communication

Simone Frigerio, Melanie Kappes, Jan Blahůt, and Grzegorz Skupinski

Abstract Clear communication of information is a compulsory issue in disaster risk management. This section highlights the development of interactive tools to constantly present the most recent geo-database with multi-scale and multi-source approaches, and user-oriented graphical interfaces for simple and quick data management. A client-server structure is used to customize geo-data accessibility rights and interaction and a WebGIS service architecture is designed to offer data accessibility and effective dissemination to the user community. Different solutions are presented using a common open source environment and interoperability plug-ins: (1) WebRiskCity is an educational kit on multi-hazard risk assessment,

S. Frigerio (✉)
Italian National Research Council – Research Institute for Geo-Hydrological Protection (CNR–IRPI), C.so Stati Uniti 4, IT-35127 Padova, Italy
e-mail: simone.frigerio@irpi.cnr.it

M. Kappes
Department of Geography and Regional Research, Geomorphic Systems and Risk Research Unit, University of Vienna, Austria Universitätsstraße 7, AU-1010 Vienna, Austria

Disaster Risk Management Unit, The World Bank, Urban, Water and Sanitation, 1818 H St. NW, Washington, DC 20433, USA

J. Blahůt
Department of Environmental and Territorial Sciences, University of Milano-Bicocca, Piazza della Scienza 1, IT-20126 Milan, Italy

Department of Engineering Geology, Institute of Rock Structure and Mechanics, Academy of Sciences of the Czech Republic, V Holešovičkách 41, 18209 Prague, Czech Republic

G. Skupinski
Laboratoire Image, Ville, Environnement, CNRS ERL 7230, Faculty of Geography, Université de Strasbourg, 3 rue de l'Argonne, F-67083 Strasbourg Cedex, France

Institut de Physique du Globe de Strasbourg, CNRS UMR 7516, EOST, Université de Strasbourg, 5 rue Descartes, F-67084 Strasbourg Cedex, France

T. van Asch et al. (eds.), *Mountain Risks: From Prediction to Management and Governance*, Advances in Natural and Technological Hazards Research 34,
DOI 10.1007/978-94-007-6769-0_15,

(2) Barcelonn@ supports risk management with interoperability on spatial data and metadata, (3) Historic@ is a prototype to spatially compare historical natural events and population trends, and (4) MultiRISK Visualisation Tool is a service to automatically publish multi-hazard risk analysis outcomes produced by the MultiRISK Modelling Tool.

Abbreviations

DBMS	Database Management System
XML	eXtensible Markup Language
GIS	Geographic Information System
GML	Geography Markup Language
GNU GPL License	GNU General Public License
HTML	Hyper Text Markup Language
HTTP	Hyper Text Transfer Protocol
OGC	Open GIS Consortium
SOAP	Simple Object Access Protocol
WebGIS	Web-based GIS
Web	World Wide Web

15.1 Introduction

In the context of management of disaster risk caused by natural hazards, the transmission and cognition of information is necessary. Consequently, an adequate communication infrastructure is indispensable. Cognition refers to 'the capacity to recognize the degree of risk to which a community is exposed and the capacity to act on that information' (Newman 2001; Comfort 2006, 2007). While a lack of communication (e.g. transmission delay, loss of information) is a minor difficulty, the risk cognition posed by different types of natural events and environmental contexts is a weak point (Weick 1995; Davis 2006; Comfort 2007). The information available concerning natural disasters is often inhomogeneous in scale, resolution and classification, provided by different institutions, not standardized and, as a consequence, hardly comparable (Waugh 2000; Maggi 2005). Furthermore, this difficulty is steadily amplified with high amounts of data (Comfort 2007).

In the last decades, the scientific community has developed new methodologies for the awareness of hazard assessment with innovative techniques (Glade et al. 2005; van Westen et al. 2008), but a lack of methods able to furnish useful and practical information with end-users still exists. Recent examples of education and training on natural hazards are the BE-SAFE-NET, Junior FLOODsite, NIMS

and NOAA[1] webplatforms. Considering the transfer of knowledge at assorted levels and aims (e.g. basic awareness for children, classroom for decision-makers, virtual training for civil protection volunteers), some communication systems draw attention to information stored as web-available data and offering different features of natural hazards and risks assessment (αPHRODITE, SICI, UNISDR Training Toolkit, EDURISK).[2] They are commonly designed in easy-to-use graphical interfaces for citizens, technicians and administrators with various levels of data access, responsibility and knowledge. The examples in literature underline an unclear 'graphical standard language' to share scientific output, inhomogeneous semantics (e.g. unclear map extension, unsuitable symbols or colour display, inappropriate and useless visible scale range) and generally expensive or complex solutions. Maceachren et al. (2005), Heil et al. (2010) and Maiyo et al. (2010) suggest standard criteria to highlight what information the decision-makers really need during crisis phases in terms of layers visualized, rapid data access modes and simplicity of interpretation. The meaning of scientific results, the explanation of available data and the awareness of people in charge are basic aims in risk governance, especially for non-expert users (McEntire and Myers 2004; Heil and Reichenbacher 2009).

In the context of risk communication like training, education, dissemination, sharing and decision-making support, the presented research has the purposes of:

1. Designing interactive and easy-to-use tools based on user-oriented maps and cartographic utilities able to manage, explain and compare effortlessly available geo-data;
2. Providing a multi-scale and multi-source box of information for natural events cognition to improve meaning, limits and advantages of geo-data in different case studies;
3. Adapting graphical interfaces to user-oriented requirements providing simple and quick data visualization, layers management, explanation of information, multi-users access.

The suggested technical solutions tried to cope with aims required and can be summarized in some tasks:

1. The design of a service to tailor geo-information tools to end-users' requirements, handling the results of the scientific community (e.g. past events collections, kinematic information, monitoring sensors, triggering factors)

[1] BE-SAFE-NET: http://www.besafenet.org/main/default.aspx
Junior FLOODsite : http://www.floodsite.net/juniorfloodsite
NIMS: www.fema.gov/emergency/nims/nims.shtm
NOAA: http://www.ngdc.noaa.gov/hazard/

[2] αPHRODITE: http://www.cimafoundation.org/aphrodite.php
SICI: http://sici.irpi.cnr.it/
UNISDR Training Toolkit http://www.uncclearn.org/unisdr-toolkit
EDURISK: http://www.edurisk.it/eng/the-project.html

in a level-headed example of risk knowledge (e.g. explanation of metadata, simplification of maps, crossed information, features comparison);
2. The sorting of data hierarchy for thematic features depending by context criteria like thematic clusters for training, scale-range clusters for dissemination or combined clusters for decision-making support;
3. The establishment of on-line guidelines to clarify meanings of data and metadata and suggesting potential interaction between data and support users;
4. The development of tools to issue specific aims of cartographic interoperability on available layers;
5. The proposition of an easy-to-access environment both for usability, data upgrading and structure customizations;
6. The avoidance of complex software environment, simplification of data management system and reduction of cost of design and maintenance.

The proposed methodology is based on Web-based services, applied on different case studies.

15.2 WebGIS and Geo-information as a Possible Practical Arrangement

Web-based services started in the late 1980s and were originally interface to systems which had to be accessed by user and not through the Web. A second wave of Web-based services was designed on the basis of simple Web technologies like Hyper Text Transfer Protocol (HTTP) and eXtensible Markup Language (XML) to implement programming interfaces and customized applications. A more recent third wave of Web-based services added lighter-weight protocols like Simple Object Access Protocol (SOAP) and ad-hoc design approaches to merge or mash-up information or services primarily for use by individuals. At the end of the 1980s, Geographic Information System (GIS) were centralized and needed expert knowledge for successful operation. In the early 1990s, GIS started to recognize the benefits of Hyper Text Markup Language (HTML), with HTTP and the World Wide Web (Web). Most of the information available in the world started to be accessible via Web towards standard protocols (e.g. HTTP, SOAP) and the same was true concerning geospatial data whose contents are more visible and open, making the accessibility of spatial features easy (Dragićević 2004). Collecting and sharing geodata via networks became a fundamental issue and the Web-based services started to be recognized by GIS community as a practical instrument to transfer spatial data (Kraak and Brown 2001; Lehto and Sarjakoski 2005). With Web connections getting faster, the information that can be transferred is amplified, hence data analysis by a widely spread group can also be accomplished in a rapid and more efficient manner even though the information may be scattered over the World. Consequently, a static visualization of geo-information is renovated in a client-server design with the development of geovisualization with cartographic

tools and interactive maps (Kraak and Brown 2001). The integration of GIS and Web started to cope with new research topics (Kraak and Brown 2001; Green and Bossomaier 2002; Peng and Tsou 2003; Dragićević 2004; Dragićević and Shivanand 2004) such as:

1. Spatial data access and dissemination in which basic GIS tools and the Web environment are combined to offer user-friendly and dynamic access to the maps towards simple visual structure. Interoperability of spatial data is provided by a Geography Markup Language code (GML) while several open standards specifications managed by the Open GIS Consortium (OGC) deal with the retrieval and access to geographical information;
2. Public user participation in spatial decision-making with interactive tools. Web-based services supply needs to interact dynamically with features and information and offer communication between geographically dispersed stakeholders;
3. Spatial data analysis, processing and modelling offered in a Web frame. Web users are enabled to obtain data, perform visual analysis and produce maps by means of specific tools and an adjusted user interface.

Henceforth, the presented research deals with the first and the second topics previously explained. The third one is not included since the basic aim needs of a common and parallel tool of knowledge and communication, in which data is continuously updated by local client application and not posed by a Web-based processing.

In few years, Web-based services were integrated with GIS systems in several solutions like Internet GIS, On-line GIS, distributed GIServices and Web-based GIS (Dragićević 2004). Web-based GIS (WebGIS) is the solution adopted because it is a capable way to access and disseminate geospatial data (Tsou 2004) collating multiple users entries over the Web (Nappi et al. 2008). With the objective to facilitate the cognition of the provided information, a WebGIS environment should offer the information structured in a manner that allows the user to gain, first, a rapid understanding of complex problems like natural risks, to exchange a wide set of file formats (maps, text, graphs, links), to use the multi-dimensional spatial information for decision-making. Second, the Web environment provides a not-time limited participation of multiple stakeholders including the general public (Evans et al. 1999; Huang et al. 2001; Peng and Tsou 2003; Burdziej 2011). The reason is that a 'WebGIS denotes a type of GIS, whose client is implemented in a Web browser' (Yang et al. 2005), therefore multi-users interaction is allowed by the same Web service, whose structure directly converge users at the same data storage avoiding any stand-alone software installation. Especially in a network of stakeholders involved in risk issues, such WebGIS services can offer visualization, exchange information produced by actors involved and gain advantage on a quick transfer of data (Romang et al. 2009; Frigerio and van Westen 2010). Furthermore, several dataset without well-defined management systems, clear mapping output and graphical tools do not guarantee either organizational performance among decision-makers and spatial planners or clarity among normal citizens (Holland 1995; Maggi 2005). This point includes the difficulties arising with crossing and

overlaying available spatial information. For instance, in a multi-hazard context it is practically impossible to communicate information on the hazard or risk level due to several natural threats in detail in one single map. A partition of information on multiple maps is necessary to clearly transmit the information inherent in the different data files. Consequently, users need adjusted and easy-to-use tools with simple interfaces and a user-friendly approach to emphasize and exploit available information.

A WebGIS architecture in an open source environment is the easy-to-use technique designed. The traditional GIS data package is integrated with cooperative, scalable and customizable solution, sharing spatial data using the web and following last year's trend in risk assessment and disaster management (Peisheng and Yang 1999; Brabhaharan et al. 2001; Fan-Chieh et al. 2007; Lehto 2007; Herrmann 2008; Balducci et al. 2009; Rivas-Medina et al. 2009; Salvati et al. 2009). It is compiled as a free open Web-based service and consequently the installation of costly software can be avoided since a Web browser is sufficient for user's interaction. A clear advantage is the ability to collect a dataset from heterogeneous sources, scales and resolutions along the network (Maiyo et al. 2010) with standard geospatial services predefined for more suitable information (e.g. by Registry Office, Regional Geo-Portal). Dataset and spatial analysis are developed by individuals but a Web-based mapping and GIS tools support a different-place collaboration for geospatial information retrieval from distributed databases. Maps are seen as a central tool in Web environment, serving as both information repositories and vehicles for communication and empowering local communities by virtual spaces for geospatial interaction (MacEachren 2001).

A proposed client-server structure supplies geo-data accessibility rights and levels of user-oriented interaction like stakeholders, technicians or students with customized profiles. Geospatial information is stored in Web clusters with thematic criteria (e.g. location, temporal range, feature type) and a visual correlation copes with different scales, metadata, attributes, classifications and online explanation. Special attention has to be paid to the clarity and readability of the maps. They are formed by layers derived from different sources (modelling output, monitoring loggers, external contribution), but their meaning has to be scientifically meaningful and practically produced. An example is the classification of a final map (e.g. hazard map, susceptibility map, multi-hazard map) that has to be simple but suitably effortless and comprehensive. A minimum number of classes should keep the map more understandable for the end-users although it is of high importance to show the uncertainty of the maps in a written or graphical way. A common structure has been proposed for different case studies to get the advantage of a similar and flexible frame to different needs of communication.

In the proposed research a WebGIS service architecture has been designed to open data accessibility and effective dissemination at multiple levels in the user community. The experiences gained in the MOUNTAIN RISKS project are presented in contexts of training, education and data interaction.

15.3 The Designed WebGIS Solutions: WebRiskCity, Barcelonn@ and Historic@

Three WebGIS solutions are set up using a common free open source environment and Database Management System (DBMS), composed of multi-source data access and geospatial plugins. The architecture is a ready-to-use WebGIS solution built on Mapserver[3] as open source environment for spatially-enabled internet application, released under the free and copyleft GNU General Public License (GNU GPL License).[4] A large list of open source softwares could be used for the purpose (e.g. Pmapper, Cartonet, Geoserver, Geonetwork) and further upgrade is continuously provided by network developers. For the planned activities a Web-based service is provided (Fig. 15.1) using SOAP[5] protocol and CartoWeb[6] as comprehensive WebGIS solution. The choice of CartoWeb is due to its clear modular and object-based structure able to customize personal visualization requirement (Frigerio and van Westen 2010). The platform has a core map-interface while users can activate other tools like spatial multi-query, annotation and labelling, drawing and

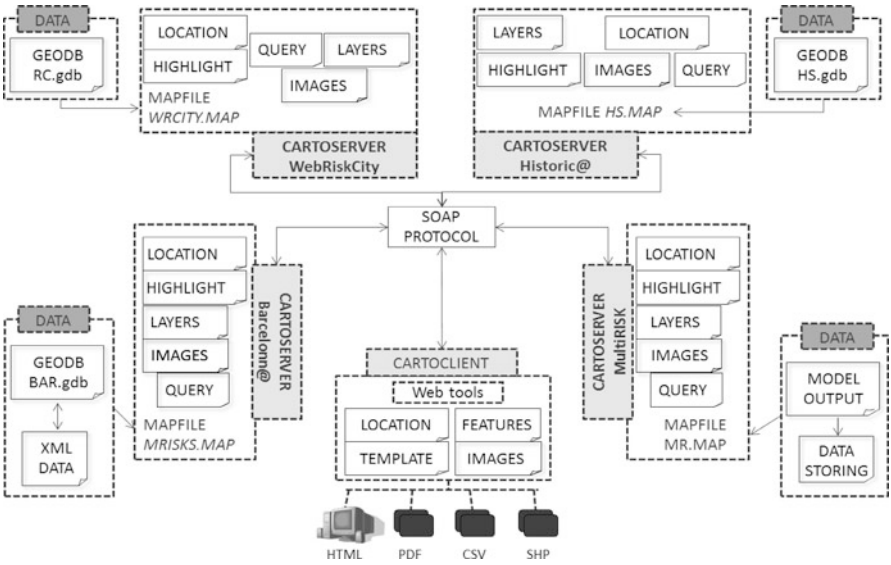

Fig. 15.1 Mapserver/Cartoweb platform. Four WebGIS with a server-side environment (CartoServer) are interacting with a client-side browser by SOAP protocols

[3]Mapserver: http://mapserver.org/

[4]GNU licence: http://www.gnu.org/licenses/gpl.html

[5]SOAP protocol: http://www.w3.org/TR/soap/

[6]CartoWeb: http://www.cartoweb.org/

measuring, PDF creation and other export formats, on-line support for features and metadata. CartoWeb is composed of a set of standard plugins activated and adapted for the project aims. The user can visualize type and resolution of the archived data, compare geo-spatial information, prepare queries according to his proper goals, download raw-data tables for outside elaboration, and create a personal layout with new-drawn shapes and labels. All the interested parties involved can use information located on a Web-based service and benefit from the meaning of published thematic features contributing to an idea of democratization of spatial data (Dragićević 2004). These advantages of Web-based service have led to a growing number of projects aimed at opening the access to spatial information and cartographic tools for both citizens and decision-makers seriously considered in last year's approach to natural risks management (Boroushaki and Malczewski 2010; Burdziej 2011).

Users can dynamically approach spatial data and this interoperability is desirable for various reasons (Hecht 2002):

1. Communication between information providers and end users is independent of geoprocessing and viewer software;
2. Database and geospatial sources regarding natural risks are growing quickly and the WebGIS offers a standardization of formats and visualizations;
3. It is more efficient and time-effective to maintain and upgrade data on one server-side allowing on-line access and interaction for users, and;
4. Multiple users including non-GIS experts can access specific sets of data with different levels and permissions.

A first training case study encloses an area of ca. 14 km^2 in Tegucigalpa (Honduras) where Hurricane Mitch caused a huge flood and an old landslide reactivation destroyed the entire neighbourhood in 1998. As a domino effect the landslide blocked the river causing serious flooding in large parts of the city for several weeks (Soeters and van Westen 1996; Mastin and Olsen 2002; Harp et al. 2002; Castellanos Abella 2008). In Barcelonnette (France) and the Consortium of Mountain Municipalities of Valtellina di Tirano (Italy), some areas are prone to mass movements and have been deeply studied (Crosta et al. 2003; Malet et al. 2003; Maquaire et al. 2003; Moine et al. 2009; Blahut et al. 2012).

Four server-side frames (Fig. 15.1) are created (CartoServer) using a common client structure (CartoClient): (1) WebRiskCity[7] is the integrated Web-based service of RiskCity, an educational kit on multi-hazard risk assessment designed in the Tegucigalpa study area; (2) Barcelonn@[8] is a WebGIS solution for risk management with interoperability on spatial data and metadata designed in the Barcelonnette study area; (3) Historic@ is a WebGIS prototype to spatially compare historical natural events and the evolution of the population designed for the Valtelinna di Tirano study area; (4) MultiRISK Visualisation Tool is a Web-based service to

[7]WebRiskCity: http://geoserver.itc.nl:8181/cartoweb3/WebRiskCity/WebRiskCity.html

[8]Barcelonn@: http://eost.u-strasbg.fr/omiv/main-page.html

upgrade and publish multi-hazard risk analysis features produced in the MultiRISK Modelling Tool. All the frames have plugins for data interoperability commonly designed on the CartoServer and distributed on each CartoClient: (1) Header (Login, language translator); (2) Mapping (Navigator and visualization maps); (3) Thematic sessions; (4) Cartographic commands (editing, querying, sketch drawing, outlining, printing, scaling); (5) Plug-ins tabs (themes, search, outline, query, print, about, help viewer), and; (6) Data clusters (layer, legends, classifications, hyperlinks).

15.3.1 RiskCity

RiskCity is a distance-education course created in a free open GIS environment for training in multi-hazard risk assessment and is designed especially for users from developing countries who should not be restricted in using the package due to the financial burdens of the software (van Westen 2008). In the course, it is possible to interact with virtual classmates, proceed step-by-step, receive instructions and support from tutors and to submit the results for every risk assessment task. The distance-education course deals with procedures in collecting, analysing and evaluating spatial information for natural and human-induced hazards. Users have access to information on earthquakes, flooding, technological hazards, and landslides. Hazard assessment procedures, generation of elements at risk databases, vulnerability assessment, qualitative and quantitative risk assessment methods, risk evaluation and risk reduction are the actions planned in the training course. Despite a lot of output provided from previous research in the study area the information required for a multi-hazard risk assessment is not complete and consequently some additional 'scholar' training features integrate the original available dataset (Frigerio and van Westen 2010).

WebRiskCity is the Web-based service designed simultaneously to RiskCity in which every feature of the education course is visualized by Web mapping and explained by an online guide as a major new trend in cartography-based transfer of knowledge (Frigerio and van Westen 2010). Users can compare their training output with published results and can simulate the usefulness of a Web-based service with interactive and user-oriented maps. WebRiskCity allows understanding of spatial features produced on the course and the requirements of stakeholders (Figs. 15.2 and 15.3).

The dataset has a clustering hierarchy of layers and maps. Tabs convoy user's activity to specific Web maps uploading automatically blocks, drop-down menus and graphical options. Seven data tabs are used (Fig. 15.3): (1) Introduction to WebRiskCity; (2) Spatial data and image interpretation; (3) Hazard assessment, (4) Elements at risk charactetisation; (5) Vulnerability assessment; (6) Risk analysis; (7) Risk reduction.

WebRiskCity has a visual-friendly and distributed frame to handle the following purposes: (1) Enhance interoperability results of RiskCity spatial analysis (e.g. script activities, mapping creation, image processing) on a public Web client-

Fig. 15.2 WebRiskCity starting page. Users can direct on visualization kit or select online guide on data type, activities required and explanation of dataset

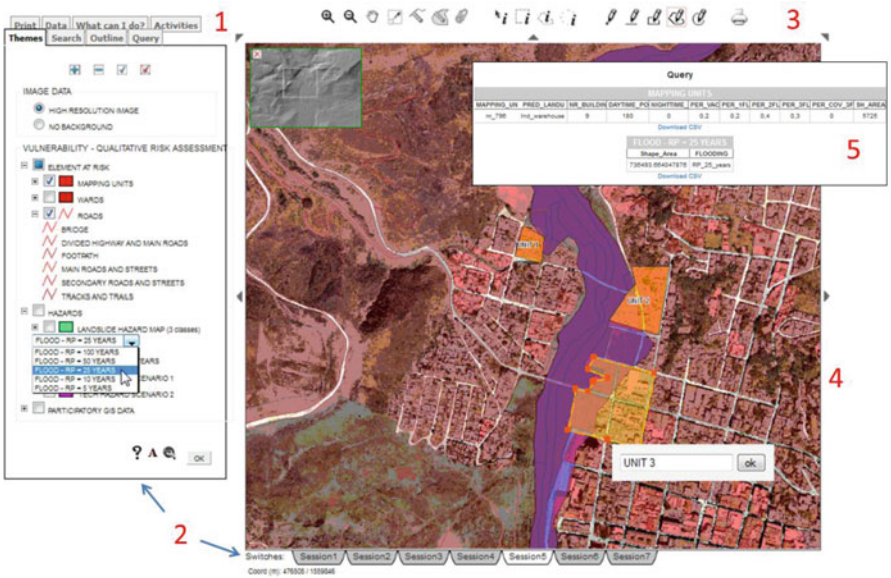

Fig. 15.3 WebRiskCity visualization: *1* tabs for instruction and plugins offered (e.g. layers management, printing, instructions, searching, outlining), *2* layer tree with charts, menu, scale dependency. The information visualized is controlled by seven data tabs synchronized with the RiskCity dataset, *3* geospatial tool kit for querying and outlining, *4* map layout, *5* query charts (CSV export is available)

side avoiding stand-alone GIS environment; (2) Provide hierarchic structure to the features fitting training concepts of distance-course; (3) Create multiple light-weight and proof-of-concept frame of sharing data (Latini and Kobben 2005); (4) Offer user-friendly tool for in-context integration of multiple risk assessment features without being a GIS expert, and; (5) Train on spatial output comparison in a context

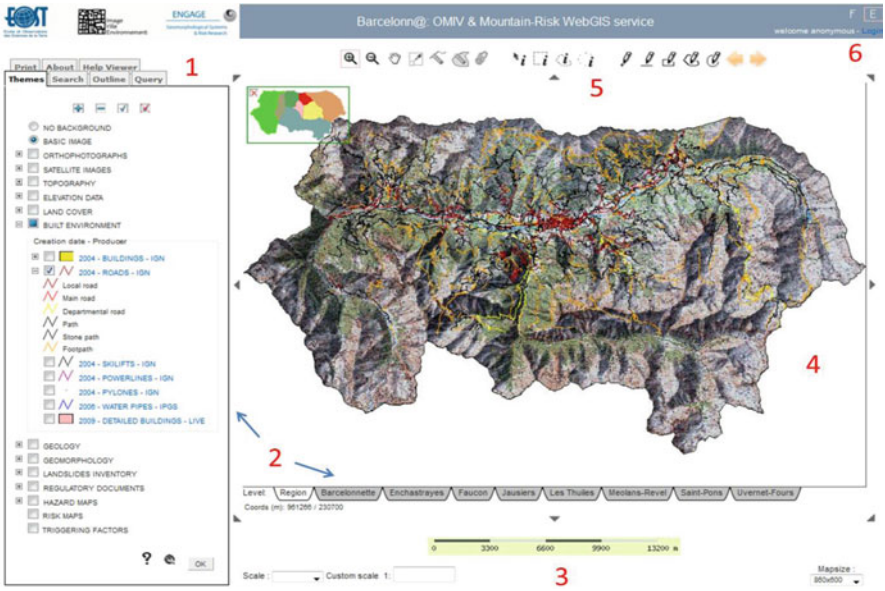

Fig. 15.4 Barcelonn@ visualization: *1* tabs for instruction and plug-in list, *2* layer tree with charts, menu, scale dependency. The information visualized is controlled by several switches. The dimension of dataset requires a split on PostgreSQL database, *3* scale bar and map size customization, *4* map layout, *5* geospatial tool kit for querying and outlining, *6* English-French translation tool

of multi-hazard risk management and disaster decision support (e.g. comparison of multi-hazard scenarios, cost-benefit analysis, estimation of buildings and population involved, potential losses, spatial multi-query on risk data).

15.3.2 Barcelonn@

Barcelonn@ is a WebGIS designed with a geo-spatial easy-to-use toolkit to supply reliable data access and transfer of information related to natural events. Data gathering, sharing, and interoperability have been the main goals in this frame, proposing a system to decrease the disparity between scientific output and stakeholders' practical needs like friendly visualization and rapid mapping feedback. The wide collection of information related to the local hazards and risks analysis (e.g. past landslide events, susceptibility maps, information on elements at risk, cadastral maps, triggering factors) enables collaborative geo-information access and comparison as a feasible support to end-users requirements (Frigerio et al. 2010b). The last years' activity in Barcelonnette study area is collected in a geodatabase integrating huge amount of geographic features, attribute tables, documents, reports and images whose spatial information is linked with external masks (Figs. 15.4 and 15.5).

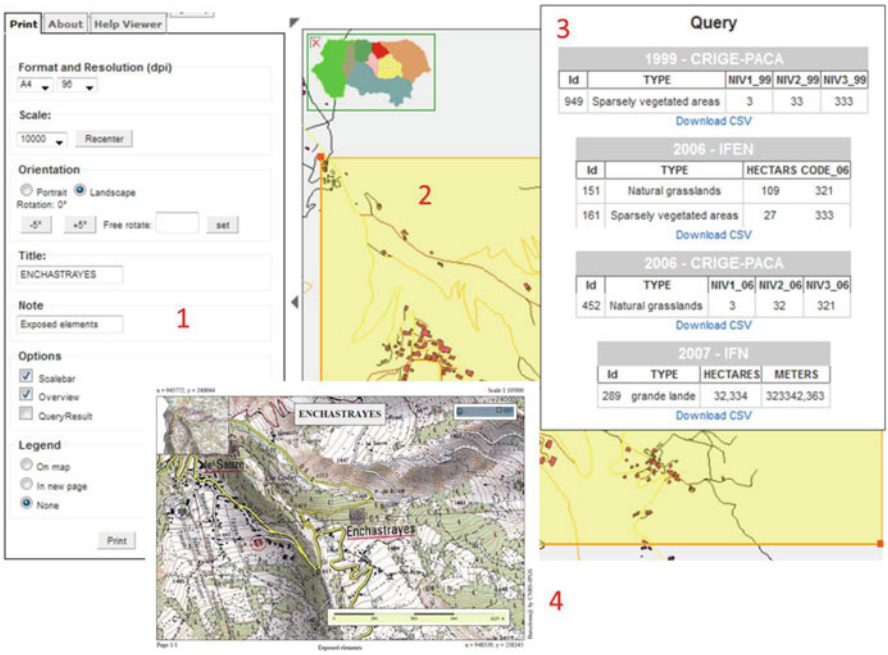

Fig. 15.5 Tab for printing tools: *1* users can customize the layout at high resolution selecting parameter of visualization, *2* shape defined on the map for screenshot capture, *3* query for multiple layers can be included in the layout, *4* final PDF generator

All published features address a metadata presented in XML and HTML format, ready-to-use on Web browser and grouped by typology clusters (Fig. 15.6). Easy to share and upgrade, metadata provide a global mirror of parameters and standards for published layers. They capture the characteristics of *Barcelonn@* geospatial dataset including: (1) Core library catalogue elements (e.g. title, abstract, author, standard used, publication date, purpose of data); (2) Geographic elements such as projection information and geographic extent, and; (3) Database elements such as attribute label definitions and attribute domain values.

In Barcelonn@ the information is arranged in geospatial thematic and metadata clusters whose contents are: (1) Orthophotographs multi-temporal catalogue; (2) Satellite images: (3) Topography; (4) Elevation data; (5) Land Cover; (6) Built environment; (7) Geology; (8) Geomorphology; (9) Landslides inventory; (10) Regulatory documents, and; (11) Hazard maps. Data groups have different storage criteria enabled by users on the Web interface: (1) Typology (e.g. contour lines and Digital Elevation Model inside the Elevation data cluster); (2) Date of production (e.g. 1984 till 2010 for satellite images); (3) Resolution (e.g. 15 m for contour lines 2001 and 10 m for contour lines 2008); (4) Producer (e.g. Institut Geographique National for Land Cover 2000 and Institut de Physique du Globe de Strasbourg for Land Cover 1931). Barcelonn@ has three levels of geodata visibility published on

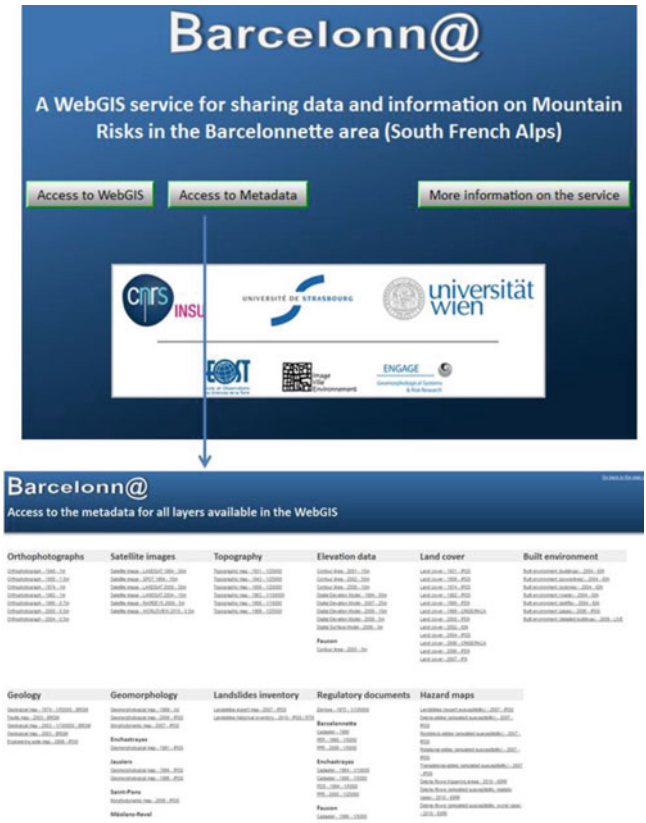

Fig. 15.6 Barcelonn@ starting page. Users can direct on visualization kit or select metadata management. All layers are listed and linked to their metadata by thematic clusters. A description of the study area is also supplied

a scale-based criterion: (1) Local single slides or debris flow catchments (Super-Sauze, La Valette, Sanières, Bourget); (2) Municipalities dataset (Barcelonnette, Enchastrayes, Faucon, Jausiers, Les Thuiles, Meolans-Revel, Saint-Pons, Uvernet-Fours), and; (3) Region dataset (Vallée de l'Ubaye).

15.3.3 Historic@

Historic@ is an ongoing WebGIS for the Community of Valtellina di Tirano whose aim is the multi-scale spatially comparison with geo-statistical criteria between the historical database of natural events and the evolution of the population. The purpose is a visual solution able to support risk perception evaluation in mountain

areas towards distribution of natural events and the population trend. The first methodological step provided a geo-spatial database, achieving: (1) Historical data on landslides and floods from 1600 to 2008 in the study area, organized by spatial location, type, date, producer and general description; (2) Registry office and past census surveys on inhabitant distribution at local scale (1:10,000). The historical catalogue supplies some tasks listed in Frigerio et al. (2010a).

The study case is historically affected by natural events and data collected from local and regional sources provides information on landslides (debris flows, mudflows, earth flows and rock falls) excluding floods whose data availability is statistically inadequate (Blahut et al. 2012). Historical data is integrated with external information (newspapers, documents) and thus spatial error or redundancy of reported events are corrected (e.g. multi-sources events with same location, different survey scale and methodology) obtaining a homogeneous database at 1:10,000 scale with standard metadata (date, type of event, damage reported, projected coordinates).

The database has collected 615 events in 505 sites with different accuracy on date of occurrence. The event-per-site ratio revealed a peak of 450 sites with single event despite 1 single site with 7 occurred events. A spatial distribution analysis compared the location of historical events with the area of occurrence and temporal information, and as matter of fact from 1983 to 2008, 195 events cover the 55 % of the entire database, especially in 1983 and 1987, including the most impressive events recorded in all of the valley (Crosta et al. 2003; Blahut et al. 2012). A deeper analysis in monthly distribution provides details on high peak level of events before 1950 concentrated in August–September–October (64 % of the events) while in the most recent period two peaks of recorded events can be distinguished (May–July and October–November) covering 77 % of the events. The incompleteness and inhomogeneous quality of the catalogue, the change of slope stability parameters (land use type, morphology) and meteorological conditions could influence the temporal pattern evaluated with a further detailed analysis. Considering the time series 1861–2010, an evaluation on population distribution at local scale highlights a temporal pattern for all community (high peak reveal 31.301 inhabitants in 1911 against a lower peak on 1931 with 28.699 inhabitants) or for single municipalities (e.g. fastest escalation on Tirano in last 80 years or Teglio as quickest reduction). Touristic improvement, social behaviour or traditional local handicraft activity are potential tasks whose meaning engages a more complex multi-disciplinary challenge in the analysis. A rising number or events for all the municipalities poses attention on a real increasing local hazard, but at a normal average of population trend should discloses a low level of landslide risk perception. Including a lot of parameters in the analysis is a compulsory challenge (triggering factors, awareness and knowledge of people about risk, accuracy of data, social approach), but a kind of easy-sharing technique and simple tools like a Web-based service can be a real support and useful instrument for this aim.

15.4 Multi-hazard Risk Analysis: The MultiRISK Visualization Tool

Multi-hazard visualization is a challenging topic since it involves a high quantity of information and a multitude of stakeholders with many different objectives and interests (Kappes et al. 2012a). Analogue maps reach their limits in a multi-hazard context since a whole set of them would be necessary to communicate the information to the different actors. GIS-tools, in contrast, offer interactive comprehension, however profound GIS and cartographic experience is necessary to deal with the multi-hazard topic. While a scientific-based analysis should provide a concrete approach to multi-hazard risk issue an impractical interface can seriously slow down data access for both stakeholders and decision-makers. A Web-based visualization of GIS-tools has the advantage for end-users of managing several maps and tables produced by spatial geoprocessing, avoiding complex overlapping, incomprehensibility of information and isolation of specific features. Consequently WebGIS provide the opportunity to share the information via the web easily with a large quantity of end-users and interested parties (MacEachren and Kraak 2001). The objective of this study is therefore to develop a visualization tool which enables the clear and interactive transmission of multi-hazard analysis information.

Related to the MultiRISK Modelling Tool, the MultiRISK Visualisation Tool is a free open WebGIS designed on CartoWeb client-server solution, generally described in the previous session. The files produced with the Modelling Tool are automatically transferred in specific folders by user-friendly charts from which the Visualisation Tool is taking the data to depict them (Fig. 15.7).

MultiRISK Visualisation Tool can automatically store and share the information, improving visibility of geospatial output, clarity of information meaning and ease on data comprehensibility toward internet browser. Thematic clusters on server-side automatically enclose the information provided by modelling tool and the geospatial features are consequently fixed inside the WebGIS.

The frame is originally compiled on localhost environment previously settled with MapServer and Apache HTTP Web Server to supply respectively a geospatial engine and Web compatibility. The choice of a stand-alone package at the beginning is due to: (1) A quick software-refresh availability during development; (2) A permanent test between client- and server-side to reduce time-consumption on platform usability; (3) A feedback from local server whose structure can easily pass to a Web-hosting service. The interface of the MultiRISK Visualization Tool consists of seven distinct tabs (Fig. 15.8) which present different aspects of the multi-dimensional analysis results (refer to Kappes et al. 2012b).

- ‘General settings’: information on the study site. The dataset includes in first place modelling input of hazard models (land use and lithology and DEM-derived layers such as hillshade, slope or planar curvature). Users get the possibility to be acquainted with the study area and geomorphological parameters (Fig. 15.9).
- ‘Single hazards’: the modelling results of each single-hazard susceptibility analysis are shown in detail to enable users to identify hazard-specific patterns.

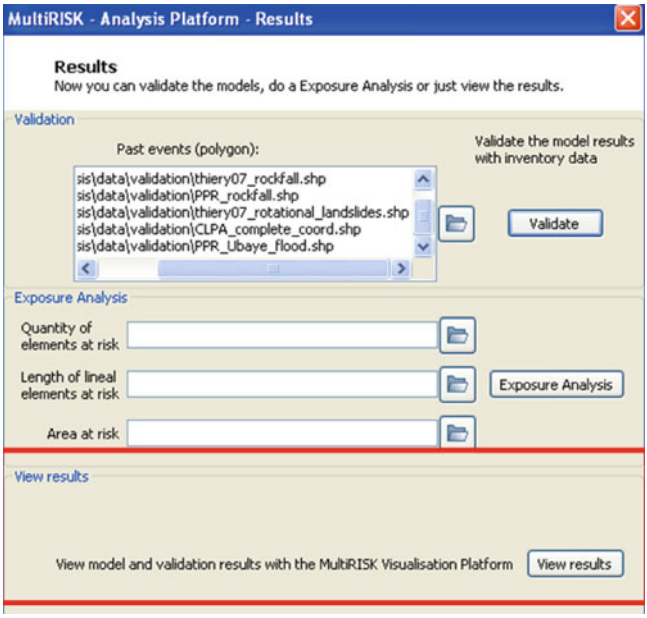

Fig. 15.7 MultiRISK Modelling Tool provides several customizations for users. They are managed by different charts and easy-to-use buttons. MultiRISK Visualisation Tool can be updated (*red shape command*) and results automatically posed on Web frame

Fig. 15.8 Thematic bar. User can select data groups and visualize the layers for each modelling task. The 'Elements at risk' data group is available for all the tabs

Overlays of multiple processes are not allowed to avoid confusion, but users can select independently checkboxes for sources and runout areas (Fig. 15.10).

– 'Overlapping hazards': up to three hazards can be overlaid to facilitate the identification of those areas susceptible to the occurrence of several processes. Each hazard is represented by a style (colour, pattern and transparency) whose combinations provide ease in overlay of processes (Fig. 15.11).
– 'Number of hazards': with the combination of four or more overlaying hazards the clearness of the depiction gets lost since too many different combinations exist. Therefore in this map only the number of overlaying hazards is presented without even indicating which ones. By a spatial query, the user can inquire which hazard combination leads to the respective number (Fig. 15.12).
– 'Past Events': visualization of past events used for the validation process with different symbology. User can select with a dropdown menu the type of hazard and choose sources or complete area involved (Fig. 15.13).
– 'Validation': the results of the validation are depicted by (1) areas modelled and recorded (true positives) (2) not modelled but recorded (false negatives) and (3)

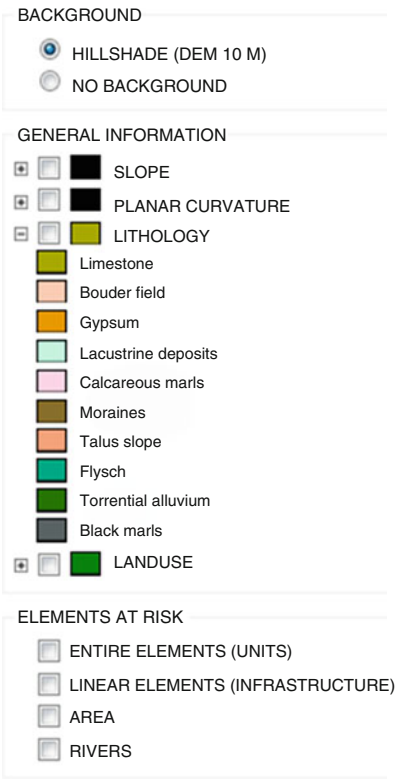

Fig. 15.9 Data groups and layer tree for the 'General settings' tab

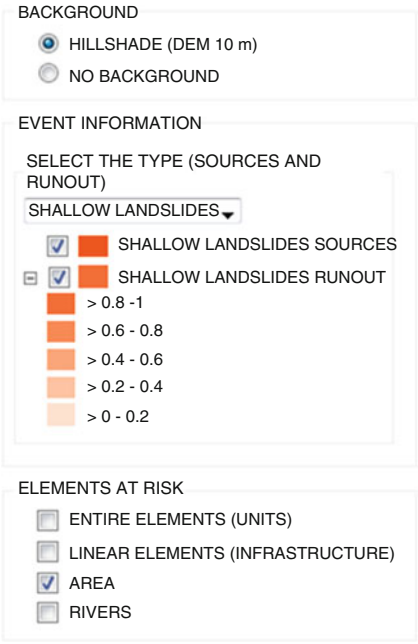

Fig. 15.10 Data groups and layer tree for the 'Single hazards' tab

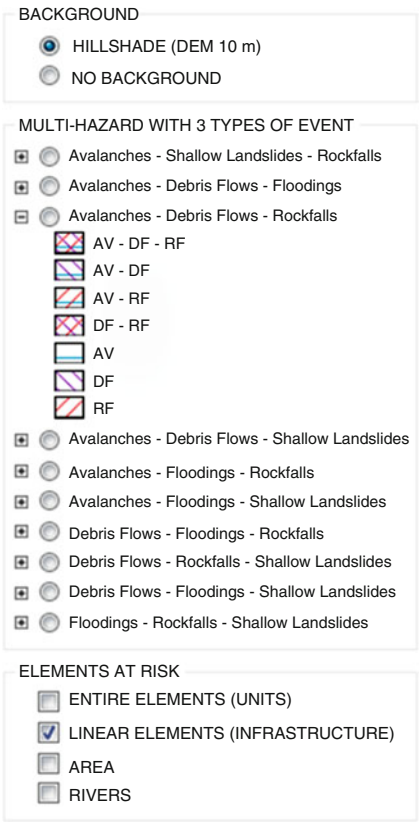

Fig. 15.11 Data groups and layer tree for the 'Overlapping hazards' tab

modelled but not recorded (false positives). Users can visualize validation maps properly for type of event and involved area (e.g. validation map only for sources in debris flow) and the pixel comparison can be illustrated in confusion matrices by hyperlink table (Fig. 15.14).

– Exposure: the elements exposed to different hazards are displayed together with their proper single-hazard areas. A drop box menu splits visualization in elements exposed to the complete susceptible area or limited to source area. By means of a hyperlink the exposure matrices offering information on the quantity of exposed elements in terms of number of affected elements, length and area compared to the total source or complete area is provided in a separate internet tab (Figs. 15.15 and 15.16).

This version of the MultiRISK Visualization Tool offers a discussion basis for further developments towards the actual needs of specific users. Additionally, a modification towards the implementation of a logon procedure and subsequent visualization of different contents adapted to the specific user group could additionally facilitate a targeted communication of the information. The level of information accessible for each user group can thereby be clearly defined and the presentation to the specific needs adjusted.

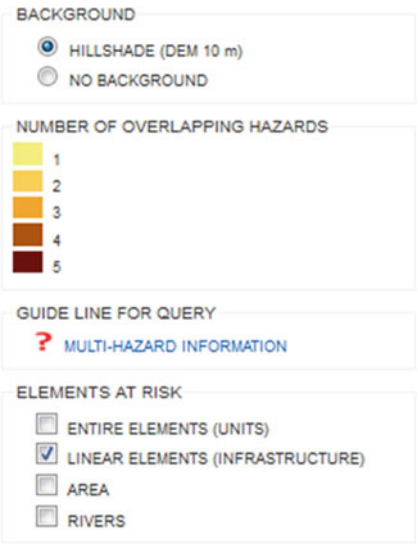

Fig. 15.12 Data groups and layer tree for the 'Number of hazards' tab

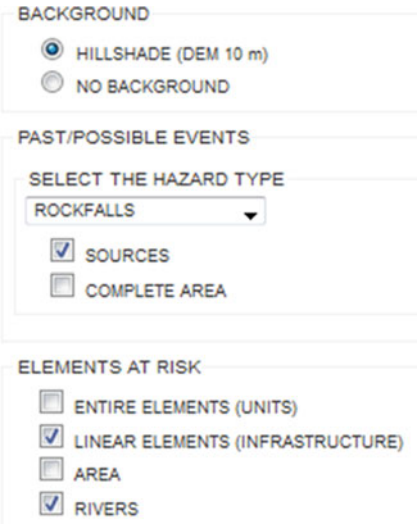

Fig. 15.13 Data groups and layer tree for the 'Past Events' tab

15.5 Conclusion

Risk cognition is a complex issue and includes perception of natural events and consequent reaction (e.g. trigger insight and emergency response). Thus preparedness and response are strictly linked to the meaning of data and the capacity to transfer correct information. We focus straightforwardly on communication technique combining solutions with GIS-tools and Web-based services. Modern visualisation tools provide a significant contribution to the dissemination of knowledge about

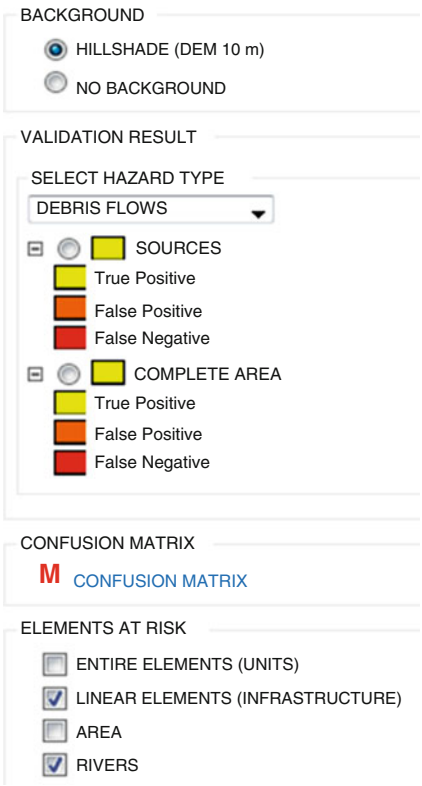

Fig. 15.14 Data groups and layer tree for the 'Validation' tab

disasters and risk communication, serving as an important source of information for both, experts and general public and highlighting interoperability in the transfer of knowledge, based on simplicity, clearness, flexibility and direct access of information. We proposed an approach for designing comprehensible and multi-user enabled interfaces (Goodchild 1999; Maceachren et al. 2005) accessible by Web browser in different contexts. The browser handling provides the possibility to customize every activity and application, pondering what is the real need of the end user in risk communication.

A common client-server structure has been designed combining a free open source environment with Web potentialities. The advantages are a customizable architecture for research tasks with no-cost development and a geographically shared service, applied for different contexts on risk communication.

WebRiskCity is a learning and training solution synchronized to the multi-risk training package RiskCity. The service offers an instrument to increase knowledge in multi-hazard assessment, combining GIS-based analysis performed on distance course and Web-based data mapping. Users can learn multi-risk methodology step-by-step in RiskCity exercises and guidelines and simulate disaster management using the output maps and Web tools. A similar structure is built on MultiRISK

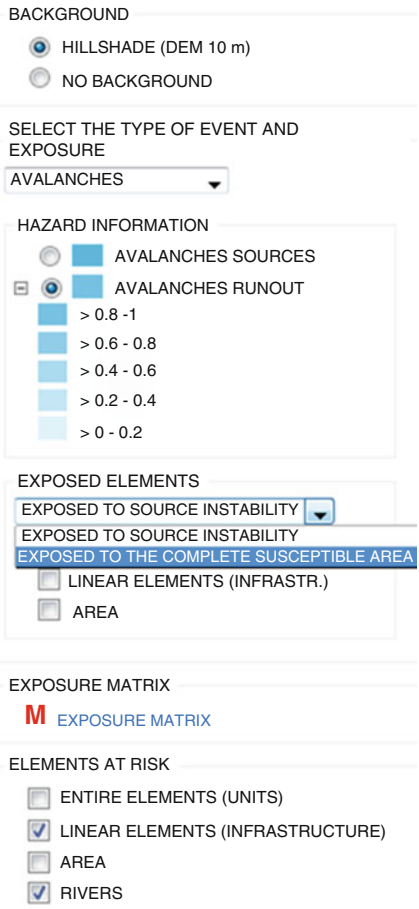

Fig. 15.15 Data groups and layer tree for the 'Exposure' tab

Visualisation Tool where a client-side environment is linked by a user-friendly interface to the modelling output supplied by MultiRISK Modelling Tool. In this case study the outcome is the synchronization client- and server-side where users can personally generate information afterwards visualized automatically by Web service. Barcelonn@ is solution for dissemination, sharing and transfer of knowledge. It is designed with a free database management system able to publish on browser a huge dataset related to natural events, provided by several agencies, produced at different scales and time range. Layers are grouped in thematic or geographical clusters to allow an organized interaction between potential decision-makers and the most complete spatial database available. Finally Historic@ is an on-going WebGIS for multi-scale spatial comparison between the historical database on distribution of natural events and the evolution of the population.

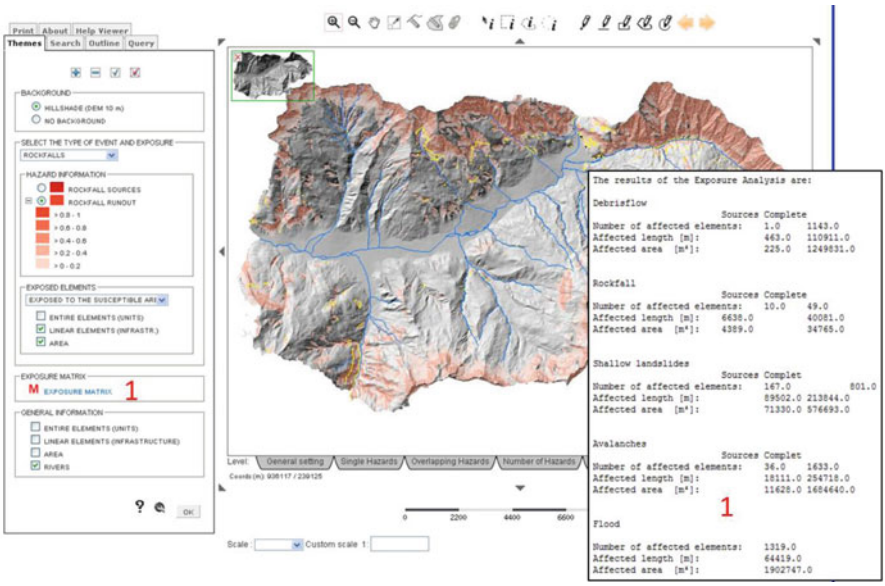

Fig. 15.16 Hyperlink to exposure matrix produced in the 'Exposure' tab. Users can compare the exposed features with the entire dataset on elements at risk in the study area whose content is available at *bottom* of all thematic tabs

However, in the field of risk communication using modern visualization tools there are still some challenges that need to be addressed such as the lack of homogeneous language (Fabrikant and Buttenfield 2001), and still not sufficient user-friendly applications. Information systems used in the field of disaster management are often not as open and comprehensive as needed to integrate and accommodate the complex data sets and the different systems. Information provided by modern visualisation tools has to be clear, readable and easy for transfer of knowledge, because correctly shared information educates and improves awareness of natural events. A Web interface proposed with easy-to-use functions is an important goal in risk communication tools and WebGIS usage, preferentially open source and customized. Key questions to improve the quality of the system are how to simultaneously display multiple layers and establish rules controlling overlays, which symbology kit, colour scheme or style to adopt, how to correctly manage overlapping property to allow a single data visualization or a 'group of layers' patterns.

Providing an interface for risk communication requires attention to the users' needs at all stages of design and development, in summary, a 'human-centred' approach. The frame proposed a system to collect the advantages of the available information inherent the natural hazards and risk, posed a graphical and helpful solution to directly interact with available dataset and requirement of final users.

References

Balducci V, Tonelli G, Reichenbach P, Guzzetti F (2009) Webgis e dissesto idrogeologico. Paesaggio Urbano 1:18–22

Blahut J, Poretti I, Sterlacchini S, De Amicis M (2012) Database of geo-hydrological disasters for civil protection purposes. Nat Hazards 60(3):1065–1083. doi:10.1007/s11069-011-9893-6

Boroushaki S, Malczewski J (2010) Measuring consensus for collaborative decision-making. A GIS-based approach. Comput Environ Urban 34(4):322–332

Brabhaharan P, Fleming MJ, Lynch R (2001) Natural hazard risk management for road networks. Part I: risk management strategies, Research report number 217. Transfund New Zealand, Wellington

Burdziej J (2011) A web-based spatial decision support system for accessibility analysis – concepts and methods. Appl Geomat (3) Online First™, Springer Link. doi: 10.1007/s12518-011-0057-x

Castellanos Abella EA (2008) Multiscale landslide risk assessment in Cuba. Dissertation (154), Utrecht University, Utrecht, ITC. ISBN: 978-90-6164-268-8

Comfort LK (2006) Cities at risk: Hurricane Katrina and the drowning of New Orleans. Urban Aff Rev 41(4):501–516

Comfort LK (2007) Crisis management in hindsight: cognition, communication, coordination, and control. Public Admin Rev 67(s1):189–197

Crosta GB, Dal Negro P, Frattini P (2003) Soil slips and debris flows on terraced slopes. Nat Hazards Earth Syst Sci 3:31–42

Davis T (2006) A failure of initiative, the final report of the select Bipartisan Committee to investigate the preparation for and response to Hurricane Katrina. Government Printing Office, Washington, DC. http://katrina.house.gov/full_katrina_report.htm. Accessed 25 Nov 2011

Dragićević S (2004) The potential of Web-based GIS. J Geogr Syst 6:79–81

Dragićević S, Shivanand B (2004) A web GIS collaborative framework to structure and manage distributed planning processes. J Geogr Syst 6(2):133–153

Evans A, Kingston R, Carver S, Turton I (1999) Web-based GIS to enhance public democratic involvement. GeoComputation '99, 24–28 July, Mary Washington College. http://virtualsociety.sbs.ox.ac.uk/reports/gis.htm

Fabrikant SI, Buttenfield BP (2001) Formalizing semantic spaces for information access. Ann Assoc Am Geogr 91:263–280

Fan-Chieh Y, Chien-Yuan C, Sheng-Chi L, Yu-Ching L, Shang-Yu W, Kei-Wai C (2007) Web-based decision support system for slopeland hazard warning. Environ Monit Assess 127:419–428

Frigerio S, van Westen CJ (2010) RiskCity and WebRiskCity: data collection, display and dissemination in a multi-risk training package. Cartogr Geogr Inf Sci 37(2):119–135

Frigerio S, Blahut J, Sterlacchini S, Poretti I (2010a) Landslides historical dataset and population distribution: Hystoric@, the experience of the Consortium of Mountain Municipalities of Valtellina di Tirano, Italy. In: Malet JP, Glade T, Casagli N (eds) Mountain risks – bringing science to society. CERG, Strasbourg

Frigerio S, Skupinski G, Puissant A, Malet JP, Rose X (2010b) An open source WebGIS platform for sharing information and communicating about risks: the Barcelonnette Basin (South French Alps) as pilot study. In: Malet JP, Glade T, Casagli N (eds) Mountain risks – bringing science to society. CERG, Strasbourg

Glade T, Anderson M, Crozier MJ (2005) Landslide hazard and risk. Wiley, Chichester

Goodchild MF (1999) Future directions in geographic information science. Geogr Inf Sci 5:1–8

Green D, Bossomaier T (2002) Online GIS and spatial metadata. Taylor & Francis, London

Harp EL, Castaneda M, Held MD (2002) Landslides triggered by Hurricane Mitch in Tegucigalpa, Honduras. USGS Open-File Report 02-0033. http://pubs.usgs.gov/of/2002/ofr-02-0033/

Hecht L (2002) Insist on interoperability. GeoWorld 15(4):22–23

Heil B, Reichenbacher T (2009) The use of guidelines to obtain usability for geographic information interfaces. In: International cartography conference 2009, Santiago de Chile

Heil B, Petzold I, Romang H, Hess J (2010) The common information platform for natural hazard in Switzerland. Nat Hazards. doi:10.1007/s11069-010-9606-6

Herrmann J (2008) Interoperable access control for geo web services. In: Nayak S, Zlatanova S (eds) Remote sensing and GIS technologies for monitoring and prediction of disasters. Springer, Berlin/Heidelberg

Holland J (1995) Hidden order: how adaptation builds complexity. Addison-Wesley, Reading

Huang B, Jiang B, Lin H (2001) An integration of GIS, virtual reality and the internet for visualization, analysis and exploration of spatial data. Int J Geogr Inf Sci 15:439–456

Kappes M, Keiler M, von Elverfeldt K, Glade T (2012a) Challenges of analyzing multi-hazard risk: a review. Nat Hazards 64(2):1925–1958

Kappes M, Gruber K, Frigerio S, Bell R, Keiler M, Glade T (2012b) A multi-hazard exposure analysis tool: the MultiRISK platform. Geomorphology 151–152:139–155

Kraak MJ, Brown A (2001) Web cartography, developments and prospects. Taylor & Francis, London

Latini M, Kobben B (2005) A web application for landslide inventory using data-driven SVG. In: van Oosterom PJM et al (eds) Proceeding of the 1st international symposium on geo-information for disaster management. Springer, Berlin, pp 1041–1054

Lehto L (2007) Real-time content transformations in a web service-based delivery architecture for geographic information. Helsinki University of Technology, Helsinki

Lehto I, Sarjakoski T (2005) Real-time generalization of XML-encoded spatial data for the web and mobile devices. Int J Geogr Inf Sci 19(8–9):957–973

MacEachren AM (2001) Cartography and GIS: extending collaborative tools to support virtual teams. Prog Hum Geogr 25(3):431–444

MacEachren AM, Kraak MJ (2001) Research challenges in geovisualization. Cartogr Geogr Inf Sci 28:3–12

Maceachren AM, Cai G, Sharma R, Rauschert I, Brewer I, Bolelli L, Shaparenko B, Fuhrmann S, Wang H (2005) Enabling collaborative geoinformation access and decision-making through a natural, multimodal interface. Int J Geogr Inf Sci 19:293–317

Maggi L (2005) Lack of communication proved crippling: rescue, safety, recovery efforts were hindered. Times-Picayune A10

Maiyo L, Kerle N, Köbben B (2010) Collaborative post-disaster damage mapping via geo web services. In: Konecny M et al (eds) Geographic information and cartography for risk and crisis management – towards better solutions, Lecture notes in geoinformation and cartography. Springer, Berlin/Heidelberg

Malet JP, Remaître A, Maquaire O, Ancey C, Locat J (2003) Flow susceptibility of heterogeneous marly formations. Implications for torrent hazard control in the Barcelonnette basin (Alpes-de-Haute-Provence, France). In: Rickenmann D, Chen CL (eds) Proceedings of the third international conference on debris-flow hazard mitigation: mechanics, prediction and assessment, Davos, Switzerland. Mill Press, Rotterdam

Maquaire O, Malet J-P, Remaître A, Locat J, Klotz S, Guillon J (2003) Instability conditions of marly hillslopes: towards landsliding or gullying? The case of the Barcelonnette basin, South East France. Eng Geol 70(1–2):109–130

Mastin MC, Olsen TD (2002) Fifty-year flood-inundation maps for Tegucigalpa, Honduras: U.S. Geological Survey Open-File Report 02-261. http://pubs.usgs.gov/of/2002/ofr02261/

McEntire DA, Myers A (2004) Preparing communities for disasters: Issues and processes for government readiness. Disaster Prev Manag 13(2):140–152

Moine M, Puissant A, Malet JP (2009) Detection of landslides from aerial and satellite images with a semi-automatic method. Application to the Barcelonnette basin (Alpes-de-Haute-Provence, France). In: Malet JP, Remaître A, Boogard TA (eds) Proceedings of the international conference 'Landslide Processes: from geomorphologic mapping to dynamic modelling'. CERG, Strasbourg

Nappi R, Alessio G, Bronzino G, Terranova C, Vilardo G (2008) Contribution of the SISCam web-based GIS to the seismotectonic study of Campania (Southern Apennines): an example of application to the Sannio-area. Nat Hazards 45:73–85

Newman MEJ (2001) The structure of scientific collaboration networks. Proc Natl Acad Sci USA 98:404–409

Peisheng Z, Yang C (1999) Studies on architecture of Web-GIS. In: Proceedings of the international symposium on digital earth. Science Press, Beijing, China

Peng Z-R, Tsou M-H (2003) Internet GIS: distributed geographic information services for the internet and wireless networks. Wiley, Hoboken

Rivas-Medina A, Gutierrez V, Gaspar-Escribano JM, Benito B (2009) Interactive web visualization tools to the results interpretation of a seismic risk study aimed at the emergency levels definition. Geophys Res Abstr 11:EGU2009–EGU12456

Romang H, Fuchs S, Holub M, Faug T, Naaim M, Tacnet J-M, Durand Y, Giraud G, Dall'Amico M, Larcher M, Rigon R, Knveldsvik V, Sandersen F, Bicchiola D, Rulli C, Bischof N, Bründl M, Rheinberger C, Rhyner J, Barbolini M, Cappabianca F (2009) Work package 5: integral risk management – best practice of integral risk management of snow avalanches, rock avalanches and debris flows in Europe. Tech Rep Irasmos – Integral Risk Management of Extremely Rapid Mass Movements

Salvati P, Calducci V, Bianchi C, Guzzetti F, Tonelli G (2009) A WebGIS for the dissemination of information on historical landslides and floods in Umbria, Italy. Geoinformatica 13:305–322

Soeters R, van Westen CJ (1996) Slope Instability. Recognition, analysis and zonation. In: Turner AK, Schuster RL (eds) Landslide: investigations and mitigation. Special Report 247. Transportation Research Board. National Research Council. National Academy Press, Washington, DC, pp 129–177

Tsou MH (2004) Integrative web-based GIS and image processing tools for environmental monitoring and natural resource management. J Geogr Syst 6:155–174

van Westen CJ (2008) RiskCity: a training package on the use of GIS for urban multi-hazard risk assessment. In: Proceedings of the First world landslide forum, 18–21 Nov 2008, Tokyo, parallel session volume. United Nation University Press, Tokyo

van Westen CJ, Castellanos Abella EA, Sekhar LK (2008) Spatial data for landslide susceptibility, hazards and vulnerability assessment: an overview. Eng Geol 102(3–4):112–131

Waugh LWJ (2000) Living with hazards, dealing with disasters: an introduction to emergency management. M.E. Sharpe Inc., Armonk

Weick KE (1995) Sensemaking in organizations. Sage Publications, Thousand Oaks

Yang CP, Wong D, Yang R, Kafatos M, Li Q (2005) Performance-improving techniques in web-based GIS. Int J Geogr Inf Sci 19(3):319–342

Index

T. van Asch et al. (eds.), *Mountain Risks: From Prediction to Management and Governance*, Advances in Natural and Technological Hazards Research 34,
DOI 10.1007/978-94-007-6769-0, © Springer Science+Business Media Dordrecht 2014